frontiers | Research Topics

Artificial polyploidy in plants, volume II

Edited by
Jen-Tsung Chen, Geoffrey Meru and Jeremy Coate

Published in
Frontiers in Plant Science

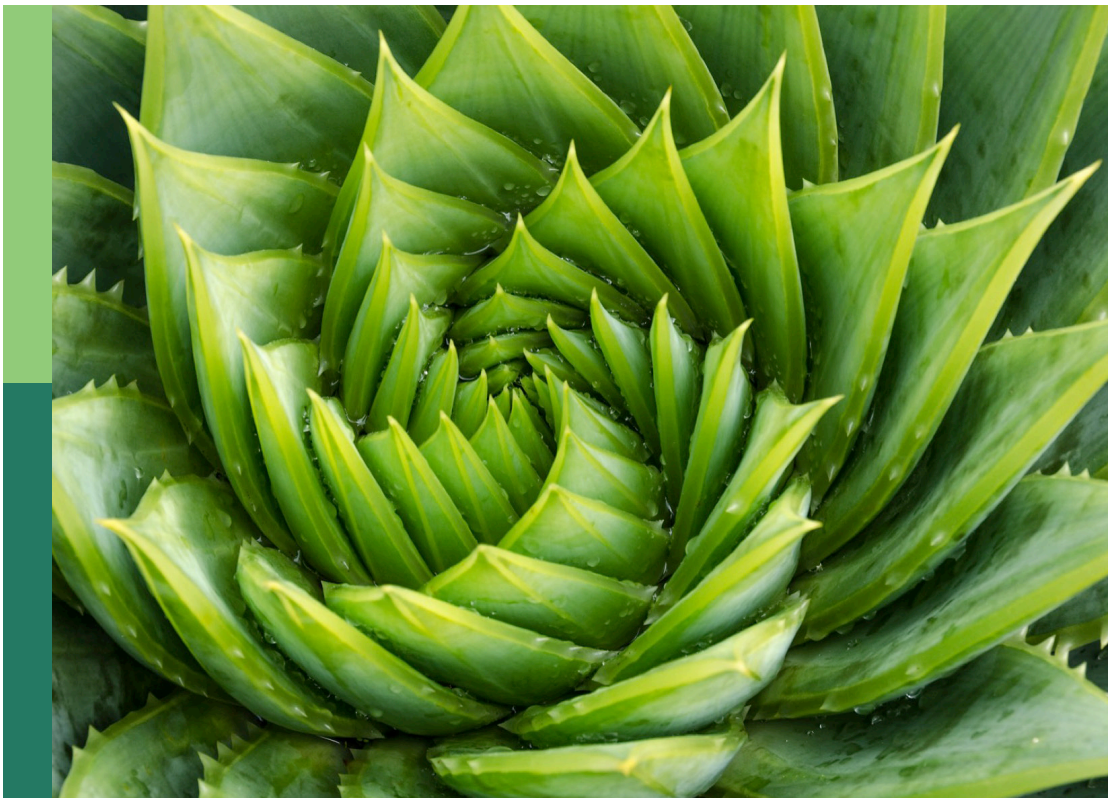

ISSN 1664-8714
ISBN 978-2-83251-468-9
DOI 10.3389/978-2-83251-468-9

About Frontiers

Frontiers is more than just an open access publisher of scholarly articles: it is a pioneering approach to the world of academia, radically improving the way scholarly research is managed. The grand vision of Frontiers is a world where all people have an equal opportunity to seek, share and generate knowledge. Frontiers provides immediate and permanent online open access to all its publications, but this alone is not enough to realize our grand goals.

Frontiers journal series

The Frontiers journal series is a multi-tier and interdisciplinary set of open-access, online journals, promising a paradigm shift from the current review, selection and dissemination processes in academic publishing. All Frontiers journals are driven by researchers for researchers; therefore, they constitute a service to the scholarly community. At the same time, the *Frontiers journal series* operates on a revolutionary invention, the tiered publishing system, initially addressing specific communities of scholars, and gradually climbing up to broader public understanding, thus serving the interests of the lay society, too.

Dedication to quality

Each Frontiers article is a landmark of the highest quality, thanks to genuinely collaborative interactions between authors and review editors, who include some of the world's best academicians. Research must be certified by peers before entering a stream of knowledge that may eventually reach the public - and shape society; therefore, Frontiers only applies the most rigorous and unbiased reviews. Frontiers revolutionizes research publishing by freely delivering the most outstanding research, evaluated with no bias from both the academic and social point of view. By applying the most advanced information technologies, Frontiers is catapulting scholarly publishing into a new generation.

What are Frontiers Research Topics?

Frontiers Research Topics are very popular trademarks of the *Frontiers journals series*: they are collections of at least ten articles, all centered on a particular subject. With their unique mix of varied contributions from Original Research to Review Articles, Frontiers Research Topics unify the most influential researchers, the latest key findings and historical advances in a hot research area.

Find out more on how to host your own Frontiers Research Topic or contribute to one as an author by contacting the Frontiers editorial office: frontiersin.org/about/contact

Artificial polyploidy in plants, volume II

Topic editors

Jen-Tsung Chen — National University of Kaohsiung, Taiwan

Geoffrey Meru — University of Florida, United States

Jeremy Coate — Reed College, United States

Citation

Chen, J.-T., Meru, G., Coate, J., eds. (2023). *Artificial polyploidy in plants, volume II*. Lausanne: Frontiers Media SA. doi: 10.3389/978-2-83251-468-9

Table of contents

frontiers | Frontiers in Plant Science

TYPE Editorial
PUBLISHED 12 January 2023
DOI 10.3389/fpls.2022.1124292

OPEN ACCESS

EDITED AND REVIEWED BY
Diego Rubiales,
Institute for Sustainable Agriculture (CSIC), Spain

*CORRESPONDENCE
Jen-Tsung Chen
jentsung@nuk.edu.tw

SPECIALTY SECTION
This article was submitted to Plant Breeding, a section of the journal Frontiers in Plant Science

RECEIVED 15 December 2022
ACCEPTED 23 December 2022
PUBLISHED 12 January 2023

CITATION
Coate JE, Chen J-T and Meru G (2023) Editorial: Artificial polyploidy in plants, Volume II.
Front. Plant Sci. 13:1124292.
doi: 10.3389/fpls.2022.1124292

Editorial: Artificial polyploidy in plants, Volume II

Jeremy E. Coate[1], Jen-Tsung Chen[2*] and Geoffrey Meru[3]

[1]Department of Biology, Reed College, Portland, OR, United States, [2]Department of Life Sciences, National University of Kaohsiung, Kaohsiung, Taiwan, [3]Horticultural Sciences Department and Tropical Research & Education Center, University of Florida, Gainesville, FL, United States

KEYWORDS

antimitotic agents, artificial polyploidy, plant biotechnology, plant breeding, whole genome duplication

Editorial on the Research Topic
Artificial polyploidy in plants, Volume II

Polyploidy (whole genome multiplication) produces a myriad of dramatic phenotypes, many of which are favored by natural and/or artificial selection. The artificial induction of polyploidy has become an invaluable method both for understanding the evolution of natural polyploid lineages and harnessing polyploidy's potential to produce traits of value to humans. The 14 studies described in the second volume of the research topic, "Artificial Polyploidy in Plants" highlight new methods for generating polyploids across a wide range of plant lineages, illustrate the range of, and recurring patterns in, polyploid phenotypes, provide new mechanistic insights into polyploid phenotypes, and illustrate the dual utility of inducing genome duplications for understanding plant evolution and improving plant agronomic traits.

Methods for generating artificial polyploids

To fully harness the utility of synthetic polyploids, it is critical to optimize methods of polyploid induction. Several studies in the current volume tackle this challenge.

Triploids are variously considered to be infertile deadends (triploid block), or important intermediates in the production of tetraploids (triploid bridge). Li et al. demonstrated that triploids in the orchid genus, *Cymbidium*, produce fertile pollen and that crosses involving triploids produce viable offspring of varying ploidies, including stable tetraploids, demonstrating that triploids are more 'bridge' than 'block' in this genus. This provides support for the idea that triploids can serve as critical intermediates in the evolution of natural polyploids, and illustrates their utility for generating synthetic polyploids.

Commercial garlic is male-sterile and cultivated asexually, limiting the ability to improve traits by traditional breeding methods. Wen et al. established an optimized protocol for *in vitro* induction of autotetraploidy in garlic (*Allium sativum*), achieving

induction rates of 21.8% by culturing explants in 0.2% colchicine for 20 days. Additionally, the authors demonstrated that tetraploids exhibited a number of novel traits, including enhanced production of secondary metabolites, and that induction of polyploidy might enhance the crop's value as a factory for pharmaceuticals.

A major challenge for *in vitro* induction of polyploidy is the frequent formation of unstable mixoploids (cytotypic mosaics). Working with *Magnolia officinalis*, Gao et al. described a novel procedure using colchicine treatment of embryonic cell aggregates to produce, in some cases, 100% tetraploid somatic embryos with no mixoploids. Cell lines and plantlets demonstrated stable ploidy throughout the somatic embryogenesis process, providing a potentially more efficient approach for trait improvement through polyploidy induction.

In addition to the use of antimitotic agents, high-temperature treatments are another method for inducing polyploidy. Liu et al. analyzed the timing of zygotic development in relation to floral bud development in *Eucalyptus urophylla* to identify the optimal timing of heat treatment for inducing zygotic doubling. They first established that zygotic mitosis initiated on day 23 post-fertilization. They then demonstrated, for the first time in *E. urophylla*, that zygotic doubling could be induced by heat treatment on days 24-26, with the highest rate of induction achieved on day 25 (additionally determining the optimal heat treatment conditions for inducing doubling). The authors further documented a range of phenotypic effects in the derived polyploids and linked these traits to changes in gene expression (see below). These data should facilitate the breeding of improved eucalyptus crops *via* polyploidy induction.

Phenotypic effects of polyploidy

Several studies in this collection illustrate the breadth of phenotypic changes induced by polyploidy. To cite a few examples, polyploids were shown to exhibit novel traits ranging from morphological (e.g., larger cells, thicker leaves, longer wood fibers), physiological (e.g., higher chlorophyll contents and photosynthetic rates) and biochemical (higher contents of secondary metabolites, chlorophyll, and hormones), to complex traits of agricultural significance (higher or lower growth rates, drought tolerance, resistance to lodging).

In some cases, the direction of these phenotypic effects varied by species. For example, though *Cymbopogon khasianus* polyploids were larger than their diploid progenitors (Vimala et al.), polyploids in other taxa exhibited reduced biomass and dwarf phenotypes [e.g., hybrid poplar (Wouters et al.), garlic (Wen et al.), hybrid sweetgum (Chen et al.)]. Often, however, several similar phenotypic effects were observed across evolutionarily distant lineages, revealing some recurring themes in the immediate consequences of polyploidy. Increased cell sizes were documented in garlic (Wen et al.), Cymbopogon (Vimala et al.), and hybrid sweetgum (Chen et al.), and drought tolerance was observed in figs (Abdolinejad and Shekafandeh) and sour jujube (Li et al.). Tolerance to drought and other stresses has emerged as a common property of polyploids, including neopolyploids, as discussed by Tossi et al.

A potentially significant source of phenotypic variation in polyploids is alterations in chromosome numbers and gene dosage associated with aneuploidy and structural changes. Zhong et al. used microsatellites and fluorescence *in situ* hybridization to study chromosomal number and structural variation in the offspring of an interploidy cross, *Populus alba* × *Populus berolinensis* 'Yinzhong'. They identified progeny representing a range of aneuploidies and structural changes which will be a useful resource for future studies on the effects of changes in gene and chromosome dosage on trait variation.

Though numerous studies, including several in this collection, have identified traits that are likely to be beneficial to the plant and/or useful to humans, it is important to keep in mind that the effects of polyploidy are, in many cases, highly variable, taxon-specific, and/or deleterious (or at least undesirable from a human-use point of view). Wouters et al. demonstrated that induction of polyploidy in hybrid poplar resulted in a propensity for their apical meristems to break, as well as in reduced biomass and increased lignin content (resulting in lower saccharification efficiency). Though this contrasted with what was observed previously in Arabidopsis, the reduced biomass was consistent with what Wen et al. observed in Allium, and what Liu et al. reported for *Eucalyptus urophylla*. Thus, just as polyploidy has mixed effects on evolutionary success in natural populations, these studies serve as a reminder that polyploidy should not be oversold as a panacea for crop improvement.

Molecular phenotypes and mechanistic insights into the consequences of polyploidy

Though numerous studies have documented a plethora of phenotypes associated with polyploidy, our understanding of the underlying molecular mechanisms lags behind. Several studies in the current collection contribute important insights on this front as well. Tossi et al., for example, undertook a comprehensive review of the mechanisms by which polyploidy confers stress tolerance. Among many mechanisms discussed, they note that epigenetic modifications and changes in hormone levels have emerged as key players in polypoid phenotypes (including tolerance to various stresses), and examples of both are reported in this collection.

Xiao et al. characterized changes to the DNA methylome of autotetraploid cassava (*Manihot esculenta*) and concluded that

variation in methylation around transposable elements acts to adaptively modulate dosage responses of protein-coding genes and lncRNA genes. Abdolinejad and Shekafandeh showed that enhanced water stress tolerance in figs was associated with elevated levels of stress hormones. Chen et al. showed that the dwarf phenotype in tetraploid hybrid sweetgum (*Liquidambar styraciflua* × *L. formosana)* correlated with differential expression of hormone biosynthetic genes, and with reduced levels of auxin, gibberellin, and brassinolide in both roots and stems. Notably, they showed that exogenous gibberellin and auxin treatments significantly promoted stem and root growth, and concluded that reduced growth in the tetraploids was a consequence of auxin and gibberellin deficiency. Interestingly, Tossie et al. describe cases in which stress response genes, including those involved in jasmonic acid biosynthesis, are primed by hypomethylation, enabling a more rapid and robust response to stress. Thus, epigenetic modifications and hormone biosynthesis have been mechanistically linked in promoting stress tolerance in polyploids.

The molecular changes that contribute to polyploid phenotypes extend beyond epigenetics and hormone biology, however. Abdolinejad and Shekafandeh, for example, showed that in addition to elevated hormone levels, drought tolerance in figs was associated with elevated levels of protective osmolytes and scavengers of reactive oxygen species, suggesting that tetraploidy induces a multi-layered stress response.

Two studies in this collection link polyploid phenotypes to transcription factors. Li et al. showed that the enhanced drought tolerance in sour jujube autotetraploids correlated with a near doubling in vessel elements and parenchyma cells and that the transcription factor, ZjVND7, which is known to play a central role in xylem vessel development, was differentially expressed between diploids and tetraploids under drought conditions. Using DAP-Seq, they found more targets of ZjVND7 in the tetraploid, with enrichment for targets involved in xylem development. Among these targets was the gene *ZjSMR1*, which had a stronger binding signal for ZjVND7 in tetraploids than in diploids under drought. They hypothesize that altered ZjVND7 activity upregulates ZjSMR1 to promote xylem vessel formation. Liu et al. found that differences in leaf chlorophyll contents between diploid and triploid *E. urophylla* correlated with changes in the expression of Golden 2-Like (GLK) transcription factors, and provided evidence that GLKs positively regulate gene co-expression networks involved in chlorophyll biosynthesis.

Conclusions and perspectives

Polyploidy induces a range of traits of value to humans, and inducing polyploidy has become an important tool in the plant breeder's toolbox (Chen et al., 2020). At the same time, generating synthetic polyploids allows researchers to step back in time to better understand the early evolution of natural polyploids. As with volume I of this Research Topic, volume II highlights several recent advances in the biology of artificial polyploidy. The 14 studies included in this volume highlight the very active and vibrant nature of ongoing research in this field, describing advances in our ability to generate polyploids, as well as in our understanding of polyploid phenotypes and how they arise. We hope this collection stimulates further work and breakthroughs on this important topic.

Author contributions

J-TC, JC and GM drafted the manuscript. All authors revised and approved the final version.

Acknowledgments

We greatly appreciate the invaluable contributions of all authors, reviewers, and Dr. Diego Rubiales, Specialty Chief Editor for Plant Breeding of Frontiers in Plant Science.

Conflict of interest

The authors declare that the research was conducted in the absence of any commercial or financial relationships that could be construed as a potential conflict of interest.

Publisher's note

Reference

Chen, J.-T., Coate, J. E., and Meru, G. (2020). Artificial polyploidy in plants. *Front. Plant Sci.* 11. doi: 10.3389/fpls.2020.621849

frontiers in Plant Science

ORIGINAL RESEARCH
published: 26 January 2022
doi: 10.3389/fpls.2021.816946

Variation of Chromosome Composition in a Full-Sib Population Derived From 2x × 3x Interploidy Cross of *Populus*

*Yu-Hang Zhong[1,2,3,4], Yun-Fei Zheng[2,3,4], Yin-Xuan Xue[1,2,3,4], Lv-Ji Wang[1,2,3,4], Jin-Wang Zhang[5], Dai-Li Li[6] and Jun Wang[1,2,3,4]**

[1] National Engineering Research Center of Tree Breeding and Ecological Remediation, Beijing Forestry University, Beijing, China, [2] Key Laboratory of Genetics and Breeding in Forest Trees and Ornamental Plants, MOE, Beijing Forestry University, Beijing, China, [3] The Tree and Ornamental Plant Breeding and Biotechnology Laboratory, National Forestry and Grassland Administration, Beijing Forestry University, Beijing, China, [4] College of Biological Sciences and Technology, Beijing Forestry University, Beijing, China, [5] Forestry and Grassland Research Institute of Tongliao City, Tongliao, China, [6] Beijing Institute of Landscape Architecture, Beijing, China

OPEN ACCESS

Edited by:
Jen-Tsung Chen,
National University of Kaohsiung, Taiwan

Reviewed by:
Mahmoud Said,
Institute of Experimental Botany, Academy of Sciences of the Czech Republic, Czechia
Rodrigo R. Amadeu,
Bayer Crop Science, United States

***Correspondence:**
Jun Wang
wangjun@bjfu.edu.cn

Specialty section:
This article was submitted to Plant Breeding, a section of the journal Frontiers in Plant Science

Received: 17 November 2021
Accepted: 27 December 2021
Published: 26 January 2022

Citation:
Zhong YH, Zheng YF, Xue YX, Wang LJ, Zhang JW, Li DL and Wang J (2022) Variation of Chromosome Composition in a Full-Sib Population Derived From 2x × 3x Interploidy Cross of Populus. Front. Plant Sci. 12:816946. doi: 10.3389/fpls.2021.816946

Interploidy cross commonly results in complex chromosome number and structural variations. In our previous study, a progeny with segregated ploidy levels was produced by an interploidy cross between diploid female parent *Populus tomentosa* × *Populus bolleana* clone TB03 and triploid male parent *Populus alba* × *Populus berolinensis* 'Yinzhong'. However, the chromosome compositions of aneuploid genotypes in the progeny were still unclear. In the present study, a microsatellite DNA allele counting–peak ratios (MAC-PR) method was employed to analyze allelic configurations of each genotype to clarify their chromosome compositions, while 45S rDNA fluorescence *in situ* hybridization (FISH) analysis was used to reveal the mechanism of chromosome number variation. Based on the MAC-PR analysis of 47 polymorphic simple sequence repeat (SSR) markers distributed across all 19 chromosomes of *Populus*, both chromosomal number and structural variations were detected for the progeny. In the progeny, 26 hypo-triploids, 1 hyper-triploid, 16 hypo-tetraploids, 10 tetraploids, and 5 hyper-tetraploids were found. A total of 13 putative structural variation events (duplications and/or deletions) were detected in 12 genotypes, involved in chromosomes 3, 6, 7, 14, 15, 16, and 18. The 46.2% (six events) structural variation events occurred on chromosome 6, suggesting that there probably is a chromosome breakpoint near the SSR loci of chromosome 6. Based on calculation of the allelic information, the transmission of paternal heterozygosity in the hypo-triploids, hyper-triploid, hypo-tetraploids, tetraploids, and hyper-tetraploids were 0.748, 0.887, 0.830, 0.833, and 0.836, respectively, indicating that the viable pollen gains of the male parent 'Yinzhong' were able to transmit high heterozygosity to progeny. Furthermore, 45S rDNA–FISH

analysis showed that specific-chromosome segregation feature during meiosis and chromosome appointment in normal and fused daughter nuclei of telophase II of 'Yinzhong,' which explained that the formation of aneuploids and tetraploids in the progeny could be attributed to imbalanced meiotic chromosomal segregation and division restitution of 'Yinzhong,' The data of chromosomal composition and structural variation of each aneuploid in the full-sib progeny of TB03 × 'Yinzhong' lays a foundation for analyzing mechanisms of trait variation relying on chromosome or gene dosages in *Populus*.

Keywords: aneuploidy, chromosome composition, heterozygosity transmission, interploidy cross, *Populus*, SSR karyotypic analysis, 45S rDNA–FISH

INTRODUCTION

Chromosome number variation, such as euploidy and aneuploidy variation, commonly leads to extensive phenotypic changes, which have been widely used in breeding programs of plants. Compared to euploids, aneuploids characterized by loss or gain of one or more individual chromosome(s) are particularly valuable for chromosome engineering breeding and cytogenetic research. According to the loss or gain of chromosome(s) from euploid, aneuploid commonly can be classified into two basic types: hypo- and hyper-euploid. Both types of aneuploids could be produced by crossing with polyploids because imbalanced meiotic chromosome segregation and chromosome elimination of polyploids can result in the formation of aneuploid gametes. In *Arabidopsis thaliana*, Henry et al. (2005) produced a swarm of different aneuploids by self-pollination of triploids, and revealed that chromosome composition and dosage variation strongly result in phenotypic changes (Henry et al., 2010). In apple, aneuploids with 35–55 chromosomes and tetraploids with 68 chromosomes were also produced from the crosses with diploids and triploids (Zhang and Park, 2009). To analyze the chromosomal function and evolutionary relationships and to locate functional genes, serial lines of monosomes, nullisomes, trisomes, and tetrasomes have all been established in wheat (Law et al., 1987). Undoubtedly, chromosome manipulation based on aneuploids has attracted increasing attention for improving the efficiency in plant breeding.

Populus is an important model for the forest tree biotechnology and genetic research (Taylor, 2002; Wullschleger et al., 2002; Jansson and Douglas, 2007). The utilization of chromosome number variation, especially polyploidization, has been proved as an important approach in *Populus* breeding programs. In the past several decades, many allotriploid poplar cultivars, such as *P.* × 'Beilinxiongzhu 1,' *P. tomentosa* 'Sanmaoyang,' *P. tremula* × *P. tremuloides* cv. Astria, *P.* × *euramericana* 'Zhonglin-46,' and *P. alba* × *P. berolinensis* 'Yinzhong' (Baumeister, 1980; Chen et al., 2004; Zhang et al., 2004, 2005; Kang, 2016), have been bred and widely used in plantations of the Northern Hemisphere owing to their favorable growth performance and pulpwood characteristics (Einspahr, 1984; Zhu et al., 1998; Kang, 2016). In aspect of aneuploidization of *Populus*, interploidy cross is a valid approach. Wang et al. (2017) produced a progeny with extensive segregation of ploidy levels, including many aneuploids, by pollinating triploid 'Yinzhong' to diploid *P. tomentosa* × *P. bolleana* clone TB03. For the aneuploids, however, their chromosome compositions were still unclear.

Several methods have been developed to analyze the chromosome compositions of aneuploids, such as cytological karyotypic analysis and marker-based dosage analysis. However, karyotypic analysis based on chromosome morphology is difficult for poplar trees owing to their small and similar chromosomes. By contrast, marker-based dosage analysis has extensive applicability. Esselink et al. (2004) developed a microsatellite DNA allele counting–peak ratios (MAC-PR) method to assign allelic configuration in *Rosa*. This method was also successfully used in the analysis of parental heterozygosity transmission of gametes in *Citrus* (Xie et al., 2015). In *Arabidopsis thaliana*, quantitative fluorescent PCR (QF-PCR) based on microsatellite and InDels markers was used to conduct molecular karyotyping and aneuploidy detection by analyzing the height of highest fluorescent peak or sum of the height of two highest peaks (Henry et al., 2006).

Recently, the fluorescence *in situ* hybridization (FISH) technique was used to position specific chromosomes in meiosis of plants. Zhao et al. (2019) found dramatically biased pairing of homoeologous chromosomes and different univalent and chromosome lagging frequencies between C- and H-subgenomes in interspecific hybrids and allotetraploid *Cucumis* × *hytivus* through oligo-painting and genomic *in situ* hybridization (GISH), concluding that the meiotic behavior harmony of subgenomes is important for meiotic evolution. In *Saccharum officinarum* × *Erianthus arundinaceus* hybrids, unequal chromosome segregation and chromosome losing were observed during meiosis based on 5S rDNA and 45S rDNA FISH analyses (Li et al., 2021). Definitely, the FISH analysis has developed into a reliable tool for tracing the chromosome behavior during meiosis of plants.

In this investigation, aiming to clarify the chromosome composition of each genotype for the TB03 × 'Yinzhong' progeny, the MAC-PR method was used to analyze the allelic configurations of each genotype based on the simple sequence repeat (SSR) markers located throughout all 19 chromosomes. The heterozygosity transferred from the male parent was also evaluated based on the allelic configurations for different ploidy groups. Furthermore, cytological records based on 45S

rDNA–FISH were conducted to reveal the mechanism of chromosome number variations. These data will help us to understand the rule of chromosome segregation of triploid 'Yinzhong'.

MATERIALS AND METHODS

Plant Materials

A total of 58 aneuploids were derived from interploidy cross between diploid female parent *Populus tomentosa* × *P. bolleana* clone TB03 and triploid male parent *P. alba* × *P. berolinensis* 'Yinzhong' (Wang et al., 2017) were used for chromosome composition analysis in the present study. All plants including parents were cultivated in greenhouse of Beijing Forestry University, Beijing, China. Young leaves were collected from these plants and stored at −80°C for DNA extraction.

Genomic DNA Extraction and Simple Sequence Repeat Genotyping

Genomic DNA of all samples was isolated from the young leaves using a DP320 DNAsecure Plant Kit (TianGen, Beijing, China) following the manufacturer's instruction. The quality and concentration of the stock DNA were checked with a NanoDrop 2000 spectrophotometer (Thermo Fisher Scientific, Wilmington, DE, United States). For SSR analysis, all stock DNA samples were diluted to a final concentration of 50 ng μl^{-1} and stored at −20°C.

SSR markers used for this study should be polymorphic between the parents and covers all chromosomes (Xie et al., 2015). According to this principle, 21 markers were selected from a database of the International *Populus* Genome Consortium[1] and published papers of Yin et al. (2009) and Du et al. (2013). In addition, 26 markers were selected from a self-designed database using the *Populus trichocarpa* genome (v3.1, available at https://phytozome-next.jgi.doe.gov/).

The SSR primer pairs (**Supplementary Table 1**) were synthesized by Sangon Biotech (Shanghai, China). Following the fluorescence-labeled TP-M13-SSR PCR method (Schuelke, 2000), the forward primer of each pair was tagged with the universal M13 sequence (5′-TGTAAAACGACGGCCAGT-3′) during synthesis. Each PCR used a 20-μl total volume

[1]http://web.ornl.gov/sci/ipgc/ssr_resource.htm

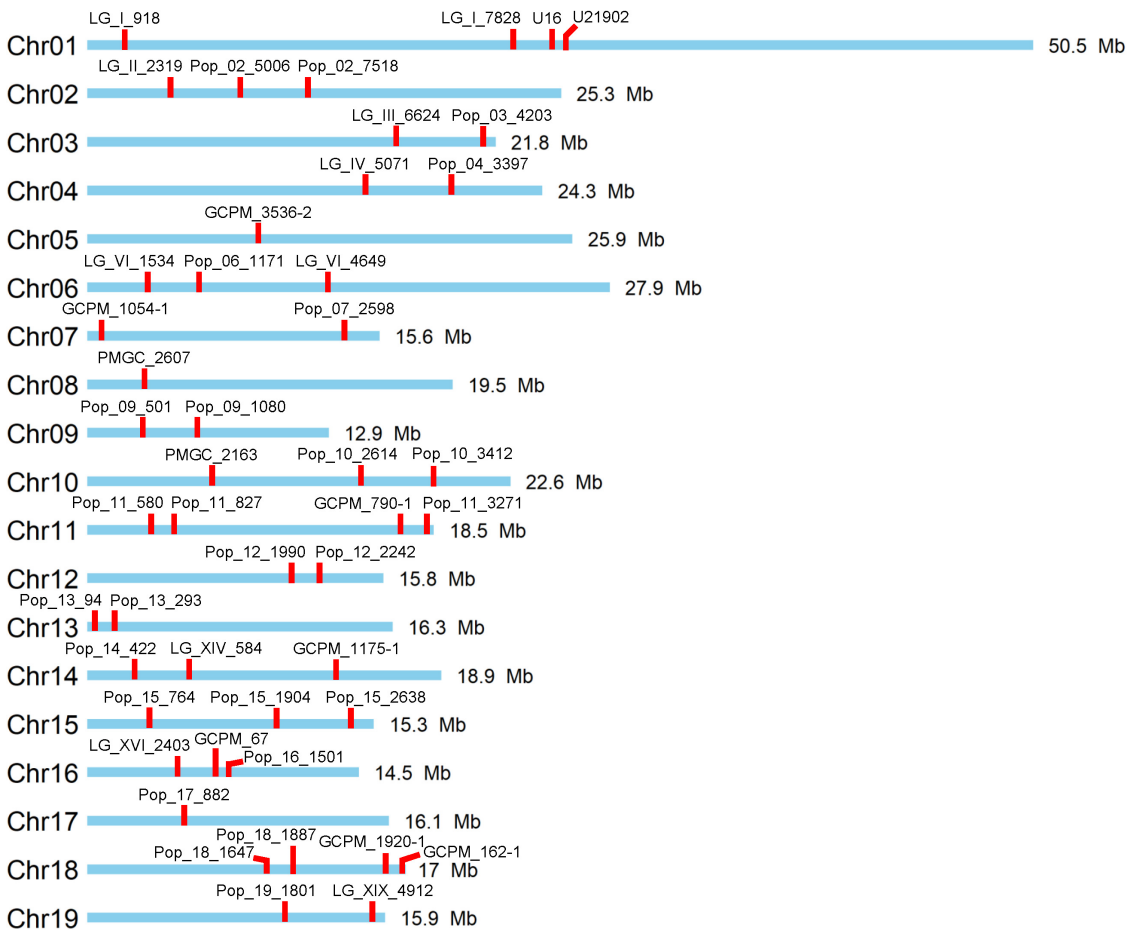

FIGURE 1 | Distribution of used 47 simple sequence repeat (SSR) markers on the 19 chromosomes of *Populus*.

containing 10 μl 2 × TSINGKE® Master Mix (with *Taq*-polymerase Tsingke, Beijing, China), 0.4 pmol forward primer, 1.6 pmol reverse primer, 1.6 pmol fluorescent-dyelabeled (FAM, HEX, TAMRA, ROX) M13 primer (Synthesized by RuiBiotech Inc., Beijing, China), and 15 ng genomic DNA. PCR amplifications were performed in a SimpliAmp™ thermal cycler (Thermo Fisher Scientific, Singapore) using the following program: 94℃ for 5 min; followed by 30 cycles of 30 s at 94℃, 45 s at 56℃, and 45 s at 72℃; then 8 cycles of 30 s at 94℃, 45 s at 53℃, and 45 s at 72℃; and a final extension at 72℃ for 10 min. Then capillary electrophoresis fluorescence-based SSR analyses were conducted on an ABI 3730xl DNA Analyzer by RuiBiotech Inc., Beijing, China, and the data were analyzed using the GeneMarker software v2.2.0 (SoftGenetics LLC, State College, PA, United States) with the default settings. The relative allelic dosage was estimated based on the MAC-PR method (Esselink et al., 2004) to assess the genotype of each sample.

45S rDNA–FISH During Meiosis of 'Yinzhong'

The male flower buds of 'Yinzhong' under meiosis were collected and fixed in Carnoy's mixture (ethanol:acetic acid = 3:1) for 24 h at 4℃. Subsequently, anthers were harvested to slide preparation. The anthers were washed for 15 min with distilled water and digested using an enzyme mixture, i.e. 3% cellulose Onozuka R-10 (Yakult Pharmaceutical, Tokyo, Japan) and 1% pectolyase Y-23 (Yakult Pharmaceutical, Tokyo, Japan) in 0.01 M citric buffer (pH 4.5), at 37℃ for 3 h. Then, the digested anthers were washed for 5 min in distilled water and squashed in a drop of 45% acetic acid on slides. After freezing in liquid nitrogen, the coverslips of the slide preparations were immediately removed. The preparations without coverslips were stored at −20℃ for FISH analysis.

According to Li et al. (2001) with some modifications, before *in situ* hybridization, the slide preparations were treated with 100 μg ml^{-1} of DNase-free RNase at 37℃ for 1 h and 1 μg ml^{-1} of Proteinase K at 37℃ for 40 min. After three 5-min washes in 2 × SSC at room temperature, the slides were post-fixed in 4% paraformaldehyde at room temperature for 10 min, washed twice in 2 × SSC for 5 min, dehydrated through a graded ethanol series (70, 90, and 100%), and air-dried. Plasmids containing 45s rDNA sequence were gifted from Dr. Guixiang Wang in Beijing Academy of Agriculture and Forestry Sciences, China. The 45S rDNA probe was labeled with DIG-11-dUTP using a standard nick translation reaction (DIG-Nick Translation Mix, Roche, Cat. No. 11745816910, Mannheim, Germany).

The fluorescence *in situ* hybridization was performed following standard protocols (Comai et al., 2003). The hybridization mixture contained 50% deionized formamide, 2 × SSC, 10% dextran sulfate, 0.1% SDS, and 2 ng μl^{-1} of labeled probe for each slide. The probe was detected by fluorescein anti-digoxigenin (Anti-Digoxigenin-Fluorescein Fab fragments, Roche, Cat. No. 11207741910, Mannheim, Germany). Chromosomes were counter stained with DAPI in VectaShield antifade mounting medium (Vector Laboratories, Burlingame, CA, United States). All slides were examined using an Olympus BX53 microscope (Olympus, Tokyo, Japan) equipped with a CoolCube 1 camera (MetaSystems, Altlussheim, Germany). Signal capturing and picture processing were performed using the Isis imaging software (MetaSystems, Altlussheim, Germany). The final image adjustment was done with Adobe Photoshop CC 2018 (Adobe Systems Incorporated, San Jose, CA, United States).

Heterozygosity Analysis

To analyze the genetic heterozygosity of population with mixed ploidy levels, GenoDive v (Meirmans and Van Tienderen, 2004) was used to calculate the observed heterozygosity (*Ho*).

RESULTS

Chromosomal Composition in Progeny

In this study, a total of 47 polymorphic SSR markers with no more than one allele shared between female parent clone TB03 and male parent 'Yinzhong' were screened for genotyping of the progeny (**Figure 1**). Out of the 47 markers, 12 markers dispersed on 11 chromosomes, including LG_I_918, Pop_02_7518, Pop_03_4203, Pop_04_3397, PMGC_2607, PMGC_2163, Pop_11_3271, Pop_13_293, GCPM_67, Pop_18_1647, GCPM_162-1, and Pop_19_1801 amplified completely different fragments between the two parents (**Table 1**). According to the allele data of the 12 markers in progeny, we found that the female parent TB03 only contributed one locus in all progeny (**Supplementary Table 2**), suggesting that the female parent TB03 only contributed normal eggs in the interploidy hybridization.

Based on the relative allelic dosage estimation of MAC-PR analysis at all loci of each sample (**Figure 2**), chromosomal compositions of all genotypes were revealed. Both chromosomal number variations and structural rearrangements were found in this progeny (**Figure 3**). In term of chromosomal number variation, all genotypes in the progeny contained at least three copies of chromosomes 1, 2, and 4. The 58 offspring were divided into 26 hypo-triploids, 1 hyper-triploid, 16 hypo-tetraploids, 10 tetraploids, and 5 hyper-tetraploids in the progeny. In the 26 hypo-triploids, the number of missed entire chromosomes ranged from 1 to 5, involved in all chromosomes except chromosomes 1, and 2 to 4. The chromosome 3 was the most frequently missed (∼13.8%) in the hypo-triploids. The unique hyper-triploid contained an extra chromosome 1. In the 16 hypo-tetraploids, the number of missed entire chromosome ranged from 1 to 3, involved in chromosomes 2, 3, 5, 9, 11, 13, 14, 16, 17, and 19. The most frequently missed entire chromosome was chromosome 9, with the frequency of 23.5%. The hyper-tetraploids included 4 4x + 1 type and 1 4x + 2 type. For the 4x + 1 type hyper-tetraploids, the gained chromosomes are involved in chromosomes 3, 5 (in two genotypes), and 9. In the unique 4x + 2 type hyper-tetraploid, there were five copies of chromosomes 1 and 9, respectively.

Structural Variation Detection

Besides the chromosomal number variation, interestingly, chromosome structural variations, such as duplications and/or

TABLE 1 | Heterozygosity analysis of each simple sequence repeat (SSR) loci and each chromosome for the mixed ploidy progeny.

Chromosome number	Locus	*Ho* for each allele	*Ho* for each chromosome
Chromosome 1	LG_I_918	0.921	0.830
	LG_I_7828	0.852	
	U16	0.875	
	U21902	0.673	
Chromosome 2	LG_II_2319	0.770	0.718
	Pop_02_5006	0.626	
	Pop_02_7518	0.759	
Chromosome 3	LG_III_6624	0.767	0.858
	Pop_03_4203	0.949	
Chromosome 4	LG_IV_5071	0.905	0.849
	Pop_04_3397	0.793	
Chromosome 5	GCPM_3536-2	0.853	0.853
Chromosome 6	LG_VI_1534	0.876	0.866
	Pop_06_1171	0.832	
	LG_VI_4649	0.891	
Chromosome 7	GCPM_1054-1	0.796	0.722
	Pop_07_2598	0.647	
Chromosome 8	PMGC_2607	0.807	0.807
Chromosome 9	Pop_09_501	0.836	0.830
	Pop_09_1080	0.824	
Chromosome 10	PMGC_2163	0.983	0.869
	Pop_10_2614	0.805	
	Pop_10_3412	0.819	
Chromosome 11	Pop_11_580	0.842	0.891
	Pop_11_827	0.908	
	GCPM_790-1	0.874	
	Pop_11_3271	0.940	
Chromosome 12	Pop_12_1990	0.871	0.855
	Pop_12_2242	0.839	
Chromosome 13	Pop_13_94	0.624	0.796
	Pop_13_293	0.968	
Chromosome 14	Pop_14_422	0.839	0.851
	LG_XIV_584	0.796	
	GCPM_1175-1	0.917	
Chromosome 15	Pop_15_764	0.859	0.782
	Pop_15_1904	0.890	
	Pop_15_2638	0.597	
Chromosome 16	LG_XVI_2403	0.822	0.912
	GCPM_67	0.991	
	Pop_16_1501	0.922	
Chromosome 17	Pop_17_882	0.874	0.874
Chromosome 18	Pop_18_1647	0.989	0.883
	Pop_18_1887	0.830	
	GCPM_1920-1	0.750	
	GCPM_162-1	0.963	
Chromosome 19	Pop_19_1801	0.960	0.934
	LG_XIX_4912	0.908	

deletions, were detected on many loci. For example, in the genotype TY02 (3x-1 type with two chromosome 18), the allelic configure on locus LG_VI_4649 was abc, but the allelic configure on loci LG_VI_1534 and Pop_06_1171 were ac and ab, respectively, suggesting that either deletion occurred on the fragments containing loci LG_VI_1534 and Pop_06_1171 in condition of three copies of chromosome 6 or duplication occurred on the fragment containing locus LG_VI_4649 in condition of two copies chromosome 6. For the genotype TY29 (tetraploid with fragment deletion on chromosome 6), loci on all chromosomes had four copies, except for the chromosome 6. Both the loci LG_VI_1534 and Pop_06_1171 on chromosome 6 showed three alleles and LG_VI_4649 had four alleles, indicating that deletion was happened on chromosome 6. As a result, all tetraploids with deletions of part chromosome were grouped into hypo-tetraploids.

According to the amplified data of total 47 loci, we detected 13 putative structural variation events in 12 genotypes. The genotype TY02 included 2 structural variation events, locating on chromosomes 6 and 7, respectively. The 13 structural variation events were dispersed on 7 different chromosomes, i.e., chromosomes 3, 6, 7, 14, 15, 16, and 18 (**Figure 3**). Six structural variation events occurred on chromosome 6, accounting for 46.2%, and two events occurred on chromosome 15.

Analysis of Heterozygosity Transmission

According to allelic variation of the 47 loci, the observed heterozygosity of the whole progeny was 0.843. The heterozygosity levels of loci were positively related with the number of alleles (r = 0.8264, p = 8.494e-13). For the different chromosomes, the maximum *Ho* was 0.934 on chromosome 19 and the minimum was 0.718 on chromosome 2 (**Table 1**). The *Ho* of the hypo-triploids, hyper-triploid, hypo-tetraploids, tetraploids, and hyper-tetraploids was 0.844, 0.862, 0.846, 0.835, and 0.843, respectively.

In the aspect of paternal heterozygosity transmission, the transmitted paternal heterozygosity in the progeny was 0.795. Based on the chromosome-specific analysis, the maximum paternal heterozygosity transmission was 0.925 of chromosome 17 and the minimum was 0.477 of chromosome 8 (**Supplementary Table 3**). The locus with the highest paternal heterozygosity transmission was LG_IV_5071 on chromosome 4 and the locus with the lowest paternal heterozygosity transmission was Pop_02-7518 on chromosome 2. The transmitted paternal heterozygosity in the hypo-triploids, hyper-triploid, hypo-tetraploids, tetraploids, and hyper-tetraploids was 0.748, 0.887, 0.830, 0.833, and 0.836, respectively, indicating that the viable pollen gains of 'Yinzhong' were able to transmit high heterozygosity to progeny.

Meiotic Specific-Chromosome Segregation Feature

To clarify the chromosome segregation feature during meiosis of 'Yinzhong,' chromosome behaviors were observed based on 45S rDNA–FISH analysis. At metaphase I of 'Yinzhong,' the pairing pattern of the 45S rDNA located chromosomes exhibited univalent (I) + bivalent (II), I + I + I, and trivalent (III) types (**Figures 4A–C**), suggesting that the 45S rDNA signals were just located three homoeologous chromosomes of 'Yinzhong'. At anaphase I, the segregation of the chromosomes commonly

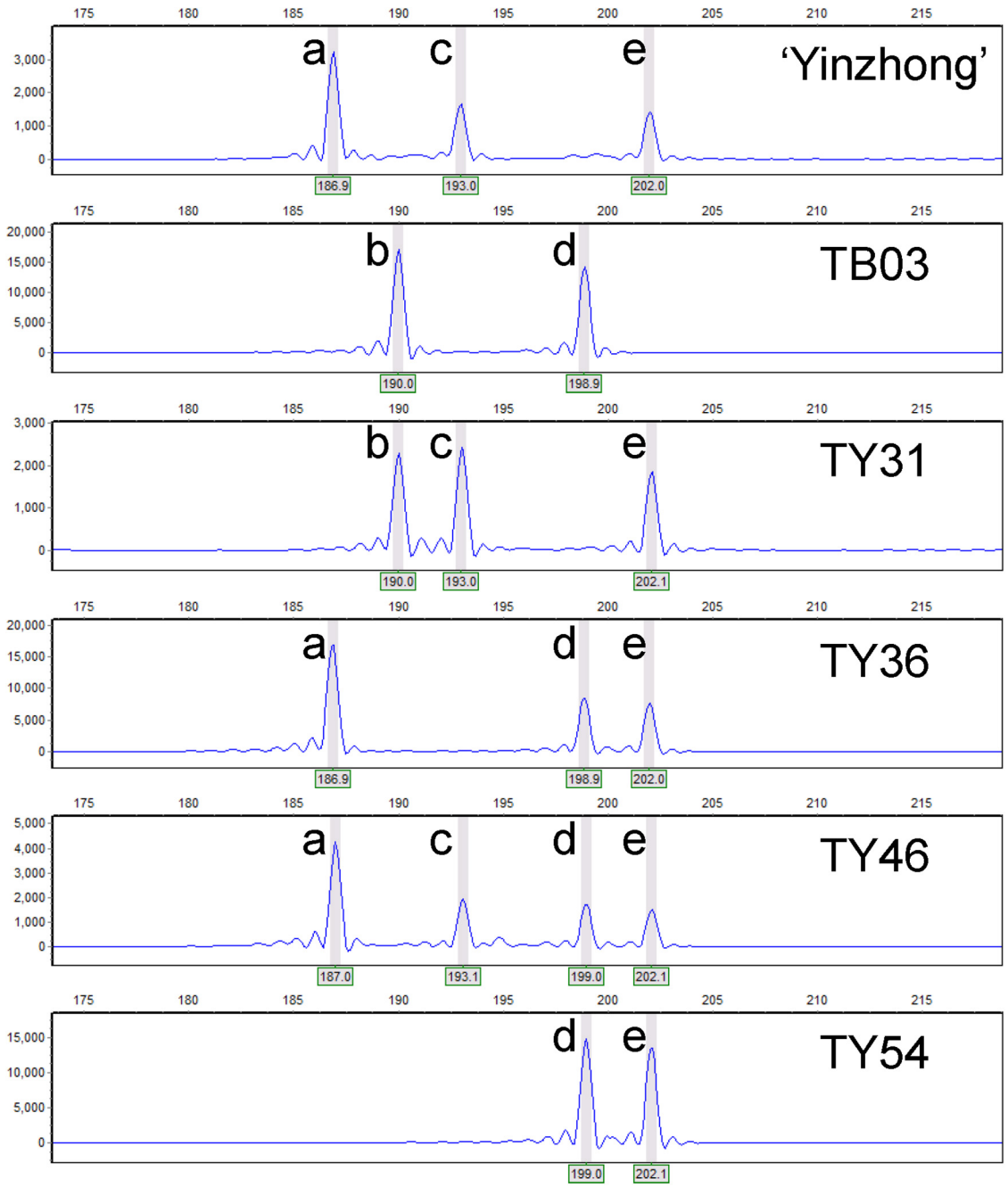

FIGURE 2 | Genotypic analyses of the parents and parts of progeny based on capillary electrophoresis of locus Pop-11-3271. Letters a–e represent the alleles at the locus Pop-11-3271.

followed the unequal 1:2 pattern in most of the cells (**Figure 4D**). One of the 45S rDNA signals also might locate on a lagging chromosome in some cells (**Figure 4E**). Interestingly, several cells with three 45S rDNA signals located in one daughter nucleus were observed (**Figure 4F**).

At anaphase II, the sister chromatids were usually segregated into daughter nuclei (**Figure 4G**). However, failed segregation of sister chromatids also was observed in several microcytes, resulting in two sister chromatids moved into the same daughter nucleus (**Figure 4H**). At telophase II, although microcytes with normal four daughter nuclei were dominant, microcytes with fused nuclei were also observed. In normal daughter nucleus, the number of 45S rDNA signals was 0–3, and in the fused nucleus, 2–4 45S rDNA signals were recorded (**Figures 4I–L**), suggesting that 0–4 dosages of 45S rDNA located chromosome will be contained in the male gametes of 'Yinzhong.'

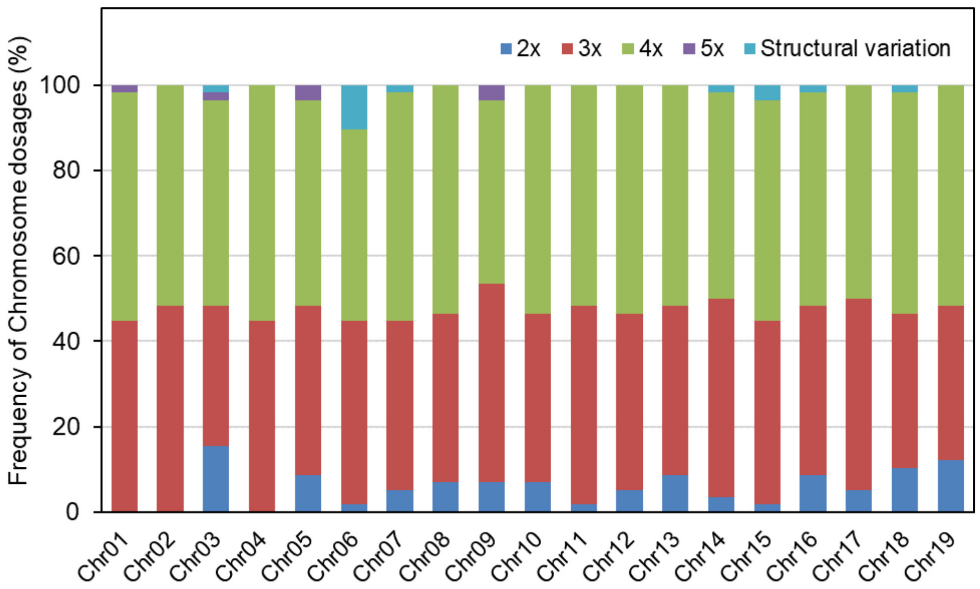

FIGURE 3 | Frequency of each chromosome dosage and occurrence of structural variations in the progeny of TB03 × 'Yinzhong.'

DISCUSSION

Microsatellite DNA allele counting–peak ratio has been proved as a feasible method for the allelic configuration analysis of polyploids in *Rosa* and *Citrus* (Esselink et al., 2004; Babaei et al., 2007; Cuenca et al., 2011; Xie et al., 2015). In the present study, the MAC-PR method was successfully used in quantification of the allele copy number of *Populus* aneuploids. According to the allele copy number of each SSR locus, the genotypes of all offspring were determined. Furthermore, the chromosomal composition and occurrence of structural variation for each genotype were clarified. Compared to cytological karyotyping based on the chromosome number and morphology, the molecular karyotyping based on the MAC-PR method exhibited higher efficiency and easier operation.

Interploidy cross is an important pathway for the creation of new germplasms with ploidy variations, although it is usually accompanied by highly reproductive barrier (Birchler, 2014; Alexander, 2020). In *Actinidia chinensis*, triploid, tetraploid, pentaploid, heptaploid, and octaploid hybrids were produced by interploidy cross between hexaploid and diploid parents (Rao et al., 2012). In the previous study on *Populus*, Wang et al. (2017) produced a progeny with segregated ploidy levels, including many aneuploids, by pollinating triploid 'Yinzhong' to diploid TB03, because of the imbalanced meiotic chromosomal segregation of the 'Yinzhong'. In the present study, the chromosomal compositions of each genotype in the TB03 × 'Yinzhong' progeny were further revealed by the MAC-PR analysis. Forty-eight of 58 genotypes were aneuploids with various chromosomal compositions, including 26 hypo-triploids, 1 hyper-triploid, 16 hypo-tetraploids, and 5 hyper-tetraploids. No hypo-diploid was found, suggesting that gamete without complete chromosome set might be sterile in *Populus* or rare hypo-diploid was aborted.

In general, triploids undergo normal meiosis to give rise to aneuploid gametes with approximate 3x/2 chromosome number. However, because of the imbalanced chromosome number, the aneuploid gametes are almost sterile (Ramsey and Schemske, 1998; Charles et al., 2010). In the present study, 26 hypo-triploids (3x–1∼5) and 1 hyper-triploid (3x + 1) were determined from the progeny of diploid "TB01" × triploid 'Yinzhong,' which probably attributed to fertilization of rarely fertile aneuploid pollen grains from normal meiosis of the male parent 'Yinzhong'. All aneuploids had chromosome numbers more than x + 3x/2, probably suggesting that the aneuploid pollen grains with chromosome number less than 3x/2 might had lower viability than that with more than 3x/2 chromosomes. The chromosome 3 was the most frequently missed (∼34.6%) in the hypo-triploids, which might suggest that the development of aneuploid embryo is not very sensitive to the copies of chromosome 3.

In a previous study, the production of unreduced pollen grains was observed in 'Yinzhong' (Wang et al., 2017). The formation of tetraploids in our study could be explained by union between normal x egg and unreduced 3x sperm. Because the imbalanced chromosome segregation commonly happens at the first meiotic division of triploids, theoretically, triploid can produce fertile unreduced 3x gametes through first meiotic division restitution (FDR) but not second meiotic division restitution (SDR). Therefore, we speculated that the unreduced pollen grains from triploid 'Yinzhong' should be FDR type. Additionally, chromosomes elimination was also observed during the meiosis of 'Yinzhong' (Wang et al., 2017), which could produce aneuploid unreduced pollen grains with loss of several chromosomes when FDR took place. In this study, the

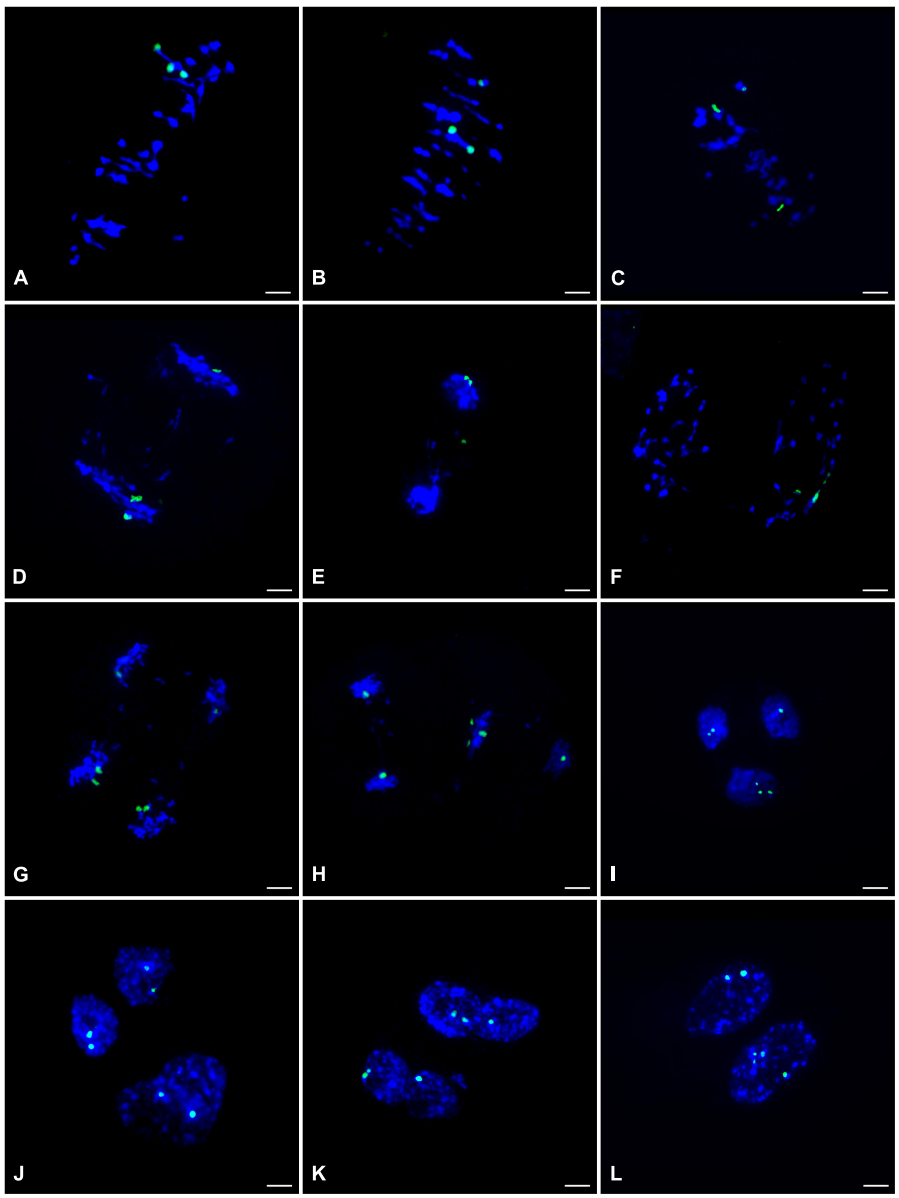

FIGURE 4 | 45S rDNA– fluorescence *in situ* hybridization (FISH) analysis during the meiosis of the male parent 'Yinzhong'. **(A)** Metaphase I cell showing one trivalent with 45S rDNA signals (green). **(B)** Metaphase I cell showing a bivalent and a univalent with 45S rDNA signals. **(C)** Metaphase I cell showing three univalents with 45S rDNA signals. **(D)** Anaphase I cell showing imbalance 45S rDNA-located chromosome segregation. **(E)** Anaphase I cell showing one 45S rDNA signal on a lagging chromosome. **(F)** Telophase I cell showing all 45S rDNA signals in one daughter nucleus, **(G)** Anaphase II cell with normal meiotic 45S rDNA-located sister chromatid segregation. **(H)** Anaphase II cell showing three 45S rDNA signals in one chromosome group. **(I)** Two normal daughter nuclei at telophase II including one and two 45S rDNA signals, respectively, and one fused nucleus including three signals. **(J)** Two normal daughter nuclei and one fused nucleus at telophase II including two 45S rDNA signals, respectively. **(K)** Telophase II with two fused nuclei including three 45S rDNA signals, respectively. **(L)** Telophase II with two fused nuclei including two and four 45S rDNA signals, respectively.

production of the hypo-tetraploids could attribute to fertilization of the aneuploid unreduced pollen grains.

It is interesting that 5 hyper-tetraploids with 1–2 extra chromosomes were determined in the progeny, suggesting that viable male gametes containing 3 chromosome sets plus 1–2 extra chromosomes took part in fertilization. The FISH analysis showed that three 45S rDNA signals were found on three homoeologous chromosomes at metaphase I stage of male parent 'Yinzhong' microsporocytes and 2–4 45S rDNA signals could be observed in fused daughter nucleus of telophase II. The fused nucleus with 4 signals probably contained unreduced chromosome number and extra one 45S rDNA signals located chromosome. Therefore, the formation of the male gametes containing unreduced chromosome number and extra chromosomes could be attributed to imbalanced meiotic chromosomal segregation and division restitution of the male

parent triploid 'Yinzhong'. According to Xin et al. (2020), the 45S rDNA FISH signals were positioned on chromosomes 8 and 14 for *P. lasiocarpa*, *P. deltoides*, and *P. trichocarpa*, on chromosome 14 for *P. tremula* × *P. tremuloides*, and *P. tomentosa*, and on chromosome 9 for *P. euphratica*. The 'Yinzhong' is an intersectional hybrid between sect. Populus and sect. Aigeiros (Zhou et al., 1992); so, we speculated that the chromosomes with the 45S rDNA signals were chromosome 8 or chromosome 14. Although the 45S rDNA located chromosome was not corresponding to the extra chromosome in the hyper-tetraploids in the present study, the FISH analysis still gave us a reasonable explanation for the cytological mechanism of the hyper-tetraploid formation.

Chromosome structural variation is an important type of chromosome aberrations, which can drive species evolution and promote plant improvement (Wijnker and de Jong, 2008; Yang et al., 2012; Danilova et al., 2017). Abnormal meiosis of allopolyploids usually results in the production of chromosome structural variations (Gou et al., 2018). In our study, chromosome structural variations, such as duplications and deletions, were detected by SSR molecular markers on many loci. Occurrence of chromosomal rearrangements is related with chromosome breakpoint regions (Lysák and Schubert, 2013). The present study showed that 46.2% structural variation events occurred on chromosome 6, probably suggesting that a chromosome breakpoint locates near the loci of chromosome 6. However, it is difficult to detect the occurrence of all structural variations, owing to the limited number and density of SSR markers. The inversion and translocation structural variation types are also impossible to be determined by SSR marker method. Molecular cytological tools, such as GISH and FISH, are effective methods to detect occurrence of chromosome structural rearrangements in plants (Lou et al., 2014; Danilova et al., 2017; Huang et al., 2018; Said et al., 2019, 2021). Lou et al. (2014) developed single-copy gene pools in *Cucumis sativus*, and analyzed chromosome rearrangements in the *Cucumis* genus by using single-copy gene-based chromosome painting method. In addition, molecular karyotyping technique depending on read-counting of DNA sequencing also was used to precisely detect abundant deletions and insertions of chromosomal segments in poplar progeny derived from crossing with gamma-irradiated pollen (Henry et al., 2015). Therefore, in order to completely analyze the structural variations in our materials, the chromosome painting and read-counting-based molecular karyotyping methods could be applied.

According to the mechanism of unreduced gamete formation, the FDR type unreduced gametes contain non-sister chromatids, which can transmit approximately 80% parental heterozygosity theoretically when crossovers occur; the SDR type unreduced gametes contain sister chromatids, which can transmit approximately 40% parental heterozygosity (Hermsen, 1984). In induced 2n eggs of *Populus*, it was found that the FDR, SDR, and postmeiotic restitution types 2n eggs transmitted 0.7480, 0.3958, and 0.3590 maternal heterozygosities, respectively (Dong et al., 2015). As the above inference, the tetraploids, hypo-tetraploids, and hyper-tetraploids should be derived from the hybridization of euploid or aneuploid unreduced pollen grains in this study. Their transmitted paternal heterozygosities reached 0.830, 0.833, and 0.836, which support our conclusion of the unreduced pollen of male parent 'Yinzhong' were FDR type.

Numerical and structural variations in chromosomes commonly result in complex phenotypic trait changes. In *Arabidopsis* aneuploids, phenotypic variation is strongly associated with chromosomal composition and dosage (Henry et al., 2010). Bastiaanse et al. (2019, 2021) found that gene dosage variations in *Populus* carrying large DNA fragmental insertions and deletions can influence morphological variation through complex changes in gene expression, and identified some dosage-sensitive genomic regions that influenced pleiotropic morphological characters. The vessel morphology in *Populus* was also affected by gene dosages (Rodriguez-Zaccaro et al., 2021). In our study, chromosomal composition and structural variation of each aneuploid for the full-sib progeny of TB03 × 'Yinzhong' were clarified, which provides a potential material for analyzing mechanisms of trait variation relying on chromosome or gene dosages. In future, an exact analysis of gene dosage variations in the aneuploids could be conducted by the read-counting-based molecular karyotyping method. Effects of gene dosage variations on trait changes of *Populus* also could be deciphered by association analysis between gene copy numbers and trait phenotypes. Additionally, after flowering, we hope that the aneuploids can play a valuable role in chromosome engineering breeding of *Populus*.

DATA AVAILABILITY STATEMENT

The datasets presented in this study can be found in online repositories. The names of the repository/repositories and accession number(s) can be found in the article/**Supplementary Material**.

AUTHOR CONTRIBUTIONS

JW conceived and designed the research. Y-HZ, Y-FZ, and Y-XX conducted the SSR experiments and analyzed the data. L-JW conducted FISH experiments. J-WZ cultivated the materials. Y-HZ and JW wrote the manuscript. All authors read and approved the manuscript.

FUNDING

This work was supported by the National Key R&D Program of China during the 14th Five-Year Plan Period (2021YFD2200104) and National Natural Science Foundation of China (31470662).

SUPPLEMENTARY MATERIAL

The Supplementary Material for this article can be found online at: https://www.frontiersin.org/articles/10.3389/fpls.2021.816946/full#supplementary-material

REFERENCES

Alexander, L. (2020). Ploidy level influences pollen tube growth and seed viability in interploidy crosses of *Hydrangea macrophylla*. *Front. Plant Sci.* 11:100. doi: 10.3389/fpls.2020.00100

Babaei, A., Tabaei-Aghdaei, S. R., Khosh-Khui, M., Omidbaigi, R., Naghavi, M. R., Esselink, G. D., et al. (2007). Microsatellite analysis of Damask rose (*Rosa damascena* Mill.) accessions from various regions in Iran reveals multiple genotypes. *BMC Plant Biol.* 7:12. doi: 10.1186/1471-2229-7-12

Bastiaanse, H., Henry, I., Tsai, H., Lieberman, M., Canning, C., Comai, L., et al. (2021). A systems genetics approach to deciphering the effect of dosage variation on leaf morphology in *Populus*. *Plant Cell* 33, 940–960. doi: 10.1093/plcell/koaa016

Bastiaanse, H., Zinkgraf, M., Canning, C., Tsai, H., Lieberman, M., Comai, L., et al. (2019). A comprehensive genomic scan reveals gene dosage balance impacts on quantitative traits in Populus trees. *Proc. Natl. Acad. Sci. U.S.A.* 116, 13690–13699. doi: 10.1073/pnas.1903229116

Baumeister, G. (1980). Beispiele der polyploidie-Züchtung. *Allg. Forestz.* 35, 697–699.

Birchler, J. A. (2014). Interploidy hybridization barrier of endosperm as a dosage interaction. *Front. Plant Sci.* 5:281. doi: 10.3389/fpls.2014.00281

Charles, J. S., Hamilton, M. L., and Petes, T. D. (2010). Meiotic chromosome segregation in triploid strains of *Saccharomyces cerevisiae*. *Genetics* 186, 537–550. doi: 10.1534/genetics.110.121533

Chen, C. B., Qi, L. W., Zhang, S. G., Han, S. Y., Li, X. L., Song, W. Q., et al. (2004). The karyotype analysis of triploid poplar. *J. Wuhan Bot. Res.* 22, 565–567.

Comai, L., Tyagi, A. P., and Lysak, M. A. (2003). FISH analysis of meiosis in *Arabidopsis* allopolyploids. *Chromosome Res.* 11, 217–226. doi: 10.1023/a:1022883709060

Cuenca, J., Froelicher, Y., Aleza, P., Juárez, J., Navarro, L., and Ollitrault, P. (2011). Multilocus half-tetrad analysis and centromere mapping in citrus: evidence of SDR mechanism for 2n megagametophyte production and partial chiasma interference in mandarin cv 'Fortune'. *Heredity* 107, 462–470. doi: 10.1038/hdy.2011.33

Danilova, T. V., Akhunova, A. R., Akhunov, E. D., Friebe, B., and Gill, B. S. (2017). Major structural genomic alterations can be associated with hybrid speciation in *Aegilops markgrafii* (Triticeae). *Plant J.* 92, 317–330. doi: 10.1111/tpj.13657

Dong, C. B., Suo, Y. J., Wang, J., and Kang, X. Y. (2015). Analysis of transmission of heterozygosity by 2n gametes in *Populus* (Salicaceae). *Tree Genet. Genomes* 11:799.

Du, F. K., Xu, F., Qu, H., Feng, S., Tang, J., and Wu, R. (2013). Exploiting the transcriptome of Euphrates Poplar, *Populus euphratica* (Salicaceae) to develop and characterize new EST-SSR markers and construct an EST-SSR database. *PLoS One* 8:e61337. doi: 10.1371/journal.pone.0061337

Einspahr, D. W. (1984). Production and utilization of triploid hybrid aspen. *Iowa State J. Res.* 58, 401–409.

Esselink, G. D., Nybom, H., and Vosman, B. (2004). Assignment of allelic configuration in polyploids using the MAC-PR (microsatellite DNA allele counting—peak ratios) method. *Theor. Appl. Genet.* 109, 402–408. doi: 10.1007/s00122-004-1645-5

Gou, X., Bian, Y., Zhang, A., Zhang, H., Wang, B., Lv, R., et al. (2018). Transgenerationally precipitated meiotic chromosome instability fuels rapid karyotypic evolution and phenotypic diversity in an artificially constructed allotetraploid wheat (AADD). *Mol. Biol. Evol.* 35, 1078–1091. doi: 10.1093/molbev/msy009

Henry, I. M., Dilkes, B. P., and Comai, L. (2006). Molecular karyotyping and aneuploidy detection in *Arabidopsis thaliana* using quantitative fluorescent polymerase chain reaction. *Plant J.* 48, 307–319. doi: 10.1111/j.1365-313X.2006.02871

Henry, I. M., Dilkes, B. P., Miller, E. S., Burkart-Waco, D., and Comai, L. (2010). Phenotypic consequences of aneuploidy in *Arabidopsis thaliana*. *Genetics* 186, 1231–1245. doi: 10.1534/genetics.110.121079

Henry, I. M., Dilkes, B. P., Young, K., Watson, B., Wu, H., and Comai, L. (2005). Aneuploidy and genetic variation in the *Arabidopsis thaliana* triploid response. *Genetics* 170, 1979–1988. doi: 10.1534/genetics.104.037788

Henry, I. M., Zinkgraf, M. S., Groover, A. T., and Comai, L. (2015). A system for dosage-based functional genomics in poplar. *Plant Cell* 27, 2370–2383. doi: 10.1105/tpc.15.00349

Hermsen, J. (1984). Mechanisms and genetic implications of 2n gamete formation. *Iowa State J. Res.* 58, 421–434.

Huang, X., Zhu, M., Zhuang, L., Zhang, S., Wang, J., Chen, X., et al. (2018). Structural chromosome rearrangements and polymorphisms identified in Chinese wheat cultivars by high-resolution multiplex oligonucleotide FISH. *Theor. Appl. Genet.* 131, 1967–1986. doi: 10.1007/s00122-018-3126-2

Jansson, S., and Douglas, C. J. (2007). *Populus*: a model system for plant biology. *Annu. Rev. Plant Biol.* 58, 435–458. doi: 10.1146/annurev.arplant.58.032806.103956

Kang, X. Y. (2016). "Polyploid induction techniques and breeding strategies in poplar," in *Polyploidy and Hybridization for Crop Improvement*, ed. A. S. Mason (Boca Raton, FL: CRC Press), 76–96. doi: 10.1201/9781315369259-5

Law, C. N., Snape, J. W., and Worland, A. J. (1987). "Aneuploidy in wheat and its uses in genetic analysis," in *Wheat Breeding: Its Scientific Basis*, ed. F. G. H. Lupton (London: Chapman and Hall Ltd), 71–108. doi: 10.1007/978-94-009-3131-2_4

Li, C. B., Zhang, D. M., Ge, S., Lu, B. R., and Hong, D. Y. (2001). Identification of genome constitution of *Oryza malampuzhaensis*, *O. minuta*, and *O. punctata* by multicolor genomic in situ hybridization. *Theor. Appl. Genet.* 103, 204–211. doi: 10.1007/s001220100563

Li, X., Huang, F., Chai, J., Wang, Q., Yu, F., Huang, Y., et al. (2021). Chromosome behavior during meiosis in pollen mother cells from *Saccharum officinarum* × *Erianthus arundinaceus* F_1 hybrids. *BMC Plant Biol.* 21:139. doi: 10.1186/s12870-021-02911-z

Lou, Q. F., Zhang, Y. X., He, Y. H., Li, J., Jia, L., Cheng, C. Y., et al. (2014). Single-copy gene-based chromosome painting in cucumber and its application for chromosome rearrangement analysis in *Cucumis*. *Plant J.* 78, 169–179. doi: 10.1111/tpj.12453

Lysák, M. A., and Schubert, I. (2013). "Mechanisms of Chromosome Rearrangements," in *Plant Genome Diversity*, Vol. Vol. 2, eds J. Greilhuber, J. Dolezel, and J. Wendel (Vienna: Springer), 137–147.

Meirmans, P. G., and Van Tienderen, P. H. (2004). GENOTYPE and GENODIVE: two programs for the analysis of genetic diversity of asexual organisms. *Mol. Ecol. Notes* 4, 792–794.

Ramsey, J., and Schemske, D. W. (1998). Pathways, mechanisms, and rates of polyploid formation in flowering plants. *Annu. Rev. Ecol. Syst.* 29, 467–501.

Rao, J. Y., Liu, Y. F., and Huang, H. W. (2012). Analysis of ploidy segregation and genetic variation of progenies of different interploidy crosses in *Actinidia chinensis*. *Acta Hortic. Sin.* 39, 1447–1456.

Rodriguez-Zaccaro, F. D., Henry, I. M., and Groover, A. (2021). Genetic regulation of vessel morphology in *Populus*. *Front. Plant Sci.* 12:705596. doi: 10.3389/fpls.2021.705596

Said, M., Holušová, K., Farkas, A., Ivanizs, L., Gaál, E., Cápal, P., et al. (2021). Development of DNA markers from physically mapped loci in *Aegilops comosa* and *Aegilops umbellulata* using single-gene FISH and chromosome sequences. *Front. Plant Sci.* 12:689031. doi: 10.3389/fpls.2021.689031

Said, M., Parada, A. C., Gaál, E., Molnár, I., Cabrera, A., Doležel, J., et al. (2019). Uncovering homeologous relationships between tetraploid *Agropyron cristatum* and bread wheat genomes using COS markers. *Theor. Appl. Genet.* 132, 2881–2898. doi: 10.1007/s00122-019-03394-1

Schuelke, M. (2000). An economic method for the fluorescent labeling of PCR fragments. *Nat. Biotech.* 18, 233–234.

Taylor, G. (2002). *Populus*: *Arabidopsis* for forestry. Do we need a model tree? Ann. Bot. 90, 681–689. doi: 10.1093/aob/mcf255

Wang, J., Huo, B., Liu, W., Li, D., and Liao, L. (2017). Abnormal meiosis in an intersectional allotriploid of *Populus* L. and segregation of ploidy levels in 2x × 3x progeny. *PLoS One* 12:e0181767. doi: 10.1371/journal.pone.0181767

Wijnker, E., and de Jong, H. (2008). Managing meiotic recombination in plant breeding. *Trends Plant Sci.* 13, 640–646. doi: 10.1016/j.tplants.2008.09.004

Wullschleger, S. D., Jansson, S., and Taylor, G. (2002). Genomics and forest biology: *Populus* emerges as the perennial favorite. *Plant Cell* 14, 2651–2655. doi: 10.1105/tpc.141120

Xie, K. D., Xia, Q. M., Wang, X. P., Liang, W. J., Wu, X. M., Grosser, J. W., et al. (2015). Cytogenetic and SSR-marker evidence of mixed disomic, tetrasomic, and intermediate inheritance in a citrus allotetraploid somatic hybrid between 'Nova' tangelo and 'HB' pummelo. *Tree Genet. Genomes* 11:112.

Xin, H., Zhang, T., Wu, Y., Zhang, W., Zhang, P., Xi, M., et al. (2020). An extraordinarily stable karyotype of the woody *Populus* species revealed by chromosome painting. *Plant J.* 101, 253–264. doi: 10.1111/tpj.14536

Yang, L. M., Koo, D. H., Li, Y. H., Zhang, X. J., Luan, F. S., Havey, M. J., et al. (2012). Chromosome rearrangements during domestication of cucumber as revealed by high-density genetic mapping and draft genome assembly. *Plant J.* 71, 895–906. doi: 10.1111/j.1365-313X.2012.05017.x

Yin, T. M., Zhang, X. Y., Gunter, L. E., Li, S. X., Wellschleger, S. D., Huang, M. R., et al. (2009). Microsatellite primer resource for *Populus* developed from the mapped sequence scaffolds of the Nisqually-1 genome. *New Phytol.* 181, 498–503. doi: 10.1111/j.1469-8137.2008.02663.x

Zhang, C. H., and Park, S. M. (2009). Aneuploid production from crosses with diploid and triploid in apple tree. *Hortic. Environ. Biotechnol.* 50, 203–207.

Zhang, S., Qi, L., Chen, C., Li, X., Song, W., Chen, R., et al. (2004). A report of triploid *Populus* of the section Aigeiros. *Silvae Genet.* 53, 69–75. doi: 10.1515/sg-2004-0013

Zhang, S. G., Chen, C. B., Han, S. Y., Li, X. L., Ren, J. Z., Zhou, Y. Q., et al. (2005). Chromosome numbers of some *Populus* taxa from China. *Acta Phytotaxon Sin.* 43, 539–544. doi: 10.1360/aps040008

Zhao, Q., Wang, Y., Bi, Y., Zhai, Y., Yu, X., Cheng, C., et al. (2019). Oligo-painting and GISH reveal meiotic chromosome biases and increased meiotic stability in synthetic allotetraploid *Cucumis ×hytivus* with dysploid parental karyotypes. *BMC Plant Biol.* 19:471. doi: 10.1186/s12870-019-2060-z

Zhou, L. J., Kang, Z. X., Geng, L. Y., and Wen, B. Y. (1992). Breeding and utilization of *Populus alba* × *P. berolinensis*. *Protect. For. Sci. Technol.* 1, 23–27.

Zhu, Z. T., Kang, X. Y., and Zhang, Z. Y. (1998). Studies on selection of natural triploid of *Populus tomentosa*. *Sci. Silvae Sin.* 34, 22–31.

Conflict of Interest: The authors declare that the research was conducted in the absence of any commercial or financial relationships that could be construed as a potential conflict of interest.

Publisher's Note: All claims expressed in this article are solely those of the authors and do not necessarily represent those of their affiliated organizations, or those of the publisher, the editors and the reviewers. Any product that may be evaluated in this article, or claim that may be made by its manufacturer, is not guaranteed or endorsed by the publisher.

frontiers in Plant Science

ORIGINAL RESEARCH
published: 28 January 2022
doi: 10.3389/fpls.2021.796215

Tetraploidy Confers Superior *in vitro* Water-Stress Tolerance to the Fig Tree (*Ficus carica*) by Reinforcing Hormonal, Physiological, and Biochemical Defensive Systems

*Ruhollah Abdolinejad and Akhtar Shekafandeh**

Department of Horticultural Science, College of Agriculture, Shiraz University, Shiraz, Iran

The fig tree is a well-adapted and promising fruit tree for sustainable production in arid and semi-arid areas worldwide. Recently, Iran's dryland fig orchards have been severely damaged due to prolonged severe and consecutive drought periods. As emphasized in many studies, ploidy manipulated plants have a significantly enhanced drought tolerance. In the current study, we compared the induced autotetraploid explants of two fig cultivars ('Sabz' and 'Torsh') with their diploid control plants for their water stress tolerance under *in vitro* conditions using different polyethylene glycol (PEG) concentrations (0, 5, 10, 15, 20, and 25%). After 14 days of implementing water stress treatments, the results revealed that both tetraploid genotypes survived at 20% PEG treatments. Only 'Sabz' tetraploid explants survived at 25% PEG treatment, while both diploid control genotypes could tolerate water stress intensity only until 15% PEG treatment. The results also demonstrated that the tetraploid explants significantly had a higher growth rate, more leaf numbers, and greater fresh and dry weights than their diploid control plants. Under 15% PEG treatment, both tetraploid genotypes could maintain their relative water content (RWC) at a low-risk level (80–85%), while the RWC of both diploid genotypes drastically declined to 55–62%. The ion leakage percentage also was significantly lower in tetraploid explants at 15% PEG treatment. According to the results, these superiorities could be attributed to higher levels of stress response hormones including abscisic acid, salicylic acid, and jasmonic acid at different PEG treatments, the robust osmotic adjustment by significantly increased total soluble sugar (TSS), proline, and glycine betaine contents, and augmented enzymatic defense system including significantly increased superoxide dismutase (SOD), catalase (CAT), ascorbate peroxidase (APX), and glutathione peroxidase (GPX) activities in tetraploid genotypes, compared to their diploid control genotypes. Consequently, the current study results demonstrated that the 'Sabz' tetraploid genotype had a significantly higher water stress tolerance than other tested genotypes.

Keywords: fig tree, synthetic tetraploids, *in vitro* water stress, superior drought tolerance, hormonal and biochemical investigations

OPEN ACCESS

Edited by:
Jen-Tsung Chen,
National University of Kaohsiung, Taiwan

Reviewed by:
Marta Ruiz Valdés,
University of California, Riverside, United States
Mohammad Bagher Hassanpouraghdam,
University of Maragheh, Iran

***Correspondence:**
Akhtar Shekafandeh
shekafan@shirazu.ac.ir

Specialty section:
This article was submitted to Plant Breeding, a section of the journal Frontiers in Plant Science

Received: *16 October 2021*
Accepted: *27 December 2021*
Published: *28 January 2022*

Citation:
Abdolinejad R and Shekafandeh A (2022) Tetraploidy Confers Superior in vitro Water-Stress Tolerance to the Fig Tree (Ficus carica) by Reinforcing Hormonal, Physiological, and Biochemical Defensive Systems. Front. Plant Sci. 12:796215. doi: 10.3389/fpls.2021.796215

Abbreviations: PEG, polyethylene glycol; ABA, abscisic acid; SA, salicylic acid; JA, jasmonic acid; UPLC-MS, ultra performance liquid chromatography–mass spectrometer.

INTRODUCTION

With the intensifying adverse effects of climate change, water stress has become a worldwide crisis and threat to agricultural development, especially in arid and semi-arid areas (Rai et al., 2011). About 41% of the Earth's terrestrial surface is considered arid lands, and it is predicted to increase from 11 to 23% by the late 21st century (Leng et al., 2020).

The fig (*Ficus carica* L.) is a fruit tree from the Moraceae family, well-adapted to the arid and semi-arid areas worldwide, including Mediterranean regions and the Middle East, due to its great tolerance to harsh climates (Flaishman et al., 2008; Falistocco, 2009). For instance, fig orchards have been established throughout Iran, and over 84% of the orchards (51,000 ha from all 60,250 ha) are in dryland (without or very little precipitation during the growing season), where the average annual rainfall is between 250 and 400 mm (Roointan et al., 2016), with a dry and warm condition for five successive months during the growing season (Mesgaran et al., 2017). During the last two decades, severe and consecutive drought periods and shifting precipitation patterns influenced by climate change have seriously damaged fig production and industry in Iran. On the other hand, fig tree breeding is associated with complexities and barriers, including the existence of three different floral forms, a significant number of parthenocarpic cultivars, and the great heterozygosity rate (Mori et al., 2017). Therefore, developing efficient breeding methods to achieve highly drought-tolerant cultivars and/or rootstocks is necessary to maintain sustainable production and future demand (Flaishman et al., 2017; Abdolinejad et al., 2020).

Both cultivars investigated in this study are the figs sought after in Iran. 'Sabz' for its high-quality fresh and dry fruits and 'Torsh' for its unique fresh taste and flavor. 'Sabz' also is the most favorite fig cultivar for dryland fig production systems due to its good tolerance to drought conditions compared to other cultivars.

Polyploidy, or entire genome multiplication, is known as a major biological phenomenon with a crucial role in plant adaptation and diversification during the evolutionary periods (Ramsey and Schemske, 2002; Soltis et al., 2009; Fox et al., 2020). Because of the significant effects on whole-plant morphology and physiology, ploidy manipulation is an efficient breeding method that has been extensively used in crop improvement (Sattler et al., 2016; Ruiz et al., 2020). Due to the multiplied gene dosage, synthetic polyploids have enhanced the tolerance of many plant species to various abiotic stresses (Wei et al., 2019), including drought (Allario et al., 2013; De Souza et al., 2017; Oliveira et al., 2017; Wei et al., 2019; Rao et al., 2020), salt (Saleh et al., 2008; Wang et al., 2013; Ruiz et al., 2016b; Khalid et al., 2020), heat (Zhang et al., 2010), cold (Oustric et al., 2018), nutrient deficiency (Oustric et al., 2019), chromium toxicity (Balal et al., 2017), boron, and chloride excess (Ruiz et al., 2016a,b). Although the underlying molecular mechanisms by which neo-polyploids increase drought tolerance have not been clearly studied (Wei et al., 2019), the abscisic acid (ABA) signaling pathways, robust osmotic adjustment, and antioxidant defense system have been reported as the major mechanisms in this process. Allario et al. (2013) reported, compared to the diploid rootstocks, the over-expression of drought-responsive genes, particularly those involved in ABA biosynthesis and signaling pathway, had a key role in increasing drought tolerance of tetraploid rootstocks of *Citrus limonia*. Furthermore, Oliveira et al. (2017) discovered that the superiority of tetraploid seedlings of 'Carrizo citrange' for H_2O_2 scavenging is due to their higher *CAT2* expression, which could be the reason for their greater drought tolerance than diploid seedlings. Wei et al. (2019) also reported that tetraploid seedlings of *Poncirus trifoliata* exhibited remarkably higher drought tolerance compared with their diploid control plants. They explained that the strong reactive oxygen species (ROS) scavenging capacity due to over-expression of the genes related to the antioxidant defense system [peroxidase (POD) and superoxide dismutase (SOD)], robust osmotic adjustment (higher sugar accumulated), as well as lower levels of ROS accumulation were the major involved mechanisms. Rao et al. (2020) compared the transcriptomic analysis of diploid and tetraploid plants of *Lycium ruthenicum* subjected to severe drought stress. They reported that the superiority of tetraploid plants over diploids is attributed to their enhanced ABA biosynthesis (up to 78.4%) and more significant osmotic proteins' expression.

In addition, morphological and anatomical alterations resulting from ploidy manipulation could also play an important role in plant drought tolerance. In this respect, polyploid plants have a larger stomata size but are less dense than diploid plants, leading to lower stomatal conductance, decreased transpiration rate, and improved photosynthetic efficiency under stressful conditions (Hias et al., 2017; Corneillie et al., 2019). Polyploidy could also effectively modify root hydraulic conductivity, which plays an important role in water status under drought stress. Polyploids may have thicker root cortex and suberin depositions, a well-known adaptive mechanism in plant systems to cope with water stress conditions, resulting in reduced transpiration rate and increased water-use efficiency (Doyle and Coate, 2019). These modifications were reported in tetraploid plants of *Citrus* spp. (Syvertsen et al., 2000; Ruiz et al., 2016a,b) and *Salix viminalis* (Dudits et al., 2016) and resulted in lower root hydraulic conductivity than their corresponding diploid plants (Ruiz et al., 2016b). In tetraploid plants of 'Carrizo' citrange, lower root hydraulic conductivity under drought stress give rise to maintaining gas exchange parameters and limiting water consumption, while diploid plants were greatly affected (Ruiz et al., 2016b; Oliveira et al., 2017).

Nowadays, implementing *in vitro* water stress experiments based on polyethylene glycol (PEG) treatments is frequently used to identify drought tolerance genotypes in higher plants (Kovalikova et al., 2020). PEG, an inert non-penetrating and non-ionic polymer with a high molecular weight (4000–8000 Da) and soluble in water, can decrease the water potential of the substrate by inducing osmotic stress without being phytotoxic (Emmerich and Hardegree, 1990; Ahmad et al., 2020) as it happens under field conditions.

The significant advantage of *in vitro* PEG-induced water stress is the possibility of precise control of any plant–environment interactions, which provide facilities to precisely study plant's defensive strategies to water stress conditions and

perform a rapid and convenient screening of drought tolerance genotypes. Thus, the results are reliable and reproducible (Peìrez-Clemente and Gomez-Cadenas, 2012). Compared to soil-based and hydroponic-based methods, it has certain fundamental advantages. Providing a constant and reproducible decline of substrate water potential that could not be obtained by the soil-based method and providing greater relevance to the natural field conditions due to performing on a solid substrate than hydroponic-based methods (Osmolovskaya et al., 2018). Despite the advantages, using high PEG concentrations may result in some limitations as it could interfere with solidifying the nutrient medium and increase the need for more agar. Also, high PEG concentration could enhance the viscosity of the medium and cause hypoxia (Osmolovskaya et al., 2018) which could be of concern in experimental design.

Climate change has intensified drought over the past decades in Iran and seriously damaged the dryland fig orchards. Therefore, using drought-tolerant rootstocks can be an effective approach to overcome this challenge. So, the main objective of this study was to compare the morphological, hormonal, physiological, and biochemical responses of tetraploid and diploid plants of two fig cultivars under induced drought tolerance and identify the most tolerant genotypes.

MATERIALS AND METHODS

Plant Materials and Water Stress Treatments

In vitro tetraploid explants of two fig cultivars ('Sabz' and 'Torsh') were obtained from our previous work (Abdolinejad et al., 2021), and their diploid control explants (as four genotypes) were used in this study to compare their responses to different water stress treatments. The uniform 4 cm explants were obtained from shoot tips pre-cultured on PGR-free MS (Murashige and Skoog, 1962) medium with 3% sucrose and 0.8% agar (**Figure 1**). To implement water stress treatments, the selected explants were cultured on the same medium supplemented with various concentrations of 0 (control), 5 (mild), 10 (moderate), 15 (high), 20 (severe), and 25 (extreme) % (w/v) of PEG 6000. The media were sterilized by 20 min autoclaving at 121°C after their pH was adjusted to 5.8. Except for explants of control and mild treatments, all other explants were initially cultured on 5% PEG concentration and gradually transferred to the target treatments in 12 h intervals to avoid high-level water stress shock. PEG was added to the media after autoclaving through the 45-μ syringe filters when the media temperature dropped to 70–80°C. All cultures were kept in a growth chamber with 24 ± 1°C temperature, 16/8 h light/darkness, and a light intensity of 40 μmol m^{-2} s^{-1} for 14 days. At the end of the experiment (14th day), all the morphological, hormonal, physiological, and biochemical measurements were performed.

Phytohormonal Analysis

The concentrations of three major stress response phytohormones, including ABA, salicylic acid (SA), and jasmonic acid (JA) in tetraploid and diploid explants, were determined according to Pan et al. (2010) with some modifications. Approximately 250 mg of leaf samples were taken from upper leaves, instantly transferred to liquid nitrogen, and then lyophilized. The samples were then ground to a fine powder in liquid nitrogen and extracted for their phytohormonal content by adding 0.5 ml of 1-propanol: distilled water: HCl (2:1:0.002 v:v:v) solution and shaking for 45 min at 3°C. Then, 1 ml of dichloromethane was added to the mixtures, and the samples were shaken for another 45 min at 3°C. The extraction solutions were centrifuged at 15,000 × *g* for 7 min. at 3°C. The lower phases (1 ml) were taken, immediately filtered (using 22 μm syringe filters), and transferred into the new tubes, then lyophilized and re-solubilized in 500 μl methanol [high performance liquid chromatography (HPLC) grade].

Ultra Performance Liquid Chromatography–Mass Spectrometer Analysis

The liquid chromatography–mass spectrometry (LC-MS) analysis was performed by an ACQUITY UPLC H-Class System device equipped with an ACQUITY QDa Mass Detector (Waters Corporation, Milford, MA, United States), with an analytical column C18 (2.1 mm × 50 mm, 1.7 μm; Waters Corporation). The flow rate was 0.5 ml/min, and injection volume of 5 μl, eluted with an isocratic mixture of 30% (v/v) HPLC-grade

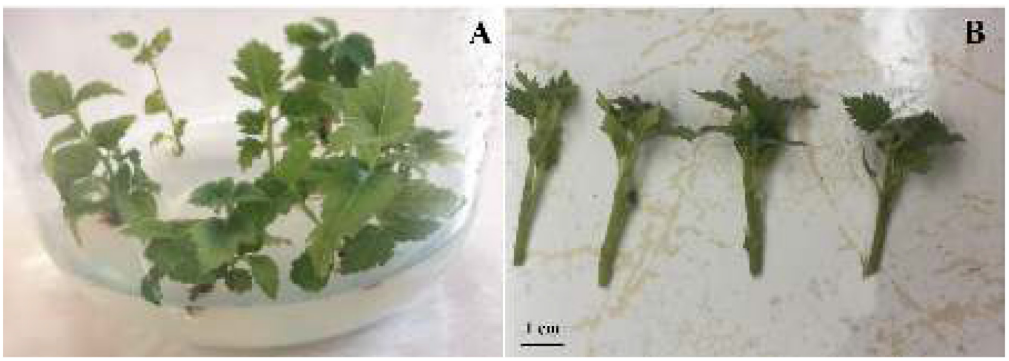

FIGURE 1 | *In vitro* pre-culture of diploid and tetraploid explants on PGR-free MS medium as the explant source for water stress experiment **(A)**, and the isolated shoot tip explants for implementation of water stress treatments **(B)**.

water and 70% (v/v) acetonitrile + 0.1% formic acid. Different concentrations of standard solutions (0.02–2000 ng/ml) for all phytohormones were prepared and used for plotting the standard curves. The data was presented as nanograms per gram lyophilized tissue (ng/g lyophilized tissue).

The Survival Rate, Growth, and Proliferation Rate, and Morphological Measurements

The survival rate percentage of explants was calculated using the following formula:

$$Survival\ rate\ (\%) = \left(\frac{Number\ of\ survived\ explants}{Total\ number\ of\ incubated\ explants}\right) \times 100$$

Shoot length was measured by a ruler and the average daily growth rate of explants was calculated as AGR (day^{-1}) using the following formula:

$$\text{Average growth rate} = \left(\frac{H2 - H1}{T}\right)$$

where H1 = First measurement, H2 = Second measurement, and T = Time interval between two measurements.

For proliferation rate, only shoots larger than 5 mm were considered, and the rate was estimated using the following formula:

$$\text{Proliferation rate} = \left(\frac{\text{Total number of shoots larger than 5 mm}}{\text{Total number of incubated explants}}\right)$$

Stem diameter was measured using a digital caliper. Leaf area was measured using a leaf area meter device (CRLA1, Iran). The fresh weight (FW) and dry weight (DW) of explants were measured using an analytical balance. For DW, the explants were oven-dried at 60°C for 48 h then weighed.

Physiological Measurements

Relative Water Content

For measuring relative water content (RWC), leaf disk samples about 2 cm in diameter were provided, and their weight was initially measured. Then the samples were immersed in distilled water for 24 h to determine the turgid weight. Leaf DW were determined after oven-drying at 65°C for 48 h. RWC was estimated using the following formula:

$$RWC\ (\%) = \left(\frac{Fresh\ weight - dry\ weight}{Turgid\ weight - dry\ weight}\right) \times 100$$

Ion Leakage

For estimating leaf ion leakage, the individual leaf samples were incubated in vials containing 10 ml of distilled water for 24 h at room temperature (22°C) on a rotary shaker (100 rpm). The initial electrical conductivity (EC1) was recorded. The samples were then autoclaved at 121°C for 20 min. After cooling the solutions, the second electrical conductivity (EC2) was recorded, and the electrolyte leakage was calculated following the formula:

$$EL\ (\%) = \left(\frac{EC1}{EC2}\right) \times 100$$

Photosynthetic Pigments Content

According to Roy et al. (2021), for estimation of the total chlorophyll and total carotenoid contents, approximately 100 mg of leaf samples were ground into fine powder in liquid nitrogen and homogenized with 10 ml of ethanol: acetone: distilled water (4.5:4.5:1) and kept at 4°C for 24 h. The mixtures were then centrifuged at 10,000 × *g* for 10 min at 4°C. Light absorbance of samples was recorded by a microplate spectrophotometer (Epoch, BioTek, United States) at 645 and 663 nm for total chlorophyll and 470 nm for total carotenoid contents. Data were presented as milligram per gram FW (mg g^{-1} FW).

Lignin Content

Lignin content was determined according to the acetyl bromide digestion method described by Iiyama and Wallis (1990). The leaf samples (100 mg) were ground into a fine powder, mixed, and heated with 20 ml distilled water at 65°C. The mixtures were passed through the 45-μ filters, and the residues were thoroughly washed with ethanol, chloroform–methanol (2:1), and acetone, then dried at 100°C for 5 min. Thereafter, 6 mg of dried samples were mixed to 5 ml of 25% acetyl bromide in a glacial acetic acid solution containing 100 μl of 70% perchloric acid and heated at 70°C for 30 min and then samples were quickly cooled on ice. The samples were treated with 5 ml of NaOH (2N) and glacial acetic acid. Light absorbance of samples was recorded by a spectrophotometer (Epoch, BioTek, United States) at 280 nm, and lignin content was presented as a percentage of the cell wall.

Biochemical Measurements

Oxidative Markers

Further in experiment, 5 g of leaf samples from all genotypes and all treatments were collected. The samples were immediately transferred to liquid nitrogen, then ground into a fine powder, and stored at −80°C to use for the following measurements.

Hydrogen Peroxide (H_2O_2) Content

According to Sarker and Oba (2018), 200 mg of leaf fine powder was mixed with 1 ml of trichloroacetic acid (TCA) (0.1%) for a while and then centrifuged at 13,000 × *g* for 10 min at 4°C. Reaction mixture including 500 μl of supernatant, 500 μl of 100 mM potassium phosphate buffer (pH = 7), and 1 ml of 1 M potassium iodide was kept in darkness for 60 min. Light absorbance of samples was recorded by a spectrophotometer (Epoch, BioTek, United States) at 390 nm, and H_2O_2 concentration was presented as micromole H_2O_2 per gram FW (μmol g^{-1} FW).

Malondialdehyde Content

Lipid peroxidation was determined by measuring the malondialdehyde (MDA) concentration in leaf tissue according to Hodges et al. (1999). In brief, 100 mg of leaf fine powder

was homogenized in 2 ml ethanol: distilled water (80% v/v) and centrifuged at 10,000 × *g* for 15 min. Then 1 ml of supernatant was mixed with 1 ml thiobarbituric acid (TBA) solution comprised of 20.0% (w/v) TCA and 0.01% butylated hydroxytoluene. The mixture was then heated at 95°C for 30 min and immediately cooled on ice and centrifuged at 7000 × *g* for 10 min. Light absorbance of samples was recorded by a spectrophotometer (Epoch, BioTek, United States) at 414, 532, and 600 nm. The MDA content was calculated using the following formula:

$$\text{MDA} = 6.45\left(\text{Abs } 532 - \text{Abs } 600\right) - 0.56\,\text{Abs } 414$$

Data were presented as micromole MDA per gram FW (μmol g^{-1} FW).

Antioxidant Enzymes Measurements

To measure the activity of antioxidant enzymes, approximately 2 g of frozen powder (−80°C) was mixed with 3 ml of extraction buffer composed of potassium phosphate buffer (50 mM, pH 7.8), 100 μM EDTA, 0.2% triton x-100, and 2% polyvinylpolypyrrolidone. The mixture was centrifuged at 13,000 × *g* for 15 min, and the supernatant was transferred to a new tube and used for further analyses (Pan et al., 2006). All operations for antioxidant enzyme activity were performed at 3°C.

Superoxide Dismutase Activity

Superoxide dismutase activity was determined according to Manquián-Cerda et al. (2016) based on its ability to inhibit the photochemical reduction of nitroblue tetrazolium (NBT). The reaction mixture consists of 300 μl of enzyme extract, 400 μl potassium phosphate buffer (100 mM, pH 7.0), 10 μl EDTA (10 mM), 50 μl methionine (260 mM), 80 μl NBT (4.2 mM), and 170 μl riboflavin (130 μM). It was illuminated by a light intensity of 60 μmol m^{-2} s^{-1}, provided by cool-white, fluorescent tubes for 15 min. Light absorbance of samples was recorded by a spectrophotometer (Epoch, BioTek, United States) at 560 nm, and SOD activity was presented as unit SOD activity per mg protein per minute (U mg^{-1} protein min^{-1}).

Catalase Activity

For catalase (CAT) activity assessment, according to Chance and Maehly (1955), 15 μl of enzyme extract was added to the 2885 μl potassium phosphate buffer (50 mM, pH 7) and 100 μl hydrogen peroxide (10 mM), to a volume of 3 ml reaction mixture. Light absorbance of samples was recorded by a spectrophotometer (Epoch, BioTek, United States) at 240 nm, and CAT activity was determined by recording the decrease in optical absorbance resulting from the H_2O_2 decomposition rate for 1 min. CAT activity was presented as unit CAT activity per milligram protein per minute (U mg^{-1} protein min^{-1}).

Ascorbate Peroxidase Activity

Ascorbate peroxidase (APX) activity was determined according to Nakano and Asada (1981). The reaction started by adding 20 μl of enzymatic extract to 1950 μl potassium phosphate buffer (50 mM, pH 0) containing 100 μM EDTA and 100 μM sodium ascorbate, and 30 μl hydrogen peroxide (2.5 mM). The decrease in light absorbance was recorded by a spectrophotometer (Epoch, BioTek, United States) at 290 nm, and the APX activity was presented as unit APX activity per milligram protein per minute (U mg^{-1} protein min^{-1}).

Glutathione Peroxidase Activity

Glutathione peroxidase (GPX) activity was determined according to Ozden et al. (2009). GPX activity was assessed by measurements of the oxidation of guaiacol in the presence of hydrogen peroxide for 2 min in 20 s intervals. The reaction mixture contained 50 μl of guaiacol (20 mM), 2900 μl of potassium phosphate buffer (10 mM, pH 7), and 50 μl of enzyme extract, and the reaction started by adding 20 μl of H_2O_2 (40 mM). Light absorbance of samples was recorded by a spectrophotometer (Epoch, BioTek, United States) at 470 nm, and GPX activity was presented as unit GPX activity per milligram protein per minute (U mg^{-1} protein min^{-1}).

Compatible Solutes Measurements

Total Soluble Sugars

The method described by Patade et al. (2012) was used for the estimation of leaf total soluble sugars (TSSs). In brief, 100 mg of lyophilized leaf tissue was first fine powder and extracted in 10 ml of ethanol: distilled water solution (8:2 v:v) and kept at room temperature for 30 min. The mixture was centrifuged at 10,000 × *g* for 15 min at 4°C. Then, the supernatant (1 ml) was mixed with 3 ml of Anthrone reagent (150 mg anthrone + 100 ml H_2SO_4 72%) and placed in a water bath (100°C) for 15 min, then immediately cooled on ice. Finally, light absorbance was recorded by a microplate spectrophotometer (Epoch, BioTek, United States) at 620 nm. Glucose was used as a standard sample, and data were presented as milligram per gram DW (mg g^{-1} DW).

Proline Content

Free proline content was measured according to Bates et al. (1973). Leaf frozen powder (−80°C) was homogenized in 3% (w/v) sulfosalicylic acid and centrifuged at 7000 × *g* for 5 min. Then, 2 ml of supernatant was reacted with 2 ml acid ninhydrin and 2 ml of glacial acetic acid and kept at 100°C for 60 min in a water bath, then immediately cooled on ice. Four milliliters of toluene was added to the mixture and vortexed for 10 s, and kept at room temperature for a while. Two phases were formed, and the supernatant was used to determine free proline content. Light absorbance was recorded by a spectrophotometer (Epoch, BioTek, United States) at 520 nm, and proline content was presented as μmol proline g^{-1} leaf FW.

Glycine Betaine Content

The method of Patade et al. (2012) was used to determine the leaf glycine-betaine content. Leaf frozen powder (200 mg) was homogenized in 3 ml of distilled water and kept on a rotary shaker for 16 h at room temperature. The sample was then filtered (45 μm filters), and the extract was mixed equally with sulfuric acid (1:1, v:v) and placed on ice for 60 min. Moreover, 500 μl of extract reacted with 200 μl of iodine-potassium iodide (KI-I_2) reagent and incubated for another 16 h at 4°C. The mixture was centrifuged at 10,000 × *g* for 5 min at 0°C, and the mixture was lyophilized. The per-iodide crystal formed was dissolved in

1 ml of 1,2-dichloroethane, and light absorbance was recorded by a spectrophotometer (Epoch, BioTek, United States) at 365 nm. The data was presented as μmol glycine-betaine g^{-1} leaf FW.

Experiment Design and Statistical Analysis

An *in vitro* experiment was carried out based on a factorial experiment including 2 genotypes × 2 ploidy levels × 6 PEG concentrations in a completely randomized design (CRD) with 10 replications (glass jars) and 5 explants per replication. Hence, a total of 1200 explants were used. At the end of the experiment, four replications were used to measure the morphological, phytohormonal, physiological, and phytochemical parameters. Data were subjected to three-way ANOVA analysis using the SAS software version 9.4 (SAS Institute, United States). Although interactions of three-way were statistically significant, the results of two-way ANOVA analysis of ploidy level × PEG treatment within each cultivar were presented to emphasize the main research hypothesis. Means were compared using the LSD test at $P < 0.05$. Log transformation was performed, where zero was observed in the data.

RESULTS

Analysis of variance showed that the interaction effects between cultivar, Ploidy level, and PEG treatments were significant for all measured traits. Therefore, the presented results for all measured parameters indicate the interaction effects. Besides, 15% PEG treatment is identified as the critical water stress level in the present study due to the diploid genotypes not surviving in higher concentrations.

Morphological Responses

The results showed that the survival rate percentage of explants at 0, 5, and 10% PEG treatments was 100% for all genotypes. While the tetraploid genotypes had 100% survival at high water stress treatment (15% PEG), the survival rate of diploid genotypes declined to 80% for cultivar Sabz and 55% for cultivar Torsh. Furthermore, the tetraploid explants of 'Sabz' displayed a significantly higher survival rate (100%) than the tetraploid explants of 'Torsh' (45%) under severe water stress treatment (20% PEG) while as there were no surviving diploid explants at this level of water stress. Interestingly, the only surviving genotype under extreme water stress treatment (25% PEG) was tetraploid explants of 'Sabz', displaying a 70% survival rate (**Table 1** and **Figure 2**).

Water stress treatments significantly suppressed the proliferation of all genotypes, so that, shoot proliferation was only observed at the control and 5% PEG treatments for all genotypes. Accordingly, the highest proliferation rate (4.8 shoots per explant) was found in tetraploid explants of 'Sabz' in the control treatment, and the lowest proliferation rate (without any

TABLE 1 | The effect of different PEG concentrations on survival rate, proliferation rate, and various morphological characteristics of tetraploid and diploid explants of 'Sabz' and 'Torsh' fig cultivars 14 days after subjecting to water stress treatments.

Cultivar	Ploidy level	PEG concentrations	Survival rate (%)	Proliferation rate	Shoot length (cm)	Growth rate (cm/d)	Stem diameter (mm)	Leaf number	Total leaf area (cm^2)	Fresh weight (g)	Dry weight (g)
'Sabz'	2×	0	100 a	3.1 b	7.02 b	0.272 b	4.52 a	6 cd	50.66 c	9.49 b	3.07 b
		5	100 a	1.12 d	5.1f d	0.145 c	3.24 d	4.5 ef	29.76 d	6.88 d	2.2 d
		10	100 a	0 e	3.7 e	0.045 de	2.48 f	3.2 fg	17.49 ef	5.21 f	1.92 e
		15	80 b	0 e	3.07 f	0.020 ef	2.03 g	1.5 h	7.61 gh	4.57 g	1.46 f
		20	0 d	–	–	–	–	–	–	–	–
		25	0 d	–	–	–	–	–	–	–	–
	4×	0	100 a	4.8 a	8.12 a	0.362 a	4.23 b	16 a	89.2 a	10.75 a	3.46 a
		5	100 a	2.8 c	6.35 c	0.232 b	3.72 c	12.75 b	67.95 b	8.15 c	2.63 c
		10	100 a	0 e	5.3 d	0.160 c	2.83 e	7.25 c	35.52 d	6.35 e	2.07 de
		15	100 a	0 e	5.27 d	0.155 c	2.43 f	4.75 de	19.8 e	6.31 e	2.03 de
		20	100 a	0 e	3.92 e	0.062 d	2.06 g	3 g	12.01 fg	3.38 h	1.24 fg
		25	70 c	0 e	3.05 f	0.002 f	1.83 h	1.5 h	4.82 hi	3.19 h	1.02 g
'Torsh'	2×	0	100 a	3.3 b	7.05 b	0.285 b	4.22 a	5.75 c	56.16 a	10.37 a	3.34 a
		5	100 a	0 d	4.85 d	0.130 d	3.41 b	3.5 d	27.31 b	7.15 c	2.3 c
		10	100 a	0 d	3.12 f	0.007 f	2.83 d	2.25 e	11.48 cd	4.61 e	1.48 e
		15	55 b	0 d	3 f	0 f	2.31 f	1.25 e	4.24 de	3.21 f	1.03 f
		20	0 c	–	–	–	–	–	–	–	–
		25	0 c	–	–	–	–	–	–	–	–
	4×	0	100 a	4.6 a	7.52 a	0.320 a	4.28 a	10 a	56.15 a	9.79 b	3.15 b
		5	100 a	2.1 c	5.77 c	0.192 c	3.31 bc	8 b	34.49 b	7.27 c	2.34 c
		10	100 a	0 d	5.1 d	0.145 d	3.15 c	5 c	18.31 c	6.05 d	1.94 d
		15	100 a	0 d	4.85 d	0.127 d	2.62 e	2 e	6.86 de	4.50 e	1.44 e
		20	45 b	0 d	3.4 e	0.022 e	2.07 g	1.25 e	3.69 e	3.08 f	0.99 f
		25	0 c	–	–	–	–	–	–	–	–

Means are present the ploidy level and PEG treatment effects tested by two-way ANOVA. Different letters in each column indicate significant differences at $P < 0.05$ using the LSD test.

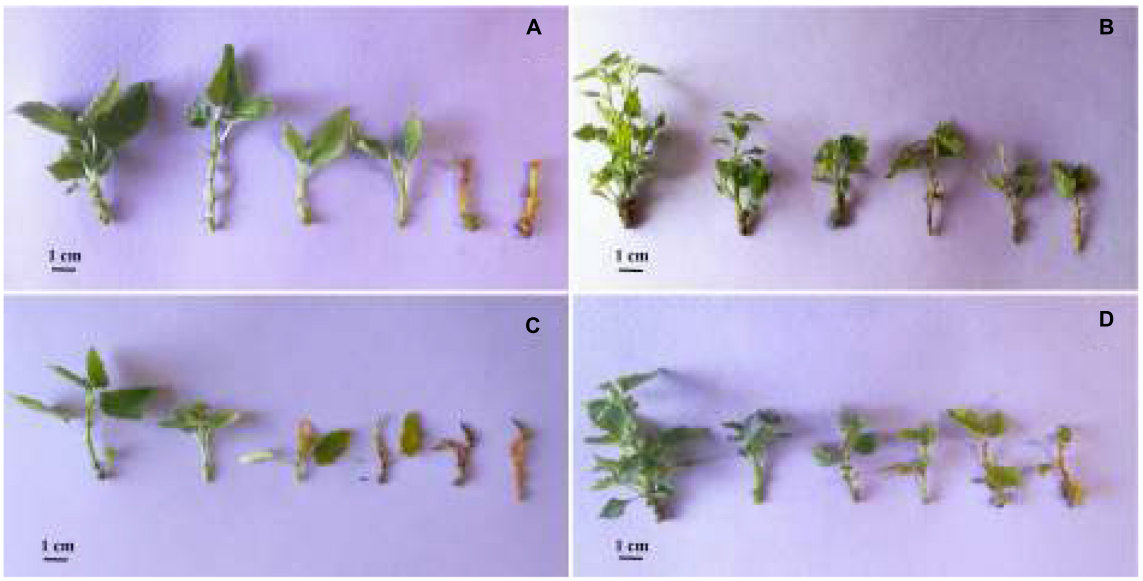

FIGURE 2 | *In vitro* responses of diploid and tetraploid explants of 'Sabz' and 'Torsh' fig cultivars, 14 days after subjecting to different water stress treatments. In each section **(A–D)**, the explants belonged to PEG treatments of 0, 5, 10, 15, 20, and 25%, from left to right, respectively. **(A)** Diploid explants of 'Sabz' cultivar, **(B)** tetraploid explants of 'Sabz' cultivar, **(C)** diploid explants of 'Torsh' cultivar, and **(D)** tetraploid explants of 'Torsh' cultivar.

lateral branch) was found in all diploid and tetraploid explants at 10, 15, 20, and 25% PEG treatments.

Water stress treatments had a significant restrictive effect on all measured morphological features for all genotypes. According to the results, tetraploid explants of both cultivars were less affected by the detrimental effects of water stress treatments at 5, 10, and 15% PEG treatments than their diploid control plants. However, the most difference between tetraploid and diploid explants of both cultivars was observed at 15% PEG treatment, where all morphological indices in tetraploid genotypes were significantly higher. In addition, morphological indices were remarkably higher in tetraploid explants of 'Sabz' than tetraploid explants of 'Torsh' at the 20% PEG treatment. At 25% PEG treatment, only tetraploid explants of 'Sabz' survived (**Table 1**).

According to the results, the shoot length in tetraploid explants of 'Sabz' and 'Torsh' was significantly higher (1.7-fold and 1.6-fold, respectively) than their diploid control plants under 15% PEG treatments. Under 20% PEG treatment, tetraploid explants of 'Sabz' had significantly higher shoot length (13% higher) than the tetraploid explants of 'Torsh'. Also, the shoot length of 'Sabz' tetraploids displayed a significant decrease at 25% PEG treatment (up to 22%) compared with 20% PEG treatment. A similar trend was observed for the growth rate of the tetraploid genotypes which were significantly higher than their diploid control plants at 15% PEG treatment (**Table 1**).

The results also demonstrated that with increasing PEG concentration, the stem diameter was notably decreased for all genotypes. However, compared to 'Sabz' and 'Torsh' diploid explants, their corresponding tetraploid explants displayed a significantly greater stem diameter under 15% PEG treatment (1.2-fold and 1.13-fold, respectively). There was no significant difference between tetraploid explants of 'Sabz' and 'Torsh' under 20% PEG treatment (**Table 1**).

As shown in **Figure 2**, tetraploid explants of both cultivars intrinsically have greater leaf numbers than their diploid control plants. The results revealed that with increasing water stress intensity, leaf number significantly declined in all genotypes. Both tetraploid genotypes had significantly greater leaf numbers at 5, 10, and 15% PEG treatments than their diploid control explants. In addition, the leaf number in 'Sabz' and 'Torsh' tetraploid explants was (3.1-fold and 1.6-fold, respectively) higher than their diploid control plants at 15% PEG treatment. At 20% PEG treatment 'Sabz' tetraploid explants had significantly greater leaf numbers (2.4-fold) than 'Torsh' tetraploid explants, and at 25% PEG treatment, 'Sabz' tetraploid explants showed a 50% decline in leaf number compared to 20% PEG treatment (**Table 1**).

Increased PEG concentrations considerably decreased the total leaf area for all genotypes compared to their control treatment. However, tetraploid genotypes showed a remarkably larger total leaf area (2.6-fold and 1.6-fold, in 'Sabz' and 'Torsh', respectively) at 15% PEG treatments than their diploid control plants. Under 20% PEG treatment, the total leaf area in tetraploid explants of 'Sabz' was significantly (up to threefold) greater than tetraploid explants of 'Torsh'. The total leaf area in 'Sabz' tetraploids was 4.82 cm^2 at 25% PEG treatment which showed a drastically decreased area (about 60%) than 20% PEG treatment (**Table 1**).

Fresh and dry weights of all genotypes significantly decreased by increasing PEG concentrations. Nevertheless, among all genotypes, the FW and DW of 'Sabz' tetraploid explants were significantly less affected by water stress treatments than the other genotypes. At 15% PEG treatment, 'Sabz' tetraploids displayed the maximum FW and DW (6.31 and 2.03 g, respectively)

compared to the other genotypes. At 20% PEG treatment, there was no significant difference between 'Sabz' and 'Torsh' tetraploid explants in relation to the FW, however, 'Sabz' tetraploids displayed a significantly higher DW (1.24 g) than 'Torsh' tetraploids (0.99 g) (**Table 1**).

Hormonal Responses

The results revealed that water stress treatments significantly increased the ABA, SA, and JA biosynthesis in all genotypes. However, hormonal biosynthesis and accumulation were significantly higher in both tetraploid genotypes than their diploid control explants (**Figures 3A–C**). ABA biosynthesis was 2-fold and 2.3-fold higher in 'Sabz' and 'Torsh' tetraploid genotypes, respectively, than their diploid control explants at 15% PEG treatment. At 20% PEG treatment, the ABA biosynthesis in 'Sabz' tetraploid explants was significantly higher (1.4-fold) than 'Torsh' tetraploid explants. As the only surviving genotype, the ABA content of 'Sabz' tetraploid explants was 8.12 ng/g LPT at 25% PEG treatment which showed a significant decrease than 20% PEG treatment (**Figure 3A**).

The SA and JA biosynthesis of tetraploid and diploid genotypes also displayed a similar increase trend with ABA at 10 and 15% PEG treatments. Tetraploid explants of 'Sabz' and 'Torsh' genotypes displayed significantly increased SA biosynthesis up to 2- and 1.7-fold at 15% PEG treatment, respectively, when compared to their diploid control plants. Under 20% PEG treatment, the SA biosynthesis was 1.7-fold higher in tetraploid explants of cultivar Sabz than tetraploid explants of cultivar Torsh. The SA content of 'Sabz' tetraploids at 25% PEG treatment (95.77 ng/g LPT) was decreased by 29.5% compared with its content at 20% PEG treatment (**Figure 3B**). JA biosynthesis also increased by 1.74-fold and 1.53 at 15% PEG treatment in tetraploid explants of cultivars Sabz and Torsh, respectively, compared to their diploid control explants. Furthermore, JA biosynthesis was 1.27-fold higher in tetraploid explants of cultivar Sabz than tetraploid explants of cultivar Torsh, and JA content in 'Sabz' tetraploid explants was 66.2 ng/g LPT at 25% PEG treatment, which showed an 18% reduction compare to 20% PEG treatment (**Figure 3C**).

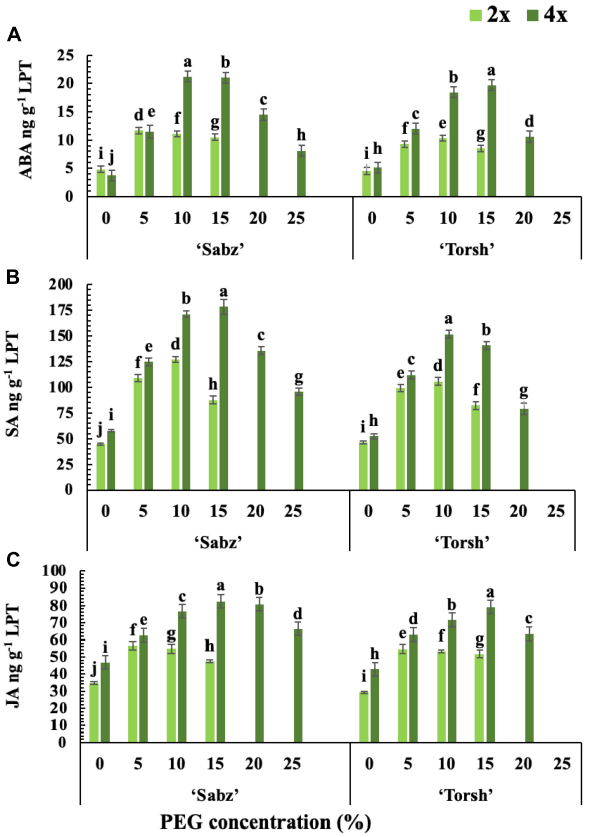

FIGURE 3 | The cumulative biosynthesis amount of three main stress response phytohormones in tetraploid and diploid explants of 'Sabz' and 'Torsh' fig cultivars 14 days after subjecting to different water stress treatments. **(A)** Abscisic acid, **(B)** salicylic acid, and **(C)** jasmonic acid. LPT, lyophilized tissue. Means represent the ploidy level and PEG treatment effects tested by two-way ANOVA. Each value represents the means ± SE. Different letters indicate significant differences at $P < 0.05$ using the LSD test.

Physiological Responses

The results demonstrated that the RWC and ion leakage of tetraploid and diploid explants of both cultivars were differently affected by water stress treatments. Indeed, in tetraploid explants, decrement in RWC and increment in ion leakage occurred gradually following an increase in water stress intensity from the control level to 20 and 25% PEG treatments. In contrast, their diploid control explants displayed a drastic RWC decrement and ion leakage increment at 10% PEG treatment (**Figures 4A,B**). At 15% PEG treatment, the RWC was 1.3-fold and 1.4-fold higher in tetraploid explants of 'Sabz' and 'Torsh', respectively, compared to their diploid counterparts (**Figure 4A**). Additionally, at 20% PEG treatment, the RWC in 'Sabz' tetraploids was 20% higher than 'Torsh' tetraploids, and at 25% PEG treatment, the RWC in 'Sabz' tetraploids was placed on the critical range of 66.25%, while 'Torsh' tetraploid explants did not survive at this level of water stress (**Figure 4A**).

The ion leakage in 'Sabz' and 'Torsh' tetraploid genotypes was 2.1- and 2-fold, respectively, less than their diploid control plants at 15% PEG treatment. Also, the ion leakage of 'Sabz' tetraploids (27.52%) was significantly less than 'Torsh' tetraploids (45.22%) at 20% PEG treatment. Furthermore, ion leakage of 'Sabz' tetraploids reached its highest percent (39.25%) at 25% PEG treatment, which was a 29.8% increase compared with 20% PEG treatment (**Figure 4B**).

According to the results, increasing water stress intensity significantly decreased the content of the photosynthetic pigments (total chlorophyll and carotenoids) in all genotypes, however, the carotenoid content was less affected by the detrimental effects of water stress treatments than chlorophyll (**Figures 4C,D**). With increasing water stress intensity, both tetraploid genotypes showed a higher ability for the biosynthesis of photosynthetic pigments. Therefore, at 15% PEG treatment, the chlorophyll content was found significantly 1.4-fold higher in both tetraploid explants than their diploid control plants. At 20% PEG treatment, tetraploid explants of 'Sabz' had significantly higher chlorophyll content (1.75 mg g^{-1} FW) than

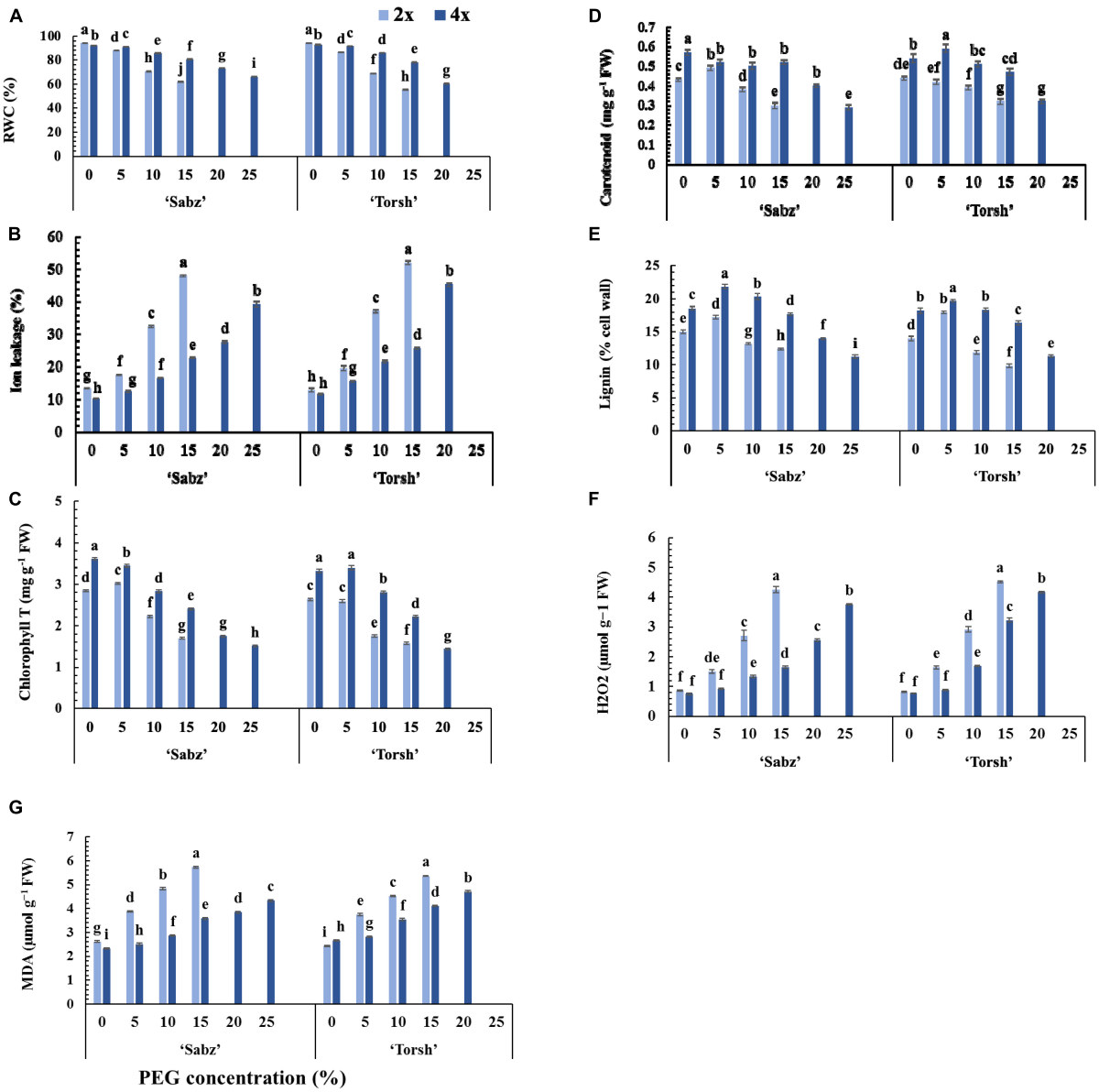

FIGURE 4 | Physiological responses of diploid and tetraploid explants of 'Sabz' and 'Torsh' fig cultivars, 14 days after subjecting to different water stress treatments. **(A)** Relative water content, **(B)** ion leakage, **(C)** total chlorophyll content, **(D)** total carotenoid content, **(E)** lignin, **(F)** hydrogen peroxide, and **(G)** malondialdehyde. Means represent the ploidy level and PEG treatment effects tested by two-way ANOVA. Each value represents the means ± SE. Different letters indicate significant differences at $P < 0.05$ using the LSD test.

tetraploid explants of 'Torsh' (1.44 mg g^{-1} FW). The chlorophyll content of 'Sabz' tetraploids was 1.51 mg g^{-1} FW, at 25% PEG treatment, displaying a 13.7% defacement than 20% PEG treatment (**Figure 4C**).

The carotenoid content was also significantly higher and up to 42 and 31% in tetraploid explants of 'Sabz' and 'Torsh', respectively, than their diploid controls at 15% PEG treatment. Besides, compared to tetraploid explants of 'Torsh' (0.32 mg g^{-1} FW), the carotenoid content was significantly higher in tetraploid explants of 'Sabz' (0.4 mg g^{-1} FW) at 20% PEG treatment. The carotenoid content of 'Sabz' tetraploids showed a decrease of 27.5% at 25% PEG treatment compared to 20% PEG treatment (**Figure 4D**).

The lignin biosynthesis in all genotypes was enhanced at 5% PEG treatment, and then it decreased by increasing PEG concentrations. The lignin content was significantly higher up to 1.4-fold and 1.6-fold in tetraploid explants of 'Sabz' and 'Torsh' cultivars, respectively, than their diploid control plant. At 20% PEG treatment, 'Sabz' tetraploids synthesized significantly more lignin (14% cell wall) than tetraploid explants of 'Torsh' (11.3% cell wall). Under 25% PEG treatment, tetraploids explants of the 'Sabz' cultivar showed 11.3% lignin

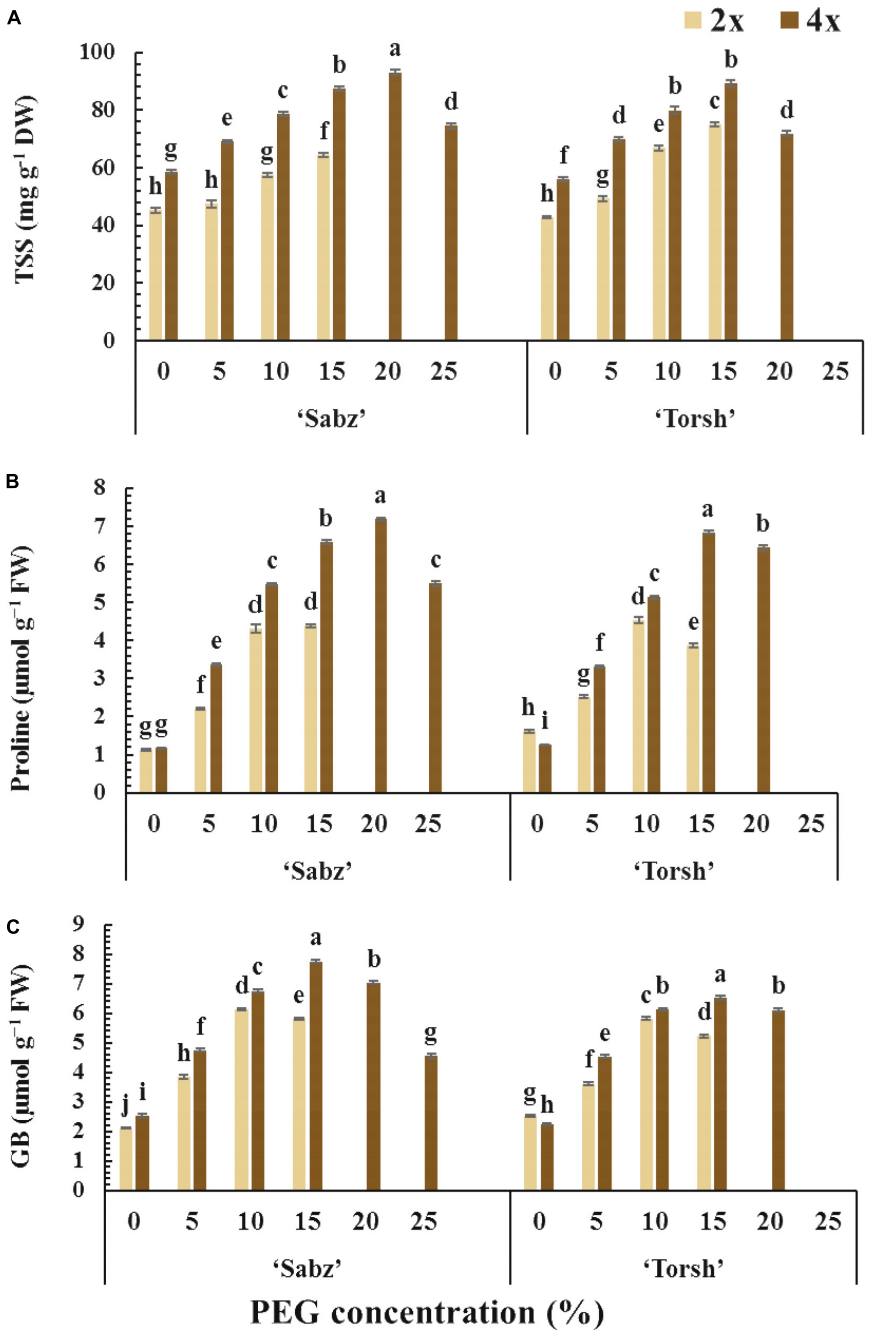

FIGURE 5 | The comparison of non-enzymatic defense system responses of tetraploid and their diploid control explants of 'Sabz' and 'Torsh' fig cultivars, 14 days after subjecting to different water stress treatments. **(A)** Total soluble sugars, **(B)** proline, and **(C)** glycine betaine. Means represent the ploidy level and PEG treatment effects tested by two-way ANOVA. Each value represents the means ± SE. Different letters indicate significant differences at $P < 0.05$ using the LSD test.

cell wall (**Figure 4E**). The results showed that H_2O_2 and MDA contents were significantly amassed in all genotypes by increasing water stress intensity. The H_2O_2 and MDA contents were notably lower in both tetraploid genotypes than their diploid control plants at 5, 10, and 15% PEG treatments (**Figures 4F,G**). At 15% PEG treatment, the H_2O_2 content was 2.5-fold and 1.4-fold lower in tetraploid explants of 'Sabz' and 'Torsh' cultivars, respectively, compared to their diploid control plants. Furthermore, the H_2O_2 content of tetraploid explants of 'Sabz' was significantly lower (1.6-fold) than tetraploid explants of 'Torsh' at 20% PEG treatment. The H_2O_2 content in tetraploid explants of 'Sabz' showed a 47.2% increase and reached 3.77 µmol g^{-1} FW at 25% PEG treatment (**Figure 4F**).

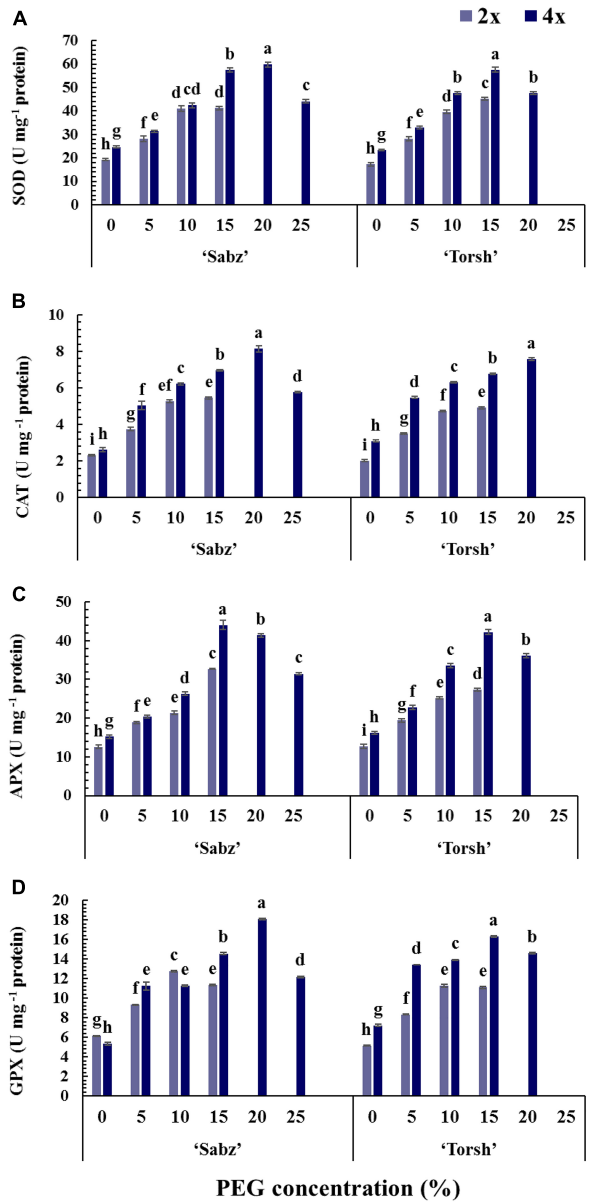

FIGURE 6 | Enzymatic activity responses of diploid and tetraploid explants of 'Sabz' and 'Torsh' fig cultivars 14 days after subjecting to different water stress treatments. **(A)** Superoxide dismutase, **(B)** catalase, **(C)** ascorbate peroxidase, and **(D)** glutathione peroxidase. Means represent the ploidy level and PEG treatment effects tested by two-way ANOVA. Each value represents the means ± SE. Different letters indicate significant differences at $P < 0.05$ using the LSD test.

Polyethylene glycol treatments increased the MDA content of all genotypes, similar to the trend of H_2O_2 content in a concentration-dependent manner. At 15% PEG treatment, the MDA content of tetraploid explants of 'Sabz' and 'Torsh' cultivars was significantly lower (1.6-fold and 1.3-fold, respectively) than their diploid control plants. The MDA content in tetraploid explants of the 'Sabz' cultivar (3.84 μmol g^{-1} FW) was significantly lower than tetraploid explants of the 'Torsh' cultivar (4.71 μmol g^{-1} FW) at 20% PEG treatment. Also, the MDA content in tetraploid explants of 'Sabz' cultivar with a gradual increase reached 4.34 μmol g^{-1} FW at 25% PEG treatment (**Figure 4G**).

Biochemical Responses

The TSS accumulation was greatly increased by increasing water stress treatments in all genotypes compared to their control treatments. Tetraploid genotypes of both cultivars ('Sabz' and 'Torsh') exhibited significantly higher TSS accumulated by 1.35-fold and 1.2-fold, respectively, than their diploid control genotypes, under 15% PEG treatment. At 20% PEG treatment, the TSS content of 'Sabz' tetraploids was significantly higher (up to 1.3-fold) than 'Torsh' tetraploids, and at 25% PEG treatment, 'Sabz' tetraploids had 74.55 mg g^{-1} DW of TSS that decreased by 19% than its content under 20% PEG treatment (**Figure 5A**).

The accumulation of proline and glycine betaine (GB) displayed a similar rising trend in all genotypes with increasing PEG concentrations. However, their accumulations were significantly higher in tetraploid genotypes than their diploid control plants at 5, 10, and 15% PEG treatments (**Figures 5B,C**). At 15% PEG treatment, the proline content of 'Sabz' and 'Torsh' tetraploids was 1.5-fold and 1.7-fold higher than their diploid control plants, respectively. In addition, at 20% PEG treatment, the proline content of 'Sabz' tetraploids was significantly greater (11% higher) than 'Torsh' tetraploids. The proline content of 'Sabz' tetraploids was 5.49 μmol g^{-1} FW at 25% PEG treatment, showing a 23% decrease than 20% PEG treatment (**Figure 5B**).

While the GB content of both tetraploid genotypes showed an increasing trend from the control to 15% PEG treatment, this trend was observed only in 5 and 10% PEG treatments in their diploid control genotypes. The GB content of 'Sabz' and 'Torsh' tetraploids was significantly higher (1.33-fold and 1.25-fold, respectively) than their diploid controls at 15% PEG treatment. At 20% PEG treatment, the GB content of 'Sabz' tetraploids was significantly higher (13% higher) than 'Torsh' tetraploids. Also, the GB content of 'Sabz' tetraploids was 4.55 μmol g^{-1} FW at 25% PEG treatment, which showed a 35% decrease than 20% PEG treatment (**Figure 5E**).

Enzymatic Activities

The enzymatic defense system, including the activity of SOD, CAT, APX, and GPX enzymes, was significantly enhanced with increasing water stress intensity in all genotypes (**Figure 6**). The results demonstrated that at 5, 10, and 15% PEG treatments, antioxidant enzymes activities were significantly higher in both tetraploid genotypes compared to their diploid control plants. Accordingly, at 15% PEG treatment, the SOD activity in 'Sabz' and 'Torsh' tetraploids was 1.4-fold and 1.27-fold higher than their diploid control explants, respectively. SOD activity was significantly higher (1.25-fold) in 'Sabz' tetraploids compared to 'Torsh' tetraploids at 20% PEG treatment. At 25% PEG treatment, SOD activity was 44.18 U mg^{-1} protein in 'Sabz' tetraploids, showing a 26% decrease than its activity at 20% PEG treatment (**Figure 6A**).

Catalase activity showed a 1.27-fold and 1.37-fold increase in 'Sabz' and 'Torsh' tetraploid genotypes compared to their diploid control genotypes under 15% PEG treatment. In addition, CAT activity in 'Sabz' tetraploids was significantly higher (6% higher) than 'Torsh' tetraploids at 20% PEG treatment. At 25% PEG treatment, CAT activity in the 'Sabz' tetraploids was 5.78 U mg^{-1} protein, which displayed a 28% decrease compared to the 20% PEG treatment (**Figure 6B**).

Ascorbate peroxidase activity was also significantly higher in 'Sabz' and 'Torsh' tetraploids by 1.34-fold and 1.54-fold, respectively, than their diploid control explants at 15% PEG treatment. At 20% PEG treatment, the APX activity of 'Sabz' tetraploids was significantly higher (up to 12.5%) than 'Torsh' tetraploids. Also, the APX activity in 'Sabz' tetraploids was 31.45 U mg^{-1} protein at 25% PEG treatment, significantly lower than its activity at 20% PEG treatment (**Figure 6C**).

Both 'Sabz' and 'Torsh' tetraploid genotypes showed a significantly greater GPX activity (1.28-fold and 1.46-fold, respectively) at 15% PEG treatment than their diploid control genotypes. Also, the GPX activity was significantly higher (19% higher) in 'Sabz' tetraploids than 'Torsh' tetraploids at 20% PEG treatment. GPX activity in 'Sabz' tetraploids was 12.19 U mg^{-1} protein at 25% PEG treatment and was significantly lower than its activity under 20% PEG treatment (**Figure 6D**).

DISCUSSION

Under natural conditions, the plant roots have a determinant role in plant water stress responses. Nevertheless, the shoot tip explants (without roots) have proved to be a good representative for an entire plant under *in vitro* conditions for abiotic stress studies, including drought and salinity (Peìrez-Clemente and Gomez-Cadenas, 2012). In this regard, shoot tip explants have recently been widely used to study various aspects of plant strategies encountering water stress conditions in many plants' species *in vitro*. As reported in *Eucalyptus tereticornis* (Singh et al., 2020), *Actinidia* spp. (Zhong et al., 2018), *Lippia alba* (De Castro et al., 2020), *Prunus* spp. (Sorkheh et al., 2011), etc. A shoot tip explant behaves like an entire plant under water stress conditions and may indicate the water stress coping mechanisms in the roots and shoots, including rapid hormonal responses, osmoprotectants accumulation, enzymatic and non-enzymatic defensive strategies (Montoliu et al., 2009; Peìrez-Clemente and Gomez-Cadenas, 2012).

Water stress significantly limits plant growth and development by affecting different morphological, hormonal, physiological, and biochemical aspects (Khalid et al., 2020). *In vitro* water stress is usually accompanied by a typical range of symptoms. In the current study, depending on genotype, various levels of leaf wilting and rolling, yellowing and necrosis of the leaf margins, leaf shedding, shoot tip dieback, and stem browning were observed by the increased water stress intensity and duration. The observations pointed that both cultivars' tetraploid explants were more resilient to the high level of water stress treatments (15, 20, and 25% PEG treatments) than their diploid control explants (**Figure 2**). For example, at 15% PEG treatment, both diploid genotypes showed severely damaged symptoms, including drastic leaf shedding, decreasing leaf area, leaf necrosis, stem browning, shoot tip dieback, as previously reported (Karimi et al., 2012; Shekafandeh and Hojati, 2013). In both tetraploid genotypes, the symptoms were less severe and limited to reduced growth, leaf numbers and area, and some degree of yellowish.

The results highlighted the superiority of both tetraploid genotypes in all tested morphological parameters at different water stress treatments than their diploid control plants (**Figure 2**). This indicates that tetraploid genotypes benefited from the adaptive strategies that alleviate the detrimental effects of water stress, especially at high levels of PEG treatments (15, 20, and 25% PEG concentrations).

In plants, water stress tolerance is highly related to the modulating and coordinating gene expression networks, especially regarding turgor maintenance, preventing cell dehydration, and cell detoxification. Various physiological and biochemical strategies are involved (Pandey and Chakraborty, 2015; Hasanuzzaman et al., 2020). As Zhang et al. (2015) reported, these strategies resulted in superior drought tolerance of two tetraploid apple cultivars ('Hanfu' and 'Gala') compared to their diploid seedlings under short term extreme drought conditions (30% PEG).

Rapid phytohormonal changes follow the formation of the first hyperosmotic signals in plant cells under water stress conditions. Drought adaptive strategies, including morphological, physiological, and biochemical modifications, are then regulated by the phytohormonal responses (Zhu, 2016). In this regard, ABA, SA, and JA are considered major stress response phytohormones (SRHs) (Yu et al., 2020). The biosynthesis, and accumulation of key SRH, ABA, increase rapidly by receiving the first hyperosmotic signals and regulating a series of downstream genes, especially overexpression of genes involving the compatible solutes, osmoprotectants, and enzymatic and non-enzymatic defensive system. ABA also regulates the closure of stomata to reduce transpiration (Pandey and Chakraborty, 2015).

The hormonal behavior analysis in this study revealed that ABA biosynthesis in tetraploid explants of both cultivars was around twofold higher than their diploid control plants under moderate and high water-stress levels. The SA and JA levels and their biosynthesis were significantly higher in tetraploid explants at the high water-stress levels than in their diploid control plants. They synergistically work with ABA to alleviate detrimental effects of water stress by triggering the downstream mechanisms, including rapid stomatal closure, over-accumulation of compatible solutes and osmoprotectants, over-activating the enzymatic antioxidant system, and increasing hydraulic conductivity of water to leaves at stressful times (Wager and Browse, 2012; Sánchez-Romera et al., 2014). Herein, 20% (severe) and 25% (extreme) PEG treatments negatively affected ABA, SA, and JA biosynthesis of tetraploid genotypes, which indicated that very high water-stress intensities could seriously disrupt their biosynthesis pathways.

Enhanced efficiency of adaptive strategies under water stress, including robust osmotic adjustment and enzymatic defense system, all influenced by augmented ABA signaling pathways as a result of chromosome doubling, have been well investigated

(Allario et al., 2013; Rao et al., 2020). However, there is not enough information about the molecular mechanisms underlying this phenomenon. Rao et al. (2020), by comparing transcriptional analysis of autotetraploid and diploid plants of *L. ruthenicum*, discovered that the substantial superiority of autotetraploids over diploid plants is mainly related to their intrinsic capability to rapidly increase ABA biosynthesis and accumulation *via* overexpression of *9-cis-epoxycarotenoid dioxygenase 1 (NCED1)* and *NCED2*, which encode pivotal biosynthetic enzymes in ABA signaling transduction pathways. Additionally, Allario et al. (2013) reported that tolerance to water stress of 4× Rangpur lime rootstocks than their 2× counterparts is because of their boosted ability for ABA biosynthesis and ABA regulatory system, which is regulated by overexpression of drought-responsive genes, including *CsNCED1*, a critical regulatory gene of ABA biosynthesis.

Increasing ion leakage is an essential index for cell membrane stability under stressful conditions, reported in all types of abiotic stresses (Santos et al., 2019). The significantly low percentage of ion leakage in tetraploid explants than their diploid control plants in the present study might be related to their superior adaptive strategies such as robust osmotic adjustment and cell detoxification systems, which lead to maintaining the cell membrane integrity and preventing its destruction (Wei et al., 2019). These augmented critical strategies resulting from chromosome doubling could also play a key role in preventing the degradation of photosynthetic pigments and plant cytokinins, which are essential for photosynthetic pigments biosynthesis (Du et al., 2020). Due to that, tetraploid explants had significantly greater chlorophyll and carotenoid contents under all water stress treatments. However, the tetraploid figs essentially produced much more photosynthetic pigments at the non-stress condition (**Figures 4C,D**).

The tetraploid explants of both cultivars contained significantly more lignin in their cell walls than their diploid control plants. Lignin content increased only at 5% PEG treatment in diploids genotypes, while it increased even at 10% PEG treatment in tetraploid genotypes compared to their control treatment. Although the lignin content declined for both tetraploid and diploid explants at higher water stress levels, the decline rate was quicker for diploids (**Figure 4E**). The increase in lignin biosynthesis is due to overexpression of *MdMYB4* and *MdVND6* genes, which are two essential genes in lignin biosynthesis pathways, resulting in lignin deposition, xylem vessel synthesis, better hydraulic conductivity, more cell wall, and membrane stability, that all lead to increasing drought adaptation (Geng et al., 2018; Xu et al., 2020). Our data support previous work across plant species that showed that severe abiotic stress, including water stress, can limit lignin biosynthesis (Moura-Sobczak et al., 2011). A decrement in the biosynthesis of lignin precursors such as caffeoyl-CoA and para-coumaryl alcohol and declined anionic peroxidase activity, have been reported as the possible reasons for lignin biosynthesis suppression (Vincent et al., 2005; Moura et al., 2010).

H_2O_2 and MDA are two well-known stress biomarkers in plant systems. Excessive water loss in plants under drought conditions gives rise to over-producing ROSs, which damage cell membranes and increase ion leakage. Increasing MDA content indicates enhanced lipid peroxidation of the cell membrane. The greater ability of tetraploid genotypes for osmotic adjustment and their robust ROS scavenging systems significantly reduces their H_2O_2 and MDA contents under high-level water stress treatments (Jaafar et al., 2012).

Osmotic adjustment through synthesis and accumulation of compatible solutes is one of the most critical plant strategies confronting water stress conditions. Compatible solutes mostly include soluble sugars (TSSs), amino acids (especially proline), and quaternary ammonium compounds (notably GB), which are rich in hydroxyls (−OH) groups that allow them to bind to H_2O molecules and protect cellular ingredients from dehydration, keeping vital functions of proteins and enzymes and preserving cell structures and membranes (Laxa et al., 2019; Hasanuzzaman et al., 2020).

As the results revealed, tetraploid genotypes in this study displayed a greater intrinsic capability for cell osmolytes accumulation than their diploid controls. This essential superiority was clearly observed (for only 'Sabz' tetraploids) at severe and extreme water stress conditions (20 and 25% PEG concentrations), where the tetraploid genotypes were capable of biosynthesis and accumulating a remarkable amount of cell osmolytes whilst their diploid controls did not tolerate such a level of water stress and died (**Figure 5**). Cell osmolytes accumulation, including TSS, proline, and GB, is well known as a central plant's strategy for confronting water stress, which functionally protects cell ingredients from excessive dehydration, as well as less generation of ROSs, ROS scavenging, and preventing cell membrane disruption (Gurrieri et al., 2020). It could be considered as a significant strategy in which tetraploid genotypes cope with water stress and display extra tolerance to severe water stress conditions compared with their diploid genotypes. Our findings support previous reports that enhanced osmolyte accumulation confers superiority to tetraploid genotypes to better tolerate water stress than diploids (Liu et al., 2011; Zhang et al., 2015; Wei et al., 2019; Oustric et al., 2020).

Stomatal closure, as one of the earliest plant responses to water stress conditions, leads to the disrupting of the thylakoid electron transport chain, which results in the overaccumulation of various forms of ROSs in cell organelles such as chloroplasts, mitochondria, peroxisomes, as well as apoplast, and plasma membranes (Laxa et al., 2019). Due to their strong tendency to react with cellular ingredients such as carbohydrates, proteins, lipids, nucleic acids, cell membranes, etc., the ROS molecules are highly detrimental for plant systems and need to be rapidly removed. Plants counteract ROSs by boosting enzymatic (SOD, CAT, APX, GPX) and non-enzymatic (phenolic compounds, non-protein amino acids) defensive systems to maintain the steady-state balance in cells (Hasanuzzaman et al., 2020). As displayed in **Figure 6**, tetraploid explants benefited from an augmented antioxidant defense system under water stress treatments compared to their diploid control plants. Obviously, under the high levels of water-stress condition, the significant superiority of SOD, CAT, APX, and GPX activity in tetraploid explants resulted in robust ROS scavenging and cell

detoxification than their diploid control plants. The antioxidant enzymes act together synergistically, in a so-called chain reaction for cell protection against ROSs toxicity (Su et al., 2017). The enhanced enzymatic antioxidant system resulting from the chromosome doubling in the current research were also reported in autotetraploid plants of *P. trifoliata* (Wei et al., 2019), 'Carrizo' citrange (Oustric et al., 2017), *Dioscorea zingiberensis* (Zhang et al., 2010), and *Robinia pseudoacacia* (Wang et al., 2013).

The vital function of the enzymatic defense system briefly includes catalyzing the conversion of two molecules of $O_2^{\bullet -}$ into H_2O_2 and O_2 by SOD enzyme and its metal isoforms (Mn-SOD, Fe-SOD, Cu, Zn-SOD, and Ni-SOD). This is followed by decomposing H_2O_2 into H_2O and O_2 by CAT, APX, GPX enzyme activities *via* mediating different substrates to protect cellular ingredients from the ROSs injuries (Mittler, 2002; Rai et al., 2011; Santos et al., 2019; Zhang et al., 2019).

CONCLUSION

In the present study, tetraploid-induced explants of two fig cultivars ('Sabz' and 'Torsh') and their diploid control plants were subjected to different *in vitro* PEG-induced water stress treatments (0, 5, 10, 15, 20, and 25%) to evaluate their water stress tolerance. The morphological, hormonal, physiological, and biochemical analysis revealed that both tetraploid genotypes exhibited superior water stress tolerance than their diploid control plants. Among the four tested genotypes, the tetraploid explants of the 'Sabz' cultivar were the only genotype that could withstand the extreme (25% PEG) water stress conditions. Tetraploid plantlets of both cultivars displayed a superior ability for maintaining their RWC and ion leakage percentages in a low-risk range compared with their diploid genotypes. They also benefit from augmented adaptive strategy systems, including remarkably higher biosynthesis of ABA, SA, and JA stress response hormones, robust osmotic adjustment (higher accumulated TSS, proline, and glycine-betaine), and a strong enzymatic defense system (notably higher SOD, CAT, APX, and GPX activities). Our results paved the way for using the ploidy manipulation method in fig tree breeding programs as an efficient breeding system to achieve new desirable characteristics with significant tolerance to abiotic stresses and to overcome the conventional breeding system's barriers of the fig tree.

DATA AVAILABILITY STATEMENT

The original contributions presented in the study are included in the article/**Supplementary Material**, further inquiries can be directed to the corresponding author.

AUTHOR CONTRIBUTIONS

RA conducted the experiments, data analyzing, and interpretation, and wrote the manuscript. AS contributed to the supervisor, research design, assistance with data interpretation, correction, and approval of the manuscript. Both authors contributed to the article and approved the submitted version.

FUNDING

This study was supported by the Shiraz University.

ACKNOWLEDGMENTS

The authors wish to thank Bahman Khahani and Ahmad Tahmasebi for their kind help in data analysis and Abolfazl Jowkar and Ali Gharaghani for the critical reading of the manuscript.

SUPPLEMENTARY MATERIAL

The Supplementary Material for this article can be found online at: https://www.frontiersin.org/articles/10.3389/fpls.2021.796215/full#supplementary-material

REFERENCES

Abdolinejad, R., Shekafandeh, A., and Jowkar, A. (2021). In vitro tetraploidy induction creates enhancements in morphological, physiological and phytochemical characteristics in the fig tree (Ficus Carica L.). *Plant Physiol. Biochem.* 166, 191–202. doi: 10.1016/j.plaphy.2021.05.047

Abdolinejad, R., Shekafandeh, A., Jowkar, A., Gharaghani, A., and Alemzadeh, A. (2020). Indirect regeneration of Ficus carica by the TCL technique and genetic fidelity evaluation of the regenerated plants using flow cytometry and ISSR. *Plant Cell. Tissue Organ Cult.* 143, 131–144. doi: 10.1007/s11240-020-01903-5

Ahmad, M. A., Javed, R., Adeel, M., Rizwan, M., and Yang, Y. (2020). PEG 6000-stimulated drought stress improves the attributes of in vitro growth, steviol glycosides production, and antioxidant activities in Stevia rebaudiana bertoni. *Plants* 9, 1–10. doi: 10.3390/plants9111552

Allario, T., Brumos, J., Colmenero-Flores, J. M., Iglesias, D. J., Pina, J. A., Navarro, L., et al. (2013). Tetraploid Rangpur lime rootstock increases drought tolerance via enhanced constitutive root abscisic acid production. *Plant Cell Environ.* 36, 856–868. doi: 10.1111/pce.12021

Balal, R. M., Shahid, M. A., Vincent, C., Zotarelli, L., Liu, G., Mattson, N. S., et al. (2017). Kinnow mandarin plants grafted on tetraploid rootstocks are more tolerant to Cr-toxicity than those grafted on its diploids one. *Environ. Exp. Bot.* 140, 8–18. doi: 10.1016/j.envexpbot.2017.05.011

Bates, L. S., Waldren, R. P., and Teare, I. D. (1973). Rapid determination of free proline for water-stress studies. *Plant Soil* 39, 205–207. doi: 10.1007/bf00018060

Chance, B., and Maehly, A. C. (1955). [136] Assay of catalases and peroxidases. {black small square}. *Methods Enzymol.* 2, 764–775. doi: 10.1016/S0076-6879(55)02300-8

Corneillie, S., De Storme, N., Van Acker, R., Fangel, J. U., De Bruyne, M., De Rycke, R., et al. (2019). Polyploidy affects plant growth and alters cell wall composition. *Plant Physiol.* 179, 74–87. doi: 10.1104/pp.18.00967

De Castro, K. M., Batista, D. S., Silva, T. D., Fortini, E. A., Felipe, S. H. S., Fernandes, A. M., et al. (2020). Water deficit modulates growth, morphology, and the essential oil profile in Lippia alba L. (Verbenaceae) grown in vitro. *Plant Cell, Tissue Organ Cult.* 141, 55–65. doi: 10.1007/s11240-020-01766-w

De Souza, J. D., De Andrade Silva, E. M., Filho, M. A. C., Morillon, R., Bonatto, D., Micheli, F., et al. (2017). Different adaptation strategies of two citrus

scion/rootstock combinations in response to drought stress. *PLoS One* 12, 1–23. doi: 10.1371/journal.pone.0177993

Doyle, J. J., and Coate, J. E. (2019). Polyploidy, the nucleotype, and novelty: The impact of genome doubling on the biology of the cell. *Int. J. Plant Sci.* 180, 1–52. doi: 10.1086/700636

Du, K., Liao, T., Ren, Y., Geng, X., and Kang, X. (2020). Molecular Mechanism of Vegetative Growth Advantage in Allotriploid Populus. *Int. J. Mol. Sci.* 21:441. doi: 10.3390/ijms21020441

Dudits, D., Török, K., Cseri, A., Paul, K., Nagy, A. V., Nagy, B., et al. (2016). Response of organ structure and physiology to autotetraploidization in early development of energy willow Salix viminalis. *Plant Physiol.* 170, 1504–1523. doi: 10.1104/pp.15.01679

Emmerich, W. E., and Hardegree, S. P. (1990). Polyethylene Glycol Solution Contact Effects on Seed Germination. *Agron. J.* 82, 1103–1107. doi: 10.2134/agronj1990.00021962008200060015x

Falistocco, E. (2009). Presence of triploid cytotypes in the common fig (Ficus carica L.). *Genome.* 52, 919–925. doi: 10.1139/G09-068

Flaishman, M. A., Peer, R., Freiman, Z. E., Izhaki, Y., and Yablovitz, Z. (2017). Conventional and molecular breeding systems in fig (Ficus carica L.). *Acta Hortic.* 1173, 1–9. doi: 10.17660/ActaHortic.2017.1173.1

Flaishman, M. A., Rodov, V., and Stover, E. (2008). The Fig: Botany, Horticulture, and Breeding. *Horticul. Rev.* 34, 113–196. doi: 10.1002/9780470380147

Fox, D. T., Soltis, D. E., Soltis, P. S., Ashman, T. L., and Van de Peer, Y. (2020). Polyploidy: A Biological Force From Cells to Ecosystems. *Trends Cell Biol.* 30, 688–694. doi: 10.1016/j.tcb.2020.06.006

Geng, D., Chen, P., Shen, X., Zhang, Y., Li, X., Jiang, L., et al. (2018). MdMYB88 and MdMYB124 Enhance Drought Tolerance by Modulating Root Vessels and Cell Walls in Apple. *Plant Physiol.* 178, 1296–1309. doi: 10.1104/pp.18.00502

Gurrieri, L., Merico, M., Trost, P., Forlani, G., and Sparla, F. (2020). Impact of Drought on Soluble Sugars and Free Proline Content in Selected Arabidopsis Mutants. *Biology* 9:367. doi: 10.3390/biology9110367

Hasanuzzaman, M., Bhuyan, M. H. M. B., Zulfiqar, F., Raza, A., Mohsin, S. M., Al Mahmud, J., et al. (2020). Reactive oxygen species and antioxidant defense in plants under abiotic stress: Revisiting the crucial role of a universal defense regulator. *Antioxidants* 9, 1–52. doi: 10.3390/antiox9080681

Hias, N., De Dauw, K., Davey, M. W., Leus, L., Van Labeke, M. C., Van Huylenbroeck, J., et al. (2017). Influence of ploidy level on the physiological response of apple to water deficit. *Acta Hortic.* 1177, 333–338. doi: 10.17660/ActaHortic.2017.1177.48

Hodges, D. M., DeLong, J. M., Forney, C. F., and Prange, R. K. (1999). Improving the thiobarbituric acid-reactive-substances assay for estimating lipid peroxidation in plant tissues containing anthocyanin and other interfering compounds. *Planta* 207, 604–611. doi: 10.1007/s004250050524

Iiyama, K., and Wallis, A. F. A. (1990). Determination of lignin in herbaceous plants by an improved acetyl bromide procedure. *J. Sci. Food Agric.* 51, 145–161. doi: 10.1002/jsfa.2740510202

Jaafar, H. Z. E., Ibrahim, M. H., and Fakri, N. F. M. (2012). Impact of soil field water capacity on secondary metabolites, phenylalanine ammonia-lyase (PAL), maliondialdehyde (MDA) and photosynthetic responses of Malaysian Kacip Fatimah (Labisia pumila Benth). *Molecules* 17, 7305–7322. doi: 10.3390/molecules17067305

Karimi, S., Hojati, S., Eshghi, S., Nazary Moghaddam, R., and Jandoust, S. (2012). Magnetic exposure improves tolerance of fig "Sabz" explants to drought stress induced in vitro. *Sci. Hortic.* 137, 95–99. doi: 10.1016/j.scienta.2012.01.018

Khalid, M. F., Hussain, S., Anjum, M. A., Ahmad, S., Ali, M. A., Ejaz, S., et al. (2020). Better salinity tolerance in tetraploid vs diploid volkamer lemon seedlings is associated with robust antioxidant and osmotic adjustment mechanisms. *J. Plant Physiol.* 244:153071. doi: 10.1016/j.jplph.2019.153071

Kovalikova, Z., Jiroutova, P., Toman, J., Dobrovolna, D., and Drbohlavova, L. (2020). Physiological responses of apple and cherry in vitro culture under different levels of drought stress. *Agronomy* 10, 1–13. doi: 10.3390/agronomy10111689

Laxa, M., Liebthal, M., Telman, W., Chibani, K., and Dietz, K. J. (2019). The role of the plant antioxidant system in drought tolerance. *Antioxidants* 8:94. doi: 10.3390/antiox8040094

Leng, X., Feng, X., and Fu, B. (2020). Driving forces of agricultural expansion and land degradation indicated by Vegetation Continuous Fields (VCF) data in drylands from 2000 to 2015. *Glob. Ecol. Conserv.* 23:e01087. doi: 10.1016/j.gecco.2020.e01087

Liu, S., Chen, S., Chen, Y., Guan, Z., Yin, D., and Chen, F. (2011). In vitro induced tetraploid of Dendranthema nankingense (Nakai) Tzvel. shows an improved level of abiotic stress tolerance. *Sci. Hortic.* 127, 411–419. doi: 10.1016/j.scienta.2010.10.012

Peìrez-Clemente, R. M., and Gomez-Cadenas, A. (2012). In vitro Tissue Culture, a Tool for the Study and Breeding of Plants Subjected to Abiotic Stress Conditions. *Recent Adv. Plant Vitr. Cult.* 2012:50671. doi: 10.5772/50671

Manquián-Cerda, K., Escudey, M., Zúñiga, G., Arancibia-Miranda, N., Molina, M., and Cruces, E. (2016). Effect of cadmium on phenolic compounds, antioxidant enzyme activity and oxidative stress in blueberry (Vaccinium corymbosum L.) plantlets grown in vitro. *Ecotoxicol. Environ. Saf.* 133, 316–326. doi: 10.1016/j.ecoenv.2016.07.029

Mesgaran, M. B., Madani, K., Hashemi, H., and Azadi, P. (2017). Iran's Land Suitability for Agriculture. *Sci. Rep.* 7, 1–12. doi: 10.1038/s41598-017-08066-y

Mittler, R. (2002). Oxidative stress, antioxidants and stress tolerance. *Trends Plant Sci.* 7, 405–410. doi: 10.1016/S1360-1385(02)02312-9

Montoliu, A., López-Climent, M. F., Arbona, V., Pérez-Clemente, R. M., and Gómez-Cadenas, A. (2009). A novel in vitro tissue culture approach to study salt stress responses in citrus. *Plant Growth Regul.* 59, 179–187. doi: 10.1007/s10725-009-9401-0

Mori, K., Shirasawa, K., Nogata, H., Hirata, C., Tashiro, K., Habu, T., et al. (2017). Identification of RAN1 orthologue associated with sex determination through whole genome sequencing analysis in fig (Ficus carica L.). *Sci. Rep.* 7, 1–15. doi: 10.1038/srep41124

Moura, J. C. M. S., Bonine, C. A. V., de Oliveira Fernandes, Viana, J., Dornelas, M. C., and Mazzafera, P. (2010). Abiotic and Biotic Stresses and Changes in the Lignin Content and Composition in Plants. *J. Integr. Plant Biol.* 52, 360–376. doi: 10.1111/j.1744-7909.2010.00892.x

Moura-Sobczak, J., Souza, U., and Mazzafera, P. (2011). Drought stress and changes in the lignin content and composition in Eucalyptus. *BMC Proc.* 5:573–587. doi: 10.1186/1753-6561-5-S7-P103

Murashige, T., and Skoog, F. (1962). A revised medium for rapid growth and bioassays with tobacco tissue cultures. *Physiol. Plant.* 15, 473–497. doi: 10.1111/j.1399-3054.1962.tb08052.x

Nakano, Y., and Asada, K. (1981). Hydrogen peroxide is scavenged by ascorbate-specific peroxidase in spinach chloroplasts. *Plant Cell Physiol.* 22, 867–880. doi: 10.1093/oxfordjournals.pcp.a076232

Oliveira, T. M., Yahmed, J., Ben, Dutra, J., Maserti, B. E., Talon, M., et al. (2017). Better tolerance to water deficit in doubled diploid 'Carrizo citrange' compared to diploid seedlings is associated with more limited water consumption. *Acta Physiol. Plant.* 39:204. doi: 10.1007/s11738-017-2497-3

Osmolovskaya, N., Shumilina, J., Kim, A., Didio, A., Grishina, T., Bilova, T., et al. (2018). Methodology of drought stress research: Experimental setup and physiological characterization. *Int. J. Mol. Sci.* 19:12. doi: 10.3390/ijms19124089

Oustric, J., Lourkisti, R., Herbette, S., Morillon, R., Paolacci, G., Gonzalez, N., et al. (2020). Effect of propagation method and ploidy level of various rootstocks on the response of the common clementine (Citrus clementina hort. ex tan) to a mild water deficit. *Agric.* 10, 1–21. doi: 10.3390/agriculture10080321

Oustric, J., Morillon, R., Luro, F., Herbette, S., Lourkisti, R., Giannettini, J., et al. (2017). Tetraploid Carrizo citrange rootstock (Citrus sinensis Osb. × Poncirus trifoliata L. Raf.) enhances natural chilling stress tolerance of common clementine (Citrus clementina Hort. ex Tan). *J. Plant Physiol.* 214, 108–115. doi: 10.1016/j.jplph.2017.04.014

Oustric, J., Morillon, R., Luro, F., Herbette, S., Martin, P., Giannettini, J., et al. (2019). Nutrient Deficiency Tolerance in Citrus Is Dependent on Genotype or Ploidy Level. *Front. Plant Sci.* 10:127. doi: 10.3389/fpls.2019.00127

Oustric, J., Morillon, R., Ollitrault, P., Herbette, S., Luro, F., Froelicher, Y., et al. (2018). Somatic hybridization between diploid Poncirus and Citrus improves natural chilling and light stress tolerances compared with equivalent doubled-diploid genotypes. *Trees - Struct. Funct.* 32, 883–895. doi: 10.1007/s00468-018-1682-3

Ozden, M., Demirel, U., and Kahraman, A. (2009). Effects of proline on antioxidant system in leaves of grapevine (Vitis vinifera L.) exposed to oxidative stress by H2O2. *Sci. Hortic.* 119, 163–168. doi: 10.1016/j.scienta.2008.07.031

Pan, X., Welti, R., and Wang, X. (2010). Quantitative analysis of major plant hormones in crude plant extracts by high-performance liquid chromatography-mass spectrometry. *Nat. Protoc.* 5, 986–992. doi: 10.1038/nprot.2010.37

Pan, Y., Wu, L. J., and Yu, Z. L. (2006). Effect of salt and drought stress on antioxidant enzymes activities and SOD isoenzymes of liquorice (Glycyrrhiza uralensis Fisch). *Plant Growth Regul.* 49, 157–165. doi: 10.1007/s10725-006-9101-y

Pandey, S., and Chakraborty, D. (2015). "Salicylic Acid and Drought Stress Response: Biochemical to Molecular Crosstalk," in *Stress Responses in Plants*, eds B. N. Tripathi and M. Muller (Switzerland: Springer International Publishing), 247–265. doi: 10.2174/1389202918666170605083319

Patade, V. Y., Bhargava, S., and Suprasanna, P. (2012). Effects of NaCl and iso-osmotic PEG stress on growth, osmolytes accumulation and antioxidant defense in cultured sugarcane cells. *Plant Cell. Tissue Organ Cult.* 108, 279–286. doi: 10.1007/s11240-011-0041-5

Rai, M. K., Kalia, R. K., Singh, R., Gangola, M. P., and Dhawan, A. K. (2011). Developing stress tolerant plants through in vitro selection-An overview of the recent progress. *Environ. Exp. Bot.* 71, 89–98. doi: 10.1016/j.envexpbot.2010.10.021

Ramsey, J., and Schemske, D. W. (2002). Neopolyploidy in flowering plants. *Annu. Rev. Ecol. Syst.* 33, 589–639. doi: 10.1146/annurev.ecolsys.33.010802.150437

Rao, S., Tian, Y., Xia, X., Li, Y., and Chen, J. (2020). Chromosome doubling mediates superior drought tolerance in Lycium ruthenicum via abscisic acid signaling. *Hortic. Res.* 7, 1–18. doi: 10.1038/s41438-020-0260-1

Roointan, R., Yadollahi, A., Sarikhani Khorami, S., Arab, M. M., and Vahdati, K. (2016). Rainfed fruit orchards in sloping lands: soil erosion reduction, water harvesting and fruit production. *Acta Hortic.* 1190, 107–112. doi: 10.17660/ActaHortic.2018.1190.18

Roy, R., Wang, J., Mostofa, M. G., and Fornara, D. (2021). Optimal water and fertilizer applications improve growth of Tamarix chinensis in a coal mine degraded area under arid conditions. *Physiol. Plant.* 172, 371–390. doi: 10.1111/ppl.13147

Ruiz, M., Oustric, J., Santini, J., and Morillon, R. (2020). Synthetic Polyploidy in Grafted Crops. *Front. Plant Sci.* 11:540894. doi: 10.3389/fpls.2020.540894

Ruiz, M., Quiñones, A., Martínez-Cuenca, M. R., Aleza, P., Morillon, R., Navarro, L., et al. (2016b). Tetraploidy enhances the ability to exclude chloride from leaves in carrizo citrange seedlings. *J. Plant Physiol.* 205, 1–10. doi: 10.1016/j.jplph.2016.08.002

Ruiz, M., Quiñones, A., Martínez-Alcántara, B., Aleza, P., Morillon, R., Navarro, L., et al. (2016a). Tetraploidy enhances boron-excess tolerance in Carrizo citrange (Citrus sinensis L. Osb. × Poncirus trifoliata L. Raf.). *Front. Plant Sci.* 7, 1–16. doi: 10.3389/fpls.2016.00701

Saleh, B., Allario, T., Dambier, D., Ollitrault, P., and Morillon, R. (2008). Tetraploid citrus rootstocks are more tolerant to salt stress than diploid. *Comptes Rendus - Biol.* 331, 703–710. doi: 10.1016/j.crvi.2008.06.007

Sánchez-Romera, B., Ruiz-Lozano, J. M., Li, G., Luu, D. T., Martínez-Ballesta, M. D. C., Carvajal, M., et al. (2014). Enhancement of root hydraulic conductivity by methyl jasmonate and the role of calcium and abscisic acid in this process. *Plant, Cell Environ.* 37, 995–1008. doi: 10.1111/pce.12214

Santos, I. C., dos Almeida, A. A. F., de, Pirovani, C. P., Costa, M. G. C., da Conceição, A. S., et al. (2019). Physiological, biochemical and molecular responses to drought conditions in field-grown grafted and ungrafted citrus plants. *Environ. Exp. Bot.* 162, 406–420. doi: 10.1016/j.envexpbot.2019.03.018

Sarker, U., and Oba, S. (2018). Catalase, superoxide dismutase and ascorbate-glutathione cycle enzymes confer drought tolerance of Amaranthus tricolor. *Sci. Rep.* 8, 1–12. doi: 10.1038/s41598-018-34944-0

Sattler, M. C., Carvalho, C. R., and Clarindo, W. R. (2016). The polyploidy and its key role in plant breeding. *Planta* 243, 281–296. doi: 10.1007/s00425-015-2450-x

Shekafandeh, A., and Hojati, S. (2013). In vitro drought effects on morphological and physiological indices of two fig (Ficus carica L.) cultivars. *Adv. Hort. Sci* 26, 131–137. doi: 10.13128/ahs-22667

Singh, D., Kaur, S., and Kumar, A. (2020). In vitro drought tolerance in selected elite clones of Eucalyptus tereticornis Sm. *Acta Physiol. Plant.* 42, 1–9. doi: 10.1007/s11738-019-3009-4

Soltis, D. E., Albert, V. A., Leebens-Mack, J., Bell, C. D., Paterson, A. H., Zheng, C., et al. (2009). Polyploidy and angiosperm diversification. *Am. J. Bot.* 96, 336–348. doi: 10.3732/ajb.0800079

Sorkheh, K., Shiran, B., Khodambshi, M., Rouhi, V., and Ercisli, S. (2011). In vitro assay of native Iranian almond species (Prunus spp. L.) for drought tolerance. Plant Cell. *Tissue Organ Cult.* 105, 395–404. doi: 10.1007/s11240-010-9879-1

Su, X., Wei, F., Huo, Y., and Xia, Z. (2017). Comparative physiological and molecular analyses of two contrasting flue-cured tobacco genotypes under progressive drought stress. *Front. Plant Sci.* 8:827. doi: 10.3389/fpls.2017.00827

Syvertsen, J. P., Lee, L. S., and Grosser, J. (2000). Limitations on Growth and Net Gas Exchange of Diploid and Tetraploid Citrus Rootstock Cultivars Grown at Elevated CO2. *J. Am. Soc. Hortic. Sci.* 125, 228–234. doi: 10.21273/JASHS.125.2.228

Vincent, D., Lapierre, C., Pollet, B., Cornic, G., Negroni, L., and Zivy, M. (2005). Water Deficits Affect Caffeate O -Methyltransferase, Lignification, and Related Enzymes in Maize Leaves. A Proteomic Investigation. *Plant Physiol.* 137, 949–960. doi: 10.1104/pp.104.050815

Wager, A., and Browse, J. (2012). Social network: JAZ protein interactions expand our knowledge of jasmonate signaling. *Front. Plant Sci.* 3:41. doi: 10.3389/fpls.2012.00041

Wang, Z., Wang, M., Liu, L., and Meng, F. (2013). Physiological and proteomic responses of diploid and tetraploid black locust (*Robinia pseudoacacia* L.) subjected to salt stress. *Int. J. Mol. Sci.* 14, 20299–20325. doi: 10.3390/ijms141020299

Wei, T., Wang, Y., Xie, Z., Guo, D., Chen, C., Fan, Q., et al. (2019). Enhanced ROS scavenging and sugar accumulation contribute to drought tolerance of naturally occurring autotetraploids in Poncirus trifoliata. *Plant Biotechnol. J.* 17, 1394–1407. doi: 10.1111/pbi.13064

Xu, W., Tang, W., Wang, C., Ge, L., Sun, J., Qi, X., et al. (2020). SiMYB56 Confers Drought Stress Tolerance in Transgenic Rice by Regulating Lignin Biosynthesis and ABA Signaling Pathway. *Front. Plant Sci.* 11:785. doi: 10.3389/fpls.2020.00785

Yu, Z., Duan, X., Luo, L., Dai, S., Ding, Z., and Xia, G. (2020). How Plant Hormones Mediate Salt Stress Responses. *Trends Plant Sci.* 25, 1–14. doi: 10.1016/j.tplants

Zhang, F., Xue, H., Lu, X., Zhang, B., Wang, F., Ma, Y., et al. (2015). Autotetraploidization enhances drought stress tolerance in two apple cultivars. *Trees - Struct. Funct.* 29, 1773–1780. doi: 10.1007/s00468-015-1258-4

Zhang, L., Wu, M., Teng, Y., Jia, S., Yu, D., Wei, T., et al. (2019). Overexpression of the glutathione peroxidase 5 (RcGPX5) gene from Rhodiola crenulata increases drought tolerance in Salvia miltiorrhiza. *Front. Plant Sci.* 9:1950. doi: 10.3389/fpls.2018.01950

Zhang, X. Y., Hu, C. G., and Yao, J. L. (2010). Tetraploidization of diploid Dioscorea results in activation of the antioxidant defense system and increased heat tolerance. *J. Plant Physiol.* 167, 88–94. doi: 10.1016/j.jplph.2009.07.006

Zhong, Y. P., Li, Z., Bai, D. F., Qi, X. J., Chen, J. Y., Wei, C. G., et al. (2018). In vitro variation of drought tolerance in five Actinidia species. *J. Am. Soc. Hortic. Sci.* 143, 226–234. doi: 10.21273/JASHS04399-18

Zhu, J. K. (2016). Abiotic Stress Signaling and Responses in Plants. *Cell* 167, 313–324. doi: 10.1016/j.cell.2016.08.029

Conflict of Interest: The authors declare that the research was conducted in the absence of any commercial or financial relationships that could be construed as a potential conflict of interest.

Publisher's Note: All claims expressed in this article are solely those of the authors and do not necessarily represent those of their affiliated organizations, or those of the publisher, the editors and the reviewers. Any product that may be evaluated in this article, or claim that may be made by its manufacturer, is not guaranteed or endorsed by the publisher.

frontiers in Plant Science

ORIGINAL RESEARCH
published: 04 February 2022
doi: 10.3389/fpls.2022.829765

Genome-Wide Identification of Direct Targets of ZjVND7 Reveals the Putative Roles of Whole-Genome Duplication in Sour Jujube in Regulating Xylem Vessel Differentiation and Drought Tolerance

*Meng Li[1,2,3], Lu Hou[1,2,3], Chenxing Zhang[1,2,3], Weicong Yang[1,2,3], Xinru Liu[1,2,3], Hanqing Zhao[1,2,3], Xiaoming Pang[1,2,3] and Yingyue Li[1,2,3]**

[1] National Engineering Laboratory for Tree Breeding, College of Biological Sciences and Technology, Beijing Forestry University, Beijing, China, [2] Key Laboratory of Genetics and Breeding in Forest Trees and Ornamental Plants, Ministry of Education, College of Biological Sciences and Technology, Beijing Forestry University, Beijing, China, [3] The Tree and Ornamental Plant Breeding and Biotechnology Laboratory of National Forestry and Grassland Administration, Beijing Forestry University, Beijing, China

OPEN ACCESS

Edited by:
Jen-Tsung Chen, National University of Kaohsiung, Taiwan

Reviewed by:
Ali Raza, Fujian Agriculture and Forestry University, China
Sezai Ercisli, Atatürk University, Turkey

***Correspondence:**
Yingyue Li
yingyueli@bjfu.edu.cn

Specialty section:
This article was submitted to Plant Breeding, a section of the journal Frontiers in Plant Science

Received: *06 December 2021*
Accepted: *12 January 2022*
Published: *04 February 2022*

Citation:
Li M, Hou L, Zhang C, Yang W, Liu X, Zhao H, Pang X and Li Y (2022) Genome-Wide Identification of Direct Targets of ZjVND7 Reveals the Putative Roles of Whole-Genome Duplication in Sour Jujube in Regulating Xylem Vessel Differentiation and Drought Tolerance. Front. Plant Sci. 13:829765. doi: 10.3389/fpls.2022.829765

The effects of whole-genome duplication span multiple levels. Previous study reported that the autotetraploid sour jujube exhibited superior drought tolerance than diploid. However, the difference in water transport system between diploids and autotetraploids and its mechanism remain unclear. Here, we found the number of xylem vessels and parenchyma cells in autotetraploid sour jujube increased to nearly twice that of diploid sour jujube, which may be closely related to the differences in xylem vessel differentiation-related ZjVND7 targets between the two ploidy types. Although the five enriched binding motifs are different, the most reliable motif in both diploid and autotetraploid sour jujube was CTTNAAG. Additionally, ZjVND7 targeted 236 and 321 genes in diploids and autotetraploids, respectively. More identified targeted genes of ZjVND7 were annotated to xylem development, secondary wall synthesis, cell death, cell division, and DNA endoreplication in autotetraploids than in diploids. SMR1 plays distinct roles in both proliferating and differentiated cells. Under drought stress, the binding signal of ZjVND7 to *ZjSMR1* was stronger in autotetraploids than in diploids, and the fold-changes in the expression of *ZjVND7* and *ZjSMR1* were larger in the autotetraploids than in the diploids. These results suggested that the targeted regulation of ZjVND7 on *ZjSMR1* may play valuable roles in autotetraploids in the response to drought stress. We hypothesized that the binding of ZjVND7 to *ZjSMR1* might play a role in cell division and transdifferentiation from parenchyma cells to vessels in the xylem. This regulation could prolong the cell cycle and regulate endoreplication in response to drought stress and abscisic acid, which may be stronger in polyploids.

Keywords: autotetraploid, drought tolerance, xylem differentiation, DNA affinity purification sequencing, VND7, sour jujube

INTRODUCTION

As important drivers of evolution, almost all eukaryotic genome sequences bear evidence of ancient whole-genome duplications events (Adams and Wendel, 2005). After whole-genome doubling, gene dose effects, modified regulatory interactions, and rapid genetic and epigenetic modifications and changes strongly affect the genome (Jackson and Chen, 2010). These changes affect gene expression, resulting in differences in traits such as those related to morphology, physiology, and adaptability (Allario et al., 2013; Zhang et al., 2015). Moreover, in the duplicated genome, paralogous copies may acquire a new function (neofunctionalization), several functions controlled by ancestral genes may be partitioned between duplicated genes (subfunctionalization), and redundant copies may accumulate mutations and lose their function, becoming pseudogenes (non-functional). These neofunctionalization, subfunctionalization, and pseudogenization processes are routes to adaptive diversification in polyploidy. In addition, gene regulatory networks involved in transcription factor (TF) pathways can be reconstructed by subfunctionalization and gene silencing (Osborn et al., 2003; De Smet and Van de Peer, 2012). Target genes bound by TFs are affected by the characteristics of the transcription factor binding site (TFBS) in the downstream promoter sequence. During polyploidization of a promoter region, some changes affect TF binding and thus alter the specifics of regulation. Recently, an instance of regulatory divergence among homologous genes via modulation of the TFBS profile was reported (Ye et al., 2016). Additionally, in *Brassica*, the change in the flowering time of allopolyploids is considered to be caused by deletion of the TFBS in the promoter region of the *SOC* homologous gene (Sri et al., 2020). However, compared with orthologs from different species, paralogs from the same species are better systems for studying the tempo, mode, and mechanisms of TFBS evolution. What is fascinating is how the number, function, and expression of TF target genes will be adjusted to balance this dose difference after a sudden homologous polyploidization. Therefore, a careful study of the target genes of TFs and their expression patterns will not only reveal the evolutionary mode of autopolyploid variation but also shed new light on the corresponding regulatory network.

NAC TFs, which compose one of the largest plant TF families, are involved in various processes, including plant organ development, secondary cell wall development, signal transduction, leaf senescence, and responses to biotic and abiotic stresses (Olsen et al., 2005; Puranik et al., 2012). These functions are mediated by NAC TFs in combination with multiple factors. In addition to the two important motifs of NACRS and CACG or CATGTG targeted by NACs (Xu et al., 2013; Han et al., 2021), many studies have shown that NAC TFs can also target a variety of additional motifs, including JUB1 binding site, NBE binding element (TTACGT), and ABRE motif (ACGTG), that participate in plant drought tolerance (Yuan et al., 2019; Shang et al., 2020; Li et al., 2021c). During plant growth and development, a sufficient number of vascular elements, especially the xylem, are essential to promote long-distance transport and alleviate the effects of drought. In this respect, a subfamily of NAC TFs related to the regulation of xylem differentiation called VASCULARRELATED NAC-DOMAIN (VND) has been discovered (Kubo et al., 2005). A previous study has shown that VND7 is one of the first-layer master transcriptional switches for xylem vessel differentiation (Endo et al., 2015). Its overexpression induces the ectopic differentiation of protoxylem-like vessels, while the functional suppression causes defects in the formation of vessel elements (Kubo et al., 2005; Yamaguchi et al., 2008). It has been reported that VND7 can bind to two specific regions—X1E1 and X1E2—of *XCP1* for programmed cell death (Yamaguchi et al., 2011). In addition, *PtrWND*, a homolog of *VND7*, has been shown to regulate the expression of genes related to xylem cell differentiation, programmed cell death, enzymes, and signal transduction pathways (Ohtani et al., 2011). Nonetheless, variations in and mechanisms of xylem vessel differentiation in polyploids remain poorly understood.

Chinese jujube (*Ziziphus jujuba* Mill.), which is native to China, is known for its nutritious, medicinally valuable, edible fruits (Guo and Shan, 2010; Keles, 2020). Excellent jujube varieties are generally propagated by grafting, and the drought and saline-alkali tolerance of these trees depends on the rootstock (Liu, 2010). Owing to its tolerance of poor environmental conditions, sour jujube (Z. *jujuba* var. *spinosa*) has been widely used as a rootstock tree (Wang and Sun, 1986). Many TFs in jujube, including WRKY (Chen et al., 2019), DREB (Zhou et al., 2019), and NAC (Li et al., 2021a). TFs, have been reported to be differentially expressed in response to drought stress, but their underlying is still unclear. In a previous study, autotetraploid sour jujube was acquired by colchicine-induced somatic cell chromosomal doubling, and superior salt resistance and drought tolerance were detected in autotetraploid sour jujube compared with diploid sour jujube (Li et al., 2019c, 2021b). Furthermore, the type and number of TFs changed between the diploid and autotetraploid plants, especially NAC TFs after salinity and drought stress. In the present study, differences in xylem vessels were characterized between diploid and autotetraploid sour jujube. A presumptive *ZjVND7* gene involved in vessel differentiation was differentially expressed between diploid and autotetraploid sour jujube under drought conditions. We were interested in determining how the numbers and functions of downstream target genes regulated by ZjVND7 changed after whole-genome duplication. Therefore, a genome-wide investigation of ZjVND7 target genes in the genomes of diploid and autotetraploid sour jujube under drought stress was conducted through DNA affinity purification sequencing (DAP-seq). Differences in binding motifs between diploid and autotetraploid plants were identified, and the enriched functions of target genes were further analyzed. In addition, *ZjSMR1* targeted by ZjVND7 was identified, and its putative effects on vessel differentiation regulation and the drought response were proposed. Our research provides evidence for the diversified adjustment of plant genomes in response to polyploidization. The putative functions of ZjVND7 and its target genes and the related genetic pathways may be useful tools for designing plant drought tolerance in the future.

MATERIALS AND METHODS

Plant Materials and Treatments

Two-year-old diploid and autotetaploid sour jujube plants growing in pots and tissue cultural seedlings maintained for more than 20 generations were preserved in the National Engineering Laboratory for Tree Breeding, Beijing Forestry University, Beijing, China. Two-year-old plants were grown outdoors, and the tissue cultural materials were grown under a 16/8 h light/dark cycle at 25 ± 2°C and under 130 μmol/m^2/s illumination. More than 50 and 30 diploid and autotetraploid tissue cultural seedlings, respectively, were cultured in rooting medium for 45 days. Then, diploids and autotetraploids displaying uniform growth were transplanted into vermiculite soil and subsequently grown in a greenhouse with a temperature of 24 ± 1°C under a 16 h photoperiod with a cool-white fluorescent light (3,000 lx). After 30 days, the diploids and autotetraploids were subjected to drought and sprayed with abscisic acid (ABA). For drought treatment, after watering through, not watered until the soil water content reaches 4% and held for 7 days. For ABA treatment, the aboveground parts of diploid sour jujube were sprayed with 10 mg/L ABA every 3 h. Mature leaves (leaf order 4–6 from the shoot apex) of diploid and autotetraploid sour jujube plants after drought treatment and after 2 and 12 h of ABA spraying were collected and snap-frozen in liquid nitrogen. For each experiment, there were four plants per replication, and each treatment was repeated three times.

Anatomical Analyses

Fourth-order leaves of 2-year-old diploids and autotetraploids were collected and cut into paraffin sections, with five biological repeats. All the leaves were preserved in FAA solution (50% ethyl alcohol, formaldehyde and glacial acetic acid V:V:V = 18:1:1). Dehydration was performed using ethanol and xylene at different concentrations. Then, the leaves were embedded in paraffin wax. The wax was cut into 8 μm sections and then dyed with safranine and fast green dyes. After decolorization with picric acid, the leaves were observed under a Nikon Eclipse Ci microscope (Nikon, Tokyo, Japan). SPSS 20.0 statistical software (IBM, New York, NY, United States) was used to analyze the number of vessels and parenchyma cells in the xylem. Significant differences were determined via *t*-tests, with * indicating $p < 0.05$ and ** indicating $p < 0.01$.

Isolation of ZjVND7 and Phylogenetic Analysis

Total RNA was extracted with a Plant RNA Kit (Omega Biotech, New York, NY, United States) and purified with RNase-free DNase set. Next, first-strand cDNA was reverse transcripted in a reaction with 1.5 μg of total RNA. The full-length coding sequence (CDS) was obtained from the *Z. jujuba* genome and cloned via PCR of the cDNA. The primer sequences used are as follows: forward, 5′-ATGGAAATGGAATCTTGTGTCCCA-3′, and reverse, 5′-CTACAAATCAGGAAAACAACCAAGA-3′. The PCR products were extracted from the gels using a Gel Extraction Kit (Tsingke, Beijing, China), and then ligated into a pMD19-T vector (Aidlab, Beijing, China) for sequencing. The orthologous genes sequences of *ZjVND7* were obtained by BLAST searches of The Arabidopsis Information Resource (TAIR) website[1]. Multiple sequence alignments were performed using ClustalW, and subsequent phylogenetic analyses were conducted with MEGAX using the maximum likelihood method (Kumar et al., 2018).

Gene Expression Levels According to qRT-PCR

To analyze gene expression levels, qRT-PCR was carried out with a 2 × SYBR Green qPCR Mix Kit (Aidlab, China) in a 25 μl volume on a 7500 Fast Real-Time instrument (Thermo Fisher, Waltham, MA, United States) using the following cycling protocol: 3 min at 94°C followed by 40 cycles of 20 s at 94°C, 20 s at 55°C, and 30 s at 72°C (signal acquisition at 72°C). *ZjActin* was used as a reference gene (Bu et al., 2016). The $2^{-\Delta\Delta Ct}$ method was used to calculate the relative gene expression levels (Livak and Schmittgen, 2001).

DAP-seq, Data Analysis and Functional Annotation

DAP-seq in diploid and autotetraploid sour jujube were performed according to the procedure published by Bartlett et al. (2017). For the DNA DAP library, fresh leaves from diploid and autotetraploid plants after drought stress were sampled, and genomic DNA was obtained using a DNA Extract Kit (Tiangen, Beijing, China) according to the manufacturer's instructions. Then, genomic DNA was fragmented to a size of 200 bp, after which end repair, A-tailing reaction, and adapter ligation were performed. To induce the binding of proteins to magnetic beads, the full-length CDS of *ZjVND7* was first reassembled into a pFN19K HaloTag T7 SP6 Flexi vector. TNT SP6 High-Yield Protein Expression System (Promega, Wisconsin, United States) was performed to express the Halo-ZjVND7 fusion protein according to the manufacturer's specifications (Promega, United States). Then, the expressed proteins were removed with Magne Halo Tag Beads (Promega, Madison, WI, United States). The protein-bound beads were then washed three times with buffer. For recognition of DNA bound to proteins, the beads were resuspended, and a DNA library was added to these reactions. The bound protein-bead-DNA complex was washed and then heated to 98°C for 10 min to denature the Halo-ZjVND7 proteins and release the bound DNA. Finally, a 50 μl PCR mixture that included 25 μl of released DNA was implemented.

An ∼200–400 bp DNA gel was cut out and extracted. The DNA was sequenced using an Illumina NavoSeq instrument with 100-bp single-end reads. For read alignment, the sequences in FASTQ files were aligned to the *Z. jujuba* 'Dongzao' genome using Bowtie 2 (Langmead and Salzberg, 2012). Read trimming and quality/repeat read filtering were further performed. For peak analysis, mapped read files (SAM or BAM format) were used to identify peaks using peak calling via MACS2

[1]https://www.arabidopsis.org/

(Zhang et al., 2008). Based on general feature format (GFF) files, the peak at 3.5 kb relative to the transcription start site (TSS) was located using Homer (Heinz et al., 2010). Genes located 2.0 kb upstream were described as target genes. These genes were annotated via the Gene Ontology (GO) database (Ashburner et al., 2000), and Kyoto Encyclopedia of Genes and Genomes (KEGG) pathway enrichment analysis was performed using KOBAS 2.0 (Xie et al., 2011). Negative control mock DAP-seq libraries (inputs) were prepared without the addition of proteins to the beads. Peaks relative to those of the negative control sample were compared, and motifs were identified using MEME-ChIP 5.0.5 (Machanick and Bailey, 2011).

Differential Expression Analysis of Diploid and Autotetraploid Sour Jujube Based on Published RNA-seq Data

In a previous study, we obtained transcriptomes from diploid and autotetraploid leaves (Li et al., 2019b). On this basis, we reanalyzed the genes that were the differential expression of genes involved in xylem differentiation, secondary cell wall development, cell cycle cell division, and cell death and that were differentially expressed between diploid and autotetraploid leaves. These differentially expressed genes were subsequently visualized in heat maps using TBtools software (Chen et al., 2020).

Subcellular Localization

ZjVND7 and *ZjSMR1* were recombined and ligated into a pYBA1152 vector labeled with eGFP using a one-step seamless cloning kit (Aidlab, China). In short, primers with overlapping sequences were designed for PCR amplification of full-length CDS sequences. Then, the gel was recycled, and a reaction (10 μl volume) was performed to ultimately connect it to the carrier according to the instructions. The correctly sequenced plasmid was transformed into *Agrobacterium*. Then, an MES suspension (OD = 0.5–1.0) was injected into 1-month-old tobacco leaves. The plants were incubated in the dark for 24 h under a 16/8 h light/dark cycle for 48h at 25 ± 2°C. The injection sites were then removed and observed under a SP8 microscope (Leica, Wetzlar, Germany).

Yeast One-Hybrid Assays

The CDS of *ZjVND7* and the 474 bp DNA fragment of the *ZjSMR1* promoter region were inserted into pB42AD and pLacZi2μ vectors (Takara, Kyoto, Japan), respectively, by seamless cloning. The primer sequences used for the 474 bp DNA fragment of the *SMR1* promoter are as follows: forward, 5′-GTAGGGAAAAATGAAAACAAAAACA-3′, and reverse, 5′-TGACAGAGTAAATTGCCATTACCGT-3′. The plasmids were transformed into yeast strain EGY48. The following four combinations were used for cotransformation: pB42AD and pLacZi2μ empty vectors; a pB42AD empty vector and p*ZjSMR1*$^{pro(474\ bp)}$:lacZ; pB42AD:*ZjVND7* and a pLacZi2μ empty vector; and pB42AD:*ZjVND7* and p*ZjSMR1*$^{pro(474\ bp)}$:*lacZ*. The transformed strains were suspended in double distilled water (ddH_2O) and then coated onto tryptophan (Trp) and uracil (Ura)-deficient synthetic dextrose (SD) medium (SD/–Trp/–Ura) for culture at 29°C. The chromogenic substrate 5-bromo-4-chloro-3-indolyl-beta-D-galactopyranoside (X-Gal) was used to characterize β-galactosidase (lacZ) reporter gene expression in the pLacZi2μ vector. The cotransformed strain was dipped and suspended in 200 μl ddH_2O and then spotted onto SD/-Trp/-Ura medium including 80 mg/L X-Gal at 29°C. The plaque was imaged as it turned blue.

RESULTS

Xylem Vessel Differences in Diploid and Autotetraploid Sour Jujube and Identification of *ZjVND7*

Based on the differences in morphology, the main veins of the leaves of autotetraploid sour jujube were significantly enlarged compared with those of diploid sour jujube (**Figures 1A,B** and **Supplementary Figure 1**). Additionally, the number of xylem vessels in autotetraploids increased to a number nearly twice that in diploids, while the xylem vessel size did not increase significantly in autotetraploids (**Figures 1A–C** and **Supplementary Figure 2**). Furthermore, the number of parenchyma cells markedly increased in autotetraploids (**Figure 1D**).

The most important physiological function of vessels is water transport. Here, when the plants were subjected to a soil water content equal to 4% field capacity for 7 days, *LOC107430472* exhibited a greater fold-changes in the autotetraploid leaves than in the diploid leaves (**Figure 1F**). Phylogenetic analysis confirmed that the protein encoded by *LOC107430472* was closely related to the *Arabidopsis thaliana* group secondary wall NACs (SWNs) and most strongly related to *VND7* (**Figure 1E**). On this basis, the *LOC107430472* was designated *ZjVND7*.

Genome-Wide Identification of the Direct Downstream Targets of ZjVND7 in Diploid and Autotetraploid Plants

To investigate the changes in ZjVND7 interactions between diploid and autotetraploid plants under drought stress. The DAP-seq was performed on diploids and autotetraploids under drought treatment. A total of 1,759/2,538 peaks of *ZjVND7* targets identified in diploid/autotetraploid sour jujube were distributed across 12 chromosomes (**Supplementary Figure 3**). The number of peaks distributed throughout the gene body and its upstream and downstream in autotetraploids was significantly greater than that in diploids, but there was no significant difference in the distribution of the detected positions. As shown in **Figures 2A,B**, within the genic peaks, ZjVND7 showed the highest preference for binding to proximal promoter regions located up to 2.0 kb upstream of the TSS. ZjVND7 also showed preferential binding to exons and distal downstream regions that constituted 8.64 and 6.82% of all the peaks, respectively, in diploid and 10.36 and 7.05% of all the peaks, respectively, in autotetraploids. In diploids, 1,495 peaks mapped to 1,370

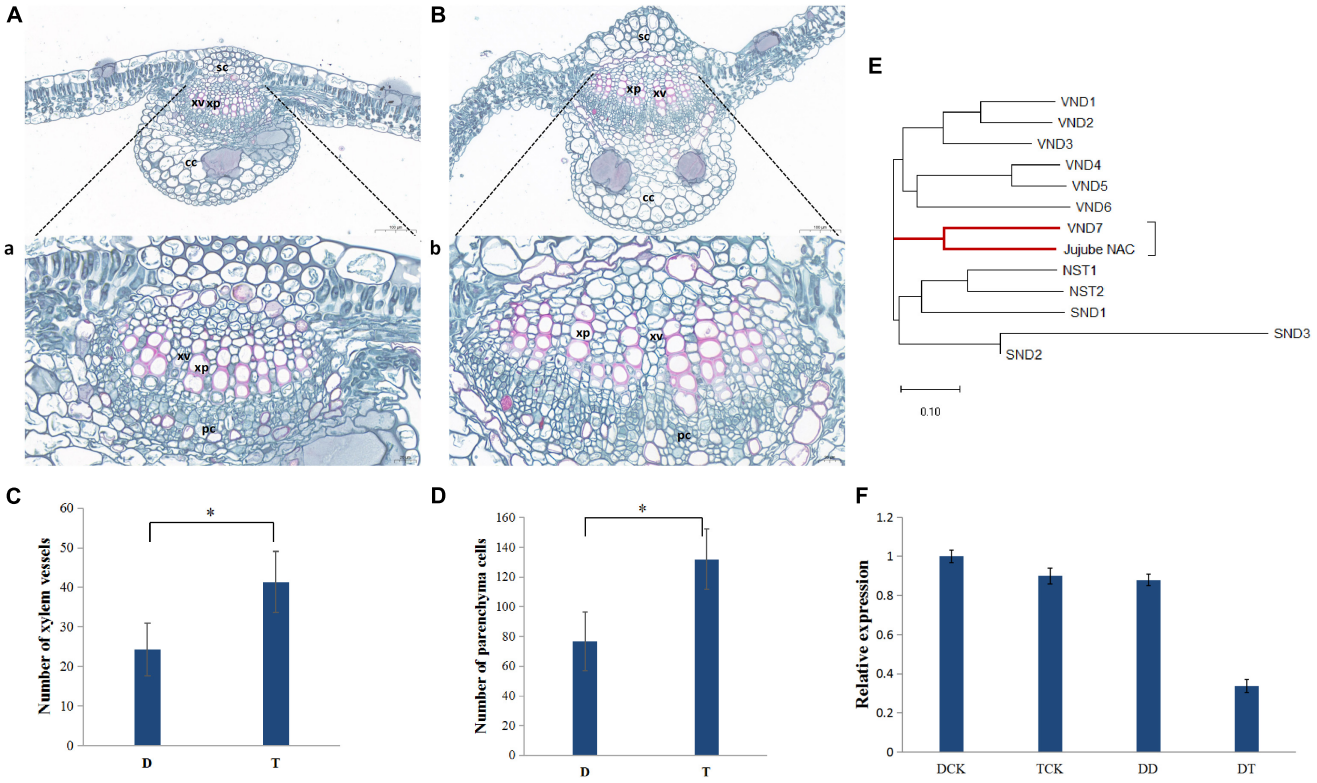

FIGURE 1 | Differences in xylem between diploid and autotetraploid sour jujube and the expression levels and phylogeny of *ZjVND7*. **(A,B)** Characterization of the anatomical structure of diploids **(A)** and autotetraploids **(B)**. a, the partial view of **(A)**; b, the partial view of **(B)**. **(C,D)** Comparison of cell numbers in xylem vessels **(C)** and xylem parenchyma **(D)** in the main veins of leaves. For the difference between D and T, * represents a significance level of 0.05. **(E)** Phylogenetic analysis of jujube LOC107430472 and the *A. thaliana SWN* genes. **(F)** Expression level of *ZjVND7* in diploid and autotetraploid sour jujube under drought stress. D, diploid; T, autotetraploid; DCK, diploid before drought treatment; TCK, autotetraploid before drought treatment; DD, diploid after drought treatment; TD, autotetraploid after drought treatment; sc, sclerenchyma cell; xp, xylem parenchyma; xv, xylem vessel; cc, collenchyma cell; pc, phloem cell.

genes, and 265 peaks were located in promoter regions of 236 jujube genes and 26 unaligned genes (**Supplementary Table 1**). In the autotetraploids, 2,135 peaks corresponded to 1,915 genes, and 375 peaks were located in the promoters of 321 jujube genes and 49 unaligned genes (**Supplementary Table 2**). The binding motifs in target genes were divided into five types in both diploid and autotetraploid sour jujube (**Figure 2C** and **Supplementary Table 3**). The results showed that the motifs in the diploids and autotetraploids were different. However, the binding motifs in both diploid and autotetraploid sour jujube have a continuous core sequence, CTTNAAG, which is conserved with core sequence published by Tamura et al. (2019).

In fact, the most reliable binding motif was not significantly different between diploids and autotetraploids (**Figures 3A,B**). Sequence analysis revealed a 19 nt motif and a TTGCTT or AAGCAA sequence, which is part of the above motif in diploids and autotetraploids. Each motif was located at a region corresponding to a peak (**Figures 3C,D**). Interestingly, both core motifs differed from the binding motifs previously found in *A. thaliana* VNDs (Zhong et al., 2010; O'Malley et al., 2016; Olins et al., 2018) and the 17 nt motif in maize NUT1 (Dong et al., 2020). This divergence in DNA-binding motifs suggests a putatively distinct downstream regulatory network among sour jujube, *A. thaliana* and maize.

ZjVND7 Putative Targeted Pathways

To explore the ZjVND7-targeted functions in diploid and autotetraploid plants, GO classification and functional enrichment analysis of these target genes were performed. As shown in **Figure 4**, target genes in both diploid and autotetraploid plants were enriched in metabolic process, developmental process, response to stimulus, and response to hormone pathways (corrected p-value < 0.05). This suggests that ZjVND7 may be related to the stress response and plant development. In addition, the target genes in diploids were markedly enriched in gametophyte development, pollen development, pollen wall assembly, response to auxin, response to ABA, and response to oxygen-containing compounds. The target genes in autotetraploids were specifically enriched in the regulation of seed germination, defense response, cell death, the regulation of hydrogen peroxide metabolic process, signal transduction, and the response to stress. Moreover, the target genes in autotetraploids were annotated to the triterpenoid metabolic process, while those in diploids were not. The number of target genes annotated to the regulation of seed germination,

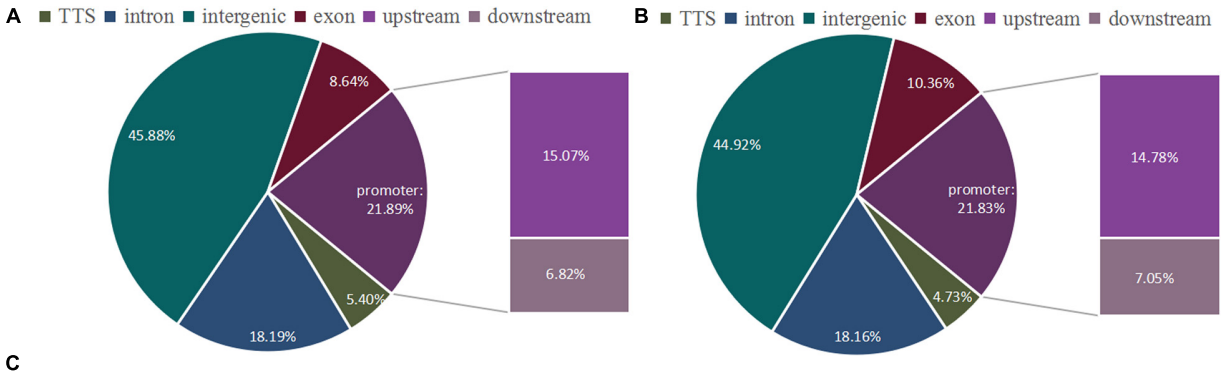

C

		-4	-3	-2	-1	1	2	3	4	5	6	7	8	9	10	11	12	13	14	15	16	17
Motif 1	D	N	T	W	D	C	T	T	N	N	W	Y	T	T	S	A	A	G	N	W		
	T	D	T	T	N	C	T	T	N	N	W	T	T	H	Y	A	A	G	H	W		
Motif 2	D	T	T	T	T	T	W	T	T	T	T	T	T	T	T	T	T	B	T	T	T	
	T	A	A	A	A	A	R	A	R	A	A	A	R	A	A	A	A	A	R	A	A	
Motif3	D															A	R	G	A	A	A	V
	T															A	W	G	C	W	T	
Motif 4	D					C	W	T	G	G	M											
	T				A	C	D	T	G													
Motif 5	D			A	G	C	T	T	S													
	T			A	T	A	T	A	T	A	B											
						C	T	T								A	A	G				

FIGURE 2 | Genome-wide distribution of ZjVND7 binding peaks and types of motifs bound to the promoter in diploid and autotetraploid sour jujube. **(A,B)** Genome-wide distribution of ZjVND7 binding peaks in diploid **(A)** and autotetraploid **(B)** plants. TSS, transcription start site. **(C)** Comparison of the ZjVND7-binding motifs in diploid and autotetraploid plants. D, diploid; T, autotetraploid.

positive regulation of cell death, regulation of hydrogen peroxide metabolic process, and immune response-activating signal transduction in autotetraploids was at least twice that in diploids. These results suggest that ZjVND7 may control a broad range of biological processes in diploid and autotetraploid sour jujube. In particular, compared with that in diploids, ZjVND7 in autotetraploids may target more pathways related to cell growth and stress signaling under drought conditions.

As shown by the KEGG annotations, the target genes in the diploid (**Supplementary Table 4**) and autotetraploid (**Supplementary Table 5**) plants were annotated in 59 and 65 pathways. A total of 27/39, 1/3, and 1/4 target genes were annotated in metabolic pathways, ABC transporters, and MAPK signaling pathway-plant pathways in diploid/autotetraploid sour jujube, respectively. The target genes in diploids were specifically annotated in 17 pathways, including carbon fixation in photosynthetic organisms and phenylalanine metabolism. In autotetraploids, targets were specifically annotated in 23 pathways, including flavonoid biosynthesis, photosynthesis, and glutathione metabolism. Taken together, these results suggest that ZjVND7 may control various stress response-related biological processes that could promote increased water transport in diploid and autotetraploid plants.

Differential Expression of Genes Related to ZjVND7 Putative Targeted Pathways

Putative target genes of VND have been reported in *A. thaliana* (Tamura et al., 2019), maize (Dong et al., 2020), and poplar (Ohtani et al., 2011). These target genes were predicted to be related to the regulation of xylem development, programmed cell death, cell wall synthesis, metabolic enzymes, and signal transduction. Similarly, the target genes of ZjVND7 detected in this study were also predicted to participate in these pathways, but there were differences in the number of target genes between diploid and autotetraploid plants. A total of 3/8, 2/5, 13/11, 5/9, 7/7, and 1/3 target genes were detected in diploid/autotetraploid plants, respectively, and may be involved in xylem development, secondary wall synthesis, ABA signaling, cell death, cell division, and DNA replication (**Figures 5A–F**).

The published RNA-seq data of the leaves of diploid and autotetraploid plants under control and drought conditions

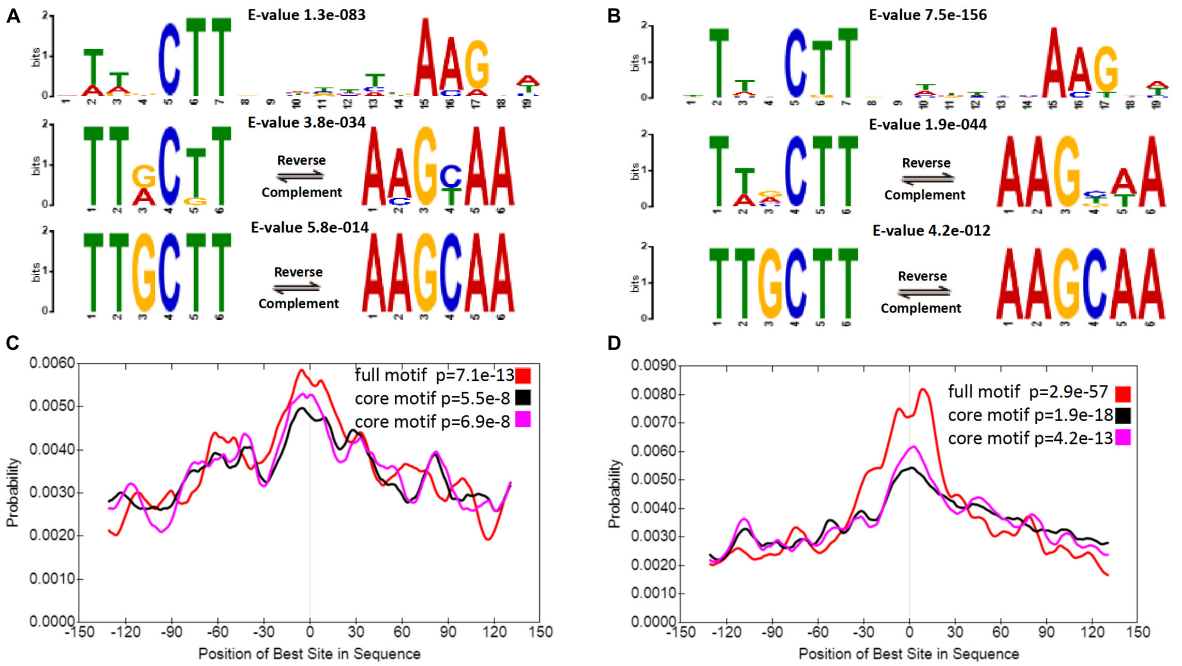

FIGURE 3 | ZjVND7-bound motifs in diploid and autotetraploid sour jujube. **(A,B)** Enriched motifs within the ZjVND7 binding peaks in diploid **(A)** and autotetraploid **(B)** plants. The *E*-value was calculated by MEME. **(C,D)** Localization of the motifs relative to the ZjVND7 peak summits in diploid **(C)** and autotetraploid **(D)** plants.

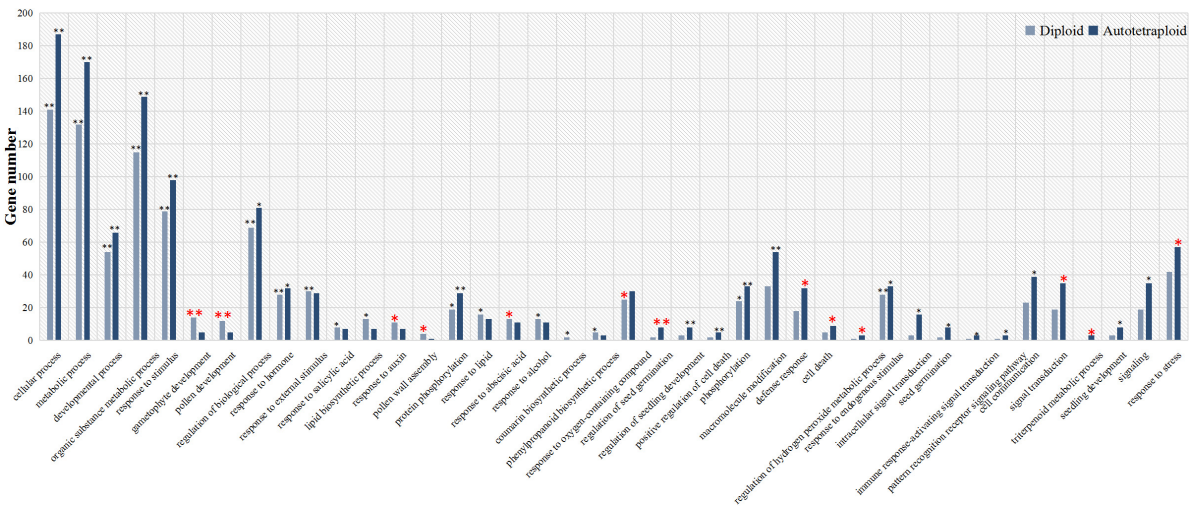

FIGURE 4 | GO functional classification of ZjVND7-targeted genes. The * indicating enriched corrected $p < 0.05$ and ** indicating enriched corrected $p < 0.01$.

were reanalyzed. Among 378 genes differentially expressed under control condition and 473 genes differentially expressed under drought conditions, 62 genes were involved in xylem differentiation, secondary cell wall development, the cell cycle and cell division, and cell death pathways, with expression fold-changes ranging from 1.6 to 6.5. In the xylem differentiation pathway, the genes encoding endoglucanase 8 and endoglucanase 17 were upregulated threefold and twofold in autotetraploids compared with diploids. In the cell cycle and cell division pathways, the gene encoding *S*-adenosylmethionine-dependent methyltransferase was upregulated twofold in the autotetraploids compared with the diploids. Taken together, these results indicated that *ZjVND7*-targeted pathways may differ in response to drought between diploid and autotetraploid sour jujube.

ZjVND7 Directly Controls the Putative Cell Division-Related *ZjSMR1*

To clarify the cause of vessel cell and parenchyma cell proliferation in autotetraploid sour jujube xylem, we investigated

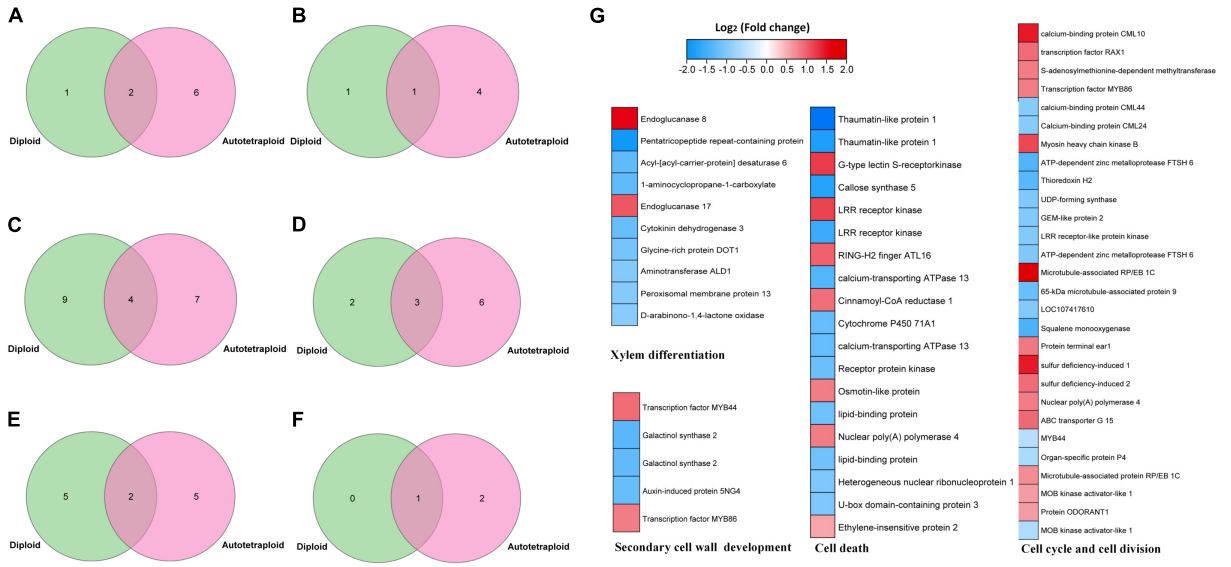

FIGURE 5 | ZjVND7-targeted genes in diploid and autotetraploid sour jujube. **(A–F)** Overlap of diploid and autotetraploid ZjVND7 target genes involved in xylem development **(A)**, secondary wall synthesis **(B)**, ABA signaling **(C)**, cell death **(D)**, cell division **(E)**, and DNA replication **(F)**. **(G)** Differential expression levels of genes involved in putative ZjVND7-targeted pathways in diploids and autotetraploids under control and drought conditions.

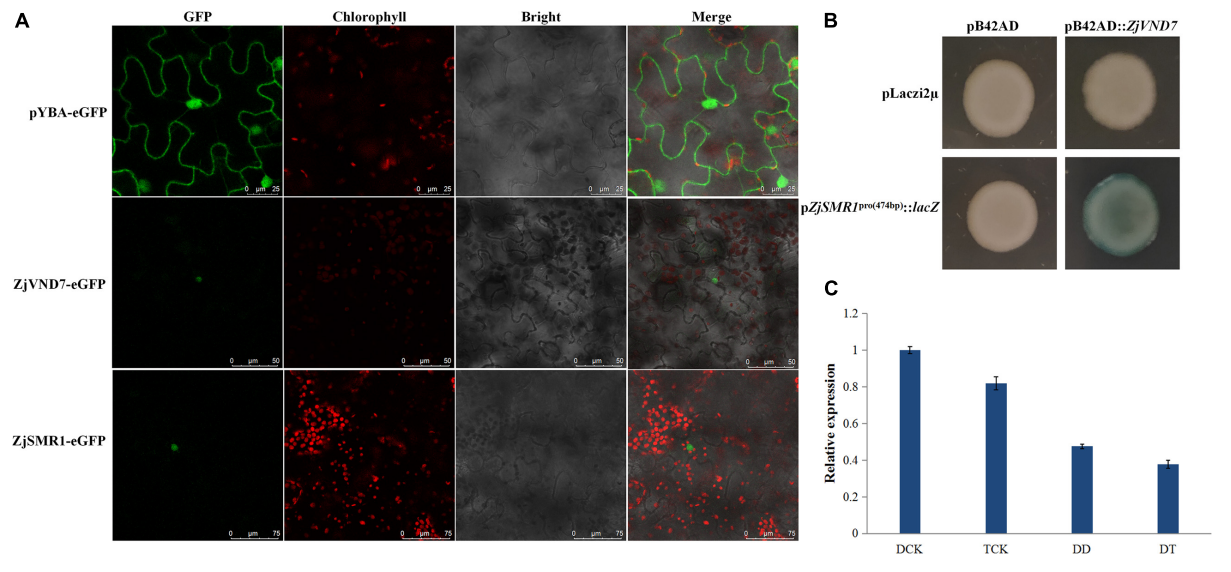

FIGURE 6 | Presumed binding of ZjVND7 to *ZjSMR1* promoter. **(A)** Cellular localization of *ZjSMR1* and *ZjVND7*. **(B)** Yeast one-hybrid validation of the interaction of ZjVND7 and the 474 bp promoter region of *ZjSMR1*. **(C)** Expression level of ZjSMR1 in diploid and autotetraploid plants under drought stress.

whether there were genes that are related to cell division and differentiation and that were also targets of *ZjVND7*. On the basis of the DAP-seq data, *ZjSMR1*, which was annotated to cell division and DNA endoreduplication was recognized as a ZjVND7 downstream target. However, this gene was detected for only one duplication of diploids (with a peak score value of 20, **Supplementary Table 1**) and for two duplications of autotetraploid with signal values of 53 and 63 (**Supplementary Table 2**), respectively. In addition, the cellular localization of *ZjSMR1* and *ZjVND7* was determined. Both *ZjVND7* and *ZjSMR1* were expressed in the nucleus, indicating the possibility of space interaction with *ZjVND7* and *ZjSMR1* in **Figure 6A**. To further verify that ZjVND7 targets *ZjSMR1*, the full-length CDS of *ZjVND7* was fused into a yeast pB42AD vector, and a 474 bp promoter region of *ZjSMR1* was fused into a pLaczi2μ vector to generate a yeast one-hybrid construct. The yeast strains of the three negative controls did not exhibit blue, while the cotransformation of pB42AD:*ZjVND7* and p*ZjSMR1*$^{pro(474\ bp)}$:*lacZ* resulted in a blue color (**Figure 6B**). Moreover, *ZjSMR1* was downregulated under drought stress

in both sour jujube ploidy types, which was consistent with the expression trend of *ZjVND7* (**Figure 6C**). Taken together, these results imply that the ZjVND7 protein can positively target *ZjSMR1*.

Through an analysis of the *cis*-elements in the *ZjSMR1* promoter, the ZjVND7-targeted ACGTG detected in autotetraploids was found to be an ABRE sequence (**Supplementary Figure 4**). Therefore, we hypothesized that the interaction between *ZjSMR1* and *ZjVND7* might occur as a response to ABA. The expression levels of *ZjSMR1* and *ZjVND7* were measured after ABA was sprayed on diploid sour jujube. The results showed that both *ZjSMR1* and *ZjVND7* were responsive to ABA treatment. The expression levels of both *ZjSMR1* and *ZjVND7* decreased significantly at 2 h after treatment and then increased at 12 h after treatment (**Supplementary Figure 5**).

DISCUSSION

Due to frequent modifications to the plant genome after polyploidization, factors affecting polyploid trait variation occur at multiple levels. At the transcriptional or posttranscriptional level, changes in alternative splicing patterns (Zhou et al., 2011), diversification of differentially expressed genes (Wei et al., 2019), and increases in the types and numbers of miRNAs after genome expansion regulate variations in plant adaptability (Liu and Sun, 2017). In addition, an increasing number of studies have confirmed that polyploidization induces changes in epigenetic modifications, including DNA methylation, histone modification, and chromosome remodeling (Ding and Chen, 2018). These epigenetic modifications have been reported in autotetraploid rice (Zhang et al., 2015), switchgrass (Yan et al., 2019), and wheat (Liu et al., 2021). Previous studies have shown that autotetraploid sour jujube at the seedling stage has advantages in terms of phenotype, photosynthesis-related physiology, and adaptability (Li et al., 2019b,c, 2021b). The pathways in response to drought and salt stress in polyploids are more diverse than those in diploids. In the present study, the expression differences of *ZjVND7* between the autotetraploid and diploid plants under drought stress may be the result of responses to alternative splicing, microRNAs, DNA methylation, and histone modifications after polyploidization. Moreover, a gene encoding *S*-adenosylmethionine-dependent methyltransferase expressed in autotetraploid sour jujube suggesting that DNA methylation may occur after polyploidization (**Figure 5**). These results imply that the mutation caused by whole-genome duplication may be an effective way to maintain genome homeostasis and survival.

In the TF regulation network, TFBSs, which are located in the promoter regions of genes, undergo a series of epigenetic regulatory mechanisms, such as nucleosome localization, histone modification, and DNA methylation, that affect the binding of TFs (Bell et al., 2011; Liu et al., 2013; Kribelbauer et al., 2019). Among them, DNA methylation of the CpG-rich promoter prevents TFs from binding to TFBSs (Bird, 2002), which alters plant traits (Gao et al., 2016). O'Malley et al. (2016) also reported that mC-all and mCG-only methylation impacted binding across all TF families. In particular, E2F family member DEL2 preferentially bound to methylated motifs (Harashima et al., 2013). In addition, changes in H3K3, H3K4, H3K9, and H3K27 modifications in polyploids have been shown cause differences in substance accumulation, photosynthetic capacity, and flowering time (Wang et al., 2006; Ni et al., 2009; Zhang et al., 2020). In the present study, the difference of targets after polyploidization could be explained from the standard DAP-seq libraries used in diploid and autotetraploid sour jujube; these libraries include secondary epigenetic modifications such as cytosine methylation, and these secondary epigenetic modifications. Such subtle targeted differences may be closely related to the growth and metabolic characteristics of diploid and autotetraploid sour jujube.

Many studies have shown that *VND7* has various functions and plays a role in the differentiation of a wide range of xylem vessels, including protoxylem, metaxylem, and fibers, in several different tissues (Yamaguchi et al., 2011). Dong et al. (2020) reported that the mutation in a *VND* homolog *NUT1* causes the thickness of the vessel wall in the protoxylem to decrease and that water transport is blocked during flowering. In the autotetraploid sour jujube, ZjVND7 targeted genes encoding endoglucanase were expressed at a greater level than in the diploids, suggesting that the endoglucanase gene in autotetraploids may be regulated by *ZjVND7*, which may further regulate cell growth and vascular differentiation (Tsabary et al., 2003; Shani et al., 2006). This could further play a greater role in autotetraploids in the response to drought stress. Most studies in plant polyploids have concluded that polyploidization is accompanied by an increase in cell volume, albeit not proportionally in all tissues (Katagiri et al., 2016). In this study, the significant increase in the number of vessels in autotetraploids compared with diploids is speculated to be induced by the greater number of parenchyma cells in xylem, suggesting that autotetraploid sour jujube have a strong capacity for transdifferentiation into xylem vessel elements. Moreover, this process may be regulated by *ZjVND7* (Yamaguchi et al., 2010). Therefore, under the condition of water shortage, autotetraploids have lower hydraulic resistance to water transport than diploids do, which may be one of the reasons for the improved drought tolerance of the autotetraploids.

The greater number of xylem vessels and parenchyma cells in autotetraploid sour jujube is further speculated to be related to the target genes associated with cell division. As a supplement to WEE1, inhibitor of premature vascular differentiation, the members of the plant-specific *SMR* gene family play a suppressive role in cell cycle checkpoint activation (Cools et al., 2011). The rapid induction of *Arabidopsis SMR1* has been proven to occur in response to drought stress, and *SMR1* reduces cell division in the roots and leaves and pushes dividing cells toward expansion, which ultimately leads to an effect on root and leaf growth (Dubois et al., 2018). The hairy body was produced by the *SMR1* overexpression line with an increased amount of nuclear DNA, while the huge endoreplication epidermal cells on the abaxial sides of the sepals were lacking in *smr1*/*lgo* mutants. These data confirm that *SMR1* is an important gene that promotes the transformation

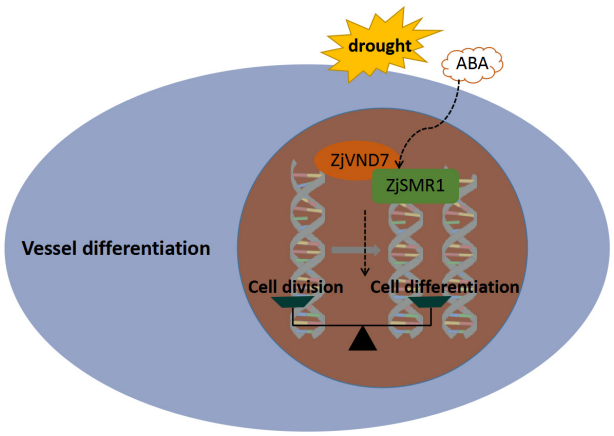

FIGURE 7 | Putative pathway through which ZjVND7 targets *ZjSMR1* in response to drought and ABA.

of cells division into endoreduplication (Roeder et al., 2010). In the present study, the regulation of putative vessel development-related ZjVND7 to *ZjSMR1* may explain the formation of more xylem parenchyma cells in the veins of autotetraploids than in those of diploids, which is a prerequisite for the greater number of vessels in autotetraploid veins. In other words, the role of *ZjVND7* in xylem vessel differentiation may be partially regulated by *ZjSMR1*. Furthermore, the stronger binding signal in autotetraploids may be due to the difference in *SMR1* motif binding between the autotetraploid and diploid plants, or to changes in the spatial structure resulting from the epigenetic modification of the promoter region. In addition, biotic and abiotic stress signals activate the signaling cascades in plants, triggering the production of reactive oxygen species and the accumulation of antimitotic hormones such as ABA and jasmonic acid. These signaling molecules also stimulate cell cycle checkpoints, resulting in impaired cell cycle G1-to-S transition; DNA replication slows down, and/or delays entry into mitosis (Reichheld et al., 2002; Swiatek et al., 2002; Kadota et al., 2005). *SMRs* respond to abiotic stress by prolonging the cell cycle and regulating endoreplication, as has been reported in *Arabidopsis* (Yi et al., 2014), rice (Peres et al., 2007), and maize (Li et al., 2019a). The binding of ZjVND7 to *ZjSMR1* may be one of the reasons for the changes in *ZjSMR1* expression, and cells may regulate the expression of *ZjSMR1* to prolong the cell cycle and regulate endoreplication, thus improving drought tolerance. In addition, we found that *ZjVND7* and *ZjSMR1* were responsive to ABA with the same expression trend, implying a positive regulatory effect (**Supplementary Figure 5**). Moreover, the targeted ABRE sequence detected in autotetraploids indicated that the binding of ZjVND7 and *ZjSMR1* may occur in response to the accumulation of antimitotic ABA and could further promote differences in vessel differentiation between diploid and autotetraploid plants (Ramachandran et al., 2021).

It is very difficult to determine whether just the secondary modifications around TFBS cause differences in gene interactions in polyploid. Recently, the DNA 3D structure or "DNA shape" characterized by the physical characteristics of large or small DNA grooves has been considered to affect TF binding (Slattery et al., 2014). However, whether these characteristics change after polyploidization needs to be further researched. Our results also provide information about many target genes functioning in xylem cell differentiation, including unique sour jujube genes without evident homologous genes in the *Arabidopsis* genome. These genes may not be conserved, and their unique significance in sour jujube needs to be further explored.

CONCLUSION

In present study, a possible functional relationship was proposed (**Figure 7**). ZjVND7 targeting *ZjSMR1* might regulate transdifferentiation from parenchyma cells into vessels in the xylem. This result might support the balancing effect between cell division and cell differentiation of xylem parenchyma, which can promote vessel differentiation by the division and enlargement of the xylem parenchyma. Therefore, more parenchyma cells were formed in autotetraploids than in diploids, and more vessel cells differentiated to mediate water transport. Moreover, ZjVND7 may regulate the expression of *ZjSMR1* to prolong the cell cycle and regulate endoreplication in response to drought stress and ABA, which may be more convincing after whole-genome duplication. However, these results are hypotheses, and the specific regulatory mechanism needs further verification.

DATA AVAILABILITY STATEMENT

The original contributions presented in the study are included in the article/**Supplementary Material**, further inquiries can be directed to the corresponding author/s.

AUTHOR CONTRIBUTIONS

YL conceived and designed the experiments, obtained the funding, and is responsible for this article. ML, LH, CZ, and WY conducted the experiments. ML, XL, and HZ collected and analyzed the data. ML wrote the manuscript. XP and YL provided the valuable suggestions on the manuscript. All authors read and approved the final manuscript.

FUNDING

This research was supported by the National Key Research and Development Program of China (2018YFD1000607) and the Fundamental Research Funds for the Central Universities (No. 2021JD02).

SUPPLEMENTARY MATERIAL

The Supplementary Material for this article can be found online at: https://www.frontiersin.org/articles/10.3389/fpls.2022.829765/full#supplementary-material

REFERENCES

Adams, K. L., and Wendel, J. F. (2005). Polyploidy and genome evolution in plants. *Curr. Opin. Plant Biol.* 8, 135–141. doi: 10.1016/j.pbi.2005.01.001

Allario, T., Brumos, J., Colmenero-Flores, J. M., Iglesias, D. J., Pina, J. A., Navarro, L., et al. (2013). Tetraploid Rangpur lime rootstock increases drought tolerance via enhanced constitutive root abscisic acid production. *Plant Cell Environ.* 36, 856–868. doi: 10.1111/pce.12021

Ashburner, M., Ball, C. A., Blake, J. A., Botstein, D., Butler, H., Cherry, J. M., et al. (2000). Gene ontology: tool for the unification of biology. the gene ontology consortium. *Nat. Genet.* 25, 25–29. doi: 10.1038/75556

Bartlett, A., O'Malley, R. C., Huang, S. C., Galli, M., Nery, J. R., Gallavotti, A., et al. (2017). Mapping genome-wide transcription-factor binding sites using DAP-seq. *Nat. Protoc.* 12, 1659–1672. doi: 10.1038/nprot.2017.055

Bell, O., Tiwari, V. K., Thoma, N. H., and Schubeler, D. (2011). Determinants and dynamics of genome accessibility. *Nat. Rev. Genet.* 12, 554–564. doi: 10.1038/nrg3017

Bird, A. (2002). DNA methylation patterns and epigenetic memory. *Genes Dev.* 16, 6–21. doi: 10.1101/gad.947102

Bu, J., Zhao, J., and Liu, M. (2016). Expression stabilities of candidate reference genes for RT-qPCR in Chinese Jujube (*Ziziphus jujuba* Mill.) under a variety of conditions. *PLoS One* 11:e0154212. doi: 10.1371/journal.pone.0154212

Chen, C., Chen, H., Zhang, Y., Thomas, H. R., Frank, M. H., He, Y., et al. (2020). TBtools: an integrative toolkit developed for interactive analyses of big biological data. *Mol. Plant* 13, 1194–1202. doi: 10.1016/j.molp.2020.06.009

Chen, X., Chen, R., Wang, Y., Wu, C., and Huang, J. (2019). Genome-Wide identification of WRKY transcription factors in Chinese jujube (*Ziziphus jujuba* Mill.) and their involvement in fruit developing, ripening, and abiotic stress. *Genes (Basel)* 10:360. doi: 10.3390/genes10050360

Cools, T., Iantcheva, A., Weimer, A. K., Boens, S., Takahashi, N., Maes, S., et al. (2011). The Arabidopsis thaliana checkpoint kinase WEE1 protects against premature vascular differentiation during replication stress. *Plant Cell* 23, 1435–1448. doi: 10.1105/tpc.110.082768

De Smet, R., and Van de Peer, Y. (2012). Redundancy and rewiring of genetic networks following genome-wide duplication events. *Curr. Opin. Plant Biol.* 15, 168–176. doi: 10.1016/j.pbi.2012.01.003

Ding, M., and Chen, Z. J. (2018). Epigenetic perspectives on the evolution and domestication of polyploid plant and crops. *Curr. Opin. Plant Biol.* 42, 37–48. doi: 10.1016/j.pbi.2018.02.003

Dong, Z., Xu, Z., Xu, L., Galli, M., Gallavotti, A., Dooner, H. K., et al. (2020). Necrotic upper tips1 mimics heat and drought stress and encodes a protoxylem-specific transcription factor in maize. *Proc. Natl. Acad. Sci. U S A.* 117, 20908–20919. doi: 10.1073/pnas.2005014117

Dubois, M., Selden, K., Bediee, A., Rolland, G., Baumberger, N., Noir, S., et al. (2018). SIAMESE-RELATED1 is regulated posttranslationally and participates in repression of leaf growth under moderate drought. *Plant Physiol.* 176, 2834–2850. doi: 10.1104/pp.17.01712

Endo, H., Yamaguchi, M., Tamura, T., Nakano, Y., Nishikubo, N., Yoneda, A., et al. (2015). Multiple classes of transcription factors regulate the expression of VASCULAR-RELATED NAC-DOMAIN7, a master switch of xylem vessel differentiation. *Plant Cell Physiol.* 56, 242–254. doi: 10.1093/pcp/pcu134

Gao, C., Zhou, G., Ma, C., Zhai, W., Zhang, T., Liu, Z., et al. (2016). Helitron-like transposons contributed to the mating system transition from out-crossing to self-fertilizing in polyploid *Brassica napus* L. *Sci. Rep.* 6:33785. doi: 10.1038/srep33785

Guo, Y., and Shan, G. (2010). *The Chinese Jujube*. Shanghai: Shanghai Scientific and Technical Publishers.

Han, T., Yan, J. W., Xiang, Y., and Zhang, A. Y. (2021). Phosphorylation of ZmNAC84 at Ser-113 enhances the drought tolerance by directly modulating ZmSOD2 expression in maize. *Biochem. Biophys. Res. Commun.* 567, 86–91. doi: 10.1016/j.bbrc.2021.06.026

Harashima, H., Dissmeyer, N., and Schnittger, A. (2013). Cell cycle control across the eukaryotic kingdom. *Trends Cell Biol.* 23, 345–356. doi: 10.1016/j.tcb.2013.03.002

Heinz, S., Benner, C., Spann, N., Bertolino, E., Lin, Y. C., Laslo, P., et al. (2010). Simple combinations of lineage-determining transcription factors prime cis-regulatory elements required for macrophage and B cell identities. *Mol. Cell.* 38, 576–589. doi: 10.1016/j.molcel.2010.05.004

Jackson, S., and Chen, Z. J. (2010). Genomic and expression plasticity of polyploidy. *Curr. Opin. Plant Biol.* 13, 153–159. doi: 10.1016/j.pbi.2009.11.004

Kadota, Y., Watanabe, T., Fujii, S., Maeda, Y., Ohno, R., Higashi, K., et al. (2005). Cell cycle dependence of elicitor-induced signal transduction in tobacco BY-2 cells. *Plant Cell Physiol.* 46, 156–165. doi: 10.1093/pcp/pci008

Katagiri, Y., Hasegawa, J., Fujikura, U., Hoshino, R., Matsunaga, S., and Tsukaya, H. (2016). The coordination of ploidy and cell size differs between cell layers in leaves. *Development* 143, 1120–1125. doi: 10.1242/dev.130021

Keles, H. (2020). Changes of some horticultural characteristics in jujube (Ziziphusjujube Mill.) fruit at different ripening stages. *Turkish J. Agriculture Forestry* 44, 391–398. doi: 10.3906/tar-1912-31

Kribelbauer, J. F., Lu, X. J., Rohs, R., Mann, R. S., and Bussemaker, H. J. (2019). Toward a mechanistic understanding of DNA methylation readout by transcription factors. *J. Mol. Biol.* Online ahead of print. doi: 10.1016/j.jmb.2019.10.021

Kubo, M., Udagawa, M., Nishikubo, N., Horiguchi, G., Yamaguchi, M., Ito, J., et al. (2005). Transcription switches for protoxylem and metaxylem vessel formation. *Genes Dev.* 19, 1855–1860. doi: 10.1101/gad.1331305

Kumar, S., Stecher, G., Li, M., Knyaz, C., and Tamura, K. (2018). MEGA X: molecular evolutionary genetics analysis across computing platforms. *Mol. Biol. Evol.* 35, 1547–1549. doi: 10.1093/molbev/msy096

Langmead, B., and Salzberg, S. L. (2012). Fast gapped-read alignment with Bowtie 2. *Nat. Methods* 9, 357–359. doi: 10.1038/nmeth.1923

Li, M., Guo, Y., Liu, S., Zhao, Y., Pang, X., and Li, Y. (2019c). Autotetraploidization in *Ziziphus jujuba* Mill. var. spinosa enhances salt tolerance conferred by active, diverse stress responses. *Environ. Exp. Botany* 165, 92–107. doi: 10.1016/j.envexpbot.2019.05.016

Li, M., Guo, Y., Liu, S., Pang, X., and Li, Y. (2019b). Physiological characteristics and transcriptomics analysis in diploid *Ziziphus jujuba* Mill. var. spinosa and its autotetraploid. *J. Beijing Forestry University* 41:11.

Li, F. F., Wang, L. C., Zhang, Z. Q., Li, T., Feng, J. J., Xu, S. T., et al. (2019a). ZmSMR4, a novel cyclin-dependent kinase inhibitor (CKI) gene in maize (*Zea mays* L.), functions as a key player in plant growth, development and tolerance to abiotic stress. *Plant Sci.* 280, 120–131. doi: 10.1016/j.plantsci.2018.03.007

Li, N., Song, Y., Li, J., Hao, R., Feng, X., and Li, L. (2021c). Transcriptome and genome re-sequencing analysis reveals differential expression patterns and sequence variation in pericarp wax metabolism-related genes in *Ziziphus jujuba* (Chinese jujube). *Sci. Horticulturae* 288:110415. doi: 10.1016/j.scienta.2021.110415

Li, M., Hou, L., Liu, S., Zhang, C., Yang, W., Pang, X., et al. (2021a). Genome-wide identification and expression analysis of NAC transcription factors in *Ziziphus jujuba* Mill. reveal their putative regulatory effects on tissue senescence and abiotic stress responses. *Industrial Crops Products* 173:114093. doi: 10.1016/j.indcrop.2021.114093

Li, M., Zhang, C., Hou, L., Yang, W., Liu, S., Pang, X., et al. (2021b). Multiple responses contribute to the enhanced drought tolerance of the autotetraploid *Ziziphus jujuba* Mill. var. spinosa. *Cell Biosci.* 11:119. doi: 10.1186/s13578-021-00633-1

Liu, B., and Sun, G. (2017). microRNAs contribute to enhanced salt adaptation of the autopolyploid *Hordeum bulbosum* compared with its diploid ancestor. *Plant J.* 91, 57–69. doi: 10.1111/tpj.13546

Liu, H., Luo, K., Wen, H., Ma, X., Xie, J., and Sun, X. (2013). Quantitative analysis reveals increased histone modifications and a broad nucleosome-free region bound by histone acetylases in highly expressed genes in human CD4+ T cells. *Genomics* 101, 113–119. doi: 10.1016/j.ygeno.2012.11.007

Liu, M. (2010). Chinese jujube: botany and horticulture. *Horticultural Rev.* 32, 229–298. doi: 10.1002/9780470767986.ch5

Liu, Y., Yuan, J., Jia, G., Ye, W., Jeffrey Chen, Z., and Song, Q. (2021). Histone H3K27 dimethylation landscapes contribute to genome stability and genetic recombination during wheat polyploidization. *Plant J.* 105, 678–690. doi: 10.1111/tpj.15063

Livak, K. J., and Schmittgen, T. D. (2001). Analysis of relative gene expression data using real-time quantitative PCR and the 2(-Delta Delta C(T)) method. *Methods* 25, 402–408. doi: 10.1006/meth.2001.1262

Machanick, P., and Bailey, T. L. (2011). MEME-ChIP: motif analysis of large DNA datasets. *Bioinformatics* 27, 1696–1697. doi: 10.1093/bioinformatics/btr189

Ni, Z., Kim, E. D., Ha, M., Lackey, E., Liu, J., Zhang, Y., et al. (2009). Altered circadian rhythms regulate growth vigour in hybrids and allopolyploids. *Nature* 457, 327–331. doi: 10.1038/nature07523

Ohtani, M., Nishikubo, N., Xu, B., Yamaguchi, M., Mitsuda, N., Goue, N., et al. (2011). A NAC domain protein family contributing to the regulation of wood formation in poplar. *Plant J.* 67, 499–512. doi: 10.1111/j.1365-313X.2011.04614.x

Olins, J. R., Lin, L., Lee, S. J., Trabucco, G. M., MacKinnon, K. J., and Hazen, S. P. (2018). Secondary wall regulating NACs differentially bind at the promoter at a CELLULOSE SYNTHASE A4 Cis-eQTL. *Front. Plant Sci.* 9:1895. doi: 10.3389/fpls.2018.01895

Olsen, A. N., Ernst, H. A., Leggio, L. L., and Skriver, K. (2005). NAC transcription factors: structurally distinct, functionally diverse. *Trends Plant Sci.* 10, 79–87. doi: 10.1016/j.tplants.2004.12.010

O'Malley, R. C., Huang, S. C., Song, L., Lewsey, M. G., Bartlett, A., Nery, J. R., et al. (2016). Cistrome and epicistrome features shape the regulatory DNA landscape. *Cell* 166:1598. doi: 10.1016/j.cell.2016.08.063

Osborn, T. C., Chris Pires, J., Birchler, J. A., Auger, D. L., Jeffery Chen, Z., Lee, H.-S., et al. (2003). Understanding mechanisms of novel gene expression in polyploids. *Trends Genet.* 19, 141–147. doi: 10.1016/s0168-9525(03)00015-5

Peres, A., Churchman, M. L., Hariharan, S., Himanen, K., Verkest, A., Vandepoele, K., et al. (2007). Novel plant-specific cyclin-dependent kinase inhibitors induced by biotic and abiotic stresses. *J. Biol. Chem.* 282, 25588–25596. doi: 10.1074/jbc.M703326200

Puranik, S., Sahu, P. P., Srivastava, P. S., and Prasad, M. (2012). NAC proteins: regulation and role in stress tolerance. *Trends Plant Sci.* 17, 369–381. doi: 10.1016/j.tplants.2012.02.004

Ramachandran, P., Augstein, F., Mazumdar, S., Nguyen, T. V., Minina, E. A., Melnyk, C. W., et al. (2021). Abscisic acid signaling activates distinct VND transcription factors to promote xylem differentiation in *Arabidopsis*. *Curr. Biol.* 31, 3153–3161.e5. doi: 10.1016/j.cub.2021.04.057

Reichheld, J. P., Vernoux, T., Lardon, F., Van Montagu, M., and Inzé, D. (2002). Specific checkpoints regulate plant cell cycle progression in response to oxidative stress. *Plant J.* 17, 647–656. doi: 10.1046/j.1365-313X.1999.00413.x

Roeder, A. H., Chickarmane, V., Cunha, A., Obara, B., Manjunath, B. S., and Meyerowitz, E. M. (2010). Variability in the control of cell division underlies sepal epidermal patterning in *Arabidopsis thaliana*. *PLoS Biol.* 8:e1000367. doi: 10.1371/journal.pbio.1000367

Shang, X., Yu, Y., Zhu, L., Liu, H., Chai, Q., and Guo, W. (2020). A cotton NAC transcription factor GhirNAC2 plays positive roles in drought tolerance via regulating ABA biosynthesis. *Plant Sci.* 296:110498. doi: 10.1016/j.plantsci.2020.110498

Shani, Z., Dekel, M., Roiz, L., Horowitz, M., Kolosovski, N., Lapidot, S., et al. (2006). Expression of endo-1,4-beta-glucanase (cel1) in Arabidopsis thaliana is associated with plant growth, xylem development and cell wall thickening. *Plant Cell Rep.* 25, 1067–1074. doi: 10.1007/s00299-006-0167-9

Slattery, M., Zhou, T., Yang, L., Dantas Machado, A. C., Gordan, R., and Rohs, R. (2014). Absence of a simple code: how transcription factors read the genome. *Trends Biochem. Sci.* 39, 381–399. doi: 10.1016/j.tibs.2014.07.002

Sri, T., Gupta, B., Tyagi, S., and Singh, A. (2020). Homeologs of *Brassica* SOC1, a central regulator of flowering time, are differentially regulated due to partitioning of evolutionarily conserved transcription factor binding sites in promoters. *Mol. Phylogenet. Evol.* 147:106777. doi: 10.1016/j.ympev.2020.106777

Swiatek, A., Lenjou, M., Van Bockstaele, D., Inze, D., and Van Onckelen, H. (2002). Differential effect of jasmonic acid and abscisic acid on cell cycle progression in tobacco BY-2 cells. *Plant Physiol.* 128, 201–211. doi: 10.1104/pp.128.1.201

Tamura, T., Endo, H., Suzuki, A., Sato, Y., Kato, K., Ohtani, M., et al. (2019). Affinity-based high-resolution analysis of DNA binding by VASCULAR-RELATED NAC-DOMAIN7 via fluorescence correlation spectroscopy. *Plant J.* 100, 298–313. doi: 10.1111/tpj.14443

Tsabary, G., Shani, Z., Roiz, L., Levy, I., Riov, J., and Shoseyov, O. (2003). Abnormal 'wrinkled' cell walls and retarded development of transgenic Arabidopsis thaliana plants expressing endo-1,4-beta-glucanase (cell) antisense. *Plant Mol. Biol.* 51, 213–224. doi: 10.1023/a:1021162321527

Wang, J., Tian, L., Lee, H. S., Wei, N. E., Jiang, H., Watson, B., et al. (2006). Genomewide nonadditive gene regulation in *Arabidopsis* allotetraploids. *Genetics* 172, 507–517. doi: 10.1534/genetics.105.047894

Wang, M., and Sun, Y. (1986). Fruit trees and vegetables for arid and semi-arid areas in north-west China. *J. Arid Environ.* 11, 3–16. doi: 10.1016/s0140-1963(18)31305-3

Wei, T., Wang, Y., Xie, Z., Guo, D., Chen, C., Fan, Q., et al. (2019). Enhanced ROS scavenging and sugar accumulation contribute to drought tolerance of naturally occurring autotetraploids in *Poncirus trifoliata*. *Plant Biotechnol. J.* 17, 1394–1407. doi: 10.1111/pbi.13064

Xie, C., Mao, X., Huang, J., Ding, Y., Wu, J., Dong, S., et al. (2011). KOBAS 2.0: a web server for annotation and identification of enriched pathways and diseases. *Nucleic Acids Res.* 39, W316–W322. doi: 10.1093/nar/gkr483

Xu, Z. Y., Kim, S. Y., Hyeon, do, Y., Kim, D. H., Dong, T., et al. (2013). The Arabidopsis NAC transcription factor ANAC096 cooperates with bZIP-type transcription factors in dehydration and osmotic stress responses. *Plant Cell* 25, 4708–4724. doi: 10.1105/tpc.113.119099

Yamaguchi, M., Goue, N., Igarashi, H., Ohtani, M., Nakano, Y., Mortimer, J. C., et al. (2010). VASCULAR-RELATED NAC-DOMAIN6 and VASCULAR-RELATED NAC-DOMAIN7 effectively induce transdifferentiation into xylem vessel elements under control of an induction system. *Plant Physiol.* 153, 906–914. doi: 10.1104/pp.110.154013

Yamaguchi, M., Kubo, M., Fukuda, H., and Demura, T. (2008). Vascular-related NAC-DOMAIN7 is involved in the differentiation of all types of xylem vessels in Arabidopsis roots and shoots. *Plant J.* 55, 652–664. doi: 10.1111/j.1365-313X.2008.03533.x

Yamaguchi, M., Mitsuda, N., Ohtani, M., Ohme-Takagi, M., Kato, K., and Demura, T. (2011). VASCULAR-RELATED NAC-DOMAIN7 directly regulates the expression of a broad range of genes for xylem vessel formation. *Plant J.* 66, 579–590. doi: 10.1111/j.1365-313X.2011.04514.x

Yan, H., Bombarely, A., Xu, B., Wu, B., Frazier, T. P., Zhang, X., et al. (2019). Autopolyploidization in switchgrass alters phenotype and flowering time via epigenetic and transcription regulation. *J. Exp. Bot.* 70, 5673–5686. doi: 10.1093/jxb/erz325

Ye, L., Wang, B., Zhang, W., Shan, H., and Kong, H. (2016). Gains and losses of cis-regulatory elements led to divergence of the *Arabidopsis* APETALA1 and CAULIFLOWER duplicate genes in the time, space, and level of expression and regulation of one paralog by the other. *Plant Physiol.* 171, 1055–1069. doi: 10.1104/pp.16.00320

Yi, D., Alvim Kamei, C. L., Cools, T., Vanderauwera, S., Takahashi, N., Okushima, Y., et al. (2014). The Arabidopsis SIAMESE-RELATED cyclin-dependent kinase inhibitors SMR5 and SMR7 regulate the DNA damage checkpoint in response to reactive oxygen species. *Plant Cell* 26, 296–309. doi: 10.1105/tpc.113.118943

Yuan, X., Wang, H., Cai, J. T., Bi, Y., Li, D. Y., and Song, F. M. (2019). Rice NAC transcription factor ONAC066 functions as a positive regulator of drought and oxidative stress response. *BMC Plant Biol.* 19:278. doi: 10.1186/s12870-019-1883-y

Zhang, C., Wang, H., Xu, Y., Zhang, S., Wang, J., Hu, B., et al. (2020). Enhanced relative electron transport rate contributes to increased photosynthetic capacity in autotetraploid pak choi. *Plant Cell Physiol.* 61, 761–774. doi: 10.1093/pcp/pcz238

Zhang, J., Liu, Y., Xia, E. H., Yao, Q. Y., Liu, X. D., and Gao, L. Z. (2015). Autotetraploid rice methylome analysis reveals methylation variation of transposable elements and their effects on gene expression. *Proc. Natl. Acad. Sci U S A.* 112, E7022–E7029. doi: 10.1073/pnas.1515170112

Zhang, Y., Liu, T., Meyer, C. A., Eeckhoute, J., Johnson, D. S., Bernstein, B. E., et al. (2008). Model-based analysis of ChIP-Seq (MACS). *Genome Biol.* 9:R137. doi: 10.1186/gb-2008-9-9-r137

Zhong, R., Lee, C., and Ye, Z. H. (2010). Global analysis of direct targets of secondary wall NAC master switches in *Arabidopsis*. *Mol. Plant* 3, 1087–1103. doi: 10.1093/mp/ssq062

Zhou, H. Y., Jia, J. P., Kong, D. C., Zhang, Z. D., Song, S., Li, Y. Y., et al. (2019). Genome-wide identification and analysis of the DREB genes and their expression profiles under abiotic stresses in Chinese jujube (*Ziziphus jujuba* Mill.). *J. Forestry Res.* 30, 1277–1287. doi: 10.1007/s11676-018-0718-2

Zhou, R., Moshgabadi, N., and Adams, K. L. (2011). Extensive changes to alternative splicing patterns following allopolyploidy in natural and resynthesized polyploids. *Proc. Natl. Acad. Sci. U S A.* 108, 16122–16127. doi: 10.1073/pnas.1109551108

Conflict of Interest: The authors declare that the research was conducted in the absence of any commercial or financial relationships that could be construed as a potential conflict of interest.

Publisher's Note: All claims expressed in this article are solely those of the authors and do not necessarily represent those of their affiliated organizations, or those of the publisher, the editors and the reviewers. Any product that may be evaluated in this article, or claim that may be made by its manufacturer, is not guaranteed or endorsed by the publisher.

frontiers | Frontiers in Plant Science

ORIGINAL RESEARCH
published: 01 April 2022
doi: 10.3389/fpls.2022.866296

Disaggregation of Ploidy, Gender, and Genotype Effects on Wood and Fiber Traits in a Diploid and Triploid Hybrid Poplar Family

Xu-Yan Huang[1,2,3,4†], Jing Shang[1,2,3,4†], Yu-Hang Zhong[1,2,3,4], Dai-Li Li[5], Lian-Jun Song[6] and Jun Wang[1,2,3,4]*

[1] National Engineering Research Center of Tree Breeding and Ecological Restoration, Beijing Forestry University, Beijing, China, [2] Key Laboratory of Genetics and Breeding in Forest Trees and Ornamental Plants, Ministry of Education, Beijing Forestry University, Beijing, China, [3] The Tree and Ornamental Plant Breeding and Biotechnology Laboratory of National Forestry and Grassland Administration, Beijing Forestry University, Beijing, China, [4] College of Biological Sciences and Technology, Beijing Forestry University, Beijing, China, [5] Beijing Institute of Landscape Architecture, Beijing, China, [6] Breeding and Propagation Base for Tree Varieties in Weixian County, Xingtai, China

Triploid breeding based on unilateral sexual polyploidization is an effective approach for genetic improvement of *Populus*, which can integrate heterosis and ploidy vigor in an elite variety. However, the phenotypic divergence of unselected allotriploids with the same cross-combination remains poorly understood, and the contributions of ploidy, gender, and genotype effects on phenotypic variation are still unclear. In this study, wood and fiber traits, including basic density (BD), lignin content (LC), fiber length (FL), fiber width (FW), and fiber length/width (FL/W), were measured based on a 10-year-old clonal trial, including full-sib diploid and triploid hybrids of (*Populus pseudo-simonii* × *P. nigra* 'Zheyin3#') × *P.* × *beijingensis*, and contributions of ploidy, gender, and genotype effects on the variation of these traits, were disaggregated to enhance our understanding of triploid breeding. We found a significant phenotypic variation for all measured traits among genotypes. All the wood and fiber traits studied here underwent strong clonal responses with high repeatabilities (0.55–0.76). The Pearson's correlation analyses based on the best linear unbiased predictors (BLUPs) revealed that BD was significantly positively correlated with FL (r = 0.65, p = 0.030), suggesting that BD could be improved together with FL during triploid breeding. The FL of the triploids was significantly larger than that of the diploids ($p < 0.001$), suggesting that ploidy strongly affected the variation of FL traits. The difference between females and males was not significant for any measured trait, implying that gender might not be a major factor for variation in these traits. Further analyses of variance components showed that genotype dominantly contributed to the variation of BD, LC, and FW traits (with 54, 62, and 53% contributions, respectively) and ploidy contributed strongly to variation in FL and FL/W (77 and 50%, respectively). The genetic coefficient of variation (CV_G) of triploids for each trait was low, suggesting that it is necessary to produce many triploids for selection or to use different *Populus* species as parents. Our findings provide new insights into the genetic effects of ploidy, gender, and genotype on wood and fiber traits within a full-sib poplar family, enhancing the understanding of the triploid breeding program of *Populus*.

Keywords: *Populus*, allotriploid, gender, genotype, wood property, fiber traits, triploid breeding

OPEN ACCESS

Edited by:
Jeremy Coate,
Reed College, United States

Reviewed by:
Xiyang Zhao,
Jilin Agricultural University, China
Jean Brouard,
Isabella Point Forestry Ltd., Canada

***Correspondence:**
Jun Wang
wangjun@bjfu.edu.cn

† These authors have contributed equally to this work

Specialty section:
This article was submitted to Plant Breeding, a section of the journal Frontiers in Plant Science

Received: *31 January 2022*
Accepted: *01 March 2022*
Published: *01 April 2022*

Citation:
Huang XY, Shang J, Zhong YH, Li DL, Song LJ and Wang J (2022) Disaggregation of Ploidy, Gender, and Genotype Effects on Wood and Fiber Traits in a Diploid and Triploid Hybrid Poplar Family. Front. Plant Sci. 13:866296. doi: 10.3389/fpls.2022.866296

INTRODUCTION

The species in the genus *Populus*, characterized by fast growth, good wood properties, strong resistance, and wide adaptability, are widely distributed over the northern hemisphere (Porth and El-Kassaby, 2015; Georgii et al., 2019). They are used not only in urban landscaping, ecological remediation, and rehabilitation of degraded lands, but also for wood and fiber production (Bannoud and Bellini, 2021). As an important source of industrial raw timber, an improvement on wood properties of *Populus* is a major focus of breeders. Wood and fiber properties, such as basic density (BD), lignin content (LC), and fiber length (FL), directly affect pulp value and paper quality.

Triploid breeding is an effective approach for the genetic improvement of tree species, which can achieve multitarget trait improvement on growth, wood properties, and stress resistance (Kang, 2020). In *Acacia*, allotriploid clones derived from crossing tetraploid *Acacia mangium* with diploid *A. auriculiformis* possessed a higher heartwood proportion and bark thickness than commercial diploid clones (Bon et al., 2020). Serapiglia et al. (2014, 2015) found that triploid genotypes of shrub willow could produce more biomass and possess lower LC than diploid genotypes. In *Populus*, some triploid varieties have been widely used for plantations, all of which exhibited favorable growth and pulpwood characteristics (van Buijtenen et al., 1958; Weisgerber et al., 1980; Zhu et al., 1995; Kang, 2016).

Unilateral sexual polyploidization based on the hybridization of uniparental 2n gametes is the main way for triploid breeding of *Populus* (Kang, 2016). Sexual polyploidization, integrating the contributions of hybridity and genome dosage, can cause extensive phenotypic variation (Fort et al., 2016). In *Populus*, therefore, understanding trait variation associated with triploidy is of considerable interest to breeders. Zhu (2006) indicated that not all triploid individuals of *Populus* are elite, so triploid breeding should follow the strategy of strong selection in a large candidate population. In hybrids of (*P. alba* × *P. glandulosa*) × *P. tomentosa*, although the 2-year seedling height and ground diameter of 12 triploids were 33 and 38% larger than those of the diploids on average, respectively, several triploid genotypes exhibited lower growth performance than the diploids (Li and Kang, 2007). Wu et al. (2013) found that the elite triploid genotypes of *P. tomentosa* hybrids had favorable wood density and fiber traits. However, the variation in wood and fiber traits of unselected allotriploids within the same cross-combination was considerable, and the contributions of ploidy and genotype on the variation of wood properties were not clarified.

As dioecious trees, members of the genus *Populus* provide opportunities to study the relationship between trait variation and sexual dimorphism in perennial woody plants. In a recent review, Melnikova et al. (2017) reviewed the sex-specific response to the stress of *Populus*, which demonstrated that the males of the *Populus* species were better adapted to the stress conditions and showed less damage, better growth, and higher photosynthetic capacity and antioxidant activity than that of the females. In *P. purdomii*, it was found that the males had a quicker energy-return strategy in high-altitude areas (Lei et al., 2016). For wood properties, in a collected natural diploid population of *P. tomentosa*, the females had a significantly larger FL and fiber width (FW) than the males on average (Du et al., 2014). However, in allotriploids, the effect of gender on wood and fiber traits remains poorly understood.

In our previous work, a full-sib family including triploid hybrids derived from crossing between induced 2n eggs of *Populus pseudo-simonii* × *P. nigra* 'Zheyin3#' and normal pollen of *P.* × *beijingensis* and diploid hybrids of the two parents were obtained (Wang et al., 2010). After cutting propagation, the diploid and triploid hybrids were planted in the trial field of Weixian County, Hebei Province, China, in 2010. In this study, the wood and fiber traits, including BD, LC, FL, FW, and fiber length/width (FL/W), were measured in the diploid and triploid hybrids, and contributions of ploidy, gender, and genotype effects on the variation of the wood and fiber traits were disaggregated. This enhanced our understanding of trait variation resulting from sexual polyploidization and provided additional data for the selection of elite genotypes.

MATERIALS AND METHODS

Plant Material

Nine diploid hybrids and 11 triploid hybrids between female parent *Populus pseudo-simonii* × *P. nigra* 'Zheyin3#' (2n = 2x = 38) and male parent *P.* × *beijingensis* (2n = 2x = 38, abbreviated as BJY) were analyzed in this study. The triploid hybrids were derived from crossing induced 2n eggs through colchicine-induced embryo sac chromosome doubling of 'Zheyin3#' with the BJY (Wang et al., 2010). All the 2n eggs were determined as post-meiotic restitution (PMR) type 2n gametes by simple sequence repeat (SSR) analysis (Dong et al., 2015). After cutting propagation, a clonal trial was established in 2010 at the Weixian County, Hebei Province, China, based on a randomized complete block design with three blocks and four ramets per plot with 3 m × 4 m tree spacing. The trial was irrigated for six times in total, in March, May, and August of the first 2 years, with no subsequent irrigation. Weed control was carried out in the first 3 years. No fertilizer was used in the field. No thinning was applied during the trial period until the time of sampling. Gender identification was carried out after flowering. In the 20 genotypes, there were 4 female diploid genotypes, 5 male diploid genotypes, 5 female triploid genotypes, and 6 male triploid genotypes. In 2019, wood samples were collected from the clonal trial. A number of three ramets (one per plot) were randomly selected from each clone for sampling. A 10-cm-thick wood disk at breast height (1.3 m) was taken from each sample tree. In total, 60 disks were harvested for laboratory measurement.

Measurement of Wood and Fiber Traits

For BD analysis, four small rectangular pith-to-bark direction wood specimens with dimensions of 40 mm radially × 20 mm tangentially × 20 mm longitudinally were cut from each disk at four directions. The seventh annual ring was located at the middle of each specimen in the radial direction. The BD was

analyzed based on the maximum moisture content method described by Smith (1954).

For intra-ring analysis of fiber properties, four matchstick-sized wood specimens were excised from the above rectangular wood specimens at the seventh and eighth rings and then macerated in a 1:1 (*v*/*v*) mixture of acetic acid and hydrogen peroxide at 60°C for 24 h. After rinsing three times with distilled water, the specimens were vibrated to scatter fibers in test tubes. Then, the fibers were stained with safranin solution and observed under an Olympus BX51 microscope. The FL and FW were measured using an ocular micrometer. More than 200 fibers were measured for each specimen. FL/W was calculated based on the FL and FW values.

The LC was measured following the standard procedure for biomass analysis developed by the National Renewable Energy Laboratory (NREL) of the United States (Sluiter et al., 2008). The LC was equal to the sum of acid-soluble LC and acid-insoluble LC. Each sample was analyzed in triplicate.

Data Statistical Analysis

Statistical analyses were performed in the R statistical environment (R Development Core Team, 2007). The results are presented in this study as mean ± SE. One-way analysis of variance (ANOVA) was performed on each trait, and the means were compared using a protected least significant difference (LSD, $p < 0.05$) to reveal the difference among genotypes. The repeatability (R^2) of each measured trait was estimated using the repeatability function in the heritability R package (version 1.3) developed by Kruijer et al. (2015). Best linear unbiased predictors (BLUPs) of each genotype, genetic coefficient of variation (CV_G), and variance components of ploidy, gender, and genotype effects were estimated by the AFEchidna R package (version 1.54) developed by Zhang et al. (2021) with model: trait ∼ 1 + ploidy + ploidy:gender + ploidy:gender: genotype. Variance contributions were calculated based on the variance components of ploidy, gender, and genotype effects, and residuals were considered as the results of environmental effects. Pearson's correlation tests were run to analyze the relationship between all trait combinations using the phenotypic data and BLUPs, respectively. Student's *t*-test were used to identify the statistical differences between diploid and triploid groups and between female and male groups nested in the two ploidy levels for all traits.

RESULTS

Basic Statistics and Variation Among Genotypes

For the full-sib diploid and triploid hybrid poplar family, the BD ranged from 320.21 to 410.35 kg m^{-3}, with an average of 355.90 ± 5.57 kg m^{-3}. The LC ranged between 25.68 and 30.33% with an average of 27.62 ± 0.24%. The FL ranged from 0.890 to 1.293 mm, with an average of 1.115 ± 0.029 mm. The FW ranged from 19.05 to 26.30 μm with an average of 22.97 ± 0.40 μm. The FL/W ranged from 41.55 to 61.53 with an average of 50.05 ± 1.29. The CV_G of the traits in this family was 7, 4, 44, 7, and 10% for BD, LC, FL, FW, and FL/W, respectively. The CV_G of BD, LC, FL, FW, and FL/W in the diploids was 7, 4, 6, 8, and 6%, respectively. The CV_G of these traits in the triploids was 5, 3, 3, 6, and 6%, respectively.

One-way ANOVA tests revealed significant differences among the genotypes in all measured traits (**Figure 1**), suggesting that genotypes affected the phenotypes of wood and fiber traits. For BD, the diploid genotypes D6 and D8 and triploid genotype T4 were significantly larger than the other genotypes. The diploid genotype D1 had the highest LC. Eight triploid genotypes, including T7, T4, T2, T6, T10, T3, T8, and T5, had longer FL, which suggests that the increased ploidy level contributed to the FL trait significantly. Three diploid genotypes (D5, D1, and D2) and four triploid genotypes (T11, T7, T1, and T6) had wider FW compared with the other genotypes. The FL/W of T4, T2, T3, and T6 was statistically equal and larger than those of the other genotypes.

Repeatabilities of Wood and Fiber Traits

Repeatabilities (R^2) for all measured traits were estimated and are shown in **Figure 2**. R^2 of the wood and fiber properties in the whole family ranged from 0.55 to 0.76, which suggests that the observed phenotypic variation of these traits in the full-sib family was strongly affected by genetic effects. BD had the highest estimated repeatability ($R^2 = 0.76$) with 95% confidence intervals ranging from 0.57 to 0.89. FL/W had the lowest estimated repeatability ($R^2 = 0.55$) with 95% confidence intervals ranging from 0.29 to 0.77.

Pearson's Correlation Between Traits

Pearson's correlations of both phenotype and BLUPs among all measured wood and fiber traits were calculated and are presented in **Figure 3**. BLUPs estimate the strength of genetic correlation between traits, which is valuable to guide plant breeding. The phenotypic correlation coefficients (*r*) between traits in the whole family ranged from −0.69 to 0.77, and the BLUP correlation coefficients ranged from −0.68 to 0.56. BD was significantly negatively correlated with FW in both phenotypic ($r = -0.69$, $p < 0.001$) and BLUP ($r = -0.64$, $p = 0.002$) levels. There was a strongly positive phenotypic correlation between FL and FL/W ($r = 0.77$, $p < 0.001$), but their BLUP correlation was not significant. Although the phenotypic correlations between BD and FL/W and between FW and FL/W were not significant, their BLUP correlations reached a significant level.

In the diploid group, BD was significantly negatively correlated with FW at both the phenotypic and BLUP levels. There were also significant negative correlations between BD and FW in diploid males. In diploid females, BD was significantly positively correlated with FL/W at both the phenotypic and BLUP levels. In the triploid group, both phenotypic and BLUP correlations between BD and FL/W and between FW and FL/W were significant, and the BD was significantly positively correlated with FL at the BLUP level. In triploid females, BD was significantly correlated with FL, FW, and FL/W. FL was strongly negatively correlated with FW and positively correlated with FL/W, and FW was strongly negatively

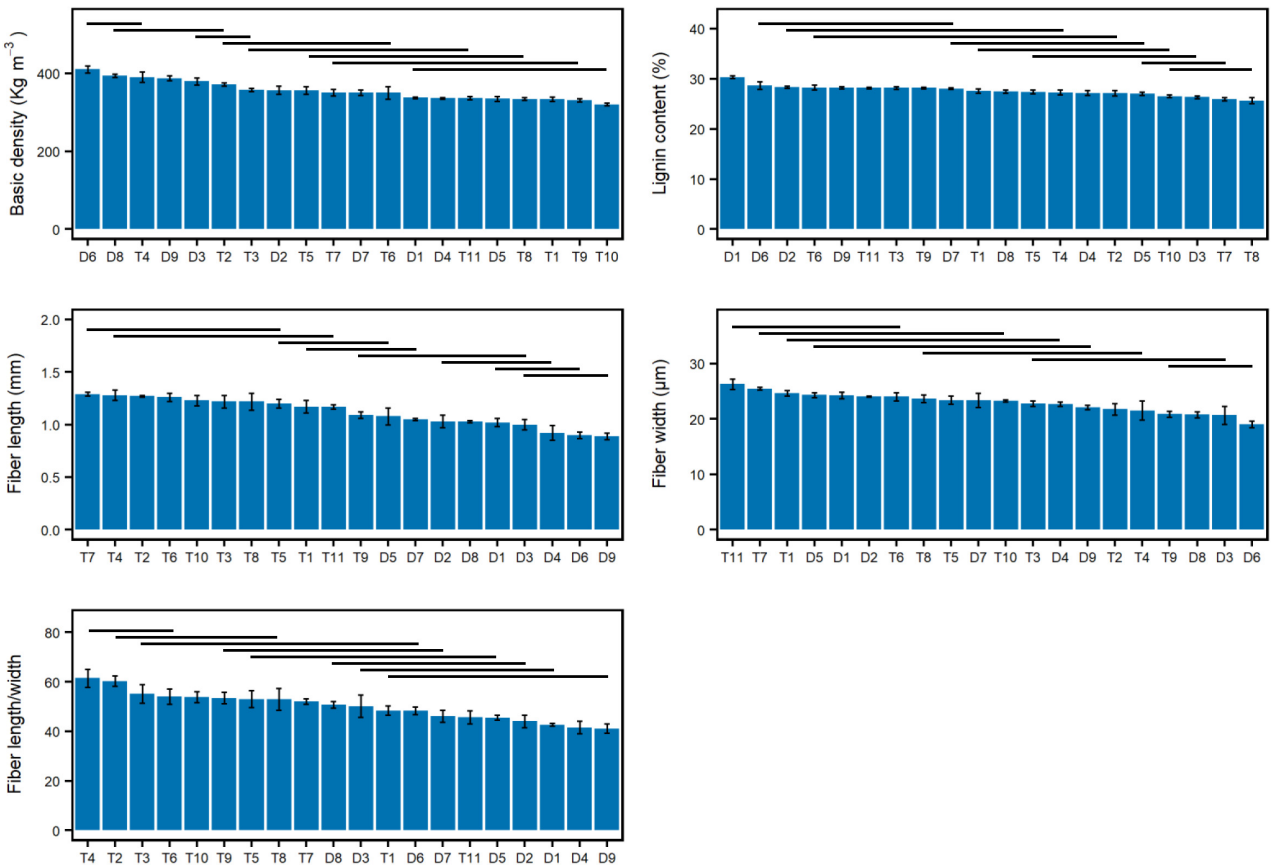

FIGURE 1 | Comparison among the genotypes for the measured wood and fiber traits. "—" covers the genotypes without a significant difference at the 0.05 level.

correlated with FL/W. However, in triploid males, there was no significant correlation between the traits no matter at phenotypic or BLUP level.

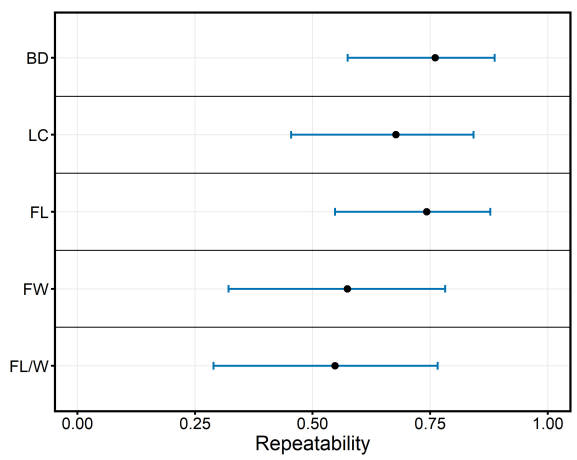

FIGURE 2 | Repeatability estimates (black dots) and 95% confidence intervals (blue bars) for wood and fiber properties. BD, Basic density; LC, Lignin content; FL, Fiber length; FW, Fiber width; FL/W, Fiber length/width.

Disaggregation of Genetic Effects

The phenotypes of the BD, LC, FL, FW, and FL/W traits of the diploid genotypes ranged from 334.66 to 410.35 kg m^{-3}, 26.37–30.33%, 0.890–1.081 mm, 19.05–24.35 μm, and 41.18–50.69, respectively. These traits of the triploid genotypes ranged from 320.21 to 390.06 kg m^{-3}, 25.68–28.29%, 1.089–1.293 mm, 20.88–26.30 μm, and 45.70–61.53, respectively. The Student's *t*-test showed that there were no statistical differences between the diploid and triploid groups on average for BD, LC, and FW traits (p = 0.157, 0.187, and 0.204, respectively). However, the FL and FL/W traits of the triploid group were significantly larger than those of the diploid group on average (**Figure 4**), which suggests that the increased ploidy level might be one of the main sources of variation for the FL and FL/W traits. Concerning the aspect of gender nested in the ploidy levels, however, no significant difference was found between females and males (p-values at 0.055–0.951), which suggests that the gender effect might not be a major factor for variation of the measured traits.

Variance contributions of genotype, ploidy, and gender effects for the wood and fiber traits were analyzed and are presented in **Figure 5**. Genotype was the major contributor to variation in BD, LC, and FW, with 54, 62, and 53% contributions, respectively. The variations in the FL and FL/W traits were mainly attributed to ploidy (77 and 50%, respectively). The gender effect nearly did

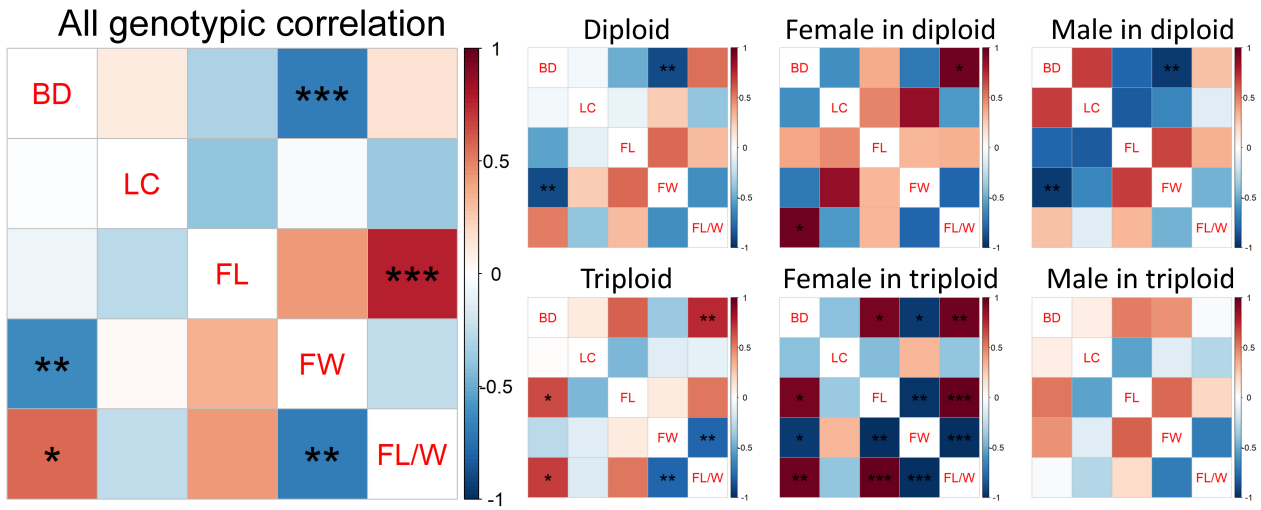

FIGURE 3 | Pearson's correlation between wood and fiber traits. The upper and lower diagonals represent phenotypic and BLUP correlations, respectively. BD, Basic density; LC, Lignin content; FL, Fiber length; FW, Fiber width; FL/W, Fiber length/width. *, **, and *** represent significance at 0.05, 0.01, and 0.001 levels, respectively.

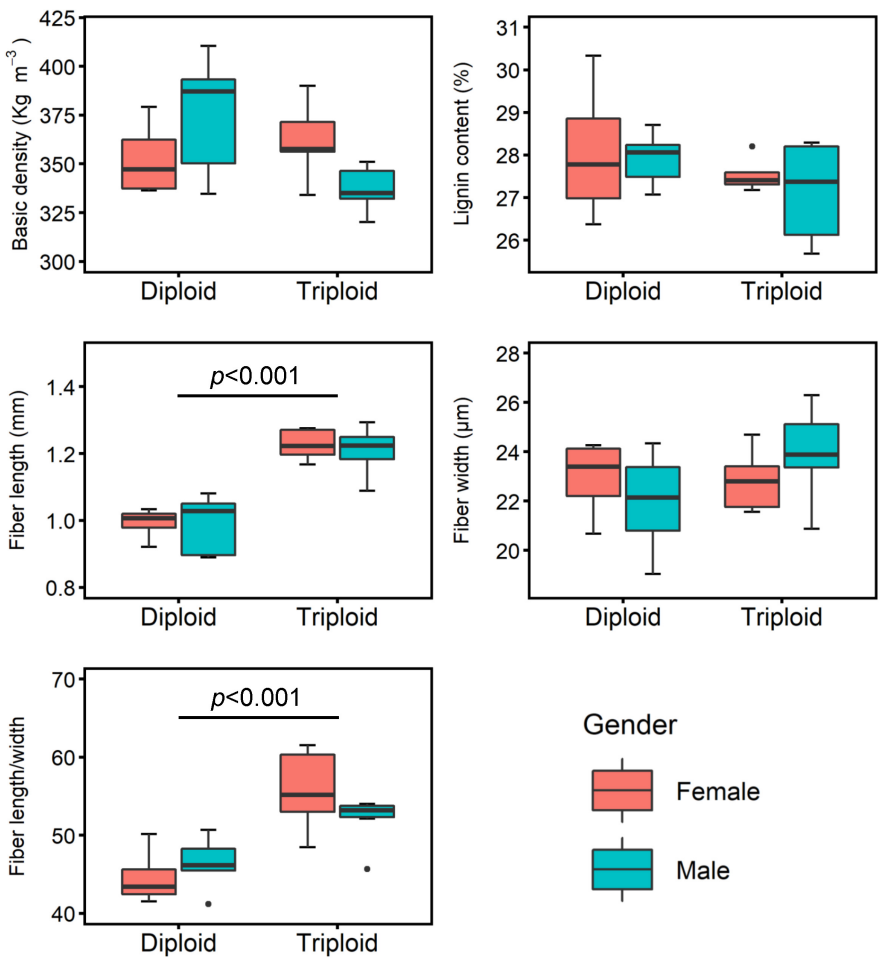

FIGURE 4 | Comparisons between diploid and triploid groups and between female and male groups within the ploidy levels for wood and fiber traits.

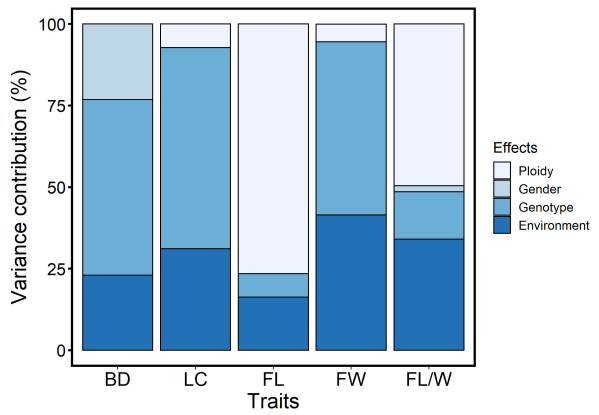

FIGURE 5 | Disaggregation of ploidy, gender, and genotype effects on woody and fiber properties based on variance contributions. BD, Basic density; LC, Lignin content; FL, Fiber length; FW, Fiber width; FL/W, Fiber length/width.

not contribute to the variation of these traits, except for the BD, which was attributed to the gender effect with 23% contribution. The environmental effects on these traits ranged from 16 to 41%.

DISCUSSION

Genus *Populus* is an important source of industrial raw timber in the northern hemisphere. In China, the lumber of *Populus* is widely used to produce pulpwood. The basic wood density, LC, and FL affect the pulp yield and paper quality (Kenney et al., 1990). Therefore, the improvement of pulpwood characteristics has attracted much attention. Triploid breeding has proved to be an effective way to improve the growth, wood properties, and abiotic stress of *Populus* (Kang, 2016). In white poplar, however, it was found that the BD of triploids was lower than that of the diploids (Kang, 2016). The low BD could decrease the yield of the pulp. In the triploid breeding program of the *Populus*, the selection of elite genotypes with high BD, low LC, and large FL are our key breeding objectives.

Polyploidization plays an important role in plant speciation and evolution and contributes to plant breeding (Van de Peer et al., 2009; De Storme and Mason, 2014; Sattler et al., 2016). According to the genomic composition, polyploid can be classified into two basic types: auto- and allopolyploid. In allopolyploids, phenotypic variation is commonly affected by both genomic heterozygosity and polyploidy. In *Arabidopsis thaliana*, the plant size of allotriploids was related to their parental genome dosage, but the tetraploid plants showed a low growth rate, suggesting that both the genotype and ploidy level contributed to variation in the plant size (Fort et al., 2016). In the present study, we took advantage of a full-sib progeny, including diploid and triploid genotypes, to provide new insights into the genetic effects of ploidy, gender, and genotype on the wood and fiber traits of *Populus*. All the wood and fiber traits studied here showed high repeatabilities (0.55–0.76). Genotype and ploidy were the main contributors to trait variation, suggesting that integration of heterosis and ploidy vigor is important for polyploid breeding. However, because the number of induced triploid hybrids is limited, and from a single parental combination, it is not known how generalizable these findings are.

An increased genome dosage is thought to cause many phenotypes associated with polyploidy, such as increased cell size, improved biomass yield, and enhanced production of secondary metabolites (Dhawan and Lavania, 1996; Kondorosi et al., 2000; Serapiglia et al., 2015; Iannicelli et al., 2020). Shang et al. (2020) found that ploidy notably affected the stomatal traits of *Populus*, but did not affect the serration number on the leaf margin and petiole length of the leaf. Triploid elite plants in white poplar hybrids showed better wood properties and fiber traits compared with diploid control (Kang, 2016). In *Eucalyptus grandis* × *E. urophylla*, triploid and tetraploid plants presented wider trunks, taller trees with longer stems, wider crowns, and higher BD compared with diploid plants (Longui et al., 2021). In our study, the diploid and triploid groups differed significantly in FL. The significant difference of FL/W between diploids and triploids could be attributed to a consequence of collinearity between FL and FL/W, because there was no significant difference in FW between the ploidy levels. Further analyses of variance components showed that ploidy contributed to the variation of FL and FL/W at 77 and 50%, respectively, indicating the huge potential of triploid breeding for the improvement of fiber traits in *Populus*.

The utilization of heterosis is an important topic of plant breeding. Compared with the selfing crops, hybridization breeding of the tree species usually results in extensive allelic segregation and assortment in the progeny due to the high heterozygosity of the parents. Generally, wood property and fiber traits vary with genotype in tree species (Zobel and van Buijtenen, 1989). Pliura et al. (2007) found significant genotypic variation in the wood density and growth traits of poplar hybrids. A remarkable difference of FL from wood disks at 1.5-m height was detected among genotypes in *Populus* (DeBell et al., 2002). In triploid white poplar, the genotype also resulted in significant differences in BD, FL, FW, and FL/W traits ($p < 0.001$, Wu et al., 2013). In our study, it was found that the wood and fiber traits varied significantly among the genotypes. The contribution of the genotype effect to the measured wood and fiber traits ranged from 7 to 62% (**Figure 5**). For the BD, LC, and FW traits, the genotype effect was the dominant source of their variation. Therefore, no matter in cross-breeding or triploid breeding of *Populus*, genotype screening in progeny based on the multiple parental combinations is important for the improvement of wood property and fiber traits.

In addition, gender dimorphism is an important evolutionary transition in many plant families (Miller and Venable, 2000). For dioecious plants, gender dimorphism may lead to phenotypic divergence. In *Silene latifolia*, the male plants had significantly wider calyx than the female plants (Yu et al., 2011). Maldonado-López et al. (2014) found that the female plants of *Spondias purpurea* showed a higher plant size and nutritional quality than the male plants. In a collected natural population of *P. tomentosa*, both FL and FW of the female group were significantly larger than those of the male group, but there

were no significant differences between the female and male groups in wood chemical compositions (Du et al., 2014). In our study, however, no statistical difference was detected between the female and male groups in any measured BD, LC, and fiber traits within the diploid or triploid groups. The analyses of variance components showed that gender explained 23% of the variation, but rarely contributed to the variation of the LC, FL, FW, and FL/W traits. The different effects of gender dimorphism between our study and the earlier ones might be attributed to the differences in species and population for investigation. Recently, male varieties of *Populus* were recommended for plantation in China, because fluff catkins of female plants may cause severe environmental pollution in rural and urban areas, even potential fire risk (Janković et al., 2021). The minor effects of gender on wood properties suggest that the selection of male genotypes might not reduce the pulp-industrial value of *Populus* in our experimental family.

An understanding of the relationships between these wood properties is of value in the development of a breeding program for the pulp and paper industry. In our study, both phenotypic and BLUP correlations between the traits were analyzed. The results showed that the phenotypic correlations had similar changes with the BLUP correlations, though the significance levels in several trait pairs varied, which reflected on the difference between the phenotypic value and BLUP-adjusted genotypic value. BLUP, presented by Henderson (1975), is a traditional method for predicting genetic parameters and has been commonly used in plant breeding (Resende, 2016). The BLUP method has good predictive accuracy for genetic parameters when the sample sizes are variable (Piepho et al., 2008). Compared with the phenotypic correlation, BLUP reflects the genetic correlation between traits, which can provide a better understanding of how traits are interrelated. In triploids, BD was significantly positively correlated with FL in BLUPs (r = 0.65, p = 0.030), suggesting that BD could be improved together with FL during triploid breeding. In the triploids of *P. tomentosa*, a significantly positive genotypic correlation between BD and FL was also found with the correlation coefficient ranging from 0.41 to 0.98 at different sites (Wu et al., 2013). There was a moderately negative BLUP correlation between LC and FL in the triploid group (r = −0.46, p = 0.159), in our study, suggesting that the selection of FL trait might lead to the decrease of LC in triploid breeding.

In this study, the CV_G for each measured trait was low, ranging from 4 to 11%, which indicates that the genetic variation is quite small for these wood traits. It means that changes from direct selection and correlated responses will be quite small for these traits in the family of our study. The CV_G values in triploids were no larger than that of the diploids in this family. In the triploids of *P. tomentosa*, the CV_G values of the wood and fiber traits were also very small, ranging from 1.4 to 6.4 at different sites (Wu et al., 2013). Therefore, to improve the wood and fiber traits, it is necessary to produce many hybrids and triploids for selection. To produce triploids of *Populus*, various methods for sexual polyploidization, such as 2n pollen induction, 2n female gamete induction, and crossing diploids with tetraploids, have been developed (Einspahr, 1984; Kang et al., 2000; Wang et al., 2010, 2012a,b; Li et al., 2019). The approach of 2n female gamete induction could produce more than 60% triploids (Wang et al., 2010, 2012a,b; Lu et al., 2013), which should be used to increase the number of triploids in this family. Alternatively, other species could be introduced as parents to improve the wood and fiber traits. In our study, the parents are both Aigeiros–Tacamahaca intersection hybrids (the female parent 'Zheyin3#' is derived from *P. pseudo-simonii* × *P. nigra* and the male parent BJY was generated by crossing *P. nigra* var *italica* with *P. cathayana*), resulting in limited variations of the traits in progeny. In future, more species, such as *P. simonii*, *P. nigra*, and *P. deltoides,* could be used for parental selection with large combining ability, and triploid induction should be conducted using the parents.

DATA AVAILABILITY STATEMENT

The original contributions presented in the study are included in the article/supplementary material, further inquiries can be directed to the corresponding author/s.

AUTHOR CONTRIBUTIONS

JW conceived and designed the research. X-YH, JS, and Y-HZ collected wood disks and conducted laboratory experiments. JS and D-LL analyzed the data. L-JS managed the field trial. X-YH, D-LL, and JW wrote and revised the manuscript. All authors read and approved the manuscript.

FUNDING

This study was funded by the National Key R&D Program of China during the 14th Five-year Plan Period (grant no. 2021YFD2200105) and the Fundamental Research Funds for the Central Universities (grant no. 2018ZY30).

ACKNOWLEDGMENTS

We thank Prof. Tong-Qi Yuan from Beijing Forestry University for his kind help on wood property investigation, Prof. Yuan-Zhen Lin from South China Agricultural University, and Prof. Li-Bo Jiang from the Shandong University of Technology for their kind help for data analysis. We also thank the editor and the reviewers for their constructive comments.

REFERENCES

Bannoud, F., and Bellini, C. (2021). Adventitious rooting in *Populus* species: update and perspectives. *Front. Plant Sci.* 12:668837. doi: 10.3389/fpls.2021.668837

Bon, P. V., Harwood, C. E., Chi, N. Q., Thinh, H. H., and Kien, N. D. (2020). Comparing wood density, heartwood proportion and bark thickness of diploid and triploid *Acacia* hybrid clones in Vietnam. *J. Trop. For Sci.* 32, 206–216. doi: 10.26525/jtfs32.2.206

De Storme, N., and Mason, A. (2014). Plant speciation through chromosome instability and ploidy change: Cellular mechanisms, molecular factors and evolutionary relevance. *Curr. Plant Biol.* 1, 10–33. doi: 10.1016/j.cpb.2014.09.002

DeBell, D. S., Singleton, R., Harrington, C. A., and Gartner, B. L. (2002). Wood density and fiber length in young *Populus* stems: relation to clone, age growth rate, and pruning. *Wood Fiber Sci.* 34, 529–539.

Dhawan, O. P., and Lavania, U. C. (1996). Enhancing the productivity of secondary metabolites *via* induced polyploidy: a review. *Euphytica* 87, 81–89. doi: 10.1186/s43141-020-00109-8

Dong, C. B., Suo, Y. J., Wang, J., and Kang, X. Y. (2015). Analysis of transmission of heterozygosity by 2n gametes in *Populus* (Salicaceae). *Tree Genet. Genom.* 11:799.

Du, Q., Xu, B., Gong, C., Yang, X., Pan, W., Tian, J., et al. (2014). Variation in growth, leaf, and wood property traits of Chinese white poplar (*Populus tomentosa*), a major industrial tree species in Northern China. *Can. J. For. Res.* 44, 326–339. doi: 10.1139/cjfr-2013-0416

Einspahr, D. W. (1984). Production and utilization of triploid hybrid aspen. *Iowa State J. Res.* 58, 401–409.

Fort, A., Ryder, P., McKeown, P. C., Wijnen, C., Aarts, M. G., Sulpice, R., et al. (2016). Disaggregating polyploidy, parental genome dosage and hybridity contributions to heterosis in *Arabidopsis thaliana*. *New Phytol.* 209, 590–599. doi: 10.1111/nph.13650

Georgii, E., Kugler, K., Pfeifer, M., Vanzo, E., Block, K., Domagalska, M. A., et al. (2019). The systems architecture of molecular memory in poplar after abiotic stress. *Plant Cell* 31, 346–367. doi: 10.1105/tpc.18.00431

Henderson, C. R. (1975). Best linear unbiased estimation and prediction under a selection model. *Biometrics* 31, 423–447. doi: 10.2307/2529430

Iannicelli, J., Guariniello, J., Tossi, V. E., Regalado, J. J., Di Ciaccio, L., van Baren, C. M., et al. (2020). The "polyploid effect" in the breeding of aromatic and medicinal species. *Sci. Hortic.* 260:108854. doi: 10.1016/j.scienta.2019.108854

Janković, B., Manić, N., and Dodevski, V. (2021). Pyrolysis kinetics of poplar fluff bio-char produced at high carbonization temperature: A mechanistic study and isothermal life-time prediction. *Fuel* 296:120637. doi: 10.1016/j.fuel.2021.120637

Kang, X. Y. (2016). ""Polyploid induction techniques and breeding strategies in poplar"," in *Polyploidy and hybridization for Crop Improvement*, ed. A. S. Mason (Boca Raton, FL: CRC Press), 76–96. doi: 10.1201/9781315369259-5

Kang, X. Y. (2020). Research progress and prospect of triploid breeding of forest trees. *Sci. Sin. Vitae* 50, 136–143. doi: 10.1360/ssv-2019-0126

Kang, X. Y., Zhu, Z. T., and Zhang, Z. Y. (2000). Breeding of triploids by the reciprocal crossing of *Populus alba* × *P. glandulosa* and *P. tomentosa* × *P. bolleana*. *J. Beijing For. Univ.* 22, 8–11.

Kenney, W. A., Sennerby-Forsse, L., and Layton, P. (1990). A review of biomass quality research relevant to the use of poplar and willow for energy conversion. *Biomass* 21, 163–188. doi: 10.1016/0144-4565(90)90063-p

Kondorosi, E., Roudier, F., and Gendreau, E. (2000). Plant cell-size control: growing by ploidy? *Curr. Opin. Plant Biol.* 3, 488–492. doi: 10.1016/s1369-5266(00)00118-7

Kruijer, W., Boer, M. P., Malosetti, M., Flood, P. J., Engel, B., Kooke, R., et al. (2015). Marker-based estimation of heritability in immortal populations. *Genetics* 199, 379–398. doi: 10.1534/genetics.114.167916

Lei, Y., Chen, K., Jiang, H., Yu, L., and Duan, B. (2016). Contrasting responses in the growth and energy utilization properties of sympatric *Populus* and *Salix* to different altitudes: implications for sexual dimorphism in Salicaceae. *Physiol. Plant.* 159, 30–41. doi: 10.1111/ppl.12479

Li, D. L., Tian, J., Xue, Y., Chen, H., and Wang, J. (2019). Triploid production *via* heat-induced diploidization of megaspores in *Populus pseudo-simonii*. *Euphytica* 215:10.

Li, Y. H., and Kang, X. Y. (2007). Triploid induction in white poplar by chromosome doubling of megaspore. *J. Beijing For. Univ.* 29, 22–25.

Longui, E. L., Custódio, G. H., Amorim, E. P., da Silva Júnior, F. G., Oda, S., and Souza, I. C. G. (2021). Differences in wood properties among *Eucalyptus grandis* and *Eucalyptus grandis* x *Eucalyptus urophylla* with different degrees of ploidy. *Res. Society Develop.* 10:e395101624035. doi: 10.33448/rsd-v10i16.24035

Lu, M., Zhang, P., and Kang, X. (2013). Induction of 2n female gametes in *Populus adenopoda* Maxim by high temperature exposure during female gametophyte development. *Breed. Sci.* 63, 96–103. doi: 10.1270/jsbbs.63.96

Maldonado-López, Y., Cuevas-Reyes, P., Sánchez-Montoya, G., Oyama, K., and Quesada, M. (2014). Growth, plant quality and leaf damage patterns in a dioecious tree species: is gender important? *Arthropod-Plant Interact.* 8, 241–251.

Melnikova, N. V., Borkhert, E. V., Snezhkina, A. V., Kudryavtseva, A. V., and Dmitriev, A. A. (2017). Sex-specific response to stress in populus. *Front. Plant Sci.* 8:1827. doi: 10.3389/fpls.2017.01827

Miller, J. S., and Venable, D. L. (2000). Polyploidy and the evolution of gender dimorphism in plants. *Science* 289, 2335–2338. doi: 10.1126/science.289.5488.2335

Piepho, H. P., Möhring, J., Melchinger, A. E., and Büchse, A. (2008). BLUP for phenotypic selection in plant breeding and variety testing. *Euphytica* 161, 209–228. doi: 10.1007/s10681-007-9449-8

Pliura, A., Zhang, S. Y., MacKay, J., and Bousquet, J. (2007). Genotypic variation in wood density and growth traits of poplar hybrids at four clonal trials. *For Ecol. Manag.* 238, 92–106. doi: 10.1016/j.foreco.2006.09.082

Porth, I., and El-Kassaby, Y. A. (2015). Using *Populus* as a lignocellulosic feedstock for bioethanol. *Biotechnology* 10, 510–524. doi: 10.1002/biot.201400194

R Development Core Team (2007). *R: a Language and Environment for Statistical Computing*. Vienna, Austria: R Foundation for Statistical Computing.

Resende, M. D. V. (2016). Software Selegen-REML/BLUP: a useful tool for plant breeding. *Crop Breed. Appl. Biotechnol.* 16, 330–339. doi: 10.1590/1984-70332016v16n4a49

Sattler, M. C., Carvalho, C. R., and Clarindo, W. R. (2016). The polyploidy and its key role in plant breeding. *Planta* 243, 281–296. doi: 10.1007/s00425-015-2450-x

Serapiglia, M. J., Gouker, F. E., Hart, J. F., Unda, F., Mansfield, S. D., Stipanovic, A. J., et al. (2015). Ploidy level affects important biomass traits of novel shrub willow (*Salix*) hybrids. *BioEnergy Res.* 8, 259–269. doi: 10.1007/s12155-014-9521-x

Serapiglia, M. J., Gouker, F. E., and Smart, L. B. (2014). Early selection of novel triploid hybrids of shrub willow with improved biomass yield relative to diploids. *BMC Plant Biol.* 14:74. doi: 10.1186/1471-2229-14-74

Shang, J., Xue, Y. X., Song, L. J., Liu, C. H., Li, D. L., Zhang, H. Y., et al. (2020). Ploidy, genotype and gender effects of functional leaf and stomatal traits on short branches in full-sib hybrids between section Tacamahaca and sect. *Aigeiros of Populus*. *J. Beijing For. Univ.* 42, 11–18.

Sluiter, A., Hames, B., Ruiz, R., Scarlata, C., Sluiter, J., Templeton, D., et al. (2008). *Determination of Structural Carbohydrates and lignin in Biomass (NREL/TP-510-42618)*. Golden, Colorado: US National Renewable Energy Laboratory.

Smith, D. M. (1954). *Maximum Moisture Content method for Determining Specific Gravity of Small Wood Samples*. Gifford Pinchot Drive: Forest Products Laboratory.

van Buijtenen, J. P., Joranson, P. N., and Einspahr, D. W. (1958). Diploid versus triploid aspen as pulpwood sources with reference to growth, chemical, physical and pulping differences. *Tappi* 41, 170–175.

Van de Peer, Y., Maere, S., and Meyer, A. (2009). The evolutionary significance of ancient genome duplications. *Nature Rev. Genet.* 10, 725–732. doi: 10.1038/nrg2600

Wang, J., Kang, X. Y., and Li, D. L. (2012a). High temperature-induced triploid production during embryo sac development in *Populus*. *Silvae Genet.* 61, 85–93. doi: 10.1515/sg-2012-0011

Wang, J., Li, D. L., and Kang, X. Y. (2012b). Induction of unreduced megaspores with high temperature during megasporogenesis in *Populus*. *Ann. For. Sci.* 69, 59–67. doi: 10.1007/s13595-011-0152-5

Wang, J., Kang, X. Y., Li, D. L., and Chen, H. W. (2010). Induction of diploid eggs with colchicine during embryo sac development in *Populus*. *Silvae Genet.* 59, 40–48. doi: 10.1515/sg-2010-0005

Weisgerber, H., Rau, H. M., Gartner, E. J., Baumeister, G., Kohnert, H., and Karner, L. (1980). 25 years of forest tree breeding in Hessen. *Allg. For.* 26, 665–712.

Wu, F., Zhang, P., Pei, J., and Kang, X. (2013). Genotypic parameters of wood density and fiber traits in triploid hybrid clones of *Populus tomentosa* at five clonal trials. *Ann. For. Sci.* 70, 751–759. doi: 10.1007/s13595-013-0307-7

Yu, Q., Ellen, E. D., Wade, M. J., and Delph, L. F. (2011). Genetic differences among populations in sexual dimorphism: evidence for selection on males in a dioecious plant. *J. Evol. Biol.* 24, 1120–1127. doi: 10.1111/j.1420-9101.2011.02245.x

Zhang, W. H., Wei, R. Y., Liu, Y., and Lin, Y. Z. (2021). AFEchidna is a R package for genetic evaluation of plant and animal breeding datasets. *BioRxiv* [prepint]. doi: 10.1101/2021.06.24.449740

Zhu, Z. T. (2006). *Genetic Improvement of Populus Tomentosa* Carr. Beijing: Chinese Forestry Publishing House.

Zhu, Z. T., Lin, H. B., and Kang, X. Y. (1995). Studies on allotriploid breeding of *Populus tomentosa* B301 clones. *Sci. Silvae Sin.* 31, 499–505.

Zobel, B. J., and van Buijtenen, J. P. (1989). *Wood variation: Its Causes and Control*. Berlin: Heidelberg: Springer.

Conflict of Interest: The authors declare that the research was conducted in the absence of any commercial or financial relationships that could be construed as a potential conflict of interest.

frontiers | Frontiers in Plant Science

ORIGINAL RESEARCH
published: 27 April 2022
doi: 10.3389/fpls.2022.870698

Induction and Characterization of Tetraploid Through Zygotic Chromosome Doubling in *Eucalyptus urophylla*

*Zhao Liu[1,2,3], Jianzhong Wang[4], Bingfa Qiu[4], Zhongcai Ma[4], Te Lu[5], Xiangyang Kang[1,2,3] and Jun Yang[1,2,3]**

[1] National Engineering Research Center of Tree Breeding and Ecological Restoration, College of Biological Sciences and Technology, Beijing Forestry University, Beijing, China, [2] Key Laboratory of Genetics and Breeding in Forest Trees and Ornamental Plants, Ministry of Education, Beijing Forestry University, Beijing, China, [3] The Tree and Ornamental Plant Breeding and Biotechnology Laboratory, National Forestry and Grassland Administration, Beijing Forestry University, Beijing, China, [4] Guangxi Dongmen Forest Farm, Chongzuo, China, [5] Science and Technology Section, Chifeng Research Institute of Forestry Science, Chifeng, China

OPEN ACCESS

Edited by:
Jen-Tsung Chen, National University of Kaohsiung, Taiwan

Reviewed by:
Sezai Ercisli, Atatürk University, Turkey
Ali Raza, Fujian Agriculture and Forestry University, China

***Correspondence:**
Jun Yang
yang_jun@bjfu.edu.cn

Specialty section:
This article was submitted to Plant Breeding, a section of the journal Frontiers in Plant Science

Received: *07 February 2022*
Accepted: *28 March 2022*
Published: *27 April 2022*

Citation:
Liu Z, Wang J, Qiu B, Ma Z, Lu T, Kang X and Yang J (2022) Induction and Characterization of Tetraploid Through Zygotic Chromosome Doubling in Eucalyptus urophylla. Front. Plant Sci. 13:870698. doi: 10.3389/fpls.2022.870698

Improvements in plant growth can bring great benefits to the forest industry. *Eucalyptus urophylla* is an important plantation species worldwide, and given that ploidy increases are often associated with plant phenotype changes, it was reasoned that its polyploidization may have good prospects and great significance toward its cultivation. In this study, the zygotic development period of *E. urophylla* was observed through paraffin sections, and a correlation between the development time of flower buds after pollination and the zygotic development period was established. On this basis, it was determined that the 25th day after pollination was the appropriate time for a high temperature to induce zygotic chromosome doubling. Then tetraploid *E. urophylla* was successfully obtained for the first time through zygotic chromosome doubling induced by high temperature, and the appropriate conditions were treating flower branches at 44°C for 6 h. The characterization of tetraploid *E. urophylla* was performed. Chromosome duplication brought about slower growing trees with thicker leaves, larger cells, higher net photosynthetic rates, and a higher content of certain secondary metabolites. Additionally, the molecular mechanisms for the variation in the tetraploid's characteristics were studied. The qRT-PCR results showed that genes mediating the tetraploid characteristics showed the same change trend as those of the characteristics, which verified that tetraploid trait variation was mainly caused by gene expression changes. Furthermore, although the tetraploid had no growth advantage compared with the diploid, it can provide important germplasm resources for future breeding, especially for the creation of triploids.

Keywords: breeding, artificial polyploidy, high-temperature treatment, zygotic development period, trait variation, molecular mechanism

INTRODUCTION

Improvements in plant growth are the main goals of tree breeders, and polyploidy has long been recognized as a major force in angiosperm evolution (Jiao et al., 2011). The evolution of most plants has involved one or more episodes of polyploidy (Soltis et al., 2009). However, the frequency of naturally occurring polyploidy is very low, which means it cannot meet the demand for tree growth improvements (Zhu et al., 1998). Nowadays, artificially induced polyploidy has been widely used for the generation and creation of new plant varieties (Lu et al., 2013; Guo et al., 2017). Compared with diploid plants, polyploidy plants usually grow robustly and have enlarged organs such as flowers, leaves, and fruits (Liu et al., 2007; Zhang et al., 2019). After polyploidization, plants often exhibit broader environmental adaptability, such as enhanced abiotic stress tolerance, and show significant increases in their potentially valuable secondary metabolite contents (Bon et al., 2020; Zhang et al., 2020). *Eucalyptus*, *Populus*, and *Salix* are fast-growing and important plantation species worldwide. *Eucalyptus* can provide a large amount of wood for industrial production. Its leaves contain oil that can be used as an effective pesticide or herbicide component (Hung et al., 2014; Dhakad et al., 2018; Stikhareva et al., 2021). Therefore, *Eucalyptus* polyploidization has good prospects and significance toward its breeding.

Although no naturally occurring *Eucalyptus* polyploids have been found, artificial mutagenesis could give rise to them (Guo et al., 2017). In previous studies on *Eucalyptus* tetraploid induction, only the use of colchicine to induce somatic chromosome doubling to obtain autotetraploids was reported, despite often obtaining a large number of mixoploids (Fernando et al., 2019; Silva et al., 2019). Compared with inducing the chromosome doubling of somatic cells, the mutagenesis approach to obtain tetraploids by treating zygotic cells after fertilization clearly shows great advantages (Lu et al., 2013; Guo et al., 2017). This is the case because tetraploids obtained by inducing chromosome doubling of zygotes develop from a single cell, and mixoploids will not be produced during the mutagenesis treatment period (Lu et al., 2013). Moreover, employing zygotes as mutagenic objects can also harness the hybrid effect produced by sexual mating design and obtain more genetic gains (Wang J. et al., 2010). Therefore, zygotic chromosome doubling induction is an important method to artificially induce tetraploidy. Colchicine, high temperature, or N_2O are often used to block normal zygote development and promote chromosome doubling to obtain tetraploids in *Populus* and other tree species (Atwood, 1936; Wang J. et al., 2010; Gordej et al., 2019). As a physical mutagenic factor, high temperature is an efficient and environmentally friendly polyploid induction method in several hardwood tree species (Li et al., 2019; Yao et al., 2020). However, there has been no report on the induction of zygotic chromosome doubling by high temperature in *Eucalyptus*.

Tetraploids have been induced successfully in many plants, but there are few reports describing the tetraploids obtained by zygotic chromosome doubling. In studies of maize, rye, and other plants, tetraploids were successfully obtained by zygotic chromosome doubling after fertilization, but the characterization of tetraploids was not performed (Kato and Birchler, 2006; Gordej et al., 2019). Tetraploids have been obtained in *Populus*, a model tree species, through somatic or zygotic chromosome doubling (Lu et al., 2013; Wu et al., 2020). Although there have been characterizations of the tetraploid obtained by somatic chromosome doubling, the tetraploid obtained by zygotic chromosome doubling is unclear (Ren et al., 2021). In *Eucalyptus*, it was reported that the growth of tree height and diameter at breast height of autotetraploids obtained by somatic chromosome doubling was slower than that of diploids, and their content of secondary metabolites such as essential oils showed no significant change compared with that of diploids (Fernando et al., 2019). However, whether the variation trend in tetraploids obtained by zygotic doubling is consistent with that in those obtained by somatic doubling is the most important issue in breeding research and industrial production and applications.

This study carried out high-temperature-induced zygotic chromosome doubling to induce *Eucalyptus urophylla* tetraploids for the first time and explored the appropriate treatment time and conditions for inducing zygotic chromosome doubling. The characteristics of the tetraploids obtained by zygotic chromosome doubling were studied. Additionally, the molecular mechanism for the variation of characteristics after polyploidization of *E. urophylla* was also studied. This study provides a new path for *Eucalyptus* germplasm innovation and a reference for the development of *Eucalyptus* polyploid breeding in the future.

MATERIALS AND METHODS

Plant Materials

Eucalyptus urophylla S. T. Blake used in this study are all from the same clone composed of 20 individual ramets. This clone was planted in a seed orchard at the Guangxi Dongmen Forest Farm (Guangxi Zhuang Autonomous Region, China) in 2015. After years of observation, the growth and the number of flowers within this clone were confirmed to be relatively consistent.

Controlled Pollination

The flower branches of *E. urophylla* with a large number of flowers were selected as alternative flower branches for experiments. Controlled pollination was carried out after observing that most operculums changed from green to yellow. Pollination was performed following the method described by Assis et al. (2005). The pollen from other *Eucalyptus* clones collected in the previous year was used for controlled pollination. After pollination, the flower branches were bagged to exclude external pollen sources, and the bags were released 2 weeks after pollination.

Observation of the Zygotic Development Process

The time of artificial pollination, when a large number of bud operculums of *E. urophylla* turned yellow, was set as 0. The flower buds were sampled every 24 h after

pollination and then immediately placed inside a centrifuge tube filled with Carnoy's fixative solution (acetic acid:ethanol, 1:3) (Tjio and Whang, 1962).

To observe mitosis in zygotes, the preserved flower buds were studied by the improved paraffin section technique described by Guo et al. (2019). Sections were observed and photographed under a microscope (BX51; Olympus) equipped with a CCD camera (DP70; Olympus).

Zygotic Chromosome Doubling Using High Temperature

According to previous research, after correlating the development time of flower buds after pollination with the development period of zygotes, flower buds with different development times after pollination were treated at 40, 44, and 48°C for 3 and 6 h using the high-temperature treatment machine (Chinese invention patent No. ZL200610113448.X). Six replicate groups for each duration at each temperature were treated, and the untreated flower buds were used as a control. After treatment, the groups were marked according to treatment temperature and duration.

Detection of Ploidy Levels

Capsules were harvested individually at maturity. Seeds were extracted and separated from the chaff by hand to permit their counting. Collected seeds were sown in the soil, and when the seedlings grew to approximately 20 cm, both flow cytometry and somatic chromosome counting were used to detect their ploidy levels according to the method of Yang et al. (2018).

Measurement of Growth Traits of Tetraploids and Diploids in *E. urophylla*

After ploidy detection, diploids from full-sib families under the same treatment conditions were selected as controls, and tetraploids and diploids underwent clonal propagation. For tetraploid and diploid clones, 10 ramets were selected for biological replicates. When the plants had grown for 6 months, their height was measured with a tape, and the ground diameter was measured with a vernier caliper. All the leaves of each ramet of the two ploidy clones were counted, and five fully expanded mature leaves of two ploidy clones were randomly selected to measure the leaf length and width and the petiole length. The leaf area was recorded by a CI-203 handheld laser leaf area meter (Li-Cor Inc., Lincoln, NE, United States). Immediately after the measurement, the fresh weight of the leaves was obtained, and after drying in the oven, the dry weight was obtained. All data were measured three times, and the average was recorded.

Leaf Anatomical Structure Analysis

The fully expanded mature leaves of diploids and tetraploids were selected as samples. Leaves were cut into 0.25 cm^2 blocks, and their middle parts (including the leaf vein) were selected for the paraffin sections to observe mesophyll cell characteristics. Sections were stained with 1% safranine solution for 1 h, then transferred to a 0.1% fast green solution for 1 min. Sections were observed and photographed under a microscope (BX51; Olympus) equipped with a CCD camera (DP70; Olympus).

Measurement of Photosynthetic Parameters

The fully expanded mature leaves of diploids and tetraploids were selected to measure their photosynthetic parameters. Net photosynthetic rate (Pn), stomatal conductance (Gs), intercellular carbon dioxide concentration (Ci), and transpiration rate (Tr) were measured using an LI-6400-02B portable photosynthesis system (Li-Cor Inc., Lincoln, NE, United States) at 8–10 o'clock on a sunny day in October 2020. All photosynthetic parameters were measured under a photosynthetic photon flux density of 1,400 mol^{-2} s^{-1}, at 60% of relative humidity, and with a CO_2 concentration of 400 μmol mol^{-1} held using a CO_2 injection system (Cha-um and Kirdmanee, 2010). The instantaneous water use efficiency (WUE_i) was calculated as Pn divided by Tr. Additionally, the chlorophyll fluorescence parameter Fv/Fm, reflecting the maximal photochemical efficiency of photosystem II (PSII), was measured on mature leaves using an MD-500 chlorophyll fluorescence spectrometer (Yi Zong Qi Technology Co. Ltd., Beijing, China).

Stomatal Analysis

The fully expanded mature leaves of diploids and tetraploids were selected for stomatal observation. The leaf epidermis was peeled off and placed on the slide. Stomatal characteristics and chloroplast numbers were observed using ultraviolet or bright-field illumination and photographed under a microscope equipped with a CCD camera (BX51 and DP70; Olympus).

Transmission Electron Microscopy Observation of Chloroplasts

The chloroplasts in the fully expanded mature leaves of diploids and tetraploids were prepared using the method of Wang et al. (2021). Chloroplast ultrastructures were observed using JEM-1010 electron microscopy (JEM-1010, Jeol Ltd., Tokyo, Japan).

Physiological Parameter Measurements

The fully expanded mature leaves of diploids and tetraploids were selected for physiological parameter measurements. For the determination of the catalase (CAT) activity, peroxidase (POD) activity, malondialdehyde (MDA) content, total protein content, and soluble sugar content, their corresponding assay kits (Catalog No. A007-1-1, A084-3-1, A003-1-2, A045-2-2, and A145-1-1, Nanjing Jiancheng Bioengineering Ins., Nanjing, China) were used according to the manufacturer's protocols.

Foliar Oil Glands Isolation

A 100-mm^2 section was excised from the middle part of fully expanded mature leaves of diploids and tetraploids and digested in pectinase, as described in Goodger et al. (2010). The leaf cuticle and attached epidermal layers were readily removed following digestion, as described in Goodger and Woodrow (2011). Foliar

TABLE 1 | Zygote development after pollination.

Time after pollination (day)	Development stages	Zygotic mitotic period
7–9	I	Double fertilization
10–22	II	Dormant zygote
23–25	III	Dormant zygote to four-cell proembryo
26–28	IV	Two-cell proembryo to multicellular embryo

oil glands were isolated from the remaining leaf tissues by disruption and sieving (Goodger and Woodrow, 2011). The oil glands and mature leaves were observed using ultraviolet and bright-field illumination, respectively, and photographed under a microscope equipped with a CCD camera (BX51 and DP70; Olympus).

qRT-PCR

The total RNA was isolated from the young, mature, and senescent leaves of *E. urophylla* using an RNAprep Pure Plant Plus Kit (Tiangen, China, cat DP441). Approximately 1.5 μg of RNA was reverse-transcribed into first-stand cDNA using a cDNA synthesis kit (Tiangen, China, cat KR106). The qRT-PCR reaction mixture consisted of 10 μl of 2 × TransStart® Tip Green qPCR SuperMix (TransGen Biotech, China, cat AQ101), 0.6 μl of forward primer, 0.6 μl of reverse primer, 2 μl of cDNA template, 0.4 μl of 50 × ROX reference dye, and 6.4 μl of RNase-free ddH_2O. qRT-PCR was performed on the Applied Biosystems 7500 Fast Real-Time PCR system for 39 cycles under the following conditions: 95°C for 15 min of pre-degeneration, 95°C for 10 s of degeneration, 58°C for 30 s of annealing, and 72°C for 30 s of extension. The samples were then heated to 95°C for 15 s and then 60°C for 1 min for dissolution curve analysis. Three technical replicates and three biological replicates were used for each sample and randomly selected gene. EuGADPH was a reference gene, and the primers used for qRT-PCR analysis are listed in **Supplementary Table 1**.

Statistical Analysis

Measurements of leaf anatomical structure, oil glands, and stomatal parameters were obtained using the ImageJ software (version 1.51, NIH, Bethesda, MD, United States). The statistical analysis of tetraploids and diploids was performed using the SPSS version 19.0 software (SPSS Inc., Chicago, IL, United States). Significant differences among means were determined by Duncan's multiple range tests at $P \leq 0.05$.

RESULTS

Correlation Between the Flower Bud Development and Zygotic Development Period

We found a relationship between the development time of flower buds after pollination and the zygotic development period. According to the zygotic mitotic period, the development time of flower buds after pollination could be divided into 4 stages (**Table 1**). The double fertilization of *E. urophylla* was observed for the first time on the 7th day after pollination. At this time, central cells with fused polar nuclei, egg cells, and synergists were observed at the micropylar end of the embryo sac (**Figure 1A**). Subsequently, the process of double fertilization was completed, and dormant zygotes with obvious nucleoli could be observed in the embryo sac (**Figure 1B**). Zygotes experienced about 12 days of dormancy, and the first mitosis of zygotes was observed on the 23rd day after pollination. At this time, zygotes were divided to form two-cell proembryos (**Figure 1C**). In the next few days, fertilized eggs continued to develop, from four-cell proembryos to multicellular embryos (**Figures 1D–G**). The fertilized polar nucleus developed as the fertilized eggs developed. After multiple

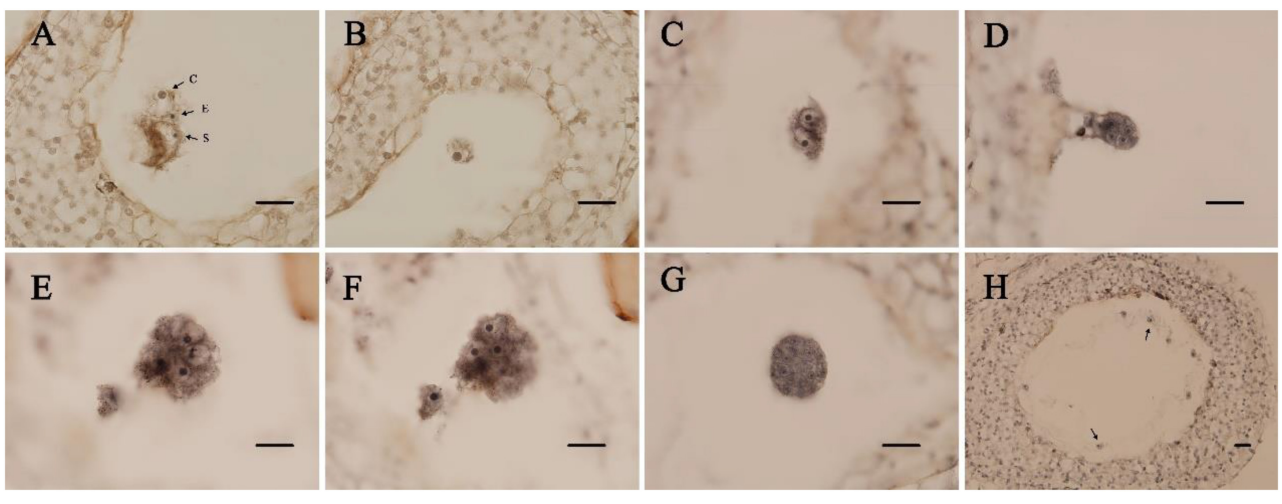

FIGURE 1 | Paraffin section of ovules in *Eucalyptus urophylla.* **(A)** Central cell (c), egg cell (e), and persistent synergid (s); **(B)** zygote; **(C)** two-cell proembryo; **(D)** four-cell proembryo; **(E,F)** eight-cell proembryo; **(G)** multicellular embryo; and **(H)** free nuclear endosperm (bar = 200 μm).

TABLE 2 | *Eucalyptus urophylla* tetraploid production *via* zygote chromosome doubling by high temperature.

Time after pollination	Treatment temperature (°C)	Treatment duration (h)	No. of seeds	No. of Seedlings	No. of tetraploid	Tetraploid production rate (%)
23rd day	40	3	87	49	0	0
		6	56	37	0	0
	44	3	65	41	0	0
		6	52	36	0	0
	48	3	–	–	–	–
		6	–	–	–	–
24th day	40	3	97	42	0	0
		6	62	35	0	0
	44	3	58	30	1	3.33
		6	48	21	0	0
	48	3	–	–	–	–
		6	–	–	–	–
25th day	40	3	129	57	0	0
		6	97	47	0	0
	44	3	77	44	0	0
		6	69	31	2	6.45
	48	3	–	–	–	–
		6	–	–	–	–
26th day	40	3	154	68	0	0
		6	92	40	0	0
	44	3	78	25	0	0
		6	75	34	1	2.9
	48	3	–	–	–	–
		6	–	–	–	–
27th day	40	3	66	27	0	0
		6	19	9	0	0
	44	3	93	34	0	0
		6	145	47	0	0
	48	3	–	–	–	–
		6	–	–	–	–
28th day	40	3	87	49	0	0
		6	156	67	0	0
	44	3	236	130	0	0
		6	99	41	0	0
	48	3	–	–	–	–
		6	–	–	–	–

rounds of mitosis, multiple free nuclear endosperms scattered in the embryo sac could be observed (**Figure 1H**).

Inducing Zygotic Chromosome Doubling Through High Temperature

Based on the results from the cytological study of zygotic development (**Figure 1**), combined with the correlation between flower bud development time after pollination and the zygotic development period (**Table 1**), an experiment inducing zygotic chromosome doubling to obtain tetraploids by high temperature was carried out. Capsules were harvested at maturity the next year. In the treatment group with a temperature of 48°C and treatment durations of 3 or 6 h, the seeds could not be harvested, and the branches had dried up. However, the seeds could be harvested from groups treated with temperatures of 40°C or 44°C for 3 or 6 h (**Table 2**).

The number of seeds and seedlings was counted. A total of 2,197 *E. urophylla* treated seeds were harvested, and 1,074 seedlings survived after sowing and transplantation into pots (**Table 2**). Using diploids as control, the ploidy levels of 1,074 seedlings were detected by flow cytometry, and a total of 4 tetraploids were detected. Then, the ploidy of 4 plants was further determined by somatic chromosome counting. The chromosome numbers of diploid *E. urophylla* are $2n = 2 \times = 22$, and the chromosome numbers of the 4 plants are $2n = 4 \times = 44$ (**Figure 2**), so they could be determined to be tetraploids. At the same time, the untreated seeds of *E. urophylla* were harvested as control groups, and no tetraploids were detected in the control groups. The results showed that tetraploids could be

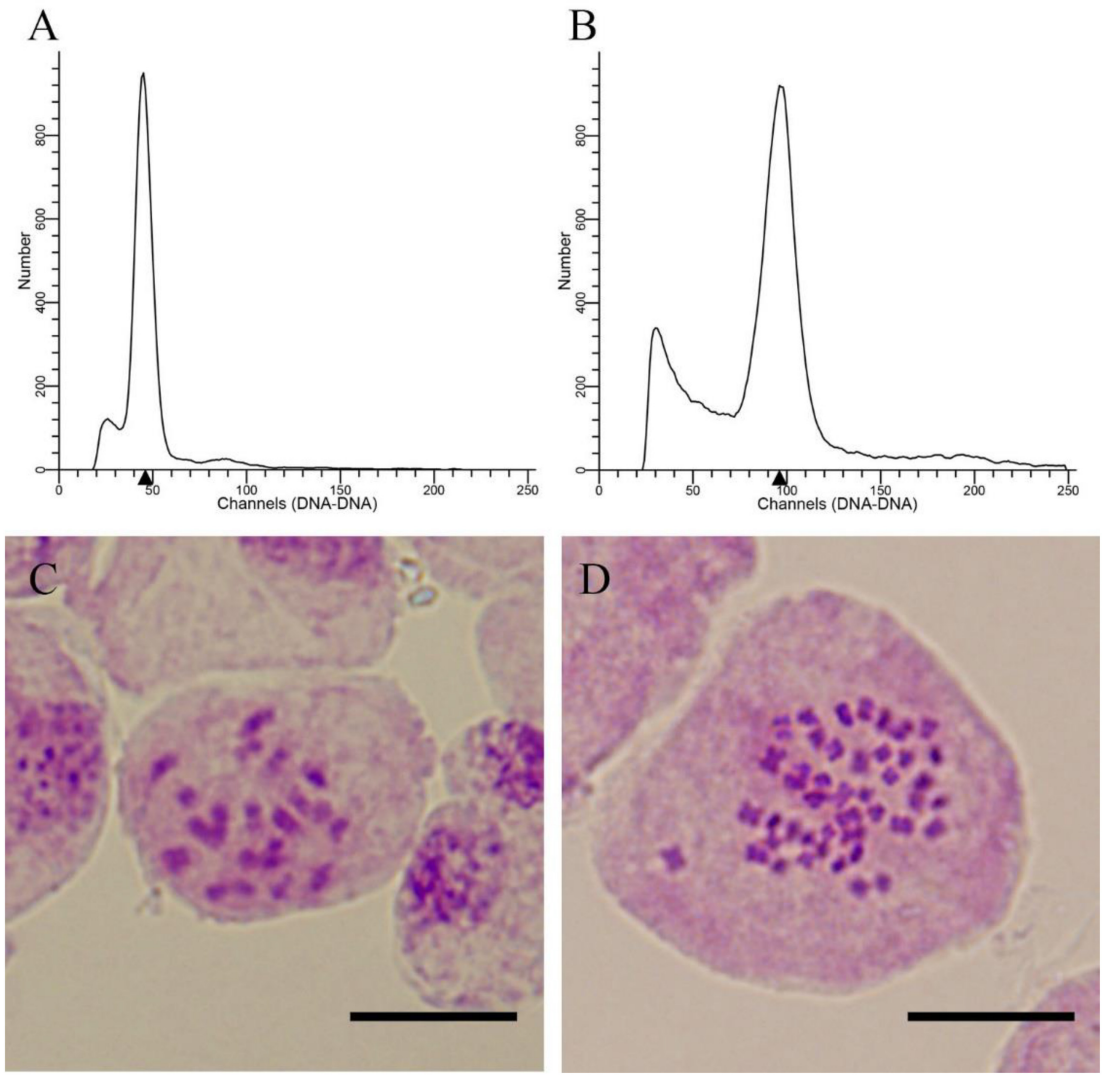

FIGURE 2 | Ploidy level detection of *E. urophylla* offspring. **(A)** Histogram of the flow cytometry results for diploids; **(B)** histogram of the flow cytometry results for the tetraploid; **(C)** somatic chromosome counting for the diploid (2n = 2 × = 22); and **(D)** somatic chromosome counting for the tetraploid (2n = 4 × = 44).

obtained from 24 to 26 days after pollination and treated at 44°C for 3 or 6 h. The appropriate conditions for inducing zygotic chromosome doubling of *E. urophylla* were treating flower branches at 44°C for 6 h on the 25th day after pollination.

Comparison of Growth Traits

Tetraploids and their diploid controls after undergoing clonal propagation were used to measure growth traits (**Figure 3** and **Table 3**). When *E. urophylla* clones grew for 6 months, there was no significant difference in plant height between the tetraploids and diploids, but the ground diameter of the tetraploids decreased significantly. The number of leaves per ramet of tetraploids was only approximately half that of diploids. Several leaf attributes also varied between diploids and tetraploids. The mean leaf length of tetraploids was 9.43 cm, an increase of 78.26% compared to that of diploids. The mean leaf width of tetraploids was 2.62 cm, which was about twice that of diploids. The petiole connecting the leaf and stem of tetraploids was also longer than that of diploids. Additionally, the leaf area of tetraploids was more than three times that of diploids. After measuring leaf parameters, the leaf's fresh mass was weighed. The leaf fresh mass of tetraploids was 344.00% higher than that of diploids. After drying, the leaf dry mass of tetraploids increased by 263.64% compared with that of diploid leaves. Taking the ratio of leaf mass to leaf area, the leaf fresh mass per unit area of tetraploid leaves increased by 19.23% compared with that of diploids, but there were no significant differences in leaf dry mass per unit area between tetraploids and diploids.

Observation of Leaf Anatomical Features

There were also differences in the leaf anatomical structure of tetraploids and diploids in *E. urophylla* (**Figure 4** and

FIGURE 3 | Morphological features of diploid and tetraploid plants in *E. urophylla.* **(A)** Clonal propagation ramet of diploids (left) and tetraploids (right); and **(B)** fully expanded leaf blades of diploids (left) and tetraploids (right).

TABLE 3 | Growth characteristics of tetraploid and diploid *Eucalyptus urophylla*.

Characteristics	Diploid	Tetraploid	Difference (%)	Significance
Plant height (cm)	74.33 ± 3.54	75.14 ± 2.84	–	NS
Ground diameter (cm)	10.50 ± 0.72	8.42 ± 0.69	−19.81	***
No. of leaves per plant	368.80 ± 29.97	165.60 ± 17.34	−55.10	***
Leaf length (cm)	5.29 ± 0.28	9.43 ± 1.47	+ 78.26	***
Leaf width (cm)	2.62 ± 0.16	5.27 ± 0.67	+ 101.15	***
Petiole length (cm)	0.72 ± 0.06	1.03 ± 0.111	+ 43.06	***
Leaf area (cm^2)	10.32 ± 1.17	35.61 ± 8.56	+ 245.06	***
Leaf fresh mass (g)	0.25 ± 0.012	1.11 ± 0.305	+ 344.00	***
Leaf dry mass (g)	0.11 ± 0.009	0.40 ± 0.111	+ 263.64	***
Leaf fresh mass per unit area (g cm^{-2})	0.026 ± 0.0013	0.031 ± 0.0015	+ 19.23	***
Leaf dry mass per unit area (g cm^{-2})	0.011 ± 0.0007	0.011 ± 0.0009	–	NS

****for $P \leq 0.001$ and NS for $P > 0.05$.*

Table 4). The leaves and veins of tetraploids were 67.40 and 129.06% thicker than those of diploids, respectively. The xylem, palisade, and sponge cells were significantly enlarged in tetraploids compared to diploids. Moreover, the palisade cell arrangement in tetraploid leaves was denser, with an average of 112 palisade cells per unit length (mm^{-1}). In addition, the area of upper and lower epithelial cells in tetraploid leaves was significantly larger than that in diploid leaves.

Measurement of Photosynthetic Characteristics

The measurement results of photosynthetic parameters of *E. urophylla* tetraploids and diploids are shown in **Table 5**. The net photosynthetic rate (Pn) of tetraploids was 14.51 μmol m^{-2} s^{-1}, significantly higher than that of diploids. The water use efficiency (WUE_i) of tetraploids was also significantly higher than that of diploids. However, there were no significant differences between tetraploids and diploids in intercellular carbon dioxide concentration (Ci), stomatal conductance (Gs), and transpiration rate (Tr). The chlorophyll fluorescence parameters were also measured on the same day. There was no significant difference in the maximal photochemical efficiency of photosystem II (PSII) between tetraploids and diploids.

Observation of Stomata and Chloroplast Characteristics

There were significant differences in the number and density of stomata on the leaves between tetraploids and diploids (**Figure 5** and **Table 6**). The stomatal size of tetraploids increased significantly, with a length of 20.16 μm and a

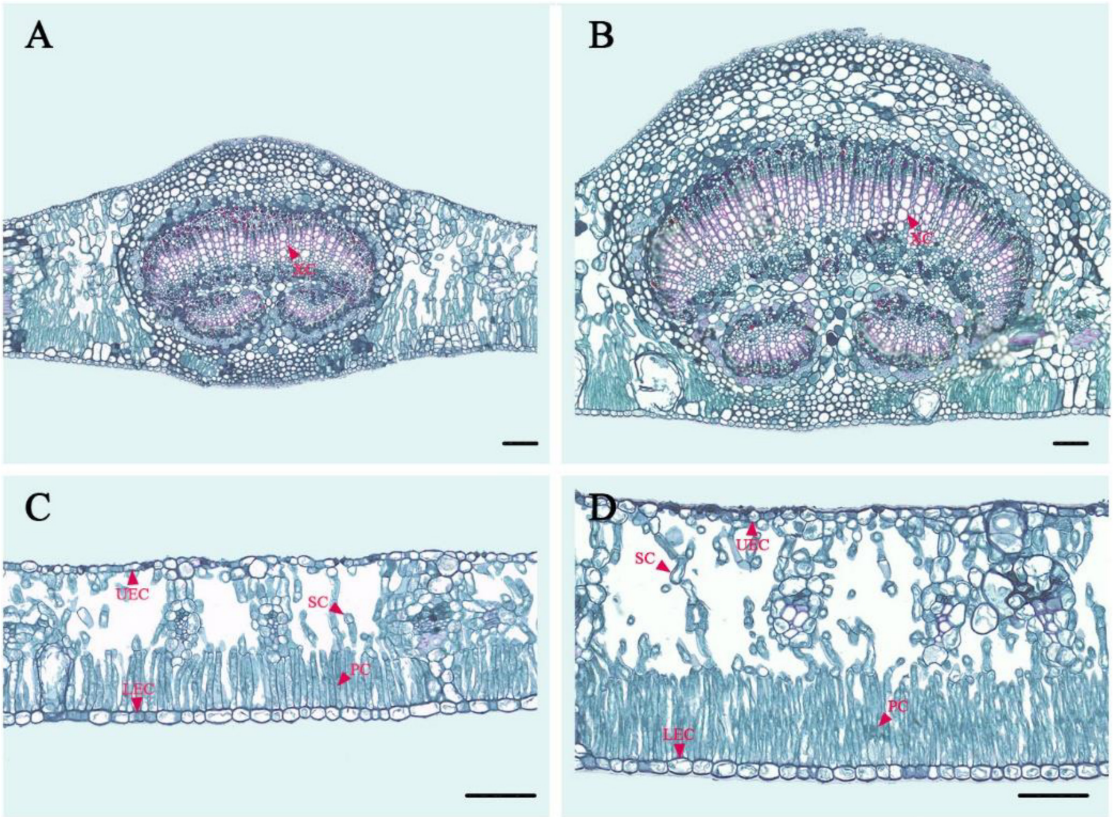

FIGURE 4 | Paraffin section of a diploid and tetraploid leaf in *E. urophylla.* **(A)** Vein anatomical structure of the diploid; **(B)** vein anatomical structure of the tetraploid; **(C)** leaf anatomical structure of the diploid; and **(D)** leaf anatomical structure of the tetraploid. XC, xylem cells; UEC, upper epidermis cells; LEC, lower epidermis cells; SC, sponge cells; PC, palisade cells.

TABLE 4 | The leaf anatomical structure of diploid and tetraploid *Eucalyptus urophylla*.

Characteristics	Diploid	Tetraploid	Difference (%)	Significance
Leaf thickness (μm)	243.11 ± 6.39	406.97 ± 3.77	+67.4	***
Veins thickness (μm)	513.16 ± 2.01	1175.43 ± 5.94	+129.06	***
Palisade cells (μm)	88.50 ± 2.39	133.21 ± 2.23	+50.52	***
Sponge cells (μm)	31.86 ± 2.73	41.42 ± 3.76	+30.01	**
Density of palisade cells (mm^{-1})	82.67 ± 2.79	112.00 ± 3.80	+35.48	***
Xylem cells (μm^2)	285.00 ± 18.47	694.00 ± 47.37	+143.51	***
Upper epidermis cells (μm^2)	452.76 ± 33.93	690.01 ± 78.29	+52.4	***
Lower epidermis cells (μm^2)	149.83 ± 60.97	299.83 ± 85.24	+100.11	***

****for $P \leq 0.001$ and **for $0.001 < P \leq 0.01$.*

width of 12.71 μm, which were 34.76 and 59.87% larger than that of diploids, respectively. However, while the stomata of tetraploids were enlarged, their stomatal density decreased by 22.67% compared with that of diploids, and there was only a mean of 360.75 stomata per mm^2 of tetraploid leaves. The mean number of chloroplasts in the guard cells of tetraploids was 17.5, which was significantly higher than that of diploids. The transmission electron microscopy results of diploid and tetraploid chloroplasts showed that the starch grains in diploid chloroplasts were fuller. Osmiophilic granules were more widely distributed in tetraploid chloroplasts, and the matrix lamella started to become loose locally, which was a manifestation of senescence and damage.

Measurement of Physiological Characteristics

The leaf physiological parameter measurements of *E. urophylla* diploids and tetraploids are shown in **Table 7**. There were significant differences in the contents of MDA, POD, and soluble sugars between tetraploids and diploids. However, there were no differences in the content of total protein and CAT between

TABLE 5 | Leaf photosynthetic parameters of diploid and tetraploid *Eucalyptus urophylla*.

Characteristics	Diploid	Tetraploid	Significance
Pn (μmol m^{-2} s^{-1})	12.53 ± 1.88	14.51 ± 1.16	*
Gs (mol m^{2} s^{-1})	0.171 ± 0.048	0.172 ± 0.024	NS
Ci (μmol m^{-1})	248.09 ± 23.50	241.2 ± 19.54	NS
Tr (mmol m^{-2} s^{-1})	4.079 ± 1.130	3.604 ± 0.431	NS
WUE_i	3.26 ± 0.85	4.08 ± 0.59	*
Fv/Fm	0.644 ± 0.037	0.627 ± 0.035	NS

**for 0.01 < P ≤ 0.05 and NS for P > 0.05.*

tetraploids and diploids. POD and soluble sugar contents were significantly elevated in tetraploids, but the MDA content decreased by 36.24% compared with that in diploids.

Observation of Oil Gland Characteristics

Under the microscope, differences in oil gland diameter and density between diploid and tetraploid leaves were observed (**Figure 6**). The mean diameter of oil glands in the leaves of tetraploids was 94.81 μm, being significantly larger than that of diploids. However, there was only a mean of 4.75 oil glands per cm^2 of tetraploid leaves, with a density that was significantly lower than that of diploid leaves.

Molecular Mechanism of Trait Variation

To deeply understand the molecular mechanism of tetraploid trait variation, several genes related to leaf growth and photosynthesis were selected for qRT-PCR (**Figure 7**). Leaf growth is a dynamic process, and according to the development time, the leaves were divided into three stages: young, mature, and senescent leaves. The expression patterns of genes controlling different traits were approximately the same in the three developmental stages of diploid and tetraploid leaves. The expression levels of *CYCD3;1*, a gene related to cell division, were relatively stable in diploid leaves but upregulated significantly in young tetraploid leaves. The expression patterns of *GRF5*, related to leaf expansion, and *LHCB4*, related to photosynthesis, were the same in diploids and tetraploids, and their expression levels were the highest in mature leaves. Compared with diploids, *GRF5* and *LHCB4* showed a higher expression across different stages in tetraploid leaves, and significant expression differences between tetraploids and diploids appeared in young and mature leaves. The expression of *PAO* related to chlorophyll degradation was gradually upregulated with the change in leaf stages, and that in tetraploid mature leaves was significantly higher than that in diploid leaves. *TMM*, the gene related to stomatal formation, showed an expression pattern opposite to that of *PAO*. The expression of *TMM* in tetraploids was lower than that in diploids

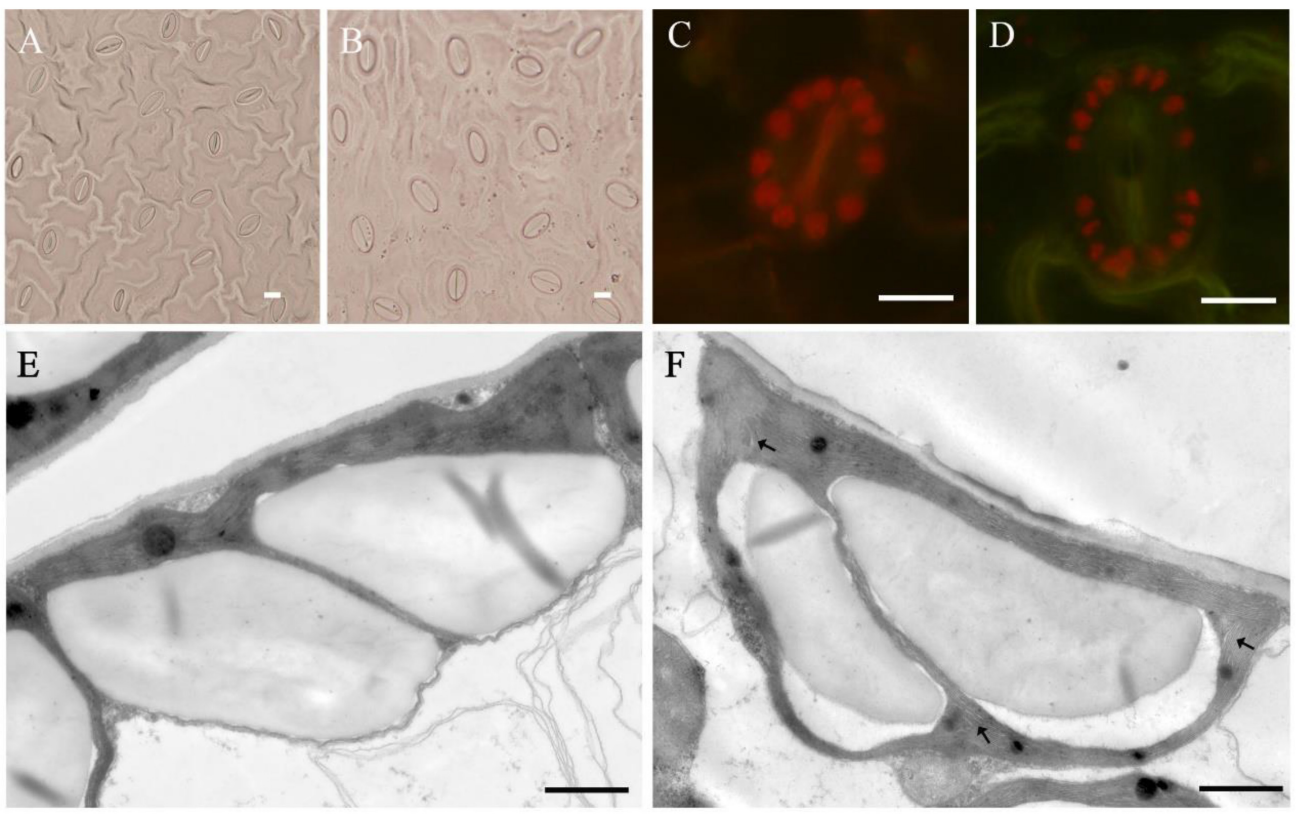

FIGURE 5 | Stomatal and chloroplast characteristics of tetraploids and diploids in *E. urophylla*. Stomata in the leaf of diploid **(A)** and tetraploid **(B)**; chloroplast number in stomata of diploid **(C)** and tetraploid **(D)**; ultrastructure of mesophyll cell chloroplasts of the diploid **(E)**; and tetraploid **(F)**. Arrows indicate sparse stroma lamella (**A–D**, bar = 10 μm; **E,F**, bar = 1 μm).

TABLE 6 | Stomatal characteristics of tetraploid and diploid *Eucalyptus urophylla*.

Ploidy	Stomatal length (μm)	Stomatal length (μm)	Stomatal density (No. mm^{-2})	No. of chloroplasts
Diploid	14.96 ± 1.19	7.95 ± 0.80	466.50 ± 23.13	11.13 ± 0.99
Tetraploid	20.16 ± 1.93	12.71 ± 0.95	360.75 ± 42.61	17.67 ± 1.35
Significance	***	***	***	***

****for $P \leq 0.001$.*

TABLE 7 | Physiological parameters of diploid and tetraploid *Eucalyptus urophylla*.

Ploidy	Protein (mg·gFW^{-1})	CAT (U·mgprot^{-1})	MDA (nmol·mgprot^{-1})	POD (U·mgprot^{-1})	Soluble sugar (mg·gFW^{-1})
Diploid	2.50 ± 0.51	325.67 ± 53.71	9.05 ± 0.86	11.61 ± 1.50	16.35 ± 0.79
Tetraploid	3.44 ± 0.49	344.57 ± 60.35	5.77 ± 0.80	16.71 ± 0.55	19.99 ± 0.83
Significance	NS	NS	***	***	**

****for $P \leq 0.001$, **for $0.001 < P \leq 0.01$, and NS for $P > 0.05$.*

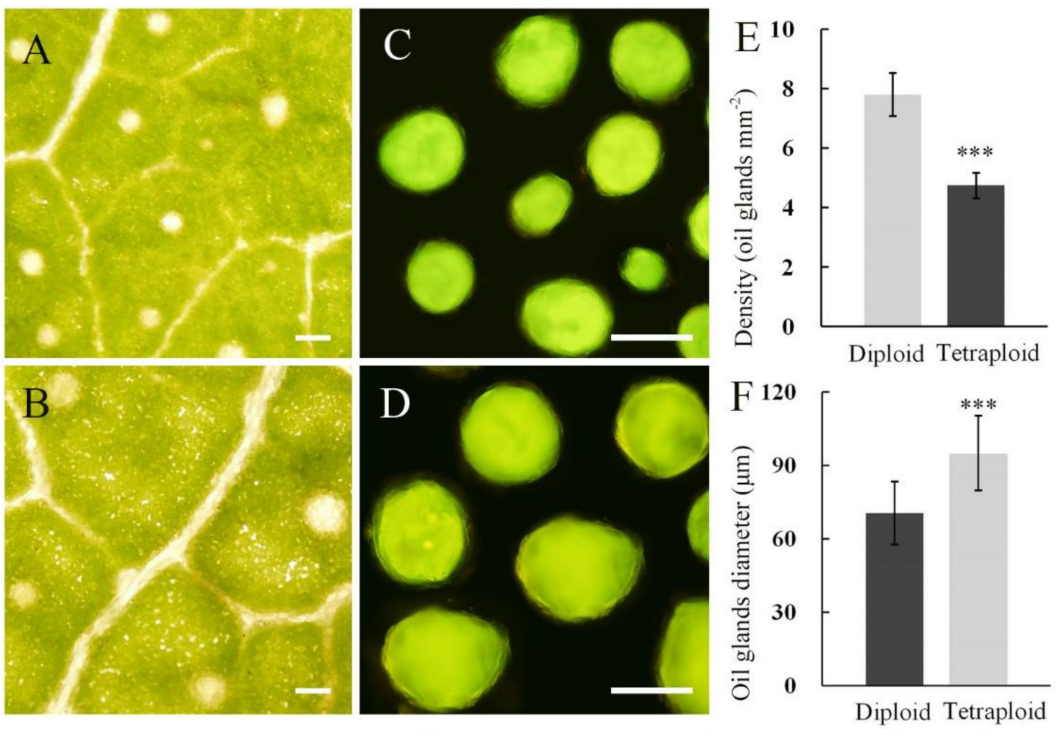

FIGURE 6 | Oil gland characteristics of *E. urophylla* tetraploids and diploids. Oil glands in the leaf of diploid **(A)** and tetraploid **(B)**; oil glands isolated from the diploid **(C)** and tetraploid **(D)** leaf; **(E)** for measurements of oil gland density; and **(F)** for measurements of oil gland diameter (bar = 100 μm). ***for $P \leq 0.001$.

during the entire leaf growth process, and especially in mature leaves, there was a significant difference between them.

DISCUSSION

Most of the previous studies on tetraploids focused on somatic chromosome doubling in *Eucalyptus* (Silva et al., 2019; Castillo et al., 2020; Moura et al., 2020). Induced zygotic chromosome doubling has been successfully applied in several plants (Randolph, 1932; Atwood, 1936; Guo et al., 2017). Surprisingly, there have been no reports on zygotic chromosome doubling to obtain *Eucalyptus* tetraploids. In this study, four *E. urophylla* tetraploids were successfully obtained by high-temperature treatment, and no mixoploidy was found in the process of ploidy level detection. Compared with somatic chromosome doubling, the polyploids obtained by zygotic chromosome doubling are stable, and there is no need to screen for mixoploidy (Lu et al., 2013). At the same time, zygotic chromosome doubling is a method to obtain polyploids by sexual reproduction. If controlled pollination is carried out before high-temperature treatment, the method has the potential

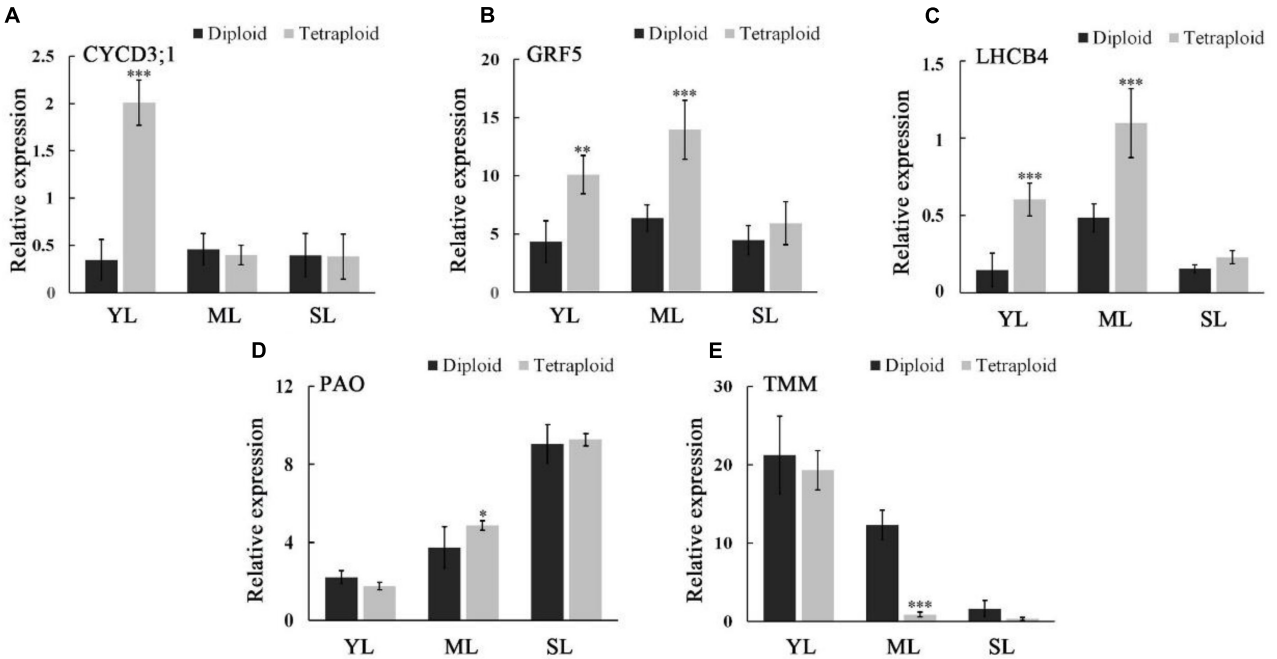

FIGURE 7 | Expressions of *CYCD3;1* **(A)**, *GRF5* **(B)**, *LHCB4* **(C)**, *PAO1* **(D)**, and *TMM* **(E)** were measured by real-time qRT-PCR in young leaves (YM), mature leaves (ML), and senescent leaves (SL) of diploids and tetraploids. ***for $P \leq 0.001$, **for $0.001 < P \leq 0.01$, and *for $0.01 < P \leq 0.05$.

to obtain multi-genotype and multi-trait polyploids (Wang J. et al., 2010; Guo et al., 2017). Additionally, zygotic chromosome doubling was induced by high temperature without any chemical mutagenic agent to avoid the risk of environmental pollution. Therefore, zygotic chromosome doubling induced by high temperature is an option for *Eucalyptus* germplasm innovation.

In this study, we explored the induction of zygotic chromosome doubling in *Eucalyptus* by high temperatures and found some factors restricting the efficiency of zygotic chromosome doubling. Previous studies have shown that the essence of chromosome doubling induced by high temperature was that high temperatures could affect spindle formation in a specific period of cell division, thus blocking the normal cell division process, and then causing chromosome doubling (Kang et al., 2000; Li et al., 2019). Therefore, the key to the successful induction of zygotic chromosome doubling of *E. urophylla* lies in the appropriate timing of mutagenesis treatment (Lu et al., 2013). In the cytological observation of zygote development, ovules in a two-cell proembryo stage and multicellular embryo stage could be observed in the same flower bud. This phenomenon of asynchronous zygotic development is common in plants (Pound et al., 2002, 2003) and seriously affects the judgment of the appropriate period of zygotic division for high-temperature treatment. At the same time, the phenomenon of asynchronous zygotic development also reduces the probability of applying the high-temperature treatment during the appropriate period of zygotic division, which greatly affects the mutagenesis efficiency and tetraploid yield. Therefore, we proposed that improving the proportion of zygotes in the appropriate division period during mutagenesis treatment to increase the tetraploid induction efficiency will be the focus of further research.

Additionally, the treatment temperature was chosen for two main reasons. One reason is that *E. urophylla* always blooms in the summer (from June to August in southern China), and the daily extreme temperature reaches 40°C, but tetraploid offspring have not been found in nature or in the untreated control groups of this study, indicating that temperatures of 40°C or lower are insufficient to induce zygotic chromosome doubling in *E. urophylla*. Our study showed that seeds could not be harvested when the treatment temperature reached 48°C, so the suitable treatment temperature for the mutagenesis of *E. urophylla* should be between 40 and 48°C. To determine the appropriate treatment conditions for zygotic chromosome doubling, the process of zygotic development of *E. urophylla* was tracked, and the treatment was performed at different temperatures. Using the pollination time as the reference, the results showed that a treatment at 44°C for 6 h on the 25th day after pollination was the most appropriate for inducing zygotic chromosome doubling in *E. urophylla*. This conclusion provides an important reference for polyploid induction in other *Eucalyptus* species.

As is the case in other polyploids, the leaf characteristics of tetraploids obtained by zygotic chromosome doubling were significantly different from those of diploids. The results showed that the leaf area of tetraploids was significantly larger than that of diploids. The observation of leaf anatomical structures found that the cell size and leaf thickness of tetraploids were also significantly increased compared with those of diploids, which may be the reason for the increase in water content in tetraploid leaves, making the leaf fresh mass per unit area of

tetraploids significantly higher than that of diploids. The increase in leaf area is a common phenomenon after polyploidization, such as that seen in tetraploid *Morus multicaulis* and *Platanus acerifolia*, which have larger leaves than diploids (Liu et al., 2007; Wang X. L. et al., 2010). However, it should be noted that the changes in leaf length and leaf width after polyploidization are not consistent. For example, Fernando et al. (2019) reported that the ratio of leaf length to leaf width of the autotetraploid *Eucalyptus polybractea* did not change compared with that of the diploid. In this study, the leaf width of tetraploids with zygotic chromosome doubling increased more than the leaf length, resulting in a change of leaf shape, which may be due to gene recombination in the process of sexual reproduction (Sattler et al., 2016). This showed that compared with the autotetraploid obtained by somatic chromosome doubling, tetraploids based on zygotic chromosome doubling have more abundant genetic variation, which is very important for breeding germplasm with high yield, good resistance, and other properties with high economic value.

The Pn of *E. urophylla* tetraploids was significantly higher than that of diploids. The Pn per unit leaf area is the product of the Pn of a single cell and the number of photosynthetic cells per unit leaf area (Warner and Edwards, 1989). If cell accumulation is changed to allow more cells per unit leaf area, the Pn per unit leaf area will increase (Warner and Edwards, 1993; Cao et al., 2018). This study found that the number of palisade cells per unit length increased significantly in the longitudinal section of tetraploid leaves. This may be the main reason for the increase in Pn of tetraploids. Additionally, the number of chloroplasts in the mesophyll cells of tetraploids is significantly higher than that of diploids, which may be another reason for the increase in Pn (Jellings and Leech, 1984; Warner et al., 1987). The enlargement of guard cells and stomatal volume caused by the polyploidization did not significantly change the Ci, Gs, and Tr of *E. urophylla*. This may be because the number of stomata per unit leaf area in tetraploids declined in proportion to the increase in stomatal size, and the parameters may be the same as in diploids, having smaller stomata but with higher stomatal density (Harrison et al., 2020). The chlorophyll fluorescence parameters of diploids did not change significantly, which was consistent with the study by Liao et al. (2016) in *Populus*. In general, chlorophyll fluorescence parameters are essentially constant in living plants unless they are exposed to extreme biological and abiotic stress conditions (Björkman and Demmig, 1987).

Growth characteristics of diploids and tetraploids were measured in *E. urophylla*, and tetraploids were found to grow more slowly. Although there was no difference in plant height between tetraploids and diploids, the basal diameter growth of tetraploids was significantly slower than that of diploids. In a previous study of *Eucalyptus polybractea*, Fernando et al. (2019) reported that tetraploids may be more susceptible to water stress affecting their growth. This study found that tetraploids with the same seedling age had fewer leaves. Leaves were the main organ for photosynthesis (Smith et al., 1997), and reductions in the number of leaves led to a decrease in the Pn of the whole plant and carbon fixation efficiency, which may be a reason for their slower growth (Offermann and Peterhansel, 2014). On the contrary, although the Pn of tetraploids increased, the Gs did not significantly change. This restricted the capacity for CO_2 absorption and limited the upper limit of improvement of Pn (Harrison et al., 2020). However, the increase in mesophyll cell size and density increased the energy required to produce cells and maintain cell functions (Nowicka et al., 2018; Siqueira et al., 2018). The increase in carbon fixation caused by the Pn increase cannot compensate for the increase in carbon metabolism caused by changes in cell size and density, which may be another reason for the slow growth of tetraploids.

After polyploidization, the physiological parameters and secondary metabolites of *E. urophylla* also changed. The MDA content decreased and the POD content increased in tetraploid leaves. Due to these contents are related to the stress resistance of plants, it can be inferred that tetraploids may have stronger environmental adaptability (Zhou et al., 2020). Additionally, an increase in soluble sugar content was detected in tetraploids. This result was also reported in the study of apple and ginger polyploidy (Xue et al., 2017; Zhou et al., 2020). This may be caused by changes in cell volume or cell wall components after polyploidization (Madadi et al., 2021). At the same time, the size of oil glands in leaves also increased with polyploidization (Fernando et al., 2019). Although the interaction between the increase in oil gland volume and the decrease in density led to no significant changes in the content of essential oils after polyploidization in *Eucalyptus polybractea*, tetraploids containing larger oil glands are a potential resource for cultivating new *Eucalyptus* varieties with higher essential oil contents.

The changes in plant characteristics after polyploidization are mainly caused by changes in gene expression. In plants, genome replication increases the complexity of genetic composition and affects plant gene expression (Scarrow et al., 2021). After polyploidization, the expression of genes related to chlorophyll synthesis in *Arabidopsis thaliana* and *Chrysanthemum nankingense* was upregulated, resulting in enhanced photosynthesis (Ni et al., 2009; Dong et al., 2017). The upregulated expression of *GRF5* in *Populus* polyploids leads to its production of leaves with a larger leaf area (Wu et al., 2021). Exploring the differences in gene expression after plant polyploidization is of great significance for analyzing the variation of polyploid traits (Du et al., 2020). In this study, genes related to leaf growth and expansion were analyzed by qRT-PCR. *CYCD3;1* plays a role in cell division and proliferation, and it was only differentially expressed in diploid and tetraploid young leaves, which indicates that a significant increase in mesophyll cells of the tetraploid mainly occurred in young leaves (Dewitte et al., 2003; de Jager et al., 2009). In *Populus*, overexpressing *CYCD3;1* could significantly increase the number of cells in leaves, but cell volume decreased (Guan et al., 2021). However, the cell volume increased after tetraploidy in *E. urophylla* (**Figures 4D**, **6F**). The upregulated expression of *GRF5* can increase cell volume (Wu et al., 2021), and the expression of *GRF5* in both young and mature tetraploid leaves was significantly higher than that in diploid leaves, which may cause the enlargement of cell volume. The increase in cell number and volume can remarkably increase plant organ size, which also

suggests that changes in plant organs after polyploidy are caused by multiple gene expression changes.

This study also quantified the genes causing the changes in Pn of tetraploid *E. urophylla*. *PAO* encodes an enzyme that catalyzes chlorophyll decomposition, and its expression positively correlates with leaf senescence (Pružinská et al., 2003, 2005). The expression of *PAO* was only significantly increased in mature tetraploid leaves at the level of $0.01\% < P < 0.05\%$. The transmission electron microscopy observation of chloroplasts also found only a slight difference between tetraploids and diploids, indicating that chlorophyll degradation may not be an important reason for the differences in the Pn of mature leaves of tetraploids and diploids. *LHCB4* encodes a protein involved in PSII composition (de Bianchi et al., 2011). The expression of *LHCB4* in both young and mature tetraploid leaves was significantly higher than that in diploid leaves. It has been speculated that the difference in the PSII formation process may be one of the reasons for the enhanced photosynthesis in tetraploids. Additionally, stomata also affect photosynthesis (Harrison et al., 2020). *TMM* is a key gene controlling stomatal development (Chowdhury et al., 2021), and the significant downregulation of its expression in tetraploids resulted in a decrease in leaf stomatal density, which restricted the upper limit of tetraploid photosynthesis. The above results provide a new perspective for understanding the changes in Pn of polyploid plants.

CONCLUSION

In this study, tetraploid *E. urophylla* was successfully obtained for the first time by inducing zygotic chromosome doubling at high temperatures, and changes in its characteristics and gene expression were studied. Although the tetraploid grew slowly, it showed some advantages, such as larger and thicker leaves, higher Pn, and higher secondary metabolite contents. Trends in the expression of genes related to trait formation were the same as those of traits, indicating that tetraploid trait variation was mainly caused by changes in gene expression. Although the tetraploid had no growth advantages, it can provide important germplasm resources for future breeding, especially for the creation of triploids.

DATA AVAILABILITY STATEMENT

The datasets presented in this study can be found in online repositories. The names of the repository/repositories and accession number(s) can be found in the article/ **Supplementary Material**.

AUTHOR CONTRIBUTIONS

JY and XK conceived and designed the research. ZL, JW, and ZM conducted the experiments. ZL, BQ, and TL collected and analyzed the data. ZL and JY wrote the manuscript. XK provided valuable suggestions on the manuscript. All authors read and approved the final manuscript.

FUNDING

This research was supported by the National Key R&D Program of China during the 14th Five-Year Plan period (2021YFD2200104) and the National Natural Science Foundation of China (31901337).

SUPPLEMENTARY MATERIAL

The Supplementary Material for this article can be found online at: https://www.frontiersin.org/articles/10.3389/fpls.2022.870698/full#supplementary-material

REFERENCES

Assis, T., Warburton, P., and Harwood, C. (2005). Artificially induced protogyny: an advance in the controlled pollination of *Eucalyptus*. *Aust. For.* 68, 27–33. doi: 10.1080/00049158.2005.10676223

Atwood, S. (1936). Tetraploid and aneuploid *Melilotus alba* aesulting from heat treatment. *Am. J. Bot.* 23, 674–677. doi: 10.2307/2436348

Björkman, O., and Demmig, B. (1987). Photon yield of O2 evolution and chlorophyll fluorescence characteristics at 77 K among vascular plants of diverse origins. *Planta* 170, 489–504. doi: 10.1007/BF00402983

Bon, P. V., Harwood, C. E., Nghiem, Q. C., Thinh, H. H., Son, D. H., and Chinh, N. V. (2020). Growth of triploid and diploid *Acacia* clones in three contrasting environments in Vietnam. *Aust. For.* 83, 265–274. doi: 10.1080/00049158.2020.1819009

Cao, Q., Zhang, X., Gao, X., Wang, L., and Jia, G. (2018). Effects of ploidy level on the cellular, photochemical and photosynthetic characteristics in Lilium FO hybrids. *Plant Physiol. Biochem.* 133, 50–56. doi: 10.1016/j.plaphy.2018.10.027

Castillo, A., López, V., Tavares, E., Santiaque, F., and Dalla, M. R. (2020). Polyploid induction of *Eucalyptus dunnii* Maiden to generate variability in breeding programs. *Agroci. Urug.* 24:381. doi: 10.31285/AGRO.24.381

Cha-um, S., and Kirdmanee, C. (2010). Effects of water stress induced by sodium chloride and mannitol on proline accumulation, photosynthetic abilities and growth characters of eucalyptus (*Eucalyptus camaldulensis Dehnh.*). *New For.* 40, 349–360. doi: 10.1007/s11056-010-9204-1

Chowdhury, M. R., Ahamed, M. S., Mas-Ud, M. A., Islam, H., Fatamatuzzohora, M., Hossain, M. F., et al. (2021). Stomatal development and genetic expression in *Arabidopsis thaliana L. Heliyon* 7:e07889. doi: 10.1016/j.heliyon.2021.e07889

de Bianchi, S., Betterle, N., Kouril, R., Cazzaniga, S., Boekema, E., Bassi, R., et al. (2011). *Arabidopsis* mutants deleted in the light harvesting protein LHCB4 have a disrupted photosystem II macrostructure and are defective in photoprotection. *Plant Cell* 23, 2659–2679. doi: 10.1105/tpc.111.087320

de Jager, S. M., Scofield, S., Huntley, R. P., Robinson, A. S., den Boer, B. G. W., and Murray, J. A. H. (2009).). Dissecting regulatory pathways of G1/S control in *Arabidopsis*: common and distinct targets of CYCD3;1, E2Fa and E2Fc. *Plant Mol. Biol.* 71, 345–365. doi: 10.1007/s11103-009-9527-5

Dewitte, W., Riou-Khamlichi, C., Scofield, S., Healy, J. M. S., Jacqmard, A., Kilby, N. J., et al. (2003). Altered cell cycle distribution, hyperplasia, and inhibited differentiation in *Arabidopsis* caused by the D-type cyclin CYCD3. *Plant Cell* 15, 79–92. doi: 10.1105/tpc.004838

Dhakad, A. K., Pandey, V. V., Beg, S., Rawat, J. M., and Singh, A. (2018). Biological, medicinal and toxicological significance of *Eucalyptus* leaf essential oil: a review. *J. Sci. Food Agric.* 98, 833–848. doi: 10.1002/jsfa.8600

Dong, B., Wang, H., Liu, T., Cheng, P., Chen, Y., Chen, S., et al. (2017). Whole genome duplication enhances the photosynthetic capacity of *Chrysanthemum*

nankingense. *Mol. Genet. Genomics* 292, 1247–1256. doi: 10.1007/s00438-017-1344-y

Du, K., Liao, T., Ren, Y., Geng, X., and Kang, X. (2020). Molecular mechanism of vegetative growth advantage in allotriploid *Populus*. *Int. J. Mol. Sci.* 21:441. doi: 10.3390/ijms21020441

Fernando, S. C., Goodger, J. Q. D., Chew, B. L., Cohen, T. J., and Woodrow, I. E. (2019). Induction and characterisation of tetraploidy in *Eucalyptus polybractea* R.T. Baker. *Ind. Crops Prod.* 140:111633. doi: 10.1016/j.indcrop.2019.111633

Goodger, J. Q., Heskes, A. M., Mitchell, M. C., King, D. J., Neilson, E. H., and Woodrow, I. E. (2010). Isolation of intact sub-dermal secretory cavities from *Eucalyptus*. *Plant Methods* 6:20. doi: 10.1186/1746-4811-6-20

Goodger, J. Q., and Woodrow, I. E. (2011). Alpha,beta-unsaturated monoterpene acid glucose esters: structural diversity, bioactivities and functional roles. *Phytochemistry* 72, 2259–2266. doi: 10.1016/j.phytochem.2011.08.026

Gordej, I. S., Lyusikov, O. M., and Gordej, I. A. (2019). Zygotic autopolyploidization of rye (*Secale cereale L.*). *Cytol. Genet.* 53, 357–362. doi: 10.3103/s0095452719050086

Guan, C., Xue, Y., Jiang, P., He, C., Zhuge, X., Lan, T., et al. (2021). Overexpression of PtoCYCD3;3 promotes growth and causes leaf wrinkle and branch appearance in *Populus*. *Int. J. Mol. Sci.* 22:1288. doi: 10.3390/ijms22031288

Guo, L., Xu, W., Zhang, Y., Zhang, J., and Wei, Z. (2017). Inducing triploids and tetraploids with high temperatures in *Populus sect. Tacamahaca*. *Plant Cell Rep.* 36, 313–326. doi: 10.1007/s00299-016-2081-0

Guo, Y., Li, X., Huang, F., Pang, X., and Li, Y. (2019). Megasporogenesis, microsporogenesis, and female and male gametophyte development in *Ziziphus jujuba* Mill. *Protoplasma* 256, 1519–1530. doi: 10.1007/s00709-019-01395-x

Harrison, E. L., Arce Cubas, L., Gray, J. E., and Hepworth, C. (2020). The influence of stomatal morphology and distribution on photosynthetic gas exchange. *Plant J.* 101, 768–779. doi: 10.1111/tpj.14560

Hung, T. D., Brawner, J. T., Meder, R., Lee, D. J., Southerton, S., Thinh, H. H., et al. (2014). Estimates of genetic parameters for growth and wood properties in *Eucalyptus pellita F. Muell.* to support tree breeding in Vietnam. *Ann. For. Sci.* 72, 205–217. doi: 10.1007/s13595-014-0426-9

Jellings, A. J., and Leech, R. M. (1984). Anatomical variation in first leaves of nine *Triticum* genotypes, and its relationship to puotosynthetic capacity. *New Phytol.* 96, 371–382. doi: 10.1111/j.1469-8137.1984.tb03573.x

Jiao, Y., Wickett, N. J., Ayyampalayam, S., Chanderbali, A. S., Landherr, L., Ralph, P. E., et al. (2011). Ancestral polyploidy in seed plants and angiosperms. *Nature* 473, 97–100. doi: 10.1038/nature09916

Kang, X. Y., Zhu, Z. T., and Zhang, Z. Y. (2000). Suitable period of high temperature treatment for 2n pollen of *Populus tomentosa* ×P .bolleana. *J. Beijing For. Univ.* 22, 1–4.

Kato, A., and Birchler, J. A. (2006). Induction of tetraploid derivatives of maize inbred lines by nitrous oxide gas treatment. *J. Hered.* 97, 39–44. doi: 10.1093/jhered/esj007

Li, D., Tian, J., Xue, Y., Chen, H., and Wang, J. (2019). Triploid production via heat-induced diploidisation of megaspores in *Populus pseudo-simonii*. *Euphytica* 215, 11–20. doi: 10.1007/s10681-018-2330-0

Liao, T., Cheng, S., Zhu, X., Min, Y., and Kang, X. (2016). Effects of triploid status on growth, photosynthesis, and leaf area in *Populus*. *Trees* 30, 1137–1147. doi: 10.1007/s00468-016-1352-2

Liu, G., Li, Z., and Bao, M. (2007). Colchicine-induced chromosome doubling in *Platanus acerifolia* and its effect on plant morphology. *Euphytica* 157, 145–154. doi: 10.1007/s10681-007-9406-6

Lu, M., Zhang, P., Wang, J., Kang, X., Wu, J., Wang, X., et al. (2013). Induction of tetraploidy using high temperature exposure during the first zygote division in *Populus adenopoda* Maxim. *Plant Growth Regul.* 72, 279–287. doi: 10.1007/s10725-013-9859-7

Madadi, M., Zhao, K., Wang, Y., Wang, Y., Tang, S., Xia, T., et al. (2021). Modified lignocellulose and rich starch for complete saccharification to maximize bioethanol in distinct polyploidy potato straw. *Carbohydr. Polym.* 265:118070. doi: 10.1016/j.carbpol.2021.118070

Moura, L. C., Xavier, A., Viccini, L. F., Batista, D. S., Matos, E. M., Gallo, R., et al. (2020). Induction and evaluation of tetraploid plants of *Eucalyptus urophylla* clones. *Aust. J. Crop Sci.* 14, 1786–1793. doi: 10.21475/ajcs.20.14.11.p2564

Ni, Z., Kim, E. D., Ha, M., Lackey, E., Liu, J., Zhang, Y., et al. (2009). Altered circadian rhythms regulate growth vigour in hybrids and allopolyploids. *Nature* 457, 327–331. doi: 10.1038/nature07523

Nowicka, B., Ciura, J., Szymańska, R., and Kruk, J. (2018). Improving photosynthesis, plant productivity and abiotic stress tolerance – current trends and future perspectives. *J. Plant Physiol.* 231, 415–433. doi: 10.1016/j.jplph.2018.10.022

Offermann, S., and Peterhansel, C. (2014). Can we learn from heterosis and epigenetics to improve photosynthesis? *Curr. Opin. Plant Biol.* 19, 105–110. doi: 10.1016/j.pbi.2014.05.010

Pound, L. M., Wallwork, M. A. B., Potts, B. M., and Sedgley, M. (2002). Early ovule development following self- and cross-pollinations in *Eucalyptus globulus Labill.* ssp. globulus. *Ann. Bot.* 89, 613–620. doi: 10.1093/aob/mcf089

Pound, L. M., Wallwork, M. A. B., Potts, B. M., and Sedgley, M. (2003). Pollen tube growth and early ovule development following self- and cross-pollination in *Eucalyptus nitens*. *Sex. Plant Reprod.* 16, 59–69. doi: 10.1007/s00497-003-0175-7

Pružinská, A., Tanner, G., Anders, I., Roca, M., and Hörtensteiner, S. (2003). Chlorophyll breakdown: Pheophorbide a oxygenase is a Rieske-type iron–sulfur protein, encoded by the accelerated cell death 1 gene. *Proc. Natl. Acad. Sci.* 100, 15259–15264. doi: 10.1073/pnas.2036571100

Pružinská, A., Tanner, G., Aubry, S., Anders, I., Moser, S., Muller, T., et al. (2005). Chlorophyll breakdown in senescent *Arabidopsis* leaves. Characterization of chlorophyll catabolites and of chlorophyll catabolic enzymes involved in the degreening reaction. *Plant Physiol.* 139, 52–63. doi: 10.1104/pp.105.065870

Randolph, L. F. (1932). Some effects of high temperature on polyploidy and other variations in maize. *Proc. Natl. Acad. Sci. U.S.A.* 18, 222–229. doi: 10.1073/pnas.18.3.222

Ren, Y., Jing, Y., and Kang, X. (2021). In vitro induction of tetraploid and resulting trait variation in *Populus alba* × *Populus* glandulosa clone 84 K. *Plant Cell Tissue Organ Cult.* 146, 285–296. doi: 10.1007/s11240-021-02068-5

Sattler, M. C., Carvalho, C. R., and Clarindo, W. R. (2016). The polyploidy and its key role in plant breeding. *Planta* 243, 281–296. doi: 10.1007/s00425-015-2450-x

Scarrow, M., Wang, Y., and Sun, G. (2021). Molecular regulatory mechanisms underlying the adaptability of polyploid plants. *Biological Reviews* 96, 394–407. doi: 10.1111/brv.12661

Silva, A. J., Carvalho, C. R., and Clarindo, W. R. (2019). Chromosome set doubling and ploidy stability in synthetic auto- and allotetraploid of *Eucalyptus*: from in vitro condition to the field. *Plant Cell Tissue Organ Cult.* 138, 387–394. doi: 10.1007/s11240-019-01627-1

Siqueira, J. A., Hardoim, P., Ferreira, P. C. G., Nunes-Nesi, A., and Hemerly, A. S. (2018). Unraveling interfaces between energy metabolism and cell cycle in plants. *Trends Plant Sci.* 23, 731–747. doi: 10.1016/j.tplants.2018.05.005

Smith, W. K., Vogelmann, T. C., DeLucia, E. H., Bell, D. T., and Shepherd, K. A. (1997). Leaf form and photosynthesis. *Am. Inst. Biol. Sci.* 47, 785–793. doi: 10.2307/1313100

Soltis, D. E., Albert, V. A., Leebens-Mack, J., Bell, C. D., Paterson, A. H., Zheng, C., et al. (2009). Polyploidy and angiosperm diversification. *Am. J. Bot.* 96, 336–348. doi: 10.3732/ajb.0800079

Stikhareva, T., Ivashchenko, A., Kirillov, V., and Rakhimzhanov, A. (2021). Floristic diversity of threatened woodlands of Kazakhstan formed by *Populus* pruinosa Schrenk. *Turk. J. Agric. For.* 45, 165–178. doi: 10.3906/tar-2006-70

Tjio, J. H., and Whang, J. (1962). Chromosome preparatons of bone marrow cells without prior in vitro culture or in vivo colchicine administration. *Stain Technol.* 37, 17–20. doi: 10.3109/10520296209114563

Wang, J., Kang, X. Y., Shi, L., Lu, Min, and Yang, J. (2010). Tetraploid induction of *Populus* hybrid in section *tacamahaca* through zygotic chromosome doubling with physical and chemical treatments. *J. Beijing For. Univ.* 32, 63–66. doi: 10.13332/j.1000-1522.2010.05.020

Wang, L. J., Cao, Q. Z., Zhang, X. Q., and Jia, G. X. (2021). Effects of polyploidization on photosynthetic characteristics in three Lilium species. *Sci. Hortic.* 284:110098. doi: 10.1016/j.scienta.2021.110098

Wang, X. L., Zhou, J. X., Yu, M. D., Li, Z. G., Jin, X. Y., and Li, Q. Y. (2010). Highly efficient plant regeneration and in vitro polyploid induction using hypocotyl explants from diploid mulberry (*Morus* multicaulis Poir.). *Vitro Cell. Dev. Biol. Plant* 47, 434–440. doi: 10.1007/s11627-010-9328-1

Warner, D. A., and Edwards, G. E. (1989). Effects of polyploidy on photosynthetic rates, photosynthetic enzymes, contents of DNA, chlorophyll, and sizes and numbers of photosynthetic cells in the C4 dicot *Atriplex confertifolia*. *Plant Physiol.* 91, 1143–1151. doi: 10.1104/pp.91.3.1143

Warner, D. A., and Edwards, G. E. (1993). Effects of polyploidy on photosynthesis. *Photosynth. Res.* 35, 135–147. doi: 10.1007/BF00014744

Warner, D. A., Ku, M. S. B., and Edwards, G. E. (1987). Photosynthesis, leaf anatomy, and cellular constituents in the polyploid C4 grass *Panicum virgatum*. *Plant Physiol.* 84, 461–466. doi: 10.1104/pp.84.2.461

Wu, J., Sang, Y., Zhou, Q., and Zhang, P. (2020). Colchicine in vitro tetraploid induction of *Populus* hopeiensis from leaf blades. *Plant Cell Tissue Organ Cult.* 141, 339–349. doi: 10.1007/s11240-020-01790-w

Wu, W., Li, J., Wang, Q., Lv, K., Du, K., Zhang, W., et al. (2021). Growth-regulating factor 5 (GRF5)-mediated gene regulatory network promotes leaf growth and expansion in poplar. *New Phytol.* 230, 612–628. doi: 10.1111/nph.17179

Xue, H., Zhang, B., Tian, J. R., Chen, M. M., Zhang, Y. Y., Zhang, Z. H., et al. (2017). Comparison of the morphology, growth and development of diploid and autotetraploid 'Hanfu' apple trees. *Sci. Hortic.* 225, 277–285. doi: 10.1016/j.scienta.2017.06.059

Yang, J., Wang, J., Liu, Z., Xiong, T., Lan, J., Han, Q., et al. (2018). Megaspore chromosome doubling in *Eucalyptus urophylla* S.T. Blake induced by colchicine treatment to produce triploids. *Forests* 9:728. doi: 10.3390/f9110728

Yao, P. Q., Li, G. H., Qiu, Y. F., and Kang, X. Y. (2020). Induction of 2n female gametes in rubber (*Hevea brasiliensis*) by high-temperature exposure during megasporogenesis as a basis for triploid breeding. *Tree Genet. Genomes* 16:24. doi: 10.1007/s11295-020-1413-y

Zhang, Y. S., Chen, J. J., Cao, Y. M., Duan, J. X., and Cai, X. D. (2020). Induction of tetraploids in 'Red Flash' caladium using colchicine and oryzalin: Morphological, cytological, photosynthetic and chilling tolerance analysis. *Sci. Hortic.* 272:109524. doi: 10.1016/j.scienta.2020.109524

Zhang, Y., Wang, B., Qi, S., Dong, M., Wang, Z., Li, Y., et al. (2019). Ploidy and hybridity effects on leaf size, cell size and related genes expression in triploids, diploids and their parents in *Populus*. *Planta* 249, 635–646. doi: 10.1007/s00425-018-3029-0

Zhou, J., Guo, F., Fu, J., Xiao, Y., and Wu, J. (2020). In vitro polyploid induction using colchicine for *Zingiber Officinale* Roscoe cv. 'Fengtou' ginger. *Plant Cell Tissue Organ Cult.* 142, 87–94. doi: 10.1007/s11240-020-01842-1

Zhu, Z. T., Kang, X. Y., and Zhang, Z. Y. (1998). Study on natural triploid selection of *Populus tomentosa*. *Sci. Silvae Sin.* 34, 22–31.

Conflict of Interest: The authors declare that the research was conducted in the absence of any commercial or financial relationships that could be construed as a potential conflict of interest.

Publisher's Note: All claims expressed in this article are solely those of the authors and do not necessarily represent those of their affiliated organizations, or those of the publisher, the editors and the reviewers. Any product that may be evaluated in this article, or claim that may be made by its manufacturer, is not guaranteed or endorsed by the publisher.

frontiers | Frontiers in Plant Science

ORIGINAL RESEARCH
published: 04 May 2022
doi: 10.3389/fpls.2022.900768

Establishing Tetraploid Embryogenic Cell Lines of *Magnolia officinalis* to Facilitate Tetraploid Plantlet Production and Phenotyping

Yanfen Gao[1,2†], Junchao Ma[1†], Jiaqi Chen[1,2], Qian Xu[1], Yanxia Jia[1], Hongying Chen[1], Weiqi Li[1] and Liang Lin[1]**

[1] Germplasm Bank of Wild Species, Kunming Institute of Botany, Chinese Academy of Sciences, Kunming, China,
[2] University of the Chinese Academy of Sciences, Beijing, China

OPEN ACCESS

Edited by:
Jen-Tsung Chen,
National University of Kaohsiung, Taiwan

Reviewed by:
Wellington Ronildo Clarindo
Wellington Clarindo,
Universidade Federal de Viçosa, Brazil
Pandiyan Muthuramalingam,
Gyeongsang National University, South Korea
Phanikanth Jogam,
Kakatiya University, India

***Correspondence:**
Liang Lin
linliang@mail.kib.ac.cn
Weiqi Li
weiqili@mail.kib.ac.cn

† These authors have contributed equally to this work and share first authorship

Specialty section:
This article was submitted to Plant Breeding, a section of the journal Frontiers in Plant Science

Received: 21 March 2022
Accepted: 14 April 2022
Published: 04 May 2022

Citation:
Gao Y, Ma J, Chen J, Xu Q, Jia Y, Chen H, Li W and Lin L (2022) Establishing Tetraploid Embryogenic Cell Lines of Magnolia officinalis to Facilitate Tetraploid Plantlet Production and Phenotyping. Front. Plant Sci. 13:900768. doi: 10.3389/fpls.2022.900768

The production of synthetic polyploids for plant breeding is compromised by high levels of mixoploids and low numbers of solid polyploid regenerants during *in vitro* induction. Somatic embryogenesis could potentially contribute to the maximization of solid polyploid production due to the single cell origin of regenerants. In the present study, a novel procedure for establishing homogeneous tetraploid embryogenic cell lines in *Magnolia officinalis* has been established. Embryogenic cell aggregate (ECA) about 100–200 μm across, and consisting of dozens of cells, regenerated into a single colony of new ECAs and somatic embryos following colchicine treatment. Histological analysis indicated that the few cells that survived some colchicine regimes still regenerated to form a colony. In some colonies, 100% tetraploid somatic embryos were obtained without mixoploid formation. New granular ECA from single colonies with 100% tetraploid somatic embryos were isolated and cultured individually to proliferate into cell lines. These cell lines were confirmed to be homogeneous tetraploid by flow cytometry. Many tetraploid somatic embryos and plantlets were differentiated from these cell lines and the stability of ploidy level through the somatic embryogenesis process was confirmed by flow cytometry and chromosome counting. The establishment of homogeneous polyploid cell lines, which were presumed to represent individual polyploidization events, might expand the phenotypic variations of the same duplicated genome and create novel breeding opportunities using newly generated polyploid plantlets.

Keywords: artificial polyploid, chromosome set doubling, embryogenic cell aggregate, colchicine, flow cytometry, *Magnolia officinalis*, somatic embryogenesis

INTRODUCTION

Artificial polyploid induction can be used for the improvement of important plant traits, in support of crop breeding strategies (Dhooghe et al., 2011; Chen et al., 2020; Niazian and Nalousi, 2020; Touchell et al., 2020). It has been widely used in the breeding of fruit trees (Zeng et al., 2006; Dutt et al., 2010), ornamental plants (Lucía et al., 2015; Tu et al., 2018), and medicinal plants

(Banyai et al., 2010; Chung et al., 2017; Chen et al., 2018). Whole genome duplication not only increases copies of existing genes but also produces genomic alterations, such as modulated gene expression and epigenetic changes that lead to various phenotypic variations (Chen et al., 2020; Niazian and Nalousi, 2020). Polyploid plants often exhibit better agronomic characteristics related to enhanced biomass, increased yield and tolerance to biotic and abiotic stresses (Niazian and Nalousi, 2020; Ruiz Valdés et al., 2020; Touchell et al., 2020).

In vitro regeneration systems provide a powerful tool for mitotic ploidy manipulation (Dhooghe et al., 2011; Touchell et al., 2020). The past two decades have seen a significant increase in the use of *in vitro* polyploid induction for a diverse range of taxa (Dhooghe et al., 2011; Niazian and Nalousi, 2020; Ruiz Valdés et al., 2020; Touchell et al., 2020). *In vitro* polyploid induction can be achieved by treating proliferative tissue with antimitotic agents followed by recovery of plantlets and screening of polyploid regenerants (Niazian and Nalousi, 2020). The success of *in vitro* polyploid induction is maximized when coupled with the development of efficient *in vitro* regeneration protocols (Touchell et al., 2020).

In vitro regeneration from preexisting meristems, such as apical meristems and nodal sections, has been predominantly used for polyploid induction of many species (Allum et al., 2007; Lucía et al., 2015; Fernando et al., 2019; Parsons et al., 2019). To obtain homogeneous polyploids using preexisting meristems, all initial cells within the three histogenic layers of the meristem need to be successfully affected. Otherwise, mixoploids or cytochimeras form, resulting in the need for serial tissue culture cycles for purification (Roux et al., 2001; Allum et al., 2007; Silva et al., 2019). The main bottlenecks of *in vitro* polyploid induction, such as low rates of solid polyploid initiation, high levels of mixoploid and low numbers of polyploid regenerants, are inherently correlated with the regeneration systems utilizing enhanced axillary shoot proliferation from preexisting meristems (Dhooghe et al., 2011; Touchell et al., 2020; Venial et al., 2020).

Somatic embryogenesis is a better regeneration system for *in vitro* polyploid induction than using preexisting meristems (Wu and Mooney, 2002; Zeng et al., 2006; Acanda et al., 2015). The single cell origin of somatic embryos from embryogenic tissues allows solid polyploid formation while eliminating the occurrence of mixoploids (Acanda et al., 2015; Sanglard et al., 2017; Venial et al., 2020). In polyploid induction based on the somatic embryogenesis system, however, the recovery of polyploid somatic embryos and plantlets is still impeded by necrosis and a reduced differentiation capacity of embryogenic tissues due to antimitotic agent toxicity (Zeng et al., 2006; Acanda et al., 2015). A decline in the relative proportion of polyploid cells in the mixed population following antimitotic agent treatment is due to the persistent lethality of the antimitotic agent and/or inferior growth ability of polyploid cells compared to diploid cells (Zeng et al., 2006). As a consequence, the proportion of polyploid somatic embryos decreases or is eventually lost during the prolonged regrowth and differentiation recovery phase post-treatment with antimitotic agents. In addition, toxicity of antimitotic agents affects the morphological development of somatic embryos and reduces their conversion into plantlets (Zeng et al., 2006; Venial et al., 2020). The induction and purification of polyploid cell lines is expected to eliminate the toxicity effect of antimitotic agents and facilitate subsequent polyploid production.

Plant embryogenic tissues can either proliferate as cell masses or differentiate into somatic embryos, depending on the presence or absence of adequate auxin in the medium (Nic-Can and Loyola-Vargas, 2016). Embryogenic tissues, following antimitotic agent treatment, usually regenerate during regrowth into a mixture of somatic embryos and new Embryogenic cell aggregates (ECAs) (Sanglard et al., 2017; Venial et al., 2020). It is clear that polyploid somatic embryos originate from cells with a duplicated chromosome set. New ECA formation can also originate from cells with a duplicated chromosome set. It is expected that polyploid cell lines could be purified and established by culturing small granular ECAs, which regenerate from embryogenic tissues following antimitotic agent treatment. This can be achieved using a medium that promotes cell proliferation, followed by screening with flow cytometry. Significant phenotypic variations between sibling polyploid clones are known to result from genetic and epigenetic changes occurring during individual polyploidization events (Podwyszyńska et al., 2021; Wójcik et al., 2022). The establishment different polyploid cell lines from the same diploid line, which are presumed to represent individual polyploidization events, might expand the phenotypic variations and create novel breeding opportunities.

Attaining a high proportion of polyploid cells in the mixed cell population following antimitotic agent treatment is a prerequisite for the purification of polyploid cell lines. This can only be achieved by use of very small ECAs instead of large tissues. In addition, synchronization of the tissue culture process before antimitotic agent treatment is also required because polyploidization is integrated with *in vitro* regeneration system (Dhooghe et al., 2011). Synchronization of somatic embryogenesis can be achieved by fractionation of the initial heterogeneous cell population, followed by the transfer of homogeneous cell clusters to a differentiation medium. In carrot, synchronized somatic embryo formation from cell clusters 31–47 μm across, and composed of 3–10 cells, reached more than 90% (Fujimura and Komamine, 1979; Osuga and Komamine, 1994). Size fractionation and plating of proembryonic masses (PEM) 38–140 μm in size on filter paper was key to mass production of synchronized and singularized yellow poplar somatic embryos (Merkle et al., 1990; Dai et al., 2004). For polyploid induction, the use of small homogeneous ECAs can allow the quick and uniform permeation of antimitotic agents, thus maximizing the proportion of affected cells. The cytotoxic effect of antimitotic agents can lead to dose dependent mortality of cells in explants. When small ECAs composed of dozens of cells are treated with antimitotic agents, the number of surviving cells can be very limited. The regeneration of somatic embryos and new ECAs from a very limited number of cells following antimitotic agent treatment could greatly facilitate the purification and establishment of polyploid cell lines.

Magnolia officinalis is a large tree found in the broad-leaved forests in central China. The cortex of *M. officinalis*,

known as "Houpo," has been used historically in Traditional Chinese Medicine (Luo et al., 2019). The main constituents are lignans, alkaloids, and volatile oils, among them the main active compounds are magnolol and honokiol (Lee et al., 2011; Yin et al., 2021). The active components of *M. officinalis* are also widely used in the cosmetics industry. *M. officinalis* is widely cultivated in China to supply cortex to the commercial market, but the plants need about 15 years of growth before production is commercially viable (Luo et al., 2019). The production of synthetic polyploids constitutes a novel opportunity to accelerate the breeding of *M. officinalis* and increase the production of active components in the cortex.

The objective of the present study was to explore an efficient procedure for establishing homogenous tetraploid embryogenic cell lines in *M. officinalis*. Tetraploid cell lines were successfully established and confirmed. The stability of ploidy level through a subsequent somatic embryogenesis process was evaluated in somatic embryos and plantlets differentiated from tetraploid cell lines. In addition, morphological changes of tetraploid somatic embryos and plantlets were assessed in relation to their diploid counterparts. This research shows the possibility of obtaining polyploid cell lines to overcome the bottlenecks of *in vitro* polyploid induction.

MATERIALS AND METHODS

Initiation and Maintenance of Embryogenic Cultures

Proembryonic masses of *M. officinalis* were initiated from mature zygotic embryos in M1 medium (**Table 1**). Seeds were surface sterilized for 10 min in a 0.5% sodium dichloroisocyanurate solution containing a drop of Tween 20 and rinsed three times with sterile deionized water. Zygotic embryos were extracted from these seeds and inoculated on M1 medium (**Table 1**) in 9-cm diameter Petri dishes. M1 medium contained woody plant medium (McCown and Lloyd, 1981) with plant growth regulators previously used for the induction of PEMs in *Liriodendron tulipifera* (Merkle et al., 1990). The cultures were maintained in darkness at 25°C and subcultured monthly until PEMs were produced. The PEMs were then maintained on M2 medium (**Table 1**) and subcultured regularly at 2 weeks intervals.

Preparation of Embryogenic Cell Aggregates and Colchicine Treatment

After 14 days culturing on fresh M2 medium (**Table 1**), the actively dividing PEMs (**Figure 1A**) were used to obtain homogeneous ECAs with a diameter of 100–200 μm. PEMs (500 mg, fresh weight) were transferred to 50 mL Erlenmeyer flasks containing 20 mL of M3 liquid medium (**Table 1**) with a sterile magnetic agitator (size 7 mm × 30 mm). Then the Erlenmeyer flask was placed in an IKA C-MAG HS7 magnetic mixer at 0°C and 1,000 rpm for dispersion (**Figure 1B**). After 10 min, ECAs with a diameter of 100–200 μm were obtained by sieving with screens with 100 and 200 μm pores (**Figure 1C**).

TABLE 1 | Tissue culture media used for embryogenic culture induction (M1), maintenance (M2), colchicine treatment (M3), and somatic embryo initiation (M4) of *Magnolia officinalis*.

	Medium			
Components	**M1**	**M2**	**M3**	**M4**
Casein hydrolysate	1 g L^{-1}	1 g L^{-1}	–	–
2, 4-D	1 mg L^{-1}	1 mg L^{-1}	–	–
6-BA	0.25 mg L^{-1}	–	–	–
Phytagel	3 g L^{-1}	3 g L^{-1}	–	3 g L^{-1}
Activated charcoal	1 g L^{-1}	1 g L^{-1}	–	1 g L^{-1}
PVP	1 g L^{-1}	1 g L^{-1}	–	–

All media contained Lloyd & McCown's Woody plant medium with vitamins and supplemented with 30 g L^{-1} sucrose. 2,4-D, 2,4-dichlorophenoxyacetic acid; 6-BA, 6-Benzylaminopurine; PVP, polyvinylpyrrolidone (MW 40, 000).

Colchicine stock solution was filter-sterilized and added to 25 mL Erlenmeyer flask containing 5 mL M3 liquid medium with ECAs to reach final colchicine concentrations (w/v) of 0, 0.05, 0.1, 0.15, and 0.2% (**Figure 1D**). The cultures were incubated on a tube rotator mixer (120 rpm) at 25°C for 24, 48, and 72 h (**Figure 1E**). Following colchicine treatment, the ECAs were rinsed three times with sterilized M3 liquid medium, 1 mL of ECAs were then plated on a layer of sterilized filter paper. The filter paper with ECAs were then placed on top of semi-solid M4 medium and maintained at 25°C under a 16 h photoperiod (**Figure 1F**).

To estimate the number of ECAs in the cell suspension, aliquots of 1 mL of cell suspension were precipitated by centrifugation, and resuspended in 0.1 mL of M3 medium and pipetted onto a glass slide. Images were taken under an OLYMPUS SZX16 microscope and the number of ECAs were counted with CellSens Dimension software.

Regeneration Following Colchicine Treatment

After plating the colchicine treated ECAs onto a piece of filter paper and cultured on semi-solid M4 medium for 4 weeks, each surviving ECA regenerated into a single colony consisting of somatic embryos and/or new ECAs (**Figure 2**). The number of somatic embryos produced per ECA was determined to evaluate the embryogenic potential of colchicine treated ECAs. Each colony was then picked up and cultured on semi-solid M4 medium without filter paper to enhance new ECA proliferation. Many granular ECAs appeared on most of colonies after 4 weeks (**Figure 2**).

For plantlet conversion, the cotyledonary somatic embryos were first transferred to 9 cm Petri dishes containing 20 mL of semi-solid M4 medium for germination. The cultures were maintained at 25°C under a 16 h photoperiod. The germinated somatic embryos were transferred to glass culture vessels containing 100 mL of semi-solid M4 medium and cultured at 25°C under a 16 h photoperiod.

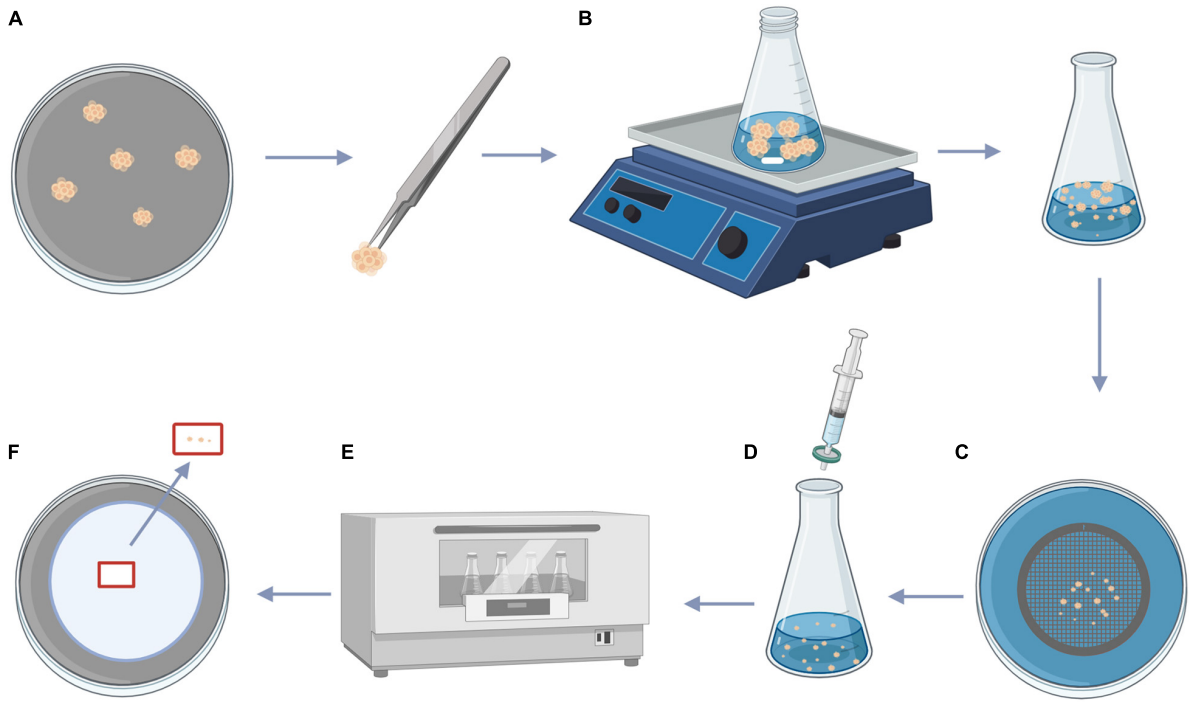

FIGURE 1 | Procedure for size fractionation of ECAs and colchicine treatment. **(A)** PEMs of *Magnolia officinalis* proliferated on M2 medium. **(B)** PEMs of *M. officinalis* were transferred to 50 mL Erlenmeyer flask containing 20 mL of M3 liquid medium with the magnetic agitator, the Erlenmeyer flask was placed in a magnetic mixer at 0°C and 1,000 rpm for dispersion. **(C)** After 10 min, the dispersed PEMs were passed through 100 and 200 μm sieves, producing a homogeneous suspension composed of ECAs with a diameter of 100–200 μm. **(D)** Filter sterilized colchicine solution was added to the ECA suspensions. **(E)** ECAs were treated with colchicine at different concentrations on an orbital shaker (100 rpm) at 25°C for 24, 48, and 72 h. **(F)** Following colchicine treatment, ECAs were washed and plated on M4 medium for somatic embryo initiation. This figure was created using BioRender (https://biorender.com/).

Fluorescein Diacetate and Propidium Iodide Staining

To trace the cellular origin of ECAs following colchicine treatment, fluorescein diacetate (FDA) and propidium iodide (PI) were used to label living cells and dead cells, respectively (**Figure 2**). ECAs were double stained immediately following grinding and sieving to assess the effect of the preparation process on the viability of cells. ECAs treated with colchicine (0.2% for 72 h) were double stained after 72 h of regeneration to indicate the position of surviving cells in the ECA, and to roughly evaluate the proportion of living cells. To stain the ECAs, 5 μL of 10 mg/mL FDA and 5 μL of 1 mg/mL PI were added to 1 mL of ECAs suspension, then incubated in the dark for 5 min. The working concentration of FDA and PI was 50 and 5 μg/mL, respectively. The ECAs were washed three times with deionized water and then observed with a 60 × oil objective by Confocal Laser Scanning Microscopy using an Olympus FV 1,000 system equipped with argon as an excitation source. FDA fluorescence was excited at 488 nm and collected with a 520–550 nm filter, PI was excited at 545 nm and collected with a 560–600 nm filter.

Flow Cytometry Analysis

Flow cytometry was used to determine the ploidy level of cell lines, somatic embryos and plantlets (**Figure 2**). For DNA content determination, a small amount of plant tissue (typically 20 mg) was placed in 1 mL ice-cold nuclei isolation buffer (WPB buffer) in a Petri dish. Using a new razor blade, the tissue was immediately chopped in the buffer, and the homogenate filtered through a 42-μm nylon mesh into a labeled sample tube. The samples were incubated with the DNA fluorochrome PI for 30 min and the relative fluorescence of the stained nuclei was then measured. The cytometer was equipped with an argon ion laser operating at 488 nm. The PI fluorescence was collected by 600 nm fluorescence-2 (FL2) filter. Parameters for data acquisition were kept constant for all samples. The results acquired were later analyzed using Cell Quest software. The average coefficient of variation values (CV) for G1 peaks were used to evaluate the results. The results with CV $<$ 5% were considered as reliable. Leaves of 24 plantlets from each of the colchicine treatments were collected to determine the ploidy level.

Chromosome Counting

The ploidy level of tetraploid plantlets and somatic embryos verified by flow cytometry were further confirmed by chromosome counting to precisely determine the number of chromosomes (**Figure 2**). Root tips and globular somatic embryos were collected and incubated in 2 mM 8-hydroxyquinoline solution for 4 h at 25°C. Subsequently, the samples were washed three times with deionized water for 5 min each, and fixed in Carnoy' s solution (ethanol: glacial acetic

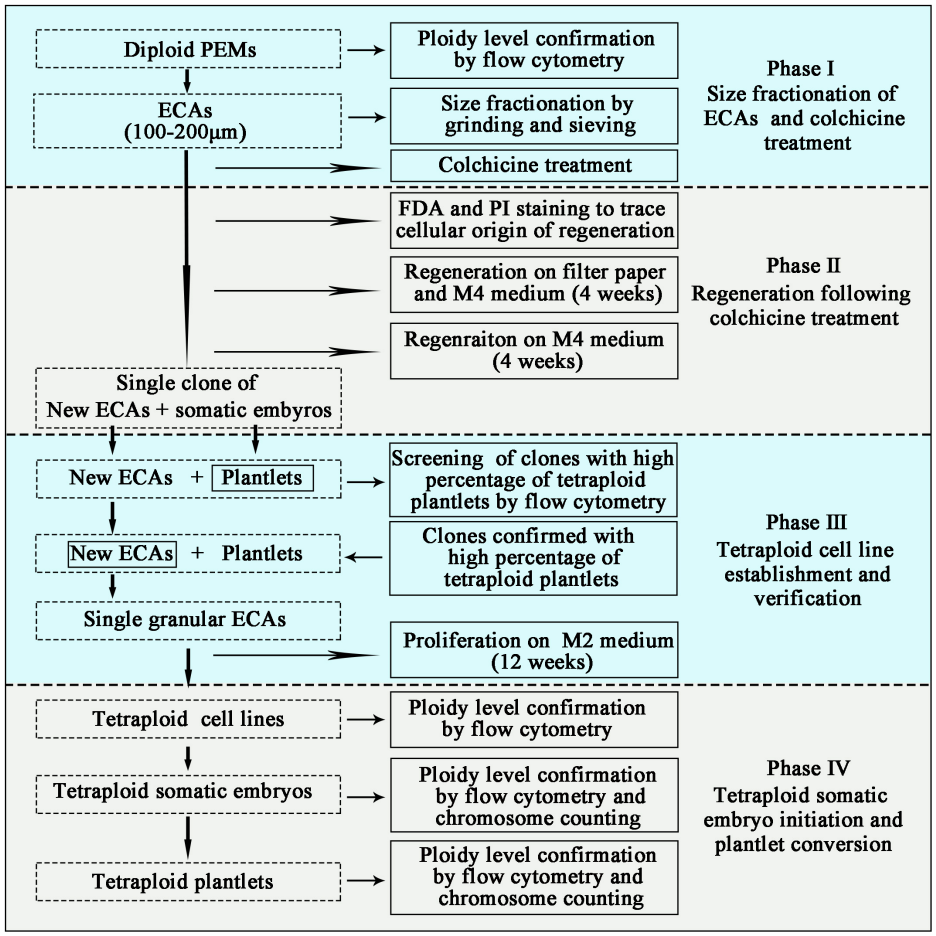

FIGURE 2 | Schematic pipeline for the establishment of tetraploid cell lines of *Magnolia officinalis*. Sequential stages of colchicine treatment, regeneration, tetraploid cell line establishment and ploidy level verification are presented.

acid = 3:1) for 24 h at 4°C. After three washes with deionized water for 5 min each, the samples were digested for 8 min at 60°C in a solution of 45% acetic acid: 1 M HCl at 1:1. After three rinses with deionized water, the digested samples were squashed in a carbol-fuchsin solution for 15 min and placed on a slide. The cells were observed and imaged using a LEICA DM1000 microscope under a 100 × oil immersion objective lens.

Stomata Characteristics

To compare the difference of stomata characteristics between diploid and tetraploid plantlets, nail polish imprints were made from the abaxial surface of leaves. Briefly, the abaxial surface of the leaves were covered with a thin layer of nail polish and allowed to dry. The polish imprints were then carefully lifted off with forceps and placed on a glass slide. The stomata were observed and imaged under LEICA DM5500 B microscope with LAS software. For evaluating the stomatal density, the number of stomata per field of view under the 40× objective was recorded in eight different images. The size of the image was measured to calculate the number of stomata per mm^2. For stomatal length and width measurements, three stomata in each image were randomly selected and measured ($n = 24$).

Establishment and Verification of Tetraploids Embryogenic Cell Lines

Flow cytometry were used for screening of clones with a high percentage of tetraploid plantlets. To establish tetraploid cell line production, single granular ECAs from the colonies confirmed with a high percentage of tetraploid plantlets were isolated and cultured individually on semi-solid M2 medium for proliferation (**Figure 2**). These cultures were maintained at 25°C in the dark and subcultured on new semi-solid M2 medium every 4 weeks. At the end of the third subculture, each single ECA proliferated into a single-ECA-derived cell line. Flow cytometry was then used to analyze the ploidy level of each single-ECA-derived cell lines (**Figure 2**).

Phenotypic Analyses

To assess the effects of polyploidization, the size of the somatic embryos and biomass of the plantlets (3 months after somatic embryo germination) regenerated from diploid and tetraploid

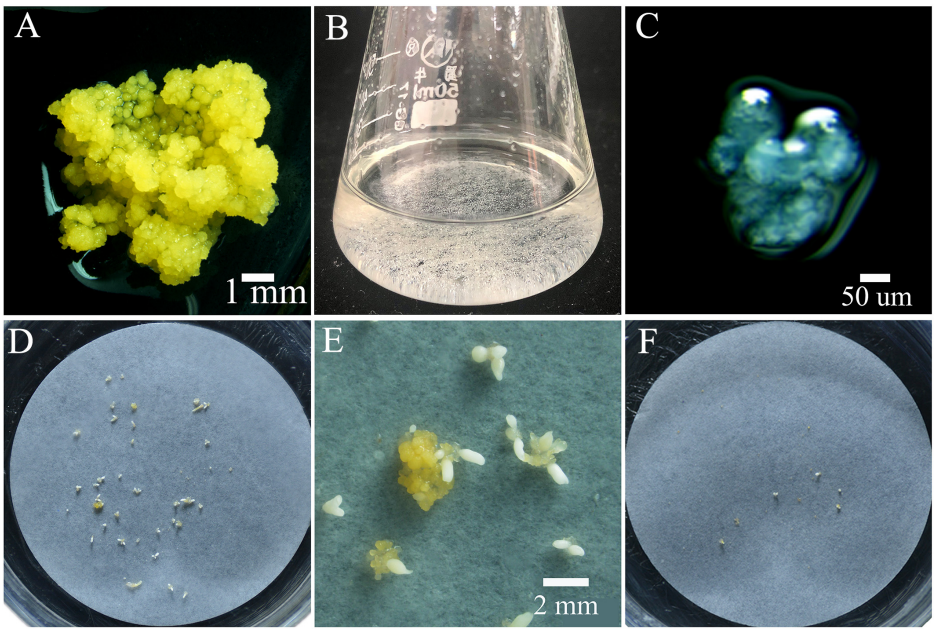

FIGURE 3 | Proembryonic masses (PEMs) and ECAs of *Magnolia officinalis* used for polyploid induction by colchicine. **(A)** PEMs of *M. officinalis* 14 days after subculture. **(B)** ECAs with a diameter of 100–200 μm suspended in M3 liquid medium in a 50 mL Erlenmeyer flask. **(C)** Microscopic observation of the ECAs with a diameter of 100–200 μm. **(D)** Somatic embryo differentiation from ECAs plated on a piece of filter paper after 4 weeks culture on M4 medium. **(E)** A magnified view of somatic embryo differentiation from ECAs plated on a piece of filter paper on M4 medium. **(F)** Regrowth and somatic embryo differentiation of ECAs treated with colchicine, 4 weeks after colchicine treatments.

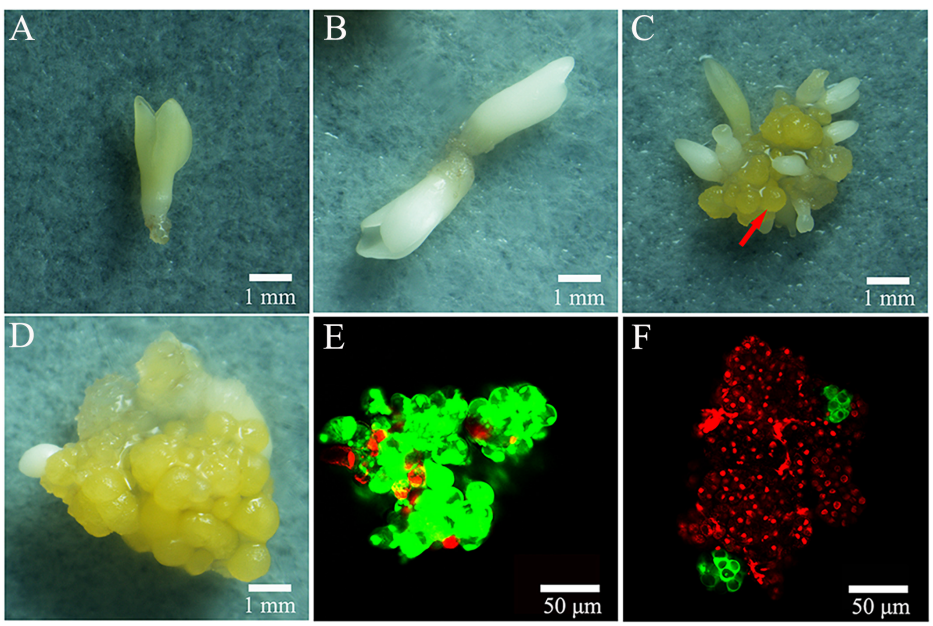

FIGURE 4 | Regeneration patterns of colchicine treated ECAs after 4 weeks regrowth culture. **(A,B)** Somatic embryo differentiation without new ECA formation. **(C)** New ECA (arrow) formation with many somatic embryos forming. **(D)** New ECA formation with scarce somatic embryo differentiation. **(E)** ECA double stained with FDA and PI. **(F)** Colchicine treated ECA (0.2% for 72 h) double stained with FDA and PI following 72 h regrowth culture.

cell lines were measured and compared. Diploid and tetraploid cell lines were used to produce somatic embryos with the same method. ECAs with a diameter of 200–450 μm were obtained and plated on a piece of filter paper and cultured on semi-solid M4 medium for somatic embryo initiation. Thirty somatic embryos initiated from diploid and tetraploid cell lines were

collected 5 weeks after somatic embryo initiation. Images were taken under an OLYMPUS SZX16 microscope. The length and diameter of somatic embryos were calculated with CellSens Dimension software. For plant conversion, germinated somatic embryos were transferred to glass culture vessels containing 100 mL of semi-solid M4 medium and cultured at 25°C under a 16 h photoperiod. Following 7 weeks culture, 12 *in vitro* plantlets of diploid and tetraploid status were collected, and the biomass was measured.

Statistical Analysis

The colchicine treatment experiment was designed with a randomized complete block design, and each treatment contained five replicates. Data were processed and analyzed with SPSS 19.0 software using Duncan's multiple range tests at $p < 0.05$. The measurement of somatic embryos, *in vitro* plantlets and stomata characteristics were analyzed with Student's *t*-test at $p < 0.05$.

RESULTS

Synchronization of the Somatic Embryogenesis Process

The PEMs of *M. officinalis* were initiated from mature zygotic embryos on semi-solid M1 medium. After initiation, PEMs were subcultured on semi-solid M2 medium for proliferation (**Figure 3A**). Somatic embryos developed following transfer of PEMs from M2 medium to semi-solid M4 medium. The PEMs were capable of producing a large number of somatic embryos over several months. However, the initiation of somatic embryos in this system was obviously not synchronized. Since highly efficient polyploid induction relies on the synchronization of the tissue culture process, efforts were made to design a system in which a high frequency of somatic embryogenesis occurred synchronously. The PEMs contained a heterogeneous population of cell aggregates of different sizes and morphologies. For synchronization of somatic embryogenesis, it was important that the cell aggregates are homogeneous in terms of cell cluster size and morphology. After grinding and dispersion of the PEMs with a magnetic agitator in liquid M3 medium, ECAs with a diameter between 100 and 200 μm (**Figures 3B,C**) were obtained by sieving with nylon screens with 100 and 200 μm pores. ECAs with a diameter between 100 and 200 μm were pipetted onto filter paper and cultured along with the filter paper on semi-solid M4 medium. Globular embryos began to appear in the second week, and there was a rapid increase in the number of somatic embryos by the third week. The somatic embryo differentiation process largely ceased after 4 weeks of culture (**Figures 3D,E**). ECAs with a diameter of 100–200 μm were the smallest cell aggregates in which embryogenesis could be efficiently induced. It was estimated that 100 ECAs produced an average of 48 somatic embryos within 4 weeks culture. This is an effective regeneration system in which somatic embryogenesis occurs efficiently and synchronously. This system was the basis for the subsequent polyploid induction experiments.

The Regeneration Patterns of Embryogenic Cell Aggregates After Colchicine Treatment

When plating the colchicine treated ECAs onto filter paper and culturing on semi-solid M4 medium, the regeneration process was not obviously delayed when compared to the control treatment without colchicine. Following 4 weeks of culture, the regeneration responses were observed and recorded (**Figure 3F**). Three types of regeneration patterns could be identified: 1, somatic embryo differentiation without new ECA formation (**Figures 4A,B**); 2, somatic embryo differentiation with new ECA formation (**Figure 4C**); and 3, new ECA formation with scarce somatic embryo differentiation (**Figure 4D**). Although the ECAs showed varying regrowth levels after they had been exposed to different colchicine treatment, these three types of regeneration patterns were observed in all the colchicine treatments. Each regeneration response was initiated from a single colchicine treated ECA which grew into one of the three types of regeneration patterns, and were denominated as single-ECA-derived colonies. When each single-ECA-derived colony was picked up and cultured on semi-solid M4 medium, the majority of them grew into a cluster of somatic embryos and new ECAs. The morphology of the somatic embryos differentiated from single-ECA-derived colonies was normal when compared with the control treatment without colchicine. We did not observe any deformed structures or abnormal morphologies which can be associated with the cytotoxic effects of colchicine. It seems that the use of very small ECAs allowed efficient rinsing of colchicine, thus minimized the carryover effect in the regeneration phase.

Confocal laser scanning microscope has been used to trace the cellular origin of the single-ECA-derived colonies. ECAs with a diameter of 100–200 μm were double stained with FDA and PI immediately after grinding and sieving. Most cells in the ECA emitted green light, indicating their live status (**Figure 4E**). A few peripheral cells of ECA emitted red light, indicated that they were injured in the grinding and sieving process (**Figure 4E**). After 72 h of regrowth culture following colchicine treatment (0.2% for 72 h), most of the cells in the colchicine treated ECA were determined to be dead as they emitted red light, evidencing the cytotoxic effect of colchicine (**Figure 4F**). However, one or two clusters of about 4–8 cells, which stained green appeared on the surface of colchicine-treated ECAs (**Figure 4F**). It was evident that these cell clusters were formed by the division of one or a very limited number of periphery cells that survived the colchicine treatment. These cell clusters grew into different types of single-ECA-derived colonies following subsequent culture.

The Regrowth Rate and Embryogenic Potential of Embryogenic Cell Aggregates After Colchicine Treatment

The regrowth rate of ECAs following various treatments were quantified after 4 weeks of regrowth culture. The control ECAs without colchicine treatment but suspended in liquid M3 medium for 24 h had a regrowth rate of 9.9% (**Figure 5**).

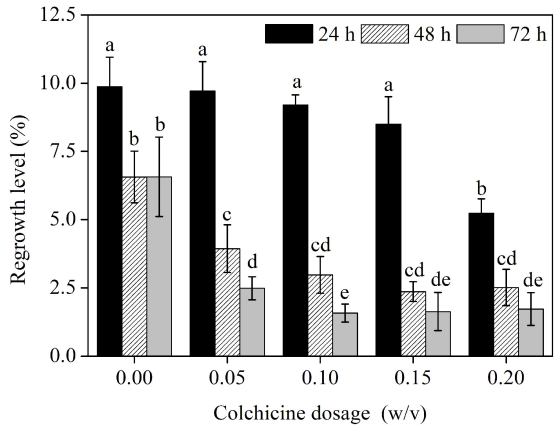

FIGURE 5 | The effects of colchicine treatments on the regrowth levels of ECAs of *Magnolia officinalis*. Data are mean ± SD of three replicates. Means with different letters are significantly different ($p < 0.05$).

This response was lower than that achieved with ECAs plated on a piece of filter paper and cultured on semi-solid M4 medium immediately after grinding and sieving (data not shown). This indicated that suspension in liquid M3 medium alone could negatively affect the regrowth ability. The regrowth rates decreased when ECAs were suspended in liquid M3 medium for 48 and 72 h, but this result was not statistically significant. Colchicine treatments at four concentrations (0.05, 0.1, 0.15, and 0.2%) for 24 h caused a slight decrease in regrowth rates compared with control ECAs without colchicine treatment but suspended in liquid M3 medium for 24 h. However, colchicine treatments at these four concentrations for 48 and 72 h led to significant reductions in regrowth when compared with colchicine treatment for 24 h and the control treatment without colchicine. Overall, the regrowth rate was negatively correlated with concentration and duration of colchicine treatments.

The embryogenic potential was determined as the average number of somatic embryos produced per ECA following 4 weeks of regrowth culture. Control and colchicine-treated ECAs produced an average of 2.2–3.7 somatic embryos, which was not statistically different (**Supplementary Table S1**). This indicates that the embryogenic potential of ECAs was not affected by the colchicine treatment.

Polyploid Analysis

The somatic embryos derived from colchicine treated ECAs germinated normally and converted into plantlets in glass culture vessels containing 100 mL of semi-solid M4 medium. Flow cytometry analysis was used to determine the ploidy level of the somatic embryo derived plantlets. With increasing concentration and duration of colchicine treatment, the number of somatic embryos and plantlets recovered decreased due to the decreased regrowth rate of ECAs. The strongest colchicine treatment in the present study (i.e., 0.2% for 72 h), yielded 24 *in vitro* plantlets, which is the minimum number among other treatments. Therefore, twenty-four plantlets have been randomly selected from the control and each colchicine treatment for flow cytometry analysis. No polyploids were detected in the control without colchicine treatment (**Table 2**). The frequency of tetraploids increased with increasing colchicine concentration and exposure time. All the plantlets (100%) regenerated from 0.2% colchicine treatment for 72 h were tetraploid (**Table 2**). Fifteen (62.6%) tetraploid plantlets were identified from the 0.15% colchicine treatment for 72 h (**Table 2**). Relatively high levels of tetraploid plantlets were also identified from ECAs treated with 0.15 and 0.2% colchicine for 48 h (**Table 2**). One plantlet (4.2%) showing an intermediate cytotype was detected in three colchicine treatments (0.05% for 72 h, 0.15% for 72 h, and 0.2% for 48 h). Mixoploid plantlets were not detected in the present study.

TABLE 2 | The ploidy level of *in vitro* plantlets regenerated from colchicine treated ECAs of *Magnolia officinalis* by somatic embryogenesis.

Colchicine concentration (% w/v)	Duration (h)	No. of diploids (%)	No. of plants with intermediate cytotype (%)	No. of tetraploids (%)
0.00	24	24 (100%)	0	0
	48	24 (100%)	0	0
	72	24 (100%)	0	0
0.05	24	24 (100%)	0	0
	48	24 (100%)	0	0
	72	22 (91.7%)	1 (4.2%)	1 (4.2%)
0.1	24	24 (100%)	0	0
	48	23 (95.8%)	0	1 (4.2%)
	72	22 (91.7%)	0	2 (8.3%)
0.15	24	24 (100%)	0	0
	48	19 (79.2%)	0	5 (20.9%)
	72	8 (33.3%)	1 (4.2%)	15 (62.6%)
0.2	24	23 (95.8%)	0	1 (4.2%)
	48	15 (62.5%)	1 (4.2%)	8 (33.4%)
	72	0	0	24 (100%)

The Establishment and Verification of Homogeneous Tetraploid Cell Lines

When colchicine treated ECAs were plated onto a piece of filter paper and cultured on semi- solid M4 medium, each surviving ECAs regenerated into a single-ECA-derived colony. Three types of regeneration response could be distinguished in single-ECA-derived colonies (**Figure 4**). Each single-ECA-derived colony was picked up with the help of a stereomicroscope and then transferred to semi-solid M4 medium without filter paper for further culture. The majority of them grew into a cluster of somatic embryos and callus, irrespective of their initial composition. Even somatic embryos without callus formation (**Figures 4A,B**) could form some callus tissue at the position of the radicle after 4 weeks of culture on semi-solid M4 medium. Somatic embryos from each single-ECA-derived colony were converted into plantlets and their ploidy levels were determined.

In the present study, high levels of tetraploid induction were obtained from several colchicine treatments. All the

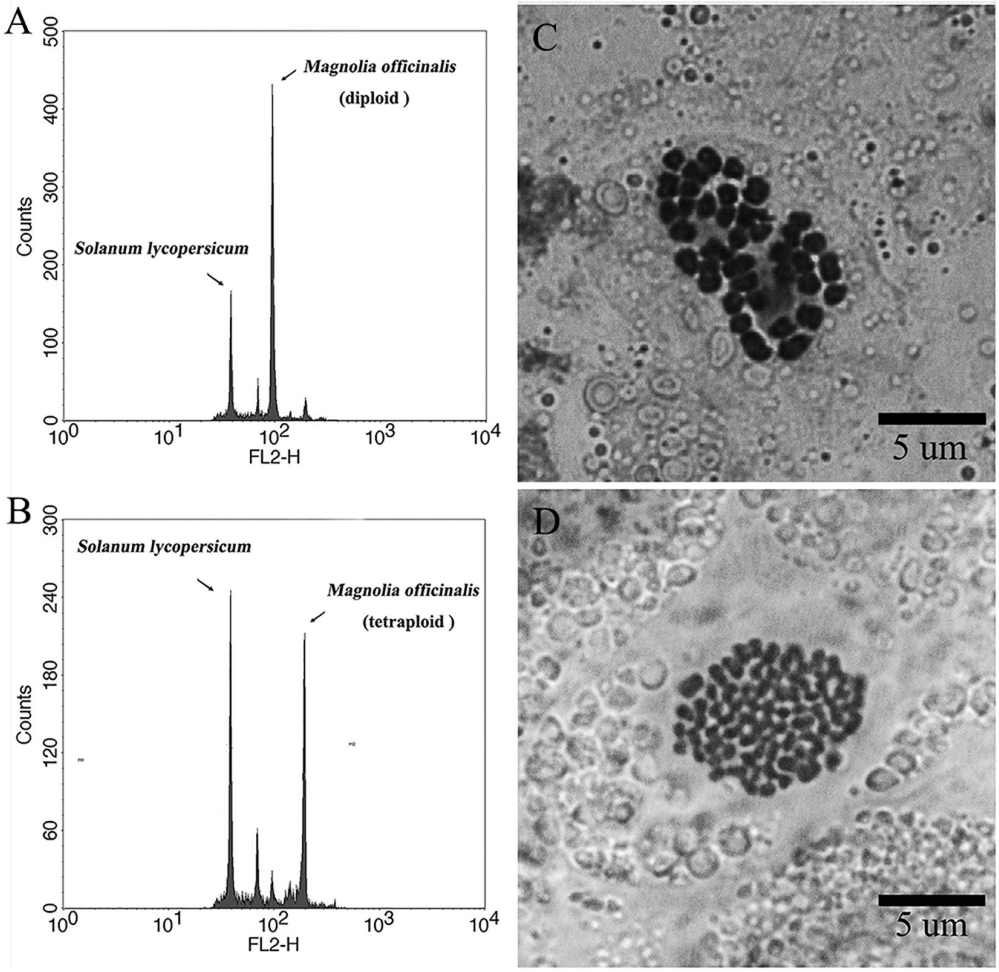

FIGURE 7 | Representative flow cytometry histograms and karyotypes of diploid and tetraploid *Magnolia officinalis*. Representative flow cytometry histograms of the nuclear DNA content in **(A)** diploid and **(B)** tetraploid leaf samples of *M. officinalis*. Chromosomes prepared from **(C)** diploid ($2n = 2\times = 38$) and **(D)** tetraploid ($2n = 4\times = 76$) samples of *M. officinalis*.

plantlets (n = 24, 100%) recovered from the treatment of ECAs with 0.2% colchicine for 72 h were determined to be tetraploid (**Table 2**). It was also established that a very limited number of cells survived colchicine treatment at 0.2% for 72 h (**Figure 4F**). These surviving cells were obviously the common cellular origin of the somatic embryos, as well as the callus tissues in the single-ECA-derived colonies. On the basis of shared cellular origin, it was assumed that tetraploid ECAs might exist in the single-ECA-derived colonies from which tetraploid somatic embryos derived plantlets were identified at high frequency. When each granular ECA (**Figure 4C** arrow) from colonies with a high percentage of tetraploid plantlets were carefully picked up under a stereomicroscope and cultured on semi-solid M2 medium, they proliferated into PEMs with a diameter of about 1 cm within 3 months. These were denominated as a cell line. By this method, 23 cell lines were established from single-ECA-derived colonies derived from colchicine treatment at 0.2% for 72 h. Flow cytometry analysis revealed that all 23 cell lines were tetraploid, and no mixoploid tissues were detected. Somatic embryos were successfully differentiated from these tetraploid cell lines and germinated into plantlets (**Figure 6**). All the somatic embryos and plantlets derived from tetraploid cell lines were determined to be tetraploid by flow cytometry (**Figures 7A,B**), indicating that ploidy stability was maintained through the somatic embryogenesis process. The ploidy level of plantlets derived from tetraploid cell lines were further confirmed by chromosome counting (**Figures 7C,D**). The diploid plantlets showed $2n$ = 38 chromosomes (**Figure 7C**) compared with $2n = 76$ in the tetraploid plantlets (**Figure 7D**).

Comparison of Somatic Embryogenesis Processes of Diploid and Tetraploid Cell Lines

The establishment of tetraploid cell lines allowed comparison to be made of somatic embryogenesis processes of tetraploid and diploid cell lines of *M. officinalis*. One representative

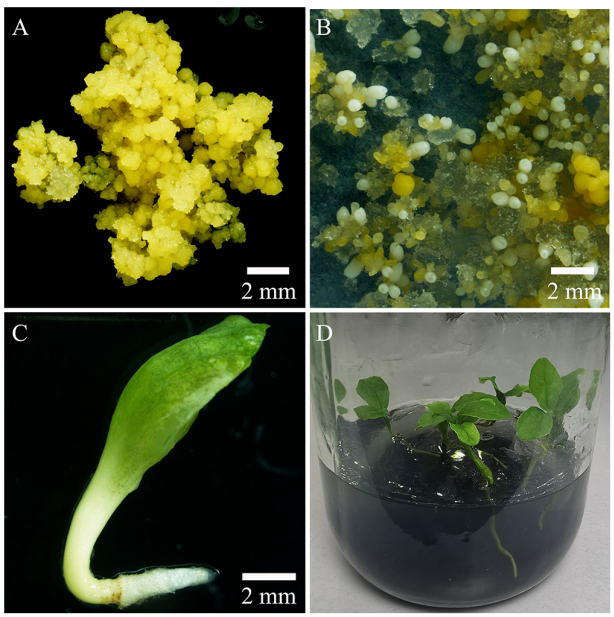

FIGURE 6 | Production of tetraploid plantlets by somatic embryogenesis. **(A)** Tetraploid embryogenic cell line of *Magnolia officinalis*. **(B)** Somatic embryo differentiation from tetraploid ECAs plated on a piece of filter paper and cultured on M4 medium for 6 weeks. **(C)** Tetraploid somatic embryo germinating on M4 medium. **(D)** Conversion of tetraploid somatic embryos into plantlets.

tetraploid cell line was selected for somatic embryo induction and comparison with the original diploid cell line. Tetraploid ECAs with a diameter of 200–450 μm were found to produce the most somatic embryos when compared with other size ranges of tetraploid ECAs, and this size range was used for the comparison following grinding and sieving of PEMs. These diploid and tetraploid ECAs were then pipetted onto a filter paper and cultured along with filter paper on semi-solid M4 medium in the same time. Globular somatic embryos started to appear in both diploid and tetraploid cell lines after 3 weeks' culture. However, the further differentiation and maturation of tetraploid somatic embryos lagged behind the diploid. Cotyledonary somatic embryos were observed at the 4th week in the diploid line. A few diploid somatic embryos even germinated precociously by the 5th week. In contrast, tetraploid somatic embryos were observed rarely by the 6th week and the majority of the somatic embryos were still in the globular stage at this time of culture. Apart from requiring extended incubation on semi-solid M4 medium, the further maturation of the tetraploid somatic embryos was normal.

Differences in embryogenic potential between diploid and tetraploid cell line of *M. officinalis* were observed. A total of 73 somatic embryos were produced by culturing 50 tetraploid ECAs with a diameter of 200–450 μm (five plates with 10 ECAs), which represented the highest embryogenic potential among other size ranges of tetraploid ECAs. However, this response was still much lower than their diploid counterpart, which produced 217 somatic embryos in 50 ECAs with a diameter of 200–450 μm in the same period. Significant differences in the morphologies of diploid (**Figure 8A**) and tetraploid (**Figure 8B**) somatic embryos were also observed. The average length and diameter of cotyledonary somatic embryos of tetraploid lines was significantly shorter and wider, respectively, than those of diploid lines (**Figure 8E**). Overall, tetraploid somatic embryos were shorter and thicker than diploid somatic embryos. This morphology difference makes it is easy to distinguish tetraploid from diploid somatic embryos *in vitro*.

Tetraploid and Diploid Phenotypes

Significant differences in morphologies between diploid and tetraploid were observed when somatic embryos converted into *in vitro* plantlets (**Figures 8C,D**). *In vitro* plantlets of tetraploid lines (**Figure 8D**) were evidently much larger than those derived from diploid lines (**Figure 8C**) in the same incubation period 3 months after somatic embryo germination. Compared to diploid line plantlets, the average fresh weight of tetraploid plantlets was increased by 136.3% (**Figure 8F**). The shoot base and root of tetraploid plantlets (**Figure 8D**) were also stronger than diploid plantlets (**Figure 8C**), although root elongation of tetraploid plantlets was delayed. Lateral root initiation was efficient in tetraploid plantlets (**Figure 8D**), but was not observed in diploid plantlets (**Figure 8C**). The nail polish imprints showed that the adaxial leave surface stomata of tetraploid plantlets were about 30% longer than diploid plantlets (**Figure 9** and **Table 3**). However, the stomatal density of tetraploid plantlet leaves declined to about 57% of that recorded for diploid plant leaves (**Figure 9** and **Table 3**).

DISCUSSION

Here, a novel procedure for the induction and establishment of homogenous tetraploid embryogenic cell lines of the species *M. officinalis* has been described. These cell lines were established from tissues treated with antimitotic agents by manipulation of the regeneration processes. The ploidy level of the synthetic tetraploid cell lines was confirmed by flow cytometry. The new tetraploid cell lines were capable of producing somatic embryos at high frequency. These somatic embryos were successfully germinated into plantlets and their ploidy level confirmed to be tetraploid by flow cytometry and chromosome counting, indicating ploidy stability of the new polyploid cell lines through the somatic embryogenesis process. Through a process of scaling-up, polyploid cell lines could provide substantial numbers of polyploid plantlets for further phenotypic evaluation and for use in breeding programs.

In the present study, several tetraploid embryogenic cell lines were successfully established and confirmed from single-ECA-derived colonies following 0.2% colchicine treatment for 72 h, which produced 100% tetraploid somatic embryos. Previous polyploid induction protocols have been designed to maximize the number of cells affected by the antimitotic agent, increase polyploid production and reduce cytochimera formation (Dhooghe et al., 2011; Touchell et al., 2020). Our results,

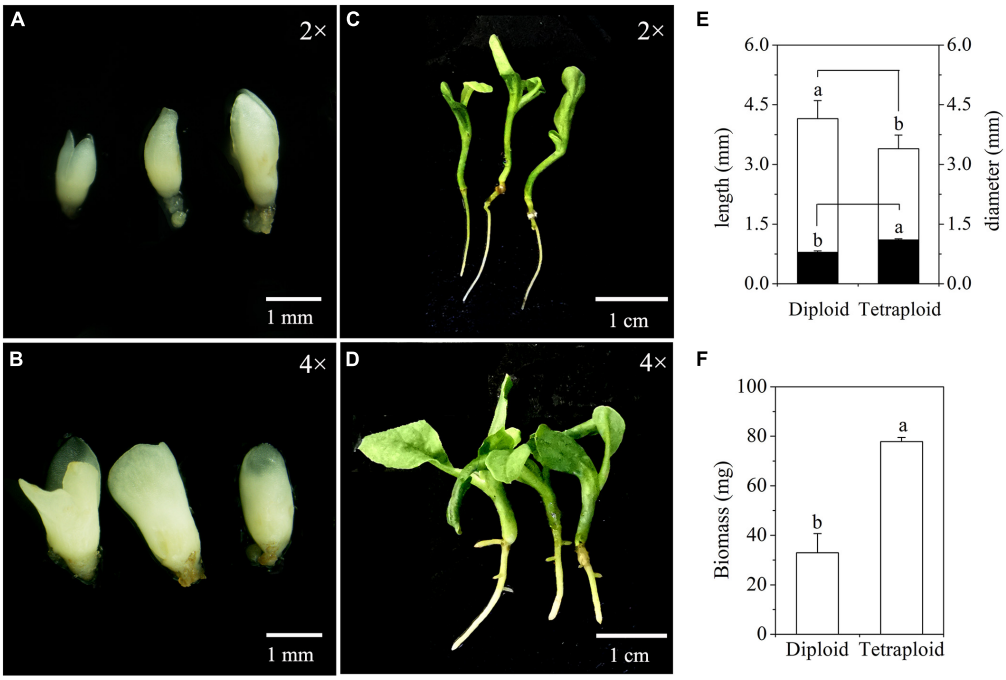

FIGURE 8 | Characterization of somatic embryos and *in vitro* plantlets derived from diploid and tetraploid embryogenic cells of *Magnolia officinalis*. Diploid **(A)** and tetraploid **(B)** somatic embryos 5 weeks after somatic embryo initiation. Diploid **(C)** and tetraploid **(D)** plantlets conversion from somatic embryos. **(E)** The length (open bars) and diameter (closed bars) of diploid and tetraploid somatic embryos of *M. officinalis* 6 weeks after somatic embryo initiation (n = 30). **(F)** The biomass of diploid and tetraploid plantlets of *M. officinalis* 3 months after somatic embryo germination (n = 12).

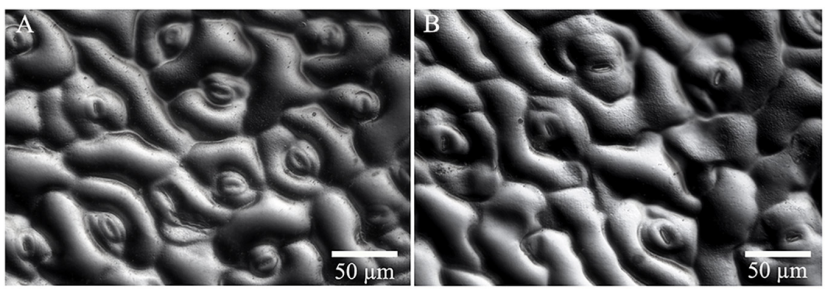

FIGURE 9 | Stomata characteristics of diploid and tetraploid leaves of *Magnolia officinalis*. Nail polish impressions showing stomata on the abaxial surface of diploid **(A)** and tetraploid **(B)** leaves.

TABLE 3 | Stomata size (n = 24) and density (n = 8) of diploid and tetraploid leaves of *Magnolia officinalis*.

	Ploidy level	
	Diploid	**Tetraploid**
Stomatal density (No./mm^2)	151.2 ± 5.9^a	86.3 ± 3.7^a
Stoma length (μm)	20.9 ± 0.3^b	29.8 ± 0.3^a
Stoma width (μm)	5.4 ± 0.1^b	6.6 ± 0.1^a

Means with different letters are significantly different (Student's t-test, $p < 0.05$).

however, suggest that regeneration from a minimal number of cells could greatly facilitate the establishment of homogeneous polyploid cell lines. Considering the high frequency production of tetraploid somatic embryos and tetraploid cell lines, it was important to confirm the cellular origin of the single-ECA-derived colonies, which were determined using histological methods. FDA and PI double staining of ECAs treated with 0.2% colchicine for 72 h and recovered for another 72 h revealed that most cells in the ECA died, while only a few of periphery cells survived and regenerated into a cluster of somatic embryos and new granular ECAs. Since somatic embryos and new granular ECAs in the specific single-ECA-derived colonies share common and limited cellular origin, it is reasonable to assume that they potentially share a common ploidy level.

In the present study, ECAs with a diameter of 100–200 μm, which possess a high potential of proliferation and

differentiation, is the key to success. ECAs with a diameter of 100–200 μm were obtained by dispersion and sieving from the initial heterogeneous embryogenic cell lines. Fractionation of size of cell clusters by sieving has been shown to synchronize somatic embryogenesis (Fujimura and Komamine, 1979; Osuga and Komamine, 1994; Kamo et al., 2004; Souza et al., 2011; Awada et al., 2020), and potentially maximizes the number of cells responsive to the antimitotic agents could facilitate greater polyploid production (Dhooghe et al., 2011). ECAs with a diameter of 100–200 μm composed of dozens of cells were the smallest cell aggregates in which somatic embryogenesis could be induced efficiently. The small and uniform size of ECAs not only permits quick and uniform permeation of antimitotic agents, but also allows efficient rinsing of antimitotic agents before regrowth culture. Therefore, the negative carryover effects of colchicine on the subsequent regrowth and differentiation were minimized, limiting the kind of abnormal growth and morphology previously reported (Zeng et al., 2006; Dutt et al., 2010; Parsons et al., 2019). The production of malformed somatic embryos during regrowth or any interruption to the process of the somatic embryogenesis were not observed in the present study, indicating that the procedure for the rinsing out of colchicine was effective. Antimitotic agent exposure can result in reduced and/or loss of embryogenic potential (Wu and Mooney, 2002; Zeng et al., 2006). However, the embryogenic potential of ECAs was not affected by the colchicine treatment when compared with control treatment in the present study. This may also be attributed to the absence of any carryover effect of colchicine during regrowth.

High levels of solid tetraploid induction without mixoploid formation were obtained in the present study. The most efficient treatment was 0.2% colchicine for 72 h, which produced 100% tetraploid plantlets in the regeneration process (**Table 2**). Colchicine treatment at 0.15% for 72 h and 0.2% for 48 h produced 62.6 and 33.4% tetraploid plantlets, respectively (**Table 2**). The development of efficient regeneration systems can facilitate an increased production of homogeneous polyploids and reduction of cytochimeras (Touchell et al., 2020). Highly efficient tetraploid plant induction has been achieved by colchicine treatment of embryogenic suspension cultures in grapevine *Vitis vinifera* cv. Mencía, with the most effective colchicine treatment generating 25% tetraploid plantlets (Acanda et al., 2015). Chromosome set doubling using cellular aggregate suspensions *via* an indirect somatic embryogenesis pathway produced 34.9% autotetraploid plantlets for *Coffea canephora* and 21.1% auto-alloctaploid plantlets for *Coffea arabica* (Venial et al., 2020). Mixoploid formation were neither found in our study with *M. officinalis*, nor in *Vitis vinifera* (Acanda et al., 2015) and *Coffea* species (Sanglard et al., 2017; Venial et al., 2020), which highlights the value of regeneration through somatic embryogenesis from a single cell origin to reduce or avoid the production of mixoploids (Acanda et al., 2015; Touchell et al., 2020; Venial et al., 2020). Conversely, all initial cells within the histogenic layers of the meristems need to be affected by the antimitotic agents to produce homogeneous polyploids using nodal segments and shoot apices; otherwise, mixoploid formation occurs (Dhooghe et al., 2011; Touchell et al., 2020). As a measure of how difficult this is, polyploid induction using multicellular meristems usually leads to a high frequency of mixoploids (Roux et al., 2001; Allum et al., 2007; Fernando et al., 2019). There is also the potential problem of reversion of putative polyploids to diploids and/or mixoploids (Allum et al., 2007; Silva et al., 2019). Overall, the present study has demonstrated how the development of an efficient regeneration system improves the production of homogeneous polyploids and reduces cytochimeras.

The manipulation of differentiation and proliferation of colchicine-treated ECAs of *M. officinalis* by the presence or absence of filter paper on semisolid M4 medium is key for the success of the method presented. Filter paper was used during the first phase of regrowth culture for somatic embryo differentiation. The use of filter paper or semi-permeable cellulose acetate membranes has been shown to enhance the induction and proper maturation and conversion of somatic embryos (Merkle et al., 1990; Niedz et al., 2002; Dutt et al., 2010). Alteration of water potential by filter paper or cellulose acetate membranes can dramatically alter the regrowth and differentiation of ECAs (Merkle et al., 1990; Niedz et al., 2002). When single-ECA-derived colonies were transferred onto semi-solid M4 medium without filter paper, the proliferation of new granular ECAs was encouraged and germination of the somatic embryos that had initially formed on the filter paper facilitated.

In the present study, somatic embryos regenerated from 0.2% colchicine treatment for 72 h could be clearly discriminated from those of control, as they are much bigger in size. This kind of "giant" somatic embryos was also observed in other colchicine regimes. When these somatic embryos were selected based on morphology characteristics and the ploidy levels were analyzed by flow cytometry, all were found to be tetraploid. After the tetraploid cell lines were established and verified, somatic embryos were produced and compared with the diploid lines. Generally, tetraploid somatic embryos were shorter and thicker in appearance than those of diploid lines. These findings suggest that the morphology of somatic embryos may be employed as a potential morphology indicator to predict ploidy level to expedite identification of putative tetraploid regenerates at an early stage before plantlet conversion. Other systems show a similar change in morphological phenotype with polyploidization. The *in vivo* autopolyploid induction system in the Chinese jujube tree (*Ziziphus jujuba* Mill.) was established by integrates *in vivo* bud regeneration *via* calluses with polyploid induction. At the mature leaf stage, not just octoploids but also tetraploid, diploid and mixoploid plants could be forecasted with a high degree of accuracy by observing the size and shape of shoots and leaves (Shi et al., 2015). A widespread consequence of polyploidy is an increase in cell size. For example, the tetraploid cell size of "Meiwa" kumquat (*Fortunella crassifolia*) is much larger than the diploid, and the two types could be clearly discriminated by size in a mixed population of diploid and tetraploid cells (Zeng et al., 2006).

Magnolia officinalis belongs to the Magnoliaceae, which consists of over 300 species in two genera–*Magnolia* L. and

Liriodendron L (Rivers et al., 2016). Many magnolia species are widely appreciated around the world as ornamental trees due to their attractive flowers and foliage. The first protocol for somatic embryogenesis of *Liriodendron tulipifera* was published nearly 40 years ago (Merkle and Sommer, 1986). Since then, many magnolia species and hybrids have been shown to be amenable to somatic embryogenesis with protocols similar to that of *Liriodendron tulipifera* (Merkle, 1999; Mata-Rosas et al., 2006; Kim et al., 2007; Park et al., 2012). The efficient method developed for the induction and establishment of polyploid embryogenic cell lines for *M. officinalis* in the present study, is based on the manipulation of the somatic embryogenesis process following antimitotic agent treatment. Our method has great potential for the creation of new polyploid germplasm for species with established somatic embryogenesis protocols, especially in the magnolia family.

CONCLUSION

Our results with *M. officinalis* demonstrate the potential of establishing polyploid embryogenic cell lines *via* induction along the somatic embryogenesis pathway. The use of very small ECAs composed of dozens of cells is highlighted. Only a few cells in the ECAs survived colchicine treatment and regenerated into single colonies. However, the dual potential of differentiation and proliferation of the ECAs was then manipulated to produce somatic embryos for ploidy analysis and new ECAs for cell line establishment, respectively. The present study shown that a high frequency of homogeneous polyploid cell lines can be established by proliferation of single new granular ECAs picked up from colonies with a high presence of polyploid somatic embryos. Somatic embryos and new ECAs in the same colonies derived from each colchicine treated ECA share a common origin from a very limited numbers of cells. The ploidy level of somatic embryos can reflect the ploidy level of cells that survived antimitotic agent treatment and regenerate. This increases the likelihood of being able to establish and purify polyploid cell lines. Our results provide insight into the potential of obtaining new polyploid embryogenic cell lines *via* polyploid induction with a somatic embryogenesis system.

DATA AVAILABILITY STATEMENT

The raw data supporting the conclusions of this article will be made available by the authors, without undue reservation.

AUTHOR CONTRIBUTIONS

LL conceived and designed the experiments and wrote the manuscript. YG, JM, and QX performed the *in vitro* tissue culture experiments and chromosome set doubling experiments and carried out the phenotypic analysis. YG, JM, and YJ performed the flow cytometry analyses. JC and YG performed the Chromosome counting experiment. LL, WL, and HC revised the manuscript. All authors contributed to the article and approved the submitted version.

FUNDING

This work was supported by grants from the Biological Resources Program, Chinese Academy of Sciences (KFJ-BRP-017-75), the Key R&D program of Yunnan Province, China (grant no. 202103AC100003), the Key Basic Research program of Yunnan Province, China (grant no. 202101BC070003). This research was facilitated by the Germplasm Bank of Wild Species, Kunming Institute of Botany, Chinese Academy of Sciences.

ACKNOWLEDGMENTS

We are grateful to Hugh W. Prtichard and Dong Liu for their review and suggestions to improve the manuscript.

SUPPLEMENTARY MATERIAL

The Supplementary Material for this article can be found online at: https://www.frontiersin.org/articles/10.3389/fpls.2022.900768/full#supplementary-material

REFERENCES

Acanda, Y., Martínez, Ó, González, M. V., Prado, M. J., and Rey, M. (2015). Highly efficient in vitro tetraploid plant production via colchicine treatment using embryogenic suspension cultures in grapevine (*Vitis vinifera* cv. Mencía). *Plant Cell Tissue Organ Cult.* 123, 547–555. doi: 10.1007/s11240-015-0859-3

Allum, J. F., Bringloe, D. H., and Roberts, A. V. (2007). Chromosome doubling in a *Rosa rugosa* Thunb. hybrid by exposure of in vitro nodes to oryzalin: the effects of node length, oryzalin concentration and exposure time. *Plant Cell Rep.* 26, 1977–1984. doi: 10.1007/s00299-007-0411-y

Awada, R., Verdier, D., Froger, S., Brulard, E., Maraschin, S., Etienne, H., et al. (2020). An innovative automated active compound screening system allows high-throughput optimization of somatic embryogenesis in *Coffea arabica*. *Sci. Rep.* 10:810. doi: 10.1038/s41598-020-57800-6

Banyai, W., Sangthong, R., Karaket, N., Inthima, P., Mii, M., and Supaibulwatana, K. (2010). Overproduction of artemisinin in tetraploid *Artemisia annua* L. *Plant Biotechnol.* 27, 427–433. doi: 10.5511/plantbiotechnology.10.0726a

Chen, E., Tsai, K.-L., Chung, H.-H., and Chen, J.-T. (2018). Chromosome doubling-enhanced biomass and dihydrotanshinone i production in *salvia miltiorrhiza*, a traditional chinese medicinal plant. *Molecules* 23:3106. doi: 10.3390/molecules23123106

Chen, J.-T., Coate, J. E., and Meru, G. (2020). Editorial: artificial polyploidy in plants. *Front. Plant Sci.* 11:621849. doi: 10.3389/fpls.2020.621849

Chung, H. H., Shi, S. K., Huang, B., and Chen, J. T. (2017). Enhanced agronomic traits and medicinal constituents of autotetraploids in anoectochilus formosanus hayata, a top-grade medicinal orchid. *Molecules* 22:13. doi: 10.3390/molecules22111907

Dai, J. L., Vendrame, W. A., and Merkle, S. A. (2004). Enhancing the productivity of hybrid yellow-poplar and hybrid sweetgum embryogenic cultures. *In Vitro Cell. Dev. Biol.Plant* 40, 376–383. doi: 10.1079/ivp2004538

Dhooghe, E., Laere, K., Eeckhaut, T., Leus, L., and Huylenbroeck, J. (2011). Mitotic chromosome doubling of plant tissues in vitro. *Plant Cell Tissue Organ Cult.* 104, 359–373. doi: 10.1007/s11240-010-9786-5

Dutt, M., Vasconcellos, M., Song, K. J., Gmitter, F. G., and Grosser, J. W. (2010). In vitro production of autotetraploid Ponkan mandarin (*Citrus reticulata Blanco*) using cell suspension cultures. *Euphytica* 173, 235–242. doi: 10.1007/s10681-009-0098-y

Fernando, S. C., Goodger, J. Q. D., Chew, B. L., Cohen, T. J., and Woodrow, I. E. (2019). Induction and characterisation of tetraploidy in *Eucalyptus polybractea* R.T. Baker. *Ind. Crops Prod.* 140:111633. doi: 10.1016/j.indcrop.2019.111633

Fujimura, T., and Komamine, A. (1979). Synchronization of somatic embryogenesis in a carrot cell suspension culture. *Plant physiol.* 64, 162–164. doi: 10.1104/pp.64.1.162

Kamo, K., Jones, B., Castillon, J., Bolar, J., and Smith, F. (2004). Dispersal and size fractionation of embryogenic callus increases the frequency of embryo maturation and conversion in hybrid tea roses. *Plant Cell Rep.* 22, 787–792. doi: 10.1007/s00299-003-0723-5

Kim, Y. W., Park, S. Y., Park, I. S., and Moon, H. K. (2007). Somatic embryogenesis and plant regeneration from immature seeds of *Magnolia obovata* Thunberg. *Plant Biotechnol. Rep.* 1, 237–242. doi: 10.1007/s11816-007-0037-0

Lee, Y. J., Lee, Y. M., Lee, C. K., Jung, J. K., Han, S. B., and Hong, J. T. (2011). Therapeutic applications of compounds in the *Magnolia* family. *Pharmacol. Ther.* 130, 157–176. doi: 10.1016/j.pharmthera.2011.01.010

Lucía, G. R., Iannicelli, J., Coviella, M. A., Bugallo, V. L., Bologna, P., Escandon, A. S., et al. (2015). A protocol for the in vitro propagation and polyploidization of an interspecific hybrid of Glandularia (G. *peruviana* × G. *scrobiculata*). *Sci. Hortic.* 184, 46–54. doi: 10.1016/j.scienta.2014.12.032

Luo, H., Wu, H., Yu, X., Zhang, X., Lu, Y., Fan, J., et al. (2019). A review of the phytochemistry and pharmacological activities of *Magnoliae officinalis* cortex. *J. Ethnopharmacol.* 236, 412–442. doi: 10.1016/j.jep.2019.02.041

Mata-Rosas, M., Jimenez-Rodriguez, A., and Chavez-Avila, V. M. (2006). Somatic embryogenesis and organogenesis in Magnolia dealbata Zucc. (*Magnoliaceae*), an endangered, endemic Mexican species. *Hortscience* 41, 1325–1329. doi: 10.21273/HORTSCI.41.5.1325

McCown, B. H., and Lloyd, G. (1981). Woody Plant Medium (WPM)-a mineral nutrient formulation for microculture for woody plant species. *Hortic. Sci.* 16:453.

Merkle, S. (1999). "Somatic embryogenesis in *magnolia* spp," in *Somatic Embryogenesis in Woody Plants*, Vol. 4, eds S. M. Jain, P. K. Gupta, and R. J. Newton (Alphen aan den Rijn: Kluwer). 387–401. doi: 10.1007/978-94-017-3032-7_15

Merkle, S. A., and Sommer, H. E. (1986). Somatic embryogenesis in tissue cultures of *Liriodendron tulipifera*. *Can. J. For. Res.* 16, 420–422. doi: 10.1139/x86-077

Merkle, S. A., Wiecko, A. T., Sotak, R. J., and Sommer, H. E. (1990). Maturation and conversion of *Liriodendron tulipifera* somatic embryos. *In Vitro Cell. Dev. Biol.* 26, 1086–1093. doi: 10.1007/bf02624445

Niazian, M., and Nalousi, A. M. (2020). Artificial polyploidy induction for improvement of ornamental and medicinal plants. *Plant Cell Tissue Organ Cult.* 142, 447–469. doi: 10.1007/s11240-020-01888-1

Nic-Can, G. I., and Loyola-Vargas, V. M. (2016). "The role of the auxins during somatic embryogenesis," in *Somatic Embryogenesis: Fundamental Aspects and Applications*, eds V. M. Loyola-Vargas and N. Ochoa-Alejo (New York, NY: Springer International Publishing). 171–182. doi: 10.1007/978-3-319-33705-0_10

Niedz, R., Hyndman, S., Wynn, E., and Bauscher, M. (2002). Normalizing sweet orange (*C. sinensis* (L.) Osbeck) somatic embryogenesis with semi-permeable membranes. *In Vitro Cell. Dev. Biol. Plant* 38, 552–557. doi: 10.1079/ivp2002331

Osuga, K., and Komamine, A. (1994). Synchronization of somatic embryogenesis from carrot cells at high frequency as a basis for the mass production of embryos. *Plant Cell Tissue Organ Cult.* 39, 125–135. doi: 10.1007/bf00033920

Park, I. S., Koiso, M., Morimoto, S., Kubo, T., Jin, H. O., and Funada, R. (2012). Plant regeneration by somatic embryogenesis from mature seeds of *Magnolia obovata*. *J. Wood Sci.* 58, 64–68. doi: 10.1007/s10086-011-1212-z

Parsons, J. L., Martin, S. L., James, T., Golenia, G., Boudko, E. A., and Hepworth, S. R. (2019). Polyploidization for the genetic improvement of *Cannabis sativa*. *Front. Plant Sci.* 10:12. doi: 10.3389/fpls.2019.00476

Podwyszyńska, M., Markiewicz, M., Broniarek-Niemiec, A., Matysiak, B., and Marasek-Ciolakowska, A. (2021). Apple autotetraploids with enhanced resistance to apple scab (*Venturia inaequalis*) due to genome duplication-phenotypic and genetic evaluation. *Int. J. Mol. Sci.* 22:527. doi: 10.3390/ijms22020527

Rivers, M., Beech, E., Murphy, L., and Oldfield, S. (2016). *The Red List of Magnoliaceae*. Richmond: Botanic Gardens Conservation International.

Roux, N., Dolezel, J., Swennen, R., and Zapata-Arias, F. J. (2001). Effectiveness of three micropropagation techniques to dissociate cytochimeras in *Musa* spp. *Plant Cell Tissue Organ Cult.* 66, 189–197. doi: 10.1023/a:1010624005192

Ruiz Valdés, M., Oustric, J., Santini, J., and Morillon, R. (2020). Synthetic polyploidy in grafted crops. *Front. Plant Sci.* 11:540894. doi: 10.3389/fpls.2020.540894

Sanglard, N. A., Amaral-Silva, P. M., Sattler, M. C., de Oliveira, S. C., Nunes, A. C. P., Soares, T. C. B., et al. (2017). From chromosome doubling to DNA sequence changes: outcomes of an improved in vitro procedure developed for allotriploid "Híbrido de Timor" (*Coffea arabica* L. × *Coffea canephora* Pierre ex A. Froehner). *Plant Cell Tissue Organ Cult.* 131, 223–231. doi: 10.1007/s11240-017-1278-4

Shi, Q.-H., Liu, P., Liu, M.-J., Wang, J.-R., and Xu, J. (2015). A novel method for rapid in vivo induction of homogeneous polyploids via calluses in a woody fruit tree (*Ziziphus jujuba Mill.*). *Plant Cell Tissue Organ Cult.* 121, 423–433. doi: 10.1007/s11240-015-0713-7

Silva, A. J., Carvalho, C. R., and Clarindo, W. R. (2019). Chromosome set doubling and ploidy stability in synthetic auto- and allotetraploid of *Eucalyptus*: from in vitro condition to the field. *Plant Cell Tissue Organ Cult.* 138, 387–394. doi: 10.1007/s11240-019-01627-1

Souza, J., Tomaz, M., Arruda, S. C., Demétrio, C., Venables, W., and Martinelli, A. (2011). Callus sieving is effective in improving synchronization and frequency of somatic embryogenesis in *Citrus sinensis*. *Biol. Plant.* 55, 703–707. doi: 10.1007/s10535-011-0171-y

Touchell, D., Palmer, I., and Ranney, T. (2020). In vitro ploidy manipulation for crop improvement. *Front. Plant Sci.* 11:722. doi: 10.3389/fpls.2020.00722

Tu, H.-Y., Zhang, A.-L., Xiao, W., Lin, Y.-R., Shi, J.-H., Wu, Y.-W., et al. (2018). Induction and identification of tetraploid *Hedychium coronarium* through thin cell layer culture. *Plant Cell Tissue Organ Cult.* 135, 395–406. doi: 10.1007/s11240-018-1472-z

Venial, L., Mendonça, M. A., Amaral-Silva, P., Canal, G., Passos, A., Ferreira, A., et al. (2020). Autotetraploid *Coffea canephora* and Auto-Alloctaploid *Coffea arabica* From In Vitro Chromosome Set Doubling: new Germplasms for *Coffea*. *Front. Plant Sci.* 11:154. doi: 10.3389/fpls.2020.00154

Wójcik, D., Marat, M., Marasek-Ciolakowska, A., Klamkowski, K., Buler, Z., Podwyszyńska, M., et al. (2022). Apple autotetraploids—phenotypic characterisation and response to drought stress. *Agronomy* 12:161. doi: 10.3390/agronomy12010161

Wu, J.-H., and Mooney, P. (2002). Autotetraploid tangor plant regeneration from in vitro *Citrus* somatic embryogenic callus treated with colchicine. *Plant Cell Tissue Organ Cult.* 70, 99–104. doi: 10.1023/a:1016029829649

Yin, Y. P., Peng, F., Zhou, L. J., Yin, X. M., Chen, J. R., Zhong, H. J., et al. (2021). The chromosome-scale genome of *Magnolia officinalis* provides insight into the evolutionary position of magnoliids. *Iscience* 24:102997. doi: 10.1016/j.isci.2021.102997

Zeng, S.-H., Chen, C.-W., Hong, L., Liu, J.-H., and Deng, X.-X. (2006). In vitro induction, regeneration and analysis of autotetraploids derived from protoplasts and callus treated with colchicine in *Citrus*. *Plant Cell Tissue Organ Cult.* 87:85. doi: 10.1007/s11240-006-9142-y

Conflict of Interest: The authors declare that the research was conducted in the absence of any commercial or financial relationships that could be construed as a potential conflict of interest.

Publisher's Note: All claims expressed in this article are solely those of the authors and do not necessarily represent those of their affiliated organizations, or those of the publisher, the editors and the reviewers. Any product that may be evaluated in this article, or claim that may be made by its manufacturer, is not guaranteed or endorsed by the publisher.

frontiers | Frontiers in Plant Science

ORIGINAL RESEARCH
published: 09 May 2022
doi: 10.3389/fpls.2022.908659

Realization of Lodging Tolerance in the Aromatic Grass, *Cymbopogon khasianus* Through Ploidy Intervention

Yerramilli Vimala[1], Umesh Chandra Lavania[2], Madhavi Singh[2], Seshu Lavania[2], Sarita Srivastava[3] and Surochita Basu[4]*

[1] Department of Botany, Chaudhary Charan Singh (CCS) University, Meerut, India, [2] Department of Botany, University of Lucknow, Lucknow, India, [3] Department of Botany, Chowdhary Mahadev Prasad (CMP) College (Constituent College of Central University of Allahabad), Prayagraj, India, [4] Department of Botany, Tripura University (A Central University), Agartala, India

Artificial polyploidy that brings about increase in cell size confers changes in histo-morphology leading to altered phenotype, causing changes in physiological attributes and enhanced concentration of secondary metabolites. The altered phenotype is generally a manifestation of tissue hardiness reflected as robust plant type. Based on a case study undertaken on an industrially important grass, *Cymbopogon khasianus* (2*n* = 60) valued for its citral rich essential oil, here we report that the artificial polyploidy not only brings about enhancement in concentration of essential oil but also facilitates lodging tolerance. The latter is contributed by ploidy mediated changes that occur to the cells and tissues in various plant organs by way of increased wall thickening, tissue enhancement and epidermal depositions that enable robust features. An exhaustive illustrated account covering various micro-/macro-morphological, skeletal and histochemical features constituting growth and development vis-a-vis ploidy mediated changes is presented highlighting the novelties realized on account of induced polyploidy.

Keywords: polyploidy and lodging tolerance, ploidy mediated histological changes, polyploidy and secondary metabolites, polyploidy breeding, aromatic grass

OPEN ACCESS

Edited by:
Jen-Tsung Chen, National University of Kaohsiung, Taiwan

Reviewed by:
Muhammad Ajmal Bashir, University of Tuscia, Italy
Yavar Vafaee, University of Kurdistan, Iran

****Correspondence:***
Umesh Chandra Lavania
lavaniauc@yahoo.co.in

Specialty section:
This article was submitted to Plant Breeding, a section of the journal Frontiers in Plant Science

Received: *30 March 2022*
Accepted: *20 April 2022*
Published: *09 May 2022*

Citation:
Vimala Y, Lavania UC, Singh M, Lavania S, Srivastava S and Basu S (2022) Realization of Lodging Tolerance in the Aromatic Grass, Cymbopogon khasianus Through Ploidy Intervention. Front. Plant Sci. 13:908659. doi: 10.3389/fpls.2022.908659

INTRODUCTION

It is an established fact that multiple cyclic episodes of whole-genome doubling or polyploidization have led to evolution and speciation in flowering plants (Wendel, 2015). The wondrous cycles of genome doubling are thought to be correlated with periods of extinction or global climate change over the geological time scale, while polyploids often thrive in harsh or disturbed environments (Van de Peer et al., 2021), and could colonize new habitats (Moraes et al., 2022). There are contrasting viewpoints about polyploidy as an evolutionary force, spanning from "evolutionary dead end" to "major player in evolution" (Lavania, 2020), but an established ecological force (Van de Peer et al., 2021). Initial models of polyploid evolution based on studies spanned over 70 years, considered autopolyploidy as an evolutionary dead end (Stebbins, 1999), but subsequent studies led to believe that polyploidy *per se* both auto- and allo- are the source for evolutionary innovation and species diversification (Van de Peer et al., 2021). Evidence accumulated on ecological niche vis-a-vis

polyploid establishment underpin that polyploids evince broader adaptability and vast ecological tolerance (teBeest et al., 2012) and owe higher invasive potential compared to their diploid relatives (Pandit et al., 2011), although the distribution of such polyploid lineages may have restricted range distribution in preferred environment (Villa et al., 2022). It is also surmised that there is differential response to both biotic interactions and abiotic stress on polyploids vs. non-polyploids (Van de Peer et al., 2021). Polyploid organisms are thought to be more resilient to extreme environments owing to increased genetic variation, bufferring effect and adaptive potential of duplicated genes (Van de Peer et al., 2017; Doyle and Coate, 2019). As such, stress response in general is an important factor in the establishment of polyploidy (Van de Peer et al., 2021).

Identification of several critical genome replication/duplication events during the periods of major environmental and climate change (Alix et al., 2017), have led to propose that environmental constraints could elicit polyploidization/genome duplication as an escape to overcome the vagaries of harsh environment as adaptive speciation and survival strategy (Levin, 2019).

While discussing the likely patterns of speciation in next 500 years, Levin (2019) opines that if the global climate undergoes major changes, then this will lead to an increase in the number of plant chromosomes, and thereby an increase in the current proportion of polyploids in angiosperms to 35–50%, and an overall proportion up to 50% of the Earth's plant species as polyploids. He further argues that such polyploidy incidences would be more pronounced in short-statured herbaceous plants. This is consistent with our earlier observations (Lavania and Srivastava, 1988, 1990), where it is observed that the subcultures of the diploid vs. autoteraploid calli when grown over a passage of monthly subcultures under stressful environment *in vitro*, exhibit differential effect to polyploidization, whereby the diploids turn into polyploids but the tetraploids retain the original ploidy status.

The polyploidy/genome doubling is considered a natural consequence to overcome abiotic stress. It is known to bring about changes in transpiration, water use efficiency, photosynthetic rate, phenology, antioxidant response, and morphology etc. that confer success to polyploids (Maherali et al., 2009; Deng et al., 2012; Soltis and Soltis, 2014). A lot has been discussed about the significance of both auto- and allo- polyploidy in conferring novelty and value addition to plants (Levin, 1983, 2002; Lavania and Vimala, 2022), especially where the plant biomass is the source of economic product, and their active metabolite components are valued in industrial applications (Lavania, 2005). It was therefore planned to explore whether polyploidy could lead to changes that confer morphological robustness from cultivation perspective, targeting a species that is cultivated through vegetative tillers under commercial cultivation, and the sexual system is deficient.

The genus *Cymbopogon* Spengel comprises a group of aromatic grasses that are either densely or loosely tufted. Although, almost all the species produce essential oil in the secretory cells present in the vegetative tissues of shoot, leaf and inflorescence, but only six species are majorly used for commercial cultivation, and the *C. khasianus* is one of them (Kumar et al., 2000; Lavania et al., 2012; Yogendra et al., 2021). Soenarko (1977) has provided detailed information on morphological, anatomical, geographical and ecological data on 55 species from taxonomic perspective, pinpointing that most of the species are perennial, where lateral branches/tillers are appressed to the main axis (culm). The perennial growth habit makes the growing tiller prone to lodging, and more so in *C. khasianus* because it becomes taller than the other species in the fast-growing season during warm and humid conditions.

The present study was undertaken to explore ploidy mediated approach to help realize genetic enhancement of an elite clone of an industrially important aromatic grass that suffers from lodging, and examine histo-morphologocal, qualitative and yield contributing characters from breeding perspective.

MATERIALS AND METHODS

Plant Material

An elite clone namely "CIM-Suwarna" of *Cymbopogon khasianus* (Hack) Stapf (ex Bor), ($2n$ = 60), developed at the CSIR-Central Institute of Medicinal and Aromatic Plants, Lucknow, India (Lal et al., 2010) was targeted to develop its clonal autotetraploids. Another clone "Krishna" of a related species *Cymbopogon flexuosus* said to produce highest concentration of lemongrass essential oil and popular in cultivation was used as a "Check."

Realization of Clonal Polyploids

The target species is an aromatic grass that sports laterally proliferating tiller formation, where meristem is basal and lay deep seated beneath the leaf sheath. As such special efforts are required for colchicine administration for induction of polyploidy. Accordingly, the clonal polyploids were developed following the experimental protocol standardized by Lavania et al. (2012). The axillary buds on fast-growing slips (tillers) were exposed to target the basal meristem, followed by immersion of bud bearing region of such slips in 0.1% (v/w) aqueous solution of colchicine in 2% DMSO for 7 h at 25°C, followed by thorough washing in running water and planting in soil. Emerging plantlets were screened for leaf stomata size, and those with uniformly and distinctly enlarged stomata, roughly twice the volume of source diploids, were selected followed by cytological screening to isolate polyploids. Both diploid and polyploid (auto-tetraploid) clones derived from the "same source tiller" were screened out through six passages of clonal propagation spread over 2 years for ploidy stability, and planted in field for further observations.

Micromorphological and Productivity Analysis

Cytologically stable autopolyploids vis-a-vis source diploids were scored for ploidy associated changes in morpho-anatomical features associated with plant biomass, cell geometry of vascular and non-vascular tissue, and essential oil secretory cells by light and fluorescence microscopy.

(i) Tissue preparation for histological examination for essential oil secretory cells: Hand cut sections of leaf and culm were prepared and incubated for 30 min at room temperature in 0.75% Schiff's reagent. The sections were then washed three times (10 min) with a freshly prepared solution of 0.5% (w/v) sodium metabisulfite in 0.1% HCl and mounted in 1N.HCl according to Lewinsohn et al. (1998). The stained sections were examined under microscope using both transmitted light and epifluorescence (blue or UV excitation). The size and frequency of essential oil glands was recorded at 40X magnification. Size of the essential oil secretory cells was calculated with the help of ocular micrometer, and cell frequency estimated by counting the number of cells/cm^2 of the leaf area. Following similar

TABLE 1 | Exomorphology, anatomy and growth related patterns affected by ploidy change (± *SE*) in the *Cymopogon khasianus*.

S. No.	Characters	Diploid	Tetraploid
1	Color (as per RHS catalog: Leaf sheath	Yellow green 146C	Yellow green 146C
2	Leaf (adaxial)	Green group N137B	Green group N137B
3	Leaf (abaxial)	Green group 137A	Green group 137A
4	Stem color	Yellow green 146D	Yellow green 146D
5	Spikelet color	Grayed green	Grayed green
6	Flowering time	Nov-Dec	September
7	Number of tillers (1 year)	97 ± 0.44	81 ± 0.65
8	Number of leaves per tiller	3–7	4–8
9	Plant height (cm)	147 ± 0.44	158 ± 0.71*
10	Culm length (cm)	228 ± 0.53	255 ± 0.63*
11	Inflorescence Length (cm)	75 ± 0.30	97 ± 0.53*
12	Number of nodes in culm	15 ± 0.41	12 ± 0.31
13	Length of internode in the middle region of culm (cm)	26.0 ± 0.48	29.5 ± 0.58*
14	Average Diameter (cm) of culm between 2nd and 3rd node	0.44 ± 0.009	0.49 ± 0.004*
15	Number of vascular bundles in the culm	115 ± 0.29	145 ± 0.88*
16	Area of the culm cross section occupied by the vascular bundles (mm^2)	6.54 ± 0.12	6.35 ± 0.09*
17	Area (L X B) of single culm vascular bundle of the 3rd concentric ring (μm^2)	22,500 ± 687	31,500 ± 814*
18	Area of Meta-xylem vessel (L × B) culm Vascular Bundle of the 3rd concentric ring (μm^2)	1,524 ± 54	1,857 ± 24*
19	Leaf mesophyll thickness/vascular thickness (μm)	165 ± 6.03/90 ± 0.0	195 ± 5.48*/115 ± 1.38*
20	Average thickness of leaf cuticle: adaxial/abaxial (μm)	3.7 ± 00/1.85 ± 0.01	5.55 ± 0.02*/3.7 ± 00*
21	Root Stele diameter (mm)	0.936 ± 0.038	1.051 ± 0.014*
22	Thickness of root vascular tissue (mm)	0.202 ± 0.005	0.244 ± 0.003*
23	Number of vascular bundles in root	18.8 ± 0.38	16.3 ± 0.21
24	Percentage of leaf vascular tissue	54.54%	58.97%
25	Average Leaf length × width (cm)	100 ± 2.0 × 1.24 ± 0.07	92 ± 1.8 × 1.31 ± 0.3
26	Average number of leaf major vein	16 ± 0.21	13 ± 0.21
27	Average distance between major veins (mm)	2.042 ± 0.026	2.210 ± 0.044*
28	Average leaf area (cm^2)	87.18 ± 0.31	49.38 ± 0.29*
29	Lumen size of essential oil containing cell (μm^2)	947 ± 21	1,747 ± 32*
30	Essential oil concentration in fresh herb (%)	0.52 ± 0.03 Citral = 82.0% Geraniol = 3.9%	0.66 ± 0.05* Citral = 85.9% Geraniol = 2.7%
31	Area of Leaf midrib in vertical section (μm^2)	742,500 ± 3,163	1,026,000 ± 1,391*
32	Average number of oil cells in leaf sheath	205 ± 0.683	178.7 ± 1.21
33	Area occupied by bulliform cell/cm^2 of leaf vertical section	0.3145 ± 0.016	0.3093 ± 0.006*
34	Area of stomatal complex (μm^2)	804.96 ± 27.9	1260.84 ± 34.8*
35	Stomatal index	27.65 ± 1.29	24.9 ± 0.802*
36	Stomatal guard cell area (μm^2)	174.1 ± 12.2	254.8 ± 35.8*
37	Size of leaf epidermal cell (μm^2)	1,911 ± 119.7	2,249 ± 90.8*
38	Phytolith size (μm^2) on leaf abaxial surface	261.07 ± 22.74	374.11 ± 21.17*
39	Phytolith frequency/mm^2 of leaf abaxial surface	106 ± 9.24	80 ± 13.3
40	Macrohair frequency/mm^2 of leaf abaxial surface	45.61 ± 1.49	31.45 ± 3.86
41	Size of macrohair (μm^2)	530.22 ± 24.73	850.97 ± 34.45*
42	Wax frequency/10μm^2 (on epidermal surface)	10.42 ± 0.11	7.63 ± 0.32

**Values significantly different with respect to diploid by Student's t-test at P = 0.05.*

staining procedures, the essential oil cells could also be seen in the surface view.

(ii) Tissue preparation for epicuticular depositions, cell geometry: To examine phytoliths on leaf surface, cleaned leaf pieces were boiled for 1–2 h by gradually raising the temperature of the waterbath from 80 to 100°C to digest the soft tissues according to Parry and Smithson (1958). Thereafter the leaf pieces were carefully washed and stained in 1% safranin in 70% glycerol, and observed under microscope for recording quantitative measurements. For recording data on cell geometry fresh leaves were scratched to clear the adaxial epidermal surface to record observations on abaxial surface.

To scan epicuticular wax deposition on leaf, the third mature leaf from a well grown tiller was excised, washed thoroughly in dH_2O distilled water, rinse dried and fixed in 5% Glutaraldehyde overnight and then transferred to phosphate buffer (pH 7.5), followed by dehydration through alcohol series. Air dried samples cut into 2–3 mm^2 pieces were loaded on SEM Aluminum stubs using double sided adhesive tape. Samples were coated in POLARON SC-7640 Sputter coater at 18 mA current for 160 s in which Gold-Palladium alloy was used as coating material. The samples were then scanned using a conventional scanning electron microscope LEO-430. The leaf abaxial surface ultra-structural details were examined and exposures were captured at desired magnifications.

To record the width of leaf mid-vein, middle region of the leaf was selected (Wilkinson, 1979). The glycerine mounts of hand-cut vertical sections (V.S.) stained in 1% safranin were examined under Nikon Eclipse Ni (Japan) microscope for anatomical characters. The measurements were recorded with a calibrated eyepiece at 100×.

(iii) Biomass and essential oil yield: For recording observations on biomass and essential oil yield, both progenitor diploid and its corresponding autopolyploid clones, along with a standard "Check" (clone Krishna of *C. flexuosus*) were grown in 10-m^2 plot with 36 hills per plot and plant to row distance 50 cm at the experimental field of the CSIR-Central Institute of Medicinal and Aromatic Plants, Lucknow, India. Data on herbage yield were taken at 4-monthly harvests over 1 year. Essential oil concentration in the leaves harvested at a similar growth stage was estimated by hydrodistillation in Clevenger's equipment adjusted to 60°C and run for 2 h, and qualitative analysis of essential oil was done by GLC.

RESULTS

Both the diploid and its corresponding autopolyploid grown under similar conditions were examined for recording the data on morphological, histological and metric traits and productivity analysis. A general account of observations recorded for morphologial and histological features is provided in **Table 1**, and the key features related to realization of sturdiness are given in **Table 2**. The data related to yield contributing characters and breeding potential of the developed polyploid clone are provided in **Table 3**. All the qualitative features related to the theme of the study are depicted in **Figures 1–5**.

TABLE 2 | Histomorphological features in the progenitor diploid and corresponding autotetraploid related to plant hardiness enabling lodging tolerance in the tetraploids.

Name of the species	Ploidy status	Hypodermal sclerenchyma thickness of culm cross section (μm) ± *SE*	Thickness of vascular region in culm cross section (mm) ± *SE*	Thickness of hypodermal sclerenchyma of leaf adaxial/abaxial (μm) ± *SE*	Average wax flake length (μm) on stomata/ epidermal surface ± *SE*	Area occupied by phytoliths (mm^2)/cm^2 of leaf abaxial surface ± *SE*	Increase in thickness of hypodermal sclerenchyma in culm in *4n* over *2n* (%)	Increase in thickness of culm vascular region (%)	Increase in hypodermal sclerenchyma of leaf in *4n* over *2n* (%)	Increase in wax flake length in *4n* over *2n* (%)	Increase in the area occupied by phytoliths in leaf in *4n* over *2n* (%)
C. khasianus	*2n*	25.9 ± 0.78	1.725 ± 0.094	89.02 ± 0.92 /69.44 ± 1.17	1.45 ± 0.095 /0.921 ± 0.062	2.82 ± 0.113	54.28	17.39	54.60	103.71	33.33
	4n	39.96 ± 0.80*	2.025 ± 0.227*	117.6 ± 1.49* /120.3 ± 0.70*	3.37 ± 0.095* /1.46 ± 0.095*	3.76 ± 0.140*					

*Values significantly different with respect to diploid by Student's *t*-test at $P = 0.05$.

TABLE 3 | Essential oil secretory channels and essential oil/biomass yield in the progenitor diploid and corresponding autotetraploid in *Cymbopogon khasianus*.

Name of the species	Ploidy status	Lumen size of essential oil-containing cell (μm^2) ± *SE*	Frequency of essential oil channels/cm^2 of leaf VS ± *SE*	Essential oil concentration in fresh herb (%) ± *SE*	Area (cm^2) covered by essential oil-producing cells/cm^2 of leaf VS ± *SE*	Number of tillers arising from a slip in 60 days ± *SE*	Fresh herb biomass (kg $10\ m^{-2}$) ± SE	Increase in essential oil channel area under cover in 4*n* over 2*n* (%)	Increase in essential oil concentration in 4*n* over 2*n* (%)	Increase in biomass yield in 4*n* over 2*n* (%)	Increase in essential oil productivity in 4*n* over 2*n* (%)
C. khasianus	2*n*	947 ± 21	3,168 ± 97	0.52 ± 0.03	0.030 ± 0.0002	13.8 ± 0.13	38.96 ± 0.23	26.67	26.92	20.30	33.99
	4*n*	1,747 ± 32*	2,175 ± 21*	0.66 ± 0.05*	0.038 ± 0.0004*	26.4 ± 0.22*	46.87 ± 0.34				
C. flexuosus—clone *Krishna*	2*n*	412 ± 17	4,419 ± 12	0.65 ± 0.02	0.018 ± 0.0001	12.3 ± 0.15	20.00 ± 0.25				

**Values significantly different with respect to diploid by Student's t-test at P = 0.05.*

It is observed that there is an overall increase in body size of the developed polyploid. This is consummated through increased cell size at all the organizational levels, including tissues, organs, and micromorphological constituents, and their associated developmental changes in cell wall thickening, and metabolic changes related to photosynthetic efficiency and secretion of secondary metabolites in the form of the essential oil. Whereas, tissue thickening enables plant sturdiness, an increased cell size adds to biomass and physiological efficiency for enhanced essential oil concentration, leading to overall lodging tolerance and enhanced productivity of the economic product. Specific details based on these observations are dealt in discussion section.

DISCUSSION

Vast data accumulated on the biology of polyploids for over more than 100 years suggest that polyploids are sturdier than diploids owing to the thicker stem and leaves and associated corresponding changes (Ramsey and Ramsey, 2014), sporting enhanced efficiency in stressed environment (Pandit et al., 2011; teBeest et al., 2012; Levin, 2019), as also offering the advantage of evolutionary novelty (Levin, 2002), and profound amenability in diverse habitats, albeit having restricted distribution (Villa et al., 2022). It is with this background that the present study was undertaken on a supposedly paleo-hexaploid ($2n = 60$) species of the *Cymbopogon* species complex (base number $\times = 10$, Soenarko, 1977; Lavania, 1988) to further enhance its biological potential by ploidy elevation for wider adaptability and enhanced productivity.

The results presented here demonstrate successful realization of genetically stable clonal autopolyploids in a commercially important aromatic grass valued for its citral rich essential oil used for its multifarious applications in aroma industry. Whereas, the target species used in this study is known to produce high biomass compared to other species of the genus, but the high biomass producing canopy *per se* is fraught with danger of lodging when challenged by intense air velocity and rains encountered in the fast-growing season. The instant induced polyploid reported here has been found to overcome such lodging challenge on account of stout stem, thicker and broader leaves realized in the polyploid owing to enhanced sclerenchyma in the vascular and epidermal regions and waxy coating/siliceous phytolith in the cuticular surface. At the same time the induced polyploid offers commercial advantage of enhanced biomass and increased concentration of essential oil, thus a dual advantage from cultivation perspective.

Comparative assay of micromorphological characters in diploids and autotetraploids reveal a clear-cut increase in the cell size reflected at all levels, including epidermal cells, vascular tissue, stomatal guard cells, essential oil secretory cells, phytolith size, cuticle thickness, and even epicuticular waxy deposition, albeit there is decrease in frequency of all such cells in per unit area. Nevertheless, there is an overall enhancement in the area occupied by the cells constituting larger tissues and organs. In particular, for the tissues contributing to economically important part, i.e., essential oil secreting cells in the source biomass, there

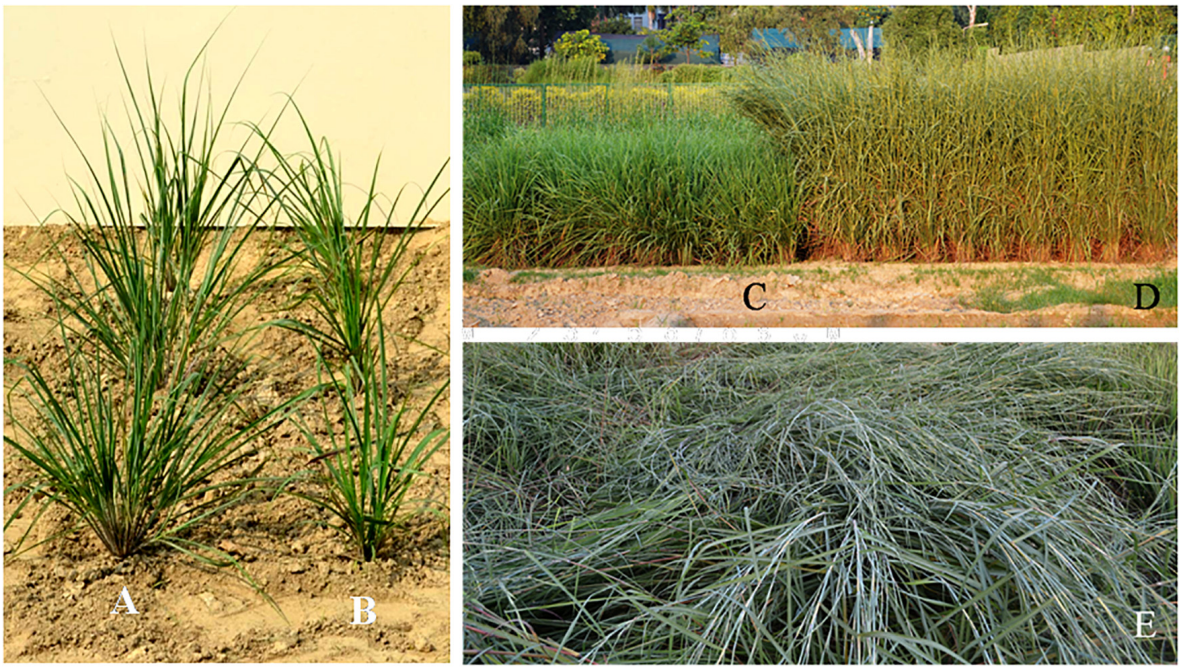

FIGURE 1 | Development of lodging tolerant autotetraploid *Cymbopogon khasianus*. **(A)** One month old plant of the tetraploid (4*n* = 120) and **(B)** corresponding source diploid (2*n* = 60). **(C–E)** Field view of fully grown plants, **(C)** check clone "Krishna", **(D)** lodging tolerant autotetraploid, and **(E)** lodging diploid progenitor.

is an overall increase in the area occupied by the essential oil secreting cells by 26.7%, and biomass yield by 20.3%, essential oil concentration by 26.9%, enabling an overall increase in essential oil productivity by 34%. At the same time the instant polyploid clone could withstand lodging pressure challenged by strong air currents and heavy rains encountered during the growing season (**Figure 1D**). Further, when compared with an elite clone "Krishna" of a related species *Cymbopogon flexuosus*—taken as "Check" (**Figure 1C**), the polyploid clone of *C. khasaianus* is superior by 237% in terms of the productivity of the economic product, i.e., citral rich essential oil.

The exhaustive data presented amply suggest that there is an overall increase in body size of the developed polyploid consummated through increased cell size at organizational levels, including tissues, organs and micromorphological constituents, and their associated developmental and metabolic changes. The major constituent components that deserve particular attention are highlighted below:-

Vascular Thickening Adds to Robustness and Lodging Tolerance

The findings presented in this study provide an exhaustive account of cell size associated comparisons between the diploid and the derived isogenic clonal polyploid (**Tables 1**, **2**). Such an elaborated account on ploidy associated changes has not been presented before. It is observed that with the increase in cell size in the tetraploid there are associated changes in the constituting tissues and organs, including cell wall thickening, secretions and waxy/siliceous phytolith depositions, and more particularly the hypodermal sclerenchyma thickness in the culm and leaf by a factor of > 50% (**Table 2**). It would be obvious that such enhanced thickening in the vascular tissues and depositions in the cuticular regions would impart physical robustness. The relative ratio toward thick walled sclerenchymatous regions would further add to robusticity, and in turn tolerance to physical pressures. Such a manifestation is in tune with the ecological behavior of neopolyploids known to demonstrate larger phenotypic and ecological ranges (Barker et al., 2012), through avoidance of competition with their established diploid parents (Hegarty et al., 2008).

The extracellular matrix constituting the cell wall is mainly composed of polysaccharides and structural proteins (Burton et al., 2010). The cell types appear to have a typical size range closely associated with function (Amodeo and Skotheim, 2016), characteristically optimized for cell fitness (Miettinen and Björklund, 2016; Vargas-Garcia et al., 2018). This is achieved through constant adjustment of cell wall composition and rearrangement of wall polysaccharides (Cosgrove, 2018; Zhang et al., 2021). Baker et al. (2017) have hypothesized that tetraploidy results in trait disintegration allowing for transgressive phenotypes emanating from changs in morphological, anatomical and physiological traits. A balanced ratio of structural components in the cell wall rearrangement facilitates wall rigidity, flexibility for cell dynamics, and enhanced potential for growth and development (Westermann, 2021), that could enable wider adaptability and robusticity to the polyploids. All this fits well in present set of things.

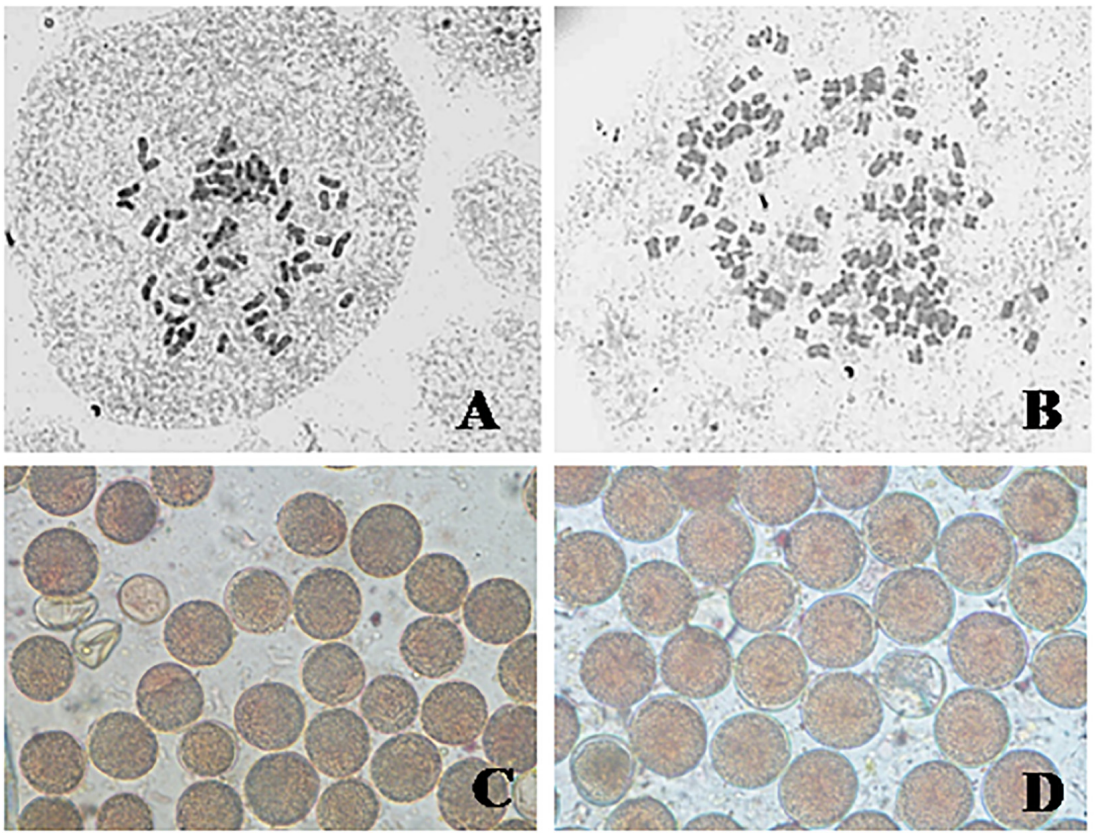

FIGURE 2 | Somatic chromosomes and pollen grains of *C. khasianus:* somatic chromosomes **(A)** source diploid (2*n* = 60) and **(B)** autotetraploid (4*n* = 120); pollen grains – **(C)** diploid, **(D)** tetraploid.

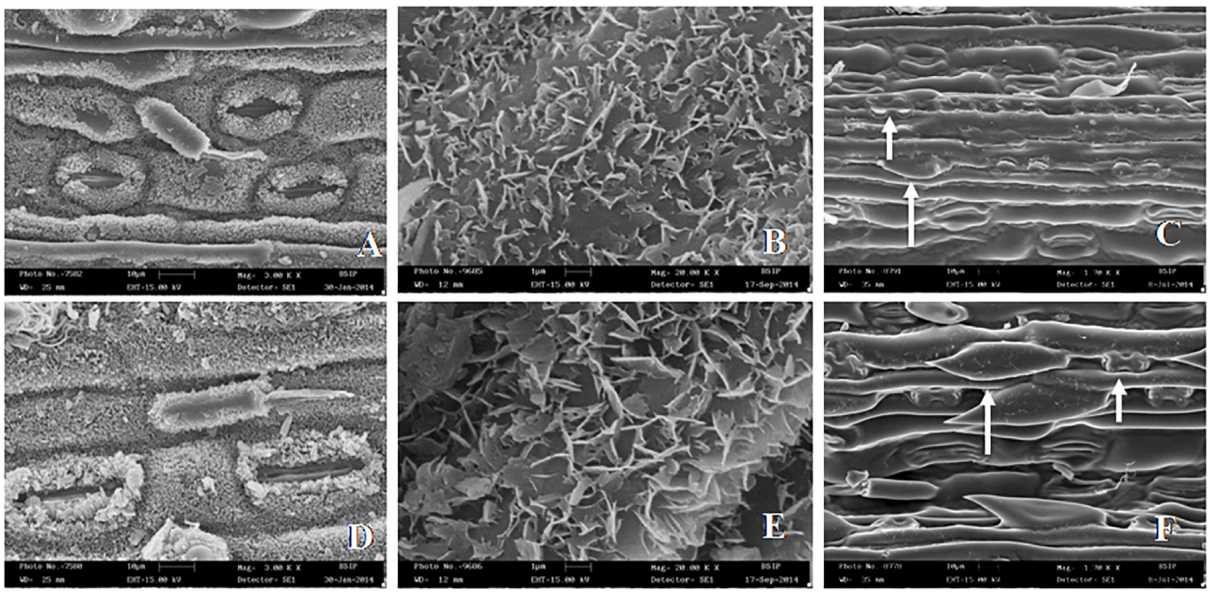

FIGURE 3 | SEM images of leaf surface features in *Cymbopogon khasianus* in the diploid (upper column) vs. autotetraploid (lower column) showing: **(A–D)**. Stomata with cuticuler wax deposition, **(B–E)**. Wax crystals, and **(C–F)**. Phytolith (small arrow) and macro-hair (large arrow).

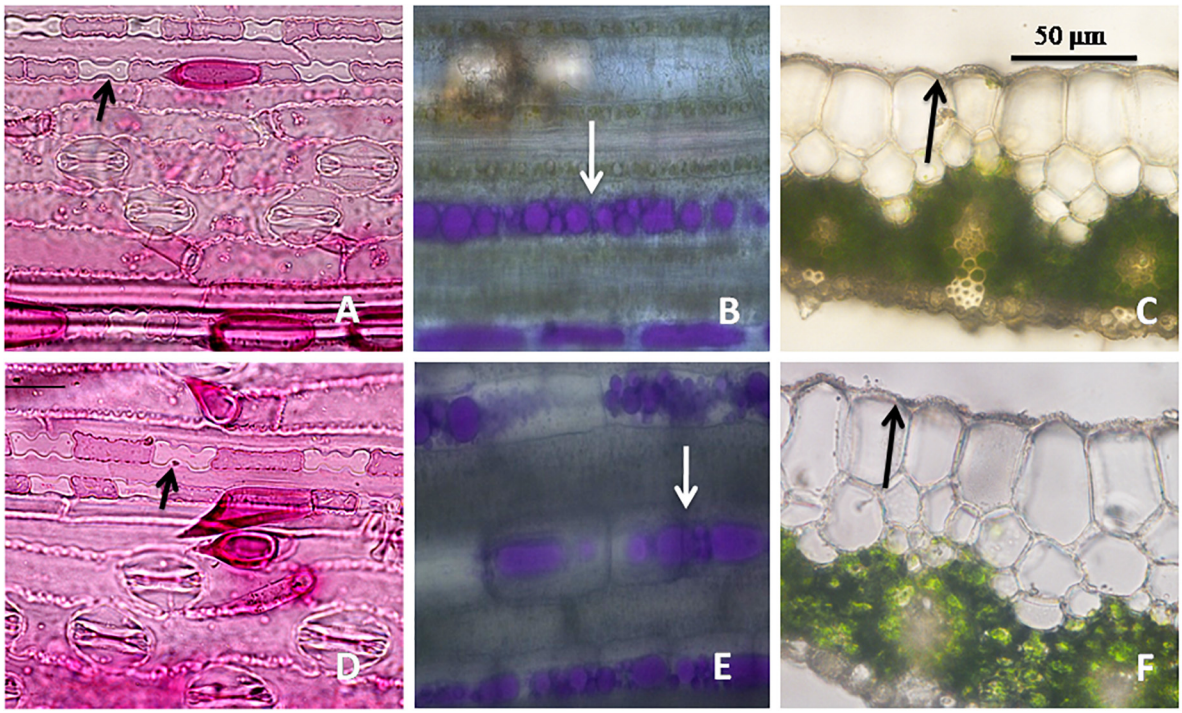

FIGURE 4 | Leaf epidermal features in *Cymbopogon khasianus* in the diploid (upper column) vs. autotetraploid (lower column) showing: **(A–D)**. Phytolith (arrow marked)/stomata, **(B–E)** secretory channels filled with essential oil (stained magenta), **(C–F)** cuticle thickness.

FIGURE 5 | VS of leaf (mid rib section) and TS of culm (partial) in the diploid (left) and tetraploid (right). Note, enhanced thickening/sclerenchymatus regions in the hypodermal and vascular bundle region in the tetraploid. Sclae bar = 200 µ.

Cell Size Contributes to Enhanced Physiological Efficiency and Increased Productivity

The key observation made out in this study is that there is an increase in cell size/wall thickening of the constituent cells of different tissues and organs on account of ploidy change. Such an effect is global and is observable in the overall organization of the polyploid clone (**Tables 1**, **2**). This is more clearly discerned in the size of stomatal guard cells, epidermal cells and essential oil secretory cells, and physiological activity in terms of chlorophyll content and waxy secretion/phytolith deposition. The increase in lumen size of the secretory cell is approximately double the volume compared to the source diploids, but in terms of overall area occupied by such cells this is accounted to ∼25%, which is also reflected in terms of essential oil concentration and yield of biomass and productivity of the economic product (**Table 3**).

A clear instance of increase in cell size as measured at the level of stomatal guard cells with ploidy change across the species has earlier been observed in *Coffea* spp. (Mishra, 1997), and in relation to essential concentration in *Cymbopogon* spp. (Janaki-Ammal and Gupta, 1966), and at autopolyploid level in different species of *Cympopogon* (Lavania et al., 2012). Extensive study undertaken by Soenarko (1977) on systematics and Lavania (1988) on cytology, lists the occurrence of natural ploidy series across the species with $2n$ = 20, 40, 60, wherein *C. khasianus* belongs to $2n$ = 60 series. A comparison of stomatal guard cells and essential oil secretory cells shows corresponding increase in cell size with ploidy series. Obviously, the stomata/essential oil secretory cells in *C. khasianus* are distinctly larger compared to natural diploids, and the same is reflected in the derived autopolyploids sporting further enlargement (Lavania et al., 2012), and is commensurate to ploidy elevation.

Doyle and Coate (2019) provide an elaborated account on the impact of genome doubling on the biology of cell vis-a-vis physiological and morphological novely. Trojak-Goluch et al. (2021) have discussed the prospective applications of artificial polyploidy in plant breeding of industrial crops. Whereas, manifestation of "gigas" effect in the phenotype is a common feature reflected in the neopolyploids but decrease in the ratio of nuclear membrane to chromatin brings more surface area to come in contact to genetic activity enabling higher physiological activity and developmental changes (Lavania et al., 2012; Doyle and Coate, 2019) in general, and secondary plant products in particular (Lavania, 2005). Since stomata are associated with various physiological activities in cell like water and CO_2 exchange, therefore, ploidy level may influence physiological activities too (Lea et al., 1977). Of course, manifestation of such effect could be genotype and species dependent (Lavania, 2005; Lavania et al., 2012).

CONCLUDING REMARKS

Artificial polyploidy is known to increase cell size in plants; axiomatically it is likely to enhance cell size of organs and tissues involved in metabolite production. However, effect of such polyploidy mediated changes could be species specific that could be inferred from micro-morphological examination of key components. *Cymbopogon* is a perennial C4 aromatic grass with numerous stiff stems arising from a short, rhizomatous root stock, indigenous to tropical and sub-tropical parts of the world. In these aromatic grasses the essential oil is stored in secretory channels that run parallel to the leaf mesophyll on the abaxial side embedded in between the vascular cylinders. The essential oil synthesis is at its maximum secretion with the onset of blooming. However, the fast growing tillers reaching the blooming stage are prone to lodging when challenged by strong winds and heavy showers. Therefore, realizing plant hardiness is considered an important requirement for optimum harvest. The present study on the development of lodging tolerant plants is an important step that could be achieved through induced polyploidy, vis-a-vis adding to enhanced productivity without causing any adverse effect (related to seed-based cultivation posed on account of autopolyploidy) on cultivation since the cultivation of this grass is done through vegetative plantation as the standard practice.

DATA AVAILABILITY STATEMENT

The raw data supporting the conclusions of this article will be made available by the authors, without undue reservation.

AUTHOR CONTRIBUTIONS

YV conceptualized and reviewed the manuscript. UL conceived the experimentation, performed the field evaluation, and drafted the manuscript. MS and SL performed micromorphological analysis and histological studies. SS and SB jointly did cytological screening. All authors contributed to the article and approved the submitted version.

FUNDING

This work was funded by the CSIR Emeritus grant to SL and INSA Senior Scientist support to UL.

REFERENCES

Alix, K., Gérard, P. R., Schwarzacher, T., and Heslop-Harrison, J. S. (2017). Polyploidy and interspecifc hybridization: partners for adaptation, speciation and evolution in plants. *Ann. Bot.* 120, 183–194. doi: 10.1093/aob/mcx079

Amodeo, A. A., and Skotheim, J. M. (2016). Cell-size control. *Cold Spring Harb. Perspect. Biol.* 8:a019083.

Baker, R. L., Yarkhunova, Y., Vidal, K., Ewers, B. E., and Weinig, C. (2017). Polyploidy and the relationship between leaf structure and function: implications for correlated evolution of anatomy, morphology, and physiology in Brassica. *BMC Plant Biol.* 17:3. doi: 10.1186/s12870-016-0957-3

Barker, M. S., Baute, G. J., and Liu, S.-L. (2012). "Duplications and turnover in plant genomes," in *Plant Genome Diversity*, Vol. 1, eds J. Greilhuber, J. Dolezel, and J. F. Wendel (Vienna: Springer), 155–169.

Burton, R., Gidley, M. J., and Fincher, G. B. (2010). Heterogeneity in the chemistry, structure and function of plant cell walls. *Nat. Chem. Biol.* 6, 724–732. doi: 10.1038/nchembio.439

Cosgrove, D. J. (2018). Diffuse growth of plant cell walls. *Plant Physiol.* 176, 16–27. doi: 10.1104/pp.17.01541

Deng, B., Du, W., Liu, C., Sun, W., Tian, S., and Dong, H. (2012). Antioxidant response to drought, cold and nutrient stress in two ploidy levels of tobacco plants: low resource requirement confers poly tolerance in polyploids? *Plant Growth Regul.* 66, 37–47. doi: 10.1007/s10725-011-9626-6

Doyle, J. J., and Coate, J. E. (2019). Polyploidy, the nucleotype, and novelty: the impact of genome doubling on the biology of the cell. *Int. J. Plant Sci.* 180, 1–52. doi: 10.1086/700636

Hegarty, M. J., Barker, G. L., Brennan, A. C., Edwards, K. J., Abbott, R. J., and Hiscock, S. J. (2008). Changes to gene expression associated with hybrid speciation in plants: further insights from transcriptomic studies in Senecio. *Philos. Trans. R. Soc. Lond. B* 363, 3055–3069.

Janaki Ammal, E. R., and Gupta, B. K. (1966). Oil content in relation to polyploidy in *Cymbopogon*. *Proc. Indian Acad. Sci. B* 64, 334–335. doi: 10.1007/bf03052137

Kumar, S., Dwivedi, S., Kukreja, A. K., Sharma, J. R., Bagchi, G. D., and (eds.). (2000). *Cymbopogon- the Aromatic Grasses Monograph*. Lucknow: Central Institute of Medicinal and Aromatic Plants.

Lal, R. K., Chandra, R., Chauhan, H. S., Misra, H. O., Singh, A., Srikrishna, S., et al. (2010). A high yielding variety of lemongrass (*Cymbopogon khasianus*) 'CIM-SUWARNA' suitable for water stress/rainfed/marginal land conditions. *J. Med. Arom. Pl. Sci.* 32, 61–63.

Lavania, U. C. (1988). Karyomorphological observations in *Cymbopogon* Sprengel. *Cytologia* 53, 517–524. doi: 10.1508/cytologia.53.517

Lavania, U. C. (2005). Genomic and ploidy manipulation for enhanced production of phyto-pharmaceuticals. *Plant Genet. Resour.* 3, 170–177. doi: 10.1079/pgr200576

Lavania, U. C. (2020). Plant speciation and polyploidy: in habitat divergence and environmental perspective. *Nucleus* 63, 1–5. doi: 10.1007/s13237-020-00311-6

Lavania, U. C., and Srivastava, S. (1988). Ploidy dependence of chromosomal variation in callus cultures of *Hyoscyamus muticus* L. *Protoplasma* 145, 55–58. doi: 10.1007/bf01323256

Lavania, U. C., and Srivastava, S. (1990). Evolutionary genomic change paralleled by diferential responses of 2× and 4× calli cultures. *Experientia* 46, 322–324. doi: 10.1007/bf01951778

Lavania, U. C., Srivastava, S., Lavania, S., Basu, S., Misra, N. K., and Mukai, Y. (2012). Autopolyploidy differentially influences body size in plants, but facilitates enhanced accumulation of secondary metabolites, causing increased cytosine methylation. *Plant J.* 71, 539–549. doi: 10.1111/j.1365-313X.2012.05006.x

Lavania, U. C., and Vimala, Y. (2022). Synthetic hybrid speciation: a resource for breeding novel lineages for secondary metabolites. *Nucleus* 65, 1–6. doi: 10.1007/s13237-022-00384-5

Lea, H. Z., Dunn, G. M., and Koch, D. W. (1977). Stomatal diffusion resistance in three ploidy levels of smooth bromegrass. *Crop Sci.* 17, 91–93. doi: 10.2135/cropsci1977.0011183x001700010026x

Levin, D. A. (1983). Polyploidy and novelty in flowering plants. *Am. Nat.* 122, 1–25. doi: 10.1086/284115

Levin, D. A. (2002). *The Role of Chromosomal Change in Plant Evolution*. New York, NY: Oxford University Press.

Levin, D. A. (2019). Plant speciation in the age of climate change. *Ann. Bot.* 124, 769–775. doi: 10.1093/aob/mcz108

Lewinsohn, E., Dudai, N., Tadmor, Y., Katzir, I., Ravid, U., Putievsky, E., et al. (1998). Histochemical localization of citral accumulation in lemongrass leaves (*Cymbopogon citratus* (D.C.) Stapf. Poaceae). *Ann. Bot* 81, 35–39. doi: 10.1006/anbo.1997.0525

Maherali, H., Walden, A. E., and Husband, B. C. (2009). Genome duplication and the evolution of physiological responses to water stress. *New Phytol.* 184, 721–731. doi: 10.1111/j.1469-8137.2009.02997.x

Miettinen, T. P., and Björklund, M. (2016). Cellular allometry of mitochondrial functionality establishes the optimal cell size. *Dev. Cell* 39, 370–382. doi: 10.1016/j.devcel.2016.09.004

Mishra, M. K. (1997). Stomatal characterization at different ploidy levels in Coffea. *Ann. Bot.* 80, 689–692. doi: 10.1006/anbo.1997.0491

Moraes, A. P., Engel, T. B. J., Forni-Martins, E. R., de Barros, F., Felix, L. P., and Cabral, J. S. (2022). Are chromosome number and genome size associated with habit and environmental niche variables? Insights from the Neotropical orchids. *Ann.Bot.* mcac021. doi: 10.1093/aob/mcac021

Pandit, M. K., Pocock, M. J. O., and Kunin, W. E. (2011). Ploidy influences rarity and invasiveness in plants. *J. Ecol.* 99, 1108–1115. doi: 10.1111/j.1365-2745.2011.01838.x

Parry, D. W., and Smithson, F. (1958). Silicification of bulliform cells in grasses. *Nature* 181, 1549–1550. doi: 10.1111/j.1438-8677.2011.00530.x

Ramsey, J., and Ramsey, T. S. (2014). Ecological studies of polyploidy in the 100 years following its discovery. *Phil.Trans. R. Soc. B.* 369:20130352. doi: 10.1098/rstb.2013.0352

Soenarko, S. (1977). The genus *Cymbopogon* Sprengel (Gramineae). *Reinwardtia* 9, 225–375.

Soltis, P. S., and Soltis, D. E. (2014). Flower diversity and angiosperm diversification. *Methods Mol. Biol.* 1110, 85–102. doi: 10.1007/978-1-4614-9408-9_4

Stebbins, G. L. (1999). A brief summary of my ideas on evolution. *Am J Bot.* 86, 1207–1208. doi: 10.2307/2656985

teBeest, M., LeRoux, J. J., Richardson, D. M., Brysting, A. K., Suda, J., Kubesová, M., et al. (2012). The more the better? The role of polyploidy in facilitating plant invasions. *Ann. Bot.* 109, 19–45. doi: 10.1093/aob/mcr277

Trojak-Goluch, A., Kawka-Lipińska, M., Wielgusz, K., and Praczyk, M. (2021). Polyploidy in industrial crops: applications and perspectives. *Plant Breed. Agronomy* 11:2574. doi: 10.3390/agronomy11122574

Van de Peer, Y., Ashman, T.-L., Soltis, P. S., and Soltis, D. E. (2021). Polyploidy: an evolutionary and ecological force in stressful times. *Plant Cell* 33, 11–26. doi: 10.1093/plcell/koaa015

Van de Peer, Y., Mizrachi, E., and Marchal, K. (2017). The evolutionary significance of polyploidy. *Nat. Rev. Genet.* 18, 411–424. doi: 10.1038/nrg.2017.26

Vargas-Garcia, C. A., Ghusinga, K. R., and Singh, A. (2018). Cell size control and gene expression homeostasis in single-cells. *Curr. Opin. Syst. Biol.* 8, 109–116. doi: 10.1016/j.coisb.2018.01.002

Villa, S., Montagna, M., and Pierce, S. (2022). Endemism in recently diverged angiosperms is associated with polyploidy. *Plant Ecol.* 223, 479–492. doi: 10.1007/s11258-022-01223-y

Wendel, J. F. (2015). The wondrous cycles of polyploidy in plants. *Am. J. Bot.* 102, 1753–1756. doi: 10.3732/ajb.1500320

Westermann, J. (2021). Two is company, but four is a party—Challenges of tetraploidization for cell wall dynamics and efficient tip-growth in pollen. *Plants* 10:2382. doi: 10.3390/plants10112382

Wilkinson, H. P. (1979). "The plant surface," in *Anatomy of the Dicotyledons*, eds C. R. Metcalf and I. Chalk (Oxford: Clarendon Press).

Yogendra, N. D., Nazeer, M., Eresha, Yadav, M. K., Baskaran, K., Pragadheesh, V. S., et al. (2021). Comparative morphological assessment of lemongrass (*Cymbopogon* spp.) cultivars for oil yield, chemical composition and quality parameters under southern region of India. *Madras Agric. J.* 108, 1–8. doi: 10.29321/MAJ.10.000564

Zhang, B., Gao, Y., Zhang, L., and Zhou, Y. (2021). The plant cell wall: Biosynthesis, construction, and functions. *J. Integr. Plant Biol.* 63, 251–272. doi: 10.1111/jipb.13055

Conflict of Interest: The authors declare that the research was conducted in the absence of any commercial or financial relationships that could be construed as a potential conflict of interest.

Publisher's Note: All claims expressed in this article are solely those of the authors and do not necessarily represent those of their affiliated organizations, or those of the publisher, the editors and the reviewers. Any product that may be evaluated in this article, or claim that may be made by its manufacturer, is not guaranteed or endorsed by the publisher.

frontiers | Frontiers in Plant Science

ORIGINAL RESEARCH
published: 22 June 2022
doi: 10.3389/fpls.2022.917910

In vitro Induction and Phenotypic Variations of Autotetraploid Garlic (*Allium sativum* L.) With Dwarfism

Yanbin Wen[1,2†], Hongjiu Liu[1†], Huanwen Meng[1], Lijun Qiao[1], Guoqing Zhang[3] and Zhihui Cheng[1]*

[1] College of Horticulture, Northwest A&F University, Xianyang, China, [2] Development Center of Fruit Vegetable and Herbal Tea, Datong, China, [3] Business School, Shanxi Datong University, Datong, China

Garlic (*Allium sativum* L.) is a compelling horticultural crop with high culinary and therapeutic values. Commercial garlic varieties are male-sterile and propagated asexually from individual cloves or bulbils. Consequently, its main breeding strategy has been confined to the time-consuming and inefficient selection approach from the existing germplasm. Polyploidy, meanwhile, plays a prominent role in conferring plants various changes in morphological, physiological, and ecological properties. Artificial polyploidy induction has gained pivotal attention to generate new genotype for further crop improvement as a mutational breeding method. In our study, efficient and reliable *in vitro* induction protocols of autotetraploid garlic were established by applying different antimitotic agents based on high-frequency direct shoot organogenesis initiated from inflorescence explant. The explants were cultured on solid medium containing various concentrations of colchicine or oryzalin for different duration days. Afterward, the ploidy levels of regenerated plantlets with stable and distinguished characters were confirmed by flow cytometry and chromosome counting. The colchicine concentration at 0.2% (w/v) combined with culture duration for 20 days was most efficient (the autotetraploid induction rate was 21.8%) compared to the induction rate of 4.3% using oryzalin at 60 μmol L^{-1} for 20 days. No polymorphic bands were detected by simple sequence repeat analysis between tetraploid and diploid plantlets. The tetraploids exhibited a stable and remarkable dwarfness effect rarely reported in artificial polyploidization among wide range of phenotypic variations. There are both morphological and cytological changes including extremely reduced plant height, thickening and broadening of leaves, disappearance of pseudostem, density reduction, and augmented width of stomatal. Furthermore, the level of phytohormones, including, indole propionic acid, gibberellin, brassinolide, zeatin, dihydrozeatin, and methyl jasmonate, was significantly lower in tetraploids than those in diploid controls, except indole acetic acid and abscisic acid, which could partly explain the dwarfness in hormonal regulation aspect. Moreover, as the typical secondary metabolites of garlic, organosulfur compounds including allicin, diallyl disulfide, and diallyl trisulfide accumulated a higher content significantly in tetraploids. The obtained dwarf genotype of autotetraploid garlic could bring new perspectives for the artificial polyploids breeding and be implemented as a new germplasm to facilitate investigation into whole-genome doubling consequences.

Keywords: autopolyploid, colchicine, dwarfness, garlic, *in vitro*, oryzalin, whole-genome duplication

OPEN ACCESS

Edited by:
Jen-Tsung Chen,
National University of Kaohsiung, Taiwan

Reviewed by:
Phanikanth Jogam,
Kakatiya University, India
Wei Seng Ho,
Universiti Malaysia Sarawak, Malaysia

***Correspondence:**
Zhihui Cheng
chengzh@nwafu.edu.cn

† These authors have contributed equally to this work

Specialty section:
This article was submitted to Plant Breeding, a section of the journal Frontiers in Plant Science

Received: *11 April 2022*
Accepted: *23 May 2022*
Published: *22 June 2022*

Citation:
Wen Y, Liu H, Meng H, Qiao L, Zhang G and Cheng Z (2022) In vitro Induction and Phenotypic Variations of Autotetraploid Garlic (Allium sativum L.) With Dwarfism. Front. Plant Sci. 13:917910. doi: 10.3389/fpls.2022.917910

INTRODUCTION

Garlic (*Allium sativum* L.) is a diploid (2n = 2x = 16) bulb crop that has been cultivated for more than 5,000 years with high global demand and economic significance (Maaß and Klaas, 1995; Ricroch et al., 2005). It is widely consumed as condiment, green vegetable, and herbal medicine with various properties, such as antibacterial, antithrombotic, antioxidant, immunomodulatory, lipid-lowering, and antidiabetic actions (Ipek et al., 2005; Tsai et al., 2012; Liu et al., 2015; Ajami and Vazirijavid, 2019).

Although fertility restoration of garlic has been achieved, the commercial garlic varieties are still sterile due to pollen degeneration and reproduced vegetatively by planting individual cloves or bulbils (Pooler and Simon, 1994; Etoh and Simon, 2002; Simon and Jenderek, 2003; Shemesh Mayer et al., 2013; Shemesh-Mayer and Kamenetsky-Goldstein, 2021), and consequently, the classical hybridization in breeding strategy and genetic studies of this economically important crop has been strictly hindered for a long time (Shemesh-Mayer et al., 2015). Its germplasm resources for improvement are severely lacking.

Polyploidy, that is, the possession of three or more complete sets of chromosomes (Ramsey and Schemske, 1998), is one of the major moving forces in the evolutionary process of higher plants which promotes speciation, biodiversity, and adaptation to environmental alterations (Wood et al., 2009; Hegarty et al., 2013; Iannicelli et al., 2020). It was estimated that about 95% of ferns, 15% of gymnosperms, and 70% of angiosperms have experienced chromosomes doubling in their evolutionary history (Masterson, 1994; Wendel, 2000). Polyploidization has been demonstrated to introduce profound phenotypic alterations including morphological (Ramsey and Schemske, 2002; Ye et al., 2010; Catalano et al., 2021), physiological (Balal et al., 2017; Mattingly and Hovick, 2021), phytochemical (Pradhan et al., 2018; Zheng et al., 2021; Tavan et al., 2022), and molecular (Adams and Wendel, 2005; Chen and Ni, 2006; Yan et al., 2019; Zhang et al., 2022) characteristics. In recent years, polyploidization has become a powerful breeding strategy to enable the development of new and improved germplasm, even cultivars. According to the origination, polyploids normally can be classified as autopolyploids and allopolyploids (Trojak-Goluch et al., 2021).

There are two underlying mechanisms for the generation of polyploids: mitotic polyploidization by doubling the whole sets of chromosomes in meristematic cells developing to mixoploid or polyploidy organisms, and meiotic polyploidization which generates 2n gametes (Ramsey and Schemske, 1998; Sattler et al., 2016). Since the pioneering artificial polyploidy induction trial documented with colchicine (Blakeslee, 1922; Blakeslee and Avery, 1937), it has gained remarkable attention for agriculture, medicine, and horticulture utilization as safe and effective breeding strategy for the improvement of desired valuable properties, especially for the vegetatively propagated plants such as garlic (Dhooghe et al., 2011; Hailu, 2021). Colchicine (natural alkaloid) and oryzalin (synthetic herbicide) were most commonly used antimitotic agents (AMA) by inhibiting the metaphase in cell division cycle. The spindle of microtubules compiled of α- and β-tubulin dimers is crucial for controlling chromosome segregation and correct polar migration during cell division (Dewitte and Murray, 2003; Wu and Akhmanova, 2017). These two AMA disturb the metaphase by associating with the α- and β-tubulin dimers, thereby reducing the attachment of new dimers on the assembly side of the microtubule, without reducing degradation of the microtubule at the disassembly end. As a result, disassembly proceeds faster than assembly and microtubules are depolymerized (Dhooghe et al., 2011, and references therein). Consequently, inhibition of this chromosome separation results in cells with doubled chromosomes. There are extensive drawbacks of colchicine including high toxicity to humans, poor binding capacity to plant tubulins, and side effects such as sterility, abnormal growth, and chromosome losses (Morejohn et al., 1987; Luckett, 1989). Meanwhile, oryzalin, with a significantly reduced toxicity for humans, is also more affinitive for plant tubulin dimers than colchicine, which can therefore be used at lower concentrations (Dolezel et al., 1994; Ascough et al., 2008). Colchicine is generally applied in a concentration range of 1.25–2.5 mM, while other antimitotic agents as oryzalin, trifluralin, or APM have a final concentration of 1–50 μM (Dhooghe et al., 2011).

It has been demonstrated that there are multi-variant factors involved in APPI procedure turning the results unpredictable and nondeterministic (Dhooghe et al., 2011; Niazian and Nalousi, 2020). These factors mainly include AMA type (Koefoed Petersen et al., 2003; Zhang Y. S. et al., 2020), concentration and exposure duration of AMA (Allum et al., 2007; Ardabili et al., 2021), plant genotype (Stanys et al., 2006; Podwyszyńska et al., 2018; Ardabili et al., 2021), and application system as *in vivo* or *in vitro* (Rubuluza et al., 2007; Eng and Ho, 2019; Parsons et al., 2019). Consequently, the interaction among aforementioned parameters is ambiguously tangled making it impossible to declare that there is one optimal overall APPI protocol regarding specific species.

Due to the absence of adequate breeding method to introduce desirable variations, it has been a long time that new garlic varieties are selected only from existing living collections through natural or induced mutations (Shemesh-Mayer and Kamenetsky-Goldstein, 2021). Increasing ploidy by artificial polyploidy induction (APPI) is an efficient way to create superior plants to sterile plants such as garlic by improving the morphology, disease resistance, adaptability to environmental stress, and yield or quality (Balal et al., 2017; Zhou et al., 2020; Kim et al., 2021; Tavan et al., 2022). In spite of few reports concerning APPI for garlic germplasm innovation (Novák, 1983; Cheng et al., 2012), they mainly focused on induction protocols with single antimitotic chemical and basic ploidy determination instead of performance evaluation, especially physiological and phytochemical characteristics. Here, we established an effective induction system of autotetraploid garlic with multiple chemicals from inflorescence explants and conducted subsequent analysis of polyploidy effects on morphology, cytology, and physiology levels in a first reported dwarfness germplasms. This research lays important groundwork and provides a new perspective for the development of novel germplasm for garlic breeding efforts.

MATERIALS AND METHODS

Plant Material

The widely grown garlic cultivar G064 was selected for artificial polyploidy induction. The healthy and uniform bulb cloves were cultivated in the garlic germplasm repository at the Horticultural Experimental Station (34°16′N, 108°4′E) of Northwest A&F University, Yangling, Shaanxi Province, China. Immature inflorescences with scape of 3 cm were collected as explant source when the ratio between scape length and pseudostem length was approximately 1 to 1.5 in late April to mid-May.

In vitro Polyploidization of Garlic

Efficient and reproducible *in vitro* regeneration protocols are a prerequisite for efficient *in vitro* polyploidization systems (Niazian and Nalousi, 2020). We have established high-frequency direct shoot organogenesis protocols from garlic inflorescence in which the scape, sheathing bract, immature bulbils and flower or primordial residue on sterilized inflorescence were removed and the remainder was trimmed into dome shape explants aseptically (Wen et al., 2020). The explants were pre-cultured on shooting medium for 2 days to initiate cell division and facilitate synchronizing the cell cycle to maximize the effect of antimitotic agents (Touchell et al., 2020; Wen et al., 2020) and then transferred to shooting medium containing 0, 125, 250, 500, 1,000, or 2,000 mg L^{-1} colchicine or 0, 15, 30, 60, 120, or 240 μmol L^{-1} oryzalin for different durations (5, 10, 15, 20, 25, or 30 days). Dimethyl sulfoxide (DMSO) (0.02%) was added to medium to increase the penetration. Four explants were cultured in one bottle. The shooting medium was used as control. After induction treatment, the treated explants were retransferred to shooting medium and cultured for 20 days. The shooting medium was composed of B5-based solid medium supplemented with 6-BA 2 mg $L^{-1}$and NAA 0.1 mg L^{-1} adjusted to pH 7.0. The regenerated shoots were calculated and cultured on rooting medium for the initiation of roots and further growth of the intact regenerated plantlets. Rooting medium was MS medium 0.5 mg L^{-1} NAA adjusted to pH 7.0. All explants were cultured at 23 ± 2°C under cool-white fluorescent light by 16-h photoperiod with light intensity of 40 μmol m^{-2} s^{-1}. The experiments were performed according to completely randomized design (CRD) with three replications per treatment (twenty explants per replicate). Data were analyzed using analysis of variance (ANOVA), and the difference between means was scored using LSD's multiple range test by statistical package of SPSS (Version 17.0).

Flow Cytometry Analysis

The determination of ploidy levels was conducted by flow cytometer (CytoFLEX, Beckman Coulter, Inc., United States). Appropriate nuclear isolation buffers are critical for preparation of suspensions of intact nuclei prior to analysis (Loureiro et al., 2006a). The Galbraith's buffer (45 mM $MgCl_2$, 20 mM MOPS, 30 mM sodium citrate, 0.1% (vol/vol) Triton X-100, adjusted to pH 7.0 with 1 M NaOH) (Galbraith et al., 1983) was selected after screening from six kinds of buffers ($MgSO_4$, Galbraith's, LB01, Otto's, GPB buffer, and Tris.$MgCl_2$) accompanied by microscopic observations of nuclei suspensions. The intact nuclear suspensions were prepared from young single leaf in each sample according to Dolezel et al. (2007) and Pellicer et al. (2021). In brief, the nuclei extractions were released by chopping 100 mg leaf tissue quickly with a brand-new razor blade in a pre-cooled 60 × 15 mm petri dish containing 0.9 ml of Galbraith's buffer followed by filtration through 30-μm nylon mesh to remove cell fragments and large tissue debris. Subsequently, 50 μl of 100 μg/ml propidium iodide (PI) and 50 μl of 100 μg/ml RNAse were added into the suspension to incubate in darkness for 10 min. PI was used to stain the nuclear DNA and RNase to eliminate the RNA and prevent the binding of PI to RNA (Loureiro et al., 2006b). Incubated samples were measured within 30 min by flow cytometer. CytoExpert 4.0 software was used for data analysis and outputting histogram of fluorescence intensities, which correspond to nuclear DNA contents. Genome sizes were measured on three non-consecutive days to ensure accuracy (Parsons et al., 2019). Four independent repetitions were performed on non-consecutive days to ensure accuracy, and at least 5,000 nuclei for each sample were analyzed.

Chromosome Counting

For the determination of chromosome numbers in putative tetraploid plantlets by FCM, young healthy roots tips were immersed in 0.05 colchicine solution for 2 h at 0 – 4°C to accumulate metaphase cells and then fixed in Carnoy's solution (ethanol: glacial acetic acid, 3: 1, v/v) for 24 h at 4°C. The fixed root tips were macerated by 1 mol/L HCL for 3 min in water bath at 60°C followed by rinsing with ice-cold water three times. The root tip cells were then excised and on a microscope slide following the squash method as described in a previous study and stained with a drop of Ziehl–Neelsen carbol fuchsin solution (Combination of 2.5 ml of melted phenol crystals, 5 ml of absolute alcohol, 0.5 g of basic fuchsin, and 50 ml of distilled water) (Lai and Lü, 2012). Cells were imaged using a compound microscope (Leica DM2000, Leica Microsystems, Heidelberg, Germany).

Molecular Variance Analysis

The regenerated tetraploid plantlets and donor plants grown in the field of G064 were randomly selected to conduct the SSR analysis. Genomic DNA was extracted from 0.25 g freeze-dried young leaves following a modified cetyltrimethyl ammonium bromide (CTAB) protocol (Murray and Thompson, 1980). The quality and quantity of extracted DNAs were examined by electrophoresis in 1% agarose gel and measured using spectrophotometer (NanoDrop™ 2000/2000c, Thermo Fisher Scientific, United States), respectively. The DNA samples were diluted to 50 ng/ml in sterile distilled water. PCR amplifications were carried in 10 ml reactions, each containing 2 ml template DNA (50 ng/ml), 0.5 ml forward primers (5 mmol/l), 0.5 ml reverse primers (5 mmol/l), 2 ml ddH_2O, and 5 ml 2 × Taq PCR Master mix (Tiangen Biotech Co., LTD., Beijing, China). The PCR program was as follows: 3 min at 95°C, 20 s denaturing

at 94°C, 20 s annealing at 68°C, and 30 s elongation at 72°C, followed by a 2°C reduction in the annealing temperature per cycle for 6 cycles. Then, the annealing temperature was reduced in each cycle by 1°C for 8 cycles from 58°C; the annealing temperature was maintained at 50°C for the remaining 20 cycles, followed by a final step at 72°C for 5 min. The amplified PCR products were separated by vertical electrophoresis on 8% polyacrylamide gel in 1 × TBE buffer at a constant 180 V for 1 h, visualized with silver staining, and photographed with a digital camera. Twenty-nine developed SSR primers (Li et al., 2021) were selected. The tests were repeated twice to ensure reliability and repeatability.

Morphological and Stomatal Characterization Analysis

Plantlets with different ploidy levels were sub-cultured for a further six months. Morphological studies of 10 diploid and tetraploid plantlets selected randomly were carried out. The well-developed functional leaves were used for measurement. The height, leaf length, leaf width, leaf thickness, leaf index, and root length were measured using an electronic digital caliper. Leaf pieces (5 mm^2) were excised after 6 h of exposure to light within the growth chamber and processed for the cryo-scanning electron microscopy (cryo-SEM) (Hitachi FlexSEM1000, Japan) according to the protocol described by Kumar et al. (2012). The stomatal length, width, and density measurements were performed using ImageJ software[1].

Hormone Assessment

For hormonal assay, the levels of various hormones including indole-3-acetic acid (IAA), zeatin (ZT), dihydrozeatin (DHZT), abscisic acid (ABA), isopentenyladenosine (IPA), Brassinosteroid (BR), Methyl Jasmonate (MeJA), and gibberellins (GA_3 and GA_4) were evaluated using enzyme-linked immunosorbent assay (ELISA) technique as described in previous studies (Yang et al., 2001; Liu et al., 2018; Liu et al., 2020). The mouse monoclonal antigens and antibodies against ZR, IAA, ABA, GA_3, and GA_4 were provided by Phytohormones Research Institute (China Agriculture University, Beijing, China). The assays were run according to manufacturer's instruction and in triplicate.

Organosulfur Compound Evaluation

The content of organosulfur compounds including allicin, diallyl disulfides (DADS), and diallyl trisulfides (DATS) was determined using liquid chromatography (HPLC) method. The detailed procedure was described by Xu et al. (2012) with modifications. Basically, 0.2 g leaf samples were extracted with 1.6 ml ethanol by Motor-Driven Tissue Grinder (Tissuelyser-II, Jingxin Co., Ltd., Shanghai, China) and incubated at 95°C for 30 min followed by filtration through 0.22-μm membrane. The filtrate was isolated by YMC-Pack ODS-A C18 column (250 mm × 4.6 mm, 5 μm) with mobile phase consisting of acetonitrile-ultrapure water (70:30, v/v). The flow rate was set as 1.0 $mL{\cdot}min^{-1}$, and the UV wavelength was 240 nm.

[1]http://rsb.info.nih.gov/ij/

RESULTS

Induction of Tetraploid Garlic With Colchicine and Oryzalin

The results of analysis of variance (ANOVA) showed the significant main effect of colchicine concentration and applied exposure durations on viability, shoot regeneration ability, and tetraploid induction rate (**Table 1**). The total explant viability and shoot regeneration ability (regenerated shoots per explant, RSE) reduced along with the increasing levels of duration time and concentration of colchicine, which is not the case for tetraploid induction rate.

The highest viability of 96.5% and RSE of 23.4 was observed from the application of 125 mg/L colchicine for 5 d but failed to induce tetraploid garlic (**Table 2**). The highest tetraploid induction rate was 21.8% achieved by highest concentration of 2,000 mg/L and 20 d duration. It is noticeable that no tetraploids were found with the concertation higher than 250 mg/L combined with the longest duration of 30 d, which was supported by the greater significance of duration (*) than that of concentration (**). Furthermore, there was significant interaction effect between concentration and duration on the viability and tetraploid induction rate except for RSE.

As for oryzalin treatment, the results also showed significant main effect from duration on viability, RSE, and tetraploid induction rate, while concentration did not present significant main effect on tetraploid induction rate (**Table 3**). Increasing concentrations and exposure durations also led to the significant reduction in viability and RSE. The most efficient way for chromosome doubling was found to be exposed to 60 μmol L^{-1}

TABLE 1 | Main effect of colchicine concentration and duration on viability of explants, shoot regeneration, and tetraploid induction rate from garlic inflorescence on solid medium.

Treatment	Viability (%)	Shoots/per explant	Tetraploid (%)
Duration(d)			
5	88.9 ± 2.9a	9.3 ± 1.2a	0.1 ± 0.5d
10	74.6 ± 4b	5.5 ± 0.9b	3.7 ± 2bc
15	60 ± 4.3c	4.2 ± 0.9c	6.2 ± 2.1bc
20	54.7 ± 3d	2.9 ± 0.7d	9.9 ± 2.7a
25	20.4 ± 3.1e	2.4 ± 1e	7.4 ± 2.4ab
30	7.3 ± 2.8f	0.9 ± 0.9f	2.8 ± 2.5c
Conc. (mg L^{-1})			
125	62.5 ± 5.5a	5.1 ± 1.8a	3.7 ± 2.3b
250	57.7 ± 5.5b	4.3 ± 1.6b	2.9 ± 2b
500	55.2 ± 5.8b	4.3 ± 1.7b	4.7 ± 2.2b
1000	44.7 ± 5.5c	3.9 ± 1.7bc	5.5 ± 2.2b
2000	34.7 ± 5.1d	3.5 ± 1.6c	8.2 ± 3a
F-test			
Duration	**	**	**
Conc.	**	**	*

*Data with different letters in the same column indicate significant difference between means at the 5% probability level by LSD. *Indicates significant difference at 0.05 level (ANOVA and LSD's multiple range test). **Indicates significant difference at 0.01 level (Two-directional ANOVA and LSD's multiple range test).*

TABLE 2 | Interaction effect of colchicine concentration and duration on viability of explants, shoot regeneration, and tetraploid induction rate from garlic inflorescence on solid medium.

Treatment		viability (%)	Shoots/per explant	Tetraploid (%)
Duration (d)	Concentration (mg L^{-1})			
0	0	100 ± 0	23.4 ± 1.4	0 ± 0
5	125	96.5 ± 1.7	11.3 ± 1.2	0 ± 0
5	250	95.2 ± 2.6	8.5 ± 0.9	0 ± 0
5	500	91.9 ± 2.7	9.5 ± 0.8	0 ± 0
5	1,000	85.3 ± 2.1	9.1 ± 0.6	0 ± 0
5	2,000	77.1 ± 2.2	7.9 ± 0.8	0.3 ± 0.7
10	125	91.7 ± 2.8	6.5 ± 1	0 ± 0
10	250	81.7 ± 1.7	5.3 ± 0.8	0 ± 0
10	500	86.8 ± 2.8	5.5 ± 0.5	3.3 ± 1.7
10	1,000	67.2 ± 3.1	5.4 ± 0.8	5.9 ± 1.4
10	2,000	45.5 ± 3.1	4.8 ± 0.8	9.2 ± 1
15	125	74.1 ± 2	5.1 ± 0.8	2.3 ± 0.4
15	250	69.7 ± 2.6	4.6 ± 0.6	3.1 ± 1
15	500	72.8 ± 2	4 ± 0.8	4.2 ± 1
15	1,000	53.4 ± 2.2	3.9 ± 0.9	10.2 ± 1
15	2,000	29.9 ± 3.4	3.3 ± 0.9	11.3 ± 2
20	125	63.3 ± 2.4	3.5 ± 0.3	2.6 ± 0.7
20	250	62.2 ± 2.1	2.5 ± 0.6	4.7 ± 1.4
20	500	55.5 ± 2.5	3 ± 0.5	10.6 ± 1.8
20	1,000	47.8 ± 2.5	2.8 ± 0.7	10 ± 0.6
20	2,000	44.6 ± 1.2	3 ± 0.5	21.8 ± 2.1
25	125	31.2 ± 1.8	2.7 ± 0.6	7.5 ± 1.4
25	250	28.6 ± 1.2	2.7 ± 0.7	5.7 ± 2.4
25	500	18.4 ± 1.4	3.2 ± 1	10.4 ± 1.3
25	1,000	13.1 ± 3.5	1.7 ± 1.2	6.7 ± 2.4
25	2,000	11 ± 1.7	1.7 ± 0.9	6.7 ± 3.4
30	125	18.3 ± 2.4	1.6 ± 0.7	10 ± 3.2
30	250	10.6 ± 2.4	1.8 ± 0.5	4.2 ± 2.7
30	500	6 ± 2.3	0.8 ± 0.9	0 ± 0
30	1,000	1.4 ± 1.6	0.3 ± 0.8	0 ± 0
30	2,000	0 ± 0	0 ± 0	0 ± 0
Duration × Conc.		**	NS	**

*Data with different letters in the same column indicate significant difference between means at the 5% probability level by LSD. **Indicates significant difference at 0.01 level (Two-directional ANOVA and LSD's multiple range test).*

oryzalin for 20 days with induction rate of 4.3% (**Table 4**). Unlike colchicine, the concentration and duration of oryzalin had no significant interaction effect on tetraploid induction rate but for viability and RSE.

Ploidy Assessment

FCM Analysis

The ploidy level of regenerated plantlets was evaluated by flow cytometry. It proved that flow cytometry was a fast and reliable screening method of ploidy level. The results indicated that linear histograms of relative nuclear DNA content of diploid control showed distinctive G0/G1 peaks at channel 0.8, whereas the induced mutant plantlets showed the same peak at channel 1.6 which was defined as putative tetraploid (**Figure 1**).

Chromosome Counting

After confirming the increase in genome size and separating tetraploid plants from diploids using flow cytometry, the microscopic chromosomal counting method was used. In this study, the chromosome number obtained for diploid plants was 2n = 2x = 16 and for tetraploid plants was 2n = 4x = 32 (**Figure 2**).

SSR Analysis

Of the 29 primers tested in SSR analysis, 28 markers presented clear, strong, and repeatable bands. These markers produced 65 scorable bands. The bands varied from one to five for each primer. No polymorphic bands were observed which indicated that neither gain nor loss of DNA sequence occurred after polyploidization of garlic in comparison with diploid (**Figure 3**).

Morphological Comparison

We found that all the autotetraploids induced from different AMA exhibited stable and similar uniform dwarf characteristics without pseudostem but densely packed leaves, and remarkably slow growth after successive culture for more than 2 years (**Figure 4**). The tetraploid showed significantly shorter and wider leaf by 1.7 and 1.5 times, respectively, which resulted in a significant decrease in leaf index compared to diploid (**Table 5**). The leaf thickness also increased by 3.5 times on average. The shorter root length was observed in tetraploids with developmental sluggish.

TABLE 3 | Main effect of oryzalin concentration and duration on viability of explants, shoot regeneration, and tetraploid induction rate from garlic inflorescence on solid medium.

Treatment	Viability (%)	Shoots/per explant	Tetraploid (%)
Duration (d)			
5	97a	18.4a	0.2d
10	91.7ab	15.8b	1.5c
15	87.7c	15.1b	2.1bc
20	78.3d	13.9c	3.2a
25	65.5e	9.5d	2.7ab
30	46.3f	8.2e	1.8bc
Conc. (μmol L^{-1})			
15	85.6a	15.6a	1.7a
30	83.1a	14.9a	1.8a
60	76.5b	14.6a	2.2a
120	74.2bc	11.7b	2.1a
240	69.4c	10.5c	1.7a
F-test			
Duration	**	**	**
Conc.	**	**	NS

*Data with different letters in the same column indicate significant difference between means at the 5% probability level by LSD. **Indicates significant difference at 0.01 level (Two-directional ANOVA and LSD's multiple range test).*

TABLE 4 | Interaction effect of oryzalin concentration and duration on viability of explants, shoot regeneration, and tetraploid induction rate from garlic inflorescence on solid medium.

Duration	Concentration	Viability (%)	Average Shoots/ per explant	Tetraploid (%)
0	0	100 ± 0	23.4 ± 1.4	0 ± 0
5	15	100 ± 0	19.5 ± 1.1	0.0 ± 0
5	30	98.3 ± 1.7	18.8 ± 0.5	0.0 ± 0
5	60	96.7 ± 1.7	18.4 ± 1.0	0.3 ± 0.3
5	120	95.0 ± 2.9	18.3 ± 0.6	0.2 ± 0.1
5	240	95.0 ± 2.9	17.1 ± 0.6	0.5 ± 0.3
10	15	96.7 ± 1.7	18.2 ± 0.6	0.8 ± 0.5
10	30	96.7 ± 1.7	15.9 ± 0.2	0.9 ± 0.5
10	60	91.7 ± 4.4	18.4 ± 1.7	1.5 ± 0.2
10	120	88.3 ± 4.4	13.5 ± 0.3	2.0 ± 0.8
10	240	85.0 ± 2.9	13.2 ± 1.2	2.4 ± 0
15	15	93.3 ± 4.4	15.5 ± 0.3	1.4 ± 0.7
15	30	91.7 ± 4.4	16.7 ± 1.4	1.6 ± 0.5
15	60	86.7 ± 1.7	17.4 ± 1.3	2.0 ± 0.4
15	120	86.7 ± 3.3	13.2 ± 1.0	2.8 ± 0.6
15	240	80.0 ± 2.9	12.6 ± 1.0	2.5 ± 0.7
20	15	78.3 ± 1.7	15.7 ± 0.7	2.8 ± 0.7
20	30	80.0 ± 0	16.1 ± 0.7	2.6 ± 0.3
20	60	81.7 ± 4.4	16.1 ± 0.5	4.3 ± 0.4
20	120	78.3 ± 3.3	11.1 ± 1.1	3.4 ± 1.1
20	240	73.3 ± 1.7	10.5 ± 1.1	2.8 ± 1.1
25	15	73.3 ± 1.7	13.1 ± 0.7	2.2 ± 0.3
25	30	73.3 ± 1.7	11.9 ± 0.8	3.4 ± 1.4
25	60	75.0 ± 5.8	9.1 ± 1.1	3.2 ± 0.9
25	120	68.3 ± 4.4	7.4 ± 0.4	2.3 ± 0.7
25	240	61.7 ± 3.3	5.9 ± 0.6	2.3 ± 0.9
30	15	71.7 ± 6.0	11.8 ± 1.3	2.7 ± 0.7
30	30	58.3 ± 4.4	10.2 ± 0.7	2.3 ± 1.2
30	60	51.7 ± 1.7	8.5 ± 1.1	2.1 ± 1.3
30	120	28.3 ± 3.3	6.7 ± 0.6	1.9 ± 0.9
30	240	21.7 ± 3.3	4.0 ± 0.8	0.0 ± 0
Duration × Conc.		*	*	NS

*Data with different letters in the same column indicate significant difference between means at the 5% probability level by LSD. *Indicates significant difference at 0.05 level (ANOVA and LSD's multiple range test).*

Stomatal Variation

Tetraploid induction led to significant changes in stomatal traits. The absence of waxy layer on leaf surface was observed (**Figure 5**). The width and area of abaxial stomata apparatus increased by 43 and 53% in tetraploids, while the density significantly reduced by 2 times. No difference was observed in the stomata length (**Table 6**).

Physiological and Sulfur-Containing Compound Evaluation

A comparison of physiological parameters in diploid and tetraploid plants showed significant differences. The content of total soluble sugar and protein increased by 172 and 166% in tetraploids, On the contrary, the amount of reduced sugar was found 1.7 times higher in diploid plants than in tetraploid (**Figure 6**). Allicin, diallyl disulfide (DADS), and diallyl trisulfide (DATS) are the main active metabolites in garlic, and HPLC analysis showed that allicin, DADS, and DATS were 50%, 44.3%, and 48.6% higher than those of diploids, respectively (**Figure 7**).

Endogenous Hormone Analysis

Compared with diploid, the contents of nine endogenous hormones in the autotetraploid garlic as indole acetic acid (IAA), indole propionic acid (IPA), gibberellin (GA_3 and GA_4), abscisic acid (ABA), brassinolide (BR), zein (ZT), dihydrozeatin (DHZT), and methyl jasmonate (MeJA) changed significantly. The elevated contents of IAA and ABA were detected in tetraploids which increased significantly, while the contents of other hormones were slightly lower than those in diploids (**Figure 8**).

DISCUSSION

Chromosome Doubling

Autopolyploidization, formed by within-species whole-genome duplication, was widely considered to be a massive mutation force in plant evolution and powerful tool to provide a broad germplasm base in breeding program (Sattler et al., 2016; Bohutínská et al., 2021). Although the artificial induction of polyploidy has been used to introduce comprehensive alterations in morphological, histological, physiological, agronomic, and genomic levels in plenty of plant species, the efficiency of specific protocols and consequences are still ambiguous (Sanwal et al., 2010; Zhang et al., 2010; Rambani et al., 2014; Ahmadi and Ebrahimzadeh, 2020; Baghyalakshmi et al., 2020; Fox et al., 2020).

Among the polyploidy induction methods, *in vitro* techniques can increase the efficiency of polyploidy induction and reduce mixoploid formation by minimizing the complex influence from internal or external factors and guarantee the multiplication of the mutant throughout the year (Touchell et al., 2020; Bhusare et al., 2021). The uniformity of environmental factors such as temperature and light can simultaneously cause meristem cell division, decrease mixoploid progeny, and increase complete tetraploid progeny (Niazian and Nalousi, 2020).

Stable and efficient regeneration system is a prerequisite for polyploidy induction or genetic manipulation (Wang et al., 2011). Nowadays, the most commonly used explants for *in vitro* polyploidy induction are shoot tips, axillary buds, petiole or leaf explants, nodal segments, roots, and callus (Trojak-Goluch et al., 2021). The main problems in mutation breeding of vegetatively propagated plants *in vitro* are the formation of chimeras and the somatic elimination (diplontic selection) of mutated sectors after mutagenic treatment (Suprasanna et al., 2015). Consequently, it is suggested that the best method for *in vitro* polyploidization is through direct adventitious shoot regeneration without pre-existence of shoot-bud or meristem tissue, because young meristematic portions are more flexible to polyploidy induction, since they provide better permeability to the antimitotic chemicals (Eng and Ho, 2019; Touchell et al., 2020). Satisfactory results of polyploidy induction are also obtained as a result of antimitotic treatment of seedlings containing intensely dividing meristematic tissues for many

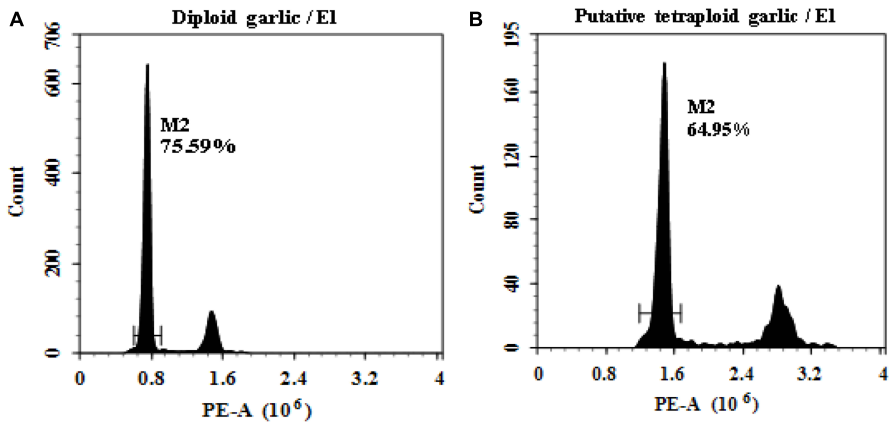

FIGURE 1 | Linea histograms of the relative fluorescence intensity of garlic with FCM. **(A)** Diploid (2n = 2x = 16). **(B)** Putative tetraploid (2n = 2x = 32).

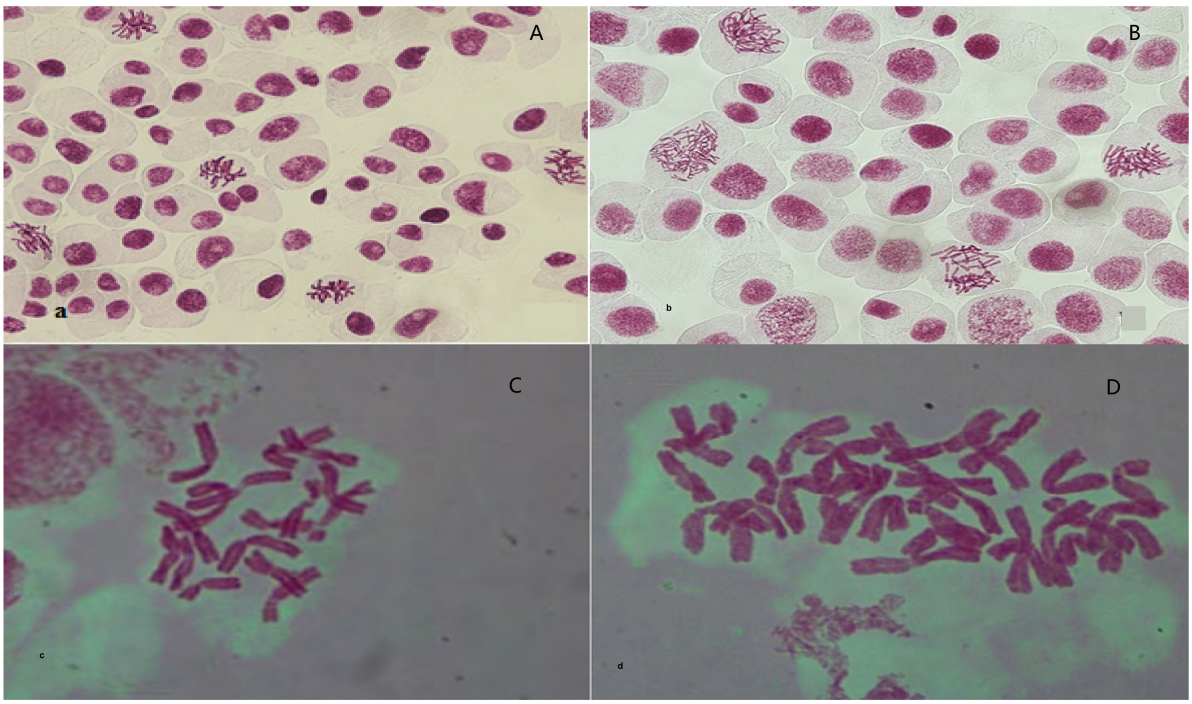

FIGURE 2 | Observation and validation of root tip chromosomes in regenerated plantlets. **(A,C)** Diploid garlic (2n = 2x = 16). **(B,D)** Tetraploid garlic (2n = 2x = 32).

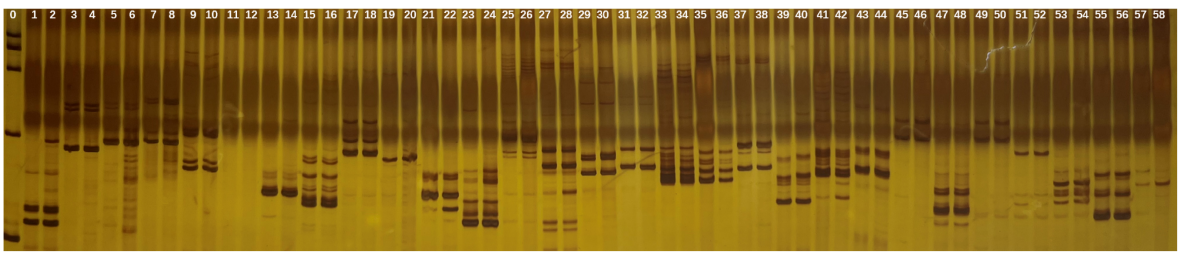

FIGURE 3 | SSR banding pattern in the tetraploid and diploid garlic plantlets by 29 primers. Lane 0: marker, odd lane: diploid garlic, even lane: tetraploid garlic.

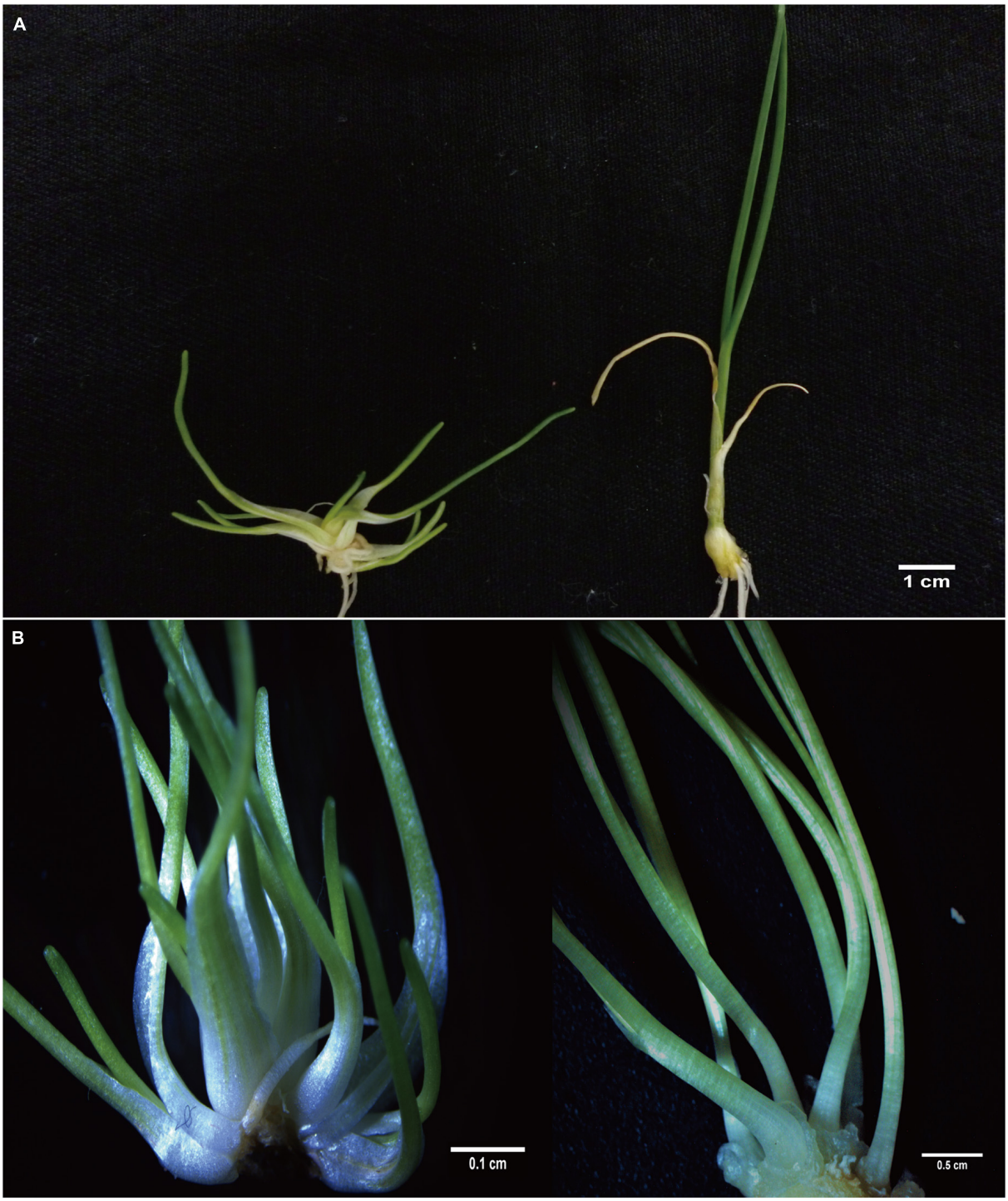

FIGURE 4 | Comparison of plant architecture and growth characteristics of diploid and tetraploid in different regeneration stages. **(A)** Developed tetraploid (left) and diploid (right) plantlet. **(B)** Newly regenerated tetraploid (left) and diploid (right) shoots.

industrial species (Trojak-Goluch et al., 2021). To establish the polyploidization system, we explored a high-frequency direct shoot organogenesis from garlic inflorescence as explant with active meristematic status, which is more amenable to ploidy alterations and in regeneration of autopolyploid shoots (Wen et al., 2020; Gantait and Mukherjee, 2021).

Utilization of suitable antimitotic chemicals is critical in polyploidy induction. Among different antimitotic agents,

TABLE 5 | Morphological characteristics of diploid and tetraploid garlic.

Morphological characteristics	Leaf length (mm)	Leaf width (mm)	Leaf index	Leaf thickness (mm)	Root length (mm)
Diploid	50.9 ± 6.2**	3.4 ± 0.3	14.9 ± 0.6**	0.4 ± 0.0	112.0 ± 2.3**
Tetraploid	18.2 ± 1.2	8.4 ± 0.4**	2.2 ± 0.1	1.8 ± 0.1**	71.4 ± 3.4

*Data are presented as mean ± SE. Data with **Indicate significant difference at 0.01 level by one-directional ANOVA and Student's t-test.*

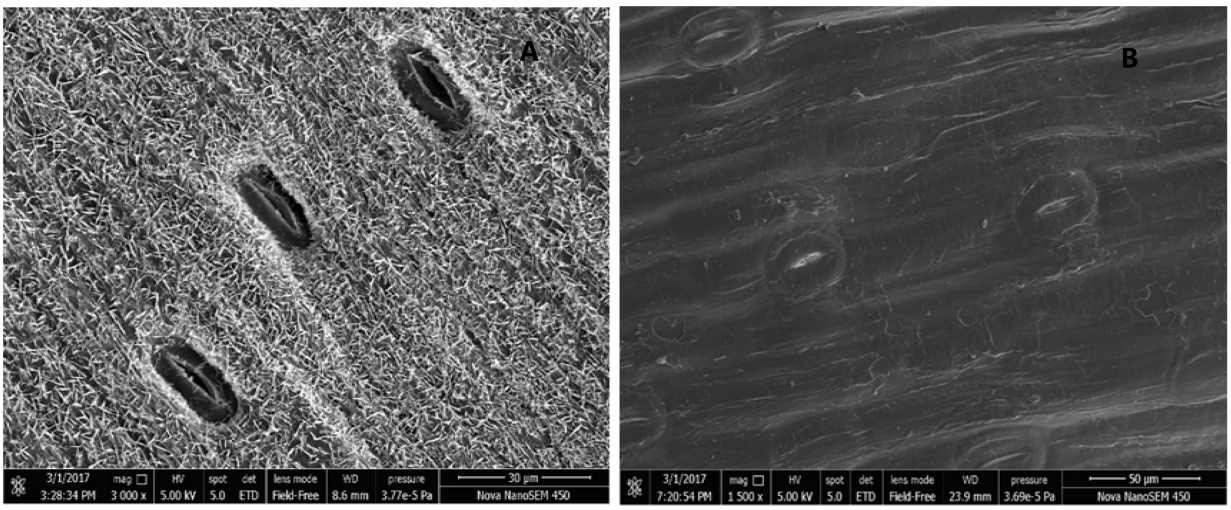

FIGURE 5 | Cryo-scanning electron micrographs of stomata. **(A)** Diploid garlic. **(B)** Tetraploid garlic.

colchicine has been the most commonly used chemical as the criteria (Dhooghe et al., 2011). However, it also causes side effects such as sterility, abnormal growth, chromosome losses or rearrangements, and gene mutation (Luckett, 1989). Moreover, due to its high affinity to microtubules of animal cells, colchicine is highly toxic to mammals and impacts negatively on the environment (Morejohn et al., 1987). Colchicine binds poorly to plant tubulins; thus, it is usually used in relatively high concentrations. For these multiple drawbacks, mitosis-inhibiting herbicides with more affinity for plant tubulin dimer have gained attraction as its alternatives (Wan et al., 1991; Häntzschel and Weber, 2010). They have outperformed colchicine for the higher efficiency of polyploidy induction in many plant species including fruit (van Duren et al., 1996; Bartish et al., 1998), vegetable (Viehmannová et al., 2009), ornamentals (Van Laere et al., 2006), agricultural crops, and forage (Quesenberry et al., 2010). However, our study demonstrated that colchicine is still the optimal mutation agent with tetraploid induction rate of 21.8% compared to 4.3% for oryzalin.

The concentration and exposure time of specific antimitotic compounds are most crucial factors. Too low doses may be ineffective, while excessively high concentrations are toxic and usually cause reduced viability even lethal. Furthermore, high concentrations and exposure times can result in higher ploidy levels than desired (Allum et al., 2007). Up to now, consistent investigation has established the agreement that in case of successful induction treatment, usually lower concentrations were accompanied by longer exposure duration and vice versa. One cannot proclaim that one antimitotic agent is the most successful (Dhooghe et al., 2011) even for certain species, because it is also significantly affected by the genotype and explant type of the donor plant (Trojak-Goluch et al., 2021). The evaluation of main and interaction effect between these two factors has yet been conducted in related research before. We demonstrated that the concentration of oryzalin had no main effect on tetraploid induction rate in agreement with its high affinity; meanwhile, the interaction effect was not observed neither. It means the duration scale setting should be paid more concise considerations.

Morphological and Hormonal Variations

Genome doubling event is a single macromutation with many phenotypic consequences (Doyle and Coate, 2020). Autopolyploids tend to be superior to their diploid parents with respect to morphological changes, genetic adaptability, and tolerance to environmental stresses (Leitch and Leitch, 2008), among which, the giga effect as bigger organs was preeminent. However, polyploids do not always exhibit higher quality and/or enlargement (Tsai et al., 2021). It illustrates that

TABLE 6 | Characteristics of stomatal apparatus in diploid and tetraploid garlic plantlets.

Ploidy level	Length (μm)	Width (μm)	Area (μm^2)	Density (mm^2)
Diploid	35.2 ± 3.2	12.2 ± 1.7	324.7 ± 50.2	1.30E-04**
Tetraploid	35.3 ± 4.2	17.4 ± 3.0**	497.1 ± 109.2**	4.55E-05

*Data are presented as mean ± SE. **Indicates significant difference at 0.01 level by one-directional ANOVA and Student's t-test.*

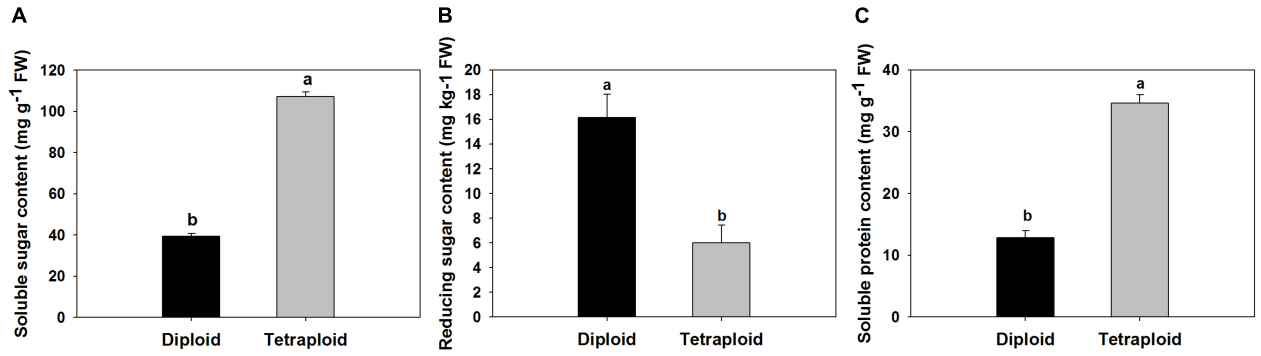

FIGURE 6 | Comparison of physiological compounds. **(A)** Soluble sugar. **(B)** Reducing sugar. **(C)** Soluble protein.

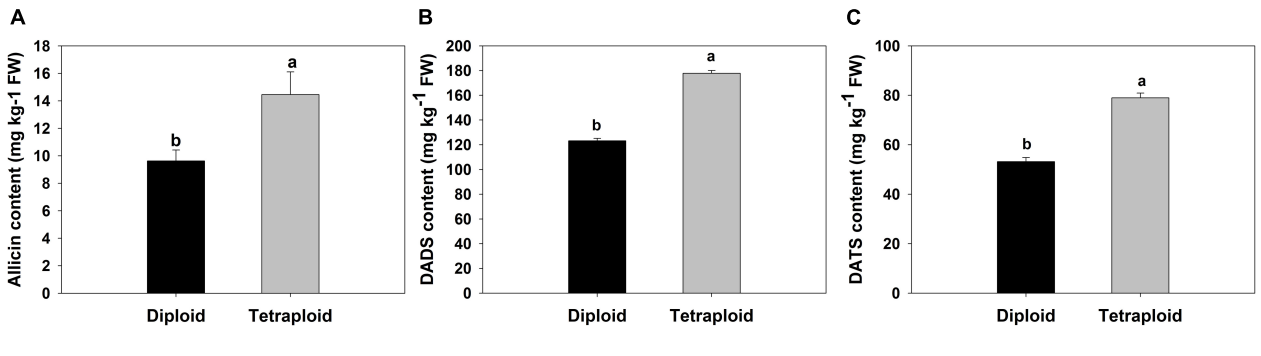

FIGURE 7 | Comparison of sulfur-containing compounds. **(A)** Allicin, **(B)** DADS. **(C)** DATS.

stochastic changes in phenotype initiated by ploidy are species-dependent (Trojak-Goluch et al., 2021). The autotetraploid garlic obtained from our study is accompanied by thicker, wider, but much shorter leaves and developmentally delayed roots reported previously (Dixit and Chaudhary, 2014; Tavan et al., 2015; Ayu et al., 2019), along with difficulty acclimating to a greenhouse environment (Roy et al., 2001; Trojak-Goluch and Skomra, 2013).

Dwarfing is the most noticeable phenotype displayed in tetraploid garlic compared to the diploid counterpart. The extreme dwarfness after tetraploidization was also reported in apple (Ma et al., 2016), cabbage (Ari et al., 2015), Chinese jujube (Wang et al., 2019), Escallonia genus (Denaeghel et al., 2018), and Z. *zamiifolia* (Seneviratne et al., 2020) following genome doubling.

Polyploidization can alter plant morphology, phenology, and physiology within only one or a few generations (te Beest et al., 2012). After more than two consecutive years of subculture, we found that newly regenerated autotetraploid garlic plantlets were still lack of pseudostem and significantly shorter than the diploid. We thus excluded the possibility that colchicine or oryzalin toxicity caused dwarfism of autotetraploid garlic.

The dwarfness of tetraploid garlic could attribute to its slower growth (Rao et al., 2019; Yan et al., 2022). Following polyploidization, individuals may experience "genomic shock" (McClintock, 1984) conferring disruption of the balance between nuclear and cytoplasmic components which inhibits the completion of mitosis and meiosis (Cavalier-Smith, 1978; Otto and Whitton, 2000; Otto, 2007; Manzoor et al., 2019). It was suggested that increasement of cell volume after polyploidization could strongly reduce cell division rate and slow down the activity of metabolism, consequently resulting in low growth rates (Cavalier-Smith, 1978; Tsukaya, 2013; Corneillie et al., 2019; Sabooni et al., 2022).

Recent reports have demonstrated that dwarfism and organ development in polyploidy were regulated by the complex interaction of various phytohormones (Kondorosi et al., 2000; Wang Y. et al., 2018). It has been reported that mutants with defects in plant hormone biosynthesis or signaling could result in dwarfism (Durbak et al., 2012; Chen et al., 2016; Wang B. et al., 2018). Most dwarfism phenotypes in plants are associated with genes involved in the biosynthesis or signaling pathways of GA, BR, and IAA (Nemhauser et al., 2006; Wang and Li, 2008; Ma et al., 2016; Wang B. et al., 2018).

The deficiency of active GAs, brassinosteroids (BRs), was detected in the dwarfism phenotype for tetraploid rice, apple, and Arabidopsis which applied with our results (Spielmeyer et al., 2002; Yin et al., 2002). Studies have convincingly demonstrated that GA deficiency specifically causes the decrease in plant height. The dwarf and semidwarf rice resulted from a deficiency in active GAs (Spielmeyer et al., 2002; Sakamoto et al., 2004). The impaired GA biosynthesis was found in the dwarf banana phenotypes (Chen et al., 2016; Shao et al., 2020). Decreased accumulation

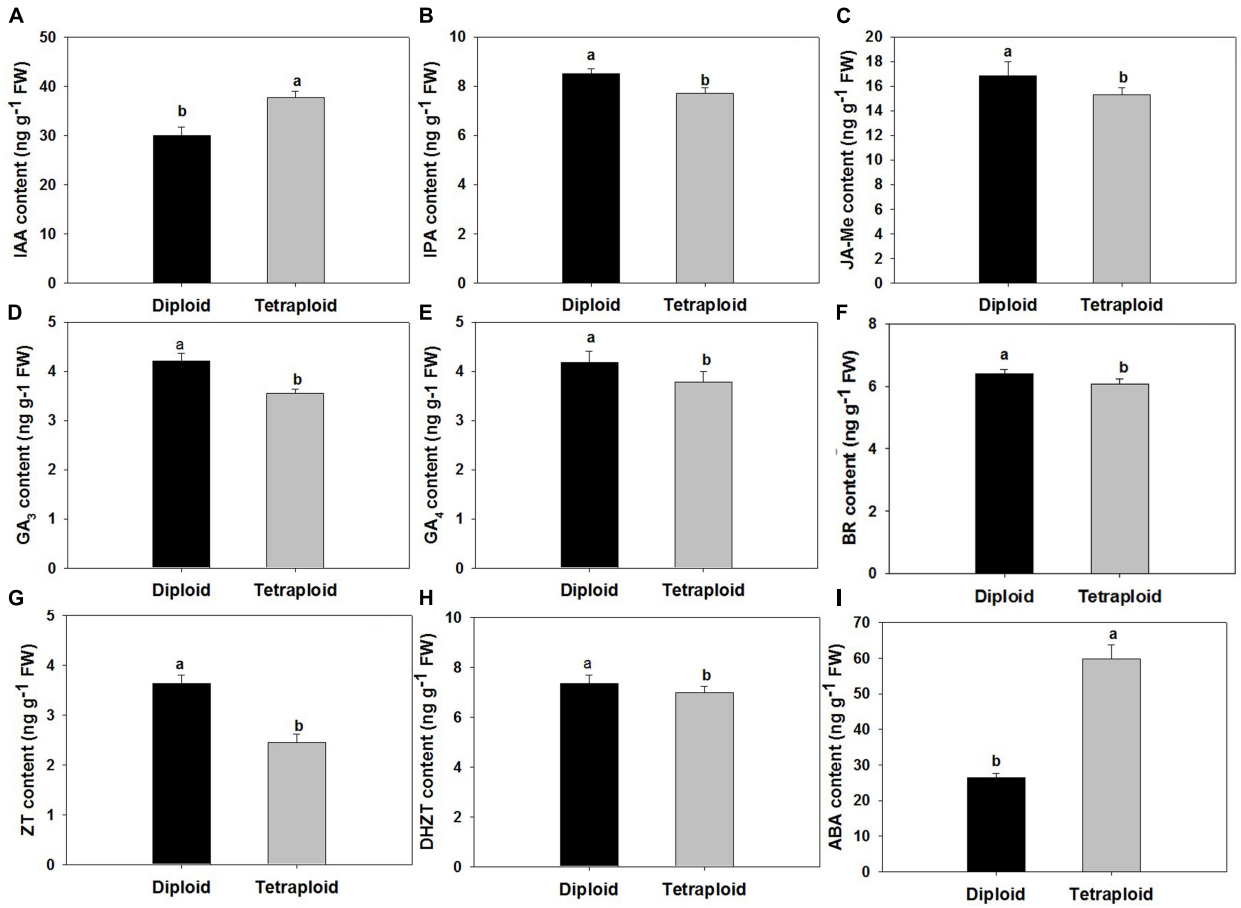

FIGURE 8 | Comparison of endogenous hormone levels. **(A)** Indole-3-acetic acid (IAA). **(B)** Isopentenyladenosine (IPA). **(C)** Methyl Jasmonate (MeJA). **(D)** Gibberellins (GA_3) **(E)** Gibberellins (GA_4). **(F)** Brassinosteroid (BR). **(G)** Zeatin (ZT). **(H)** Dihydrozeatin (DHZT). **(I)** Abscisic acid (ABA).

of GAs can suppress additional cell divisions and decrease the size of the division zone thereby inhibiting leaf growth and contributing to the semidwarf phenotype in maize (Nelissen et al., 2012; Zhang J. et al., 2020). The mutants defective in BR synthesizing genes also reduce plant height in rice, sorghum, and barley (Fujioka et al., 1998; Dockter and Hansson, 2015; Hirano et al., 2017). This could be attributed to the inhibition of genes, transcription factors, or enzymes related to BR synthesis and signal transduction pathways which affect the cell elongation or expansion (Nakamura et al., 2006; Zhao et al., 2022).

The IAA and ABA contents were significantly higher in tetraploid dwarf garlic. The significantly higher IAA was found in the dwarf bananas which likely regulated GA biosynthesis by negative feedback (Deng et al., 2021). IAA was also found to induce the overexpression of OsIAA1 gene (member of Aux/IAA and auxin response factor), leading to shorter plant and loose architecture distinctively in rice (Song et al., 2009). ABA accumulation by higher transcript level of the ABA pathway genes exhibited the dwarf yellowing phenotype in pear which is also consistent with our findings (Pang et al., 2019). It was illustrated that high concentrations of ABA not only inhibit cell division in the apical meristems but also repress the elongation of roots (Bai et al., 2009; Takatsuka and Umeda, 2014). Expression of key genes related to ABA was significantly upregulated in cabbage dwarf mutant (Xing et al., 2020). Controversially, the higher IAA but lower ABA contents in dwarf autotetraploid Chinese Cabbage was found (Wang Y. et al., 2018). In addition to the abovementioned hormones, the low content of MeJA also caused dwarf traits in rice (Gan et al., 2015).

Our results of various endogenous hormones in diploid and tetraploid garlic provided partial explanation of morphological alterations (Maru et al., 2021). It should be noted that the factors affecting plant height are complex and diverse. Noticeably, Xing et al. (2020) implied that the change in phytohormones is due to but not the cause of the dwarf trait in polyploidy cabbage. Further studies of transcriptome analysis are worth pursuing to facilitate a better understanding of dwarfism mechanism in tetraploid garlic.

Functional Metabolites

It is widely acknowledged that multiplication of genome bestows conspicuous enhancement of nutritional and secondary metabolites yield, which has contributed to a significant commercial value for industrial and medicinal importance (Gantait and Mukherjee, 2021). The significantly higher bioactive

constituents of total flavonoid and gastrodin in all parts of tetraploid *Anoectochilus formosanus Hayata* were evaluated compared with the diploid (Chung et al., 2017). It also demonstrated a dramatic change in secondary metabolism (terpene composition) related to an increase in the ploidy level in Eucalyptus germplasms (da Silva et al., 2021). Nevertheless, in *Solanum bulbocastanum*, the lower contents of phenylpropanoids, tryptophan, and tyrosine were found in tetraploids than in diploids (Caruso et al., 2011). This indicates that genome doubling does not increase the accumulation of high-value bioactive compounds all the time. In this study, the dwarfing tetraploid plantlets showed higher levels of allicin, DADS, and DATS than diploid counterpart, suggesting the potentiality as a breeding method in garlic for abundant production of pharmaceuticals.

CONCLUSION

In this study, a successful *in vitro* polyploidization protocol was established with colchicine and oryzalin in garlic. The colchicine led to the highest tetraploid induction rate of 21.8% with the application of 200 mg/L for 20 days. The unexpected dwarfing tetraploids were characterized for their morphological traits and phytochemical variations. This is the first report suggesting that chromosome doubling could impart garlic with dwarfism. Our study provides a valuable germplasm resource to broaden the elucidation of polyploidization consequences, as well as the genetic studies and possible major breakthrough for future improvement of Allium species.

DATA AVAILABILITY STATEMENT

The raw data supporting the conclusions of this article will be made available by the authors, without undue reservation.

AUTHOR CONTRIBUTIONS

YW conceived the idea, designed and performed the experiment, and prepared the draft manuscript. HL participated in the design of the study, carried out experiments, and reviewed the manuscript. HM contributed to analysis of the data. LQ conducted molecular variance analysis. GZ contributed to data analysis, revising, and funding acquisition for publication. This work was conducted under the supervision of ZC who provided significant intelligence to the manuscript revision. All authors contributed to the article and approved the submitted version.

FUNDING

This research was supported by the Education Development Fund project of Northwest A&F University (2017) and the National Public Welfare Industry (Agriculture) Special Project (200903018-7).

ACKNOWLEDGMENTS

We greatly appreciate dedicated efforts from journal editor and reviewers. We also thank Datong development and reform commission for publication support.

REFERENCES

Adams, K. L., and Wendel, J. F. (2005). Novel patterns of gene expression in polyploid plants. *Trends Genet.* 21, 539–543. doi: 10.1016/j.tig.2005.07.009

Ahmadi, B., and Ebrahimzadeh, H. (2020). *In vitro* androgenesis: spontaneous vs. artificial genome doubling and characterization of regenerants. *Plant Cell Rep.* 39, 299–316. doi: 10.1007/s00299-020-02509-z

Ajami, M., and Vazirijavid, R. (2019). "Chapter 3.17 - garlic (*Allium sativum* L.)," in *Nonvitamin and Nonmineral Nutritional Supplements*, eds S. M. Nabavi and A. S. Silva (Academic Press), 227–234. doi: 10.1016/B978-0-12-812491-8.00033-3

Allum, J. F., Bringloe, D. H., and Roberts, A. V. (2007). Chromosome doubling in a *Rosa rugosa Thunb*. hybrid by exposure of *in vitro* nodes to oryzalin: the effects of node length, oryzalin concentration and exposure time. *Plant Cell Rep.* 26, 1977–1984. doi: 10.1007/s00299-007-0411-y

Ardabili, G. S., Zakaria, R. A., Zare, N., and Namazi, L. G. (2021). Induction of autotetraploidy in bride rose poppy (*Papaver fugax* poir.) by colchicine treatment of seeds and seedlings. *Cytologia* 86, 15–19. doi: 10.1508/cytologia.86.15

Ari, E., Djapo, H., Mutlu, N., Gurbuz, E., and Karaguzel, O. (2015). Creation of variation through gamma irradiation and polyploidization in vitex agnus-castus L. *Sci. Horticult.* 195, 74–81. doi: 10.1016/j.scienta.2015.08.039

Ascough, G. D., van Staden, J., and Erwin, J. E. (2008). Effectiveness of colchicine and oryzalin at inducing polyploidy in watsonia lepida N.E. brown. *HortSci. Horts* 43, 2248–2251. doi: 10.21273/hortsci.43.7.2248

Ayu, G., Elimasni, M., and Nurwahyuni, I. (2019). Effect of concentration and duration of colchicine treatment to garlic (*Allium sativum* L.) Cv. doulu. *Int. J. Sci. Technol. Res.* 8, 172–175.

Baghyalakshmi, K., Shaik, M., Mohanrao, M. D., Shaw, R. K., Lavanya, C., Manjunatha, T., et al. (2020). Development and characterization of tetraploid castor plants. *Plant Genet. Res. Charact. Utilizat.* 18, 98–104. doi: 10.1017/s1479262120000039

Bai, L., Zhang, G., Zhou, Y., Zhang, Z., Wang, W., Du, Y., et al. (2009). Plasma membrane-associated proline-rich extensin-like receptor kinase 4, a novel regulator of Ca signalling, is required for abscisic acid responses in *Arabidopsis thaliana*. *Plant J.* 60, 314–327. doi: 10.1111/j.1365-313X.2009.03956.x

Balal, R. M., Shahid, M. A., Vincent, C., Zotarelli, L., Liu, G., Mattson, N. S., et al. (2017). Kinnow mandarin plants grafted on tetraploid rootstocks are more tolerant to Cr-toxicity than those grafted on its diploids one. *Environ. Exp. Bot.* 140, 8–18. doi: 10.1016/j.envexpbot.2017.05.011

Bartish, I. V., Korkhovoy, V. I., Fomina, Y. L., and Lim, Y. K. (1998). A new approach to obtain polyploid forms of apple. *Acta Horticult.* 484, 561–564. doi: 10.17660/ActaHortic.1998.484.95

Bhusare, B. P., John, C. K., Bhatt, V. P., and Nikam, T. D. (2021). Colchicine induces tetraploids in *in vitro* cultures of *Digitalis lanata* Ehrh.: enhanced production of biomass and cardiac glycosides. *Industr. Crops Prod.* 174:114167. doi: 10.1016/j.indcrop.2021.114167

Blakeslee, A. F. (1922). Variations in datura due to changes in chromosome number. *Am. Natur.* 56, 16–31. doi: 10.1086/279845

Blakeslee, A. F., and Avery, A. G. (1937). Methods of inducing doubling of chromosomes in plants: by treatment with colchicine. *J. Heredity* 28, 393–411. doi: 10.1093/oxfordjournals.jhered.a104294

Bohutínská, M., Alston, M., Monnahan, P., Mandáková, T., Bray, S., Paajanen, P., et al. (2021). Novelty and convergence in adaptation to whole

genome duplication. *Mol. Biol. Evolu.* 38, 3910–3924. doi: 10.1093/molbev/msab096

Caruso, I., Lepore, L., De Tommasi, N., Dal Piaz, F., Frusciante, L., Aversano, R., et al. (2011). Secondary metabolite profile in induced tetraploids of wild solanum commersonii dun. *Chem. Bio.* 8, 2226–2237. doi: 10.1002/cbdv.201100038

Catalano, C., Abbate, L., Motisi, A., Crucitti, D., Cangelosi, V., Pisciotta, A., et al. (2021). Autotetraploid emergence via somatic embryogenesis in vitis vinifera induces marked morphological changes in shoots, mature leaves, and stomata. *Cells* 10:1336. doi: 10.3390/cells10061336

Cavalier-Smith, T. (1978). Nuclear volume control by nucleoskeletal DNA, selection for cell volume and cell growth rate, and the solution of the DNA C-value paradox. *J. Cell Sci.* 34, 247–278. doi: 10.1242/jcs.34.1.247

Chen, J., Xie, J., Duan, Y., Hu, H., Hu, Y., and Li, W. (2016). Genome-wide identification and expression profiling reveal tissue-specific expression and differentially-regulated genes involved in gibberellin metabolism between williams banana and its dwarf mutant. *BMC Plant Biol.* 16:123. doi: 10.1186/s12870-016-0809-1

Chen, Z. J., and Ni, Z. (2006). Mechanisms of genomic rearrangements and gene expression changes in plant polyploids. *BioEssays* 28, 240–252. doi: 10.1002/bies.20374

Cheng, Z., Zhou, X. J., Khan, M. A., Su, L., and Meng, H. W. (2012). *In vitro* induction of tetraploid garlic with trifluralin. *Genet. Mol. Res.* 3, 2620–2628. doi: 10.4238/2012.July.10.13

Chung, H. H., Shi, S. K., Huang, B., and Chen, J. T. (2017). Enhanced agronomic traits and medicinal constituents of autotetraploids in *Anoectochilus formosanus* hayata, a top-grade medicinal orchid. *Molecules* 22:1907. doi: 10.3390/molecules22111907

Corneillie, S., De Storme, N., Van Acker, R., Fangel, J. U., De Bruyne, M., De Rycke, R., et al. (2019). Polyploidy affects plant growth and alters cell wall composition. *Plant Physiol.* 179, 74–87. doi: 10.1104/pp.18.00967

da Silva, A. J., Clarindo, W. R., Simiqueli, G. F., Praça-Fontes, M. M., Mendes, L. A., Martins, G. F., et al. (2021). Short-term changes related to autotetraploidy in essential oil composition of eucalyptus benthamii maiden & cambage and its applications in different bioassays. *Sci. Rep.* 11:24408. doi: 10.1038/s41598-021-03916-2

Denaeghel, H. E. R., Van Laere, K., Leus, L., Lootens, P., Van Huylenbroeck, J., and Van Labeke, M. C. (2018). The variable effect of polyploidization on the phenotype in escallonia. *Front. Plant Sci.* 9:354. doi: 10.3389/fpls.2018.00354

Deng, B., Wang, X., Long, X., Fang, R., Zhou, S., Zhang, J., et al. (2021). Plant hormone metabolome and transcriptome analysis of dwarf and wild-type banana. *J. Plant Growth Regul.* doi: 10.1007/s00344-021-10447-7

Dewitte, W., and Murray, J. A. (2003). The plant cell cycle. *Ann. Rev. Plant Biol.* 54, 235–264. doi: 10.1146/annurev.arplant.54.031902.134836

Dhooghe, E., Van Laere, K., Eeckhaut, T., Leus, L., and Van Huylenbroeck, J. (2011). Mitotic chromosome doubling of plant tissues *in vitro*. *Plant Cell Tissue Organ Cult.* 104, 359–373. doi: 10.1007/s11240-010-9786-5

Dixit, V., and Chaudhary, B. R. (2014). Colchicine-induced tetraploidy in garlic (*Allium sativum* L.) and its effect on allicin concentration. *J. Horticul. Sci. Biotechnol.* 89, 585–591. doi: 10.1080/14620316.2014.11513124

Dockter, C., and Hansson, M. (2015). Improving barley culm robustness for secured crop yield in a changing climate. *J. Exp. Bot.* 66, 3499–3509. doi: 10.1093/jxb/eru521

Dolezel, J., Greilhuber, J., and Suda, J. (2007). Estimation of nuclear DNA content in plants using flow cytometry. *Nat. Protocols* 2, 2233–2244. doi: 10.1038/nprot.2007.310

Dolezel, J., Lucretti, S., and Schubert, I. (1994). Plant chromosome analysis and sorting by flow cytometry. *Crit. Rev. Plant Sci.* 13, 275–309.

Doyle, J. J., and Coate, J. E. (2020). Autopolyploidy: an epigenetic macromutation. *Am. J. Bot.* 107, 1097–1100. doi: 10.1002/ajb2.1513

Durbak, A., Yao, H., and McSteen, P. (2012). Hormone signaling in plant development. *Curr. Opin. Plant Biol.* 15, 92–96. doi: 10.1016/j.pbi.2011.12.004

Eng, W. H., and Ho, W. S. (2019). Polyploidization using colchicine in horticultural plants: a review. *Sci. Horticult.* 246, 604–617. doi: 10.1016/j.scienta.2018.11.010

Etoh, T., and Simon, P. W. (2002). "Diversity, fertility and seed production of garlic," in *Allium Crop Science: Recent Advances*, eds H. D. Rabinowitch and L. Currah (Wallingford: CABI Publishing), 101–118. doi: 10.1079/9780851995106.0101

Fox, D. T., Soltis, D. E., Soltis, P. S., Ashman, T. L., and Van de Peer, Y. (2020). Polyploidy: a biological force from cells to ecosystems. *Trends Cell Biol.* 30, 688–694. doi: 10.1016/j.tcb.2020.06.006

Fujioka, S., Noguchi, T., Takatsuto, S., and Yoshida, S. (1998). Activity of brassinosteroids in the dwarf rice lamina inclination bioassay. *Phytochemistry* 49, 1841–1848. doi: 10.1016/S0031-9422(98)00412-9

Galbraith, D. W., Harkins, K. R., Maddox, J. M., Ayres, N. M., Sharma, D. P., and Firoozabady, E. (1983). Rapid flow cytometric analysis of the cell cycle in intact plant tissues. *Science* 220, 1049–1051. doi: 10.1126/science.220.4601.1049

Gan, L., Wu, H., Wu, D., Zhang, Z., Guo, Z., Yang, N., et al. (2015). Methyl jasmonate inhibits lamina joint inclination by repressing brassinosteroid biosynthesis and signaling in rice. *Plant Sci.* 241, 238-245. doi: 10.1016/j.plantsci.2015.10.012

Gantait, S., and Mukherjee, E. (2021). Induced autopolyploidy—a promising approach for enhanced biosynthesis of plant secondary metabolites: an insight. *J. Genet. Eng. Biotechnol.* 19:4. doi: 10.1186/s43141-020-00109-8

Hailu, M. G. (2021). Garlic micro-propagation and polyploidy induction *in vitro* by colchicine. *Plant Breed. Biotechnol.* 9, 1–19. doi: 10.9787/PBB.2021.9.1.1

Häntzschel, K. R., and Weber, G. (2010). Blockage of mitosis in maize root tips using colchicine-alternatives. *Protoplasma* 241, 99–104. doi: 10.1007/s00709-009-0103-2

Hegarty, M., Coate, J., Sherman-Broyles, S., Abbott, R., Hiscock, S., and Doyle, J. (2013). Lessons from natural and artificial polyploids in higher plants. *Cytogenet Genome Res.* 140, 204–225. doi: 10.1159/000353361

Hirano, K., Kawamura, M., Araki-Nakamura, S., Fujimoto, H., Ohmae-Shinohara, K., Yamaguchi, M., et al. (2017). Sorghum DW1 positively regulates brassinosteroid signaling by inhibiting the nuclear localization of BRASSINOSTEROID INSENSITIVE 2. *Sci. Rep.* 7:126. doi: 10.1038/s41598-017-00096-w

Iannicelli, J., Guariniello, J., Tossi, V. E., Regalado, J. J., Di Ciaccio, L., van Baren, C. M., et al. (2020). The "polyploid effect" in the breeding of aromatic and medicinal species. *Sci. Horticult.* 260:108854. doi: 10.1016/j.scienta.2019.108854

Ipek, M., Ipek, A., Almquist, S. G., and Simon, P. W. (2005). Demonstration of linkage and development of the first low-density genetic map of garlic, based on AFLP markers. *Theor. Appl. Genet.* 110, 228–236. doi: 10.1007/s00122-004-1815-5

Kim, H. E., Han, J. E., Lee, H., Kim, J. H., Kim, H. H., Lee, K. Y., et al. (2021). Tetraploidization increases the contents of functional metabolites in *Cnidium officinale*. *Agron. Basel* 11:1561. doi: 10.3390/agronomy11081561

Koefoed Petersen, K., Hagberg, P., and Kristiansen, K. (2003). Colchicine and oryzalin mediated chromosome doubling in different genotypes of *Miscanthus sinensis*. *Plant Cell Tissue Organ Cult.* 73, 137–146. doi: 10.1023/A:1022854303371

Kondorosi, E., Roudier, F., and Gendreau, E. (2000). Plant cell-size control: growing by ploidy? *Curr. Opin. Plant Biol.* 3, 488–492. doi: 10.1016/S1369-5266(00)00118-7

Kumar, A. S., Lakshmanan, V., Caplan, J. L., Powell, D., Czymmek, K. J., Levia, D. F., et al. (2012). Rhizobacteria *Bacillus* subtilis restricts foliar pathogen entry through stomata. *Plant J.* 72, 694–706. doi: 10.1111/j.1365-313X.2012.05116.x

Lai, M., and Lü, B. (2012). "Tissue preparation for microscopy and histology," in *Comprehensive Sampling and Sample Preparation*, ed. J. Pawliszyn (Oxford: Academic Press), 53–93. doi: 10.1016/B978-0-12-381373-2.00070-3

Leitch, A. R., and Leitch, I. J. (2008). Genomic plasticity and the diversity of polyploid plants. *Science* 320, 481–483. doi: 10.1126/science.1153585

Li, X., Qiao, L., Chen, B., Zheng, Y., Zhi, C., Zhang, S., et al. (2021). SSR markers development and their application in genetic diversity evaluation of garlic (*Allium sativum* L.) germplasm. *Plant Div.* doi: 10.1016/j.pld.2021.08.001

Liu, H., Wen, Y., Cui, M., Qi, X., Deng, R., Gao, J., et al. (2020). Histological, physiological and transcriptomic analysis reveal gibberellin-induced axillary meristem formation in garlic (*Allium sativum*). *Plants* 9:970. doi: 10.3390/plants9080970

Liu, L., Wang, Z., Liu, J., Liu, F., Zhai, R., Zhu, C., et al. (2018). Histological, hormonal and transcriptomic reveal the changes upon gibberellin-induced parthenocarpy in pear fruit. *Hortic. Res.* 5:1. doi: 10.1038/s41438-017-0012-z

Liu, T., Zeng, L., Zhu, S., Chen, X., Tang, Q., Mei, S., et al. (2015). Large-scale development of expressed sequence tag-derived simple sequence repeat

markers by deep transcriptome sequencing in garlic (*Allium sativum* L.). *Mol. Breed.* 35:204. doi: 10.1007/s11032-015-0399-x

Loureiro, J., Rodriguez, E., Dolezel, J., and Santos, C. (2006a). Comparison of four nuclear isolation buffers for plant DNA flow cytometry. *Ann. Bot.* 98, 679–689. doi: 10.1093/aob/mcl141

Loureiro, J., Rodriguez, E., Dolezel, J., and Santos, C. (2006b). Flow cytometric and microscopic analysis of the effect of tannic acid on plant nuclei and estimation of DNA content. *Ann. Bot.* 98, 515–527. doi: 10.1093/aob/mcl140

Luckett, D. J. (1989). Colchicine mutagenesis is associated with substantial heritable variation in cotton. *Euphytica* 42, 177–182. doi: 10.1007/BF00042630

Ma, Y., Xue, H., Zhang, L., Zhang, F., Ou, C., Wang, F., et al. (2016). Involvement of auxin and brassinosteroid in dwarfism of autotetraploid apple (malus×domestica). *Sci. Rep.* 6:26719. doi: 10.1038/srep 26719

Maaß, H. I., and Klaas, M. (1995). Infraspecific differentiation of garlic (*Allium sativum* L.) by isozyme and RAPD markers. *Theor. Appl. Genet.* 91, 89–97. doi: 10.1007/BF00220863

Manzoor, A., Ahmad, T., Bashir, M. A., Hafiz, I. A., and Silvestri, C. (2019). Studies on colchicine induced chromosome doubling for enhancement of quality traits in ornamental plants. *Plants (Basel)* 8:194. doi: 10.3390/plants8070194

Maru, B., Parihar, A., Kulshrestha, K., and Vaja, M. (2021). Induction of polyploidy through colchicine in cotton (*Gossypium herbaceum*) and its conformity by cytology and flow cytometry analyses. *J. Genet.* 100:52. doi: 10.1007/s12041-021-01297-z

Masterson, J. (1994). Stomatal size in fossil plants: evidence for polyploidy in majority of angiosperms. *Science* 264, 421–424. doi: 10.1126/science.264.5157.421

Mattingly, K. Z., and Hovick, S. M. (2021). Autopolyploids of *Arabidopsis thaliana* are more phenotypically plastic than their diploid progenitors. *Ann. Bot.* XX, 1–13. doi: 10.1093/aob/mcab081

McClintock, B. (1984). The significance of responses of the genome to challenge. *Science* 226, 792–801. doi: 10.1126/science.15739260

Morejohn, L. C., Bureau, T. E., Tocchi, L. P., and Fosket, D. E. (1987). Resistance of rosa microtubule polymerization to colchicine results from a low-affinity interaction of colchicine and tubulin. *Planta* 170, 230–241. doi: 10.1007/BF00397893

Murray, M. G., and Thompson, W. F. (1980). Rapid isolation of high molecular weight plant DNA. *Nucleic Acids Res.* 8, 4321–4325. doi: 10.1093/nar/8.19.4321

Nakamura, A., Fujioka, S., Sunohara, H., Kamiya, N., Hong, Z., Inukai, Y., et al. (2006). The role of OsBRI1 and its homologous genes, OsBRL1 and OsBRL3, in rice. *Plant Physiol.* 140, 580–590. doi: 10.1104/pp.105.072330

Nelissen, H., Rymen, B., Jikumaru, Y., Demuynck, K., Van Lijsebettens, M., Kamiya, Y., et al. (2012). A local maximum in gibberellin levels regulates maize leaf growth by spatial control of cell division. *Curr. Biol.* 22, 1183–1187. doi: 10.1016/j.cub.2012.04.065

Nemhauser, J. L., Hong, F., and Chory, J. (2006). Different plant hormones regulate similar processes through largely nonoverlapping transcriptional responses. *Cell* 126, 467–475. doi: 10.1016/j.cell.2006.05.050

Niazian, M., and Nalousi, A. M. (2020). Artificial polyploidy induction for improvement of ornamental and medicinal plants. *Plant Cell Tissue Organ Culture* 142, 447–469. doi: 10.1007/s11240-020-01888-1

Novák, F. (1983). Production of garlic (*Allium sativum* L.) tetraploids in shoot-tip *in vitro* culture. *Z Pflanzenzuchtg* 91, 329–333.

Otto, S. P. (2007). The evolutionary consequences of polyploidy. *Cell* 131, 452–462. doi: 10.1016/j.cell.2007.10.022

Otto, S. P., and Whitton, J. (2000). Polyploid incidence and evolution. *Ann. Rev. Genet.* 34, 401–437. doi: 10.1146/annurev.genet.34.1.401

Pang, H., Yan, Q., Zhao, S., He, F., Xu, J., Qi, B., et al. (2019). Knockout of the S-acyltransferase gene, PbPAT14, confers the dwarf yellowing phenotype in first generation pear by ABA accumulation. *Int. J. Mol. Sci.* 20:6347. doi: 10.3390/ijms20246347

Parsons, J. L., Martin, S. L., James, T., Golenia, G., Boudko, E. A., and Hepworth, S. R. (2019). Polyploidization for the genetic improvement of cannabis sativa. *Front. Plant Sci.* 10:476. doi: 10.3389/fpls.2019.00476

Pellicer, J., Powell, R. F., and Leitch, I. J. (2021). The application of flow cytometry for estimating genome size, ploidy level endopolyploidy, and reproductive modes in plants. *Methods Mol. Biol.* 2222, 325–361. doi: 10.1007/978-1-0716-0997-2_17

Podwyszyńska, M., Trzewik, A., and Marasek-Ciolakowska, A. (2018). *In vitro* polyploidisation of tulips (*Tulipa gesneriana* L.) — phenotype assessment of tetraploids. *Sci. Horticult.* 242, 155–163. doi: 10.1016/j.scienta.2018.07.007

Pooler, M. R., and Simon, P. W. (1994). True seed production in garlic. *Sexual Plant Rep.* 7, 282–286. doi: 10.1007/BF00227710

Pradhan, S. K., Gupta, R. C., and Goel, R. K. (2018). Differential content of secondary metabolites in diploid and tetraploid cytotypes of *Siegesbeckia orientalis* L. *Nat. Produ. Res.* 32, 2476–2482. doi: 10.1080/14786419.2017.1423298

Quesenberry, K. H., Dampier, J. M., Lee, Y. Y., Smith, R. L., and Acuña, C. A. (2010). Doubling the chromosome number of bahiagrass via tissue culture. *Euphytica* 175, 43–50. doi: 10.1007/s10681-010-0165-4

Rambani, A., Page, J. T., and Udall, J. A. (2014). Polyploidy and the petal transcriptome of *Gossypium*. *BMC Plant Biol.* 14:3. doi: 10.1186/1471-2229-14-3

Ramsey, J., and Schemske, D. W. (1998). Pathways, mechanisms, and rates of polyploid formation in flowering plants. *Ann. Rev. Ecol. Evol. Syst.* 29, 467–501. doi: 10.1146/annurev.ecolsys.29.1.467

Ramsey, J., and Schemske, D. W. (2002). Neopolyploidy in flowering plants. *Ann. Rev. Ecol. Syst.* 33, 589–639. doi: 10.1146/annurev.ecolsys.33.010802.150437

Rao, S., Kang, X., Li, J., and Chen, J. (2019). Induction, identification and characterization of tetraploidy in *Lycium ruthenicum*. *Breed Sci.* 69, 160–168. doi: 10.1270/jsbbs.18144

Ricroch, A., Yockteng, R., Brown, S. C., and Nadot, S. (2005). Evolution of genome size across some cultivated *Allium* species. *Genome* 48, 511–520. doi: 10.1139/g05-017

Roy, A., Leggett, G., and Koutoulis, A. (2001). *In vitro* tetraploid induction and generation of tetraploids from mixoploids in hop (*Humulus lupulus* L.). *Plant Cell Rep.* 20, 489–495. doi: 10.1007/s002990100364

Rubuluza, T., Nikolova, R. V., Smith, M. T., and Hannweg, K. (2007). *In vitro* induction of tetraploids in *Colophospermum mopane* by colchicine. *South Afr. J. Bot.* 73, 259–261. doi: 10.1016/j.sajb.2006.12.001

Sabooni, N., Gharaghani, A., Jowkar, A., and Eshghi, S. (2022). Successful polyploidy induction and detection in blackberry species by using an *in vitro* protocol. *Sci. Horticult.* 295:110850. doi: 10.1016/j.scienta.2021.110850

Sakamoto, T., Miura, K., Itoh, H., Tatsumi, T., Ueguchi-Tanaka, M., Ishiyama, K., et al. (2004). An overview of gibberellin metabolism enzyme genes and their related mutants in rice. *Plant Physiol.* 134, 1642–1653. doi: 10.1104/pp.103.033696

Sanwal, S. K., Rai, N., Singh, J., and Buragohain, J. (2010). Antioxidant phytochemicals and gingerol content in diploid and tetraploid clones of ginger (*Zingiber officinale* roscoe). *Sci. Horticult.* 124, 280–285. doi: 10.1016/j.scienta.2010.01.003

Sattler, M. C., Carvalho, C. R., and Clarindo, W. R. (2016). The polyploidy and its key role in plant breeding. *Planta* 243, 281–296. doi: 10.1007/s00425-015-2450-x

Seneviratne, K. A. C. N., Kuruppu Arachchi, K. A. J. M., Seneviratne, G., and Premarathna, M. (2020). Zamioculcas zamiifolia novel plants with dwarf features and variegated leaves induced by colchicine. *Ceylon J. Sci.* 49:203. doi: 10.4038/cjs.v49i2.7741

Shao, X., Wu, S., Dou, T., Zhu, H., Hu, C., Huo, H., et al. (2020). Using CRISPR/Cas9 genome editing system to create *MaGA20ox2* gene-modified semi-dwarf banana. *Plant Biotechnol. J.* 18, 17–19. doi: 10.1111/pbi.13216

Shemesh Mayer, E., Winiarczyk, K., Błaszczyk, L., Kosmala, A., Rabinowitch, H. D., and Kamenetsky, R. (2013). Male gametogenesis and sterility in garlic (*Allium sativum* L.): barriers on the way to fertilization and seed production. *Planta* 237, 103–120. doi: 10.1007/s00425-012-1748-1

Shemesh-Mayer, E., Ben-Michael, T., Rotem, N., Rabinowitch, H. D., Doron-Faigenboim, A., Kosmala, A., et al. (2015). Garlic (*Allium sativum* L.) fertility: transcriptome and proteome analyses provide insight into flower and pollen development. *Front. Plant Sci.* 6:271. doi: 10.3389/fpls.2015.00271

Shemesh-Mayer, E., and Kamenetsky-Goldstein, R. (2021). "Traditional and novel approaches in garlic (*Allium sativum* L.) breeding," in *Advances in Plant Breeding Strategies: Vegetable Crops: Volume 8: Bulbs, Roots and Tubers*, eds J. M. Al-Khayri, S. M. Jain, and D. V. Johnson (Cham: Springer International Publishing), 3–49. doi: 10.1007/978-3-030-66965-2_1

Simon, P. W., and Jenderek, M. M. (2003). Flowering, seed production, and the genesis of garlic breeding. *Plant Breed. Rev.* 2003, 211–244. doi: 10.1002/9780470650226.ch5

Song, Y., You, J., and Xiong, L. (2009). Characterization of OsIAA1 gene, a member of rice aux/IAA family involved in auxin and brassinosteroid hormone responses and plant morphogenesis. *Plant Mol. Biol.* 70, 297–309. doi: 10.1007/s11103-009-9474-1

Spielmeyer, W., Ellis, M. H., and Chandler, P. M. (2002). Semidwarf (sd-1), "green revolution" rice, contains a defective gibberellin 20-oxidase gene. *Proc. Natl. Acad. Sci. U.S.A.* 99, 9043–9048. doi: 10.1073/pnas.132266399

Stanys, V., Weckman, A., Staniene, G., and Duchovskis, P. (2006). *In vitro* induction of polyploidy in japanese quince (*Chaenomeles japonica*). *Plant Cell Tissue Organ Culture* 84, 263–268. doi: 10.1007/s11240-005-9029-3

Suprasanna, P., Mirajkar, S. J., and Bhagwat, S. G. (2015). "Induced mutations and crop improvement," *in Plant Biology and Biotechnology: Volume I: Plant Diversity, Organization, Function and Improvement*, eds B. Bahadur, M. Venkat Rajam, L. Sahijram, and K. V. Krishnamurthy (New Delhi: Springer India), 593–617. doi: 10.1007/978-81-322

Takatsuka, H., and Umeda, M. (2014). Hormonal control of cell division and elongation along differentiation trajectories in roots. *J. Exp. Bot.* 65, 2633–2643. doi: 10.1093/jxb/ert485

Tavan, M., Azizi, A., Sarikhani, H., Mirjalili, M. H., and Rigano, M. M. (2022). Induced polyploidy and broad variation in phytochemical traits and altered gene expression in *Salvia multicaulis*. *Sci. Horticult.* 2022:291. doi: 10.1016/j.scienta.2021.110592

Tavan, M., Mirjalili, M. H., and Karimzadeh, G. (2015). *In vitro* polyploidy induction: changes in morphological, anatomical and phytochemical characteristics of *Thymus persicus* (*Lamiaceae*). *Plant Cell Tissue Organ Culture* 122, 573–583. doi: 10.1007/s11240-015-0789-0

te Beest, M., Le Roux, J. J., Richardson, D. M., Brysting, A. K., Suda, J., Kubesová, M., et al. (2012). The more the better? The role of polyploidy in facilitating plant invasions. *Ann. Bot.* 109, 19–45. doi: 10.1093/aob/mcr277

Touchell, D. H., Palmer, I. E., and Ranney, T. G. (2020). *In vitro* ploidy manipulation for crop improvement. *Front. Plant Sci.* 11:722. doi: 10.3389/fpls.2020.00722

Trojak-Goluch, A., Kawka-Lipińska, M., Wielgusz, K., and Praczyk, M. (2021). Polyploidy in industrial crops: applications and perspectives in plant breeding. *Agronomy* 11:2574. doi: 10.3390/agronomy11122574

Trojak-Goluch, A., and Skomra, U. (2013). Artificially induced polyploidization in *Humulus lupulus* L. and its effect on morphological and chemical traits. *Breed. Sci.* 63, 393–399. doi: 10.1270/jsbbs.63.393

Tsai, C. W., Chen, H. W., Sheen, L. Y., and Lii, C. K. (2012). Garlic: health benefits and actions. *BioMedicine* 2, 17–29. doi: 10.1016/j.biomed.2011.12.002

Tsai, Y. T., Chen, P. Y., and To, K. Y. (2021). Induction of polyploidy and metabolic profiling in the medicinal herb wedelia chinensis. *Plants* 10:1232. doi: 10.3390/plants10061232

Tsukaya, H. (2013). Does ploidy level directly control cell size? Counterevidence from *Arabidopsis genetics*. *PLoS One* 8:e83729. doi: 10.1371/journal.pone.0083729

van Duren, M., Morpurgo, R., Dolezel, J., and Afza, R. (1996). Induction and verification of autotetraploids in diploid banana (*Musa acuminata*) by *in vitro* techniques. *Euphytica* 88, 25–34. doi: 10.1007/BF00029262

Van Laere, K., Van Huylenbroeck, J., and Van BockStaele, E. (2006). Breeding strategies to increase genetic variability within *Hibiscus syriacus*. *Acta Horticult. Leuven Belgium Soc. Horticult. Sci.* 714, 75–81.

Viehmannová, I., Cusimamani, E. F., Bechyne, M., Vyvadilová, M., and Greplová, M. (2009). *In vitro* induction of polyploidy in yacon (*Smallanthus sonchifolius*). *Plant Cell Tissue Organ Culture* 97, 21–25. doi: 10.1007/s11240-008-9494-6

Wan, Y., Duncan, D. R., Rayburn, A. L., Petolino, J. F., and Widholm, J. M. (1991). The use of antimicrotubule herbicides for the production of doubled haploid plants from anther-derived maize callus. *Theor. Appl. Genet.* 81, 205–211. doi: 10.1007/bf00215724

Wang, B., Smith, S. M., and Li, J. (2018). Genetic regulation of shoot architecture. *Ann. Rev. Plant Biol.* 69, 437–468. doi: 10.1146/annurev-arplant-042817-040422

Wang, L., Luo, Z., Wang, L., Deng, W., Wei, H., Liu, P., et al. (2019). Morphological, cytological and nutritional changes of autotetraploid compared to its diploid counterpart in Chinese jujube (*Ziziphus jujuba* mill.). *Sci. Horticult.* 249, 263–270. doi: 10.1016/j.scienta.2019.01.063

Wang, X. L., Zhou, J. X., Yu, M. D., Li, Z. G., Jin, X. Y., and Li, Q. Y. (2011). Highly efficient plant regeneration and *in vitro* polyploid induction using hypocotyl explants from diploid mulberry (*Morus multicaulis* poir.). *Vitro Cell. Dev. Biol. Plant* 47, 434–440. doi: 10.1007/s11627-010-9328-1

Wang, Y., and Li, J. (2008). Molecular basis of plant architecture. *Annu. Rev. Plant Biol.* 59, 253–279. doi: 10.1146/annurev.arplant.59.032607.092902

Wang, Y., Huang, S., Liu, Z., Tang, X., and Feng, H. (2018). Changes in endogenous phytohormones regulated by microRNA-target mRNAs contribute to the development of Dwarf autotetraploid Chinese cabbage (*Brassica rapa* L. ssp. pekinensis). *Mol. Genet. Geno.* 293, 1535–1546. doi: 10.1007/s00438-018-1480-z

Wen, Y. B., Liu, X. X., Liu, H. J., Wu, C. N., Meng, H. W., and Cheng, Z. H. (2020). High-frequency direct shoot organogenesis from garlic (*Allium sativum* L.) inflorescence and clonal fidelity assessment in regenerants. *Plant Cell Tissue Organ Culture* 141, 275–287. doi: 10.1007/s11240-020-01785-7

Wendel, J. F. (2000). Genome evolution in polyploids. *Plant Mol. Biol.* 42, 225–249. doi: 10.1023/A:1006392424384

Wood, T. E., Takebayashi, N., Barker, M. S., Mayrose, I., Greenspoon, P. B., and Rieseberg, L. H. (2009). The frequency of polyploid speciation in vascular plants. *Proc. Natl. Acad. Sci. U.S.A.* 106, 13875–13879. doi: 10.1073/pnas.0811575106

Wu, J., and Akhmanova, A. (2017). Microtubule-organizing centers. *Ann. Rev. Cell Dev. Biol.* 33, 51–75. doi: 10.1146/annurev-cellbio-100616-060615

Xing, M., Su, H., Liu, X., Yang, L., Zhang, Y., Wang, Y., et al. (2020). Morphological, transcriptomics and phytohormone analysis shed light on the development of a novel dwarf mutant of cabbage (*Brassica oleracea*). *Plant Sci.* 290:110283. doi: 10.1016/j.plantsci.2019.110283

Xu, L. H., Wang, J. Q., Zhang, Q. Y., Li, X. M., Qiu, C. H., and Yuan, L. W. (2012). Determination of allicin in dietary supplement by HPLC. *Acta Agric. Zhejiang.* 24:717. doi: 10.3969/j.issn.1004-1524.2012.04.033

Yan, H., Bombarely, A., Xu, B., Wu, B., Frazier, T. P., Zhang, X., et al. (2019). Autopolyploidization in switchgrass alters phenotype and flowering time via epigenetic and transcription regulation. *J. Exp. Bot.* 70, 5673–5686. doi: 10.1093/jxb/erz325

Yan, Y. J., Qin, S. S., Zhou, N. Z., Xie, Y., and He, Y. (2022). Effects of colchicine on polyploidy induction of Buddleja lindleyana seeds. *Plant Cell Tissue Organ Cult.* 149, 735–745. doi: 10.1007/s11240-022-02245-0

Yang, J., Zhang, J., Wang, Z., Zhu, Q., and Wang, W. (2001). Hormonal changes in the grains of rice subjected to water stress during grain filling. *Plant Physiol.* 127, 315–323. doi: 10.1104/pp.127.1.315

Ye, Y. M., Tong, J., Shi, X. P., Yuan, W., and Li, G. R. (2010). Morphological and cytological studies of diploid and colchicine-induced tetraploid lines of crape myrtle (*Lagerstroemia indica* L.). *Sci. Horticult.* 124, 95–101. doi: 10.1016/j.scienta.2009.12.016

Yin, Y., Cheong, H., Friedrichsen, D., Zhao, Y., Hu, J., Mora-Garcia, S., et al. (2002). A crucial role for the putative *Arabidopsis* topoisomerase VI in plant growth and development. *Proc. Natl. Acad. Sci. U.S.A.* 99, 10191–10196. doi: 10.1073/pnas.152337599

Zhang, F., Qu, L., Gu, Y., Xu, Z. H., and Xue, H. W. (2022). Resequencing and genome-wide association studies of autotetraploid potato. *Mol. Horticult.* 2:6. doi: 10.1186/s43897-022-00027-y

Zhang, J., Zhang, X., Chen, R., Yang, L., Fan, K., Liu, Y., et al. (2020). Generation of transgene-free semidwarf maize plants by gene editing of gibberellin-oxidase20-3 using CRISPR/Cas9. *Front. Plant Sci.* 11:01048. doi: 10.3389/fpls.2020.01048

Zhang, X. Y., Hu, C. G., and Yao, J. L. (2010). Tetraploidization of diploid dioscorea results in activation of the antioxidant defense system and increased heat tolerance. *J. Plant Physiol.* 167, 88–94. doi: 10.1016/j.jplph.2009.07.006

Zhang, Y. S., Chen, J. J., Cao, Y. M., Duan, J. X., and Cai, X. D. (2020). Induction of tetraploids in 'Red Flash' caladium using colchicine and oryzalin: morphological, cytological, photosynthetic and chilling tolerance analysis. *Sci. Horticult.* 272:109524. doi: 10.1016/j.scienta.2020.109524

Zhao, X., Sun, X. F., Zhao, L. L., Huang, L. J., and Wang, P. C. (2022). Morphological, transcriptomic and metabolomic analyses of sophora davidii mutants for plant height. *BMC Plant Biol.* 22:144. doi: 10.1186/s12870-022-03503-1

Zheng, X., Xiao, H., Su, J., Chen, D., Chen, J., Chen, B., et al. (2021). Insights into the evolution and hypoglycemic metabolite biosynthesis of autotetraploid cyclocarya paliurus by combining genomic, transcriptomic and metabolomic analyses. *Indust. Crops Prod.* 173:114154. doi: 10.1016/j.indcrop.2021.114154

Zhou, J., Guo, F., Fu, J., Xiao, Y., and Wu, J. (2020). *In vitro* polyploid induction using colchicine for zingiber officinale roscoe cv. 'fengtou' ginger. *Plant Cell Tissue Organ Culture* 142, 87–94. doi: 10.1007/s11240-020-01842-1

Conflict of Interest: The authors declare that the research was conducted in the absence of any commercial or financial relationships that could be construed as a potential conflict of interest.

Publisher's Note: All claims expressed in this article are solely those of the authors and do not necessarily represent those of their affiliated organizations, or those of the publisher, the editors and the reviewers. Any product that may be evaluated in this article, or claim that may be made by its manufacturer, is not guaranteed or endorsed by the publisher.

frontiers | Frontiers in Plant Science

ORIGINAL RESEARCH
published: 27 June 2022
doi: 10.3389/fpls.2022.924044

Comparative Transcriptomic, Anatomical and Phytohormone Analyses Provide New Insights Into Hormone-Mediated Tetraploid Dwarfing in Hybrid Sweetgum (*Liquidambar styraciflua* × *L. formosana*)

Siyuan Chen[1], Yan Zhang[1,2], Ting Zhang[1], Dingju Zhan[3], Zhenwu Pang[3], Jian Zhao[1] and Jinfeng Zhang[1]**

[1]National Engineering Research Center of Tree Breeding and Ecological Restoration, Key Laboratory of Genetics and Breeding in Forest Trees and Ornamental Plants, Ministry of Education, The Tree and Ornamental Plant Breeding and Biotechnology Laboratory of National Forestry and Grassland Administration, College of Biological Sciences and Biotechnology, Beijing Forestry University, Beijing, China, [2]College of Landscape Architecture, Beijing University of Agriculture, Beijing, China, [3]Guangxi Bagui Forest and Flowers Seedlings Co., Ltd., Nanning, China

OPEN ACCESS

Edited by:
Geoffrey Meru,
University of Florida, United States

Reviewed by:
Wei Seng Ho,
Universiti Malaysia Sarawak, Malaysia
Helene S. Robert Boisivon,
Central European Institute of Technology (CEITEC), Czechia

***Correspondence:**
Jian Zhao
zhaojian0703@bjfu.edu.cn
Jinfeng Zhang
zjf@bjfu.edu.cn

Specialty section:
This article was submitted to Plant Breeding, a section of the journal Frontiers in Plant Science

Received: 20 April 2022
Accepted: 24 May 2022
Published: 27 June 2022

Citation:
Chen S, Zhang Y, Zhang T, Zhan D, Pang Z, Zhao J and Zhang J (2022) Comparative Transcriptomic, Anatomical and Phytohormone Analyses Provide New Insights Into Hormone-Mediated Tetraploid Dwarfing in Hybrid Sweetgum (*Liquidambar styraciflua* × *L. formosana*). *Front. Plant Sci.* 13:924044. doi: 10.3389/fpls.2022.924044

Polyploid breeding is an effective approach to improve plant biomass and quality. Both fast growth and dwarf types of *in vitro* or *ex vitro* plants are produced after polyploidization. However, little is known regarding the dwarf type mechanism in polyploids grown *in vitro*. In this study, the morphological and cytological characteristics were measured in tetraploid and diploid hybrid sweetgum (*Liquidambar styraciflua* × *L. formosana*) with the same genetic background. RNA sequencing (RNA-Seq) was used to analyse shoot and root variations between tetraploid and diploid plants; important metabolites were validated. The results showed that the shoot and root lengths were significantly shorter in tetraploids than in diploids after 25 d of culture. Most tetraploid root cells were wider and more irregular, and the length of the meristematic zone was shorter, while tetraploid cells were significantly larger than diploid cells. Differentially expressed genes (DEGs) were significantly enriched in the plant growth and organ elongation pathways, such as plant hormone biosynthesis and signal transduction, sugar and starch metabolism, and cell cycles. Hormone biosynthesis and signal transduction genes, such as *YUCCA*, *TAA1*, *GH3*, *SAUR*, *CPS*, *KO*, *KAO*, *GA20ox*, *GA3ox*, *BAS1* and *CYCD3*, which help to regulate organ elongation, were generally downregulated. The auxin, gibberellin, and brassinolide (BL) contents in roots and stems were significantly lower in tetraploids than in diploids, which may greatly contribute to slow growth in the roots and stems of tetraploid regenerated plants. Exogenous gibberellic acid (GA_3) and indole-3-acetic acid (IAA), which induced plant cell elongation, could significantly promote growth in the stems and roots of tetraploids. In summary, comparative transcriptomics and metabolite analysis showed

that the slow growth of regenerated tetraploid hybrid sweetgum was strongly related to auxin and gibberellin deficiency. Our findings provide insights into the molecular mechanisms that underlie dwarfism in allopolyploid hybrid sweetgum.

Keywords: polyploidization, RNA-seq, dwarf, plant hormone, hybrid sweetgum

INTRODUCTION

Polyploidy or genome doubling results from the merging of more than two full sets of chromosomes (Comai, 2005; Song and Chen, 2015); polyploidization substantially contributes to plant evolution, new species formation, and plant genetic improvement (Leitch and Leitch, 2008; Jiao et al., 2011). After chromosome doubling, polyploid plants often exhibit multiple variations and generally develop large organs, strong resistance, high crop yield, wood quality, and ornamental value (Zhu et al., 1995; Leitch and Leitch, 2008; Tiku et al., 2014). However, after polyploidization, the changes in plant height differ among species; there is usually a fast growing type (Ni et al., 2009; Miller et al., 2012; Dai et al., 2015; Liao et al., 2016) and a dwarf type (Mu et al., 2012; Tokumoto et al., 2016; Xue et al., 2017). Similar to fast growth, dwarfing is a common phenomenon in tetraploid plants, especially woody plants. It remains unclear why specific species exhibit fast or slow growth after chromosome doubling. Dwarf tetraploid plants have a high ornamental value (Ye et al., 2010); they are often favoured in courtyard and urban landscapes where space may be limited. Such plants often exhibit strong resistance to abiotic and biotic stresses (Tan et al., 2015) and can be used as parents for triploid production.

In addition, fast growth (Gantait et al., 2011; Salma et al., 2018) and slow growth (Gu et al., 2005; Rao et al., 2019) polyploids have been observed *in vitro*. Regenerated plants of tetraploid *Lagerstroemia indica* (Tong, 2007), *Ziziphus jujube* (Gu et al., 2005), *Punica granatum* (Shao et al., 2003), and *Lycium ruthenicum* (Rao et al., 2019) exhibit dwarfing or shortened roots, which can affect regeneration efficiency. The transcriptional expression levels of fast and slow-growing polyploids may substantially change after polyploidization (Cheng et al., 2015; Ma et al., 2016). However, there have been few reports (Ma et al., 2016) concerning the molecular mechanism that underlies the *in vitro* dwarf polyploid type. Moreover, to promote stem and root elongation by improving culture conditions or medium formulation, there is a need to understand which genes and metabolites substantially change in tetraploid plants.

Organ elongation is an important process in plant tissue culture. The degree of difficulty in modifying organ length varies among species (Bizet et al., 2015). Light intensity, agar concentration, growth regulators, and nutrients can affect the lengths of adventitious shoots, stem segments, and roots in tissue culture. Plant hormones have critical effects on organ lengths *in vitro*; for example, auxin, gibberellin, and brassinolide (BL) can promote root or stem elongation (Su et al., 2011). Tong (2007) found that a diploid medium was unsuitable for *in vitro* tetraploid plants. After polyploidization, plants exhibit altered hormone synthesis and changes in the levels of metabolites related to signal transduction genes (Mu et al., 2012; Ma et al., 2016).

Forest trees of *Liquidambar* spp. have important economic and ecological value (Harlow et al., 1996; Merkle and Battle, 2000; Zheng et al., 2015). Chinese sweetgum (*Liquidambar formosana* Hance) is mainly used for ornamental and medicinal purposes (Chen et al., 2020). American sweetgum (*Liquidambar styraciflua* L.) is an important feedstock for the timber and paper industries in South America. In a previous study, several clones of hybrid sweetgum demonstrated obvious heterosis in terms of growth rate and wood density (Merkle et al., 2010). For allotetraploid species, the advantages of some traits have been linked to heterosis (Fuentes et al., 2014). Tetraploid hybrid sweetgum (*L. styraciflua* × *L. formosana*; Zhang et al., 2017) has been reported to show dwarf traits (Unpublished). Some new varieties of sweetgum, such as the dwarfing cultivar 'Gumball', have a shrubby appearance (maximum height of 4.5 m) (Sommer et al., 1999).

What are the key contributors to the dwarf resulting from genome doubling in hybrid sweetgum? Whether the roots and stems of tetraploid hybrid sweetgum have mutated; whether endogenous hormones in plants, the most important factors affecting plant growth, change their regulatory mechanism after polyploidy; whether the growth of dwarf tetraploid can be promoted by application of exogenous plant growth regulators. To answer those questions, in this study, *in vitro* tetraploid hybrid sweetgum was compared with diploid hybrid sweetgum. Morphological changes in stems and roots were observed at various growth stages; organ variations of tetraploid hybrid sweetgum were analysed at the phenotypic, cytological, and molecular levels. Histological analysis, phytohormone analysis and transcriptome sequencing were also performed to identify mechanisms responsible for the variation.

MATERIALS AND METHODS

Plant Material and Determination of Ploidy Level

Three genotypes (Z1, Z2, and Z3) of diploid hybrid sweetgum (D1, D2, and D3) and their tetraploid counterparts (T1, T2, and T3; same genetic background) were used as research material in the present study. *In vitro* diploid and tetraploid families were obtained by hybridization (*L. styraciflua* × *L. formosana*). Artificial tetraploids were acquired from *in vitro* shoot regeneration *via* colchicine treatment, as previously described (Zhang et al., 2017). To acquire sufficient clones for each genotype, all materials were derived from tissue culture propagation. Plantlets were rooted in half-strength woody plant medium supplemented with 2.0 mg/L indole butyric acid, 0.1 mg/L naphthaleneacetic acid,

2.0 g/L agar, 4.0 g/L polygel, and 30 g/L sucrose, called primitive rooting medium. The pH was adjusted to 5.8 prior to autoclaving. Vigorously growing leaves of all genotypes were collected; the ploidy level was analysed using a Cyflow Ploidy Analyser (Partec, Görlitz, SN, Germany). Ploidy level was determined in accordance with the methods described by Zhang et al. (2017).

Plant Height Measurement

To maintain consistency, adventitious shoots at the same regeneration time were excised and cut to approximately 1.5 cm for rooting. The rooting medium contained half-strength woody plant medium supplemented with 2.0 mg/L indole butyric acid and 0.1 mg/L naphthaleneacetic acid; it was placed in a culture bottle with 50 ml medium. The phenotypes of the plantlets were measured after 0, 25, 50, and 70 d of subculture: 0–25 d was stage I, 25–50 d was stage II, and 50–70 d was stage III. In addition to plant height, ground diameter, number of stem nodes, root length, number of roots, leaf area, petiole length, and number of leaves were measured. The primary root diameter was measured by ImageJ.[1] Three biological replicates were performed; each consisted of three genotypes, including three to five plantlets for each genotype.

Anatomical Analysis

Leaves (second or third leaf position), roots, stems, and shoot tips of diploid and tetraploid plants at 25, 50, and 70 d were prepared as paraffin sections. Materials were immobilised in formaldehyde alcohol acetic acid solution (5 ml 38% formaldehyde +5 ml glacial acetic acid +90 ml 50% ethanol, 1:1:18, by vol.) for 24 h. The materials were dehydrated in ethanol and pellucidum in xylene, then embedded in paraffin. The slices had a thickness of 8 mm; they were stained with saffron and solid green. All materials were observed under a biomicroscope (BX43, Olympus, Tokyo, Japan) and photographed by an image acquisition and analysis system (DP73, Olympus). The following items were observed: the thicknesses of leaves, spongy tissues, palisade tissues, and main veins; stem diameter and the thicknesses of epidermis, cortex, and vascular column; root diameter, epidermis cortex radius, and central column diameter; upper column diameter and cell transection area of leaf xylem, as well as cell transection areas of the lower epidermis, spongy tissue, and palisade tissue; cell transection areas of xylem, cortex, and phloem, as well as stem pith; and cell transection areas of xylem, epidermis, and root cortex. Three biological replicates were obtained. Each section was randomly measured for 20–30 cells, with three to five replicate measurements. All measurements were performed using ImageJ software.

RNA Extraction

Four types of RNA were extracted (each containing three genotypes): diploid stem (DS), tetraploid stem (TS), diploid root (DR), and tetraploid root (TR). Three biological replicates were used for total RNA extraction. The 12 samples were named DS-1, DS-2, DS-3, TS-1, TS-2, TS-3, DR-1, DR-2, DR-3, TR-1, TR-2, and TR-3, respectively. All materials were collected after 50 d of subculture, immediately frozen in liquid nitrogen, and stored at −80°C until RNA extraction. RNA extraction was performed in accordance with the methods described by Zhang et al. (2019). RNA purity was checked using a NanoPhotometer® spectrophotometer (IMPLEN, CA, United States). RNA concentrations were measured using a Qubit® RNA Assay Kit in a Qubit®2.0 fluorometer (Life Technologies, Carlsbad, CA, United States).

Sequencing and Data Analysis

The construction and sequencing of a cDNA library were performed by Shanghai OE Biotech. Co., Ltd. (China); fragments with lengths of 150–200 bp were selected using an AMPure XP system (Beckman Coulter, Beverly, MA, United States). Library quality was assessed on a bioanalyzer (2100, Agilent, Santa Clara, CA, United States). Nine cDNA libraries were sequenced on a Hiseq 2000 platform (Illumina, CA, United States). High-quality reads were assembled *de novo* using Trinity software (Grabherr et al., 2011). The final unique consensus sequences were regarded as unigenes. For gene annotation, BLAST was used to align the unigenes to the National Center for Biotechnology Information (NCBI) nonredundant protein database (Nr), NCBI non-redundant nucleotide database (Nt), Swiss-Prot protein database (Swiss-Prot), protein families database (Pfam), Kyoto Encyclopaedia of Genes and Genomes (KEGG), and Clusters of Orthologous Groups of proteins (COG). Gene Ontology (GO)[2] annotation was performed using Blast2GO software (version 2.5; Gotz et al., 2008) based on the results of Nr and Pfam annotation. Fragments per kilobase per million base pairs (FPKM) values were used to evaluate the expression patterns of unigenes with the thresholds of $|\log_2\text{Ratio}| \geq 1.0$ and false discovery rate ≤ 0.001.

Analysis of DEGs

GO enrichment analysis (corrected $p < 0.05$) of the DEGs was performed with the GOseq R package after the data had been evaluated using the Kolmogorov–Smirnov test. KEGG pathways were assigned to the unigenes and pathway maps using the online KEGG Automatic Annotation Server[3] with the bidirectional best-hit method (Moriya et al., 2007). KOBAS software (Mao et al., 2005) was used to determine DEG enrichment in KEGG pathways.

Gene Clustering and Visualization

Heat maps were used to visualise gene expression; the maps were constructed using $\log_2$-transformed FPKM values in MeV v4.8.1 (Saeed et al., 2003), with Pearson's correlation as a similarity metric.

qPCR Validation and Expression Analysis

Quantitative real-time polymerase chain reaction (qPCR) was conducted in accordance with the methods described by Zhang et al. (2019). Primer sequences are listed in **Supplementary Table S1**. 18s rRNA was used as the endogenous reference gene; relative expression levels were calculated using the $2^{-\Delta\Delta Ct}$ method (Livak and Schmittgen, 2001).

[1]http://rsb.info.nih.gov/ij/

[2]http://www.geneontology.org/

[3]http://www.genome.jp/kegg/kaas/

Soluble Sugar and Starch Content Measurement

Soluble sugar content was determined by the anthrone colorimetry method (Fukao et al., 2006). Fructose (Fructose assay kit A085-1-1), sucrose (Sucrose measurement kit A099-1-1), glucose (Glucose kit a154-1-1), and starch (Starch content kit A148-1-1) contents were measured using an assay kit (Nanjing Jiancheng Biotechnology Company, Nanjing, China). Units were expressed as mg metabolites per g of plant tissue. The experiment was conducted with three biological and three technical replicates.

Measurement and Statistical Analysis of IAA, GA_3, and BL Concentrations

Endogenous IAA, GA_3, and BL were measured by liquid chromatography-mass spectrometry. Tetraploid and diploid stems and roots (leaves removed) were collected after 50 d of growth, then frozen in liquid nitrogen. IAA and GA_3 detection methods were adopted from the work by Chen et al. (2012); the BL detection method was adopted from the work by Ding et al. (2013). Quantum triple quadrupole liquid chromatography-mass spectrometry (Thermo Fisher Scientific, Waltham, MA, United States) was used for plant hormone detection; three biological replicates were included in this experiment.

Exogenous Hormone Addition

Adventitious shoots of tetraploid hybrid sweetgum were incubated in three types of new media for 0, 30, or 40 d. Each new medium contained one hormone: 1.5 mg/L IAA, 0.5 mg/L GA_3, or 0.1 mg/L epibrassinolide. After determination of the optimal replacement time, the adventitious shoots were placed in rooting media that contained different hormones; eight combinations were used (**Supplementary Table S2**). There were three replicates in each treatment; each replicate contained 10 plantlets, including five genotypes. Each adventitious shoot was cut to a length of approximately 1.5 cm. After 60–70 d of growth (i.e., when the plant stopped growing), the plant height, ground diameter, internode number, main root number, and root length were measured.

Statistical Analyses

Significant differences among treatments were evaluated by Duncan's multiple range test using a threshold of $p < 0.05$, after a homogeneity test had been conducted; all statistical analyses were performed using SPSS version 18.0 (SPSS Inc., Chicago, IL, United States). Histograms and line graphs were constructed using Microsoft Excel 2010 software (Microsoft Corp., Redmond, WA, United States).

RESULTS

Morphological Description of Regenerated Tetraploids and Diploids

The ploidy levels of three genotypes were determined by flow cytometry before morphological and molecular examinations (**Figure 1A**). The phenotypes of tetraploid and diploid plants were measured after they had been cultured in rooting medium for 0, 25, 50, and 70 d (**Table 1**; **Figure 1B**). The results showed that there were no significant differences in ploidy among the plants.

In stage I, the height of tetraploids only increased by 1.93 mm, while the diploids grew rapidly; in stage II, a significant difference was apparent (**Figure 1B**). In stage III, the plant growth rates of both tetraploid and diploid plants were less than the rates in stage II (increases of 0.93 and 4.77 mm, respectively). At 50 d, the plant height and number of internodes were significantly shorter and fewer, respectively, in tetraploids than in diploids. In all three stages, the stem diameter was always larger in tetraploids than in diploids, but the difference was not statistically significant at 50 or 70 d. There were significantly fewer tetraploid leaves than diploid leaves at 25 d, and the area of tetraploid leaves was less than the area of diploid leaves at 50 d; however, there was no significant difference in petiole length at any developmental stage. The rooting times

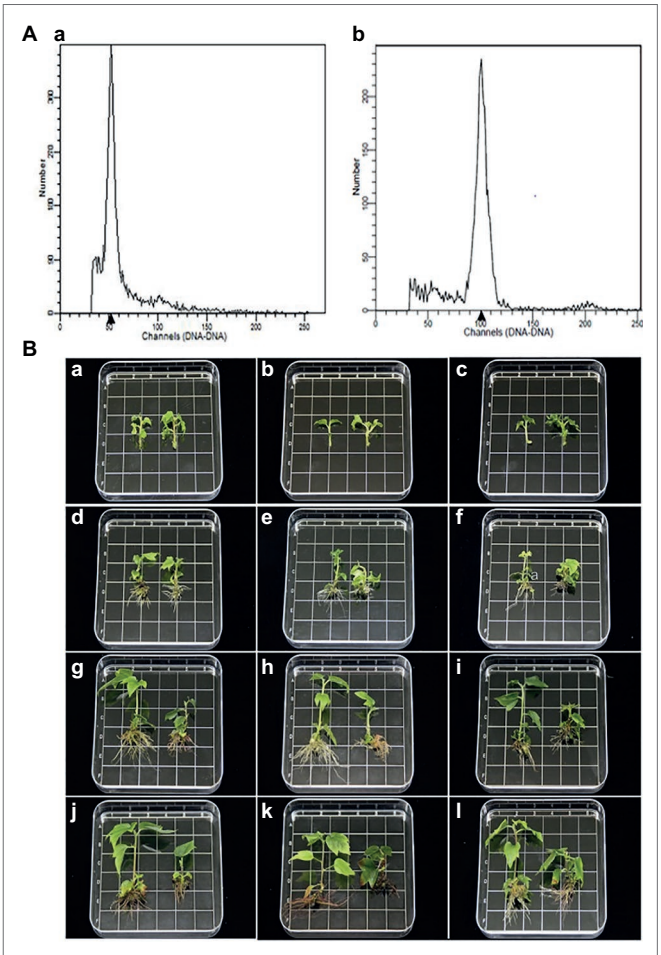

FIGURE 1 | (A) Histograms of flow cytometry findings for *Liquidambar styraciflua* × *Liquidambar formosana*: **a** diploid plant (control); **b** tetraploid plant. **(B)** Morphological comparison of diploid and tetraploid hybrid sweetgum plants at various developmental stages of *in vitro* growth. **a,d,g,j** Z1; **b,e,h,k** Z2; **c,f,i,l** Z3. **a–c**: 0 d; **d–f**: 25 d; **g–i**: 50 d; **j–l** 70 d. **a–l** tetraploid on the right and diploid on the left in each picture. Area of each square: $1 \times 1 = 1\ cm^2$.

TABLE 1 | *In vitro* growth statistics of diploid and tetraploid hybrid sweetgum plants at various developmental stages.

	0		25 d		50 d		70 d	
	2X	4X	2X	4X	2X	4X	2X	4X
Plant height (mm)	15 ± 0c	15 ± 0c	19.35 ± 0.67c	17.5 ± 1.3c	36.28 ± 5.56b	19.14 ± 1.22c	41.05 ± 4.65a	20.07 ± 1.3c
Number of internodes	2.89 ± 0.19d	3.33 ± 0cd	4.11 ± 0.69b	4 ± 0.33bc	5.44 ± 0.51a	3.89 ± 0.38bc	5.89 ± 0.38a	4.22 ± 0.19b
Stem diameter (mm)	1.24 ± 0.05c	1.47 ± 0.04bc	1.24 ± 0.12c	1.54 ± 0.09b	1.44 ± 0.3bc	1.48 ± 0.09bc	1.81 ± 0.07a	1.94 ± 0.17a
Root length (mm)	\	\	7.68 ± 1.72c	4.92 ± 0.66d	11.32 ± 1.62b	6.37 ± 1.03cd	14.15 ± 0.81a	6.49 ± 0.8cd
Root number	\	\	14.78 ± 2.5b	9 ± 0.33c	21.44 ± 2.22a	10.44 ± 1.35c	20.11 ± 2.59a	9.67 ± 0.33c
Number of leaves	4 ± 0.58f	4.44 ± 0.38ef	6.33 ± 0.58bc	5.44 ± 0.19d	6.78 ± 0.19ab	5.11 ± 0.38de	7.44 ± 0.51a	5.78 ± 0.19cd
Leaf area (mm^2)	18.74 ± 1.12c	23.67 ± 1.26c	19.99 ± 2.81c	28.54 ± 2.56c	63.32 ± 5.12b	57.5 ± 5.1b	87.05 ± 9.33a	84.25 ± 9.73a
Petiole length (mm)	2.09 ± 0.32bc	1.78 ± 0.02c	1.82 ± 0.11c	2.16 ± 0.3bc	2.49 ± 0.14b	2.25 ± 0.07bc	3.98 ± 0.33a	3.74 ± 0.6a

Data are represented as means ± standard errors of three replicates. Different lowercase letters indicate significant differences among treatments, as determined by Duncan's test ($p < 0.05$).

of tetraploid and diploid plants were similar; the root number and length were significantly fewer and shorter, respectively, in tetraploids than in diploids (**Table 1**; **Figure 1B**). These results showed that diploid growth was rapid in stage II, while tetraploid growth was not. Regenerated tetraploid plants were shorter and could grow fewer new buds after upper stem segments had been cut.

Histological Observations of Leaves, Stems, and Roots of Regenerated Tetraploids and Diploids

Observation of the second or third leaf positions of tetraploid and diploid plants showed that tetraploid leaves were significantly thicker than diploid leaves (**Figure 2A**; **Supplementary Table S3**). Tetraploid veins were also thicker than diploid veins, but this difference was not statistically significant at stage III. Palisade tissue and spongy tissue were also thicker in tetraploids than in diploids. The areas of xylem transverse cells, upper epidermal cells, lower epidermal cells, spongy tissue cells, and palisade tissue cells were larger in tetraploids than in diploids (**Supplementary Table S4**).

The shoot tissue thickness and cell size were greater in tetraploids than in diploids. The tissue thickness and cell area increased with as the number of culture days increased (**Figure 2B**; **Supplementary Tables S5** and **S6**). The shoot diameter, epidermal thickness, stem cortex thickness, and vascular column thickness were not significantly different between tetraploids and diploids, although epidermal thickness differed at 70 d. There were significant differences between tetraploids and diploids in terms of xylem cells at all three stages, cortex cells at 70 d, and phloem cells at both 50 and 70 d. **Figure 2B** shows that the apical meristem cells in diploid and tetraploid plants divided vigorously at 25 d; most diploid apical meristem cells continued to vigorously divide at 50 and 70 d (**Figures 3Ac,e**). However, most tetraploids exhibited a dormant bud apex at 50 d (**Figure 3Ad**). At 70 d, the apical uds were completely dormant and the bud scale structure was present (**Figure 3Af**). Therefore, the slow growth rate of the apical meristem may have contributed to shorter plant height in tetraploids than in diploids.

The root diameter and root tissue thickness at 25 and 50 d were larger in tetraploids than in diploids, with the exception of cylinder diameter at 70 d. The root diameter at 50 and 70 d, and the thicknesses of the epidermis and cortex at all three stages, significantly differed between tetraploids and diploids (**Figure 3B**; **Supplementary Tables S7** and **S8**). The areas of xylem cells, epidermal cells, and cortical cells were significantly greater in tetraploids at all three stages. The apical meristematic cells of new diploid and tetraploid roots divided vigorously at 25 d of rooting culture (**Figures 3Ca,b**); the apical meristematic cells of diploid roots continued to vigorously divide at 50 d. However, most tetraploids exhibited increased root cell width and irregular shapes at 50 d (**Figures 3Cc,d**); the length of the root meristematic zone also decreased in tetraploids. The proportion of malformed roots was 81.33%. Complete coleoptile structure was not detected. These results indicated that root cell shape and root structure began to change after stage II in tetraploids; their longitudinal elongation ability significantly decreased.

Transcriptome Sequencing and Assembly

Twelve samples were analysed in this study. The original quality score (Q30) of each sample was 93.45–95.07%, the effective data were 6.26–6.90 G, the mean guanine-cytosine (GC) content was 46.50%, and 6.81–7.48 G raw bases were obtained by sequencing (**Supplementary Table S9**). In total, 4 526,576 to 4 677,234 clean reads (**Supplementary Table S9**) were obtained after low-quality sequences had been filtered out. Furthermore, 60,187 Unigenes were assembled, with a total length of 5 200,279 bp and mean length of 917 bp (**Supplementary Table S10**). Of these sequences, 0.24–63.82% were annotated in seven databases: Nr, Swiss-Prot, KEGG, COG, evolutionary genealogy of genes: Non-supervised Orthologous Groups (eggNOG), GO, and Pfam (**Supplementary Table S11**).

Analysis of DEGs

Statistical analysis of FPKM values in each group is shown in **Supplementary Table S12** and **Figure 4A**. Overall, 14,095 and 13,117 DEGs were identified in tetraploid stems and roots, respectively, compared with diploid plants (**Figure 4B**). The

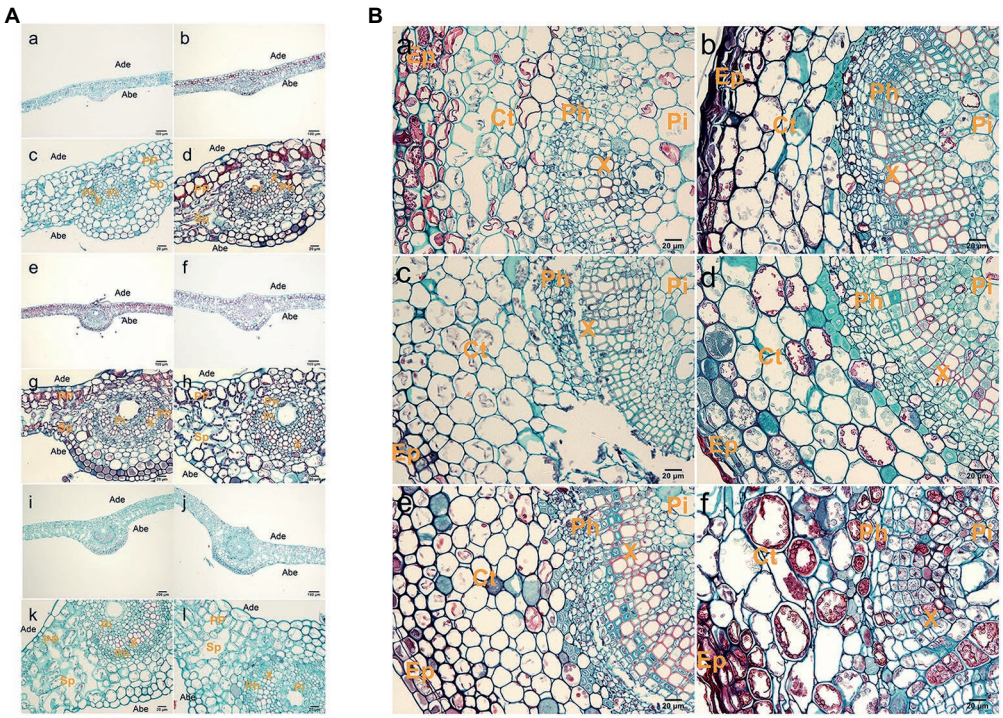

FIGURE 2 | Histological observations of leaves and stems. **(A)** Anatomy of a leaf cross section from hybrid sweetgum. **a**,**c**,**e**,**g**,**i**,**k** Cross-section of a diploid leaf; **b**,**d**,**f**,**h**,**g**,**l** cross section of a tetraploid leaf. **a–d** 25 d; **e–h** 50 d; **i–l**: 70 d. Ade: adaxial epidermis; Abe: abaxial epidermis; PP: palisade parenchyma; Sp: spongy parenchyma; Pi: pith; Ph: phloem; X: xylem. Bars are 200 μm in **a,b,e,f,i,j**; they are 20 μm in **c,d,g,h,k,l**. **(B)** Anatomy of a stem cross section from hybrid sweetgum. **a**,**c**,**e** Cross section of a diploid shoot; **b**,**d**,**f** cross-section of a tetraploid shoot. **a**,**b** 25 d; **c**,**d** 50 d; **e**,**f** 70 d. Ct: cortex; Ep: epidermis; Pi: pith; Ph: phloem; X: xylem. Bars are 200 μm in **a,b,e,f**; they are 20 μm in **c**,**d**.

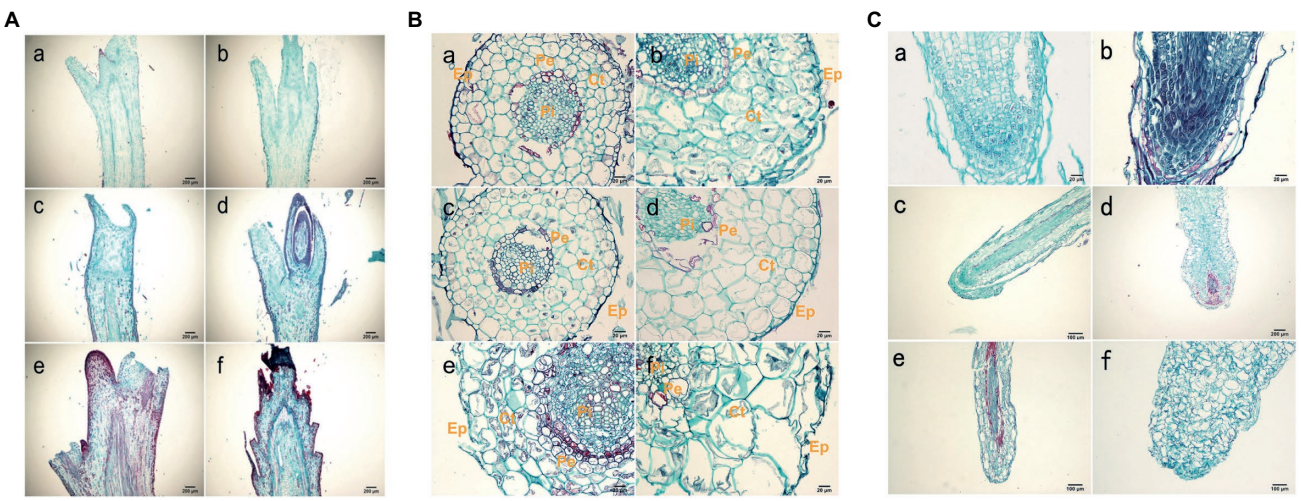

FIGURE 3 | Histological observations of roots. **(A)** Anatomy of a shoot tip longitudinal-section from hybrid sweetgum. **a,c,e** Cross-section of a diploid shoot tip; **b,d,f** crosssection of a tetraploid shoot tip. **a,b** 25 d; **c,d** 50 d; **e,f** 70 d. Each bar is 200 μm. **(B)** Anatomy of a typical root cross section from hybrid sweetgum. **a,c,e** Cross-section of a diploid root; **b,d,f** cross-section of tetraploid roots. **a,b** 25 d; **c,d** 50 d; **e,f** 70 d. Ep: epidermis; Ct: cortex; Pi: pith; CC: central cylinder; Pe: pericycle. Bars are 100 μm in **a,b,e,f**; they are 20 μm in **c,d**. **(C)** Anatomy of a typical root tip longitudinal-section from hybrid sweetgum. **a,c,e** Cross-section of diploid root tips; **b,d,f** cross-section of tetraploid roof tips. **a,b** 25 d; **c,d** 50 d; **e,f** 70 d. Each bar is 200 μm.

qPCR results on selected genes were similar to the RNA-Seq data, which indicated that the results of RNA-Seq were reliable (**Figure 5**). In stems, 7,425 and 6,670 DEGs were upregulated and downregulated, respectively; in roots, 4,160 and 8,957 DEGs were upregulated and downregulated, respectively—these values constituted 31.71 and 68.29% of all DEGs, respectively

(**Figure 4C**). Thus, gene expression was generally downregulated in the tetraploid roots of hybrid sweetgum.

Analysis of DEG Enrichment in GO and KEGG Pathways

Gene ontology was used to analyse the DEGs of tetraploid and diploid stems and roots from three perspectives: biological process (BP), cell component (CC), and molecular function (MF). For stems and roots, DEGs were enriched in biosynthesis and signal transduction pathways, cell cycle, and carbon metabolism. For shoots, upregulated DEGs were enriched in guanosine triphosphate metabolic process (GO:0046039), gibberellin catabolic process (GO:0045487), other hormone biosynthesis and metabolic pathways, secondary metabolite biosynthetic process (GO:0044550), starch catabolic process (GO:0005983), and alkaloid metabolic process (GO:0009820; **Supplementary Table S13**). For shoots, downregulated DEGs were mainly enriched in histone phosphorylation (GO:0016572), cellular response to far red light (GO:0071490), cellular response to red light (GO:0071491), and histone kinase activity (H3-S10 specific; GO:0035175; **Supplementary Table S14**). For roots, upregulated DEGs were significantly enriched in maintenance of seed dormancy by abscisic acid (GO:0098755), response to low light intensity stimulus (GO:0009645), cellular response to freezing (GO:0071497), priming of cellular response to stress (GO:0080136), cellular response to boron-containing substance deprivation (GO:0080169), other stress response pathways, and NADH dehydrogenase complex (plastoquinone) assembly (GO:0010258; **Supplementary Table S15**). For roots, downregulated DEGs were mainly involved in septin ring assembly (GO:0000921) and cell cycle (GO:0007089), (GO:0071931, GO:2000045, GO:2000134; **Supplementary Table S16**).

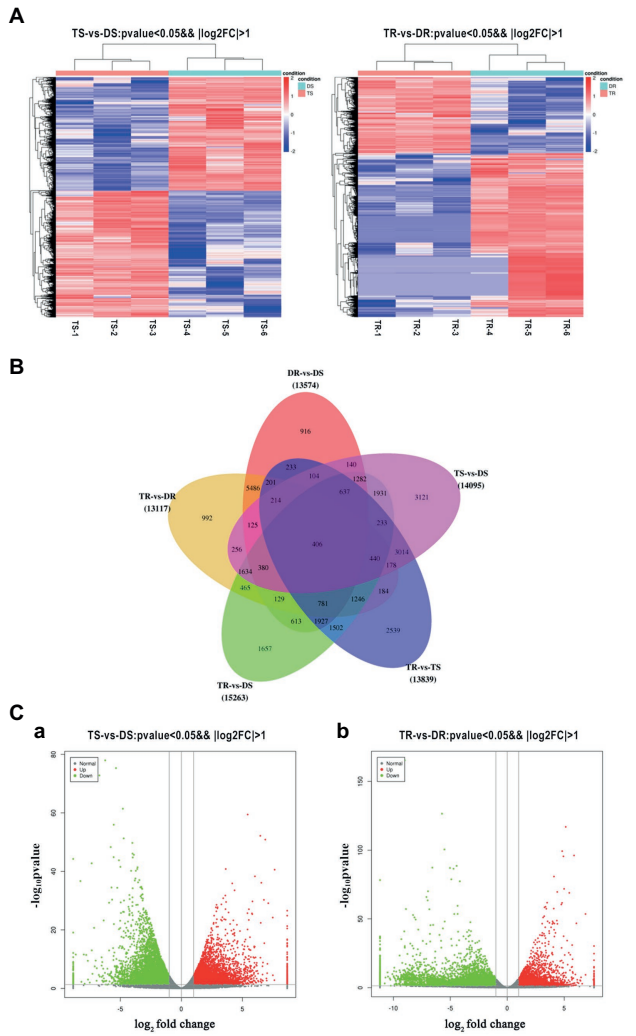

FIGURE 4 | (A) Heatmap of DEG expression profiles (RNA-Seq) in tetraploid vs. diploid shoots. Left: DEGs were derived from TS-1_TS-2_ TS-3_vs DS-1_ DS-2_ DS-3. Right: DEGs were derived from TR-1_ TR-2_ TR-3_vs DR-1_ DR-2_ DR-3. Thresholds for DEG selection in the heatmap are $p < 0.05$ and $|\log_2\text{FoldChange}| > 2$. **(B)** Venn diagram analysis comparing five groups of DEGs. **(C)** Volcano plot of DEGs. **a,b** Represent the number of DEGs that were up- or downregulated for TS vs. DS and TR vs. DR, respectively. Grey indicates unigenes with similar expression patterns, red indicates significantly upregulated unigenes, and green indicates significantly downregulated unigenes. The x-axis is the $\log_2$FoldChange, and the y-axis is the $\log_{10}P$-value.

KEGG Analysis of DEGs

The KEGG database was used to identify biological pathways that were enriched in DEGs (**Figure 6**; **Supplementary Tables S17** and **S18**). DEGs in tetraploid and diploid stems and roots were enriched in 47 and 72 biological pathways ($p < 0.05$), respectively. These pathways included gibberellin, auxin, brassinosteroids, salicylic acid, and ethylene pathways, such as plant hormone signal transduction (ko04075), diterpene biosynthesis (ko00904), brassinosteroids biosynthesis (ko00905) and carotenoid biosynthesis (ko00906); they also included secondary metabolite pathways, such as phenylpropionic acid synthesis (ko00940), flavonoid biosynthesis (ko00941), starch and sugar metabolism (ko00500), fatty acid synthesis and metabolism related to energy synthesis and metabolism (ko00071, ko01212, ko00061), cell cycle (ko04110), and apoptosis (ko04210).

DEGs Related to Plant Hormones in Stems and Roots

Plant hormone biosynthesis and signal transduction pathways include auxin, gibberellin, cytokinin, BL, abscisic acid, ethylene, jasmonic acid and salicylic acid synthesis and transduction. Many important genes involved in auxin, gibberellin, and BL biosynthesis and signal transduction pathways were downregulated in tetraploids (**Figure 7A**). In shoots, the auxin biosynthesis genes *YUCCA* (*Indole-3-pyruvate monooxygenase YUCCA*) and *TAA1* (*Tryptophan aminotransferase of Arabidopsis1*) and the auxin influx carrier *AUX1* (*Auxin1*) were downregulated; *SAUR* (*Small auxin up RNA*), *IAA* (*Indole-3-acetic acid*), and *GH3* (*Gretchen hagan 3*) were generally downregulated (**Figure 7A**). Multiple gibberellin biosynthesis genes were also downregulated, including *CPS* (*Copalyl*

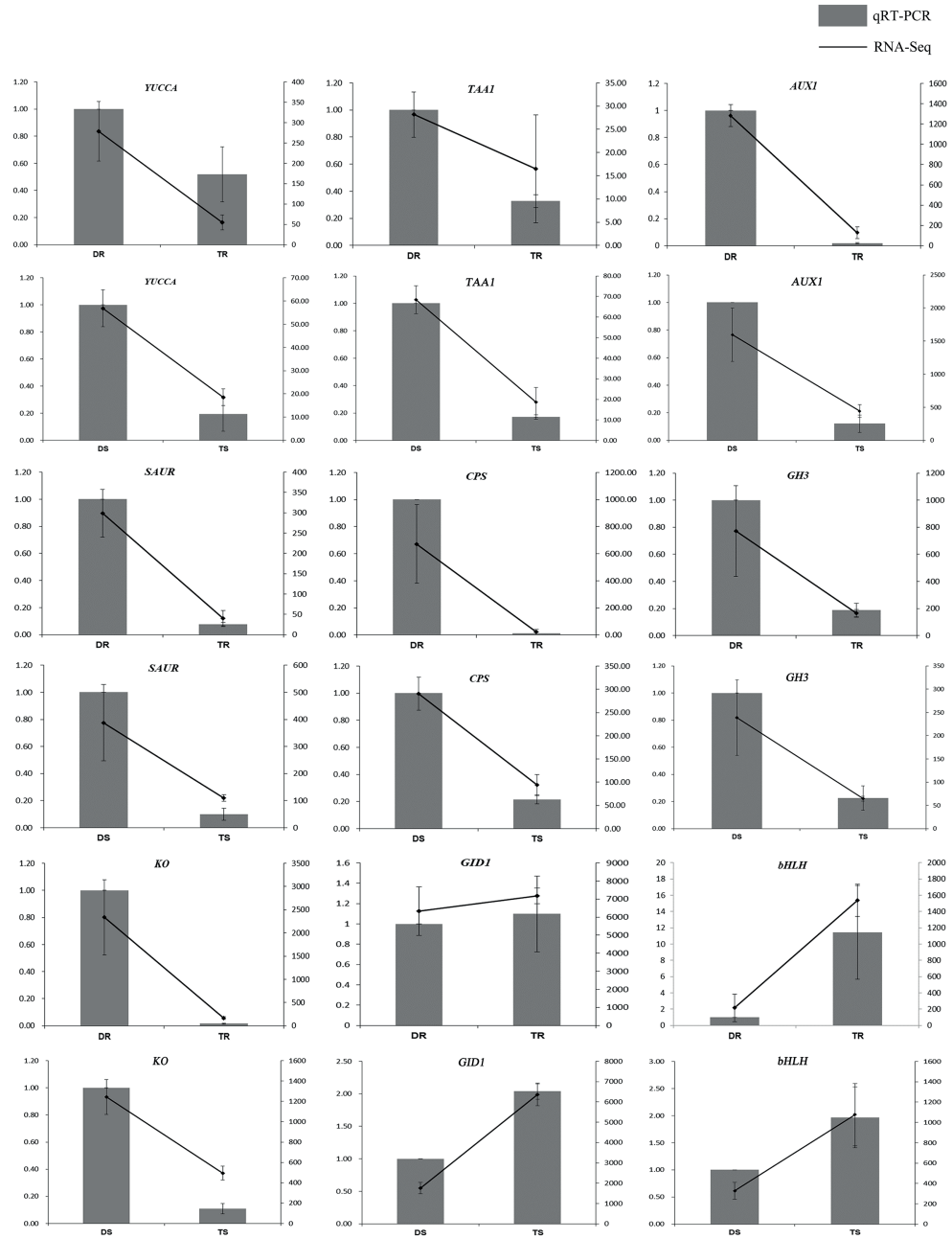

FIGURE 5 | Comparison of expression profiles of nine representative genes as measured by RNA-seq and qRT-PCR. Columns represent expression determined by qRT-PCR (left y-axis), while lines represent expression by RNA-seq in FPKM values (right y-axis). The x-axis in each chart represents different plant materials. For qRT-PCR assay, the mean was calculated from three biological replicates each with three technical replicates ($n = 9$). For RNA-seq, each point is the mean of three biological replicates.

pyrophosphate synthase), *KAO* (*Kaurenoic acid oxidase*), *KO* (*Kaurene oxidase*), *GA20ox* (*GA20-oxidase*), *GA2ox* (*GA2-oxidase*), and *GA3ox* (*GA3-oxidase*). The *GID1* (*GA-insensitive dwarf1*) gene, which contributes to positive regulation of gibberellin signal transduction, was upregulated; its negative regulation counterpart, *DELLA*, was generally downregulated. The BL biosynthesis and signal transduction genes *BAS1* (*phyB-4 activation-tagged suppressor 1*) and *CYCD3* (*Cyclin D3;1*) were downregulated. *ABA*, *PYL* (*Pyrabactin resistance 1-like*), the negative regulation *SnRKs* (*SNF1-related protein kinases*; TRINITY_DN36419_c0_g1_i1_3, TRINITY_DN39068_c1_g1_i10_3, TRINITY_DN44648_c2_g3_i1_1, TRINITY_ DN46092 _ c1 _g1_i3_1)—which negatively regulates abscisic acid signal transduction—and *PP2C* (*Protein phosphatase 2C*; TRINITY_DN34392_c0_g1_i3_2 and TRINITY_DN37551_c0_g1 _i6_2) were downregulated. However, the positive

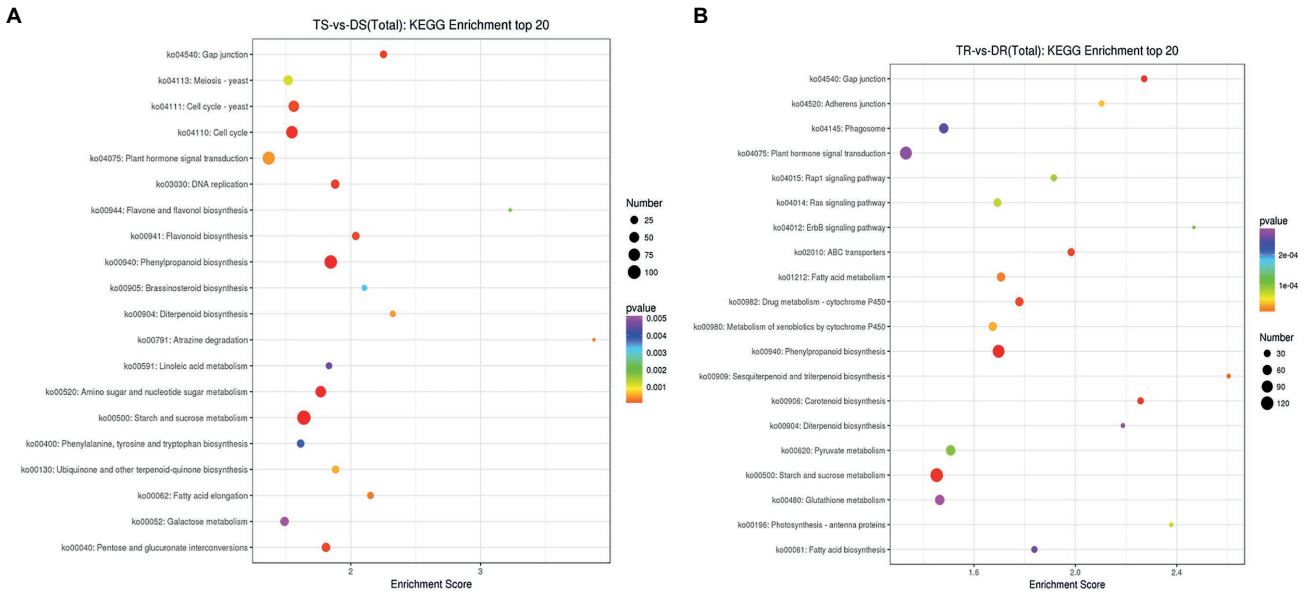

FIGURE 6 | Map of KEGG enrichment analysis results for DEGs. **(A)** TS vs. DS; **(B)** TR vs. DR.

regulation counterpart, *ABF* (*Abscisic acid responsive elements-binding factor*), was generally downregulated.

Similar to stems, the auxin biosynthesis genes *YUCCA* and *KYNU* (*kynureninase*), auxin signal transduction genes *AUX/IAA* (auxin/indole-3-acetic acid), *SAUR*, *GH3* (TRINITY_DN35023 _c0_g1_i1_1, TRINITY_DN42653_c0_g1_i1_1) and *IAA* were downregulated in roots, while auxin influx carrier *AUX1* was also similarly downregulated. The gibberellin biosynthesis biosynthetic genes (e.g., *CPS*, *KO*, *KAO*, *GA20ox*, and *GA3ox*) were all downregulated. However, *GID1*, which positively regulates gibberellin signal transduction, was upregulated; *DELLA*, its negative regulation counterpart, was downregulated. For ABA, except CYP707A3, the biosynthesis genes *AAO3* and *ABA2* were downregulated, while *NCED* (*9-cis-epoxycarotenoid dioxygenase*) was generally downregulated. In contrast to stems, with the exception of *PP2C*, the signal transduction genes *PYL*, *SnRKs*, and *ABF* were generally downregulated (**Figure 7B**).

DEGs Related to Starch and Sucrose Biosynthesis and Metabolism

In stems and roots, there were 42 and 65 DEGs related to starch and sugar metabolism, respectively (**Figure 8**); most were downregulated. In stems, sacA, *SS* (*Starch synthase*), glgA, otsB, GN1_2_3, GN4, GN5_6, SPS1 (*Sucrose-phosphate synthase1*), and *SUS* (*Sucrose synthase*) were downregulated; TPS (*Trehalose 6-phosphate synthase*) was upregulated. In roots, *TPS*, *SS* (TRINITY_DN 37738_c0_g1_i1_2, TRINITY_DN40072_c0_g1_i1_1, TRINITY_DN44913_c0_g2 _i1 _4), *sac* (TRINITY _DN 17363 _c 0_g1_i1_2, TRINITY_DN35727_c0_g1_i12_2, TRINITY_DN36819_c0_g1_i2_3, TRINITY_DN46169_c0_g1_i15_1), *otsB*, *GN1_2 _3*, and *GN5_6* were downregulated.

DEGs Related to Cell Cycles in Stems and Roots

There were 76 and 49 genes involved in regulating cell cycles (ko04110) in stems and roots, respectively (**Figure 8**). In stems, these genes were generally downregulated, except *ATM* (*Ataxia telangiectasia mutated*), *CDK2* (*cyclin-dependent kinase 2*), *CDC6* (cell division control protein 6), *CDC7*, *CDC20*, *CDC45*, *E2F3*, *Bub1*, *Bub3*, *CycA* (*Cyclin A*), *Orc1-Orc3*, and *Orc5*; notably, *Orc6*—a contributor to cell proliferation and cell cycle regulation—was generally downregulated. In roots, except for two genes, the DEGs were downregulated in tetraploids, including *ATM*, *BUB1*, *CDC20*, *CDC45*, *CUL1* (*Cullin 1*), *SKP1* (*S-phase kinase-associated protein 1*), and *GSK3B* (*glycogen synthase kinase 3 beta*). These genes have important roles in regulating cell size and cell number. Therefore, the generally larger cells of tetraploid hybrid sweetgum, compared to diploid hybrid sweetgum, may be related to significant changes in cell cycle genes.

Analysis of the Hormone and Sugar Contents of Tetraploids and Diploids

The IAA, GA_3, and BL contents of diploid and tetraploid roots and stems cultured in rooting medium for 50 d were measured; the results are shown in **Figure 9A**. The endogenous auxin, gibberellin, and BL levels were significantly lower in tetraploids than in diploids, consistent with the results of the transcriptome analysis. Compared with diploids, only the glucose contents significantly differed in tetraploids (**Figure 9B**). The result showed that although starch and sugar biosynthesis genes were downregulated in tetraploid plants, the starch and soluble sugar contents did not significantly decrease. Therefore, gene expression and sugar accumulation were not synchronised at this stage.

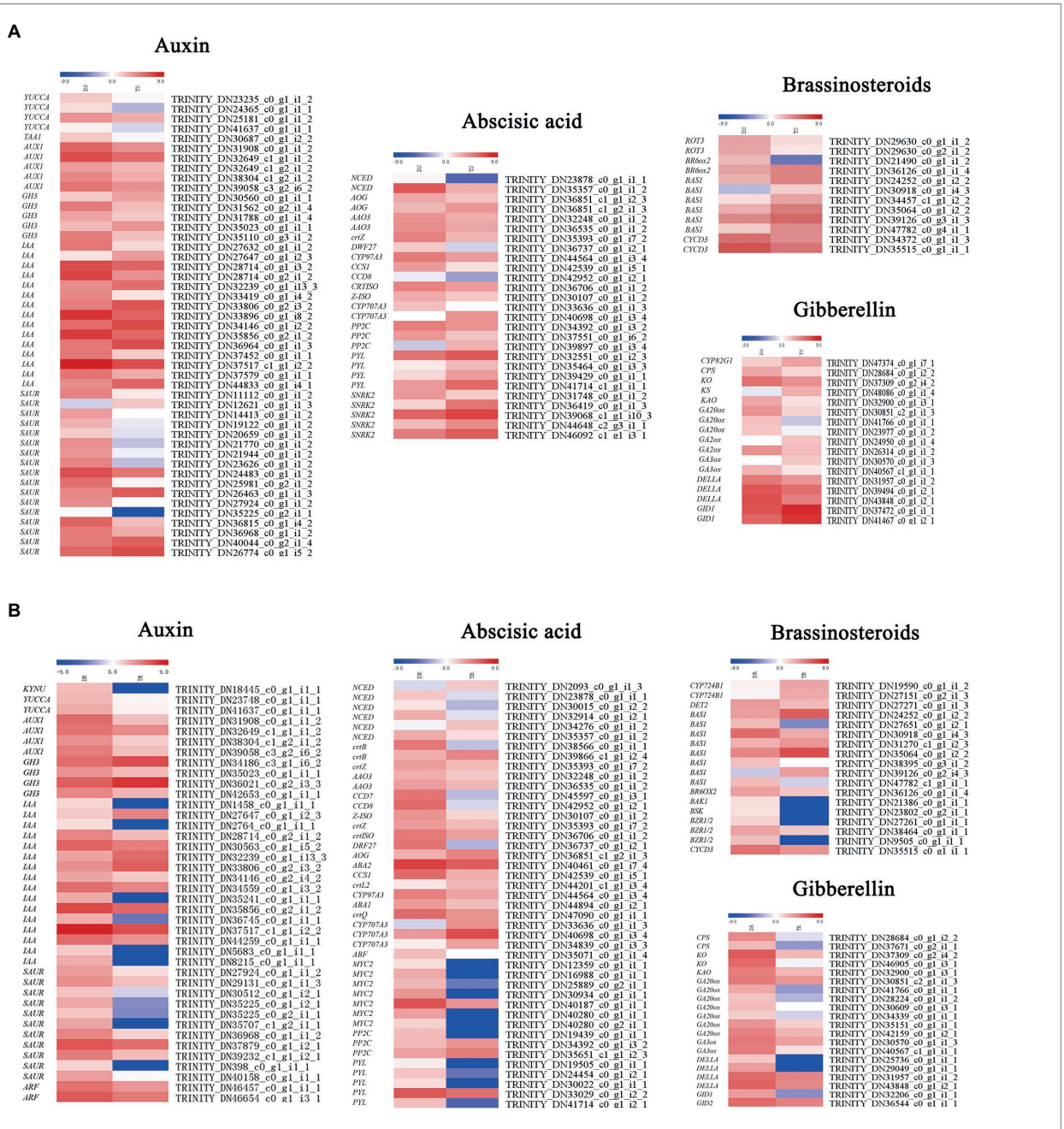

FIGURE 7 | Heat maps depicting differential expression patterns of genes involved in plant hormone synthesis and signal transduction: **(A)** shoots, **(B)** roots.

Effects of Exogenous Hormones on Plant Growth

To verify the effects of IAA, GA_3, and BL on elongation in tetraploids, the effect of the timing of tetraploid transplantation into new medium was investigated. As shown in **Supplementary Table S19**, the growth of regenerated tetraploid plants was only significantly promoted at the initial stage when the rooting medium was supplemented with 0.5 mg/L GA_3 or 1.5 mg/L IAA. These results showed that the timing of addition of exogenous hormones significantly affected the growth of regenerated plants. As time elapsed without replacement of the medium, the elongation effect gradually decreased.

After determination of the optimal medium replacement time, the effects of media containing different hormone ratios on tetraploid growth were investigated. The results showed that the greatest plant height was 4.42 cm in a rooting medium supplemented with 0.5 mg/L GA_3; the plant height, ground diameter, root length, and leaf area were significantly increased compared with tetraploid hybrid sweetgum grown in primitive rooting medium, but the number of roots did not significantly

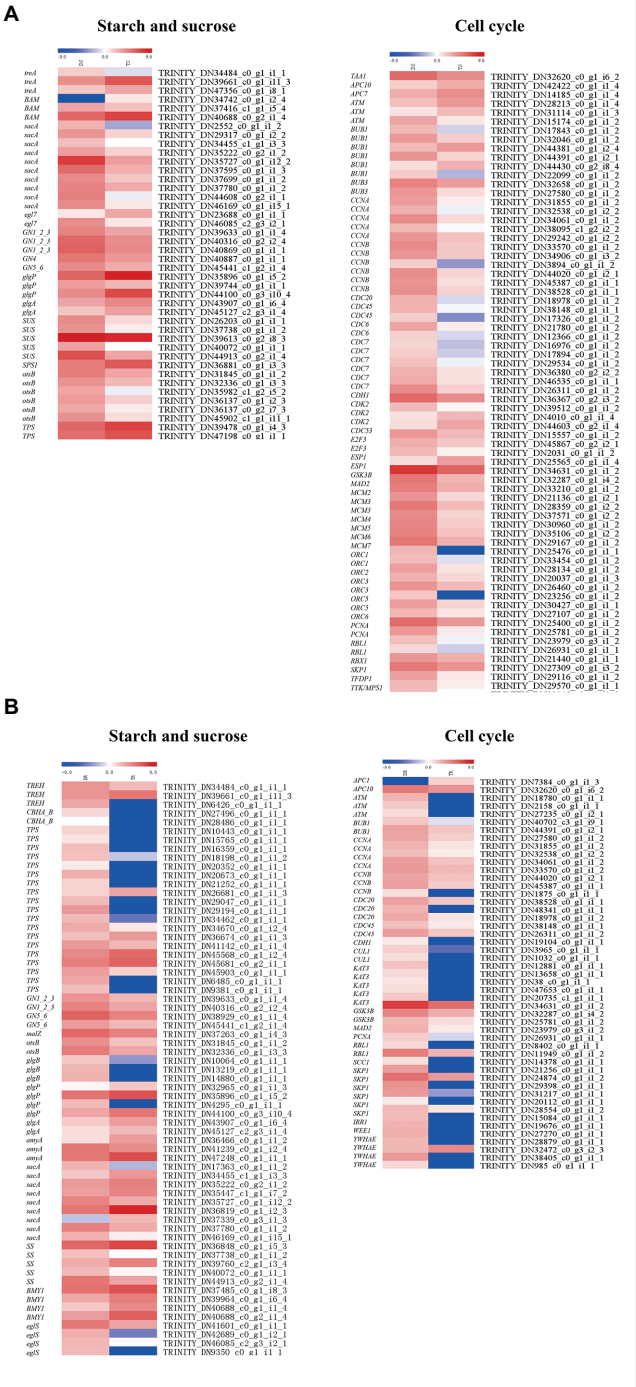

FIGURE 8 | Heat maps depicting DEGs involved in starch and sucrose biosynthesis and metabolism and cell cycles: **(A)** shoots, **(B)** roots.

differ (**Figure 10**; **Supplementary Table S20**). The plants placed in a medium with the addition of 0.5 mg/L GA_3 combined with 1.5 mg/L IAA had the largest leaf area and greatest number of main roots. Therefore, GA_3 was the hormone that most strongly supported stem elongation (**Supplementary Table S20**). The effects of BR alone or in combination with GA_3 or IAA were weaker than the effects of other two hormones. These results indicated that the height of tetraploid plants could be significantly increased by adding an appropriate concentration of GA_3 to the growth media. In addition, the stem segments used for subcultures could be rooted and elongated normally in the medium. Therefore, *in vitro* micro-cutting could be used to subculture and expand tetraploid plants. Additionally, 0.5 mg/L GA_3 was added to the tetraploid adventitious bud elongation medium; it demonstrated a strong effect on adventitious bud elongation (**Figure 10**).

DISCUSSION

Tetraploid hybrid sweetgum regenerated plants exhibited obvious morphological variations, with shorter stems and roots than diploid plants. Furthermore, the stem diameter and internode length were thicker and shorter, respectively, in tetraploids than in diploids. These observations were consistent with previous findings in some herbs, fruit trees, and timber trees (Nilanthi et al., 2009; Tan et al., 2015; Xu et al., 2018). However, with the exceptions of stems and roots, the other organs of dwarf tetraploids did not necessarily exhibit a growth disadvantage. The plant height was shorter in tetraploid apples than in diploid apples, but the leaf and flower organs were obviously larger in tetraploid apples (Xue et al., 2017). Thus, plant height is not necessarily positively related to the sizes of other organs. In addition, Corneillie et al. (2019) found that in *Arabidopsis thaliana*, the leaf area, stem length, and dry weight were greater in tetraploid plants than in plants with other ploidy levels; as the ploidy level increased, hexaploid and octoploid plants gradually exhibited less growth. The ploidy level at which optimal growth is reached differs among species.

The proliferation and enlargement rates of apical and intersegment meristematic cells have considerable effects on elongation and development in roots and stems (Takatsuka and Umeda, 2014). The relationships among organ size, cell size, and cell number remain unresolved (Tsukaya, 2008; Li et al., 2012). Previous studies have suggested that plant organ sizes are determined by both cell size and cell number (Krizek, 2009; Gonzalez et al., 2012). Generally, plant cell sizes significantly increase after chromosome doubling. Endoreduplication is considered an important cause of polyploid cell enlargement (Tsukaya, 2008). The numbers of cells vary among species and ploidy levels. Compared with diploids, triploid *Populus* plants showed a significant increase in cell area, but the number of cells did not decrease (Zhang et al., 2019). A similar observation was reported in a study of *A. thaliana* (Li et al., 2012). However, cell area was larger in octoploid *Arabidopsis* plants than in diploid plants, but the smaller number of cells resulted in a smaller leaf area (Levan, 1939). These results indicated that the cell size was greater in tetraploids than in diploids, but the tetraploid plants had dwarfing characteristics.

In the present study, tetraploid hybrid sweetgum root cells exhibited increased width and irregular shape, the tetraploid root meristematic zone length decreased, and no obvious coleoptile sheath or complete coleoptile structure were observed. Few observations of root malformation have been reported in tetraploid regenerated plants; however, in apples, the ratio of

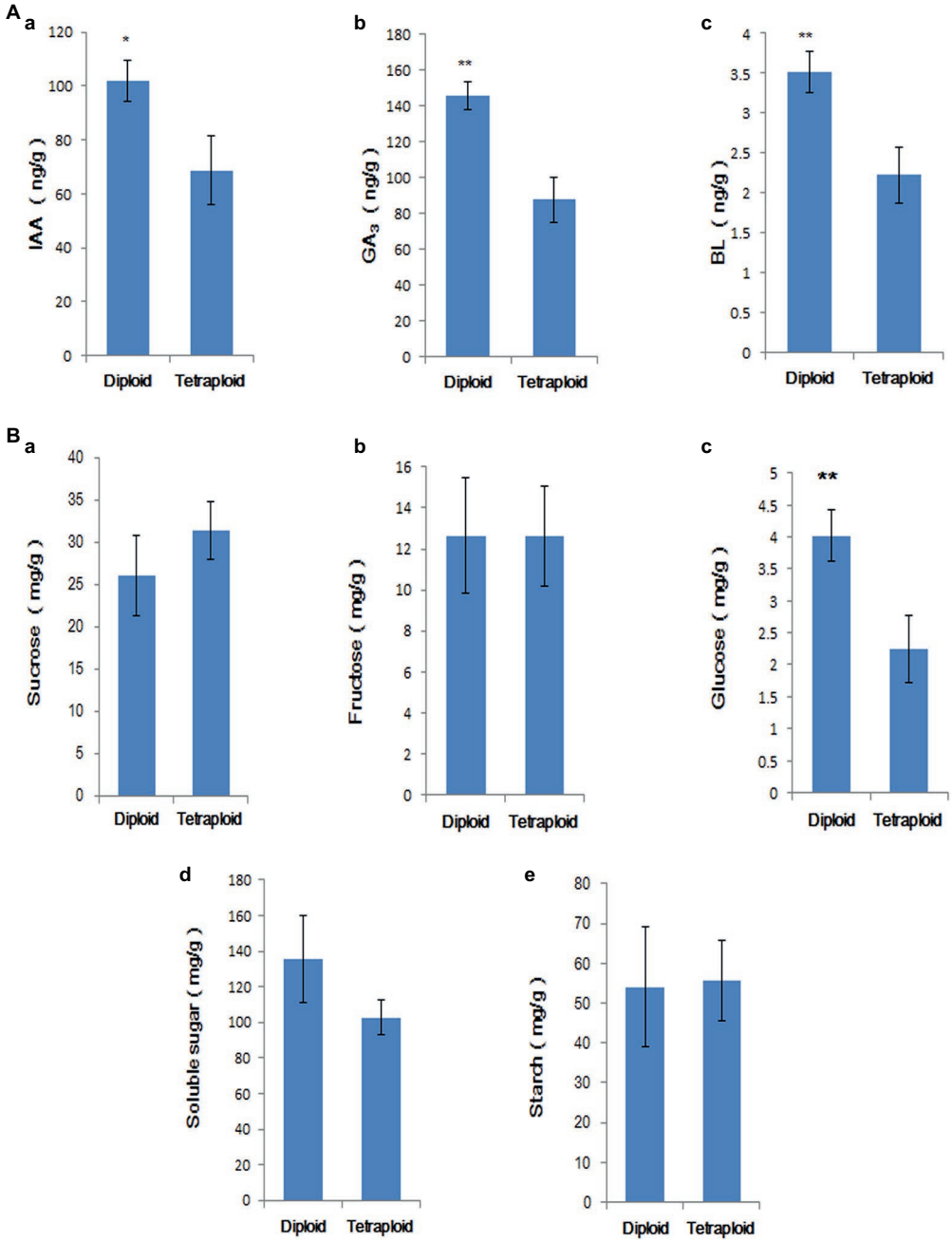

FIGURE 9 | (A) Comparison of IAA (a), GA_3 (b), and BR (c) contents in tetraploid and diploid stems and roots. '*' indicates $p < 0.05$, '**' indicates $p < 0.01$. **(B)** Comparison of sucrose (a), fructose (b), glucose (c), soluble sugar (d), and starch contents (e) in tetraploid and diploid stems and roots. '**' indicates $p < 0.01$.

length to width of parenchyma cells is altered in the stem cortex (Ma et al., 2016). Compared with diploids, the apical bud entered dormancy earlier; it was difficult for most plants to exit dormancy and continue to elongate, which may explain why tetraploid regenerated plants were shorter than diploid plants. Sun et al. (2016) found that only a few individuals had autumn shoot growth, but none of these individuals were diploid. Changes in the content and proportion of endogenous hormones in plants are closely related to bud dormancy (Tanino, 2004; Ruttink et al., 2007), especially the ratio of gibberellin to abscisic acid (Rinne et al., 2011). In this study, the morphological variations of roots and stems may be closely related to hormone levels in tetraploid hybrid sweetgum; changes in the hormone ratio may lead to premature dormancy in tetraploid regenerated plants.

After polyploidization, growth conditions usually change *in vitro*; thus, the original medium for diploids is often unsuitable for tetraploid plant growth. For example, *Lagerstroemia crassipes*

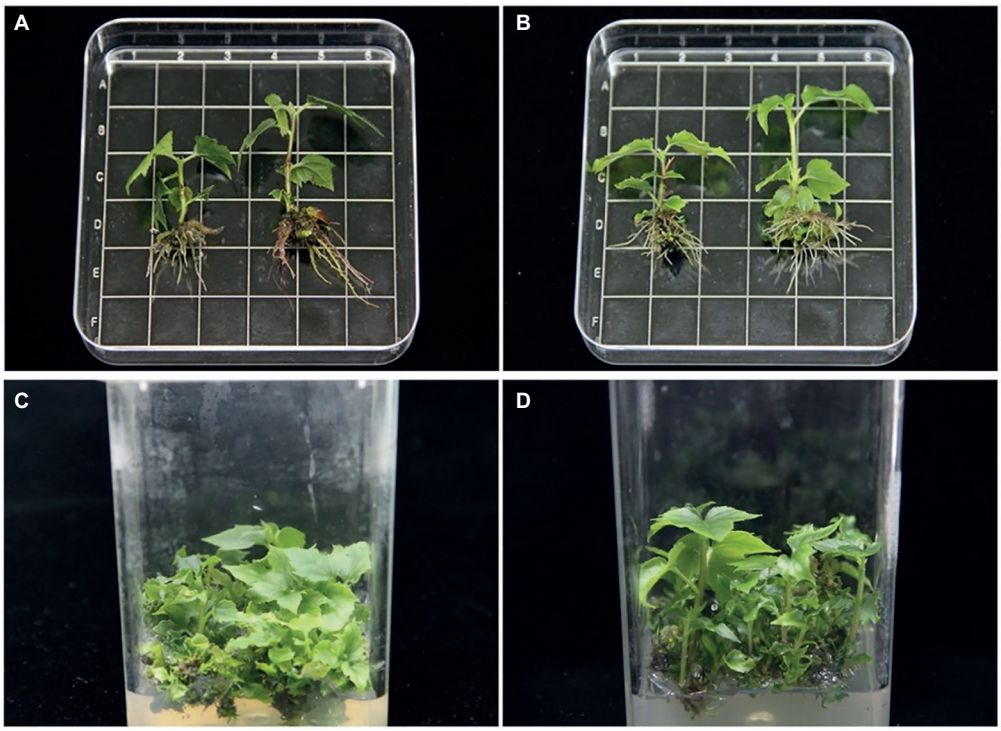

FIGURE 10 | Effects of GA_3 and IAA on shoot and root lengths of tetraploid hybrid sweetgum Z4 grown *in vitro* **(A,B)**. **(A)** Control on the left (primitive rooting medium) and rooting medium supplemented with 0.5 mg/L GA_3 on the right. **(B)** Control on the left (primitive rooting medium) and rooting medium supplemented with 0.5 mg/L GA_3 and IAA on the right. Area of each square: $1 \times 1 = 1\ cm^2$. Effects of GA_3 on adventitious bud length in tetraploid hybrid sweetgum **(C,D)**. **(C)** Control. **(D)** Development of adventitious shoots in medium supplemented with 0.5 mg/L GA_3.

is difficult to root in an original culture medium (Tong, 2007). Root and stem elongation is an important process in plant tissue culture, but the elongation of adventitious shoots and plantlets is problematic in many species. Plant hormones (e.g., auxin, gibberellin, and BL) are the most important factors that affect the lengths of regenerated organs; such hormones can promote *in vitro* plant elongation (Sasaki, 2002; Zhang et al., 2013, 2018). The concentrations of auxin hormones (e.g., IAA and indole butyric acid) added to the medium have a significant effect on root length elongation (Nandagopal and Kumari, 2007). In this study, the rooting medium supplemented with IAA alone promoted roots of tetraploid hybrid sweetgum elongation; it also increased plant height. This result may have occurred because, although the polar transport of auxin occurs from top to bottom, the growth processes of underground and aboveground parts often interact. An increase in underground growth can provide more water, inorganic salts, organic substances, and hormones for the shoots (Agren and Franklin, 2003). In this study, the number of roots was significantly fewer in tetraploids than in diploids; a similar phenomenon has been reported, but in *Gerbera jamesonii*, the plant height was significantly greater in tetraploids than in diploids (Gantait et al., 2011). Therefore, tetraploid plant height may not be directly proportional to root number.

In the present study, gibberellin had effects on root and stem of tetraploid hybrid sweetgum elongation; however, the induction of root thinning by gibberellin may have been related to the gradient change in roots. Eiichi (2012) suggested that the gibberellin-mediated-concentration dependent-stimulation of elongation is important for regulating plant height and root length; GA_3 could also significantly promote elongation in adventitious buds of sweetgum (Wang et al., 2018b).

Brassinolide also has important roles in promoting cell elongation, cell enlargement, and vascular tissue differentiation (Clouse, 2002). Previous studies have shown that BL can promote both lateral stem expansion and vertical stem growth (Sasse, 1997). Clouse and Sasse (1998) found that a low concentration of BL helped to accelerate cell division, whereas high concentrations had the opposite effect. In the present study, the addition of 0.1 mg/L BL did not have a significant effect on the lengths of roots and stems. Therefore, the concentration range is presumably unsuitable for tetraploid hybrid sweetgum elongation.

Previous studies have shown that reduced expression levels of genes with positive regulatory roles in gibberellin, auxin, and BL biosynthesis and signal transduction are important causes of plant dwarfing (Li et al., 2017; Ju et al., 2018; Wang et al., 2018a). Ma et al. (2016) suggested that changes in the auxin and BL contents in tetraploid apples might contribute to plant height variation. In the present study, the DEGs of tetraploid and diploid hybrid sweetgum stems and roots were also highly enriched in the hormone synthesis and signal transduction pathways, which were related to auxin, gibberellin, and BL levels.

Although the auxin synthesis pathway has not been fully analysed, an in-depth analysis of the indole-3-pyruvate pathway has been conducted. In the present study, the significant downregulation of *YUCCA* and *TAA1* genes of tetraploid hybrid sweetgum had important effects on auxin biosynthesis. TAA participates in the transformation of tryptophan (Trp) into indole-3-pyruvate, while YUCs participate in the transformation of indole-3-pyruvate into IAA (Tao et al., 2008; Won et al., 2011; Zhao, 2012). *YUC* and *TAA* genes affect the growth of the *yuc* and *tar* mutants of *A. thaliana*, which have very short hypocotyls and roots (Won et al., 2011). Auxin signal transduction genes are classified into *AUX*/*IAA*, *SAUR*, and *GH3* groups (Guilfoyle and Hagen, 2007), which have important roles in plant growth and development. *AUX/IAA* is an early auxin response gene, and its protein product can specifically bind to auxin response factor (ARF), thereby regulating the expression of auxin response genes; in the *A. thaliana* mutant *AUX*/*IAA*, the lengths of the stem and hypocotyl are altered; apical dominance and root formation are also modified (Liscum and Reed, 2002). In the present study, auxin signal transduction genes (e.g., *AUX*/*IAA*, *GH3*, and *SAUR*) and auxin influx carrier *AUX1* (Swarup and Bhosale, 2019) were substantially downregulated in roots and stems.

Gibberellin biosynthesis genes also affect cell division and elongation, thereby influencing plant stem and root elongation. In this study, the *CPS*, *KAO*, *KO*, *GA20ox*, *GA2ox*, and *GA3ox* genes were generally downregulated in tetraploid hybrid sweetgum. These genes are involved in the three main steps of gibberellin synthesis. First, ent-kobaki pyrophosphate synthase (CPS) and ent-kaurene synthase catalyse the formation of ent-kaurene from yak's geranyl pyrophosphate. Second, ent-kaurene catalyses the formation of GA12 and GA53 by ent-kaurene oxidase (KO) and ent-kaurenoic acid oxidase (KAO). Third, the oxidases GA20ox, GA2ox, and GA3ox eventually catalyse GA12 and GA53 to form GA1 and GA4 (Hedden and Phillips, 2000). Gibberellin and auxin are closely related and have significant interaction (Depuydt and Hardtke,

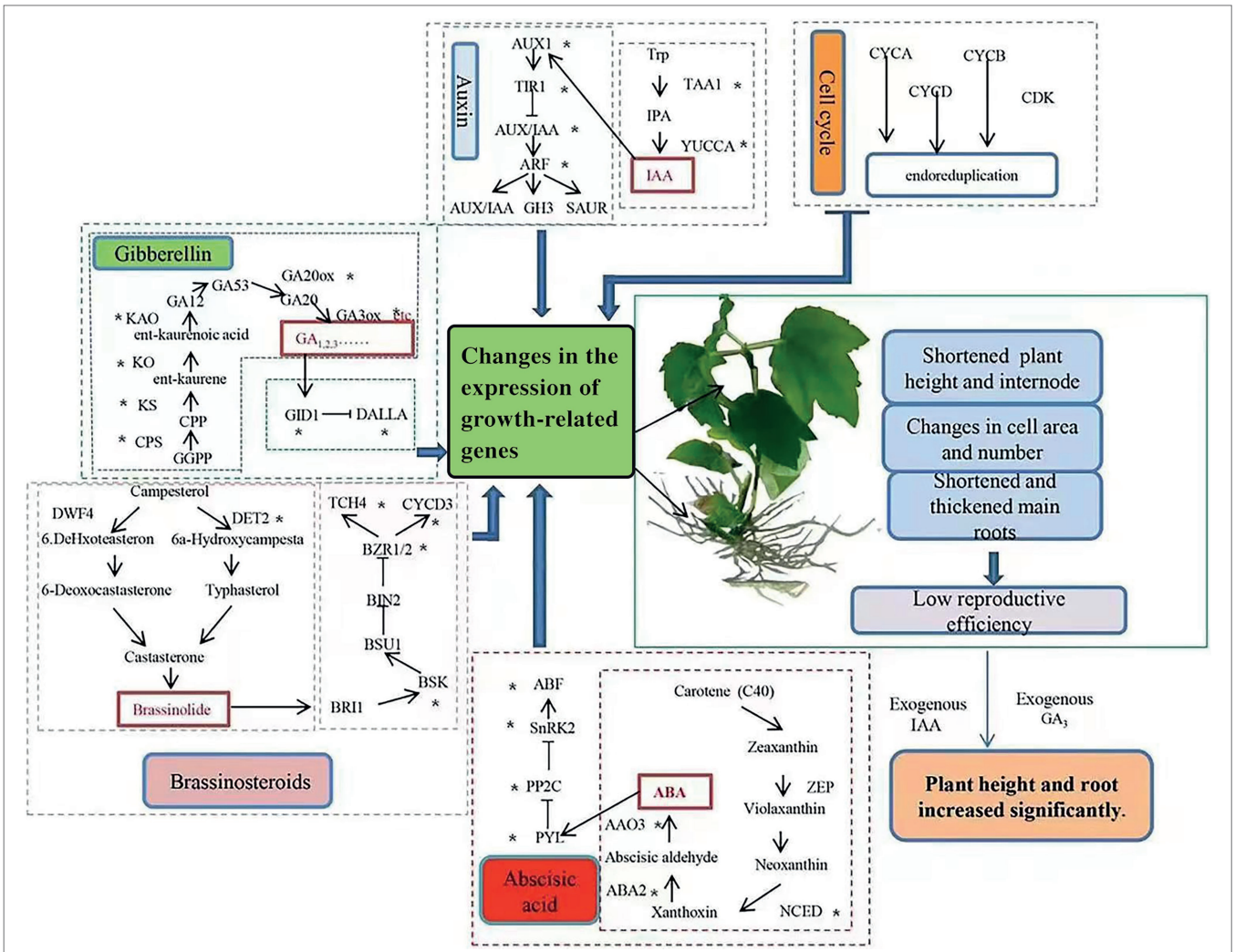

FIGURE 11 | Effects of changes in endogenous hormone biosynthesis and signal transduction genes and supplementation with exogenous hormones on tetraploid hybrid sweetgum growth. '*' indicates DEG enrichment in roots or stems.

2011; Willige et al., 2011). Auxin reportedly can promote root growth in *A. thaliana* by acting on the gibberellin responsive protein, DELLA (Fu and Harberd, 2003). *GID1* and *DELLA* have key roles in gibberellin signal transduction. After activation by gibberellin, the gibberellin receptor GID1 binds to DELLA *via* the E3 ubiquitination pathway, which leads to degradation of the DELLA protein and thus eliminates growth inhibition (Sun, 2010). However, in maize, *DELLA* deletion mutants showed dwarfing traits (Lawit et al., 2010). Therefore, although DELLA is a negative regulator, it is indispensable.

Changes in the expression patterns of BL biosynthesis and signal transduction genes also have significant effects on plant height and root length. *DET2*, *ROT3*, and *BR6ox1* are important BL biosynthesis genes (Noguchi et al., 2000; He et al., 2005). A balanced BR signal is necessary to maintain the root meristem (Takatsuka and Umeda, 2014). The root meristem length of the *bri1-116* mutant is decreased, but overexpression of the cell cycle gene *CYCD3;1* inhibits this decrease (Gonzalez-Garcia et al., 2011). The overexpression of the mutant *BZR1* significantly promoted hypocotyl elongation and increased plant height (Wang et al., 2002).

Previous studies have shown that epigenetic changes are important sources of transcriptional variation after polyploidization (Ni et al., 2009; Chen, 2013). The downregulation of the auxin signal transduction gene *MdARF3* in tetraploid apples may be related to upregulation of the negative regulator *MiR390*; it may affect auxin signal transduction (Ma et al., 2016). Therefore, significant changes in the expression levels of hormone-related genes in tetraploid hybrid sweetgum may be related to the upregulation or downregulation of small RNA genes.

Based on our findings, we constructed a schematic of the effects of changes in endogenous hormone biosynthesis and signal transduction genes, as well as supplementation with exogenous hormones, on growth in tetraploid hybrid sweetgum (**Figure 11**). As discussed previously, reduced expression levels of genes in gibberellin, auxin, BL and other hormone biosynthesis and signal transduction are important causes of tetraploid hybrid sweetgum dwarfing. Furthermore, the down-regulated expression of important genes involved in cell cycle may also have an impact on tetraploid hybrid sweetgum. Exogenous GA_3 and IAA, which induced plant cell elongation, could significantly promote growth in the stems and roots of tetraploids. It is currently unclear why some species exhibit two different phenotypes (i.e., fast growth or slow growth) after polyploidization. Species evolution and genome duplication induce gene redundancy. Epigenetic modification models differ among species; such models may influence the expression patterns of genes related to growth and development. This complex problem should be investigated in future studies.

CONCLUSION

To our knowledge, this is the first investigation of the polyploid molecular mechanism in the dwarf type of hybrid sweetgum grown *in vitro*. Genes that promote organ growth (e.g., auxin, gibberellin, and BL biosynthesis) and genes involved in signal transduction were downregulated. These changes may be the main cause of root and stem variations in tetraploids, which lead to slower growth in tetraploids than in diploids. Both IAA and GA_3 can significantly promote shoot and root elongation in dwarf tetraploid hybrid sweetgum. Our findings provide insights into the molecular mechanisms that underlie dwarfism in allopolyploid hybrid sweetgum.

DATA AVAILABILITY STATEMENT

The data presented in the study are deposited in the NCBI repository, accession number PRJNA831658.

AUTHOR CONTRIBUTIONS

JZhan and JZhao designed the study. YZ and SC conducted the experiments, analysed the data, and drafted the manuscript. SC, YZ, TZ, JZhao, and ZP critically reviewed and improved the manuscript. All authors contributed to the article and approved the submitted version.

FUNDING

This work was supported by National Forestry and Grassland Administration Promotion Project of China (2020133102); Scale-up Propagation Technology Promotion *via* Somatic Embryogenesis of Sweetgum Forestry Science and Technology Innovation Special Project of Jiangxi Province (2019-16); the Fundamental Research Funds for the Central Universities (2019ZY39); Major Science and Technology Special Project of Xuchang, Henan province, China (20170112006).

SUPPLEMENTARY MATERIAL

The Supplementary Material for this article can be found online at: https://www.frontiersin.org/articles/10.3389/fpls.2022.924044/full#supplementary-material

REFERENCES

Agren, G. I., and Franklin, O. (2003). Root: shoot ratios, optimization and nitrogen productivity. *Ann. Bot.* 92, 795–800. doi: 10.1093/aob/mcg203

Bizet, F., Hummel, I., and Bogeat-Triboulot, M.-B. (2015). Length and activity of the root apical meristem revealed in vivo by infrared imaging. *J. Exp. Bot.* 66, 1387–1395. doi: 10.1093/jxb/eru488

Chen, Z. J. (2013). Genomic and epigenetic insights into the molecular bases of heterosis. *Nat. Rev. Genet.* 14, 471–482. doi: 10.1038/nrg3503

Chen, S. Y., Dong, M. L., Zhang, Y., Qi, S. Z., Liu, X. Z., Zhang, J. F., et al. (2020). Development and characterization of simple sequence repeat markers for, and genetic diversity analysis of Liquidambar formosana. *Forests* 11:203. doi: 10.3390/f11020203

Chen, M.-L., Fu, X.-M., Liu, J.-Q., Ye, T.-T., Hou, S.-Y., Huang, Y.-Q., et al. (2012). Highly sensitive and quantitative profiling of acidic phytohormones using derivatization approach coupled with nano-LC-ESI-Q-TOF-MS analysis. *J. Chromatogr. B-Analytical Technol. Biomed. Life Sci.* 905, 67–74. doi: 10.1016/j.jchromb.2012.08.005

Cheng, S., Huang, Z., Li, Y., Liao, T., Suo, Y., Zhang, P., et al. (2015). Differential transcriptome analysis between Populus and its synthesized allotriploids driven by second-division restitution. *J. Integr. Plant Biol.* 57, 1031–1045. doi: 10.1111/jipb.12328

Clouse, S. D. (2002). Brassinosteroid signaling: novel downstream components emerge. *Curr. Biol.* 12, R485–R487. doi: 10.1016/s0960-9822(02)00964-8

Clouse, S. D., and Sasse, J. M. (1998). Brassinosteroids: essential regulators of plant growth and development. *Annu. Rev. Plant Physiol. Plant Mol. Biol.* 49, 427–451. doi: 10.1146/annurev.arplant.49.1.427

Comai, L. (2005). The advantages and disadvantages of being polyploid. *Nat. Rev. Genet.* 6, 836–846. doi: 10.1038/nrg1711

Corneillie, S., De Storme, N., Van Acker, R., Fangel, J. U., De Bruyne, M., De Rycke, R., et al. (2019). Polyploidy affects plant growth and alters Cell Wall composition. *Plant Physiol.* 179, 74–87. doi: 10.1104/pp.18.00967

Dai, F., Wang, Z., Luo, G., and Tang, C. (2015). Phenotypic and Transcriptomic analyses of Autotetraploid and diploid mulberry (*Morus alba* L.). *Int. J. Mol. Sci.* 16, 22938–22956. doi: 10.3390/ijms160922938

Depuydt, S., and Hardtke, C. S. (2011). Hormone signalling crosstalk in plant growth regulation. *Curr. Biol.* 21, R365–R373. doi: 10.1016/j.cub.2011.03.013

Ding, J., Mao, L.-J., Wang, S.-T., Yuan, B.-F., and Feng, Y.-Q. (2013). Determination of endogenous Brassinosteroids in plant tissues using solid-phase extraction with double layered cartridge followed by high-performance liquid chromatography-tandem mass spectrometry. *Phytochem. Anal.* 24, 386–394. doi: 10.1002/pca.2421

Eiichi, T. (2012). Tall or short? Slender or thick? A plant strategy for regulating elongation growth of roots by low concentrations of gibberellin. *Ann. Bot.* 110, 373–381. doi: 10.1093/aob/mcs049

Fu, X. D., and Harberd, N. P. (2003). Auxin promotes Arabidopsis root growth by modulating gibberellin response. *Nature* 421, 740–743. doi: 10.1038/nature01387

Fuentes, I., Stegemann, S., Golczyk, H., Karcher, D., and Bock, R. (2014). Horizontal genome transfer as an asexual path to the formation of new species. *Nature* 511, 232–235. doi: 10.1038/nature13291

Fukao, T., Xu, K. N., Ronald, P. C., and Bailey-Serres, J. (2006). A variable cluster of ethylene response factor-like genes regulates metabolic and developmental acclimation responses to submergence in rice(W). *Plant Cell,* 18, 2021–2034. doi: 10.1105/tpc.106.043000

Gantait, S., Mandal, N., Bhattacharyya, S., and Das, P. K. (2011). Induction and identification of tetraploids using in vitro colchicine treatment of *Gerbera jamesonii* bolus cv. Sciella. *Plant Cell Tissue Org. Cult.* 106, 485–493. doi: 10.1007/s11240-011-9947-1

Gonzalez, N., Vanhaeren, H., and Inze, D. (2012). Leaf size control: complex coordination of cell division and expansion. *Trends Plant Sci.* 17, 332–340. doi: 10.1016/j.tplants.2012.02.003

Gonzalez-Garcia, M.-P., Vilarrasa-Blasi, J., Zhiponova, M., Divol, F., Mora-Garcia, S., Russinova, E., et al. (2011). Brassinosteroids control meristem size by promoting cell cycle progression in Arabidopsis roots. *Development* 138, 849–859. doi: 10.1242/dev.057331

Gotz, S., Garcia-Gomez, J. M., Terol, J., Williams, T. D., Nagaraj, S. H., Nueda, M. J., et al. (2008). High-throughput functional annotation and data mining with the Blast2go suite. *Nucleic Acids Res.* 36, 3420–3435. doi: 10.1093/nar/gkn176

Grabherr, M. G., Haas, B. J., Yassour, M., Levin, J. Z., Thompson, D. A., Amit, I., et al. (2011). Full-length transcriptome assembly from RNA-Seq data without a reference genome. *Nat. Biotechnol.* 29, 644–652. doi: 10.1038/nbt.1883

Gu, X. F., Yang, A. F., Meng, H., and Zhang, J. R. (2005). In vitro induction of tetraploid plants from diploid Zizyphus jujuba mill. cv. Zhanhua. *Plant Cell Rep.* 24, 671–676. doi: 10.1007/s00299-005-0017-1

Guilfoyle, T. J., and Hagen, G. (2007). Auxin response factors. *Curr. Opin. Plant Biol.* 10, 453–460. doi: 10.1016/j.pbi.2007.08.014

Harlow, W., Harrar, E., Hardin, J. W., and White, F. M. (1996). *Textbook of Dendrology. 8th Edn*. New York, NY, United States: McGraw-Hill, 534.

He, J. X., Gendron, J. M., Sun, Y., Gampala, S. S. L., Gendron, N., Sun, C. Q., et al. (2005). BZR1 is a transcriptional repressor with dual roles in brassinosteroid homeostasis and growth responses. *Science* 307, 1634–1638. doi: 10.1126/science.1107580

Hedden, P., and Phillips, A. L. (2000). Gibberellin metabolism: new insights revealed by the genes. *Trends Plant Sci.* 5, 523–530. doi: 10.1016/s1360-1385(00)01790-8

Jiao, Y., Wickett, N. J., Ayyampalayam, S., Chanderbali, A. S., Landherr, L., Ralph, P. E., et al. (2011). Ancestral polyploidy in seed plants and angiosperms. *Nature* 473, 97–100. doi: 10.1038/nature09916

Ju, Y., Feng, L., Wu, J., Ye, Y., Zheng, T., Cai, M., et al. (2018). Transcriptome analysis of the genes regulating phytohormone and cellular patterning in Lagerstroemia plant architecture. *Sci. Rep.* 8:15162. doi: 10.1038/s41598-018-33506-8

Krizek, B. A. (2009). Making bigger plants: key regulators of final organ size. *Curr. Opin. Plant Biol.* 12, 17–22. doi: 10.1016/j.pbi.2008.09.006

Lawit, S. J., Wych, H. M., Xu, D., Kundu, S., and Tomes, D. T. (2010). Maize DELLA proteins dwarf plant8 and dwarf plant9 as modulators of plant development. *Plant Cell Physiol.* 51, 1854–1868. doi: 10.1093/pcp/pcq153

Leitch, A. R., and Leitch, I. J. (2008). Perspective – genomic plasticity and the diversity of polyploid plants. *Science* 320, 481–483. doi: 10.1126/science.1153585

Levan, A. (1939). Tetraploidy and octaploidy induced by colchicines in diploid *Petunia*. *Hereditas* 25, 109–131. doi: 10.1111/j.1601-5223.1939.tb02689.x

Li, W., Katin-Grazzini, L., Gu, X., Wang, X., El-Tanbouly, R., Yer, H., et al. (2017). Transcriptome analysis reveals differential gene expression and a possible role of gibberellins in a shade-tolerant mutant of perennial ryegrass. *Front. Plant Sci.* 8:868. doi: 10.3389/fpls.2017.00868

Li, X., Yu, E., Fan, C., Zhang, C., Fu, T., and Zhou, Y. (2012). Developmental, cytological and transcriptional analysis of autotetraploid Arabidopsis. *Planta* 236, 579–596. doi: 10.1007/s00425-012-1629-7

Liao, T., Cheng, S., Zhu, X., Min, Y., and Kang, X. (2016). Effects of triploid status on growth, photosynthesis, and leaf area in Populus. *Trees-Struct. Funct.* 30, 1137–1147. doi: 10.1007/s00468-016-1352-2

Liscum, E., and Reed, J. W. (2002). Genetics of aux/IAA and ARF action in plant growth and development. *Plant Mol. Biol.* 49, 387–400. doi: 10.1023/a:1015255030047

Livak, K. J., and Schmittgen, T. D. (2001). Analysis of relative gene expression data using real-time quantitative PCR and the 2(-Delta Delta C(T)) method. *Methods* 25, 402–408. doi: 10.1006/meth.2001.1262

Ma, Y., Xue, H., Zhang, L., Zhang, F., Ou, C., Wang, F., et al. (2016). Involvement of Auxin and Brassinosteroid in dwarfism of Autotetraploid apple (Malus x domestica). *Sci. Rep.* 6:26719. doi: 10.1038/srep26719

Mao, X. Z., Cai, T., Olyarchuk, J. G., and Wei, L. P. (2005). Automated genome annotation and pathway identification using the Kegg Orthology (Ko) as a controlled vocabulary. *Bioinformatics* 21, 3787–3793. doi: 10.1093/bioinformatics/bti430

Merkle, S. A., and Battle, P. J. (2000). Enhancement of embryogenic culture initiation from tissues of mature sweetgum trees. *Plant Cell Rep.* 19, 268–273. doi: 10.1007/s002990050010

Merkle, S., Montello, P., Kormanik, T., and Le, H. (2010). Propagation of novel hybrid sweetgum phenotypes for ornamental use via somatic embryogenesis. *Propag. Ornam. Plants* 10, 220–226.

Miller, M., Zhang, C., and Chen, Z. J. (2012). Ploidy and hybridity effects on growth vigor and gene expression in *Arabidopsis thaliana* hybrids and their parents. *G3* 2, 505–513. doi: 10.1534/g3.112.002162

Moriya, Y., Itoh, M., Okuda, S., Yoshizawa, A. C., and Kanehisa, M. (2007). KAAS: An automatic genome annotation and pathway reconstruction server. *Nucleic Acids Res.* 35, W182–W185. doi: 10.1093/nar/gkm321

Mu, H.-Z., Liu, Z.-J., Lin, L., Li, H.-Y., Jiang, J., and Liu, G.-F. (2012). Transcriptomic analysis of phenotypic changes in birch (*Betula platyphylla*) Autotetraploids. *Int. J. Mol. Sci.* 13, 13012–13029. doi: 10.3390/ijms131013012

Nandagopal, S., and Kumari, B. R. (2007). Effectiveness of auxin induced in vitro root culture in chicory. *J. Cent. Euro. Agricult.* 8:8.

Ni, Z., Kim, E.-D., Ha, M., Lackey, E., Liu, J., Zhang, Y., et al. (2009). Altered circadian rhythms regulate growth vigour in hybrids and allopolyploids. *Nature* 457, 327–331. doi: 10.1038/nature07523

Nilanthi, D., Chen, X.-L., Zhao, F.-C., Yang, Y.-S., and Wu, H. (2009). Induction of Tetraploids from petiole explants through colchicine treatments in *Echinacea purpurea* L. *J. Biomed. Biotechnol.* 2009, 1–7. doi: 10.1155/2009/343485

Noguchi, T., Fujioka, S., Choe, S., Takatsuto, S., Tax, F. E., Yoshida, S., et al. (2000). Biosynthetic pathways of brassinolide in Arabidopsis. *Plant Physiol.* 124, 201–210. doi: 10.1104/pp.124.1.201

Rao, S., Kang, X., Li, J., and Chen, J. (2019). Induction, identification and characterization of tetraploidy in Lycium ruthenicum. *Breed. Sci.* 69, 160–168. doi: 10.1270/jsbbs.18144

Rinne, P. L. H., Welling, A., Vahala, J., Ripel, L., Ruonala, R., Kangasjarvi, J., et al. (2011). Chilling of dormant buds Hyperinduces flowering locus T and recruits GA-inducible 1,3-beta-Glucanases to reopen signal conduits and release dormancy in Populus. *Plant Cell* 23, 130–146. doi: 10.1105/tpc.110.081307

Ruttink, T., Arend, M., Morreel, K., Storme, V., Rombauts, S., Fromm, J., et al. (2007). A molecular timetable for apical bud formation and dormancy induction in poplar. *Plant Cell* 19, 2370–2390. doi: 10.1105/tpc.107.052811

Saeed, A. I., Sharov, V., White, J., Li, J., Liang, W., Bhagabati, N., et al. (2003). Tm4: a free, open-source system for microarray data management and analysis. *BioTechniques* 34, 374–378. doi: 10.2144/03342mt01

Salma, U., Kundu, S., Hazra, A. K., Ali, M. N., and Mandal, N. (2018). Augmentation of wedelolactone through in vitro tetraploid induction in *Eclipta alba* (L.) Hassk. *Plant Cell Tissue Org. Cult.* 133, 289–298. doi: 10.1007/s11240-018-1381-1

Sasaki, H. (2002). Brassinolide promotes adventitious shoot regeneration from cauliflower hypocotyl segments. *PCTOC* 71, 111–116. doi: 10.1023/A:1019913604202

Sasse, J. M. (1997). Recent progress in brassinosteroid research. *J Physiologia Plantarum.* 100, 696–701. doi: 10.1034/j.1399-3054.1997.1000333.x

Shao, J. Z., Chen, C. L., and Deng, X. X. (2003). In vitro induction of tetraploid in pomegranate (*Punica granatum*). *Plant Cell Tissue Org. Cult.* 75, 241–246. doi: 10.1023/a:1025871810813

Sommer, S. E., Wetzstein, S. Y., and Brown, S. L. (1999). Shoot growth and histological response of dwarf sweetgum to gibberellin. *J. Horticult. Sci. Biotechnol.* 74, 618–621. doi: 10.1080/14620316.1999.11511163

Song, Q., and Chen, Z. J. (2015). Epigenetic and developmental regulation in plant polyploids. *Curr. Opin. Plant Biol.* 24, 101–109. doi: 10.1016/j.pbi.2015.02.007

Su, Y.-H., Liu, Y.-B., and Zhang, X.-S. (2011). Auxin-Cytokinin interaction regulates meristem development. *Mol. Plant* 4, 616–625. doi: 10.1093/mp/ssr007

Sun, T.-P. (2010). Gibberellin-Gid1-Della: A pivotal regulatory module for plant growth and development. *Plant Physiol.* 154, 567–570. doi: 10.1104/pp.110.161554

Sun, R. X., Lin, F. R., Huang, P., and Zheng, Y. Q. (2016). Moderate genetic diversity and genetic differentiation in the relict tree liquidambar formosana hance revealed by genic simple sequence repeat markers. *Front. Plant Sci.* 7. doi: 10.3389/fpls.2016.01411

Swarup, R., and Bhosale, R. (2019). Developmental roles of AUX1/LAX Auxin influx carriers in plants. *Front. Plant Sci.* 10:1306. doi: 10.3389/fpls.2019.01306

Takatsuka, H., and Umeda, M. (2014). Hormonal control of cell division and elongation along differentiation trajectories in roots. *J. Exp. Bot.* 65, 2633–2643. doi: 10.1093/jxb/ert485

Tan, F.-Q., Tu, H., Liang, W.-J., Long, J.-M., Wu, X.-M., Zhang, H.-Y., et al. (2015). Comparative metabolic and transcriptional analysis of a doubled diploid and its diploid citrus rootstock (C. junos cv. Ziyang Xiangcheng) suggests its potential value for stress resistance improvement. *BMC Plant Biol.* 15:89. doi: 10.1186/s12870-015-0450-4

Tanino, K. K. (2004). Hormones and endodormancy induction in woody plants. *J. Crop Improv.* 10, 157–199.

Tao, Y., Ferrer, J.-L., Ljung, K., Pojer, F., Hong, F., Long, J. A., et al. (2008). Rapid synthesis of auxin via a new tryptophan-dependent pathway is required for shade avoidance in plants. *Cell* 133, 164–176. doi: 10.1016/j.cell.2008.01.049

Tiku, A. R., Razdan, M. K., and Raina, S. N. (2014). Production of triploid plants from endosperm cultures of *Phlox drummondii*. *Biol. Plant.* 58, 153–158. doi: 10.1007/s10535-013-0372-7

Tokumoto, Y., Kajiura, H., Takeno, S., Harada, Y., Suzuki, N., Hosaka, T., et al. (2016). Induction of tetraploid hardy rubber tree, Eucommia ulmoides, and phenotypic differences from diploid. *Plant Biotechnol.* 33, 51–57. doi: 10.5511/plantbiotechnology.15.1219a

Tong, J. (2007). *[D] Studies on Polyploid Induction Induction of Lagerstroemia indica by Colchicne*. Wuhan: Huazhong Agricultural University.

Tsukaya, H. (2008). Controlling size in multicellular organs: focus on the leaf. *PLoS Biol.* 6, e174–e1376. doi: 10.1371/journal.pbio.0060174

Wang, T., Liu, L., Wang, X., Liang, L., Yue, J., and Li, L. (2018a). Comparative analyses of anatomical structure, Phytohormone levels, and gene expression profiles reveal potential dwarfing mechanisms in Shengyin bamboo (*Phyllostachys edulis* f. tubaeformis). *Int. J. Mol. Sci.* 19:1697. doi: 10.3390/ijms19061697

Wang, Z. Y., Nakano, T., Gendron, J., He, J., Chen, M., Vafeados, D., et al. (2002). Nuclear-localized Bzr1 mediates brassinosteroid-induced growth and feedback suppression of brassinosteroid biosynthesis. *Dev. Cell* 2, 505–513. doi: 10.1016/s1534-5807(02)00153-3

Wang, Z., Zhang, Y., Qi, S., Zhu, J., Yuan, W., Zhang, Y., et al. (2018b). Tissue culture regeneration of hybrid *Liquidambar styraciflua*×*L. formosana*. *J. Beijing For. Univ.* 40, 42–49.

Willige, B. C., Isono, E., Richter, R., Zourelidou, M., and Schwechheimer, C. (2011). Gibberellin regulates pin-formed abundance and is required for Auxin transport-dependent growth and development in *Arabidopsis thaliana*. *Plant Cell* 23, 2184–2195. doi: 10.1105/tpc.111.086355

Won, C., Shen, X., Mashiguchi, K., Zheng, Z., Dai, X., Cheng, Y., et al. (2011). "Conversion of tryptophan to indole-3-acetic acid by tryptophan aminotransferase of Arabidopsis and YUCCAs in Arabidopsis." *Proceedings of the National Academy of Sciences of the United States of America* 108, 18518–18523. doi: 10.1073/pnas.1108436108

Xu, C., Zhang, Y., Huang, Z., Yao, P., Li, Y., and Kang, X. (2018). Impact of the leaf cut callus development stages of Populus on the Tetraploid production rate by colchicine treatment. *J. Plant Growth Regul.* 37, 635–644. doi: 10.1007/s00344-017-9763-x

Xue, H., Zhang, B., Tian, J.-R., Chen, M.-M., Zhang, Y.-Y., Zhang, Z.-H., et al. (2017). Comparison of the morphology, growth and development of diploid and autotetraploid 'Hanfu' apple trees. *Sci. Hortic.* 225, 277–285. doi: 10.1016/j.scienta.2017.06.059

Ye, Y. M., Tong, J., Shi, X. P., Yuan, W., and Li, G. R. (2010). Morphological and cytological studies of diploid and colchicine-induced tetraploid lines of crape myrtle (*Lagerstroemia indica* L.). *Sci. Hortic.* 124, 95–101. doi: 10.1016/j.scienta.2009.12.016

Zhang, C., Fu, S., Tang, G., Hu, X., and Guo, J. (2013). Factors influencing direct shoot regeneration from mature leaves of *Jatropha curcas*, an important biofuel plant. *In Vitro Cell. Dev. Biol. Plant* 49, 529–540. doi: 10.1007/s11627-013-9530-z

Zhang, Y., Wang, B., Guo, L., Xu, W., Wang, Z., Li, B., et al. (2018). Factors influencing direct shoot regeneration from leaves, petioles, and plantlet roots of triploid hybrid Populus sect. Tacamahaca. *J. For. Research* 29, 1533–1545. doi: 10.1007/s11676-017-0559-4

Zhang, Y., Wang, B., Qi, S., Dong, M., Wang, Z., Li, Y., et al. (2019). Ploidy and hybridity effects on leaf size, cell size and related genes expression in triploids, diploids and their parents in Populus. *Planta* 249, 635–646. doi: 10.1007/s00425-018-3029-0

Zhang, Y., Wang, Z., Qi, S., Wang, X., Zhao, J., Zhang, J., et al. (2017). In vitro Tetraploid induction from leaf and petiole explants of hybrid Sweetgum (*Liquidambar styraciflua* x Liquidambar formosana). *Forests* 8:264. doi: 10.3390/f8080264

Zhao, Y. (2012). Auxin biosynthesis: a simple two-step pathway converts tryptophan to Indole-3-acetic acid in plants. *Mol. Plant* 5, 334–338. doi: 10.1093/mp/ssr104

Zheng, Y., Pan, B., and Itoh, T. (2015). Chemical induction of traumatic gum ducts in Chinese sweetgum, liquidambar formosana. *IAWA J.* 36, 58–68. doi: 10.1163/22941932-00000085

Zhu, Z., Lin, H., and Kang, X. (1995). Studies on allotriploid breeding of *Populus tomentosa* B301 clones. *Scientia Silvae Sinicae* 31, 499–505.

Conflict of Interest: DZ and ZP are employed by Guangxi Bagui Forest and Flowers Seedlings Co., Ltd.

The remaining authors declare that the research was conducted in the absence of any commercial or financial relationships that could be construed as a potential conflict of interest.

be evaluated in this article, or claim that may be made by its manufacturer, is not guaranteed or endorsed by the publisher.

frontiers | Frontiers in Plant Science

ORIGINAL RESEARCH
published: 04 July 2022
doi: 10.3389/fpls.2022.915056

DNA Methylome and LncRNAome Analysis Provide Insights Into Mechanisms of Genome-Dosage Effects in Autotetraploid Cassava

*Liang Xiao[1], Liuying Lu[1], Wendan Zeng[1], Xiaohong Shang[1], Sheng Cao[1] and Huabing Yan[1,2]**

[1] Cash Crops Research Institute, Guangxi Academy of Agricultural Sciences, Nanning, China, [2] State Key Laboratory for Conservation and Utilization of Subtropical Agro-Bioresources, Guangxi University, Nanning, China

Whole genome duplication (WGD) increases the dosage of all coding and non-coding genes, yet the molecular implications of genome-dosage effects remain elusive. In this study, we generated integrated maps of the methylomes and lncRNAomes for diploid and artificially generated autotetraploid cassava (*Manihot esculenta* Crantz). We found that transposable elements (TEs) suppressed adjacent protein coding gene (PCG)-expression levels, while TEs activated the expression of nearby long non-coding RNAs (lncRNAs) in the cassava genome. The hypermethylation of DNA transposons in mCG and mCHH sites may be an effective way to suppress the expression of nearby PCGs in autotetraploid cassava, resulting in similar expression levels for most of PCGs between autotetraploid and diploid cassava. In the autotetraploid, decreased methylation levels of retrotransposons at mCHG and mCHH sites contributed to reduced methylation of Gypsy-neighboring long intergenic non-coding RNAs, potentially preserving diploid-like expression patterns in the major of lncRNAs. Collectively, our study highlighted that WGD-induced DNA methylation variation in DNA transposons and retrotransposons may be as direct adaptive responses to dosage of all coding-genes and lncRNAs, respectively.

Keywords: autotetraploid cassava, genome-dosage effect, DNA-methylation, lncRNA expression, protein coding gene expression, transposon

OPEN ACCESS

Edited by:
Jeremy Coate,
Reed College, United States

Reviewed by:
Zhi Zou,
Institute of Tropical Bioscience and Biotechnology, Chinese Academy of Tropical Agricultural Sciences, China
Chuanliang Deng,
Henan Normal University, China

***Correspondence:**
Huabing Yan
h.b.yan@hotmail.com

Specialty section:
This article was submitted to Plant Cell Biology, a section of the journal Frontiers in Plant Science

Received: *14 April 2022*
Accepted: *02 June 2022*
Published: *04 July 2022*

Citation:
Xiao L, Lu L, Zeng W, Shang X, Cao S and Yan H (2022) DNA Methylome and LncRNAome Analysis Provide Insights Into Mechanisms of Genome-Dosage Effects in Autotetraploid Cassava. Front. Plant Sci. 13:915056. doi: 10.3389/fpls.2022.915056

INTRODUCTION

Polyploidy or whole genome duplication (WGD), is the heritable condition of possessing multiple sets of chromosomes co-occurring in a nucleus, with four being the most common (Comai, 2005; Madlung and Wendel, 2013). During the last several decades, there has been a resurgence of interest in the study of polyploid evolution, particularly the genetic and genomic consequences of polyploidy (Gaeta et al., 2007; Salmon et al., 2010; Shi et al., 2012; Renny-Byfield and Wendel, 2014; Visger et al., 2019). Polyploidy can result in considerable changes in both coding and non-coding gene expression caused by the increasing of the number of alleles at each locus, which provides a molecular basis for adaptation (Doyle et al., 2008; Salmon and Ainouche, 2010; Zhang et al., 2019; Tao et al., 2021). Two forms of polyploidy are often considered in

plants (Ramsey and Schemske, 1998): allopolyploidy species are traditionally considered to arise *via* interspecific hybridization and subsequent doubling of non-homologous genomes (AABB) (Xu et al., 2009; Kraitshtein et al., 2010), whereas autopolyploids arise within a single species by doubling of structurally similar, homologous genomes (AAAA) (Havananda et al., 2011; Liu and Sun, 2017). Although past views pointed that autopolyploidy is likely rare, increasing evidences indicated that autopolyploid taxa might be more common and the appearance of autotetraploidy plants in nature might be significantly underestimated (Ramsey and Schemske, 2002; Soltis et al., 2003; Soltis and Soltis, 2009; Parisod et al., 2010; Barker et al., 2016), despite potential weaknesses, such as sterility, aneuploidy, genomic and epigenetic instabilities (Comai, 2005; Madlung and Wendel, 2013). In newly formed polyploids, genome doubling events increase the dosage of all coding and non-coding genes (the number of gene copies). A large number of transcriptome studies reported that in the early stages after genome doubling *per se*, synthesized autopolyploids expressed only a small fraction of protein coding genes (PCGs) and long non-coding RNA (lncRNA) of all loci at different level relative to the diploid, named genome-dosage effect (also referred to dosage response) (Martelotto et al., 2005; Stupar et al., 2007; Parisod et al., 2010; Yu et al., 2010; Allario et al., 2011; Del Pozo and Ramirez-Parra, 2014; Xiao et al., 2019). However, the putative mechanisms for this process is largely unknown. Autopolyploids, especially artificial lines, ruling out disturbances from incompatible genomes, offer an extraordinary opportunity to understand mechanisms of genome-dosage effect.

Doubling a set of chromosome cause "genome shock," associated with dramatic changes in the epigenetic modifications (Chen, 2013; Song and Chen, 2015). DNA methylation provides an effective mean for a polyploid cell to overcome "genomic shock" caused by WGD (Chen, 2013). Cytosine methylation is a common feature of epigenetic regulation that influences many molecular processes, including embryogenesis (Rival et al., 2013), transposable elements (TEs) activity (Saze and Kakutani, 2011; Ibarra et al., 2012), and gene expression (Zilberman et al., 2007). Plant genomes are often methylated in CG, CHG, and CHH (H = A, T, or C) contexts (Law and Jacobsen, 2010). Many studies in allopolyploid crop species indicated that gene expression is altered more by interspecific hybridization than by polyploidization (Shaked et al., 2001; Madlung et al., 2002; Kraitshtein et al., 2010). However, to date, there are almost no reports on DNA methylation variations to reveal the impact on PCGs expression responding to autotetraploidization except in rice (*Oryza sativa* ssp. Indica) (Zhang et al., 2015).

The complement of TEs within any one genome typically includes both class I retrotransposon and class II DNA transposons (Feschotte et al., 2002). TEs make up a substantial fraction of mature lncRNA transcripts, they are also enriched in the vicinity of lncRNAs, where they frequently contribute to their transcriptional regulation (Kapusta et al., 2013; Wang et al., 2016). Zhao et al. (2018) reported that demethylated *LINEs*/TEs might distinctively impact lncRNAs expression in polyploid cotton interspecific F_1 hybrid in genomic shock caused by interspecific hybrid and WGD. Nevertheless, the impact on the lncRNAs expression of whole genome caused by WGD, especially TE-overlapped lncRNAs, remains largely unknown.

Cassava (*Manihot esculenta* Crantz), a perennial shrub of the Euphorbiaceae family, is one of the most important food and energy crops in the world and is ranked the third most consumed carbohydrate source and for millions of people in the tropics (Raven et al., 2006). The cassava genome is highly heterozygous because of its outcrossing nature and broad tropical distribution (Fregene et al., 2003; Siqueira et al., 2010). Previously, we obtained an autotetraploid cassava (4x) from the diploid cultivar (2x), which was produced by colchicine-induced (Zhou et al., 2017). Here, we generated integrated maps of methylomes and lncRNAomes in autotetraploid cassava and its donor parent, both of which were independently clonally propagated for 2 years, in order to evaluate the short-term impact of intraspecies genome duplication on the expression of PCGs and lncRNAs of whole genomes.

MATERIALS AND METHODS

Plant Materials

An autotetraploid cassava line (2n = 4x = 72) was artificially created by the cultivar "Xinxuan 048" (2n = 2x = 36) using aqueous colchicine solution (Zhou et al., 2017). The ploidy levels of the generated autoploid plants were detected by the flow cytometry analysis, and then chromosome counting in root-tip cells confirmed the results of flow cytometry analysis by Zhou et al. (2017). The plant architecture screening was carried out for the first two generations. Stem-propagated plants from each 2x and 4x cassava were sown and grown in plastic pots with a photoperiod of 16/8 h (day/night) in the greenhouse of Guangxi Academy of Agricultural Sciences (GXAAS). At ∼60 days after planting, 2x and 4x cassava plants have equal numbers of leaves at this stage, the fifth leave (counting from the top of the plant) of nine individual plants of each cytotype were sampled. Three plants each biological replicate were included and each cytotype has triplicates. The collected leaves were immediately frozen in liquid nitrogen, and stored at −80°C until total DNA and RNA extractions were performed.

DNA Extraction

Genomic DNA was extracted according to a plant genomic DNA kit [TIANGEN BIOTECH (Beijing) Co., Ltd., China, code number: DP305] following the manufacturer's instructions. After genomic DNAs were extracted from the samples, DNA concentration and integrity were detected by NanoPhotometer® spectrophotometer (IMPLEN, CA, United States) and Agarose Gel Electrophoresis, respectively.

Library Construction, Sequencing, and Data Filtering

The DNA libraries for Bisulfite sequencing (BS-seq) were prepared. Briefly, genomic DNAs were fragmented into 100–300 bp by Sonication (Covaris, MA, United States) and purified with MiniElute PCR Purification Kit (QIAGEN, MD,

United States). The fragmented DNAs were end repaired and a single "A" nucleotide was added to the 3′ end of the blunt fragments. Then the genomic fragments were ligated to methylated sequencing adapters. Fragments with adapters were bisulfite converted using Methylation-Gold kit (ZYMO, CA, United States), unmethylated cytosine is converted to uracil during sodium bisulfite treatment. Finally, the converted DNA fragments were PCR amplified and sequenced using Illumina HiSeq^{TM} 2500 by Gene Denovo Biotechnology Co. (Guangzhou, China).

To get high quality clean reads, the reads containing more than 10% of unknown nucleotides and low quality reads containing more than 40% of low quality (Q-value ≤ 20) bases were removed from the raw reads generated from Illumina HiSeq^{TM} 2500.

Transposable Element Annotation

Transposable elements were annotated by running RepeatMasker[1] against a cassava reference genome sequence (v6.1[2]). In detail, Tandem repeats finder (Benson, 1999) software was used to predict tandem repeats. Prediction method of Interpersed repeat was as following: (1) Considering some repeat sequences often have specific sequence characteristics, such as long terminal repeats (LTRs) transposon, which is characterized by symmetric LTR at both ends, we predicted LTR transposons through LTR_FINDER (Xu and Wang, 2007), Helitron transposon by Helitroscanner (Xiong et al., 2014), MITE transposon by MITE-Hunter (Han and Wessler, 2010). LINE by MGEscan-non-LTR (Lee et al., 2016). (2) Since the repeat sequence has multiple copies in the genome, multiple copies of the repeat sequence in the genome can be found through mutual alignment within the genome sequence. First, three softwares PILER (Edgar and Myers, 2005), RepeatScout (Price et al., 2005), and RepeatModeler (Bao and Eddy, 2002) were used to obtain preliminary *de novo* prediction results, and then sequences classified as DNA and LINE are extracted and merged into one file. The redundancy of the filtering sequence itself, and the filtering standard identity >90%. (3) Homology construction based on the principles of structure prediction and *de novo* (*de novo*), a repeat sequence database was constructed, which was combined with Repbase database as the final repeat sequence database. Then RepeatMasker (Tarailo-Graovac and Chen, 2009) software was used to predict the repeat sequence of sequencing data based on the constructed repeat sequence database. Collectively, a dataset of 12,592 TEs was used for further analysis (**Supplementary Table 1**).

Methylation Level Analysis

The obtained clean reads were mapped to cassava reference genome using BSMAP software (Xi and Li, 2009) (version: 2.90) using default setting. We used a custom Perl script to call methylated cytosines (mC) and these methylated cytosines were tested with the correction algorithm described in Lister et al. (2008). The overall methylation levels were calculated using a BSMAP package script according to the ratio of reads (mC)/[reads (mC) + reads (non-mC)]. The methylation level was calculated based on methylated cytosine percentage in the whole genome, in each chromosome and in different regions of the genome for each sequence context (CG, CHG, and CHH). To assess different methylation patterns in different genomic regions, the methylation profile at flanking 2-kb regions and PCGs (lncRNAs or TEs) body was plotted based on the average methylation levels for each window.

Analysis of Differentially Methylated Regions

To determine the differentially methylated regions (DMRs) between 2x and 4x cassava cytotypes, the minimum read coverage to call a methylation status for a base was set to 4. DMRs for CG, CHG, and CHH context according to different criteria: (1) for all C, numbers in a window $\geq$ 20, absolute value of the difference in methylation ratio $\geq$ 0.2, and $q \leq 0.05$; (2) for CG, numbers of GC in a window $\geq$ 5, absolute value of the difference in methylation ratio $\geq$ 0.25, and $q \leq 0.05$; (3) for CHG, numbers in each window $\geq$ 5, absolute value of the difference in methylation ratio $\geq$ 0.25, and $q \leq 0.05$; (4) for CHH, numbers in a window $\geq$ 15, absolute value of the difference in methylation ratio $\geq$ 0.25, and $q \leq 0.05$.

LncRNA-seq and Data Analysis

Transcriptome sequencing was performed with the same leaf used for BS-seq for each of the diploid and autopolyploid cassava. Total RNA was extracted from 100 mg of tissue using TRIzol reagent (Invitrogen) according to the manufacturer's instructions. The rRNAs were removed with Ribo-Zero rRNA Removal Kit (Plant) (Illumina, item number: MRZPL1224) to retain mRNAs and ncRNAs. The enriched mRNAs and ncRNAs were fragmented into short fragments by using fragmentation buffer and reverse transcribed into cDNA with random primers. Second-strand cDNA were synthesized by DNA polymerase I, RNase H, dNTP (dUTP instead of dTTP) and buffer. Next, the cDNA fragments were purified with QIAquick PCR extraction kit (QIAGEN, Venlo, Netherlands), end repaired, poly(A) added, and ligated to Illumina sequencing adapters. Then UNG (Uracil-N-Glycosylase) was used to digest the second-strand cDNA. The digested products were size selected by agarose gel electrophoresis, PCR amplified, and sequenced using Illumina HiSeq^{TM} 4000 (PE150) by Gene Denovo Biotechnology Co. (Guangzhou, China). After removing sequences containing adapters, poly-N and low quality reads, clean reads were aligned to the cassava reference genome (v6.1, see text footnote 2) by HISAT2 (version 2.1.0) with "-rna-strandness RF" and other parameters set as a default (Kim et al., 2013). The reconstruction of transcripts was carried out using Stringtie (version 1.3.4), which together with HISAT2 (Pertea et al., 2015, 2016). To identify novel genes, all of the reconstructed transcripts were mapped to the cassava reference genome and were divided into 12 categories by using Cuffcompare (Trapnell et al., 2012). Gene abundances were quantified using RSEM (v 1.2.19) (Li and Dewey, 2011) and PCG- and lncRNA-expression levels were normalized using FPKM (Fragments Per Kilobase of transcript

[1]http://repeatmasker.org

[2]https://phytozome.jgi.doe.gov/pz/portal.html#

per Million reads). Two softwares CPC (version 0.9-r2) and CNCI (version 2) (Kong et al., 2007; Sun et al., 2013) were used to assess the protein-coding potential of novel transcripts by default parameters. The intersection of both non-protein-coding potential results and non-protein annotation results were chosen as lncRNAs.

Differential expression analysis of PCGs and lncRNAs was performed by DESeq2 (Love et al., 2014) software between two different cytotypes. We used a false discovery rate (FDR) < 0.05 and fold change ≥ 2 as the thresholds to determine significant differences in PCG and lncRNA expression.

RESULTS

Single Base-Resolution Maps of DNA Methylation for Diploid and Autotetraploid Cassava

In order to investigate the potential role of DNA methylation in response to autotetraploidy, the methylomes of diploid (2x) and autotetraploid (4x) cassava leaves were decoded and analyzed. Genome mapping analysis showed that overall, 113,078,644 (73.50%), 109,732,951 (73.44%), and 111,434,206 (74.25%) clean reads from the three diploid biological replicates, and 119,723,975 (74.70%), 96,864,854 (75.06%), and 110,185,024 (75.65%) clean reads from the three autotetraploid biological replicates, were mapped to the genome. The sequence depth of all the samples were more than 24×. More than 99% of cytosines were altered, which indicated that a high rate of conversion (**Supplementary Table 2**). In addition, Pearson correlation coefficients between the three replicates of 2x and 4x were found to be between 0.96 and 0.97 (**Supplementary Figure 1**). All the data indicated that the quality of sequencing was satisfactory to subsequent analysis. 2x and 4x cassava showed no significant differences in overall methylation levels, regardless of sequence context, across all the sequenced C sites, the 2x and 4x genome presented 67.09 and 66.94% mCGs, 49.03 and 48.67% mCHG, and 5.88 and 5.74% mCHH, respectively (T-test, $P > 0.05$) (**Supplementary Figure 2**). At the chromosome-scale scale, it was discovered that the methylation levels of three contexts were all predominantly highly pericentromeric heterochromatin regions and methylation levels of all three contexts in 2x and 4x cassava were similar to one another (**Supplementary Figure 3**).

Landscape of Protein Coding Genes, Long Non-coding RNAs, and Transposable Elements Methylation

To characterize the DNA methylation patterns in different cassava genomic regions, we constructed the methylation profiles within PCGs, lncRNAs, and TEs, together with 2-kb regions flanking the genes, using the same lengths cut-off. Methylation patterns in PCGs in our study are generally similar to those in soybean (Song et al., 2013), the peak of CG methylation in the PCGs body was higher than that in the flanking regions (**Figure 1A**). In contrast, CHG methylation had a similar tendency to CHH methylation in that obviously lowered levels were observed in body regions compared with upstream or downstream regions (**Figure 1A**). There were no methylation differences in CG and CHG contexts between PCGs from 2x and 4x cassava (T-test, mCG P-value = 0.390, mCHG P-value = 0.451). The difference methylation level of mCHH (T-test, P-value < 0.05) could be negligible because the highest methylation level of mCHH is only about 1.5% in PCG bodies in both 2x and 4x cassava. The results suggested that WGD may not have widespread influence over methylation state of PCG bodies. The methylation state of lncRNA in all three contexts were higher than those of PCG, moreover, 4x cassava had decreased CG, CHG, and CHH methylation levels relative to 2x across lncRNA body regions and flanking regions (T-test, mCG P-value = 0.151, mCHG P-value = 0.018, mCHH P-value = 0.044) (**Figure 1B**), suggesting WGD may have widespread influence on methylation levels of lncRNAs bodies together with 2-kb flanking regions in CHG and CHH contexts, rather than CG context. As is seen in **Figure 1C**, consistent with rice and other plant species (Lister et al., 2009; Feng et al., 2010; Zemach et al., 2010), average methylation level of TEs was much higher than that of PCGs and lncRNAs. 4x cassava had decreased methylation levels in CHG and CHH contexts relative to 2x cassava in TE bodies, there is no significance difference of mCG methylation level in TE bodies between 2x and 4x cassava (T-test, mCG P-value = 0.455, mCHG P-value = 1.59E−13, mCHH P-value = 1.58E−93) (**Figure 1C**).

Consequently, we detected the methylation differences of the two classes of TEs. All the 13 orders of TEs had unique average methylation distribution, and exhibited hypermethylation state in body regions than flanking regions in all three contexts. SINE, Stowaway, Harbinger and other_DNA TE types make up a small fraction of the genome (<0.2% each) and were not considered for further analysis (**Supplementary Table 3**). 4x cassava exhibited hypomethylation levels in mCHG and mCHH sites in body regions of Copia and Gypsy, respectively (T-test, Copia mCHG P-value = 0.042, mCHH P-value = 1.41E−06; Gypsy mCHG P-value = 3.86E−05, mCHH P-value = 2.97E−40) (**Figures 1D,E**). We also found that body regions of Helitron and hAT from 4x cassava had increased CG methylation levels (T-test, Helitron P-value = 0.027, hAT P-value = 0.032). Moreover, body regions of *MITE* from 4x cassava were hypermethylated in CG and CHH contexts (mCG P-value = 0.041, mCHH P-value = 0.030) (**Figures 1F,G**).

Further, we found that TEs accounted for 60% of the cassava genome, class II TEs were inclined to localize in euchromatin regions near PCGs (Wang et al., 2014; Bredeson et al., 2016). On the other hand, TEs tended to locate in the intronic sequences or the flanking regions of the PCGs, however, only a small portion of PCGs have TEs in their introns (Wang et al., 2014, 2015). In this case, we speculated that genome-wide changes of TEs methylation levels may affect expression or activities of neighboring PCGs that were inserted and surrounded by class II TEs after WGD, given that WGD may not have widespread influence over methylation state of PCG bodies (**Figure 1A**). On the other hand, TE-overlapped lncRNAs made up 60% of all detected lncRNAs (**Supplementary Figure 4A**), and class I TEs-overlapped lncRNA

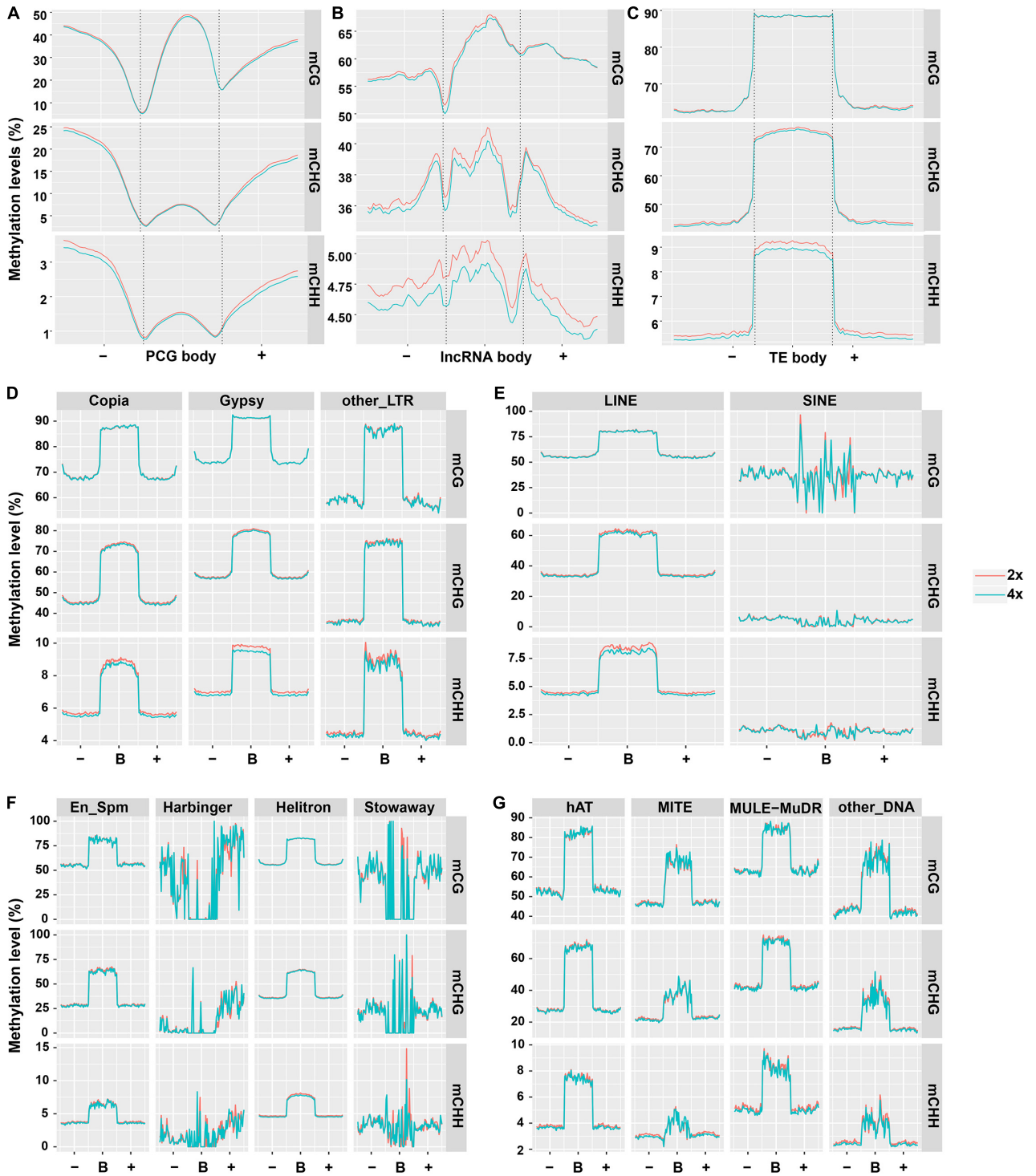

FIGURE 1 | DNA methylation patterns in PCGs, lncRNAs, and TEs. Average methylation level distributions over **(A)** PCGs, **(B)** lncRNAs, and **(C)** TEs. Average methylation level distribution over **(D,E)** class I TEs and **(F,G)** class II TEs. The average level for each 100-bp interval is plotted. The dashed lines for the PCG, lncRNA, and TE regions indicate the transcriptional start (left) and end (right) sites.

accounted for 54% (**Supplementary Figure 4B**), supporting the statement that substantial portion of lncRNAs are either derived from TEs or contain TEs remnants (Kapusta et al., 2013; Wang et al., 2016, 2017). Consequently, we hypothesized that genome-wide alteration of class I TEs methylation levels may affect nearby lncRNAs expression as a result of

autotetraploidization. Therefore, it was sensible and necessary to combine TE methylation and PCG and lncRNA expression to examine the epigenetic responses to WGD.

Gene Methylation Is Associated With Gene Activity

In view of the difference of methylation between 2x and 4x cassava after genome doubling, we attempted to understand whether PCG- and lncRNA-expression levels were influenced by DNA methylation. A total of 33,030 PCGs and 13,517 lncRNAs analyzed from the lncRNA-seq data in "Xinxuan 048" were divided into four quartiles from high-expressed group, low-expressed group, middle-expressed group, and none-expressed group based on their expression levels according to the criteria of Yan et al. (2018). As is shown in **Figure 2A**, in PCGs body regions, the highest mCG methylation levels were not detected in the highly expressed PCGs, but instead in those that are middle highly expressed in 2x and 4x cassava. In PCGs body, PCGs with no expressed displayed the lowest mCG methylation levels. High-expressed PCGs displayed the lowest CHG methylation levels, middle-expressed PCGs showed the second highest CHG methylation levels, and PCGs with non-expressed displayed the highest methylation level in the 2x and 4x cassava (**Figure 2B**). The same correlation was found between mCHH methylation and PCGs activity (**Figure 2C**). The results suggested that mCG levels in the PCGs body regions were positively correlated to PCGs expression level, whereas there is a negative correlation between CHG and CHH methylation levels and PCG expression in 2x and 4x cassava. As is shown in **Figure 2D**, there was no clear relationship between DNA methylation of mCG and lncRNA expression. In lncRNAs body together with upstream regions and downstream regions, lncRNAs with high-expressed showed the highest CHG methylation levels, middle-expressed lncRNAs displayed the second highest CHG methylation levels, and lncRNAs with non-expressed displayed almost the same relative low methylation level as that of the low-expressed lncRNAs in 2x and 4x, respectively (**Figure 2E**). The highest mCHH methylation levels were not detected in the highly expressed lncRNAs, but instead in those that are middle highly expressed in 2x and 4x cassava (**Figure 2F**). Together, though no correlation was observed between CG methylation and lncRNA-expression levels, CHG methylation levels in lncRNA body were positively correlated with lncRNA expression.

Transposons With Changed DNA Methylation Caused by Whole Genome Duplication Altered the Expression of Nearby Protein Coding Genes and Long Non-coding RNA

To better understand gene-expression pattern influenced by DNA methylation and the relationships with TEs, total RNA was extracted from leaves to generate lncRNA-seq data. Comparison of gene-expression level between 2x and 4x cassava indicated that only 359 PCGs and 402 lncRNAs were differentially expressed,

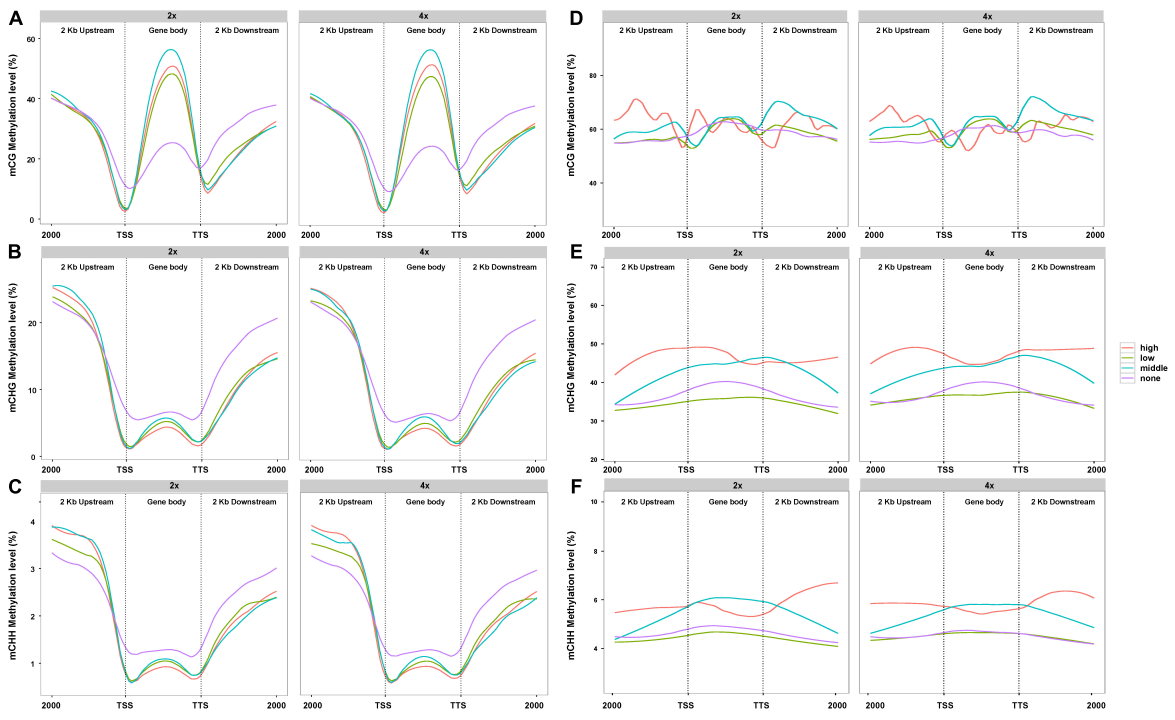

FIGURE 2 | Association between DNA methylation level and PCGs expression in 2x and 4x cassava. Effect of DNA methylation of **(A)** mCG, **(B)** mCHG, and **(C)** mCHH on genome-wide PCGs expression. Effect of DNA methylation of **(D)** mCG, **(E)** mCHG, and **(F)** mCHH on global lncRNAs expression.

respectively. That is, relative to the diploid, few PCGs and lncRNAs were significantly differentially expressed in 4x cassava despite doubled gene dosage (Wilcoxon rank sum test, PCG *P*-value = 0.5062, *n* = 33,030; lncRNA *P*-value = 0.003689, *n* = 13,517) (**Supplementary Figure 5**). Compared with 2x cassava, there were 173 PCGs up-regulated, and there were 186 PCGs down-regulated (**Supplementary Figure 5A**); there were 204 lncRNAs up-regulated, and 198 lncRNAs down-regulated in 4x cassava (**Supplementary Figure 5B**).

Consequently, we further asked whether and how TEs may affect expression of neighboring genes that were involved in WGD-induced variation in cassava. As is seen in **Figure 3A**, approximately 48% of PCGs had TEs inserted into their bodies and most of the TE insertions were class II. About 28 and 62% of PCGs were inserted by DNA transposons within bodies and 8-kb flanking regions, respectively. About 40% of lncRNAs had TEs into their bodies, 80% of lncRNAs were inserted by TEs within 2 kb, 94% lncRNAs overlapped with TEs within 4-kb flanking regions. Most of the TEs inserted into lncRNAs were retrotransposons, 25 and 52% of lncRNAs had retrotransposons insertion into their bodies and within 8-kb flanking regions, respectively (**Figure 3B**). Moreover, we found that in 2x and 4x cassava, PCGs without neighboring TEs were expressed at higher levels than those inserted or surrounded by TEs [*T*-test, Body-TE *P*(2x) value = 2.2E−16, *P*(4x) value = 2.2E−16; Flank-TE *P*(2x) value = 2.2E−16, *P*(4x) value = 2.2E−16] (**Figure 3C**). The expression levels of lncRNAs inserted or surrounded by TEs were higher than those without nearby TEs in 2x and 4x cassava [*T*-test, Body-TE *P*(2x) = 2.2E−16, *P*(4x) = 1.489E−7; Flank-TE *P*(2x) = 2.2E−16, *P*(4x) = 0.0057] (**Figure 3D**). The average PCG-expression level was positively correlated with the distance to the closest TE (**Figure 3E**), for both 2x and 4x cassava, in contrast, the average lncRNA-expression level was negatively correlated with the distance to the closet TE (**Figure 3F**). In addition, the average PCG-expression level was negatively correlated with the number of TEs within 4-kb flanking regions (**Figure 3G**), however, lncRNA-expression level was positively correlated with the number of TEs within 4-kb flanking regions in 2x and 4x cassava (**Figure 3H**). Collectively, these results indicated that PCG-expression levels were suppressed by the abundance and physical distances from adjacent TEs, and lncRNA-expression levels were activated by the abundance and physical distances from proximal TEs in cassava.

Considering expression level of adjacent genes were negatively correlated with the state of methylated TEs in *Arabidopsis* and rice (Hollister and Gaut, 2009; Zhang et al., 2015), we compared DNA methylation of TEs from the whole genome, gene body, and flanking 4-kb regions between 2x and 4x cassava. Methylation of class II TEs, for both PCGs and lncRNAs, were lower than that of class I TEs for all three contexts, and methylation levels of TEs or class II TEs for PCGs in 4x cassava were higher than those of 2x except for flanking TEs in CHH context (*T*-test, **Supplementary Table 4** and **Figure 4A**). Compared with 2x cassava, TEs inserted in lncRNA bodies from 4x cassava exhibited hypomethylation level in the CHG context (*T*-test, **Supplementary Table 5**). Class I TEs inserted in lncRNA bodies or surrounding lncRNAs from 4x cassava showed hypomethylation state exhibited hypomethylation level in the

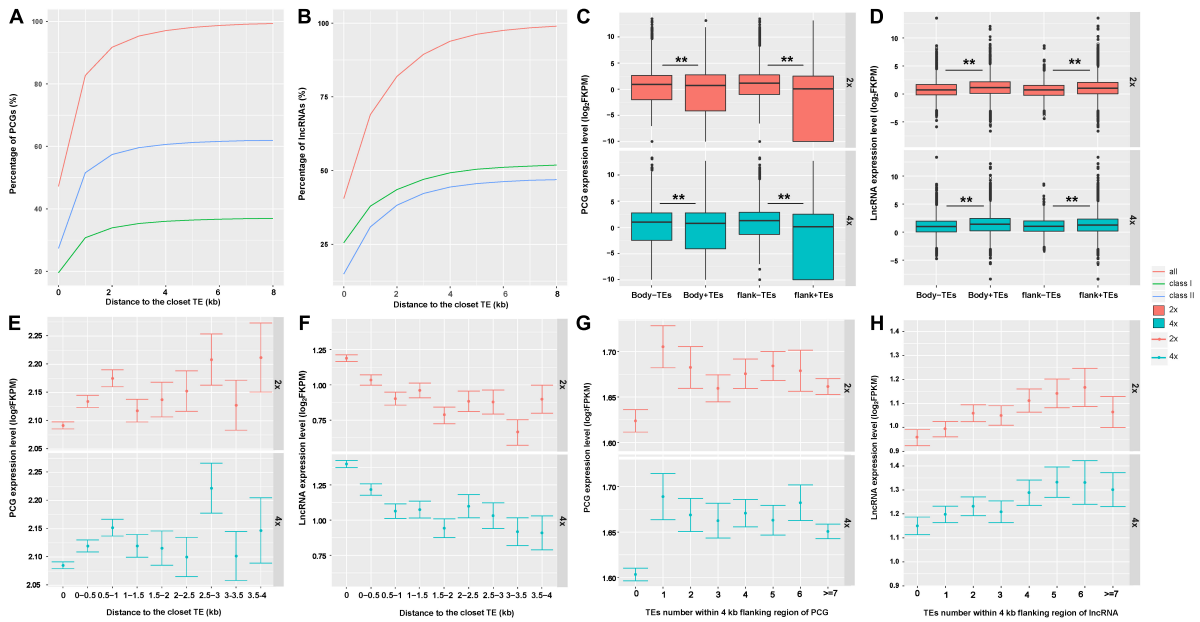

FIGURE 3 | Transposable elements altered expression of neighboring PCGs and lncRNAs in cassava. The percentage of **(A)** PCGs and **(B)** lncRNAs inserted by TEs in their bodies and within 8-kb flank regions. The expression levels of **(C)** PCGs and **(D)** lncRNAs inserted by TEs or not. "+" means TEs inserted in this region; **P*-value < 0.05; ***P*-value < 0.01. **(E)** PCGs and **(F)** lncRNAs expression level related to the distance to the closest TE. "0" indicates genes overlapped with TEs in body regions. Error bars indicates SEM. The expression levels of **(G)** PCGs and **(H)** lncRNAs related to the number of neighboring TEs.

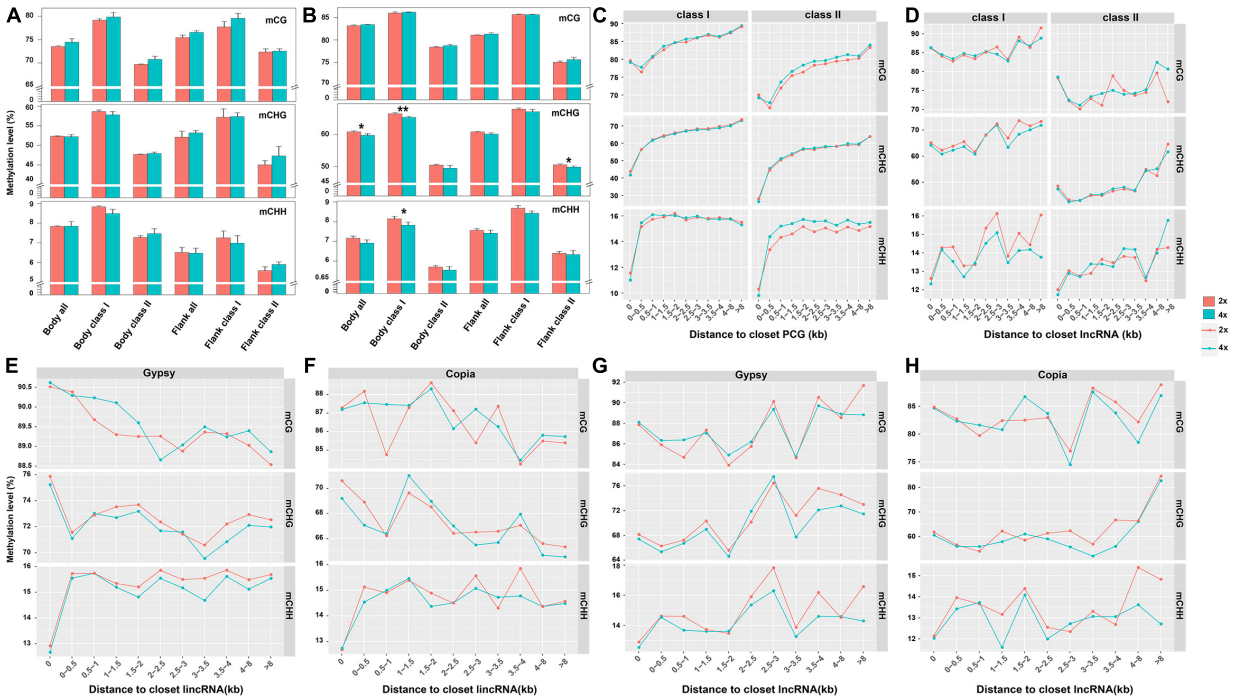

FIGURE 4 | DNA methylation level related to the distance from the closest PCG and lncRNA. DNA methylation of TEs from **(A)** PCG and **(B)** lncRNA body of whole genome, together with flanking 4-kb regions. Upper represented mCG, middle represented mCHG and lower presented mCHH. TE methylation level related to the distance from the closest **(C)** PCG and **(D)** lncRNA. **(E)** *Gypsy* and **(F)** *Copia* methylation level related to the distance from the closest lincRNA. **(G)** *Gypsy* and **(H)** *Copia* methylation level related to the distance from the closest lncRNA. *P-value < 0.05; **P-value < 0.01.

CHG and CHH context (T-test, **Supplementary Table 5** and **Figure 4B**).

We divided PCG-flanking regions into different bins and compared methylation levels between two TE classes located within them (**Figure 4C**). Obviously, methylation levels of class II TEs nearby PCGs were lower than that of class I TEs in all three contexts. The CG methylation levels of class II TEs gradually decreased with increased distances from PCGs, and the valley of CG methylation levels of TEs appeared within 0.5-kb flanking regions. For mCHG and mCHH sites, class II TEs methylation levels gradually increased with increased distances from PCGs. Notably, for mCHG and mCHH sites, 4x cassava exhibited decreased class II TEs methylation levels in PCGs body regions, consisting with hypomethylation levels of PCGs body regions in CHG and CHH contexts in 4x cassava (**Figure 1A**). In contrast, 4x cassava exhibited hypermethylation in CG and CHH contexts in PCG-flanking regions of class II TEs. The annotation of the hypermethylation CG and CHH level of class II TEs related to the distance from the closest PCGs which were not significant differentially expressed between 2x and 4x cassava were listed in **Supplementary Tables 6, 7**, respectively. To sum up, hypermethylation of class II TEs near PCGs in CG and CHH contexts, may be a direct response factor to overcome genomic shock following WGD in 4x cytotype cassava.

Parallelly, we divided lncRNA-flanking regions into different bins and compared methylation levels between two TE classes located within them (**Figure 4D**). Similar with that of PCGs, methylation levels of class II TEs nearby lncRNA in all three contexts were lower than those of class I TEs. The profile of methylation levels of class I TEs did not show always rising for lncRNAs, which was different from that of PCGs. The CHG methylation levels of class I TEs had the same dynamic change with that of CHH methylation levels with increased distances from lncRNAs excluding within 0- to 0.5-kb flanking regions. The CG methylation levels of class I TEs appeared to be higher in 4x cassava than that of 2x in 0- to 2.5-kb regions, however, CG methylation levels of class I TEs were lower in 4x in the flanking regions after 0- to 2.5-kb regions. Critically, in 4x cassava, class I TEs exhibited hypomethylation state in CHG and CHH contexts in lncRNA-flanking regions, with the exception that CHG methylation state in ∼1.5- to 3.0-kb lncRNA-flanking regions observed in 4x cassava was the same as that of 2x, and this result was consistent with the genome-wide methylation level of the five types of class I TEs (**Figures 1D,E**). The annotation of the hypomethylation CHG and CHH level of class I TEs related to the distance from the closest lncRNAs that were not significant differentially expressed between 2x and 4x cassava were listed in **Supplementary Tables 8, 9**, respectively. Taking together, reduction of CHG and CHH methylation levels of class I TEs nearby lncRNAs in 4x cassava may be a mechanism that suppressed expression of adjacent lncRNAs in 4x cassava with double alleles from the diploid line responding to genome-wide lncRNA dosage effects after WGD.

Further, we found that lincRNAs (or called intergenic lncRNA) accounted for the largest proportion (42%) of the whole lncRNAs (**Supplementary Figure 6**), the lncRNA loci contained more Gypsy and Copia segments than the other TEs at the exon and intron sequences together with 8-kb flanking regions in the cassava genome (**Supplementary Figure 7**). Gypsy showed the largest proportion of lncRNA-overlapped TEs, followed by Copia, due to its largest share of TEs in the cassava genome (**Supplementary Figure 7**). In order to understand whether the hypomethylated state of Gypsy or Copia was the effector overcoming genome shock in 4x cassava, we depicted the correlation diagram of the DNA methylation level of Gypsy and Copia related to the distance from the closest lncRNA and lincRNA in 2x and 4x cassava, respectively (**Figures 4E–H**). The results indicated that the profile of Gypsy methylation levels related to the closest lncRNA was found to be almost the same with that of class I TEs related to the closet lncRNA (**Figure 4E**).

Comparisons of Differentially Methylated Regions Between 2x and 4x Cassava

To investigate the potential effect of WGD, we identified a total number of 922 CG, 608 CHG and 51 CHH DMRs (**Figure 5A**). A total of 64.92% of mCG sites were hypermethylated, while 43.09% of mCHG and 17.05% of mCHH sites exhibited hypermethylation in 4x cassava (**Figure 5A**).

At the whole-genome level, most DMRs came from the mCG context, hardly any CHH hyper-DMRs existed in 4x cassava (**Figure 5B**). The number of CG hyper-DMRs in 4x cassava was twice as much as in 2x cassava, while the number of CHG-DMRs and CHH-DMRs in 4x is less than that in 2x (**Figure 5B**). Genome-wide analysis showed that DMR of all three contexts were inclined to localize in intergenic and TEs regions rather than PCGs and lncRNAs (**Figure 5C**). Comparison with 2x cassava, 4x cassava exhibited CHG hyper-DMR and no CHH hyper-DMR within lncRNAs (**Figure 5C**). Analysis of PCG-flanking and lncRNA-flanking 4-kb regions revealed that the distribution of DMRs was similar to that throughout the whole genome (**Figure 5C**).

DISCUSSION

Many diploid crops such as rice (*O. sativa*), maize (*Zea mays*), soybean, poplar (*Populus trichocarpa*) are actually paleo-polyploids that have undergone ancient WGD events during their evolution (Jiang et al., 2013; Ren et al., 2018). Allopolyploid models have provided numerous clues to understand polyploidy formation, however, they can be confounded by the entanglement of both WGD and hybridization (Qin et al., 2021). Conversely, autopolyploids have made changes *via* WGD, ruling out disturbances from incompatible genomes. Newly resynthesized polyploids, which can be induced by colchicine, have enabled biologists to provide insights into genomic changes that occur in response to autotetraploidization.

Large-scale variations of DNA methylation have been found in allopolyploid plants (Lukens et al., 2006; Jiang et al., 2021; Yin et al., 2021). However, relatively little is known about the effects of autopolyploidization. Our findings showed that TEs methylation variations restrained expression of nearby PCGs and lncRNAs, indicating that it is an effective way to overcome genomic shock.

TEs, nearly ubiquitous in lncRNAs, represent a major force shaping the lncRNA repertoire of plants and animals, through their capacity to move and spread in genomes in a lineage-specific fashion (Loewer et al., 2010; Kapusta et al., 2013). In our study, most of the insertions into lncRNAs were retrotransposons in the cassava genome, which coincided with the results from previous studies (Golicz et al., 2018; Zhao et al., 2018; Lv et al., 2019). LncRNAs are highly hypomethylated in the CHG and

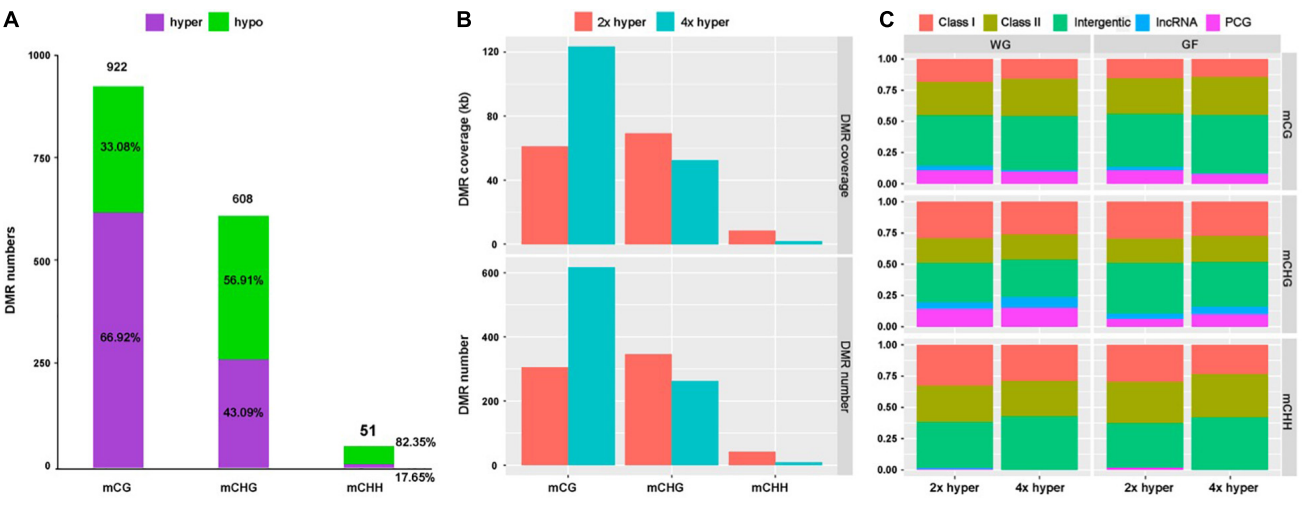

FIGURE 5 | Differentially methylated region distribution. **(A)** DMR numbers of all three contexts and proportions of hyper- and hypo-methylated regions in all three contexts for 4x cassava compared with 2x. **(B)** Genome coverage and number of defined hypermethylation DMRs. **(C)** Distribution of hypermethylation DMRs in the whole-genome (WG) and gene-flanking 4-kb regions (GF).

CHH contexts, partially reflecting hypomethylation patterns in the CHG and CHH contexts of genome-wide class I TEs and class I TEs inserted or surrounding lncRNAs in 4x cassava. Therefore, the impact of polyploidization on DNA methylation pattern of class I TEs partially reflected the impact of WGD on methylation pattern of lncRNAs.

The previous results from *Arabidopsis* and rice, indicated that the number, distance of TEs, and methylation levels of TE affected nearby PCG activity (Hollister and Gaut, 2009; Wang et al., 2013; Zhang et al., 2015). Our study further confirmed that although there were 28% PCGs inserted by class II TEs within their bodies, most of PCGs were inserted by class II TEs within 4-kb flanking regions. 4x cassava displayed hypermethylation of class II TEs in CG context in PCG-flanking regions, which is consistent with increased genome-wide CG methylation level of class II TEs. It is probable that autopolyploidization acts as an effector that may stimulate TE activities. After short-term generations, neoautopolyploids survivors may gradually and adapt to WGD through many mechanisms, one of which could be the TEs hypermethylation or hypomethylation that would have effects on nearby PCGs or lncRNAs. In the case of lncRNAs, this would entail a fitness trade off between keeping TEs inactivated and suppressing proximal lncRNA-expression levels. These results suggested that genome-wide epigenetic silencing through DNA methylation of TEs might play prominent roles in adapting to genomic shock following WGD.

It should be noted, however, that though few genes are differentially expressed between diploid and tetraploid cassava, our data do not provide direct measures of gene dosage responses (Coate and Doyle, 2010, 2015; Loven et al., 2012). Thus, the extent to which the TE methylation changes we observe have restored diploid-like expression levels in the tetraploid are unknown. Additional transcriptomic analyses that enable estimation of expression per gene copy (Loven et al., 2012; Visger et al., 2019) will be required to address this open question. In our study, we have analyzed a single autotetraploid event, generated from a single cultivar, and this may not be representative of what would be observed in other, independent doubling events. For example, we found that increasing CG and CHH methylation levels of class II TEs near PCGs in 4x cassava may suppress expression of adjacent PCGs. In contrast, compared with the diploid rice, increasing methylation status of class II TEs in mCHG and mCHH sites restrained expression levels of nearby PCGs in an artificial synthesized rice tetraploid with a relatively stable genome (Zhang et al., 2015), and the methylation levels of class II TEs that surrounded PCGs in all three contexts were reduced in the colchicine induced autopolyploid switchgrass that was vegetatively propagated for 3 years (Yan et al., 2019). Therefore, we speculate that different species may adopt different methylation responses, which may be related with the stages after WGD. Additionally, CHH methylation of TEs may be more sensitive than CG and CHG methylation in modulating the expression of nearby genes. Overall, methylation level variation of TEs may be a beneficial strategy to help neoautopolyploids to conquer the early challenges caused by WGD in autopolyploid plants.

DATA AVAILABILITY STATEMENT

The original contributions presented in this study are publicly available. This data can be found here: https://www.ncbi.nlm.nih.gov/bioproject/, PRJNA728761.

AUTHOR CONTRIBUTIONS

LX and HY planned to conceive this project. LL and WZ provided valuable suggestions on the research design. LX and XS analyzed the data. SC prepared the samples. LX wrote the manuscript. HY revised the manuscript. All authors read and approved the final manuscript.

FUNDING

This work was supported by the National Key Research and Development Program of China (Grant No. 2019YFD1000500), National Natural Science Foundation of China (Grant No. 31960440), Guangxi Natural Science Foundation (Grant No. 2020GXNSFAA259085), Key Projects of Guangxi Natural Science Foundation (Grant No. 2020GXNSFDA297031), Guangxi Science and Technology Base and Talents Special Project (GuikeAD19245053), and Guangxi Academy of Agricultural Sciences Scientific and Development Foundation (Guinongke2021JM65).

ACKNOWLEDGMENTS

We thank XZ (Chinese Academy of Tropical Agricultural Sciences) and JS (Guangxi University) for critically suggestions.

SUPPLEMENTARY MATERIAL

The Supplementary Material for this article can be found online at: https://www.frontiersin.org/articles/10.3389/fpls.2022.915056/full#supplementary-material

Supplementary Figure 1 | Pearson correlation coefficients between and within groups.

Supplementary Figure 2 | The methylation level of CG, CHG, and CHH sequence contexts in 2x and 4x cassava.

Supplementary Figure 3 | Comparison of chromosome distribution between 2x and 4x cassava. Methylation level in 80-kb windows throughout chromosomes in the leaf tissue. The green and purple lines mean "+" strand, and the red and blue lines means "−" strand.

Supplementary Figure 4 | The proportion of TE-overlapped lncRNA in this study.

Supplementary Figure 5 | The percentage of differential expressed **(A)** PCGs and **(B)** lncRNAs between 2x and 4x cassava.

Supplementary Figure 6 | The proportion of different types of lncRNAs detected in this study.

Supplementary Figure 7 | Distribution of TEs in different lncRNAs features in cassava genome.

REFERENCES

Allario, T., Brumos, J., Colmenero-Flores, J. M., Tadeo, F., Froelicher, Y., Talon, M., et al. (2011). Large changes in anatomy and physiology between diploid Rangpur lime (*Citrus limonia*) and its autotetraploid are not associated with large changes in leaf gene expression. *J. Exp. Bot.* 62, 2507–2519. doi: 10.1093/jxb/erq467

Bao, Z., and Eddy, S. R. (2002). Automated de novo identification of repeat sequence families in sequenced genomes. *Genome Res.* 12, 1269–1276. doi: 10.1101/gr.88502

Barker, M. S., Arrigo, N., Baniaga, A. E., Li, Z., and Levin, D. A. (2016). On the relative abundance of autopolyploids and allopolyploids. *New Phytol.* 210, 391–398. doi: 10.1111/nph.13698

Benson, G. (1999). Tandem repeats finder: a program to analyze DNA sequences. *Nucleic Acids Res.* 27, 573–580. doi: 10.1093/nar/27.2.573

Bredeson, J., Lyons, J., Prochnik, S., Wu, G., Ha, C. M., Edsinger-Gonzales, E., et al. (2016). sequencing wild and cultivated cassava and related species reveals extensive interspecific hybridization and genetic diversity. *Nat. Biotechnol.* 34, 562–571. doi: 10.1038/nbt.3535

Chen, Z. J. (2013). Genomic and epigenetic insights into the molecular bases of heterosis. *Nat. Rev. Genet.* 14, 471–482. doi: 10.1038/nrg3503

Coate, J. E., and Doyle, J. J. (2010). Quantifying whole transcriptome size, a prerequisite for understanding transcriptome evolution across species: an example from a plant allopolyploid. *Genome Biol. Evol.* 2, 534–546. doi: 10.1093/gbe/evq038

Coate, J. E., and Doyle, J. J. (2015). Variation in transcriptome size: are we getting the message? *Chromosoma* 124, 27–43. doi: 10.1007/s00412-014-0496-3

Comai, L. (2005). The advantages and disadvantages of being polyploidy. *Nat. Rev. Genet.* 6, 836–846. doi: 10.1038/nrg1711

Del Pozo, J. C., and Ramirez-Parra, E. (2014). Deciphering the molecular bases for drought tolerance in *Arabidopsis autotetraploids*. *Plant Cell Environ.* 37, 2722–2737. doi: 10.1111/pce.12344

Doyle, J. J., Flagel, L. E., Paterson, A. H., Rapp, R. A., Soltis, D., Soltis, P., et al. (2008). Evolutionary genetics of genome merger and doubling in plants. *Annu. Rev. Genet.* 42, 443–461. doi: 10.1146/annurev.genet.42.110807.091524

Edgar, R. C., and Myers, E. W. (2005). PILER: identification and classification of genomic repeats. *Bioinformatics* 21, i152–i158. doi: 10.1093/bioinformatics/bti1003

Feng, S. H., Cokus, S. J., Zhang, X. Y., Chen, P. Y., Bostick, M., Goll, M. G., et al. (2010). Conservation and divergence of methylation patterning in plants and animals. *Proc. Natl. Acad. Sci. U.S.A.* 107, 8689–8694. doi: 10.1073/pnas.1002720107

Feschotte, C., Jiang, N., and Wessler, S. R. (2002). Plant transposable elements: where genetics meets genomics. *Nat. Rev. Genet.* 3, 329–341. doi: 10.1038/nrg793

Fregene, M. A., Suarez, M., Mkumbira, J., Kulembeka, H., Ndedya, E., Kulaya, A., et al. (2003). Simple sequence repeat marker diversity in cassava landraces: genetic diversity and differentiation in an asexually propagated crop. *Theor. Appl. Genet.* 107, 1083–1093. doi: 10.1007/s00122-003-1348-3

Gaeta, R. T., Pires, J. C., Iniguez-Luy, F., Leon, E., and Osborn, T. C. (2007). Genomic changes in resynthesized Brassica napus and their effect on gene expression and phenotype. *Plant Cell* 19, 3403–3417. doi: 10.1105/tpc.107.054346

Golicz, A. A., Singh, M. B., and Bhalla, P. L. (2018). The long intergenic noncoding RNA (lincRNA) landscape of the soybean genome. *Plant Physiol.* 176, 2133–2147. doi: 10.1104/pp.17.01657

Han, Y., and Wessler, S. R. (2010). MITE-Hunter: a program for discovering miniature inverted-repeat transposable elements from genomic sequences. *Nucleic Acids Res.* 38:e199. doi: 10.1093/nar/gkq862

Havananda, T., Brummer, E. C., and Doyle, J. J. (2011). Complex patterns of autopolyploid evolution in alfalfa and allies (*Medicago sativa*; Leguminosae). *Am. J. Bot.* 98, 1633–1646. doi: 10.3732/ajb.1000318

Hollister, J. D., and Gaut, B. S. (2009). Epigenetic silencing of transposable elements: a trade-off between reduced transposition and deleterious effects on neighboring gene expression. *Genome Res.* 19, 1419–1428. doi: 10.1101/gr.091678.109

Ibarra, C. A., Feng, X. Q., Schoft, V. K., Hsieh, T., Uzawa, R., Rodrigues, J. A., et al. (2012). Active DNA demethylation in plant companion cells reinforces transposon methylation in gametes. *Science* 337, 1360–1364. doi: 10.1126/science.1224839

Jiang, W. K., Liu, Y. L., Xia, E. H., and Gao, L. Z. (2013). Prevalent role of gene features in determining evolutionary fates of whole-genome duplication duplicated genes in flowering plants. *Plant Physiol.* 161, 1844–1861. doi: 10.1104/pp.112.200147

Jiang, X. Y., Song, Q. X., Ye, W. X., and Chen, Z. J. (2021). Concerted genomic and epigenomic changes accompany stabilization of *Arabidopsis allopolyploids*. *Nat. Ecol. Evol.* 5, 1382–1393. doi: 10.1038/s41559-021-01523-y

Kapusta, A., Kronenberg, Z., Lynch, V. J., Zhuo, X., Ramsay, L., Bourque, G., et al. (2013). Transposable elements are major contributors to the origin, diversification, and regulation of vertebrate long noncoding RNAs. *PLoS Genet.* 9:e1003470. doi: 10.1371/journal.pgen.1003470

Kim, D., Pertea, G., Trapnell, C., Pimentel, H., Kelley, R., and Salzberg, S. L. (2013). TopHat2: accurate alignment of transcriptomes in the presence of insertions, deletions and gene fusions. *Genome Biol.* 14:R36. doi: 10.1186/gb-2013-14-4-r36

Kong, L., Zhang, Y., Ye, Z. Q., Liu, X. Q., Zhao, S. Q., Wei, L. P., et al. (2007). CPC: assess the protein-coding potential of transcripts using sequence features and support vector machine. *Nucleic Acids Res.* 35, W345–W349. doi: 10.1093/nar/gkm391

Kraitshtein, Z., Yaakov, B., Khasdan, V., and Kashkush, K. (2010). Genetic and epigenetic dynamics of a retrotransposon after allopolyploidization of wheat. *Genetics* 186, 801–812. doi: 10.1534/genetics.110.120790

Law, J. A., and Jacobsen, S. E. (2010). Establishing, maintaining and modifying DNA methylation patterns in plants and animals. *Nat. Rev. Genet.* 11, 204–220. doi: 10.1038/nrg2719

Lee, H., Lee, M., Ismail, W. M., Ismail, W. M., Rho, M., Fox, G. C., et al. (2016). MGEScan: a Galaxy-based system for identifying retrotransposons in genomes. *Bioinformatics* 32, 2502–2504. doi: 10.1093/bioinformatics/btw157

Li, B., and Dewey, C. N. (2011). RSEM accurate transcript quantification from RNA-Seq data with or without a reference genome. *BMC Bioinformatics* 12:323. doi: 10.1186/1471-2105-12-323

Lister, R., O'Malley, R. C., Tonti-Filippini, J., Gregory, B. D., Berry, C. C., Harvey Millar, A., et al. (2008). Highly integrated single-base resolution maps of the epigenome in *Arabidopsis*. *Cell* 133, 523–536. doi: 10.1016/j.cell.2008.03.029

Lister, R., Pelizzola, M., Dowen, R. H., David Hawkins, R., Hon, G., Tonti-Filippini, J. L., et al. (2009). Human DNA methylomes at base resolution show widespread epigenomic differences. *Nature* 462:315. doi: 10.1038/nature08514

Liu, B. B., and Sun, G. L. (2017). microRNAs contribute to enhanced salt adaptation of the autopolyploid *Hordeum bulbosum* compared with its diploid Ancestor. *Plant J.* 91, 57–69. doi: 10.1111/tpj.13546

Loewer, S., Cabili, M. N., Guttman, M., Loh, Y. H., Thomas, K., Park, I. H., et al. (2010). Large intergenic non-coding RNA-RoR modulates reprogramming of human induced pluripotent stem cells. *Nat. Genet.* 42, 1113–1117. doi: 10.1038/ng.710

Love, M. I., Huber, W., and Anders, S. (2014). Moderated estimation of fold change and dispersion for RNA-seq data with DESeq2. *Genome Biol.* 15:550. doi: 10.1186/s13059-014-0550-8

Loven, J., Orlando, D. A., Sigova, A. A., Lin, C. Y., Rahl, P. B., Burge, C. B., et al. (2012). Revisiting global gene expression analysis. *Cell* 151, 476–482. doi: 10.1016/j.cell.2102.10.012

Lukens, L. N., Pires, J. C., Leon, E., Vogelzang, R., Oslach, L., and Osborn, T. (2006). Patterns of sequence loss and cytosine methylation within a population of newly resynthesized *Brassica napus* allopolyploids. *Plant Physiol.* 140, 336–348. doi: 10.1104/pp.105.066308

Lv, Y. D., Hu, F. Q., Zhou, Y. F., Wu, F. L., and Gaut, B. S. (2019). Maize transposable elements contribute to long non-coding RNAs that are regulatory hubs for abiotic stress response. *BMC Genomics* 20:864. doi: 10.1186/s12864-019-6245-5

Madlung, A., Masuelli, R. W., Watson, B., Reynolds, S. H., Davison, J., and Comai, L. (2002). Remodeling of DNA methylation and phenotypic and transcriptional changes in synthetic *Arabidopsis allotetraploids*. *Plant Physiol.* 129, 733–746. doi: 10.1104/pp.003095

Madlung, A., and Wendel, J. F. (2013). Genetic and epigenetic aspects of polyploid evolution in plants. *Cytogenet. Genome Res.* 140, 270–285. doi: 10.1159/000351430

Martelotto, L. G., Ortiz, J. P. A., Stein, J., Espinoza, F., Quarin, C. L., and Pessino, S. C. (2005). A comprehensive analysis of gene expression alterations in a newly synthesized *Paspalum notatum* autotetraploid. *Plant Sci.* 169, 211–220. doi: 10.1016/j.plantsci.2005.03.015

Parisod, C., Holderegger, R., and Brochmann, C. (2010). Evolutionary consequences of autopolyploidy. *New Phytol.* 186, 5–17. doi: 10.1111/j.1469-8137.2009.03142.x

Pertea, M., Kim, D., Pertea, G. M., Leek, J. T., and Salzberg, S. L. (2016). Transcript-level expression analysis of RNA-seq experiments with HISAT, StringTie and Ballgown. *Nat. Protoc.* 11, 1650–1657. doi: 10.1038/nprot.2016.095

Pertea, M., Pertea, G. M., Antonescu, C. M., Chang, T., Mendell, J., and Salzberg, S. L. (2015). StringTie enables improved reconstruction of a transcriptome from RNA-seq reads. *Nat. Biotechnol.* 33, 290–295. doi: 10.1038/nbt.3122

Price, A. L., Jones, N. C., and Pevzner, P. A. (2005). De novo identification of repeat families in large genomes. *Bioinformatics* 21, i351–i358. doi: 10.1093/bioinformatics/bti1018

Qin, J. X., Mo, R. R., Li, H. X., Ni, Z. F., Sun, Q. X., and Liu, Z. S. (2021). The transcriptional and splicing changes caused by hybridization can be globally recovered by genome doubling during allopolyploidization. *Mol. Biol. Evol.* 38:2513. doi: 10.1093/molbev/msab045

Ramsey, J., and Schemske, D. W. (1998). Pathways, mechanisms, and rates of polyploid formation in flowering plants. *Annu. Rev. Ecol. Syst.* 29, 467–501.

Ramsey, J., and Schemske, D. W. (2002). Neopolyploidy in flowering plants. *Annu. Rev. Ecol. Evol. Syst.* 33, 589–639. doi: 10.1146/annurev.ecolsys.33.010802.150437

Raven, P., Fauquet, C., Swaminathan, M. S., Borlaug, N., and Samper, C. (2006). Where next for genome sequencing? *Science* 311, 468–468. doi: 10.1126/science.311.5760.468b

Ren, R., Wang, H. F., Guo, C., Zhang, N., Zeng, L. P., Chen, Y. M., et al. (2018). Widespread whole genome duplications contribute to genome complexity and species diversity in angiosperms. *Mol. Plant* 11, 414–428. doi: 10.1016/j.molp.2018.01.002

Renny-Byfield, S., and Wendel, J. F. (2014). Doubling down on genomes: polyploidy and crop plants. *Am. J. Bot.* 101, 1–15. doi: 10.3732/ajb.1400119

Rival, A., Ilbert, P., Labeyrie, A., Torres, E., Doulbeau, S., Personne, A., et al. (2013). Variations in genomic DNA methylation during the long-term in vitro proliferation of oil palm embryogenic suspension cultures. *Plant Cell Rep.* 32, 359–368. doi: 10.1007/s00299-012-1369-y

Salmon, A., and Ainouche, M. L. (2010). Polyploidy and DNA methylation: new tools available. *Mol. Ecol.* 19, 213–215. doi: 10.1111/j.1365-294X.2009.04461.x

Salmon, A., Flagel, L., Ying, B., Udall, J. A., and Wendel, J. F. (2010). Homoeologous nonreciprocal recombination in polyploid cotton. *New Phytol.* 186, 123–134. doi: 10.1111/j.1469-8137.2009.03093.x

Saze, H., and Kakutani, T. (2011). Differentiation of epigenetic modifications between transposons and genes. *Curr. Opin. Plant Biol.* 14, 81–87. doi: 10.1016/j.pbi.2010.08.017

Shaked, H., Kashkush, K., Ozkan, H., Feldman, M., and Levy, A. A. (2001). Sequence elimination and cytosine methylation are rapid and reproducible responses of the genome to wide hybridization and allopolyploidy in wheat. *Plant Cell* 13, 1749–1759. doi: 10.1105/TPC.010083

Shi, X. L., Ng, D. W. K., Zhang, C. Q., Comai, L., Ye, W. X., and Chen, Z. J. (2012). Cis- and trans- regulatory divergence between progenitor species determines gene-expression novelty in *Arabidopsis allopolyploids*. *Nat. Commun.* 3:950. doi: 10.1038/ncomms1954

Siqueira, M. V. B. M., Pinheiro, T. T., Borges, A., Valle, T. L., Zatarim, M., and Veasey, E. A. (2010). Microsatellite polymorphisms in cassava landraces from the Cerrado biome, Mato Grosso do Sul, Brazil. *Biochem. Genet.* 48, 879–895. doi: 10.1007/s10528-010-9369-5

Soltis, D. E., Soltis, P. S., and Tate, J. A. (2003). Advances in the study of polyploidy since Plant speciation. *New Phytol.* 161, 173–191. doi: 10.1046/j.1469-8137.2003.00948.x

Soltis, P. S., and Soltis, D. E. (2009). The role of hybridization in plant speciation. *Annu. Rev. Plant Biol.* 60, 561–588. doi: 10.1146/annurev.arplant.043008.092039

Song, Q. X., and Chen, Z. J. (2015). Epigenetic and developmental regulation in plant polyploids. *Curr. Opin. Plant Biol.* 24, 101–109. doi: 10.1016/j.pbi.2015.02.007

Song, Q. X., Lu, X., Li, Q. T., Chen, H., Hu, X. Y., Ma, B., et al. (2013). Genome-wide analysis of DNA methylation in soybean. *Mol. Plant* 6, 1961–1974. doi: 10.1093/mp/sst123

Stupar, R. M., Bhaskar, P. B., Yandell, B. S., Rensink, W. A., Hart, A. L., Ouyng, S., et al. (2007). Phenotypic and transcriptomic changes associated with potato autopolyploidization. *Genetics* 176, 2055–2067. doi: 10.1534/genetics.107.074286

Sun, L., Luo, H. T., Bu, D. C., Zhao, G. G., Yu, K. T., Zhang, C. H., et al. (2013). Utilizing sequence intrinsic composition to classify protein-coding and long non-coding transcripts. *Nucleic Acids Res.* 41:e166. doi: 10.1093/nar/gkt646

Tao, X. Y., Li, M. L., Zhao, T., Feng, S. L., Zhang, H. L., Wang, L. Y., et al. (2021). Neofunctionalization of a polyploidization-activated cotton long intergenic non-coding RNA DAN1 during drought stress regulation. *Plant Physiol.* 186, 2152–2168. doi: 10.1093/plphys/kiab179

Tarailo-Graovac, M., and Chen, N. (2009). Using RepeatMasker to identify repetitive elements in genomic sequences. *Curr. Protoc. Bioinformatics* 25:410. doi: 10.1002/0471250953.bi0410s25

Trapnell, C., Roberts, A., Goff, L., Pertea, G., Kim, D., Kelley, D. R., et al. (2012). Differential gene and transcript expression analysis of RNA-seq experiments with TopHat and Cufflflinks. *Nat. Protoc.* 7, 562–578. doi: 10.1038/nprot.2012.016

Visger, C. J., Wong, G. K., Soltis, P. S., and Soltis, D. E. (2019). Divergent gene expression levels between diploid and autotetraploid *Tolmiea* relative to the total transcriptome, the cell, and biomass. *Am. J. Bot.* 106, 280–291. doi: 10.1002/ajb2.1239

Wang, D., Qu, Z. P., Yang, L., Zhang, Q. Z., Liu, Z. H., Do, T., et al. (2017). Transposable elements (TEs) contribute to stress-related long intergenic noncoding RNAs in plants. *Plant J.* 90, 133–146. doi: 10.1111/tpj.13481

Wang, H. F., Beyene, G., Zhai, J. X., Feng, S. H., Fahlgren, N., Taylor, N. J., et al. (2015). CG gene body DNA methylation changes and evolution of duplicated genes in cassava. *Proc. Natl. Acad. Sci. U.S.A.* 112, 13729–13734. doi: 10.1073/pnas.1519067112

Wang, W. Q., Feng, B. X., Xiao, J. F., Xia, Z. Q., Zhou, X. C., Li, P. H., et al. (2014). Cassava genome from a wild ancestor to cultivated varieties. *Nat. Commun.* 5:5110. doi: 10.1038/ncomms610

Wang, X., Ai, G., Zhang, C. L., Cui, L., Wang, J. F., Li, H. X., et al. (2016). Expression and diversification analysis reveals transposable elements play important roles in the origin of Lycopersicon-specific lncRNAs in tomato. *New Phytol.* 209, 1442–1455. doi: 10.1111/nph.13718

Wang, X., Weigel, D., and Smith, L. M. (2013). Transposon variants and their effects on gene expression in *Arabidopsis*. *PLoS Genet.* 9:e1003255. doi: 10.1371/journal.pgen.1003255

Xi, Y., and Li, W. (2009). BSMAP: whole genome bisulfite sequence MAPping program. *BMC Bioinform.* 10:1. doi: 10.1186/1471-2105-10-232

Xiao, L., Shang, X. H., Cao, S., Xie, X. Y., Zeng, W. D., Lu, L. Y., et al. (2019). Comparative physiology and transcriptome analysis allows for identification of lncRNAs imparting tolerance to drought stress in autotetraploid cassava. *BMC Genomics* 20:514. doi: 10.1186/s12864-019-5895-7

Xiong, W., He, L., Lai, J., Dooner, H. K., and Du, C. (2014). HelitronScanner uncovers a large overlooked cache of Helitron transposons in many plant genomes. *Proc. Natl. Acad. Sci. U.S.A.* 111, 10263–10268. doi: 10.1073/pnas.1410068111

Xu, Y., Zhong, L., Wu, X., Fang, X., and Wang, J. (2009). Rapid alterations of gene expression and cytosine methylation in newly synthesized *Brassica napus* allopolyploids. *Planta* 229, 471–483. doi: 10.1007/s00425-008-0844-8

Xu, Z., and Wang, H. (2007). LTR_FINDER: an efficient tool for the prediction of full-length LTR retrotransposons. *Nucleic Acids Res.* 35, W265–W268. doi: 10.1093/nar/gkm286

Yan, H. D., Bombarely, A., Xu, B., Frazier, T. P., Wang, C. R., Chen, P. L., et al. (2018). siRNAs regulate DNA methylation and interfere with gene and lncRNA expression in the heterozygous polyploid switchgrass. *Biotechnol. Biofuels* 11:208. doi: 10.1186/s13068-018-1202-0

Yan, H. D., Bombarely, A., Xu, B., Wu, B. C., Frazier, T. P., Zhang, X. Q., et al. (2019). Autopolyploidization in switchgrass alters phenotype and flowering

time via epigenetic and transcription regulation. *J. Exp. Bot.* 70, 5673–5686. doi: 10.1093/jxb/erz325

Yin, L. Q., Zhu, Z. D., Huang, L. J., Luo, X., Li, Y., Xiao, C. W., et al. (2021). DNA repair- and nucleotide metabolism-related genes exhibit differential CHG methylation patterns in natural and synthetic polyploids (*Brassica napus* L.). *Hoticult. Res.* 8:142. doi: 10.1038/s41438-021-00576-1

Yu, Z., Haberer, G., Matthes, M., Rattei, T., Mayer, K., Gierl, A., et al. (2010). Impact of natural genetic variation on the transcriptome of autotetraploid *Arabidopsis thaliana*. *Proc. Natl. Acad. Sci. U.S.A.* 107, 17809–17814. doi: 10.1073/pnas.1000852107

Zemach, A., McDaniel, I. E., Silva, P., and Zilberman, D. (2010). Genome-wide evolutionary analysis of eukaryotic DNA methylation. *Science* 328, 916–919. doi: 10.1126/science.1186366

Zhang, J., Liu, Y., Xia, E. H., Yao, Q. Y., Liu, X. D., and Gao, L. Z. (2015). Autotetraploid rice methylome analysis reveals methylation variation of transposable elements and their effects on gene expression. *Proc. Natl. Acad. Sci. U.S.A.* 112, E7022–E7029. doi: 10.1073/pnas.1515170112

Zhang, K., Wang, X. W., and Cheng, F. (2019). Plant polyploidy: origin, evolution, and its influence on crop domestication. *Horticult. Plant J.* 5, 231–239. doi: 10.1016/j.hpj.2019.11.003

Zhao, T., Tao, X. Y., Feng, S. L., Wang, L. Y., Hong, H., Ma, W., et al. (2018). LncRNAs in polyploid cotton interspecific hybrids are derived from transposon neofunctionalization. *Genome Biol.* 19:195. doi: 10.1186/s13059-018-1574-2

Zhou, H. W., Zeng, W. D., and Yan, H. B. (2017). In vitro induction of tetraploids in cassava variety 'Xinxuan 048' using colchicine. *Plant Cell Tissue Organ Cult.* 128, 723–729. doi: 10.1007/s11240-016-1141-z

Zilberman, D., Gehring, M., Tran, R. K., Ballinger, T., and Henikoff, S. (2007). Genome-wide analysis of *Arabidopsis thaliana* DNA methylation uncovers an interdependence between methylation and transcription. *Nat. Genet.* 39, 61–69. doi: 10.1038/ng1929

Conflict of Interest: The authors declare that the research was conducted in the absence of any commercial or financial relationships that could be construed as a potential conflict of interest.

Publisher's Note: All claims expressed in this article are solely those of the authors and do not necessarily represent those of their affiliated organizations, or those of the publisher, the editors and the reviewers. Any product that may be evaluated in this article, or claim that may be made by its manufacturer, is not guaranteed or endorsed by the publisher.

frontiers | Frontiers in Plant Science

TYPE Original Research
PUBLISHED 28 July 2022
DOI 10.3389/fpls.2022.952877

OPEN ACCESS

EDITED BY
Jen-Tsung Chen,
National University of Kaohsiung, Taiwan

REVIEWED BY
Phanikanth Jogam,
Kakatiya University,
India
Ali Raza,
Fujian Agriculture and Forestry University,
China
Pandiyan Muthuramalingam,
Gyeongsang National University,
South Korea

*CORRESPONDENCE
Jun Yang
yang_jun@bjfu.edu.cn

SPECIALTY SECTION
This article was submitted to Plant Breeding, a section of the journal Frontiers in Plant Science

RECEIVED 25 May 2022
ACCEPTED 30 June 2022
PUBLISHED 28 July 2022

CITATION
Liu Z, Xiong T, Zhao Y, Qiu B, Chen H, Kang X and Yang J (2022) Genome-wide characterization and analysis of Golden 2-Like transcription factors related to leaf chlorophyll synthesis in diploid and triploid *Eucalyptus urophylla*. *Front. Plant Sci.* 13:952877. doi: 10.3389/fpls.2022.952877

Genome-wide characterization and analysis of Golden 2-Like transcription factors related to leaf chlorophyll synthesis in diploid and triploid *Eucalyptus urophylla*

Zhao Liu[1,2,3], Tao Xiong[4], Yingwei Zhao[4], Bingfa Qiu[4], Hao Chen[1,2,3], Xiangyang Kang[1,2,3] and Jun Yang[1,2,3]*

[1]National Engineering Research Center of Tree Breeding and Ecological Restoration, College of Biological Sciences and Technology, Beijing Forestry University, Beijing, China, [2]Key Laboratory of Genetics and Breeding in Forest Trees and Ornamental Plants, Ministry of Education, Beijing Forestry University, Beijing, China, [3]Beijing Laboratory of Urban and Rural Ecological Environment, Beijing Forestry University, Beijing, China, [4]Guangxi Dongmen Forest Farm, Chongzuo, China

Golden 2-Like (*GLK*) transcription factors play a crucial role in chloroplast development and chlorophyll synthesis in many plant taxa. To date, no systematic analysis of *GLK* transcription factors in tree species has been conducted. In this study, 40 *EgrGLK* genes in the *Eucalyptus grandis* genome were identified and divided into seven groups based on the gene structure and motif composition. The *EgrGLK* genes were mapped to 11 chromosomes and the distribution of genes on chromosome was uneven. Phylogenetic analysis of *GLK* proteins between *E. grandis* and other species provided information for the high evolutionary conservation of *GLK* genes among different species. Prediction of *cis*-regulatory elements indicated that the *EgrGLK* genes were involved in development, light response, and hormone response. Based on the finding that the content of chlorophyll in mature leaves was the highest, and leaf chlorophyll content of triploid *Eucalyptus urophylla* was higher than that of the diploid control, *EgrGLK* expression pattern in leaves of triploid and diploid *E. urophylla* was examined by means of transcriptome analysis. Differential expression of *EgrGLK* genes in leaves of *E. urophylla* of different ploidies was consistent with the trend in chlorophyll content. To further explore the relationship between *EgrGLK* expression and chlorophyll synthesis, co-expression networks were generated, which indicated that *EgrGLK* genes may have a positive regulatory relationship with chlorophyll synthesis. In addition, three *EgrGLK* genes that may play an important role in chlorophyll synthesis were identified in the co-expression networks. And the prediction of miRNAs targeting *EgrGLK* genes showed that miRNAs might play an important role in the regulation of *EgrGLK* gene expression. This research provides valuable information for further functional characterization of *GLK* genes in *Eucalyptus*.

KEYWORDS

chlorophyll synthesis, co-expression networks, *EgrGLK*, miRNA, polyploid, transcriptome analysis

Introduction

Golden 2-Like (*GLK*) transcription factors are members of the GARP family (Riechmann et al., 2000; Xiao et al., 2019). Most *GLK* genes contain two highly conserved domains: a MYB DNA-binding domain and a C-terminal (GCT) box (Rossini et al., 2001). A *GLK* gene was first identified in maize (*Zea mays* L.) and, subsequently, numerous *GLK* genes were detected in *Arabidopsis thaliana*, rice (*Oryza sativa* L.), and tomato (*Solanum lycopersicum*; Fitter et al., 2002; Powell et al., 2012; Bhutia et al., 2020). The *GLK* transcription factors play crucial roles in chloroplast development and chlorophyll synthesis in many plant taxa (Bravo-Garcia et al., 2009; Chen et al., 2016).

Although the function of *GLK* genes is conserved, different genetic regulatory mechanisms may operate in different species. There are three types of chloroplasts in C_4 plants: C_4 bundle sheath cells, C_4 and C_3 mesophyll cells (Langdale and Nelson, 1991). The spatially tissue-specific expression of different *GLK* genes in maize might represent a specialization required for the development of distinct bundle sheath and mesophyll chloroplasts (Rossini et al., 2001). However, in *Cleome gynandra*, different *GLK* genes are both expressed in bundle sheath and mesophyll cells (Wang et al., 2013). In the C_3 plant *Arabidopsis*, *GLK* genes play a redundant role in regulating chloroplast development. Single-insertion mutants showed normal phenotypes in most photosynthetic tissues, whereas in double mutants all photosynthetic tissues and chloroplasts were pale green (Fitter et al., 2002). In addition, two typical *GLK* genes were found in tomato, both of which are expressed in the leaves, but only one is predominantly expressed in fruit (Powell et al., 2012; Nguyen et al., 2014). In many plant species, *GLK* genes act as transcriptional regulators of chloroplast development. However, to date, no study of *GLK* genes in forest tree species has been conducted.

Eucalyptus is a genus of fast-growing tree species that are widely planted around the world (Booth et al., 2017; Deng et al., 2020). These trees provide raw materials for pulp and paper manufacturing, and have the advantage of fixing large amounts of atmospheric carbon (Pérez et al., 2006; Hii et al., 2017; Vilasboa et al., 2019). Compared with diploid individuals, polyploid plants usually exhibit superior growth and carbon absorption, which reflects improved photosynthetic efficiency after polyploidization (Liao et al., 2016; Li et al., 2019). Therefore, polyploid *Eucalyptus* is potentially important to improve plant biomass accumulation and to mitigate global warming. Photosynthesis occurs mainly in chloroplasts (Gan et al., 2019). *GLK* family genes are associated with chloroplast development and chlorophyll synthesis in many plant taxa (Chen et al., 2016). However, after whole-genome duplication, the gene dosage effect and epigenetic modification may affect gene expression and ultimately lead to trait variation (Allario et al., 2013; Zhang et al., 2015). For example, in triploid poplar, genes associated with chlorophyll synthesis are upregulated as a result of the gene dosage effect, which lead to increase in chlorophyll content (Du et al., 2020). The effect of *GLK* genes on chloroplast development and chlorophyll synthesis in *Eucalyptus* of different ploidies remains to be studied.

In this study, 40 *GLK* family genes were identified by genome-wide analysis of the genome of *Eucalyptus grandis*. The chromosomal distribution, phylogenetic relationships, conserved motifs, intron and exon structure, and *cis*-acting regulatory elements of *GLK* genes were analyzed. In combination with analysis of the chlorophyll content in *E. urophylla* of different ploidies, the effect of *GLK* family genes on chlorophyll synthesis was studied based on RNA-sequencing data and co-expression network analysis. In addition, putative miRNAs targeting *EgrGLK* genes were also been predicted. The results are important to enhance understanding of the *GLK* gene family and provide a reference for studying the molecular mechanism of the increase in chlorophyll content in polyploid plants.

Materials and methods

Identification of *GLK* genes in *Eucalyptus grandis*

The analysis done in this study was presented in Supplementary Figure S1 in the form of flow chart. To identify the *GLK* genes of *E. grandis*, genomic data were downloaded from the Phytozome database.[1] Using published *GLK* protein sequences from *Arabidopsis*, maize, and tomato as query sequences (Liu et al., 2016; Alam et al., 2022; Wang et al., 2022), the *GLK* protein sequences in the *E. grandis* reference genome were identified with the BLASTP tool (*E*-value: $1e^{-5}$). The identified sequences were submitted to the SMART online tool[2] and the NCBI Web CD-Search Tool[3] for further confirmation of *GLK* proteins. The protein sequences that included a *GLK* domain (PF00249) were retained and designated *EgrGLK*. The physical parameters and subcellular localization of these proteins were predicted with the ExPASy[4] and WoLF PSORT[5] online tools.

Chromosomal location and gene duplication

The location of genes on chromosome and the analysis of gene duplication can provide us with more genetic information about the *EgrGLK* genes. Information on the chromosomal location of each *EgrGLK* gene was extracted from the Phytozome database and the identified *EgrGLK* genes were mapped to individual chromosomes using TBtools (Chen et al., 2020). The

1 https://phytozome-next.jgi.doe.gov
2 http://smart.embl-heidelberg.de
3 https://www.ncbi.nlm.nih.gov/Structure/bwrpsb/bwrpsb.cgi
4 https://web.expasy.org/compute_pi
5 https://www.genscript.com/wolf-psort.html

duplication landscape of *EgrGLK* genes and cross-species collinearity of *GLK* genes was confirmed with MCScanX software (Wang et al., 2012). The parameters non-synonymous mutations (K_a), synonymous mutations (K_s) and estimated evolutionary constraints (K_a/K_s) among the *EgrGLK* genes were calculated using TBtools (Chen et al., 2020).

Phylogenetic analysis

To explore the evolutionary relationships of *GLK* proteins in plants, a phylogenetic tree was constructed derived from the *EgrGLK* protein sequences and published *GLK* protein sequences from *Arabidopsis*, maize, and tomato. A multiple sequence alignment of the sequences was generated with ClustalX (Thompson et al., 1997). A phylogenetic tree with 1,000 bootstrap replicates was generated using the neighbor-joining method with MEGAX software (Kumar et al., 2018). The tree was manipulated with the iTOL online tool.[6]

Analysis of gene structure, conserved motifs, and *cis*-acting regulatory elements

Structure, conserved motifs and *cis*-elements of genes can provide important information for understanding gene function. The structure of the *EgrGLK* genes was analyzed with the GSDS platform[7] for prediction of introns and exons. The conserved motifs of the *EgrGLK* proteins were predicted using the MEME Suite online tool.[8] The identified motifs were annotated using the NCBI Web CD-Search Tool. The nucleotide sequence 2000 bp upstream of the start codon for the *EgrGLK* genes was extracted from the *E. grandis* reference genome, and the sequences were submitted to the PlantCARE database[9] for prediction of *cis*-acting regulatory elements. Conserved motifs, gene structure, and *cis*-element information were visualized using TBtools (Chen et al., 2020).

Measurement of chlorophyll content

To explore the effect of polyploidization on chlorophyll content in plant leaves, triploid *E. urophylla* obtained by sexual polyploidization and its diploid control were used as materials for measurement of chlorophyll content (Yang et al., 2018). Five clones of triploid and diploid *E. urophylla* were selected. Young leaves at the shoot tips, fully expanded mature leaves, and senescent leaves were randomly selected. The chlorophyll content was determined following the method described by Du et al. (2020). Fresh leaf tissue (1 g), 5 ml of 95% ethanol, and a small amount of quartz sand and calcium carbonate were mixed and ground into a homogenate. An additional 5 ml of 95% ethanol was added and ground further. After standing for 3 min, the homogenate was filtered into a 50 ml brown volumetric flask and diluted to 50 ml with 95% ethanol. Absorbance (A) was measured at 645 and 663 nm using a spectrophotometer (Ultrospec 6300 Pro, Biochrom, Cambridge, United Kingdom). The chlorophyll content (mg/g) was calculated with the formula $8.02 \times A_{663} + 20.20 \times A_{645}$.

Transcriptome analysis

In order to reveal the reasons for the changes of chlorophyll content in plant leaves after polyploidization, terminal buds, young leaves, mature leaves, and senescent leaves were collected from the triploid and diploid *E. urophylla* clones. Total RNA was extracted using the TRIzol Kit (Invitrogen, Carlsbad, CA, United States). The cDNA libraries were prepared using the TruSeq Stranded Total RNA HT Sample Prep Kit (Illumina, San Diego, CA, United States). Following the manufacturer's recommended protocol, transcriptome sequencing was performed on an Illumina HiSeq 4000 platform by Lc-bio technologies Co., Ltd. (Hangzhou, China). The abundance of transcripts was expressed as reads per kilobase per million mapped reads. The transcriptome data for *EgrGLK* genes was $\log_2$-transformed. The expression patterns and differential expression among *E. urophylla* clones of different ploidies were visualized by means of a heatmap with TBtools (Chen et al., 2020). In addition, *EgrGLK* genes in leaves were annotated based on the GO database[10] to understand their functions.

Co-expression network construction

Co-expression networks were generated to identify which *EgrGLK* genes might play an important role in chlorophyll synthesis. Transcriptome data for genes associated with chlorophyll synthesis and *EgrGLK* genes were subjected to a Pearson correlation analysis. Genes with a Pearson correlation coefficient within the appropriate range ($r \geq 0.6$ or ≤ -0.6) were selected to generate a co-expression network using Cytoscape software (Kohl et al., 2011).

qRT-PCR

To determine the reliability of the RNA-seq data, 5 *EgrGLK* genes in leaves were selected for qRT-PCR analysis. Terminal

6 http://itol.embl.de/
7 http://gsds.gao-lab.org/
8 http://meme-suite.org/meme/
9 http://bioinformatics.psb.ugent.be/webtools/plantcare/html/
10 http://www.geneontology.org

buds, young leaves, mature leaves, and senescent leaves of triploid and diploid *E. urophylla* were used for qRT-PCR analysis. qPCR was subsequently performed using a TransStart® Tip Green qPCR SuperMix (TransGen Biotech, Beijing, China) in 25 μl volume on the 7500 Fast real-time PCR system (Thermo Fisher, Singapore) according to the manufacturer's instructions. Three technical replicates and three biological replicates were performed on all reactions. The primers and reference gene used for qRT-PCR analysis are listed in Supplementary Table S1.

Prediction of miRNAs targeting *EgrGLK* genes

To understand the regulation of gene expression at the post-transcriptional level, we predicted the putative miRNAs targeting *EgrGLK* genes. The miRNA sequences of *E. grandis* were downloaded from a previous study, and the miRNAs found in leaves were used for analysis (Lin et al., 2018). The miRNAs targeting *EgrGLK* genes were predicted by submitting the miRNAs and *EgrGLK* genes to psRNATarget.[11] Cytoscape was used to establish the regulatory network of miRNAs and *EgrGLK* genes (Kohl et al., 2011).

Results

Identification and analysis of *GLK* genes in *Eucalyptus grandis*

A total of 40 putative *GLK* proteins were identified in the *E. grandis* genome database (Table 1 and Supplementary Table S2). The online tools NCBI Web CD-Search and SMART were used to verify the identity of the proteins to ensure that they contained conserved *GLK* domains (Supplementary Table S3). The verified proteins were designated *EgrGLK1* to *EgrGLK40*. The molecular weight and isoelectric point of each *EgrGLK* protein are listed in Table 1. The proteins ranged in size from 102 aa (*EgrGLK16*) to 689 aa (*EgrGLK12*). The molecular weight ranged from 11.69 kDa (*EgrGLK16*) to 74.96 kDa (*EgrGLK12*). The isoelectric point ranged from 4.77 (*EgrGLK4*) to 10.22 (*EgrGLK16*). In addition, 38 of the 40 *EgrGLK* proteins were predicted to be localized in the nucleus.

Chromosomal location and duplication of *EgrGLK* genes

Based on chromosomal position data, the 40 *EgrGLK* genes were mapped to 11 chromosomes (Figure 1). The distribution of *EgrGLK* genes on chromosome was uneven. Chr1 carried eight genes, whereas Chr9 contained only one gene. The longest chromosome, Chr3, contained three genes, only one gene more than the shortest chromosome (Chr10). The number of *EgrGLK* genes on the other chromosomes ranged from three to five. Thus, no correlation between chromosome length and *EgrGLK* gene number was apparent. Investigation of potential duplication events identified five duplicated pairs of *EgrGLK* genes as the products of segmental duplication (Figure 1 and Supplementary Table S4). In addition, the synteny relationships were displayed by comparing the genome of *E. grandis* with those of the other three species (Figure 2). These species include two dicotyledons (*Arabidopsis* and tomato) and one monocotyledon (maize). A total of 41, 39 and 9 homologous gene pairs were identified between *E. grandis* and the three species, respectively. To estimate the type of evolutionary selection on the duplicated *EgrGLK* genes, the K_a, K_s, and K_a/K_s ratio among the gene pairs were calculated (Supplementary Table S4), which indicated that all gene pairs were subject to purifying selection ($K_a/K_s < 1$).

Phylogenetic relationships of *EgrGLK* proteins

To explore the evolutionary relationships of *GLK* proteins in plants and classify the identified *EgrGLK* proteins, a neighbor-joining tree was constructed. The *EgrGLK* proteins were clustered into seven groups based on their grouping with *Arabidopsis*, maize, and tomato *GLK* proteins (Figure 3). The *GLK* proteins from all four species were clustered in each group, but the 40 *EgrGLK* proteins were unevenly distributed. Eight *EgrGLK* proteins were clustered in group VII, which was double the number of *EgrGLK* proteins in groups IV and VI. Six, six, seven, and five *EgrGLK* proteins were included in groups I, II, III, and V, respectively. *EgrGLK* proteins were distributed in each group, which provided information on the orthologous relationships and strong evolutionary conservation among *GLK* proteins of different species.

Analysis of gene structure and conserved motifs of *EgrGLK* genes

To further explore evolutionary relationships among the *EgrGLK* genes, a phylogenetic tree was generated for the 40 *EgrGLK* protein sequences. The proteins were resolved into seven groups (Figure 4A). The conserved motifs of the proteins were analyzed using the online MEME tool, and the conserved sequences of each motif are shown in Supplementary Table S5. Seven putative motifs were functionally annotated, which were defined as MYB-SHAQKYF for motif 1, components of the conserved *GLK* domain for motifs 2 and 10, MYB-CC-LHEQLE for motif 3, and the REC superfamily for motifs 4, 5, and 7. No functional annotation was assigned for the remaining three putative motifs (Figure 4B). The MYB-SHAQKYF motif was observed to be a component of the conserved *GLK* domain. All *EgrGLK* proteins contained motifs 1 and 2, which indicated that these two motifs constituted the basic

11 http://plantgrn.noble.org/psRNATarget

TABLE 1 Physical parameters of *GLK* transcription factors in *Eucalyptus grandis*.

Name	Gene ID	Chromosome	Start	End	PI	Mw (kDa)	Strand	CDS length (bp)	Protein length (aa)	Location
EgrGLK1	Eucgr.A00189.1.v2.0	Chr01	7805221	7809813	5.81	72504.39	+	2,007	669	Nuclear
EgrGLK2	Eucgr.A01323.1.v2.0	Chr01	8233113	8239446	5.21	53070.55	+	1,455	485	Nuclear
EgrGLK3	Eucgr.A01857.1.v2.0	Chr01	33608330	33612765	6.01	50954.1	–	1,404	468	Nuclear
EgrGLK4	Eucgr.A01921.1.v2.0	Chr01	34530669	34532062	4.77	19053.88	–	516	172	Nuclear
EgrGLK5	Eucgr.A02031.1.v2.0	Chr01	35741939	35746799	5.83	24059.79	+	639	213	Nuclear
EgrGLK6	Eucgr.A02082.1.v2.0	Chr01	36277691	36280320	6.82	41747.57	+	1,134	378	Nuclear
EgrGLK7	Eucgr.A02201.1.v2.0	Chr01	37382917	37384778	9.25	32763.84	–	930	310	Nuclear
EgrGLK8	Eucgr.A02444.1.v2.0	Chr01	39776908	39779403	7.63	42957.85	–	1,155	385	Nuclear
EgrGLK9	Eucgr.B02155.1.v2.0	Chr02	40667707	40672664	5.20	40932.61	–	1,116	372	Nuclear
EgrGLK10	Eucgr.B02313.1.v2.0	Chr02	42073119	42074948	4.77	37255.93	–	1,011	337	Nuclear
EgrGLK11	Eucgr.B02627.1.v2.0	Chr02	46202988	46206837	8.19	31746.74	–	861	287	Nuclear
EgrGLK12	Eucgr.C00380.1.v2.0	Chr03	6065170	6069823	5.61	74964.13	–	2,067	689	Nuclear
EgrGLK13	Eucgr.C04050.1.v2.0	Chr03	83173778	83177867	7.60	55374.64	+	1,512	504	Nuclear
EgrGLK14	Eucgr.C04155.1.v2.0	Chr03	78649962	78652848	6.60	52138.75	+	1,440	480	Nuclear
EgrGLK15	Eucgr.D00972.2.v2.0	Chr04	21132122	21137252	6.50	33078.83	+	927	309	Nuclear
EgrGLK16	Eucgr.D01346.1.v2.0	Chr04	17250462	17250970	10.22	11689.9	+	306	102	Mitochondrial
EgrGLK17	Eucgr.D02225.1.v2.0	Chr04	35765713	35770752	9.33	41990.75	+	1,128	376	Nuclear
EgrGLK18	Eucgr.D02611.1.v2.0	Chr04	40020902	40024966	9.04	32064.09	–	882	294	Nuclear
EgrGLK19	Eucgr.E00234.1.v2.0	Chr05	2267724	2273201	9.14	43135.71	–	1,167	389	Nuclear
EgrGLK20	Eucgr.E00246.1.v2.0	Chr05	2412510	2421762	9.17	38620.75	–	1,041	347	Nuclear
EgrGLK21	Eucgr.E00308.1.v2.0	Chr05	2880990	2887358	5.50	62253.87	–	1,674	558	Nuclear
EgrGLK22	Eucgr.E02754.1.v2.0	Chr05	48944350	48945391	5.59	21601.73	+	573	191	Nuclear
EgrGLK23	Eucgr.E04232.1.v2.0	Chr05	74981964	74988000	5.69	36040.02	+	990	330	Nuclear
EgrGLK24	Eucgr.F02896.1.v2.0	Chr06	41128595	41132747	6.70	49407.98	+	1,353	451	Nuclear
EgrGLK25	Eucgr.F04055.1.v2.0	Chr06	51329899	51336284	5.62	54973.18	+	1,497	499	Nuclear
EgrGLK26	Eucgr.F04475.1.v2.0	Chr06	57276036	57278443	6.59	39694.62	+	1,077	359	Nuclear
EgrGLK27	Eucgr.G01503.1.v2.0	Chr07	24195911	24199198	6.48	44709.24	–	1,224	408	Nuclear
EgrGLK28	Eucgr.G02094.1.v2.0	Chr07	40710921	40719657	5.99	72986.17	–	2,034	678	Nuclear
EgrGLK29	Eucgr.G02343.1.v2.0	Chr07	44100593	44103437	7.04	43255.47	–	1,185	395	Nuclear
EgrGLK30	Eucgr.G02494.1.v2.0	Chr07	45799252	45801435	6.57	39241.02	+	1,062	354	Nuclear
EgrGLK31	Eucgr.H00055.1.v2.0	Chr08	4287466	4292435	6.08	33816.32	–	942	314	Cytoplasmic
EgrGLK32	Eucgr.H01993.1.v2.0	Chr08	20710917	20713708	6.00	48317.01	+	1,278	426	Nuclear
EgrGLK33	Eucgr.H04693.1.v2.0	Chr08	65832185	65836257	5.64	64221.54	–	1719	573	Nuclear
EgrGLK34	Eucgr.I01178.1.v2.0	Chr09	22723451	22725940	5.59	40274.79	–	1,113	371	Nuclear
EgrGLK35	Eucgr.J00182.1.v2.0	Chr10	1909756	1911619	8.59	45164.48	+	1,215	405	Nuclear
EgrGLK36	Eucgr.J01904.1.v2.0	Chr10	24412949	24413573	9.37	15323.26	–	411	137	Nuclear
EgrGLK37	Eucgr.K01056.1.v2.0	Chr11	13546489	13549812	6.12	48814.58	–	1,380	460	Nuclear
EgrGLK38	Eucgr.K01476.1.v2.0	Chr11	18158377	18161567	7.00	45984.74	+	1,260	420	Nuclear
EgrGLK39	Eucgr.K01670.1.v2.0	Chr11	19659447	19661493	6.43	32447.42	–	906	302	Nuclear
EgrGLK40	Eucgr.K02966.2.v2.0	Chr11	37110402	37113349	6.48	41802.11	+	1,101	367	Nuclear

GLK domain associated with the typical function. The proteins contained different motifs in accordance with the phylogenetic grouping. Motif 3 was only detected in group I, motifs 4, 5, and 7 were coincident in group VII, and motifs 6 and 9 were mostly present in groups IV and III, respectively. Motif 8 was only detected in *EgrGLK19*, *EgrGLK20*, and *EgrGLK28*. Motif 10 was only identified in group VI, which was the only group to contain three conserved *GLK* motifs. In general, proteins in the same group contained basically the same conserved motifs, indicating that these proteins perform similar functions within a group.

To examine the structural variation among the *EgrGLK* genes, the exon–intron organization of each *EgrGLK* gene was assessed based on the phylogenetic classification (Figure 4C). Differences in the number of introns between genes were observed in different groups. No introns were detected in group V, and the gene (*EgrGLK21*) with the most introns was classified in group VI. In

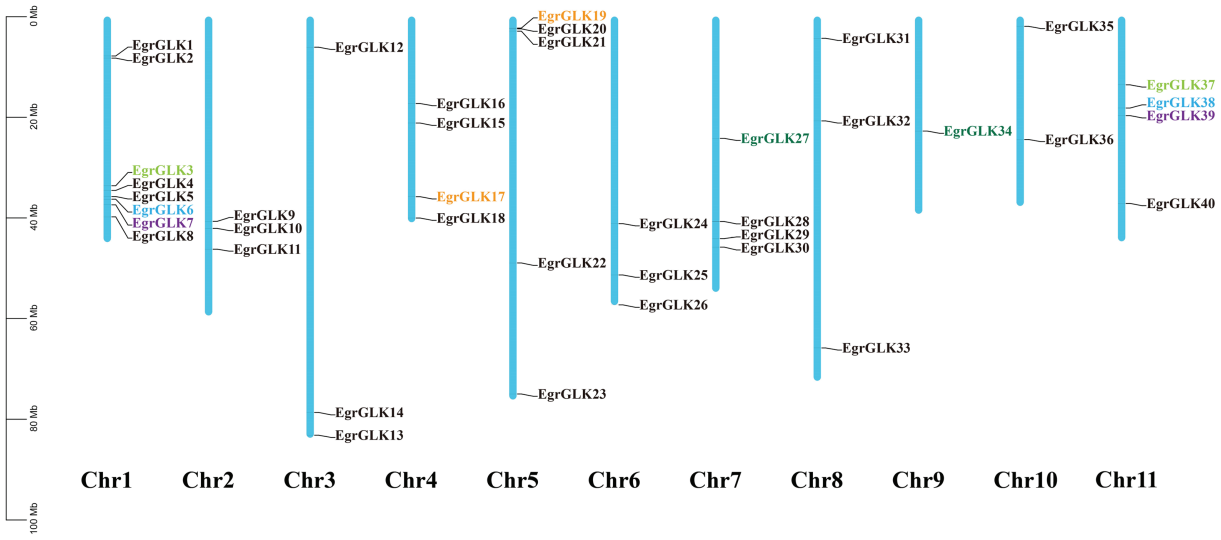

FIGURE 1
Chromosomal location of *EgrGLK* genes in *Eucalyptus grandis*. Genes of the same color represents a pair of segmented duplicated genes, and genes of different colors represent different gene pairs. No segmental duplication in black genes.

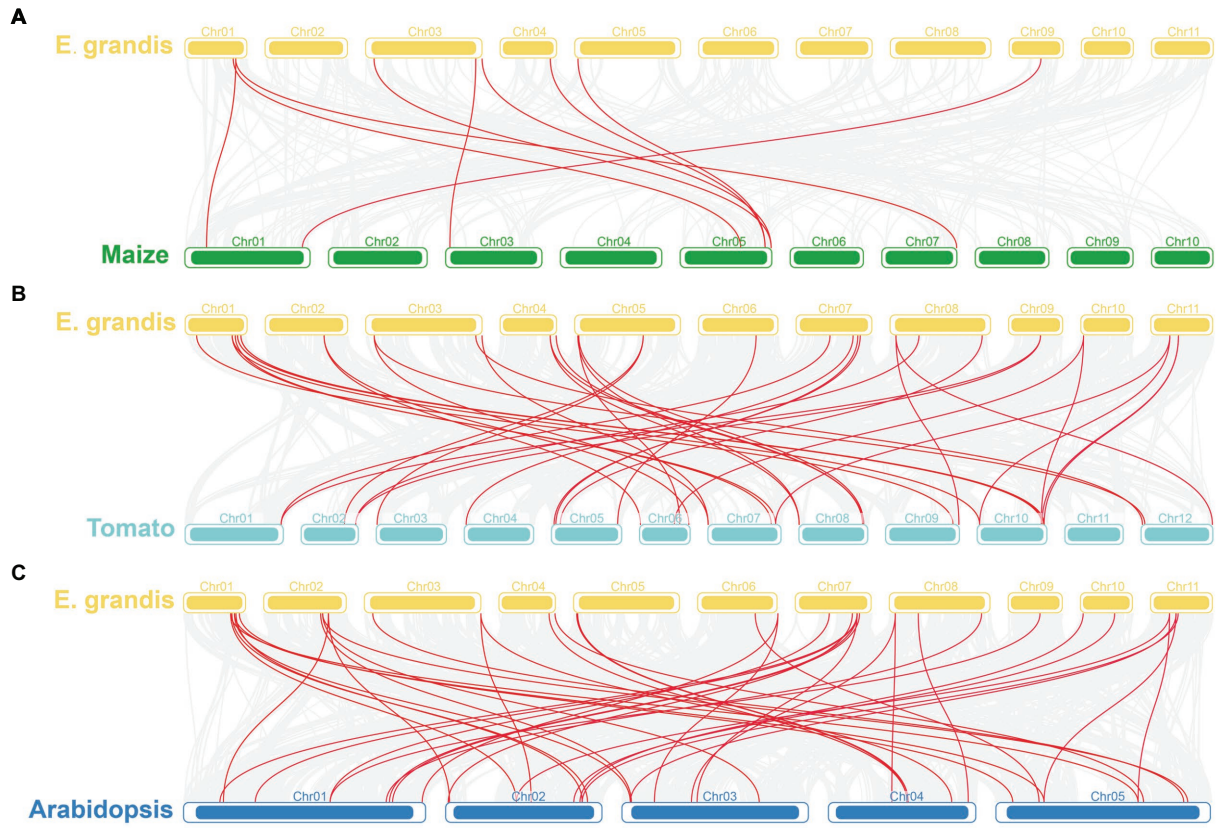

FIGURE 2
Synteny analysis of *GLK* genes in different plants. Synteny analyses of *GLK* genes between *E. grandis* and maize **(A)**, tomato **(B)**, and *Arabidopsis* **(C)**. Red lines indicate the homologous *GLK* genes between *E. grandis* genome and other plant genomes.

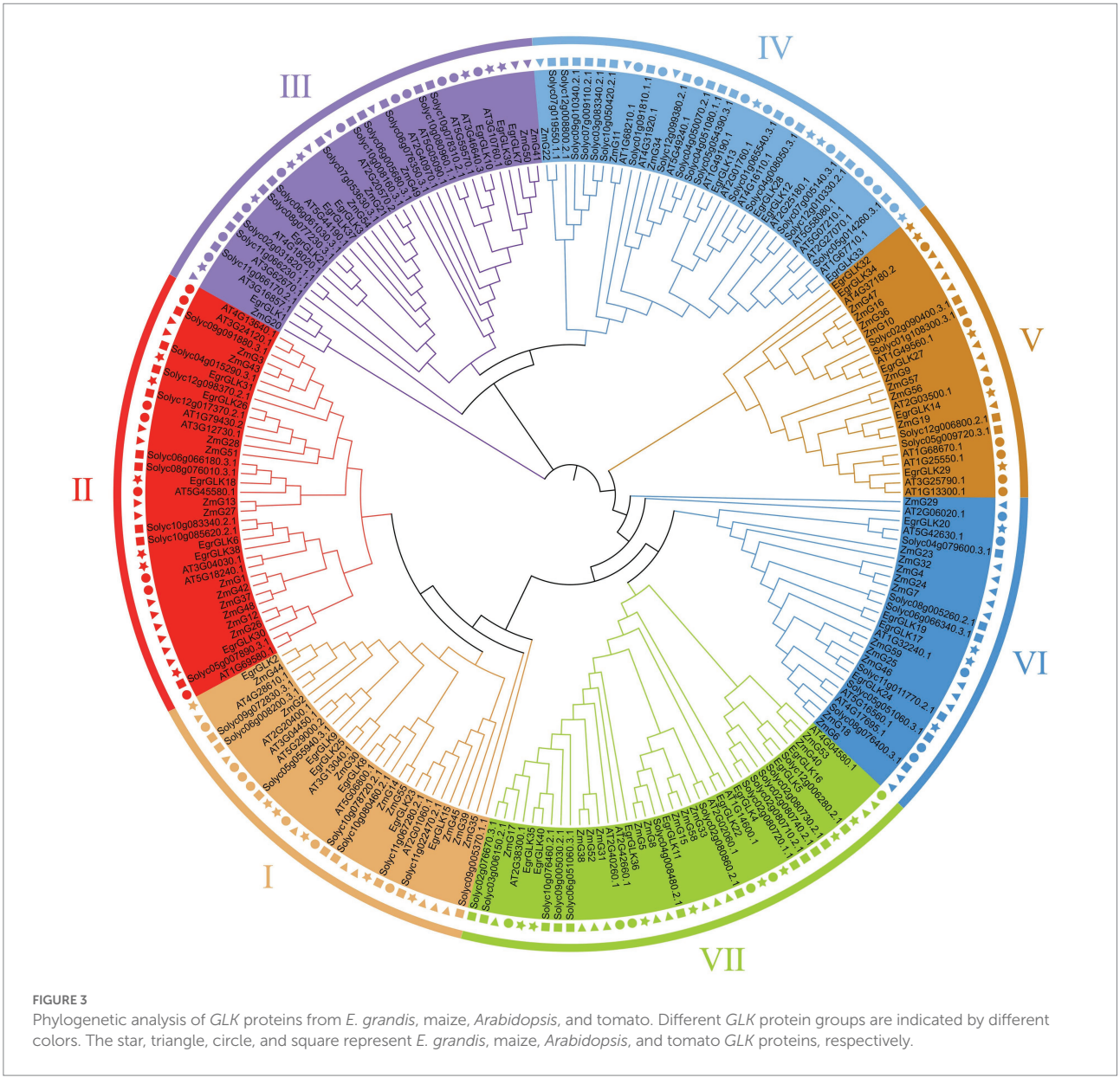

FIGURE 3
Phylogenetic analysis of *GLK* proteins from *E. grandis*, maize, *Arabidopsis*, and tomato. Different *GLK* protein groups are indicated by different colors. The star, triangle, circle, and square represent *E. grandis*, maize, *Arabidopsis*, and tomato *GLK* proteins, respectively.

group II, the intron number ranged from one to five. In addition, most *EgrGLK* genes that were clustered in the same phylogenetic group showed similar exon–intron structures.

Analysis of *cis*-regulatory elements in the promoter regions of *EgrGLK* genes

The presence of *cis*-acting regulatory elements in promoter regions is important for the expression of downstream target genes and the regulation of transcription factor interaction. Therefore, *cis*-regulatory elements related to development, light response, and hormone response in the promoter regions of the *EgrGLK* genes were investigated (Supplementary Table S6 and Figure 5). The most abundant putative *cis*-elements were involved in hormone response and comprised ABRE, CGTCA-motif, TGACG-motif, TCA-element, TATC-box, and AuxRR-core elements. The ABRE elements were distributed in the promoter regions of 33 *EgrGLK* genes and are involved in abscisic acid response. The CGTCA-motif and TGACG-motif are involved in methyl jasmonate response; thus, *cis*-regulatory elements responsive to methyl jasmonate were the most frequent. Three types of light-responsive elements were identified, namely ACE, G-box, and C-box. Among all *cis*-regulatory elements identified, G-box elements were the most widely distributed and were identified in 34 *EgrGLK* genes, which indicated that many *EgrGLK* genes may be sensitive to light. In addition, five *cis*-elements involved in development were identified, comprising CAT-box, circadian, GCN4-motif, RY-element, MSA-like elements and motif I elements. These elements are involved in plant growth, cell division, and diverse plant-specific

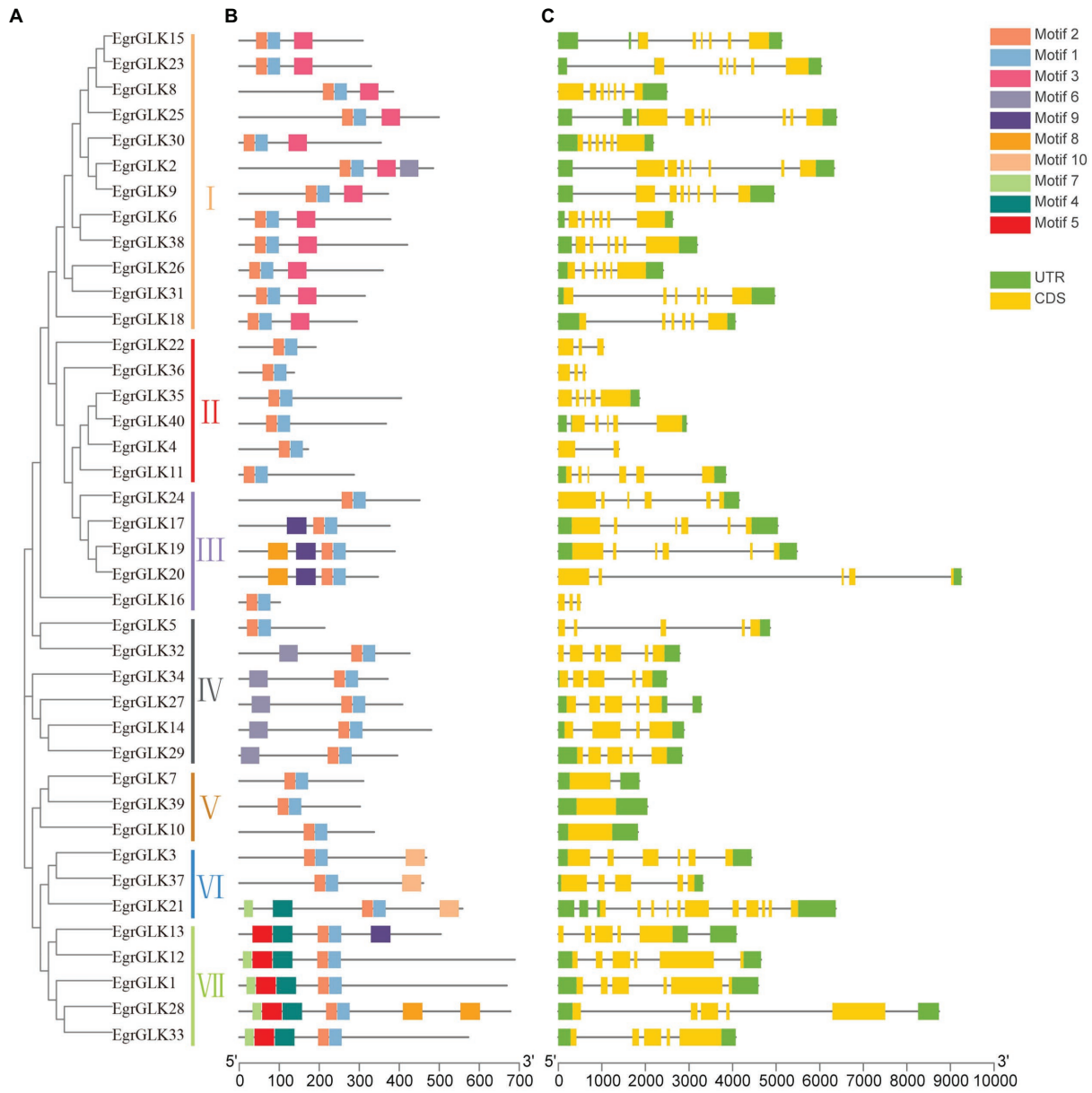

FIGURE 4
Phylogenetic tree, conserved motifs, and gene structure of *EgrGLK* genes of *E. grandis*. **(A)** Phylogenetic reconstruction for *EgrGLK* proteins. **(B)** Ten conserved motifs indicated by different colors. **(C)** Gene structure with exons and introns indicated.

tissues. Notably, many *cis*-regulatory elements consisted of two or more copies in the 2 kb upstream region, which may enhance their binding to the corresponding transcription factors.

Leaf chlorophyll content of diploid and triploid *Eucalyptus urophylla*

Triploid *E. urophylla* and its diploid control were used to measure the chlorophyll content in young, mature, and senescent leaves (Figure 6). The trend in chlorophyll content of the different leaves of the diploid and triploid clones was identical. With increase in leaf age, the chlorophyll content initially increased and then decreased, thus the chlorophyll content was highest in mature leaves. The leaf chlorophyll content was higher in the triploid than in the diploid, and in young and mature leaves the chlorophyll content of the triploid was significantly higher than that of the diploid.

Expression analysis of *EgrGLK* genes in leaves of diploid and triploid *Eucalyptus urophylla*

To explore the influence of *EgrGLK* gene expression on chlorophyll synthesis in diploid and triploid *E. urophylla*,

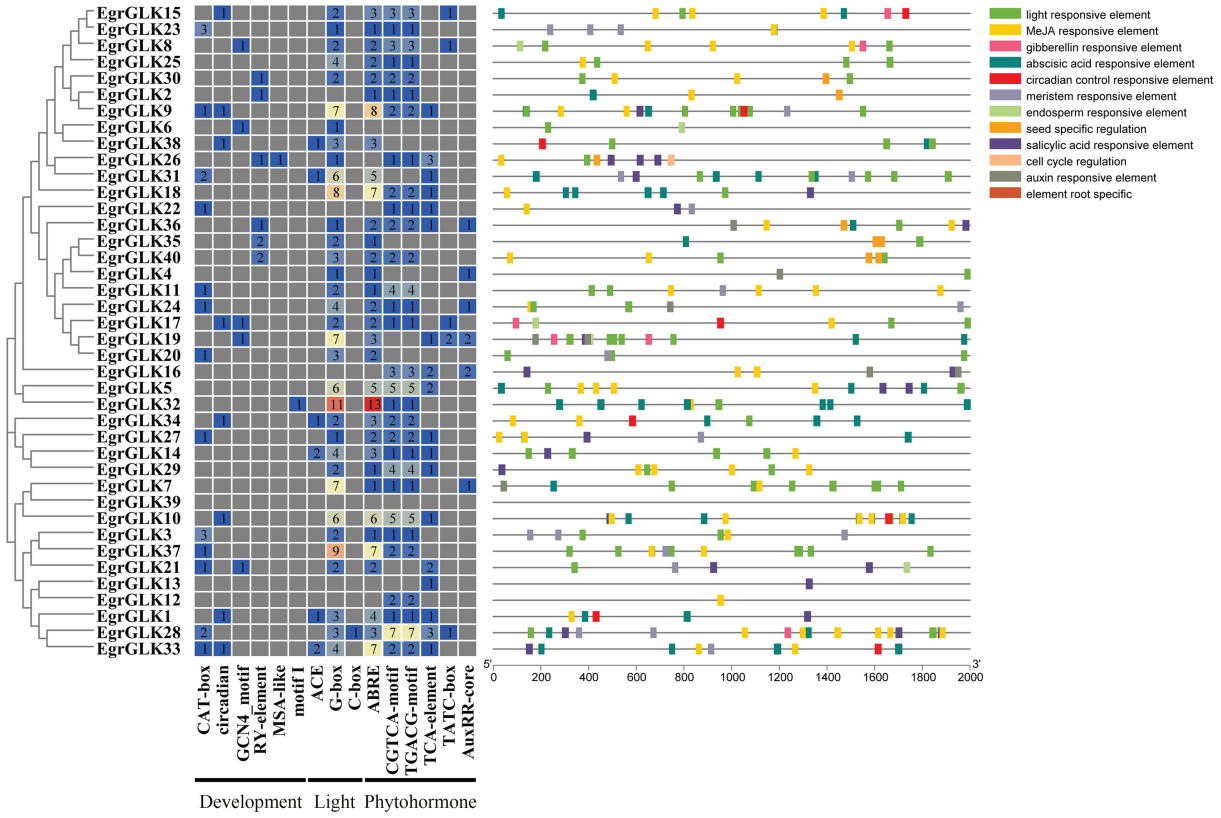

FIGURE 5
Analysis of *cis*-acting regulatory element in promoter regions of *EgrGLK* genes of *E. grandis*. Numerals in different color boxes indicate the number of the main *cis*-elements of *EgrGLK* genes. *Cis*-elements of different responsive types are indicated by different colors.

transcriptome data from leaves of four developmental stages (terminal buds, young leaves, mature leaves, and senescent leaves) were used to analyze the transcript abundance. The transcripts of 36 *EgrGLK* genes were detected in the leaves. Then, the GO term classification and enrichment analysis of 36 *EgrGLK* genes were performed. The first twenty GO terms were shown in the Supplementary Figure S2 according to the significance of enrichment. And the most enriched five GO terms were 'regulation of transcription', 'DNA-binding transcription factor activity', 'transcription', 'DNA binding' and 'nucleus'. Among them, there were 35 and 33 *EgrGLK* genes involved in 'nucleus' and 'regulation of transcription', respectively, indicating that *EgrGLK* genes mainly functions as transcription factors in the nucleus.

The expression data for these 36 *EgrGLK* genes were $\log_2$-transformed and used to generate a clustered heatmap to visualize the expression patterns at each leaf developmental stage (Figure 7). The 36 *EgrGLK* genes were divided into four and three groups in diploid and triploid *E. urophylla*, respectively. Ten *EgrGLK* genes were included in group I of the diploid and 15 *EgrGLK* genes were included in group I of the triploid, which exhibited low transcript levels at each developmental stage. Group IV of the diploid and group III of the triploid contained 15 and 10 *EgrGLK* genes, respectively, and exhibited relatively high transcription levels. Group III of the diploid and group II of the triploid contained eight and 11 *EgrGLK* genes, respectively, and these genes exhibited high transcript abundance in all analyzed leaves, hinting that these genes were essential in *E. urophylla* leaves. It was noteworthy that *EgrGLK6*, *EgrGLK35*, and *EgrGLK40* were grouped in group II of the diploid. These three genes showed low transcript abundance in terminal buds and young leaves, and high expression levels in mature and senescent leaves. The same expression patterns of *EgrGLK6*, *EgrGLK35*, and *EgrGLK40* were observed in leaves of the triploid; however, the differential expression of these three *EgrGLK* genes in the triploid was more moderate than in the diploid, hence they were not clustered into a separate group. In general, the expression patterns of most *EgrGLK* genes in leaves of the diploid and triploid were approximately identical.

Differential expression analysis of *EgrGLK* genes in leaves of diploid and triploid *Eucalyptus urophylla*

To further explore the effect of differential expression of *EgrGLK* genes on chlorophyll synthesis in leaves of *E. urophylla* of different ploidies, the expression data for the *EgrGLK* genes in diploid *E. urophylla* leaves were used as the control group, and the fold change in expression between triploid leaves and diploid

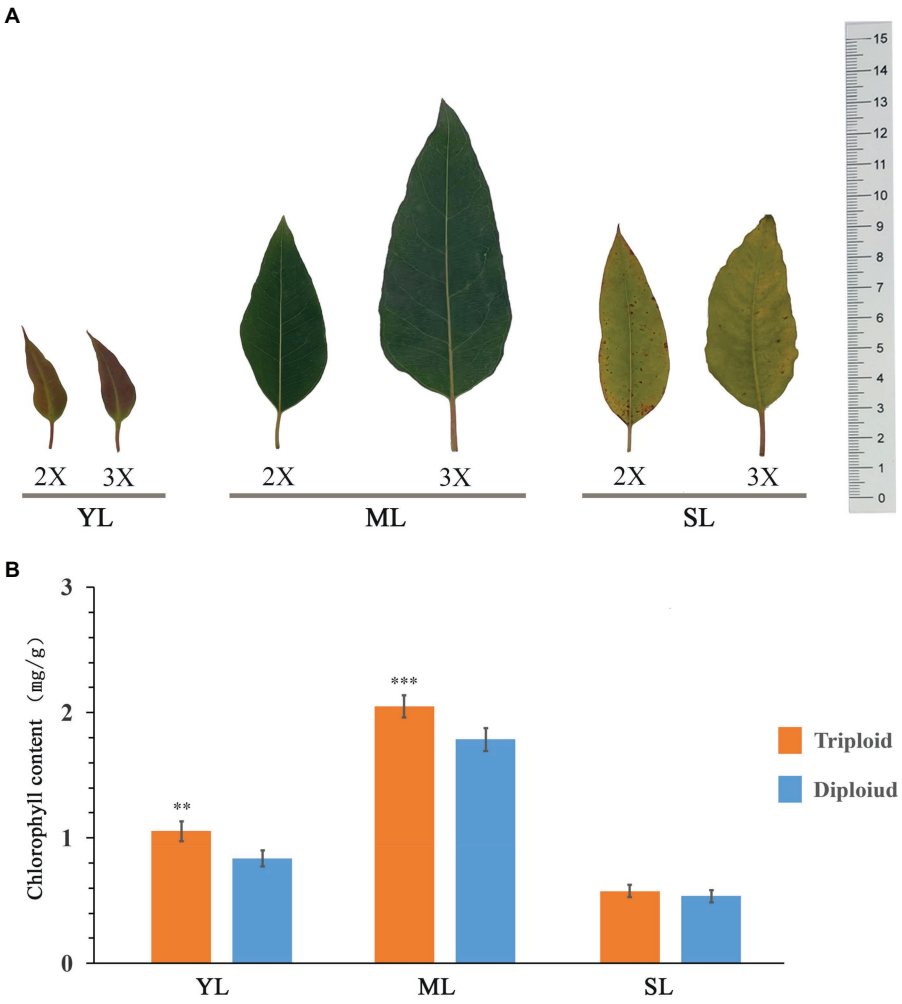

FIGURE 6
Measurement of chlorophyll content in leaves of *E. urophylla*. Phenotype **(A)** and chlorophyll content **(B)** of young leaves (YL), mature leaves (ML), and senescent leaves (SL) of diploid (2X) and triploid (3X) clones.

leaves was used to generate heat maps (Figure 8). More than half of the *EgrGLK* genes were down-regulated in terminal buds of triploid *E. urophylla*. In contrast, 30, 24, and 28 *EgrGLK* genes were upregulated in young, mature, and senescent leaves of triploid *E. urophylla* (Supplementary Table S7). Among the genes highly expressed in leaves that were common to diploid and triploid *E. urophylla* (Figure 7, *EgrGLK23*, *EgrGLK30*, *EgrGLK3*, *EgrGLK37*, *EgrGLK15*, *EgrGLK25*, and *EgrGLK39*), *EgrGLK3*, *EgrGLK15*, *EgrGLK25*, *EgrGLK37* and *EgrGLK39* were upregulated in triploid young (1.03, 1.05, 1.10, 1.01 and 1.04 fold change, respectively), mature (1.77, 1.22, 2.03, 1.48 and 1.46 fold change, respectively), and senescent leaves (1.04, 1.13, 1.91, 1.24 and 1.84 fold change, respectively), and down-regulated in triploid terminal buds (Figure 8). Three genes were highly expressed only in the triploid, of which *EgrGLK1* and *EgrGLK9* showed the same differential expression pattern as the common highly expressed genes, and the other gene (*EgrGLK27*) was upregulated in all analyzed leaves. To further confirm the effect of polyploidization on gene expression, genes upregulated in triploid including *EgrGLK3*, *EgrGLK15*, *EgrGLK25*, *EgrGLK37* and *EgrGLK39* were selected for qRT-PCR analysis (Supplementary Figure S3). Correlation analysis showed that there was a high correlation coefficient between qRT-PCR and RNA-seq ($R^2 = 0.826$, $p < 0.01$), indicating that the differential expression of *EgrGLK* genes among different ploidies was reliable. Differential expression of *EgrGLK* genes provided preliminary information for the study of chlorophyll synthesis and leaf development of *E. urophylla* with different ploidies.

Co-expression network analysis

Transcriptome data for genes associated with chlorophyll synthesis and the *EgrGLK* genes were used for a correlation analysis to explore the role of *EgrGLK* genes in chlorophyll synthesis (Supplementary Table S8). The transcriptome data for

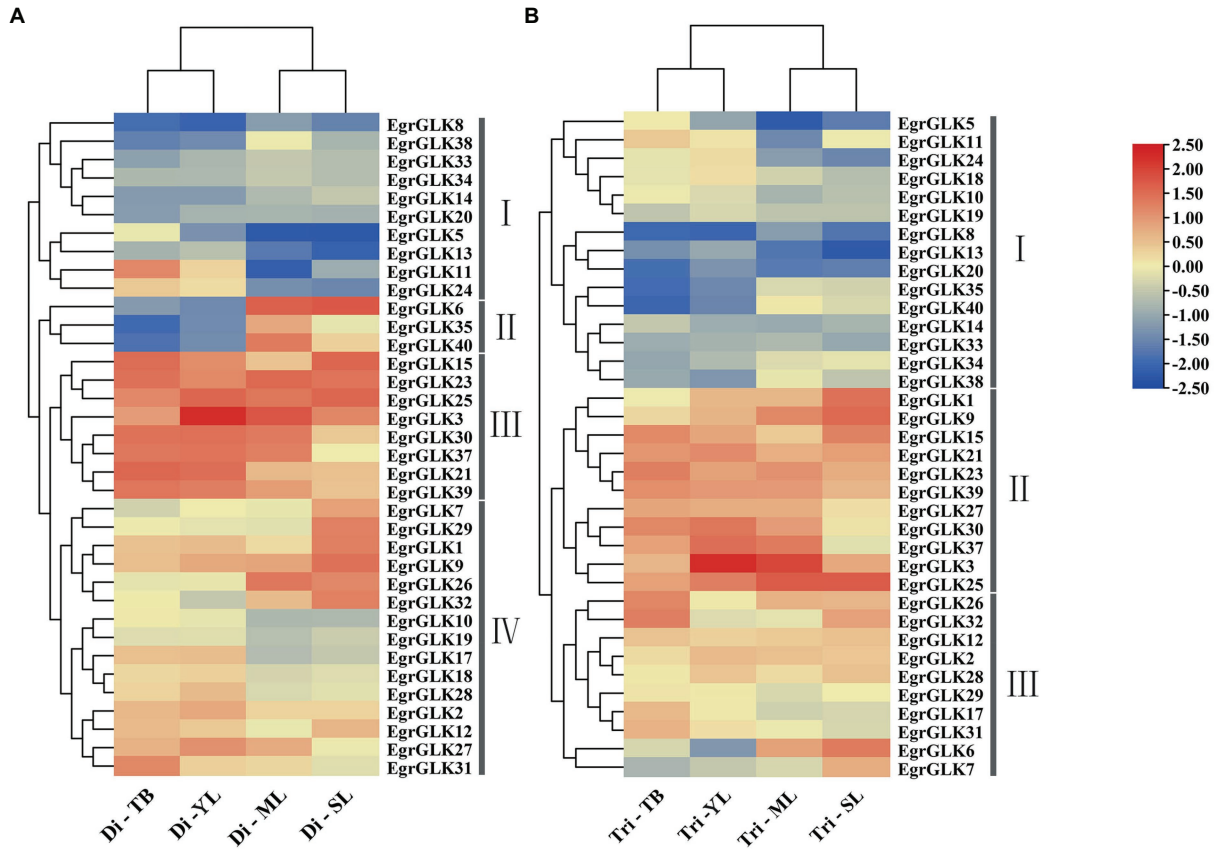

FIGURE 7
Expressions patterns of *EgrGLK* genes in leaves of *E. urophylla*. The expression patterns of *EgrGLK* genes in the terminal bud (TB), young leaves (YL), mature leaves (ML), and senescent leaves (SL) of diploid **(A)** and triploid **(B)** clones.

chlorophyll synthesis related genes and *EgrGLK* genes that were highly correlated ($r \geq 0.6$ or ≤ -0.6) were used to generate co-expression networks (Figure 9). Twenty-five *EgrGLK* genes and 21 chlorophyll synthesis related genes were involved in the positive correlation co-expression network, forming a total of 115 correlation network lines. Among these genes, *EgrGLK3* and *EgrGLK37* were correlated with 17 and 16 chlorophyll synthesis related genes, respectively. The negative correlation co-expression network incorporated 14 *EgrGLK* genes and 16 chlorophyll synthesis related genes, forming a total of 36 correlation network lines. Among these genes, *EgrGLK32* was correlated to 10 chlorophyll synthesis related genes. These results showed that *EgrGLK* genes and chlorophyll synthesis related genes were mainly positively correlated, and thus that *EgrGLK* genes may play a positive regulatory role in chlorophyll synthesis.

Prediction of miRNAs targeting *GLK* genes

In plants, microRNAs (miRNAs) have been found to play important roles in the regulation of gene expression at the post-transcriptional level. We predicted the miRNAs targeting *EgrGLK* genes to further reveal the possible reasons for the differential expression of *EgrGLK* genes in different ploidies. In previous studies, 179 miRNAs were found in leaves (Lin et al., 2018), of which 85 miRNAs from 23 families were involved in the regulation of 31 *EgrGLK* genes (Supplementary Table S9). According to the targeting relationship between miRNAs and *EgrGLK* genes, 12 regulatory networks were generated and they were divided into 5 groups (Figure 10). Figure 10A showed the most complex regulatory network containing 52 miRNAs and 16 *EgrGLK* genes, while six miRNAs in Figure 10E showed the simplest regulatory network in the type of one-to-one target gene. *EgrGLK3*, *EgrGLK32* and *EgrGLK37* has been identified as the genes that play an important role in chlorophyll synthesis, and there were nine, four and one miRNAs targeting these three genes, respectively. In addition, five *EgrGLK* genes including *EgrGLK10*, *EgrGLK27*, *EgrGLK35*, *EgrGLK29*, *EgrGLK31* with the most targeting relationships were found and they were regulated by 15, 11, 8, 8 and 8 miRNAs, respectively. These results suggest that miRNAs play an important role in the regulation of *EgrGLK* gene expression.

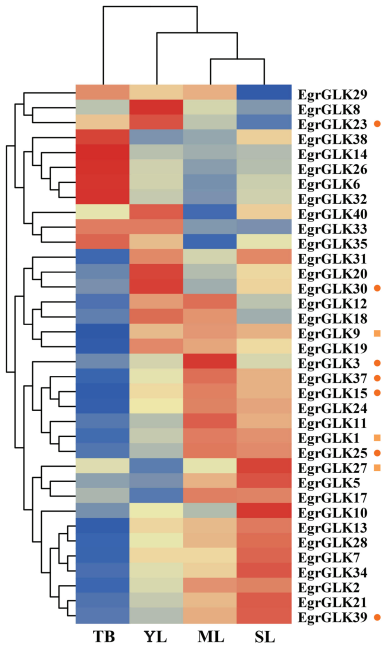

FIGURE 8
Differential expression of *EgrGLK* genes in the terminal bud (TB), young leaves (YL), mature leaves (ML), and senescent leaves (SL) of diploid and triploid clones. Circles represent highly expressed genes common to the diploid and triploid clones, and squares represent genes highly expressed only in the triploid clone.

Discussion

In this study, 40 *EgrGLK* genes were identified in the *E. grandis* genome (Supplementary Table S2). The number of *EgrGLK* genes was less than the number of *GLK* genes identified in Arabidopsis (55), maize (59), and tomato (66) (Liu et al., 2016; Alam et al., 2022; Wang et al., 2022). It was suspected that some *EgrGLK* genes were lost during evolution (Du et al., 2022). It was observed that the number of *GLK* family members was independent of genome size. The diversity of *GLK* family members in different species may be influenced by genome duplication events, such as whole-genome duplication, segmental duplication, or tandem duplication (Zhang, 2003; Chang and Duda., 2012). In the present study, five segmental duplication gene pairs were identified among the *EgrGLK* genes, indicating that segmental duplication was the main contributor to expansion of *GLK* genes in *E. grandis* (Figure 1). It has previously been reported that segmental duplication is more common than tandem duplication in the *GLK* gene family, thus the former might play an important role in chloroplast evolution (Song et al., 2016; Wu et al., 2016). The synteny relationships of *GLK* genes between *E. grandis* and other species showed that the number of homologous gene pairs between *E. grandis* and dicotyledons was much more than that between *E. grandis* and monocotyledons, indicating that *GLK* gene family has been amplified after differentiation between dicotyledon and monocotyledon (Figure 2). The *EgrGLK* genes were classified into seven groups based on a phylogenetic analysis (Figure 3), which

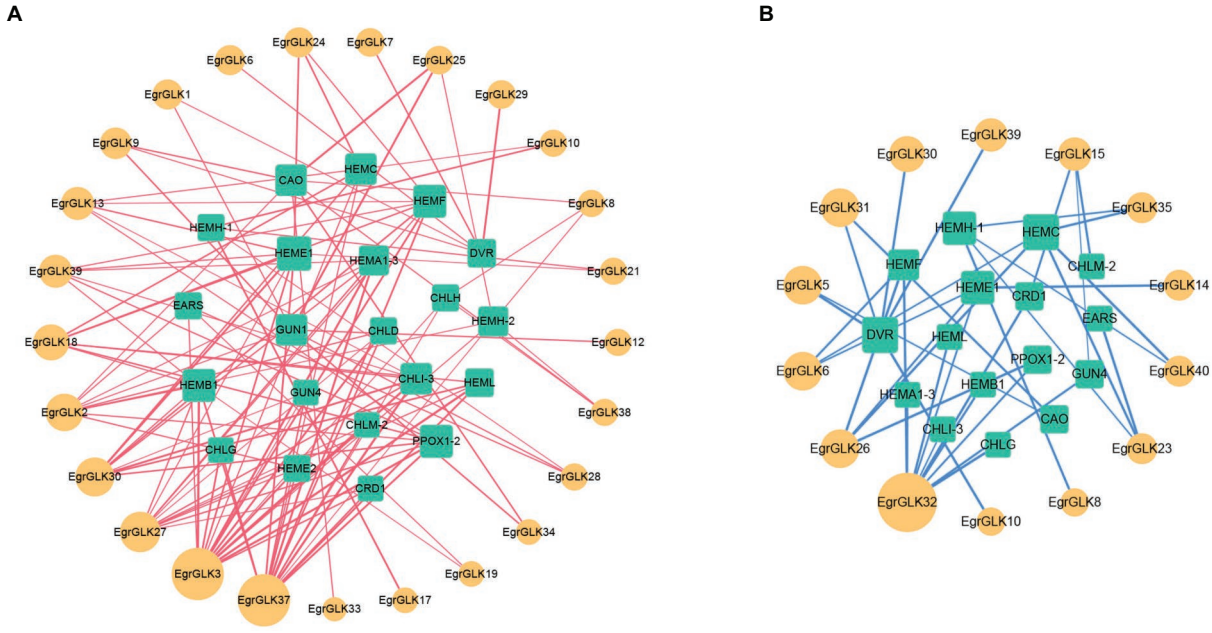

FIGURE 9
Co-expression network of *EgrGLK* genes and chlorophyll synthesis related genes. Positive correlation network **(A)** and negative correlation network **(B)** between *EgrGLK* genes and chlorophyll synthesis related genes. Circles represent *EgrGLK* genes, squares represent chlorophyll synthesis related genes, and the size of the circle or square represents the number of relationships between genes.

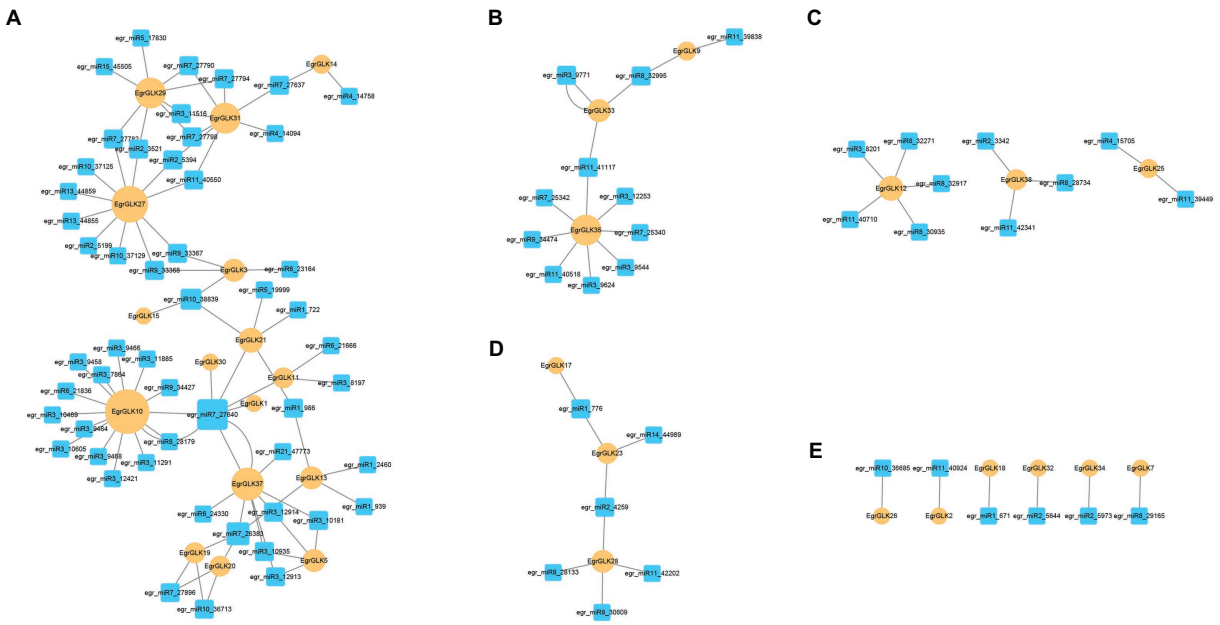

FIGURE 10
Regulatory networks were divided into **(A–E)** according to the number of targeting relationship between miRNAs and *EgrGLK* genes.

was consistent with the classification of *GLK* genes in Arabidopsis (Alam et al., 2022). This result indicated that, although some *EgrGLK* genes were lost during evolution, the sufficient genetic diversity has been retained in *E. grandis*.

As previously reported, the structural characteristics of gene families may reflect their evolutionary trends (Haas et al., 2008; Nie et al., 2022), whereas the conserved motifs reflect their protein-specific functions (Lai et al., 1998; Yang et al., 2021). The 40 *EgrGLK* genes were divided into seven groups, and the gene structure and motif arrangement of the genes in the same group were similar (Figure 4). This finding indicated that the *EgrGLK* genes in the same group might have similar functions (Li et al., 2022; Liang et al., 2022). In the current study, seven motifs were functionally annotated using the NCBI Web CD-Search Tool, which have also been detected in the *GLK* family members in tobacco (Qin et al., 2021). Thus, excluding the *GLK* motifs, other motifs detected in the *GLK* proteins were also relatively conserved. Moreover, group VI was the only group that contained three conserved *GLK* motifs; this phenomenon may enhance the regulatory role of these three *EgrGLK* genes as transcription factors.

The *cis*-acting elements may be activated by *trans*-acting elements to regulate the activity of the target genes (Valli et al., 2022). Among the *cis*-acting elements detected in the promoter regions of *EgrGLK* genes (Figure 5), elements associated with development were only sporadically distributed in the promoter regions, whereas elements involved in light response and hormone response were observed in the promoter regions of almost all *EgrGLK* genes. The motifs involved in methyl jasmonate response comprised the CGTCA-motif and TGACG-motif, which were the most frequent *cis*-regulatory elements identified. These motifs play important roles in multiple physiological processes, including development, senescence, and response to diverse environmental stresses (Browse and Howe, 2008; Wang et al., 2011). The G-box was indicated to be the most widely distributed element. The G-box element may be unique to light regulation and is a ubiquitous element in functionally diverse genes (Menkens et al., 1995; Waters et al., 2009). These results suggested that *EgrGLK* genes are controlled by light and phytohormones (Nakamura et al., 2009; Lupi et al., 2019). The diversity of types, quantity, and distribution of *cis*-acting elements in the gene promoters reflects the complex response regulatory mechanism and complex evolutionary relationships of the *EgrGLK* genes.

The *GLK* genes play an important role in chloroplast development and chlorophyll synthesis (Fitter et al., 2002; Chen et al., 2016). The expression pattern of *GLK* family genes in *E. urophylla* leaves that differ in chlorophyll content was studied to explore the effect of the genes on chlorophyll synthesis. The chlorophyll content in young and mature leaves of triploid *E. urophylla* was significantly higher than that of the diploid clone. Such an increase in chlorophyll content has been observed in other polyploid plants, such as *Populus* and *Rhododendron fortunei* (Liao et al., 2016; Mo et al., 2020). Thirty-six *EgrGLK* genes were expressed in leaves of both diploid and triploid *E. urophylla*. The *EgrGLK* genes not expressed in the leaves might be tissue-specific genes (Deveaux et al., 2003; Lim et al., 2012). The 36 *EgrGLK* genes in the diploid and triploid clones were divided into four and three groups, respectively, based on transcriptome data. The genes *EgrGLK6*, *EgrGLK35*, and

EgrGLK40 in leaves of the diploid were clustered in group II, but did not form a separate group in the triploid (Figure 7). The promoter regions of these *EgrGLK* genes in group II of the diploid contained *cis*-acting elements associated with the seed and endosperm (Figure 5). Triploids are characterized by sterility and thus whether the differential expression pattern of these three genes is associated with triploid sterility requires further study (Fujiwara and Beachy, 1994). Except for group II, other groups in the diploid showed the same expression pattern as in the triploid, which could be divided into low, relatively high, or high expression levels based on the expression data (Figure 7). Compared with the diploid, three additional genes in the triploid were clustered into the high-expression-level group. The high expression levels of a greater number of genes in polyploids might be caused by the participation of duplicated genes derived from whole-genome duplication (Jackson and Chen, 2010; Roulin et al., 2013). The high expression levels of *EgrGLK1*, *EgrGLK9*, and *EgrGLK27* in the triploid may be one factor that promotes the increase in chlorophyll content in leaves of triploid *E. urophylla*.

The differential expression of *GLK* genes in leaves also affects chloroplast development and chlorophyll synthesis (Nguyen et al., 2014). In Arabidopsis, overexpression of *GLK* genes increases the chlorophyll content in leaves (Waters et al., 2009). In the present study, *EgrGLK* genes were differentially expressed in triploid and diploid *E. urophylla* leaves (Figure 8). In the terminal bud, most *EgrGLK* genes in the triploid were down-regulated compared with the diploid, whereas in young, mature, and senescent leaves, more than two-thirds of the *EgrGLK* genes were up-regulated in the triploid. The down-regulation of *EgrGLK* genes in the terminal bud of the triploid did not affect the chlorophyll content of mature leaves, and the chlorophyll content of mature leaves was significantly higher in the triploid than in the diploid (Figure 6). The chlorophyll content in leaves increases gradually with increase in leaf age before the leaves are fully developed and attain maturity (Bertamini and Nedunchezhian, 2002; Du et al., 2020). This is consistent with the present results for *E. urophylla*, indicating that the chlorophyll content might be associated with the expression of *EgrGLK* genes during leaf development. The chlorophyll content of young, mature, and senescent leaves of the triploid was higher than that of diploid. The differential expression of *EgrGLK* genes in leaves of *E. urophylla* of different ploidies was consistent with the trend in chlorophyll content. To further verify the relationship between *EgrGLK* gene expression and chlorophyll synthesis, co-expression networks of the *EgrGLK* genes and chlorophyll synthesis related genes were generated (Figure 9). The networks indicated that *EgrGLK* genes may positively regulate chlorophyll synthesis (Waters et al., 2008; Brand et al., 2014; Zubo et al., 2018). In addition, based on the number of correlations between *EgrGLK* genes and chlorophyll synthesis related genes, three important *EgrGLK* genes were identified. *EgrGLK37* and *EgrGLK3* were involved in the positive correlation network and *EgrGLK32* was included in the negative correlation network (Figure 9). Among these genes, *EgrGLK37* and *EgrGLK3* showed high expression levels in leaves, whereas *EgrGLK32* showed relatively high expression levels in leaves (Figure 7). The present results provide a reference for further studies of the relationship between *EgrGLK* genes and chlorophyll synthesis.

Mature miRNA combines with the RNA-induced silencing complex, which interacts with target genes to regulate the expression of genes by inhibiting gene translation or degrading targeted mRNAs (Baulcombe, 2004). In this study, 85 miRNAs targeting *EgrGLK* genes were predicted, which is almost half of the miRNAs in leaves found in previous study (Lin et al., 2018). *EgrGLK10*, *EgrGLK27*, *EgrGLK29*, *EgrGLK31*, *EgrGLK35 and EgrGLK37* are all regulated by more than eight miRNAs, of which five *EgrGLK* genes do not belong to the group with high transcription level (Figure 7). The result confirmed the inhibitory effect of miRNA on gene expression (Pappas Mde et al., 2015; Unnikrishnan and Shankaranarayana, 2020). *EgrGLK37* is a gene regulated by nine miRNAs but with high expression level. And it is speculated that *EgrGLK37* may also be affected by other regulatory mechanisms, such as lncRNA (Lin et al., 2019; Chen et al., 2021). In addition, *EgrGLK37* was also found to be associated with the most chlorophyll related genes in the co-expression network, indicating that *EgrGLK37* may play an important role in the gene expression regulation network. In this study, three types of miRNAs were found, including one to multiple target genes, one to one target gene and multiple miRNAs to a common target gene, which is consistent with the results found in previous miRNA studies (Lin et al., 2018). Differential expression of *EgrGLK* genes among different ploidies have been proved in our study and the regulation of miRNA may also be one of the reasons for the change of gene expression after plant polyploidization.

Conclusion

In this study, *GLK* transcription factors of *E. grandis* were systematically analyzed using bioinformatic methods. Forty *EgrGLK* genes were identified in the *E. grandis* genome and were divided into seven groups according to the gene structure and motif composition. The number of *EgrGLK* genes is less than the number of *GLK* genes identified in other species, but the sufficient genetic diversity has been retained in *E. grandis*, which indicates that *GLK* proteins exhibit strong evolutionary conservation across diverse species. Analysis of phenotypic and transcriptome data for leaves at different developmental stages in diploid and triploid *E. urophylla* revealed a positive correlation between *EgrGLK* genes and chlorophyll synthesis. On the basis of a differential expression analysis, it was speculated that the increase in chlorophyll content in leaves of triploid *E. urophylla* may be caused by up-regulation of *EgrGLK* gene expression. In addition, three *EgrGLK* genes that may play an important role in chlorophyll synthesis were identified. The present research provides valuable information for further functional

characterization of *EgrGLK* genes in *Eucalyptus*. In the future, increasing the expression of *GLK* gene in plants by polyploidy or other methods may promote photosynthesis and growth of plants, which is of great value to improve plant yield.

Data availability statement

The data presented in the study are deposited in the GEO repository, accession number GSE207860.

Author contributions

JY and XK conceived and designed the research. ZL, TX, and YZ conducted the experiments. ZL, BQ, and HC collected and analyzed the data. ZL and JY wrote the manuscript. XK provided the valuable suggestions on the manuscript. All authors contributed to the article and approved the submitted version.

Funding

This research was supported by the National Natural Science Foundation of China (31901337) and the National Key R&D Program of China during the 14th Five-year Plan Period (2021YFD2200105).

Conflict of interest

The authors declare that the research was conducted in the absence of any commercial or financial relationships that could be construed as a potential conflict of interest.

Publisher's note

All claims expressed in this article are solely those of the authors and do not necessarily represent those of their affiliated organizations, or those of the publisher, the editors and the reviewers. Any product that may be evaluated in this article, or claim that may be made by its manufacturer, is not guaranteed or endorsed by the publisher.

Supplementary material

The Supplementary materials for this article can be found online at: https://www.frontiersin.org/articles/10.3389/fpls.2022.952877/full#supplementary-material

References

Alam, I., Wu, X., Yu, Q., and Ge, L. (2022). Comprehensive genomic analysis of G2-Like transcription factor genes and their role in development and abiotic stresses in *Arabidopsis*. *Diversity* 14, 228. doi: 10.3390/d14030228

Allario, T., Brumos, J., Colmenero-Flores, J. M., Iglesias, D. J., Pina, J. A., Navarro, L., et al. (2013). Tetraploid Rangpur lime rootstock increases drought tolerance via enhanced constitutive root abscisic acid production. *Plant Cell Environ.* 36, 856–868. doi: 10.1111/pce.12021

Baulcombe, D. (2004). RNA silencing in plants. *Nature* 431, 356–363. doi: 10.1038/nature02874

Bertamini, M., and Nedunchezhian, N. (2002). Leaf age effects on chlorophyll, Rubisco, photosynthetic electron transport activities and thylakoid membrane protein in field grown grapevine leaves. *J. Plant Physiol.* 159, 799–803. doi: 10.1078/0176-1617-0597

Bhutia, K. L., Nongbri, E. L., Gympad, E., Rai, M., and Tyagi, W. (2020). In silico characterization, and expression analysis of rice Golden 2-Like (OsGLK) members in response to low phosphorous. *Mol. Biol. Rep.* 47, 2529–2549. doi: 10.1007/s11033-020-05337-2

Booth, T. H., Jovanovic, T., and Arnold, R. J. (2017). Planting domains under climate change for *Eucalyptus pellita* and *Eucalyptus urograndis* in parts of China and South East Asia. *Aust. For.* 80, 1–9. doi: 10.1080/00049158.2016.1275101

Brand, A., Borovsky, Y., Hill, T., Rahman, K. A., Bellalou, A., Van Deynze, A., et al. (2014). CaGLK2 regulates natural variation of chlorophyll content and fruit color in pepper fruit. *Theor. Appl. Genet.* 127, 2139–2148. doi: 10.1007/s00122-014-2367-y

Bravo-Garcia, A., Yasumura, Y., and Langdale, J. A. (2009). Specialization of the Golden2-like regulatory pathway during land plant evolution. *New Phytol.* 183, 133–141. doi: 10.1111/j.1469-8137.2009.02829.x

Browse, J., and Howe, G. A. (2008). New weapons and a rapid response against insect attack. *Plant Physiol.* 146, 832–838. doi: 10.1104/pp.107.115683

Chang, D., and Duda, T. F. Jr. (2012). Extensive and continuous duplication facilitates rapid evolution and diversification of gene families. *Mol. Biol. Evol.* 29, 2019–2029. doi: 10.1093/molbev/mss068

Chen, C., Chen, H., Zhang, Y., Thomas, H. R., Frank, M. H., He, Y., et al. (2020). TBtools: an integrative toolkit developed for interactive analyses of big biological data. *Mol. Plant* 13, 1194–1202. doi: 10.1016/j.molp.2020.06.009

Chen, M., Ji, M., Wen, B., Liu, L., Li, S., Chen, X., et al. (2016). Golden 2-Like transcription factors of plants. *Front. Plant Sci.* 7, 1509. doi: 10.3389/fpls.2016.01509

Chen, H., Li, J., Qiu, B., Zhao, Y., Liu, Z., Yang, J., et al. (2021). Long non-coding RNA and its regulatory network response to cold stress in *Eucalyptus urophylla* S.T.Blake. *Forests* 12, 836. doi: 10.3390/f12070836

Deng, X., Guo, S., Sun, L., and Chen, J. (2020). Identification of short-rotation *Eucalyptus* plantation at large scale using multi-satellite imageries and cloud computing platform. *Remote Sens.* 12, 2153. doi: 10.3390/rs12132153

Deveaux, Y., Peaucelle, A., Roberts, G. R., Coen, E., Simon, R., Mizukami, Y., et al. (2003). The ethanol switch: a tool for tissue-specific gene induction during plant development. *Plant J.* 36, 918–930. doi: 10.1046/j.1365-313X.2003.01922.x

Du, K., Liao, T., Ren, Y., Geng, X., and Kang, X. (2020). Molecular mechanism of vegetative growth advantage in alotriploid *Populus*. *Int. J. Mol. Sci.* 21, 441. doi: 10.3390/ijms21020441

Du, K., Xia, Y., Zhan, D., Xu, T., Lu, T., Yang, J., et al. (2022). Genome-wide identification of the *Eucalyptus urophylla* GATA gene family and its diverse roles in chlorophyll biosynthesis. *Int. J. Mol. Sci.* 23, 5251. doi: 10.3390/ijms23095251

Fitter, D. W., Martin, D. J., Copley, M. J., Scotland, R. W., and Langdale, J. A. (2002). GLK gene pairs regulate chloroplast development in diverse plant species. *Plant J.* 31, 713–727. doi: 10.1046/j.1365-313X.2002.01390.x

Fujiwara, T., and Beachy, R. N. (1994). Tissue-specific and temporal regulation of a β-conglycinin gene: roles of the RY repeat and other cis-acting elements. *Plant Mol. Biol.* 24, 261–272. doi: 10.1007/BF00020166

Gan, P., Liu, F., Li, R., Wang, S., and Luo, J. (2019). Chloroplasts-beyond energy capture and carbon fixation: tuning of photosynthesis in response to chilling stress. *Int. J. Mol. Sci.* 20, 5046. doi: 10.3390/ijms20205046

Haas, B. J., Salzberg, S. L., Zhu, W., Pertea, M., Allen, J. E., Orvis, J., et al. (2008). Automated eukaryotic gene structure annotation using EVidenceModeler and the program to assemble spliced alignments. *Genome Biol.* 9, R7–R21. doi: 10.1186/gb-2008-9-1-r7

Hii, S. Y., Ha, K. S., Ngui, M. L., Ak Penguang, S., Duju, A., Teng, X. Y., et al. (2017). Assessment of plantation-grown *Eucalyptus pellita* in Borneo, Malaysia for solid wood utilisation. *Aust. For.* 80, 26–33. doi: 10.1080/00049158.2016.1272526

Jackson, S., and Chen, Z. J. (2010). Genomic and expression plasticity of polyploidy. *Curr. Opin. Plant Biol.* 13, 153–159. doi: 10.1016/j.pbi.2009.11.004

Kohl, M., Wiese, S., and Warscheid, B. (2011). Cytoscape: software for visualization and analysis of biological networks. *Methods Mol. Biol.* 696, 291–303. doi: 10.1007/978-1-60761-987-1_18

Kumar, S., Stecher, G., Li, M., Knyaz, C., and Tamura, K. (2018). MEGA X: molecular evolutionary genetics analysis across computing platforms. *Mol. Biol. Evol.* 35, 1547–1549. doi: 10.1093/molbev/msy096

Lai, E. C., Burks, C., and Posakony, J. W. (1998). The K box, a conserved 3′ UTR sequence motif, negatively regulates accumulation of enhancer of split complex transcripts. *Development* 125, 4077–4088. doi: 10.1242/dev.125.20.4077

Langdale, J. A., and Nelson, T. (1991). Spatial regulation of photosynthetic development in C_4 plants. *Trends Genet.* 7, 191–196. doi: 10.1016/0168-9525(91)90435-S

Li, Y., Yang, J., Song, L., Qi, Q., Du, K., Han, Q., et al. (2019). Study of variation in the growth, photosynthesis, and content of secondary metabolites in *Eucommia* triploids. *Trees* 33, 817–826. doi: 10.1007/s00468-019-01818-5

Li, X., Zhao, L., Zhang, H., Liu, Q., Zhai, H., Zhao, N., et al. (2022). Genome-wide identification and characterization of CDPK family reveal their involvements in growth and development and abiotic stress in sweet potato and its two diploid relatives. *Int. J. Mol. Sci.* 23, 3088. doi: 10.3390/ijms23063088

Liang, Y., Xia, J., Jiang, Y., Bao, Y., Chen, H., Wang, D., et al. (2022). Genome-wide identification and analysis of bZIP gene family and resistance of TaABI5 (TabZIP96) under freezing stress in wheat (*Triticum aestivum*). *Int. J. Mol. Sci.* 23, 2351. doi: 10.3390/ijms23042351

Liao, T., Cheng, S., Zhu, X., Min, Y., and Kang, X. (2016). Effects of triploid status on growth, photosynthesis, and leaf area in *Populus*. *Trees* 30, 1137–1147. doi: 10.1007/s00468-016-1352-2

Lim, C. J., Lee, H. Y., Kim, W. B., Lee, B.-S., Kim, J., Ahmad, R., et al. (2012). Screening of tissue-specific genes and promoters in tomato by comparing genome wide expression profiles of *Arabidopsis* orthologues. *Mol. Cells* 34, 53–59. doi: 10.1007/s10059-012-0068-4

Lin, Z., Li, Q., Yin, Q., Wang, J., Zhang, B., Gan, S., et al. (2018). Identification of novel miRNAs and their target genes in *Eucalyptus grandis*. *Tree Genet. Genomes* 14, 1–9. doi: 10.1007/s11295-018-1273-x

Lin, Z., Long, J., Yin, Q., Wang, B., Li, H., Luo, J., et al. (2019). Identification of novel lncRNAs in *Eucalyptus grandis*. *Ind. Crop. Prod.* 129, 309–317. doi: 10.1016/j.indcrop.2018.12.016

Liu, F., Xu, Y., Han, G., Zhou, L., Ali, A., Zhu, S., et al. (2016). Molecular evolution and genetic variation of G2-Like transcription factor genes in maize. *PLoS One* 11:e0161763. doi: 10.1371/journal.pone.0161763

Lupi, A. C. D., Lira, B. S., Gramegna, G., Trench, B., Alves, F. R. R., Demarco, D., et al. (2019). *Solanum lycopersicum* Golden 2-Like transcription factor affects fruit quality in a light- and auxin-dependent manner. *PLoS One* 14:e0212224. doi: 10.1371/journal.pone.0212224

Menkens, A. E., Schindler, U., and Cashmore, A. R. (1995). The G-box: a ubiquitous regulatory DNA element in plants bound by the GBF family of bZIP proteins. *Trends Biochem. Sci.* 20, 506–510. doi: 10.1016/S0968-0004(00)89118-5

Mo, L., Chen, J., Lou, X., Xu, Q., Dong, R., Tong, Z., et al. (2020). Colchicine-induced polyploidy in *Rhododendron fortunei* Lindl. *Plan. Theory* 9, 424. doi: 10.3390/plants9040424

Nakamura, H., Muramatsu, M., Hakata, M., Ueno, O., Nagamura, Y., Hirochika, H., et al. (2009). Ectopic overexpression of the transcription factor OsGLK1 induces chloroplast development in non-green rice cells. *Plant Cell Physiol.* 50, 1933–1949. doi: 10.1093/pcp/pcp138

Nguyen, C. V., Vrebalov, J. T., Gapper, N. E., Zheng, Y., Zhong, S., Fei, Z., et al. (2014). Tomato Golden2-Like transcription factors reveal molecular gradients that function during fruit development and ripening. *Plant Cell* 26, 585–601. doi: 10.1105/tpc.113.118794

Nie, Y. M., Han, F. X., Ma, J. J., Chen, X., Song, Y. T., Niu, S. H., et al. (2022). Genome-wide TCP transcription factors analysis provides insight into their new functions in seasonal and diurnal growth rhythm in *Pinus tabuliformis*. *BMC Plant Biol.* 22, 167. doi: 10.1186/s12870-022-03554-4

Pappas Mde, C., Pappas, G. J. Jr., and Grattapaglia, D. (2015). Genome-wide discovery and validation of *Eucalyptus* small RNAs reveals variable patterns of conservation and diversity across species of Myrtaceae. *BMC Genomics* 16, 1113. doi: 10.1186/s12864-015-2322-6

Pérez, S., Renedo, C. J., Ortiz, A., Mañana, M., and Silió, D. (2006). Energy evaluation of the *Eucalyptus globulus* and the *Eucalyptus nitens* in the north of Spain (Cantabria). *Thermochim. Acta* 451, 57–64. doi: 10.1016/j.tca.2006.08.009

Powell, A. L. T., Nguyen, C. V., Hill, T., Cheng, K. L., Figueroa-Balderas, R., Aktas, H., et al. (2012). Uniform ripening encodes a Golden 2-Like transcription factor regulating tomato fruit chloroplast development. *Science* 336, 1711–1715. doi: 10.1126/science.1222218

Qin, M., Zhang, B., Gu, G., Yuan, J., Yang, X., Yang, J., et al. (2021). Genome-wide analysis of the G2-like transcription factor genes and their expression in different senescence stages of tobacco (*Nicotiana tabacum* L.). *Front. Genet.* 12:626352. doi: 10.3389/fgene.2021.626352

Riechmann, J. L., Heard, J., Martin, G., Reuber, L., Jiang, C.-Z., Keddie, J., et al. (2000). *Arabidopsis* transcription factors: genome-wide comparative analysis among eukaryotes. *Science* 290, 2105–2110. doi: 10.1126/science.290.5499.2105

Rossini, L., Cribb, L., Martin, D. J., and Langdale, J. A. (2001). The maize Golden2 gene defines a novel class of transcriptional regulators in plants. *Plant Cell* 13, 1231–1244. doi: 10.1105/tpc.13.5.1231

Roulin, A., Auer, P. L., Libault, M., Schlueter, J., Farmer, A., May, G., et al. (2013). The fate of duplicated genes in a polyploid plant genome. *Plant J.* 73, 143–153. doi: 10.1111/tpj.12026

Song, H., Wang, P., Lin, J.-Y., Zhao, C., Bi, Y., and Wang, X. (2016). Genome-wide identification and characterization of WRKY gene family in peanut. *Front. Plant Sci.* 7:534. doi: 10.3389/fpls.2016.00534

Thompson, J. D., Gibson, T. J., Plewniak, F., Jeanmougin, F., and Higgins, D. G. (1997). The CLUSTAL_X windows interface: flexible strategies for multiple sequence alignment aided by quality analysis tools. *Nucleic Acids Res.* 25, 4876–4882. doi: 10.1093/nar/25.24.4876

Unnikrishnan, B. V., and Shankaranarayana, G. D. (2020). Insights into microRNAs and their targets associated with lignin composition in *Eucalyptus camaldulensis*. *Plant Gene* 24:100248. doi: 10.1016/j.plgene.2020.100248

Valli, H., Prasanna, D., Rajput, V. S., Sridhar, W., Sakuntala, N. N. V., Harshavardhan, P., et al. (2022). Cis elements: added boost to the directed evolution of plant genes. *J. Pure Appl. Microbiol.* 16, 663–668. doi: 10.22207/jpam.16.1.68

Vilasboa, J., Da Costa, C. T., and Fett-Neto, A. G. (2019). Rooting of eucalypt cuttings as a problem-solving oriented model in plant biology. *Prog. Biophys. Mol. Biol.* 146, 85–97. doi: 10.1016/j.pbiomolbio.2018.12.007

Wang, P., Fouracre, J., Kelly, S., Karki, S., Gowik, U., Aubry, S., et al. (2013). Evolution of Golden 2-Like gene function in C_3 and C_4 plants. *Planta* 237, 481–495. doi: 10.1007/s00425-012-1754-3

Wang, Y., Liu, G. J., Yan, X. F., Wei, Z. G., and Xu, Z. R. (2011). MeJA-inducible expression of the heterologous JAZ2 promoter from Arabidopsis in *Populus trichocarpa* protoplasts. *J. Plant Dis. Prot.* 118, 69–74. doi: 10.1007/BF03356384

Wang, Y., Tang, H., Debarry, J. D., Tan, X., Li, J., Wang, X., et al. (2012). MCScanX: a toolkit for detection and evolutionary analysis of gene synteny and collinearity. *Nucleic Acids Res.* 40:e49. doi: 10.1093/nar/gkr1293

Wang, Z. Y., Zhao, S., Liu, J. F., Zhao, H. Y., Sun, X. Y., Wu, T. R., et al. (2022). Genome-wide identification of Tomato Golden 2-Like transcription factors and abiotic stress related members screening. *BMC Plant Biol.* 22, 82. doi: 10.1186/s12870-022-03460-9

Waters, M. T., Moylan, E. C., and Langdale, J. A. (2008). GLK transcription factors regulate chloroplast development in a cell-autonomous manner. *Plant J.* 56, 432–444. doi: 10.1111/j.1365-313X.2008.03616.x

Waters, M. T., Wang, P., Korkaric, M., Capper, R. G., Saunders, N. J., and Langdale, J. A. (2009). GLK transcription factors coordinate expression of the photosynthetic apparatus in *Arabidopsis*. *Plant Cell* 21, 1109–1128. doi: 10.1105/tpc.108.065250

Wu, S., Wu, M., Dong, Q., Jiang, H., Cai, R., and Xiang, Y. (2016). Genome-wide identification, classification and expression analysis of the PHD-finger protein family in *Populus trichocarpa*. *Gene* 575, 75–89. doi: 10.1016/j.gene.2015.08.042

Xiao, Y., You, S., Kong, W., Tang, Q., Bai, W., Cai, Y., et al. (2019). A GARP transcription factor anther dehiscence defected 1 (*OsADD1*) regulates rice anther dehiscence. *Plant Mol. Biol.* 101, 403–414. doi: 10.1007/s11103-019-00911-0

Yang, X., Guo, T., Li, J., Chen, Z., Guo, B., and An, X. (2021). Genome-wide analysis of the MYB-related transcription factor family and associated responses to abiotic stressors in *Populus*. *Int. J. Biol. Macromol.* 191, 359–376. doi: 10.1016/j.ijbiomac.2021.09.042

Yang, J., Wang, J., Liu, Z., Xiong, T., Lan, J., Han, Q., et al. (2018). Megaspore chromosome doubling in *Eucalyptus urophylla* S.T. Blake induced by colchicine treatment to produce triploids. *Forests* 9, 728. doi: 10.3390/f9110728

Zhang, J. (2003). Evolution by gene duplication: an update. *Trends Ecol. Evol.* 18, 292–298. doi: 10.1016/S0169-5347(03)00033-8

Zhang, J., Liu, Y., Xia, E. H., Yao, Q. Y., Liu, X. D., and Gao, L. Z. (2015). Autotetraploid rice methylome analysis reveals methylation variation of transposable elements and their effects on gene expression. *Proc. Natl. Acad. Sci. U. S. A.* 112, E7022–E7029. doi: 10.1073/pnas.1515170112

Zubo, Y. O., Blakley, I. C., Franco-Zorrilla, J. M., Yamburenko, M. V., Solano, R., Kieber, J. J., et al. (2018). Coordination of chloroplast development through the action of the GNC and GLK transcription factor families. *Plant Physiol.* 178, 130–147. doi: 10.1104/pp.18.00414

frontiers | Frontiers in Plant Science

TYPE Review
PUBLISHED 22 August 2022
DOI 10.3389/fpls.2022.869423

OPEN ACCESS

EDITED BY
Jeremy Coate,
Reed College,
United States

REVIEWED BY
Guanjing Hu,
Iowa State University,
United States
Diego Hojsgaard,
Leibniz Institute of Plant Genetics and Crop Plant Research (IPK), Germany

*CORRESPONDENCE
Sandra Irene Pitta-Álvarez
sandrapitta-alvarez@conicet.gov.ar;
spitta1959@gmail.com
Irene Baroli
ibaroli10@gmail.com
Humberto Fabio Causin
ssvhfc@gmail.com

†These authors have contributed equally to this work and share first authorship

‡These authors have contributed equally to this work and share senior authorship

§These authors have contributed equally to this work and share last authorship

SPECIALTY SECTION
This article was submitted to Plant Breeding, a section of the journal Frontiers in Plant Science

RECEIVED 04 February 2022
ACCEPTED 25 July 2022
PUBLISHED 22 August 2022

CITATION
Tossi VE, Martínez Tosar LJ, Laino LE, Iannicelli J, Regalado JJ, Escandón AS, Baroli I, Causin HF and Pitta-Álvarez SI (2022) Impact of polyploidy on plant tolerance to abiotic and biotic stresses.
Front. Plant Sci. 13:869423.
doi: 10.3389/fpls.2022.869423

Impact of polyploidy on plant tolerance to abiotic and biotic stresses

Vanesa E. Tossi[1,2†], Leandro J. Martínez Tosar[1,2,3†], Leandro E. Laino[1‡], Jesica Iannicelli[4,5‡], José Javier Regalado[1,2‡], Alejandro Salvio Escandón[4‡], Irene Baroli[5,6*§], Humberto Fabio Causin[6*§] and Sandra Irene Pitta-Álvarez[1,2*§]

[1]Laboratorio de Cultivo Experimental de Plantas y Microalgas, Departamento de Biodiversidad y Biología Experimental (DBBE), Facultad de Ciencias Exactas y Naturales, Universidad de Buenos Aires, Ciudad Universitaria, Int. Güiraldes y Cantilo, Buenos Aires, Argentina, [2]Facultad de Ciencias Exactas y Naturales, Consejo Nacional de Investigaciones Científicas y Tecnológicas (CONICET), Universidad de Buenos Aires, Instituto de Micología y Botánica (INMIBO), Ciudad Universitaria, Int. Güiraldes y Cantilo, Buenos Aires, Argentina, [3]Departamento de Biotecnología, Alimentos, Agro y Ambiental (DEBAL), Facultad de Ingeniería y Ciencias Exactas, Universidad Argentina de la Empresa (UADE), Buenos Aires, Argentina, [4]Instituto Nacional de Tecnología, Agropecuaria (INTA), Instituto de Genética "Ewald A. Favret", Buenos Aires, Argentina, [5]Facultad de Ciencias Exactas y Naturales, Consejo Nacional de Investigaciones Científicas y Tecnológicas (CONICET), Universidad de Buenos Aires, Instituto de Biodiversidad y Biología Experimental (IBBEA), Ciudad Universitaria, Int. Güiraldes y Cantilo, Buenos Aires, Argentina, [6]Departamento de Biodiversidad y Biología Experimental (DBBE), Facultad de Ciencias Exactas y Naturales, Universidad de Buenos Aires, Ciudad Universitaria, Int. Güiraldes y Cantilo, Buenos Aires, Argentina

Polyploidy, defined as the coexistence of three or more complete sets of chromosomes in an organism's cells, is considered as a pivotal moving force in the evolutionary history of vascular plants and has played a major role in the domestication of several crops. In the last decades, improved cultivars of economically important species have been developed artificially by inducing autopolyploidy with chemical agents. Studies on diverse species have shown that the anatomical and physiological changes generated by either natural or artificial polyploidization can increase tolerance to abiotic and biotic stresses as well as disease resistance, which may positively impact on plant growth and net production. The aim of this work is to review the current literature regarding the link between plant ploidy level and tolerance to abiotic and biotic stressors, with an emphasis on the physiological and molecular mechanisms responsible for these effects, as well as their impact on the growth and development of both natural and artificially generated polyploids, during exposure to adverse environmental conditions. We focused on the analysis of those types of stressors in which more progress has been made in the knowledge of the putative morpho-physiological and/or molecular mechanisms involved, revealing both the factors in common, as well as those that need to be addressed in future research.

KEYWORDS

abiotic stress, biotic stress, polyploids, whole genome duplication, stress tolerance, plant breeding

Introduction

Most plant lineages have undergone whole genome duplication (WGD) events in their past (Bowers et al., 2003; Paterson et al., 2004; Pfeil et al., 2005; Burleigh et al., 2008; Van de Peer et al., 2009; Shi et al., 2010; Ruprecht et al., 2017), with some lineages experiencing repeated doubling events. The fact that polyploidy shows such a remarkable high frequency of occurrence among plant species is compelling from an adaptive point of view. Comparative distributions of gene duplication times and orthologue divergence times suggest 244 ancient WGD events across *Viridiplantae* (Leebens-Mack et al., 2019). The expansions (along with subsequent possible contractions; Simonin and Roddy, 2018) in gene families after WGDs contributed to the dynamic evolution of metabolic, regulatory and signaling networks in polyploids (Maere et al., 2005; Hanada et al., 2008). This plasticity may represent opportunities for adaptation, especially under fluctuations in the selective pressure exerted by the environment, or it may simply provide significant variation for neofunctionalization and the evolution of new species (Schranz et al., 2012). But apart from this alleged role in adaptation and/or speciation in natural conditions, humanity has managed to harness the adaptive potential of genome duplications and applied it to the enhancement of stress resistance and crop production in domestic environments (Renny-Byfield and Wendel, 2014).

The evidence suggesting that environmental robustness is enhanced after WGDs (e.g., Ramsey, 2011; Madlung, 2013; Diallo et al., 2016) is supported by the fact that many WGD events can be historically correlated with periods of dramatic environmental change, usually leading to mass extinctions (Fawcett et al., 2009; Vanneste et al., 2014a,b; Cannon et al., 2015; Huang et al., 2016; Lohaus and Van de Peer, 2016; Yu et al., 2017). For example, the Cretaceous-Paleogene boundary (66 Mya) is linked to several cataclysmic events causing major climatic changes that ultimately led to the loss of roughly two thirds of animal and plant biodiversity (Petersen et al., 2016). Interestingly, this era gave rise to a wave of WGD events that affected most taxa in plants (mainly in angiosperms, and more limitedly in gymnosperms and non-seed vascular plants; Mable et al., 2011). Retention of gene duplicates after WGDs in this period appears to correlate with functions linked to adaptation to low temperatures and darkness, two environmental factors believed to be of great influence at the time (Wu et al., 2020b). It has been suggested that at least a fraction of this apparent enrichment in WGDs taking place around certain cataclysmic global events might have actually preceded the environmental turmoil by millions of years (Robertson et al., 2017; Van de Peer et al., 2021 and references therein). However, the multiplicity of dating correlations between WGDs and events of worldwide dramatic environmental change strongly supports the notion of a causative link between the two, i.e., that polyploidization might notably enhance plant fitness in the midst of harsh stressful conditions.

Provokingly, the adaptive potential derived from the plasticity shown by natural polyploids in the face of the stress imposed by environmental changes can also be regarded as a two-way phenomenon, in which the environmental stress can also facilitate the occurrence of WGD events. The production of unreduced gametes is the main mechanism that gives rise to polyploidy in nature (Chen and Ni, 2006; Soltis and Soltis, 2009). Interestingly, the frequency of occurrence of unreduced gametes has been observed to be significantly increased by changes in environmental stressors such as temperature (Mason et al., 2011; Pecrix et al., 2011; De Storme et al., 2012), nutrient shortage and leaf wounding (e.g., Sora et al., 2016), and virus-induced disease (Kostoff, 1933). Though these observations remain to be validated for other types of stress, this adds plausibility to a causative effect of general environmental changes on the frequency of WGD events.

Polyploids can be classified as autopolyploids or allopolyploids, and these can be either natural or artificial (chemically-induced; Meru, 2012; Hegarty et al., 2013). Autopolyploids result from the doubling of one chromosome set within one species; whereas in allopolyploids, chromosome sets of different species can combine through hybridization events and, subsequently, increase their number through duplication events. During polyploidization, structural and functional changes in genomes such as chromosomal rearrangements (Osborn et al., 2003; Chen et al., 2007; Xie et al., 2010; Xiong et al., 2011; Wang et al., 2012), gene loss (Buggs et al., 2009, 2012; Emery et al., 2018), epigenetic reprogramming (i.e., DNA methylation and histone modifications; e.g., Jackson and Chen, 2010; Sehrish et al., 2014; Yoo et al., 2014; Zhou et al., 2021), and miRNAome alterations (Liu and Sun, 2019), can have a huge impact on gene expression. Among the many genomic responses to merging and/or doubling, changes in the activity of transposable elements (TEs) seem to play a key role in the adaptation to different stresses by modification of the expression of stress-related genes (Quadrana et al., 2019). Environmental changes or stress can result in the proliferation of highly mutagenic TEs due to a transient relief of gene silencing (Kashkush et al., 2003; Madlung et al., 2005; Tittel-Elmer et al., 2010; Lopes et al., 2013; Willing et al., 2015; Springer et al., 2016; Edger et al., 2017), and also to the presence of specific activator sequences in TE promoters (Galindo-González et al., 2017). Particularly, genomic TE content frequently increases after polyploidization events, usually affecting specific TE families which may be more susceptible to activation (McClintock, 1984; Yaakov and Kashkush, 2012). While genome shock caused by interspecific hybridization has been considered as the main trigger of changes in genomic (and conversely TE) dynamics (see Hegarty et al., 2006; Parisod et al., 2009), long terminal repeat (LTR) retrotransposons have been shown to be activated following WGD also in autopolyploids (Bardil et al., 2015). TEs contain internal promoters to facilitate their own expression, therefore, the insertion of TEs within or close to genes can alter the expression of neighboring genes by providing additional transcription factor binding sites or alternative promoters and splicing signals (Lisch, 2013). Interestingly, TE integrations are frequently not random, and it has been shown that some LTR-retrotransposons preferentially target environmentally responsive genes (Quadrana

et al., 2019), generating new genetic or epigenetic variability that could facilitate adaptation to stressful conditions. In particular, TE-driven upregulation of stress-responsive genes has been reported in the case of aluminum tolerance genes, as well as in genes involved in the response to diseases in pepper and wheat (reviewed in Blasio et al., 2022), among others (see also below).

An interestingly feedback regulation between polyploidy-induced epigenetic modifications and stress-responsive gene expression changes has been recently proposed by Wang et al. (2021), as a general mechanism for polyploid plants and crops to respond and adapt to environmental and climate challenges during evolution and domestication. In this context, it is worth mentioning that stress response in plants involves priming, which is an adaptive strategy to increase survival capacity in response to rapidly changing environments. Upon stress, plants can evoke many changes at physiological, metabolic, transcriptional, and epigenetic levels, which allow them to augment responses that help increase stress tolerance (e.g., Schwachtje et al., 2019). Particularly, changes in DNA methylation have been involved in priming by altering the expression of TEs proximal to stress-related genes, whose transcription in turn was affected, altering plant susceptibility against biotic stress (e.g., Le et al., 2014). In line with these findings, Wang et al. demonstrated that, in rice plants, polyploidy may repress proximal TEs through histone modifications, leading to CHH hypomethylation by the RNA-directed DNA methylation (RdDM) pathway. Under salt stress (the first salt treatment), CHH hypomethylation "primes" stress-related genes, including those in jasmonic acid (JA) biosynthesis and related signaling pathways, for more rapid and stronger activation in tetraploid than in diploid plants, thus improving salt-stress tolerance in the former. In turn, highly expressed stress-related genes may derepress neighboring TEs, triggering CHH hypermethylation to further silence these TEs. After stress removal, the abundance of JA-related gene transcripts in tetraploids returns to a level similar to that in diploid plants, while the hypomethylated state of CHH from tetraploids before the first salt treatment is also partially retained. After recurrent salt stress, tetraploid stress-related genes are more strongly induced and subsequently hypermethylated in a process similar to the one mentioned above, thus enhancing their adaptation to the imposed stress condition.

In addition to providing new regulatory sequences, TEs can also be the source of small RNAs (sRNAs) that affect gene expression (Nieto Feliner et al., 2020). Small RNAs, including microRNAs (miRNAs) and different classes of small interfering RNAs (siRNAs) are endogenous 21–22 nt-long RNAs which play an essential role in regulating gene expression in different developmental processes, by targeting mRNAs for repression at the transcriptional and post-transcriptional level (Bartel, 2004; He and Hannon, 2004; Khraiwesh et al., 2012). MicroRNAs involved in the regulation of the expression of stress-related genes in a protective fashion have been detected in different plant species. Notably, when plants undergo WGD, miRNA families expand (Maher et al., 2006; Ha et al., 2009; Kenan-Eichler et al., 2011), and the study of the differential expression of known miRNAs or the detection of novel miRNAs in polyploids could be crucial for the understanding of how polyploidy can render species more tolerant to stressful environments.

Considering the significant challenges humanity is facing in relation to food supply and climate change, understanding the role that polyploidy plays in enhancing plant tolerance to various types of stress and in expanding the range of conditions for plant establishment may lead to better breeding and crop-improvement strategies. In the next sections we will review the current literature regarding the association between plant polyploidy and tolerance to different abiotic and biotic stresses, with an emphasis on the distinct mechanisms responsible for these effects, where available. We will examine whether WGD may be directly related to improved stress tolerance and we will evaluate the impact of ploidy level on plant survival and production, particularly in crop species with intrinsic agronomic value or that are essential for different industrial processes. Given the wide range of environmental stress factors faced by plants, we focused on those factors in which the most progress has been made in the knowledge of the putative morpho-physiological and/or molecular mechanisms involved, revealing aspects in common, as well as remaining questions that need to be addressed in future research. A summary of the cited as well as other related studies and their primary conclusions can be found Supplementary Tables 1–5.

Genome duplication and abiotic stress tolerance

Water deficit stress

Impact of water deficit stress

Water availability is one of the main environmental factors limiting growth and development in plants (Bohnert et al., 1995; Bray, 1997; Gupta et al., 2020), rendering drought tolerance a major challenge for agriculture and ecosystem health, especially in the context of climate change and increasing food demand, and making this kind of abiotic stress the most studied worldwide. The fact that a doubling of the drought risk for world crop production has been predicted (Li et al., 2009b), emphasizes the need to design new crop management techniques and the development of more drought tolerant plant varieties. Drought is a difficult term to define but, in general, plants will be under water deficit stress when the available soil water is insufficient to meet their demand. This imbalance can be dynamic and may provoke short-term physiological acclimation responses or lead to long-term adaptive mechanisms (Chaves et al., 2003; Verslues et al., 2006). The latter may involve drought avoidance strategies, such as early flowering, in order to complete the life cycle before the start of the dry season. In the short term, water deficit affects primarily the physiological processes of transpiration and photosynthesis, and, because it influences cell expansion, cell division, plant hydraulics, hormone homeostasis and gene expression, it can lead to

long-term changes on vegetative growth and reproductive development (Tardieu et al., 2018). The magnitude and consequences of the damage due to water deficit will depend on the time of initiation, duration and intensity of the drought. In crops, when it occurs during the reproductive stage, drought can result in yield losses of more than 40% (Boyer, 1982).

The evidence strongly indicates that polyploidy promotes drought tolerance in plants (see Supplementary Table 1). However, the literature is not conclusive in terms of a single mechanism by which WGD can lead to such tolerance. Some component of it is most certainly due to the larger cell size caused by polyploidy, affecting not only the size of the roots for water absorption and the thickness of leaves for water release, but also the size and number of stomata and of xylem vessels, which together control the capacity for water movement in the continuum soil–plant-atmosphere, and hence, the plant's response to water deficit. On the other hand, transcriptomic results point to gene dosage or gene transcription effects on the content of abscisic acid and its signaling components, metabolic changes leading to osmolyte accumulation, as well as an increase in antioxidant capacity, allowing the polyploid plant to cope with the higher risk of oxidative damage caused by water deficit and closed stomata.

In the following sections we examine the available information regarding the effect of polyploidy on the main processes and traits that are known to be involved in the response to water deficit.

Anatomical changes and resource allocation

Plants deploy multiple strategies in response to water deficit stress to attain different degrees of tolerance (Bohnert et al., 1995; Gupta et al., 2020). Most tolerant plants respond to drought by reducing the rate of water loss, either physiologically by decreasing stomatal conductance or anatomically by increasing the leaf cuticle thickness or by reducing the exposed leaf area, for example through leaf rolling or abscission or by increasing mesophyll thickness. Probably owing to their larger cell size, polyploid plants are known to constitutively show some of those alterations leading to tissue water conservation, a fact that could partially explain their observed drought tolerance. For example, Li et al. (1996) reported a significant increase in the thickness of the lower and upper leaf epidermis and a higher degree of pubescence in drought-tolerant pentaploid and hexaploid *Betula papyrifera*, compared to the diploid. Similar observations were made when comparing tetraploid *Lonicera japonica* (Li et al., 2009a) and tetraploid apple (Wójcik et al., 2022) with their respective diploids, and in these cases the tetraploids also showed a thicker palisade tissue.

Another strategy by which plants maintain a balance between water uptake and transpiration entails modifying the resource allocation from shoots to roots, by developing a deeper root system which enables them to explore larger soil volumes (Poorter et al., 2012). Reports on the impact of polyploidy on root biomass or architecture are very scarce, and hence make it impossible to generalize. A significant constitutive increase in root/shoot biomass ratio has been shown in tetraploid *Citrus limonia* (Allario et al., 2011), which could lead to enhanced drought tolerance, however, to our knowledge this has not been tested. In *A. thaliana* tetraploids, a 20% root biomass increase has been observed, although in this case the effect was dependent on culture conditions (Del Pozo and Ramirez-Parra, 2014) and the tetraploid's tolerance to water deficit may have been conferred by hormonal rather an anatomical changes (see below).

Water transport capacity

Plants subjected to water deficit also respond by altering hydraulic conductivity, either through the modification of xylem conducting properties and suberization of the endodermis, or by regulating the expression and function of aquaporins, which are membrane intrinsic proteins that control the cell's water permeability and whose transcription and activation respond to environmental cues (Steudle, 2000; Ehlert et al., 2009; Chaumont and Tyerman, 2014; Tardieu et al., 2018). The impact of polyploidy on cell size can lead to increased xylem vessel diameter, which can improve the hydraulic conductivity of the tissue (Ruiz et al., 2020). But even though larger xylem vessels can be more efficient in water transport, they are also more vulnerable to cavitation under drought. In *Chamerion angustifolium*, a herbaceous perennial with natural diploid and tetraploid genotypes occupying different ecological niches, Maherali et al. (2009) found that the drought tolerant tetraploids had larger xylem vessels and higher xylem hydraulic conductivity than diploids, which would allow the former to deplete soil moisture more efficiently before the decrease in soil water potential induces stomatal closure. In contrast, Guo et al. (2016) have shown that *C. angustifolium* natural hexaploids, which also display larger xylem conduits than the diploid, were less tolerant to drought, presumably due to a higher susceptibility to the risk of embolisms caused by water deficit. Thus, at the moment nothing conclusive can be stated about the effect of increased vessel diameter on the drought tolerance reported for some polyploids.

The bigger cell size and more active metabolism of polyploids (Doyle and Coate, 2019) can lead to roots with thicker cortexes or more heavily suberized endodermis, both factors that limit the radial hydraulic conductivity of roots and diminish water uptake, delaying plant mortality under drought by conserving the resource in the soil for longer periods (Steudle, 2000). Allario et al. (2011) reported a doubling of the root cortex width in tetraploid *Citrus limonia*, but provide no information on whether this correlates with tolerance to water deficit. On the other hand, the presence of thicker suberin in the root endodermis has been correlated with enhanced tolerance to water deficit in tetraploid citrus rootstocks (see Ruiz et al., 2020 and references therein).

Regarding the potential influence of polyploidy on water transport mediated by aquaporins, whole-genome transcriptomic studies have not revealed significant changes in aquaporin gene expression upon drought stress in *Citrus limonia* (Allario et al., 2011, 2013) nor *A. thaliana* (Del Pozo and Ramirez-Parra, 2014), nor in apple polyploids (Wójcik et al., 2022). Moreover, Zhang et al. (2015) reported that, while the aquaporin genes *MdPIP1: 1*

and *MdTIP1: 1* were upregulated in leaves of apple seedlings subjected to water deficit, their expression levels were consistently lower in tetraploid than in diploid genotypes. Thus, the evidence to date does not suggest that aquaporins mediate the cases of drought tolerance conferred by polyploidy.

Regulation of osmolyte content

At the cellular level, plants can maintain turgor under water deficit conditions by accumulating osmotically active metabolites in a process known as osmotic adjustment. Most of the literature on polyploids and water deficit do not provide measurements of osmolyte accumulation but rather report the leaf relative water content, which is an indirect indicator of osmotic adjustment in tissues (Mullan and Pietragalla, 2012). Several authors reported on higher relative water content in polyploids in comparison with diploids, either when well-watered (Tal and Gardi, 1976) or under water deficit conditions (Xiong et al., 2006; Allario et al., 2011; Del Pozo and Ramirez-Parra, 2014; Zhang et al., 2015). In agreement with this notion, Khalid et al. (2021) and Lourkisti et al. (2022), observed an enhanced accumulation of osmolytes under water deficit in different polyploid citrus species. Another, older study on naturally occurring *Betula papyrifera* polyploids showed that they were more capable of maintaining turgor at low tissue water potentials than the corresponding diploids, although the authors did not provide direct evidence on the existence of osmotic adjustment (Li et al., 1996).

Stomatal function and transpiration rates

Stomatal pores are the main sites of water loss at the whole plant level. While stomatal closure helps to conserve water, it can also impose limits to photosynthetic CO_2 uptake, thus leading to decreased biomass accumulation and crop yield (Tardieu et al., 2018). Changes in stomatal conductance as well as in anatomical features like stomatal size, density and/or distribution have been proposed as the most important mechanisms of control of water use efficiency (defined as the amount of carbon gained relative to the amount of water used; see Hetherington and Woodward, 2003; Lawson and Blatt, 2014; Franks et al., 2015; Leakey et al., 2019). Stomatal movements are driven by changes in turgor pressure, a process that is under the control of the hormone abscisic acid (ABA), among other factors (Wilkinson and Davies, 2002).

Stomatal size and density vary within species and are controlled in part by environmental cues, including light quality/intensity, and CO_2 partial pressure (Faralli et al., 2019). Lower stomatal densities correlate with lower transpiration rates, and significant improvement of water use efficiencies have been demonstrated in transgenic plants with fewer stomata (Franks et al., 2015; Hughes et al., 2017). Regarding polyploidy, it is widely accepted that genome size correlates positively with stomatal size and negatively with stomatal density (Beaulieu et al., 2008), and fewer and larger stomata have been found in most, if not all, polyploids analyzed to date. The observation that polyploidy and reduced transpiration rates may be linked was made early on (Chen and Tang, 1945; Tal and Gardi, 1976), and many reports show that this in turn could have a positive impact on tolerance to water deficit by delaying wilting (Supplementary Table 1; Allario et al., 2011, 2013; Del Pozo and Ramirez-Parra, 2014). Most of the available evidence to explain how the lower transpiration rates come about in polyploids points to two main factors: fewer and larger stomata on the leaf epidermis and differential levels of ABA accumulation, transport or sensitivity. It has also been shown that the size of stomata influences the kinetics of stomatal movements, probably by affecting surface-to-volume ratios of guard cells and the efficiency of solute transport to drive movement, with smaller stomata responding more rapidly to environmental or hormonal stimuli (Drake et al., 2013). However, comparative information on stomatal kinetics for the larger stomata of polyploids is very limited, with one report in *A. thaliana* showing that natural and synthetic tetraploids, although possessing stomata of similar size, differed in stomatal kinetics and overall conductance (Monda et al., 2016).

ABA homeostasis

The regulation of transpiration by ABA involves long-distance transport from roots to shoots, and local modulation of ABA concentration at the stomatal guard cells (Wilkinson and Davies, 2002; Chaves et al., 2003; Kuromori et al., 2018). Besides the structural effect that lower stomatal densities can have on stomatal conductance and water conservation, several lines of evidence also highlight the existence of an altered ABA homeostasis in polyploids, suggesting that changes in ABA regulation may be related to their enhanced tolerance to drought. In *A. thaliana*, genome duplication does not appear to cause significant differences in ABA concentration *per se* (Monda et al., 2016), however, several reports have shown a constitutive upregulation in tetraploids of a number of genes involved in ABA metabolism and signaling, as well as other genes involved in the response to drought (Del Pozo and Ramirez-Parra, 2014, 2015; Li et al., 2017). Moreover, although several drought-induced genes (bearing ABA-responsive motifs) are greatly upregulated under drought treatment in both diploid and tetraploid genotypes, some of these transcripts are over-represented in the absence of drought in tetraploids (Del Pozo and Ramirez-Parra, 2014), suggesting that, at least in this species, polyploids may be primed for stress tolerance by having a pre-activated ABA response. Similarly, and compared with the corresponding diploids, constitutively increased ABA concentrations were found in roots of tetraploid *Citrus limonia* (Allario et al., 2013) and in leaves of tetraploid *Lycium ruthenicum* (Rao et al., 2020). Since whole-genome transcriptomic comparisons of diploids with their polyploids grown under normal growing conditions have been restricted to these few species, it is not possible at the moment to generalize about such a priming effect.

Antioxidant capacity

Severe water deficit conditions can affect cellular redox homeostasis and lead to symptoms of progressive oxidative stress (Tardieu et al., 2018). Low internal CO_2 partial pressure in leaves

of droughted plants (due to closed stomata) can increase the accumulation of reactive oxygen species (ROS) derived from overreduction of the photosynthetic electron transport chain, and from the stimulation of the photorespiratory pathway. A frequently reported response of plants exposed to severe drought (and other types of stress, see below) involves changes in the expression and activities of major antioxidant enzymes such as superoxide dismutase (SOD), catalase (CAT), and/or ascorbate and guaiacol peroxidases (APX and POD), as well as changes in key ROS scavengers such as ascorbate and glutathione (Pan et al., 2006; Noctor et al., 2014; Demidchik, 2015). Several reports point to a higher antioxidant activity in polyploids. Yang et al. (2014) showed that the improved drought tolerance of two lines of colchicine-induced rice tetraploids correlated with increased antioxidant capacity when compared to the diploid line. Similar results were reported by Deng et al. (2012) when comparing *Nicotiana benthamiana* octaploids and diploids subjected to similar degrees of water deficit. An increased ROS detoxification capacity was also found in tetraploid *A. thaliana* (Li et al., 2017). More recently, this enhanced antioxidant capacity was reported in synthetic autotetraploid apple, which showed higher APX expression than the diploid under drought (Wójcik et al., 2022), and in autotetraploid *Ziziphus jujuba*, where the higher activity of antioxidant enzymes correlated with a lower degree of oxidative damage to cell membranes (Li et al., 2021). Taken together, these findings suggest the involvement of gene dosage or other gene-expression altering effects in the regulation of antioxidant capacity. However, the apparent relationship between ROS detoxification efficiency and the expression of genes involved in the antioxidant response upon drought exposure in polyploids is far from being resolved. Del Pozo and Ramirez-Parra (2014) performed a whole transcriptome expression analysis in *Arabidopsis* and showed that tetraploidy enhances the expression of genes involved in the response to oxidative stress under well-watered conditions, irrespective of the ecotype considered. However, when plants were subjected to drought, the same genes, and also ABA responsive genes, were down-regulated in the tetraploids compared to diploids (Del Pozo and Ramirez-Parra, 2014). Similarly, in a series of experiments performed on *Citrus limonia* diploid and autotetraploid lines, the enhanced drought tolerance of the tetraploid was not associated with large changes in gene expression levels between genotypes, with genes participating in ROS detoxification being down-rather than up-regulated in the tetraploid when compared to the diploid line (Allario et al., 2011, 2013). These results may seem contradictory, but the underlying cause of drought stress tolerance in polyploids may be that gene duplication and gene dosage lead to constitutively higher content of ABA, ROS scavengers and ROS detoxifying enzymes, which may in turn raise the threshold at which the polyploid genotypes start to experience drought stress and express drought-related genes. It is also important to keep in mind that, generally, the comparisons were made in experiments designed not to provide the same degree of water deficit (i.e., same soil water potential) to the contrasting genotypes, but rather after a fixed time period following the cessation of normal watering. Thus, data interpretation may be confounded by the fact that polyploids with low transpiration rates consume less pot water than their diploid counterparts, and thus delay the onset of the soil water deficit necessary for the display of stress symptoms. Controlled drought experiments in which gene expression is evaluated simultaneously with changes in soil water potential are necessary to solve this conundrum.

Temperature stress

Temperature is a key determinant for the geographic distribution of organisms. Particularly, plants can be found within an approximate thermal range of −10°C to 60°C, defined by the freezing point of intracellular water and the temperature of protein denaturation (Fitter and Hay, 2002). Depending on the species, there is an optimum temperature range where growth and developmental processes occur at the highest rate, and beyond which plants should display different responses to cope with either the cold or the heat stress imposed.

Temperature-associated stress affects several developmental processes along the life cycle of plants (Hedhly, 2011). Chilling temperatures, for instance, thermodynamically lower the fluidity of biomembranes and cause marked disturbances in many physiological processes such as water and nutrient uptake, photosynthesis and respiration, all of which severely impair plant productivity (Jouyban et al., 2013). On the other hand, high temperatures can also alter membrane permeability, protein and cytoskeleton stability and chromatin structure, negatively affect respiration and photosynthesis, and impact on floral development and pollen viability, thus decreasing overall plant growth and/or fruit or seed yield (Bita and Gerats, 2013; Dwivedi et al., 2017; Rieu et al., 2017). In the case of crops, it has been reported that the impact of one degree-Celsius increase in global mean temperature would reduce maize, rice, wheat and soybean yields between 3.1% and 7.4% (Zhao et al., 2017a). Given the present context of global warming, strategies aimed to improve plant tolerance and crop yield in the face of increasing temperatures are needed, which makes polyploidy a promising alternative (see Supplementary Table 2).

In the following sections we summarize the research works addressing the effect of polyploidy on plant responses to either cold or high temperature stress, and then we discuss the advances in the knowledge of the possible genetic and/or molecular underlying mechanisms.

Cold stress responses

Different lines of evidence suggest that polyploidization is associated with the expansion of gene families involved in the cold temperature response, an association usually related to the direct effects of cold on diploid and polyploid gamete formation (te Beest et al., 2012). Since cold temperatures may contribute to the formation of polyploidy, cold tolerance may be important for the

survival of newly formed polyploids. Increases in cold stress tolerance have been reported for polyploids of several plant species such as *Hedyotis caerulea*, *Lolium perenne*, *Nicotiana benthamiana, Plumbago articulata,* among others (Sugiyama, 1998; Huang et al., 2007; Deng et al., 2012; Jiang et al., 2020). In colchicine-induced octaploids of *N. benthamiana*, survival time under cold stress increased about 70% when compared to tetraploids, apparently due to an enhancement in oxidative stress management by means of lower H_2O_2 production and a higher ROS scavenging capacity, both under stressful and stress-free conditions. In addition, octaploids showed a higher net rate of photosynthesis than tetraploids under decreased endogenous CO_2 availability (Deng et al., 2012).

A synthetic tetraploid of the ornamental/medicinal shrub *Plumbago auriculata* also showed higher tolerance to a short-term cold stress treatment (24 h, 5°C) than its diploid counterpart (Jiang et al., 2020). This response was associated to anatomical changes in root and, particularly, leaf tissues in the tetraploid (e.g., thickened spongy mesophyll, widened leaf stomata, and an increased guard cell size), which contributed to enhance photosynthetic activity (as estimated by chlorophyll fluorescence parameters) under cold stress. On the other hand, the tetraploid genotype showed a significantly lower level of lipid peroxidation than the diploid, suggesting a better stability of the membrane system, probably due to an enhanced ROS-scavenging capacity.

The correlation between ploidy level and enhanced temperature-stress tolerance is not always straightforward. Lagibo et al. (2005) conducted a comparative analysis of frost tolerance in garden pansy (*Viola* × *wittrockiana* Gams) among different genotypes with multiple levels of ploidy (10x, 14x, and 16x), under field conditions. Two standard octaploid cultivars were used as controls. The authors analyzed changes in pigment content and used chlorophyll fluorescence parameters to evaluate plant tolerance to low and sub-zero temperatures. While a positive correlation was found between ploidy level and pigment production (which is suggestive of greater photochemical activity in polyploids), the genotypes under study responded to frost independently of their ploidy level: hexadecaploids were ranked as sensitive to intermediate, followed by 12x (sensitive), while 10x and 14x genotypes were as tolerant as the 8x controls. These results strongly suggest that physiological and/or molecular mechanisms other than pigment production should be evaluated to better assess the effect of ploidy level on frost tolerance in this species.

Heat stress responses

Regarding heat stress, an increased tolerance to supraoptimal temperatures has been also reported in polyploids of different plant species. For instance, *Dioscorea zingiberensis* tetraploids show enhanced tolerance to high temperatures, in part due to a higher content of antioxidants (particularly ascorbic acid and glutathione) and higher antioxidant enzyme activity than in the diploid (Zhang et al., 2010). Xu et al. (2011) further showed that this species responds with a ploidy-dependent pattern of transcriptomic changes under high temperature conditions, which might contribute to the evolutionary success of polyploids in warmer niches (see Section "Advances in the knowledge of genomic and molecular mechanisms underlying temperature-stress tolerance in polyploids").

Similarly, in a study aimed at comparing the effect of ploidy level on morphological traits, metabolite content, and heat stress-associated gene expression in the medicinal crop *Cnidium officinale*, Kim et al. (2021) reported that synthetic autotetraploids had a higher tolerance to a heat-shock treatment compared to diploids (measured as a lower increase in the expression of a heat-stress marker). Although the mechanistic basis for this response was not elucidated, the higher thermal resistance of the autotetraploid could be related to an increased content of phenolic compounds with strong antioxidant activity (particularly naringin, salicylic acid and gentisic acid) as a result of polyploidization.

Finally, Wei et al. (2020) failed to observe the increase in heat tolerance usually associated with polyploidy, when comparing synthetic autotetraploids and their respective diploids from two wild *Fragaria vesca* subspecies. The authors suggest that their results can be explained by a resource allocation toward growth and clonal reproduction in the greenhouse environment where the trial was conducted. In those conditions, the observed elevated cell injury under heat-stress in the polyploids was positively correlated with the increase in clonal reproduction in response to genome doubling. This clearly reinforces the idea that stress tolerance following genome doubling is not only taxon-but also environment-dependent.

Advances in the knowledge of genomic and molecular mechanisms underlying temperature-stress tolerance in polyploids

Stressful conditions can have considerable effects on the expression of duplicated genes after a WGD event. This might lead to an overall transcriptional reprogramming enabling a phenotypic plasticity that confers an adaptive advantage to polyploids. For instance, Dong and Adams (2011) demonstrated that heat treatment induced differential expression of three specific homologous genes. In a similar line of evidence, Liu and Adams (2007) reported that only one of the alcohol dehydrogenase homologs in allopolyploid cotton was specifically expressed under cold stress. More recently, Lee and Adams (2020) conducted a thorough transcriptomic analysis on *Brassica napus* (a natural allotetraploid) under cold, heat and drought conditions, and found that stress (especially cold stress) favored gene expression in one parental subgenome (*B. rapa*), while alternative splicing alterations were more frequently found on the other parental subgenome (*B. oleracea*). These results are suggestive of a process where stressful thermal conditions could be a driving force for the preservation of certain homologs in polyploids *via* subfunctionalization.

In an attempt to deepen the knowledge of the molecular mechanisms underlying the increased tolerance to high temperatures in *D. zyngiberensis* polyploids (see above), Xu et al.

(2011) compared transcriptomic changes through sequence-related amplified polymorphism (SRAP)-cDNA and SRAP analysis in diploid and synthetic autotetraploids, prior and after heat-stress. The study revealed that tetraploids developed an "activation transcriptome response" pattern (i.e., a higher proportion of overexpressed transcripts over silenced ones) under high temperature stress, in contrast to a "random transcriptome response" pattern (i.e., a similar ratio of silenced to activated transcripts) found in diploids. According to SRAP analysis, the differences in expression patterns were not due to genetic changes after WGD, but rather to epigenetic and/or post-transcriptional regulatory mechanisms. Although the functional role of the affected genes was not elucidated, it is suggested that the observed ploidy-dependent pattern of transcriptomic response might in part explain the higher temperature tolerance reported for tetraploids. Further research will be necessary to test this hypothesis as well as to reveal more details regarding the molecular mechanisms involved.

In a study on the sequenced genomes of representative species of the Brassicaceae and several model plants (including monocots such as *Oryza sativa* and *Zea mays*, the basal angiosperm *Amborella trichopoda,* the lycophyte *Selaginella moellendorffii* and the moss *Physcomitrella patens*), Song et al. (2020) performed comparative analyses of cold-regulated genes (*CRGs*) to explore their retention, positive selection, expression and involvement in regulatory networks after polyploidy. The authors found that in 17 of the 21 plant species analyzed, polyploidization was the predominant mechanism by which *CRG* homologs originated, accounting for 46%–96% of these homologs in each genome. Most *CRGs* belong to transcription factor families, and their regulatory networks were much larger in plant genomes affected by more polyploidization events. Based on their analyses, the authors conclude that polyploidy plays an important role in resisting the stress imposed by cold. Nevertheless, and despite the available evidence (summarized in Supplementary Table 2), investigations on the underlying molecular mechanisms for increased cold/heat tolerance in polyploids is still scarce, and further research is essential for a better understanding of the role of WGD in this phenomenon.

Salinity stress

Impact of salt stress

Soil salinization is a serious global threat to agricultural production (Ivushkin et al., 2019), especially in arid and semi-arid areas (Shannon, 1998; Martinez-Beltran and Manzur, 2005). At present, salinity affects more than 1 billion hectares of cultivated land, distributed all over the world and involving more than 100 countries (FAO and ITPS, 2015). According to the Fifth Assessment Report of the United Nations Intergovernmental Panel on Climate Change (AR5-IPCC 2015), larger areas will be affected by salinity-related problems in the near future, due, among other causes, to the rise in sea level. In this context, the development of crops more resistant to salinity stress will be fundamental to sustain agricultural production. Different publications show that natural or induced polyploids of some species are more tolerant to salinity stress than diploids (Supplementary Table 3). Thus, polyploidization may have an important role in the development of crops more resistant to this type of stress.

In the following sections we discuss the main physiological mechanisms involved in the acclimation or adaptation responses to salinity stress, and we then discuss recent advances in the knowledge of the genetic and/or molecular processes underlying the effect of polyploidy on salinity stress tolerance.

Salt stress response mechanisms

Among the multiple negative effects caused by salinity stress, the most relevant are water deficit, membrane permeability alterations, ion toxicity, nutrient deficiency and free radical imbalances, all of which affect plant growth, morphology, and survival (Zhu, 2001; Golldack et al., 2014; Zhang et al., 2014; Lu et al., 2017). It is worth noting that several adaptations found in halophytes can also be found in both natural and induced polyploid plants (Supplementary Table 3). Plants use different physiological mechanisms to neutralize Na^+ toxicity, such as limiting its entry into the roots, shuttling it from the cytosol to the apoplastic space, actively accumulating Na^+ into vacuoles, or controlling Na^+ transport in the xylem (Kumari et al., 2015; Mishra and Tanna, 2017). In general, plants that can maintain an adequate cellular ionic balance, but particularly a high K^+/Na^+ ratio, are more tolerant to salinity (Munns and Tester, 2008; Pan et al., 2016). This is particularly evident in *A. thaliana,* where a study involving numerous accessions, including haploid genotypes, natural diploids and natural or induced autotetraploids, showed that ploidy was a significant determinant of leaf K^+ concentration (Chao et al., 2013). Moreover, under moderate salt stress conditions (200 mM NaCl), the increment in leaf K^+ concentration in tetraploid leaves was accompanied by a decrease in Na^+ accumulation, thus enhancing both K^+/Na^+ ratio and salinity tolerance in these genotypes (Chao et al., 2013). This salinity tolerance is not limited to autopolyploids. Polyploid species of the genus *Brassica* were also shown to be more salt-tolerant than their diploid ancestors; this was shown both in allotetraploids (Meng et al., 2011) and autotetraploids (Ashraf et al., 2001).

The role of root cells

Using a reciprocal grafting technique, Rus et al. (2006) showed that *A. thaliana* root cells control leaf K^+ concentration and, consequently, the tolerance to saline stress. Similarly, Chao et al. (2013) demonstrated that the ploidy level of root grafts can exert control over the leaf K^+ concentration regardless of the ploidy level of the rest of the plant. Even though the mechanism involved has not been clearly elucidated, polyploid rootstocks can be used to increase tolerance to saline stress while maintaining the desired agronomic traits of diploid grafts. An example of this can be found

in citrus crops, where the capacity of polyploid rootstocks to exclude Cl-from leaves increased the tolerance to moderate salinity stress (Bañuls et al., 1990; Bañuls and Primo-Millo, 1992, 1995; Saleh et al., 2008).

Reducing the outflow of K^+ induced by NaCl in root cells may contribute to maintain K^+/Na^+ homeostasis in this organ (Shabala and Pottosin, 2014). Potassium outflow from root cells is mediated by three different types of channels: depolarization-activated outward-rectifying K^+-permeable channels (DA-KORCs), weakly voltage-dependent non-selective cation channels (NSCCs) and reactive oxygen species (ROS)-activated K^+-permeable channels (including KORCs and NSCCs; Shabala et al., 2016). Another possible mechanism to maintain K^+/Na^+ ratio under salinity stress is Na^+ exclusion from the cytosol, which is mediated by a plasma membrane Na^+/H^+ antiporter, named salt overly sensitive 1 (SOS1), whose activation is mediated by Ca^{2+} (Sun et al., 2009; Maathuis, 2014; Zhu, 2016). ROS also have an important role in the regulation of Na^+ homeostasis through the stabilization of SOS1 mRNA (Chung et al., 2008), as well as the increase of cytosolic Ca^{2+} concentration due to the activation of plasma membrane Ca^{2+}-permeable channels (Sun et al., 2010; Ma et al., 2012) and the increase in the activity of plasma membrane H^+/ATPase (Zhang et al., 2007; Niu et al., 2018). Polyploidization was shown to affect many of these processes, and, as mentioned above, strategies aimed at maintaining the cellular ion balance, a high K^+/Na^+ ratio, and low levels of toxic ions in leaves and meristematic tissues appear to be a hallmark of such adaptations. Depending on the species, this may involve the regulation of the expression, the activity and/or the sensitivity of specific ion channels in order to particularly facilitate either Na^+ exclusion, K^+ and Ca^{2+} absorption or retention, as well as to regulate Ca^{2+}- dependent signaling pathways (Lu et al., 2006). A summary of the findings reported so far on the impact of ploidy levels on some of these mechanisms (as well as others, see below) can be found in Supplementary Table 3 references therein.

Antioxidants and osmoregulatory metabolites

Another adaptation that plants present to prevent the effects of salinity stress is to stimulate the production of osmotically active metabolites and of enzymatic and/or non-enzymatic antioxidants aimed to counteract the increment of ROS (Hasegawa et al., 2000; Yamada et al., 2005; Munns and Tester, 2008). Under salt stress, several polyploid species showed significant differences in the production of key antioxidants such as glutathione and proline, as well as greater superoxide dismutase (SOD) and peroxidase (POD) activity than the diploid controls (Supplementary Table 3). These changes were correlated with lower contents of malondialdehyde (MDA), a commonly used indicator of lipid peroxidation and membrane damage (Liu et al., 2011; Jiang et al., 2013; Tu et al., 2014; Fan et al., 2016a). On the other hand, transcriptomic and metabolomic studies also highlight the upregulation of metabolic pathways involved not only in antioxidant defense, but also in the synthesis of free amino acids (usually proline, but also methionine, aspartic acid, and arginine, among others), organic acids (e.g., oxaloacetic acid, fumaric acid), polyhydric alcohols (myoinositol, inositol), soluble sugars, polyamines, flavonoids and/or late embryogenesis abundant (LEA) proteins (which are rich in hydrophilic amino acids), as biochemical mechanisms to protect cells from dehydration damage, both in salt-tolerant diploids (e.g., Li et al., 2021; Qin et al., 2022 and references therein) as well as in polyploids (Wang et al., 2018; Sicilia et al., 2019; Zhao et al., 2022; see also below).

Advances in the knowledge of genomic and molecular mechanisms underlying salinity-stress tolerance in polyploids

Recent comparative proteomic and genomic analysis between polyploid plants and their diploid ancestors under high salinity conditions reveal that proteins involved in numerous processes like photosynthesis, stress and defense, energy, metabolism, transcription/translation, and transport may be differentially expressed among genotypes (Podda et al., 2013; Wang et al., 2013b; Deng et al., 2017). A sugar transporter, a chloroplastic ATP synthase delta subunit, and enzymes involved in photosynthesis and ROS scavenging are among the most relevant found to be upregulated in polyploid genotypes of the species studied. Transcriptomic analyses also support the proteomic results, though differences exist depending on the species and experimental conditions tested. For example, in *Paulownia australis* plants treated with 0.2%–0.6% (i.e., 35–100 mM) NaCl solutions for 15 days, the expression of unigenes related to ion transporters, ROS-scavenging system, proline and soluble carbohydrate synthesis, and transcription factors significantly differed between autotetraploid and diploid genotypes (Dong et al., 2017). On the other hand, in two different transcriptomic analyses performed on leaves of *P. tomentosa* diploid and autotetraploid plants grown at different combinations of salt levels and treatment periods, the differentially expressed unigenes (DEU) were assigned to metabolic pathways such as "plant hormone signal transduction," "RNA transporter," "protein processing in endoplasmic reticulum," "photosynthesis process" and "plant-pathogen interaction," among others (Fan et al., 2016a; Zhao et al., 2017b). Interestingly, changes in the expression levels of transcription factors related to stress responses, such as NAC, MYB, bHLH, GRAS, WRKY, and AP2/EREBP were particularly substantial (Zhao et al., 2017b). In addition to the above-mentioned processes, changes in the expression of DEUs involved in osmoregulation (mostly coding for LEA proteins), have been reported between polyploid and diploid genotypes of *P. fortunae* (Wang et al., 2018) and various species from the genus *Agave* (Tamayo-Ordóñez et al., 2016) after exposure to salt stress. The accumulation of LEA proteins may improve salinity tolerance, as they have important roles in preventing desiccation damage and might contribute to the upregulation of certain antioxidant enzymes (Dalal et al., 2009; Huang et al., 2018). Finally, Xue et al. (2015) studied the expression of two aquaporin genes (*MdPIP1: 1* and *MdTIP1: 1*) in leaves from diploid and autotetraploid apple

trees and found that their expression was significantly higher in the polyploids, which also displayed more tolerance to salinity stress than the diploids (note that this is in contrast with the results observed by Zhang et al. (2015) under drought stress mentioned previously) (see sub-section Water transport capacity in section Water deficit stress). The contribution of aquaporins to salinity tolerance has been demonstrated in transgenic plants with constitutive expression of different aquaporin family members (Sreedharan et al., 2013; Xu et al., 2014).

Changes in the expression of miRNAs appear also to contribute to the enhanced tolerance to salt stress of polyploid genotypes. Fan et al. (2016b) and Liu and Sun (2017) studied the differential expression of miRNAs in tetraploid and diploid leaves of *Paulownia fortunei* and *Hordeum bulbosum*, respectively, under salinity conditions. In *P. fortunei*, 10 conserved and 10 novel miRNAs were found to be differentially expressed between the studied genotypes, and the predicted target transcripts of at least eight of these miRNAs corresponded to genes associated with the response to salinity stress. In a survey of changes in the miRNAome of diploid and tetraploid barley (*Hordeum bulbosum*) plants under control (CK) and salt stress conditions, Liu and Sun (2017) reported that 13 miRNAs were differentially expressed due to the genome duplication *per se*. Of these, nine miRNAs were overexpressed in tetraploid CK compared with those in diploid CK plants, while 4 miRNAs were downregulated in the tetraploid as compared with those in the diploid. Interestingly, five of the miRNAs affected by genome duplications were also associated with salt stress. In fact, among these five miRNAs, four (miR171i, miR479, miR5048-5p and miR6196) were upregulated in tetraploid CK compared with those in diploid CK, but miR171i, miR479 and miR5048-5p were downregulated and miR6196 was upregulated in diploid Na-stressed plants with respect to its control. Interestingly, miR528b-3p was only detected in the tetraploid genotype and was downregulated under the stress treatment as compared with the tetraploid CK. The targets of these miRNAs are involved in protection of the photosynthetic machinery against oxidative stress, osmotic stress-activated phospholipid signaling and salt stress response (Liu and Sun, 2017). In view of the results, the authors concluded that, under salt stress, tetraploids have a more elaborate miRNA–target interaction compared with that in diploids, which can help tetraploids to better deal with salt stress while maintaining normal growth. This would be in agreement with physiological data indicating that *H. bulbosum* tetraploids have a stronger ability to retain water and prevent water loss, resulting in better survival under salt stress.

Nutritional stress

Like any other living organism, plants rely on an adequate supply of certain inorganic minerals for optimal development and growth. Nitrogen and phosphorus are macronutrients essential for photosynthesis, metabolism, growth and development, seed yield, and protein and nucleic acid synthesis, among other fundamental processes (Day and Ludeke, 1993; Zhang et al., 2018). Potassium is essential for osmotic and ionic equilibrium and stomatal movements, is involved in chlorophyll biosynthesis and photosynthesis, and it can enhance the resistance of crops to drought, disease and cold (e.g., Wang et al., 2013a; see also sections 1.1 and 1.3). Calcium is also fundamental for cell wall stability, ion homeostasis, the activity of different enzymes, and as a secondary messenger in numerous signaling pathways, among other biological functions (Thor, 2019). As well as for macronutrients, an adequate supply of micronutrients such as iron, copper, manganese, zinc, nickel and molybdenum is necessary for the functioning of key metabolic enzymes and redox systems, while others like boron are important for cell wall synthesis, pollen tube elongation and carbohydrate transport (Assunção et al., 2022). If left unattended, soil deficiencies in any of these and other nutrients can have a severe impact on agricultural productivity and on the nutritious quality of foods. On the other hand, mineral excess, particularly of micronutrients, may lead to the development of toxicity symptoms, which in turn negatively affects plant growth and yield (Assunção et al., 2022). Mineral nutrient acquisition is directly dependent on the demand of the plant (which is conditioned by the growth rate and the internal concentration of the nutrient) and water availability. Increased carbon allocation to root growth and upregulation of specific transporters are among the most frequent responses of plants to nutrient shortage (Lambers and Oliveira, 2019).

In the following sections we examine the available information regarding the effect of polyploidy on plant responses to cope with nutrient deficiency or excess, and in Supplementary Table 4 we summarize the main processes and conclusions discussed.

Plant responses to mineral deficiency

Although the unambiguous translation of an increased ploidy level into an actual enhancement of the overall tolerance of plants to nutritional stress is not sufficiently supported in every case under study, it is interesting to note that an early work from Grant (1952) reported that the rate of polyploid production (due to poor pairing at meiosis) in *Gilia* hybrids grown in low-nutrient conditions was seven-fold greater than that of plants grown in high-nutrient conditions.

Nitrogen starvation is among the main factors limiting plant growth. On the other hand, the abuse of nitrogen (and other mineral-based) fertilizers was shown to have adverse impacts not only on farming, but on the ecosystem as a whole (Kotschi, 2015; Rahman and Zhang, 2018). Hence, strategies aimed at developing crop genotypes with increased N use efficiency are an important alternative to reduce the amount of soil N supplementation. The link between N uptake efficiency and ploidy level is not an obvious one, since some polyploids show higher N contents than their diploid progenitors, while others do not (Noggle, 1946). Under low-nitrogen levels, N assimilation and shoot accumulation in a synthetic allohexaploid wheat was increased with respect to its tetraploid and diploid parents (Yang et al., 2018). This allohexaploid showed a higher root/shoot biomass ratio, higher H^+ efflux and higher

expression of genes lined to N uptake, which may account for the observed differences in tolerance to N deficiency (see Supplementary Table 4). Leps et al. (1980) reported that, in nodulated alfalfa (*Medicago sativa*), tetraploids had higher N fixation rates than diploids during the first 10 days of growth. Interestingly, after that time, both tetraploid and diploid plants fixed N at equal rates. However, increasing the ploidy of alfalfa plants from tetraploid to octaploid did not result in increased N fixation activity or N content.

The efficiency with which roots acquire other nutrients, such as sulfate and potassium, was found to be higher in wheat and sugar beet (but not in tomato) with higher ploidy level (Cacco et al., 1976), compared with their diploid counterparts. The authors correlated the observed uptake efficiency to the level of environmental adaptation of the plants under analysis. In a screen for *Arabidopsis* mutants showing tolerance to nutrient deficiencies, Kasajima et al. (2010) isolated one line that was tolerant to boron deficiency. Ploidy analysis showed this line to be an autotetraploid, although the original screening population was diploid. Furthermore, independently isolated autotetraploid lines were also tolerant to boron deficiency, suggesting that autotetraploidization improves tolerance to boron shortage.

As for most types of environmental stress, nutrient deficiency can increase the susceptibility to oxidative damage, as nutrients are needed for the maintenance of antioxidant activity and cell redox homeostasis (Kandlbinder et al., 2004). In an attempt to develop new citrus rootstocks that require less fertilizer, Oustric et al. (2019) compared the effect of genotype and ploidy level on tolerance to nutrient deficiency in a group of commonly used citrus rootstocks. The experiment was performed on four citrus diploid (2x) seedlings and their four doubled diploid (4x) counterparts. An allotetraploid form was also included in the study. Four-years old trees of each genotype grown under optimal nutrient conditions were divided into two blocks, and irrigated with either the growing fertilizer solution (control) or irrigation water (nutrient deficiency) for a period of 8 months. After analyzing a series of morpho-physiological traits along the experimental period in order to characterize nutrient deficiency symptoms, antioxidant capacity and the level of oxidative damage in the different genotypes, the authors concluded that autotetraploidization did not systematically improve the tolerance to nutrient deficiency, since only one of the 4x seedlings tested showed a significantly different response when compared to its 2x counterpart. Interestingly, the allotetraploid was found as the only resistant genotype, suggesting that allotetraploidization would be a means for increasing tolerance to nutrient deficiency in citrus rootstocks. A better accumulation and/or remobilization of mineral elements related to photosynthesis activity, together with a better performance of the non-enzymatic and enzymatic antioxidant system would account for the increased resistance/tolerance to nutrient deprivation observed in these polyploids.

Plant responses to mineral excess

Tetraploidization can alter root anatomy, which in turn can lead to alterations in the capacity for nutrient uptake. Ruiz et al. (2016) described root abnormalities (shorter length, larger diameter, fewer root hairs, etc.) in tetraploid citrus plants, in comparison to their diploid counterparts (see Supplementary Table 4). While expression of boron transporters was not modified by ploidy, these anatomical root alterations might have been responsible for a decreased boron uptake, leading to boron-excess tolerance in the tetraploid.

In a thorough study by Schlaepfer et al. (2010) native (2x and 4x) and invasive (4x) specimens of *Solidago gigantea* (Asteraceae) were compared in their growth performance and overall response to calcium excess. Diploids grown with additional calcium showed reduced biomass accumulation, whereas tetraploids were not affected. Unfortunately, the physiological and/or molecular mechanism underlying the observed responses remain to be elucidated.

Finally, it is worth mentioning that polyploidization in naturally occurring metal hyperaccumulator plants was shown to expand their habitat (e.g., Prasad and de Oliveira Freitas, 2003; Paape et al., 2020). Hence, the use of either natural or synthetic polyploids could be useful as a genetic tool to develop strategies for the phytoremediation of heavy-metal polluted soils.

UV-B stress

UV radiation is classified in UV-A, -B and-C, according to its wavelength range. While most UV-C radiation is absorbed by the ozone layer, UV-A and UV-B reach the Earth's surface and cause cellular damage by triggering photochemical alterations in DNA sequences and the accumulation of ROS (Hideg et al., 2013). UV-B alone is responsible for a 5% annual reduction in global agricultural production (Ballare et al., 2001; Caldwell et al., 2007). Throughout evolution, plants have developed a number of strategies to avoid and/or cope with the damage caused by UV-B radiation. Examples of these are cuticle thickening, the accumulation of pigments that act as "chemical shields" (e.g., flavonoids, betalains), production and/or activation of antioxidant enzymes and metabolites which neutralize ROS, and the upregulation of photolyases which repair cyclobutyl pyrimidine dimers that accumulate in the DNA (Chen et al., 2019). The plant response to UV-B radiation can be triggered either specifically, by activation of the UV-B receptor UVR8, or nonspecifically *via* ROS accumulation (Rizzini et al., 2011; Wu et al., 2016; O'Hara et al., 2019).

There are extremely few publications linking tolerance to UV-B stress and polyploidy. Hase et al. (2006) reported that tetraploid Arabidopsis plants grow significantly more than their diploid counterparts under UV-B irradiation. Given this difference cannot be linked to a differential accumulation of pyrimidine dimers in both plants, DNA repair mechanisms were ruled out as a relevant phenomenon responsible for the relative tolerance observed in tetraploids. *Pachycladon cheesemanii* is an allotetraploid perennial herb closely related to Arabidopsis. When both plant species were cultivated under

UV-B radiation, Arabidopsis' growth was significantly reduced, while the growth of *Pachycladon* was less affected. Chlorophyll content-usually considered a marker of UV-B tolerance-was significantly increased in *Pachycladon* after UV-B treatment while chlorophyll content in Arabidopsis Col-0 was not. Although the expression levels of genes belonging to the UVR8-dependent pathway were mildly increased in *Pachycladon* under UV-B irradiation, those related to the UVR8-independent pathway broadly increased. This suggests the enhanced UV-B tolerance shown by *Pachycladon* could rely on a yet not fully described UVR8-independent mechanism (Dong et al., 2019).

Finally, it is worth mentioning that the synthesis of flavonoids and other UV-B-absorbing metabolites was shown to be augmented in certain polyploids (Talei and Fotokian, 2020; Wu et al., 2020a), and polyploids also tend to have a higher ROS detoxification capacity than diploids under different stress conditions (see for example Sections "Antioxidant capacity", "Temperature stress", "Antioxidants and osmoregulatory metabolites," and "Plant responses to mineral deficiency").

Impact of endopolyploidy in the UV-B response

Endopolyploidy is a general term describing the multiplication of nuclear DNA within the cell. In plants, this takes place *via* several mechanisms, but mainly through the process of endoreduplication, which involves the replication of DNA without intervening cell divisions and it is often closely associated with specific cell types, organs, and developmental stages (Leitch and Dodsworth, 2017). This phenomenon is widespread among plant taxa, and it has been suggested that it may play some role in stress tolerance (Adachi et al., 2011).

UV-B radiation has been identified as a positive climatic predictor for a high incidence of endopolyploidy (Gegas et al., 2014). During the UV-B response, the endocycle regulation is mediated by UVR8 (Wargent et al., 2009) and by the atypical E2F transcription factor DP-E2F-like 1 (E2Fe/DEL1). Radziejwoski et al. (2011) demonstrated that E2Fe/DEL1 is a transcriptional repressor of PHR1, a photolyase involved in DNA repair. Upon UV-B irradiation the expression of E2Fe/DEL1 is downregulated, which in turn favors PHR1 activity. Better DNA repair allows plants to rapidly resume the endocycle, contributing in this manner to UV-B radiation resistance by compensating the stress induced reduction in cell number by ploidy-dependent cell growth.

The *uvi4* (UV-B-insensitive 4) mutation promotes the progression of endoreduplication during leaf and hypocotyl development. Hase et al. (2006) showed that the fresh weight of *uvi4* Arabidopsis mutants grown under supplemental UV-B light is two-fold greater than that of the wild type plants grown in the same conditions. In addition, Gegas et al. (2014), have demonstrated that Arabidopsis accessions with an increased level of endopolyploidy are more UV-B-tolerant (as evaluated by fresh weight gain). Hence, the authors suggest that the endopolyploidization contributes to sustaining plant growth under high incident UV radiation.

Increasing our knowledge on the physiological and/or molecular mechanisms underlying the enhanced UV-B tolerance of polyploids will be of the utmost value both to improve crop production, as well as to extend the range of cultivation of species of interest to either higher altitudes, or to regions where increments in the amounts of UV radiation due to alterations in stratospheric ozone are expected (e.g., Bais et al., 2018).

Genomic duplication and biotic stress tolerance

Pests, parasites and pathogens like bacteria, fungi, oomycetes, and nematodes, cause biotic stress in plants, leading to disease or low yield. It is estimated that between 20% and 40% of crop yield is lost globally to pests and disease (Douglas, 2018). Among pathogens, biotrophic fungi can colonize different plant organs and cause leaf spots and tumors, whereas necrotrophs can release toxins that kill the host cells. Viral infections generally do not kill the host plant but produce a systemic damage leading to stunted growth and malformations. Parasitic nematodes can cause severe root damage and can also act as vectors for viral transmission (Schumann and D'Arcy, 2006). Insect pests have high agronomic impact on crop yield because they cause direct damage and are also responsible for the transmission of plant diseases. Resistance to pathogens and/or insect herbivores may be affected by polyploidization (see Supplementary Table 5). This trait is interesting not only for the development of new varieties but also from an evolutionary point of view.

Apart from the central role of polyploidization in contributing to the biodiversification of flowering plants, Levin (1983) suggested that newly formed polyploid lineages are more resistant to pathogens than their diploid progenitors. This effect can be quite strong and, in the case of perennial species with recurrent polyploid formation, may last indefinitely, potentially providing a general explanation for the successful establishment of novel polyploid lineages (Oswald and Nuismer, 2007). However, this hypothesis has been challenged by studies on herbivory resistance in sympatrically growing diploid and autotetraploid individuals of *Heuchera grossulariifolia* (Thompson et al., 1997; Nuismer and Thompson, 2001), demonstrating that novel polyploid lineages may not receive a uniform or consistent relief from herbivory in the whole set of insect-plant interactions analyzed (see also below). Therefore the authors conclude that it seems unlikely that the evolutionary diversification and success of polyploids resulted from increased resistance to this type of biotic stress.

Different aspects in the morphology and/or development of polyploids have been related to the differential resistance/susceptibility to biotic stress observed among genotypes. For instance, polyploid *Stenotaphrum* genotypes, typically showing enhanced resistance to the nematode *Belonolaimus longicaudatus*, tend to have thicker primary roots than diploids (Busey et al., 1993, see Supplementary Table 5). Interestingly, tetraploid plants

of *H. grossulariifolia* were shown to be more susceptible to the attack of *Greya politella* than the diploids, probably due to a change in their flowering time. In fact, the tetraploids flower earlier and partially overlap the flowering of *Lithophragma parviflorum* (another host of *G. politella*), whereas the flowering of diploids generally does not. Hence, there is more of a chance for some females from the local *L. parviflorum* feeding subpopulations of *G. politella* to lay their eggs in tetraploid *H. grossulariifolia* plants than in the diploids (Thompson et al., 1997).

Metabolic differences produced by autopolyploidy can have profound effects for the development and ecological interactions of plant neopolyploids (Vergara et al., 2016). Alkaloids, terpenes, and other classes of secondary products may confer resistance to pathogens and herbivory (Levin, 1983). Similarly, changes in the concentration of metabolites related to the tricarboxylic acid (TCA) cycle and γ-aminobutyric acid (GABA) could have important adaptive consequences for the specific ecology of diploids and their polyploid counterparts (Van de Peer et al., 2017).

Recent advances in the study of the interaction between diploid *Arabidopsis thaliana* and synthetic autotetraploids with the phyllosphere microbiome have shed some light on the mechanisms underlying this interaction. It has been observed that there is no difference in the establishment of the synthetic microbiome, neither its composition nor its diversity is significantly affected with respect to host ploidy. Also, at the gene expression level, autotetraploid plants show active defenses constitutively independent of pathogen colonization, whereas diploid plants show a high number of defense-related genes that are differentially expressed in the presence or absence of pathogens (Mehlferber et al., 2022).

Unfortunately, the information available on the physiological and/or molecular mechanisms underlying most of the reported responses is comparatively scarce or nil, so further experimental approaches will be of great help to draw conclusive inferences regarding the effect of polyploidy on biotic stress tolerance.

Conclusion

Polyploidy plays an important evolutionary role in natural populations. This role can be attributed to a number of consequences of polyploidization that promote phenotypic and/or fitness alterations, such as mutation buffering, increased allelic diversity and heterozygosity, dosage effects, and sub-or neofunctionalization of duplicated genes. Although some controversy regarding this view still exists (e.g., Arrigo and Barker, 2012; Soltis et al., 2014), the overwhelming abundance of polyploid species in nature strongly suggests that polyploidy indeed confers some degree of adaptive advantage. After polyploidization, far-reaching genetic and epigenetic changes in the genome ensue, such as chromosomal rearrangements, amplification of repetitive sequences, loss of DNA sequences, methylation re-patterning and general chromatin remodeling. There are also additive changes due to heterozygosity and gene dosage. Despite the fact that some of the physiological consequences of these alterations are still far from being fully understood, there is a growing body of evidence advancing plausible mechanistic explanations, which support the notion that polyploidy can help plants to improve their tolerance to a wide range of environmental stressors (see Supplementary Tables). In fact, though generalizations should be made with caution, more than 90% of the reviewed experimental data point toward a net positive impact of ploidy level on the ability of plants to cope with different kinds of stress. This would seem to apply to both auto and allopolyploids, even though differential responses due to the genome duplication process have been reported depending on the type of stress and species considered. In view of this, and considering that certain plant species have been used by different authors as a model to test the role of polyploidy against a variety of stressors, it is tempting to advance the notion that WGD events have the potential to enhance the plant's ability to cope with environmental stress *in general*. Nevertheless, more systematic studies that perform a comparative analysis of responses to different types of stress in the same species and under similar general conditions (see for example Deng et al., 2012) are necessary, in order to adequately address this notion.

In the face of rapid climatic and other environmental changes at the global scale, understanding the impact of polyploidization in plant evolution and ecological interactions is of an uttermost relevance, as this knowledge might rapidly become an important tool for the breeding of economically important crops, helping us to pave the way for harnessing more efficient uses of artificial polyploidization to obtain genotypes with increased tolerance to diverse biotic and abiotic stresses.

Author contributions

All the authors made substantial contributions to the conception or design of the work and to the acquisition and interpretation of data for the review. SIP-Á, HFC, and IB agree to be accountable for all aspects of the work in ensuring that questions related to the accuracy or integrity of any part of the work are appropriately investigated and resolved. All authors contributed to the article and approved the submitted version.

Funding

The work was supported in part by CONICET, Argentina (grant PIP 11220200101935CO, to IB).

Acknowledgments

We thank all the reviewers and the Guest Associate Editor for their comments and suggestions, which significantly improved the article.

Conflict of interest

The authors declare that the research was conducted in the absence of any commercial or financial relationships that could be construed as a potential conflict of interest.

Publisher's note

All claims expressed in this article are solely those of the authors and do not necessarily represent those of their affiliated organizations, or those of the publisher, the editors and the reviewers. Any product that may be evaluated in this article, or claim that may be made by its manufacturer, is not guaranteed or endorsed by the publisher.

Supplementary material

The Supplementary Material for this article can be found online at: https://www.frontiersin.org/articles/10.3389/fpls.2022.869423/full#supplementary-material

References

Adachi, S., Minamisawa, K., Okushima, Y., Inagaki, S., Yoshiyama, K., Kondou, Y., et al. (2011). Programmed induction of endoreduplication by DNA double-strand breaks in Arabidopsis. *Proc. Natl. Acad. Sci. U. S. A.* 108, 10004–10009. doi: 10.1073/pnas.1103584108

Allario, T., Brumos, J., Colmenero-Flores, J. M., Iglesias, D. J., Pina, J. A., Navarro, L., et al. (2013). Tetraploid Rangpur lime rootstock increases drought tolerance *via* enhanced constitutive root abscisic acid production. *Plant Cell Environ.* 36, 856–868. doi: 10.1111/pce.12021

Allario, T., Brumos, J., Colmenero-Flores, J. M., Tadeo, F., Froelicher, Y., Talon, M., et al. (2011). Large changes in anatomy and physiology between diploid Rangpur lime (*Citrus limonia*) and its autotetraploid are not associated with large changes in leaf gene expression. *J. Exp. Bot.* 62, 2507–2519. doi: 10.1093/jxb/erq467

Arrigo, N., and Barker, M. S. (2012). Rarely successful polyploids and their legacy in plant genomes. *Curr. Opin. Plant Biol.* 15, 140–146. doi: 10.1016/j.pbi.2012.03.010

Ashraf, M., Nazir, N., and McNeilly, T. (2001). Comparative salt tolerance of amphidiploid and diploid Brassica species. *Plant Sci.* 160, 683–689. doi: 10.1016/S0168-9452(00)00449-0

Assunção, A. G. L., Cakmak, I., Clemens, S., González-Guerrero, M., Nawrocki, A., and Thomine, S. (2022). Micronutrient homeostasis in plants for more sustainable agriculture and healthier human nutrition. *J. Exp. Bot.* 73, 1789–1799. doi: 10.1093/jxb/erac014

Bais, A. F., Lucas, R. M., Bornman, J. F., Williamson, C. E., Sulzberger, B., Austin, A. T., et al. (2018). Environmental effects of ozone depletion, UV radiation and interactions with climate change: UNEP Environmental Effects Assessment Panel update 2017. *Photochem. Photobiol. Sci.* 17, 127–179. doi: 10.1039/C7PP90043K

Ballare, C. L., Rousseaux, M. C., Searles, P. S., Zaller, J. G., Giordano, C. V., Robson, T. M., et al. (2001). Impacts of solar ultraviolet-B radiation on terrestrial ecosystems of Tierra del Fuego (southern Argentina): an overview of recent progress. *J. Photochem. Photobiol. B* 62, 67–77. doi: 10.1016/S1011-1344(01)00152-X

Bañuls, J., Legaz, F., and Primo-Millo, E. (1990). Effect of salinity on uptake and distribution of chloride and sodium in some citrus scion-rootstock combinations. *J. Hortic. Sci.* 65, 715–724. doi: 10.1080/00221589.1990.11516113

Bañuls, J., and Primo-Millo, E. (1992). Effects of chloride and sodium on gas exchange parameters and water relations of citrus plants. *Physiol. Plant.* 86, 115–123. doi: 10.1111/j.1399-3054.1992.tb01319.x

Bañuls, J., and Primo-Millo, E. (1995). Effects of salinity on some citrus scion-rootstock combinations. *Ann. Bot.* 76, 97–102. doi: 10.1006/anbo.1995.1083

Bardil, A., Tayale, A., and Parisod, C. (2015). Evolutionary dynamics of retrotransposons following autopolyploidy in the buckler mustard species complex. *Plant J.* 82, 621–631. doi: 10.1111/tpj.12837

Bartel, D. P. (2004). MicroRNAs: genomics, biogenesis, mechanism, and function. *Cell* 116, 281–297. doi: 10.1016/S0092-8674(04)00045-5

Beaulieu, J. M., Leitch, I. J., Patel, S., Pendharkar, A., and Knight, C. A. (2008). Genome size is a strong predictor of cell size and stomatal density in angiosperms. *New Phytol.* 179, 975–986. doi: 10.1111/j.1469-8137.2008.02528.x

Bita, C. E., and Gerats, T. (2013). Plant tolerance to high temperature in a changing environment: scientific fundamentals and production of heat stress-tolerant crops. *Front. Plant Sci.* 4, 1–18. doi: 10.3389/fpls.2013.00273

Blasio, F., Prieto, P., Pradillo, M., and Naranjo, T. (2022). Genomic and meiotic changes accompanying Polyploidization. *Plan. Theory* 11, 125. doi: 10.3390/plants11010125

Bohnert, H. J., Nelson, D. E., and Jensen, R. G. (1995). Adaptations to environmental stresses. *Plant Cell* 7, 1099–1111. doi: 10.2307/3870060

Bowers, J. E., Chapman, B. A., Rong, J., and Paterson, A. H. (2003). Unravelling angiosperm genome evolution by phylogenetic analysis of chromosomal duplication events. *Nature* 422, 433–438. doi: 10.1038/nature01521

Boyer, J. S. (1982). Plant productivity and environment. *Science* 218, 443–228. doi: 10.1126/science.218.4571.443

Bray, E. A. (1997). Plant responses to water deficit. *Trends Plant Sci.* 2, 48–54. doi: 10.1016/S1360-1385(97)82562-9

Buggs, R. J. A., Chamala, S., Wu, W., Tate, J. A., Schnable, P. S., Soltis, D. E., et al. (2012). Rapid, repeated, and clustered loss of duplicate genes in allopolyploid plant populations of independent origin. *Curr. Biol.* 22, 248–252. doi: 10.1016/j.cub.2011.12.027

Buggs, R. J. A., Doust, A. N., Tate, J. A., Koh, J., Soltis, K., Feltus, F. A., et al. (2009). Gene loss and silencing in *Tragopogon miscellus* (Asteraceae): comparison of natural and synthetic allotetraploids. *Heredity* 103, 73–81. doi: 10.1038/hdy.2009.24

Burleigh, J. G., Bansal, M. S., Wehe, A., and Eulenstein, O. (2008). *Locating Multiple Gene Duplications Through Reconciled Trees. Research in Computational Molecular Biology* Berlin, Heidelberg Springer, 273–284.

Busey, P., Glibin-Davis, R. M., and Center, B. J. (1993). Resistance in Stenotaphrum to the sting nematode. *Crop Sci.* 33, 1066–1070. doi: 10.2135/cropsci1993.0011183X003300050038x

Cacco, G., Ferrari, G., and Lucci, G. C. (1976). Uptake efficiency of roots in plants at different ploidy levels. *J. Agric. Sci.* 87, 585–589. doi: 10.1017/S0021859600033219

Caldwell, M. M., Bornman, J. F., Ballaré, C. L., Flint, S. D., and Kulandaivelu, G. (2007). Terrestrial ecosystems, increased solar ultraviolet radiation, and interactions with other climate change factors. *Photochem. Photobiol. Sci.* 6, 252–266. doi: 10.1039/b700019g

Cannon, S. B., McKain, M. R., Harkess, A., Nelson, M. N., Dash, S., Deyholos, M. K., et al. (2015). Multiple polyploidy events in the early radiation of nodulating and nonnodulating legumes. *Mol. Biol. Evol.* 32, 193–210. doi: 10.1093/molbev/msu296

Chao, D. Y., Dilkes, B., Luo, H., Douglas, A., Yakubova, E., Lahner, B., et al. (2013). Polyploids exhibit higher potassium uptake and salinity tolerance in Arabidopsis. *Science* 341, 658–659. doi: 10.1126/science.1240561

Chaumont, F., and Tyerman, S. D. (2014). Aquaporins: highly regulated channels controlling plant water relations. *Plant Physiol.* 164, 1600–1618. doi: 10.1104/pp.113.233791

Chaves, M. M., Maroco, J. P., and Pereira, J. S. (2003). Understanding plant responses to drought – from genes to the whole plant. *Funct. Plant Biol.* 30, 239–264. doi: 10.1071/FP02076

Chen, L., Lou, Q., Zhuang, Y., Chen, J., Zhang, X., and Wolukau, J. N. (2007). Cytological diploidization and rapid genome changes of the newly synthesized allotetraploids *Cucumis* × *hytivus*. *Planta* 225, 603–614. doi: 10.1007/s00425-006-0381-2

Chen, Z., Ma, Y., Weng, Y., Yang, R., Gu, Z., and Wang, P. (2019). Effects of UV-B radiation on phenolic accumulation, antioxidant activity and physiological changes in wheat (*Triticum aestivum* L.) seedlings. *Food Bioscience* 30:100409. doi: 10.1016/j.fbio.2019.04.010

Chen, Z. J., and Ni, Z. (2006). Mechanisms of genomic rearrangements and gene expression changes in plant polyploids. *BioEssays* 28, 240–252. doi: 10.1002/bies.20374

Chen, S., and Tang, P. S. (1945). Studies on colchicine-induced autotetraploid barley. III. Physiological studies. *Am. J. Bot.* 32, 177–179. doi: 10.1002/j.1537-2197.1945.tb05104.x

Chung, J. S., Zhu, J. K., Bressan, R. A., Hasegawa, P. M., and Shi, H. (2008). Reactive oxygen species mediate Na^+-induced SOS1 mRNA stability in Arabidopsis. *Plant J.* 53, 554–565. doi: 10.1111/j.1365-313X.2007.03364.x

Dalal, M., Tayal, D., Chinnusamy, V., and Bansal, K. C. (2009). Abiotic stress and ABA-inducible Group 4 LEA from *Brassica napus* plays a key role in salt and drought tolerance. *J. Biotechnol.* 139, 137–145. doi: 10.1016/j.jbiotec.2008.09.014

Day, A. D., and Ludeke, K. L. (1993). "Phosphorus as a plant nutrient," in *Plant Nutrients in Desert Environments. Adaptations of Desert Organisms* (Berlin, Heidelberg: Springer).

De Storme, N., Copenhaver, G. P., and Geelen, D. (2012). Production of diploid male gametes in Arabidopsis by cold-induced destabilization of postmeiotic radial microtubule arrays. *Plant Physiol.* 160, 1808–1826. doi: 10.1104/pp.112.208611

Del Pozo, J. C., and Ramirez-Parra, E. (2014). Deciphering the molecular bases for drought tolerance in Arabidopsis autotetraploids. *Plant Cell Environ.* 37, 2722–2737. doi: 10.1111/pce.12344

Del Pozo, J. C., and Ramirez-Parra, E. (2015). Whole genome duplications in plants: an overview from Arabidopsis. *J. Exp. Bot.* 66, 6991–7003. doi: 10.1093/jxb/erv432

Demidchik, V. (2015). Mechanisms of oxidative stress in plants: from classical chemistry to cell biology. *Environ. Exp. Bot.* 109, 212–218. doi: 10.1016/j.envexpbot.2014.06.021

Deng, M., Dong, Y., Zhao, Z., Li, Y., and Fan, G. (2017). Dissecting the proteome dynamics of the salt stress induced changes in the leaf of diploid and autotetraploid *Paulownia fortunei*. *PLoS One* 12:e0181937. doi: 10.1371/journal.pone.0181937

Deng, B., Du, W., Liu, C., Sun, W., Tian, S., and Dong, H. (2012). Antioxidant response to drought, cold and nutrient stress in two ploidy levels of tobacco plants: low resource requirement confers polytolerance in polyploids? *Plant Growth Regul.* 66, 37–47. doi: 10.1007/s10725-011-9626-6

Diallo, A. M., Nielsen, L. R., Kjaer, E. D., Petersen, K. K., and Raebild, A. (2016). Polyploidy can confer superiority to west African *Acacia senegal* (L.) Willd. Trees. *Front. Plant Sci.* 7, 821. doi: 10.3389/fpls.2016.00821

Dong, S., and Adams, K. (2011). Differential contributions to the transcriptome of duplicated genes in response to abiotic stresses in natural and synthetic polyploids. *New Phytol.* 190, 1045–1057. doi: 10.1111/j.1469-8137.2011.03650.x

Dong, Y., Fan, G., Zhao, Z., Xu, E., Deng, M., Wang, L., et al. (2017). Transcriptome-wide profiling and expression analysis of two accessions of *Paulownia australis* under salt stress. *Tree Genet. Genomes* 13, 97. doi: 10.1007/s11295-017-1179-z

Dong, Y., Gupta, S., Sievers, R., Wargent, J. J., Wheeler, D., Putterill, J., et al. (2019). Genome draft of the Arabidopsis relative *Pachycladon cheesemanii* reveals novel strategies to tolerate New Zealand's high ultraviolet B radiation environment. *BMC Genomics* 20, 1–14. doi: 10.1186/s12864-019-6084-4

Douglas, A. E. (2018). Strategies for enhanced crop resistance to insect pests. *Annu. Rev. Plant Biol.* 69, 637–660. doi: 10.1146/annurev-arplant-042817-040248

Doyle, J. J., and Coate, J. E. (2019). Polyploidy, the Nucleotype, and novelty: the impact of genome doubling on the biology of the cell. *Int. J. Plant Sci.* 180, 11–52. doi: 10.1086/700636

Drake, P. L., Froend, R. H., and Franks, P. J. (2013). Smaller, faster stomata: scaling of stomatal size, rate of response, and stomatal conductance. *J. Exp. Bot.* 64, 495–505. doi: 10.1093/jxb/ers347

Dwivedi, S. K., Basu, S., Kumar, S., Kumar, G., Prakash, V., Kumar, S., et al. (2017). Heat stress induced impairment of starch mobilisation regulates pollen viability and grain yield in wheat: study in eastern indo-Gangetic Plains. *Field Crops Res.* 206, 106–111. doi: 10.1016/j.fcr.2017.03.006

Edger, P. P., Smith, R., McKain, M. R., Cooley, A. M., Vallejo-Marin, M., and Yuan, Y. (2017). Subgenome dominance in an interspecific hybrid, synthetic allopolyploid, and a 140-year-old naturally established neo-allopolyploid monkeyflower. *Plant Cell* 29, 2150–2167. doi: 10.1105/tpc.17.00010

Ehlert, C., Maurel, C., Tardieu, F., and Simonneau, T. (2009). Aquaporin-mediated reduction in maize root hydraulic conductivity impacts cell turgor and leaf elongation even without changing transpiration. *Plant Physiol.* 150, 1093–1104. doi: 10.1104/pp.108.131458

Emery, M., Willis, M. M. S., Hao, Y., Barry, K., Oakgrove, K., Peng, Y., et al. (2018). Preferential retention of genes from one parental genome after polyploidy illustrates the nature and scope of the genomic conflicts induced by hybridization. *PLoS Genet.* 14:e1007267. doi: 10.1371/journal.pgen.1007267

Fan, G., Li, X., Deng, M., Zhao, Z., and Yang, L. (2016b). Comparative analysis and identification of miRNAs and their target genes responsive to Salt stress in diploid and tetraploid *Paulownia fortune* seedlings. *PLoS One* 11:e0149617. doi: 10.1371/journal.pone.0149617

Fan, G., Wang, L., Deng, M., Zhao, Z., Dong, Y., Zhang, X., et al. (2016a). Changes in transcript related to osmosis and intracellular ion homeostasis in *Paulownia tomentosa* under salt stress. *Front. Plant Sci.* 7, 384. doi: 10.3389/fpls.2016.00384

FAO and ITPS (2015). Status of the World's soil resources (SWSR) – Main report. Food and agriculture Organization of the United Nations and Intergovernmental Technical Panel on soils, Rome, Italy.

Faralli, M., Matthews, J., and Lawson, T. (2019). Exploiting natural variation and genetic manipulation of stomatal conductance for crop improvement. *Curr. Opin. Plant Biol.* 49, 1–7. doi: 10.1016/j.pbi.2019.01.003

Fawcett, J. A., Maere, S., and Van de Peer, Y. (2009). Plants with double genomes might have had a better chance to survive the cretaceous–tertiary extinction event. *Proc. Natl. Acad. Sci. U. S. A.* 106, 5737–5742. doi: 10.1073/pnas.0900906106

Fitter, A., and Hay, R. (2002). *Environmental physiology of plants*, *3rd Edn*. London, San Diego: Academic Press.

Franks, P. J., W. Doheny-Adams, T., Britton-Harper, Z. J., and Gray, J. E. (2015). Increasing water-use efficiency directly through genetic manipulation of stomatal density. *New Phytol.* 207, 188–195. doi: 10.1111/nph.13347

Galindo-González, L., Mhiri, C., Deyholos, M. K., and Grandbastien, M. A. (2017). LTR-retrotransposons in plants: engines of evolution. *Gene* 160, 67–75. doi: 10.1016/j.gene.2017.04.051

Gegas, V. C., Wargent, J. J., Pesquet, E., Granqvist, E., Paul, N. D., and Doonan, J. H. (2014). Endopolyploidy as a potential alternative adaptive strategy for Arabidopsis leaf size variation in response to UV-B. *J. Exp. Bot.* 65, 2757–2766. doi: 10.1093/jxb/ert473

Golldack, D., Li, C., Mohan, H., and Probst, N. (2014). Tolerance to drought and salt stress in plants: unraveling the signaling networks. *Front. Plant Sci.* 5, 151. doi: 10.3389/fpls.2014.00151

Grant, V. (1952). Cytogenetics of the hybrid *Gilia millefoliata* × *achilleaefolia*. I. Variations in meiosis and polyploidy rate as affected by nutritional and genetic conditions. *Chromosoma* 5, 372–390.

Guo, W., Yang, J., Sun, X. D., Chen, G. J., Yang, Y. P., and Duan, Y. W. (2016). Divergence in eco-physiological responses to drought mirrors the distinct distribution of *Chamerion angustifolium* cytotypes in the Himalaya-Hengduan mountains region. *Front. Plant Sci.* 7, 1329. doi: 10.3389/fpls.2016.01329

Gupta, A., Rico-Medina, A., and Caño-Delgado, A. I. (2020). The physiology of plant responses to drought. *Science* 368, 266–269. doi: 10.1126/science.aaz7614

Ha, M., Lu, J., Tian, L., Ramachandran, V., Kasschau, K. D., and Chapman, E. J. (2009). Small RNAs serve as a genetic buffer against genomic shock in Arabidopsis interspecific hybrids and allopolyploids. *Proc. Natl. Acad. Sci. U. S. A.* 106, 17835–17840. doi: 10.1073/pnas.0907003106

Hanada, K., Zou, C., Lehti-Shiu, M. D., Shinozaki, K., and Shiu, S.-H. (2008). Importance of lineage specific expansion of plant tandem duplicates in the adaptive response to environmental stimuli. *Plant Physiol.* 148, 993–1003. doi: 10.1104/pp.108.122457

Hase, Y., Trung, K. H., Matsunaga, T., and Tanaka, A. (2006). A mutation in the uvi4 gene promotes progression of endo-reduplication and confers increased tolerance towards ultraviolet B light. *Plant J.* 46, 317–326. doi: 10.1111/j.1365-313X.2006.02696.x

Hasegawa, P. M., Bressan, R. A., Zhu, J. K., and Bohnert, H. J. (2000). Plant cellular and molecular responses to high salinity. *Annu. Rev. Plant Biol.* 51, 463–499. doi: 10.1146/annurev.arplant.51.1.463

He, L., and Hannon, G. J. (2004). MicroRNAs: small RNAs with a big role in gene regulation. *Nat. Rev. Genet.* 5, 522–531. doi: 10.1038/nrg1379

Hedhly, A. (2011). Sensitivity of flowering plant gametophytes to temperature fluctuations. *Environ. Exp. Bot.* 74, 9–16. doi: 10.1016/j.envexpbot.2011.03.016

Hegarty, M. J., Barker, G. L., Wilson, I. D., Abbott, R. J., Edwards, K. J., and Hiscock, S. J. (2006). Transcriptome shock after interspecific hybridization in senecio is ameliorated by genome duplication. *Curr. Biol.* 16, 1652–1659. doi: 10.1016/j.cub.2006.06.071

Hegarty, M., Coate, J., Sherman-Broyles, J. S., Abbott, R., Hiscock, S., and Doyle, J. (2013). Lessons from natural and artificial Polyploids in higher plants. *Cytogenet. Genome Res.* 140, 204–225. doi: 10.1159/000353361

Hetherington, A., and Woodward, I. (2003). The role of stomata in sensing and driving environmental change. *Nature* 424, 901–908. doi: 10.1038/nature01843

Hideg, É., Jansen, M. A., and Strid, Å. (2013). UV-B exposure, ROS, and stress: inseparable companions or loosely linked associates? *Trends Plant Sci.* 18, 107–115. doi: 10.1016/j.tplants.2012.09.003

Huang, Y.-M., Hsueh-Mei, C., Jenn-Che, W., and Wen-Liang, C. (2007). The distribution and habitats of the Pteris fauriei complex in Taiwan. *Taiwania* 521, 49–58. doi: 10.6165/tai.2007.52(1).49

Huang, L., Jia, J., Zhao, X., Zhang, M., Huang, X., Ji, E., et al. (2018). The ascorbate peroxidase APX1 is a direct target of a zinc finger transcription factor ZFP36 and a late embryogenesis abundant protein OsLEA5 interacts with ZFP36to co-regulate OsAPX1 in seed germination in rice. *Biochem. Biophys. Res. Commun.* 495, 339–345. doi: 10.1016/j.bbrc.2017.10.128

Huang, C. H., Zhang, C., Liu, M., Hu, Y., Gao, T., Qi, J., et al. (2016). Multiple polyploidization events across Asteraceae with two nested events in the early history revealed by nuclear phylogenomics. *Mol. Biol. Evol.* 33, 2820–2835. doi: 10.1093/molbev/msw157

Hughes, J., Hepworth, C., Dutton, C., Dunn, J. A., Hunt, L., Stephens, J., et al. (2017). Reducing stomatal density in barley improves drought tolerance without impacting on yield. *Plant Physiol.* 174, 776–787. doi: 10.1104/pp.16.01844

Ivushkin, K., Bartholomeus, H., Arnold, K., Bregt, A. K., Pulatov, A., Kempen, B., et al. (2019). Global mapping of soil salinity change. *Remote Sens. Environ.* 231:111260. doi: 10.1016/j.rse.2019.111260

Jackson, S., and Chen, Z. J. (2010). Genomic and expression plasticity of polyploidy. *Curr. Opin. Plant Biol.* 13, 153–159. doi: 10.1016/j.pbi.2009.11.004

Jiang, A., Gan, L., Tu, Y., Ma, H., Zhang, J., Song, Z., et al. (2013). The effect of genome duplication on seed germination and seedling growth of rice under salt stress. *Australian J. Crop Sci.* 7, 1814–1821.

Jiang, Y., Liu, S., Hu, J., He, G., Liu, Y., Chen, X., et al. (2020). Polyploidization of *Plumbago auriculata* lam. In vitro and its characterization including cold tolerance. *Plant Cell Tissue Organ Cult.* 140, 315–325. doi: 10.1007/s11240-019-01729-w

Jouyban, Z., Hasanzade, R., and Sharafi, S. (2013). Chilling stress in plants. *Int. J. Agric. Crop Sci. (IJACS)* 5, 2961–2968.

Kandlbinder, A., Finkemeier, I., Wormuth, D., Hanitzsch, M., and Dietz, K.-J. (2004). The antioxidant status of photosynthesizing leaves under nutrient deficiency: redox regulation, gene expression and antioxidant activity in *Arabidopsis thaliana*. *Physiol. Plant.* 120, 63–73. doi: 10.1111/j.0031-9317.2004.0272.x

Kasajima, I., Yoshizumi, T., Ichikawa, T., Matsui, M., and Fujiwara, T. (2010). Possible involvement of ploidy in tolerance to boron deficiency in *Arabidopsis thaliana*. *Plant Biotechnol.* 27, 435–445. doi: 10.5511/plantbiotechnology.10.0728a

Kashkush, K., Feldman, M., and Levy, A. A. (2003). Transcriptional activation of retrotransposons alters the expression of adjacent genes in wheat. *Nature Genet.* 33, 102–106. doi: 10.1038/ng1063

Kenan-Eichler, M., Leshkowitz, D., Tal, L., Noor, E., Melamed-Bessudo, C., Feldman, M., et al. (2011). Wheat hybridization and polyploidization results in deregulation of small RNAs. *Genetics* 188, 263–272. doi: 10.1534/genetics.111.128348

Khalid, M. F., Vincent, C., Morillon, R., Anjum, M. A., Ahmad, S., and Hussain, S. (2021). Different strategies lead to a common outcome: different water-deficit scenarios highlight physiological and biochemical strategies of water-deficit tolerance in diploid versus tetraploid Volkamer lemon. *Tree Physiol.* 41, 2359–2374. doi: 10.1093/treephys/tpab074

Khraiwesh, B., Zhu, J. K., and Zhu, J. (2012). Role of miRNAs and siRNAs in biotic and abiotic stress responses of plants. *Biochim. Biophys. Acta* 1819, 137–148. doi: 10.1016/j.bbagrm.2011.05.001

Kim, H.-E., Han, J.-E., Lee, H., Kim, J.-H., Kim, H.-H., Lee, K.-Y., et al. (2021). Tetraploidization increases the contents of functional metabolites in *Cnidium officinale*. *Agronomy* 11, 1561. doi: 10.3390/agronomy11081561

Kostoff, D. (1933). A contribution to the sterility and irregularities in the meiotic processes caused by virus diseases. *Genetica* 15, 103–114. doi: 10.1007/BF01591853

Kotschi, J. (2015). *A Soiled Reputation. Adverse Impacts of Mineral Fertilizers in Tropical Agriculture*. Germany Heinrich Böll Stiftung (Heinrich Böll Foundation), WWF.

Kumari, A., Das, P., Parida, A. K., and Agarwal, P. (2015). Proteomics, metabolomics, and ionomics perspectives of salinity tolerance in halophytes. *Front. Plant Sci.* 6, 537. doi: 10.3389/fpls.2015.00537

Kuromori, T., Seo, M., and Shinozaki, K. (2018). ABA transport and plant water stress responses. *Trends Plant Sci.* 23, 513–522. doi: 10.1016/j.tplants.2018.04.001

Lagibo, A. D., Kobza, F., and Suchánková, P. (2005). Polyploidy effects on frost tolerance and winter survival of garden pansy genotypes. *Hort. Sci.* 32, 138–146.

Lambers, H., and Oliveira, R. S. (2019). *Plant Physiological Ecology* Springer Nature Cham, Switzerland.

Lawson, T., and Blatt, M. R. (2014). Stomatal size, speed, and responsiveness impact on photosynthesis and water use efficiency. *Plant Physiol.* 164, 1556–1570. doi: 10.1104/pp.114.237107

Le, T. N., Schumann, U., Smith, N. A., Tiwari, S., Au, P. C., Zhu, Q. H., et al. (2014). DNA demethylases target promoter transposable elements to positively regulate stress responsive genes in Arabidopsis. *Genome Biol.* 15, 458. doi: 10.1186/s13059-014-0458-3

Leakey, A. D. B., Ferguson, J. N., Pignon, C. P., Wu, A., Jin, Z., Hammer, G. L., et al. (2019). Water use efficiency as a constraint and target for improving the resilience and productivity of C 3 and C 4 crops. *Annu. Rev. Plant Biol.* 70, 781–808. doi: 10.1146/annurev-arplant-042817-040305

Lee, J. S., and Adams, K. L. (2020). Global insights into duplicated gene expression and alternative splicing in polyploid *Brassica napus* under heat, cold, and drought stress. *Plant Genome. Nov.* 13:e20057. doi: 10.1002/tpg2.20057

Leebens-Mack, J. H., Barker, M. S., Carpenter, E. J., Deyholos, M. K., Gltzendanner, M. A., Graham, S. E., et al. (2019). One thousand plant transcriptomes and the phylogenomics of green plants. *Nature* 574, 679–685. doi: 10.1038/s41586-019-1693-2

Leitch, I. J., and Dodsworth, S. (2017). "Endopolyploidy in plants," in *eLS* (Chichester: John Wiley & Sons, Ltd).

Leps, W. T., Brill, W. J., and Bingham, E. T. (1980). Effect of alfalfa ploidy on nitrogen fixation 1. *Crop Sci.* 20, 427–430. doi: 10.2135/cropsci1980.001118 3X002000040002x

Levin, D. A. (1983). Polyploidy and novelty in flowering plants. *Am. Nat.* 122, 1–25. doi: 10.1086/284115

Li, W.-L., Berlyn, G. P., and Ashton, P. M. S. (1996). Polyploids and their structural and physiological characteristics relative to water deficit in *Betula papyrifera* (Betulaceae). *Am. J. Bot.* 83, 15–20. doi: 10.1002/j.1537-2197.1996.tb13869.x

Li, W. D., Biswas, D. K., Xu, H., Xu, C. Q., Wang, X. Z., Liu, J. K., et al. (2009a). Photosynthetic responses to chromosome doubling in relation to leaf anatomy in *Lonicera japonica* subjected to water stress. *Funct. Plant Biol.* 36, 783–792. doi: 10.1071/FP09022

Li, M., Xu, G., Xia, X., Wang, M., Yin, X., Zhang, B., et al. (2017). Deciphering the physiological and molecular mechanisms for copper tolerance in autotetraploid Arabidopsis. *Plant Cell Rep.* 36, 1585–1597. doi: 10.1007/s00299-017-2176-2

Li, Y., Ye, W., Wang, M., and Yan, X. (2009b). Climate change and drought: a risk assessment of crop-yield impacts. *Clim. Res.* 39, 31–46. doi: 10.3354/cr00797

Li, M., Zhang, C., Hou, L., Yang, W., Liu, S., Pang, X., et al. (2021). Multiple responses contribute to the enhanced drought tolerance of the autotetraploid *Ziziphus jujuba* Mill. Var. spinosa. *Cell Biosci.* 11, 1–20. doi: 10.1186/s13578-021-00633-1

Lisch, D. (2013). How important are transposons for plant evolution? *Nat. Rev. Genet.* 14, 49–61. doi: 10.1038/nrg3374

Liu, Z., and Adams, K. L. (2007). Expression partitioning between genes duplicated by polyploidy under abiotic stress and during organ development. *Curr. Biol.* 17, 1669–1674. doi: 10.1016/j.cub.2007.08.030

Liu, S., Sumei, C., Yu, C., Zhiyong, G., Dongmei, Y., and Fad, C. (2011). In vitro induced tetraploid of *Dendranthema nankingense* (Nakai) Tzvel. Shows an improved level of abiotic stress tolerance. *Sci. Hort.* 127, 411–419. doi: 10.1016/j.scienta.2010.10.012

Liu, B., and Sun, G. (2017). MicroRNAs contribute to enhanced salt adaptation of the autopolyploid *Hordeum bulbosum* compared with its diploid ancestor. *Plant J.* 91, 57–69. doi: 10.1111/tpj.13546

Liu, B., and Sun, G. (2019). Transcriptome and miRNAs analyses enhance our understanding of the evolutionary advantages of polyploidy. *Crit. Rev. Biotechnol.* 39, 173–180. doi: 10.1080/07388551.2018.1524824

Lohaus, R., and Van de Peer, Y. (2016). Of dups and dinos: evolution at the K/Pg boundary. *Curr. Opin. Plant Biol.* 30, 62–69. doi: 10.1016/j.pbi.2016.01.006

Lopes, F. R., Jjingo, D., da Silva, C. R., Andrade, A. C., Marraccini, P., Teixeira, J. B., et al. (2013). Transcriptional activity, chromosomal distribution and expression effects of transposable elements in Coffea genomes. *PLoS One* 8:e78931. doi: 10.1371/journal.pone.0078931

Lourkisti, R., Froelicher, Y., Morillon, R., Berti, L., and Santini, J. (2022). Enhanced photosynthetic capacity, osmotic adjustment and antioxidant defenses contribute to improve tolerance to moderate water deficit and recovery of triploid citrus genotypes. *Antioxidants.* 11, 562. doi: 10.3390/antiox11030562

Lu, B., Ding, R., Zhang, L., Yu, X., Huang, B., and Chen, W. (2006). Molecular cloning and characterization of a novel calcium-dependent protein kinase gene IiCPK2 responsive to polyploidy from tetraploid *Isatis indigotica*. *J. Biochem. Mol. Biol.* 39, 607–617. doi: 10.5483/bmbrep.2006.39.5.607

Lu, Y., Lei, J. Q., Zeng, F. J., Zhang, B., Liu, G. J., Liu, B., et al. (2017). Effect of NaCl-induced changes in growth, photosynthetic characteris-tics, water status and enzymatic antioxidant system of *Calligonum caput-medusae* seedlings. *Photosynthetica* 55, 96–106. doi: 10.1007/s11099-016-0234-6

Ma, L., Zhang, H., Sun, L., Jiao, Y., Zhang, G., Miao, C., et al. (2012). NADPH oxidase AtrbohD and Atrboh F function in ROS-dependent regulation of Na^+/K^+ homeostasis in Arabidopsis under salt stress. *J. Exp. Bot.* 63, 305–317. doi: 10.1093/jxb/err280

Maathuis, F. J. (2014). Sodium in plants: perception, signalling, and regulation of sodium fluxes. *J. Exp. Bot.* 65, 849–858. doi: 10.1093/jxb/ert326

Mable, B. K., Alexandrou, M. A., and Taylor, M. I. (2011). Genome duplication in amphibians and fish: an extended synthesis. *J. Zool.* 284, 151–182. doi: 10.1111/j.1469-7998.2011.00829.x

Madlung, A. (2013). Polyploidy and its effect on evolutionary success: old questions revisited with new tools. *Heredity* 110, 99–104. doi: 10.1038/hdy.2012.79

Madlung, A., Tyagi, A. P., Watson, B., Jiang, H., Kagochi, T., Doerge, R. W., et al. (2005). Genomic changes in synthetic Arabidopsis polyploids. *Plant J.* 41, 221–230. doi: 10.1111/j.1365-313X.2004.02297.x

Maere, S., De Bodt, S., Raes, J., Casneuf, T., Montagu, M. V., Kuiper, M., et al. (2005). Modeling gene and genome duplications in eukaryotes. *Proc. Natl. Acad. Sci. U. S. A.* 102, 5454–5459. doi: 10.1073/pnas.0501102102

Maher, C., Stein, L., and Ware, D. (2006). Evolution of Arabidopsis microRNA families through duplication events. *Genome Res.* 16, 510–519. doi: 10.1101/gr.4680506

Maherali, H., Walden, A. E., and Husband, B. C. (2009). Genome duplication and the evolution of physiological responses to water stress. *New Phytol.* 184, 721–731. doi: 10.1111/j.1469-8137.2009.02997.x

Martinez-Beltran, J., and Manzur, C., (2005). "Overview of salinity problems in the world and FAO strategies to address the problem." in *Proceedings of the International Salinity Forum*. Riverside, California. pp. 311–313.

Mason, A. S., Nelson, M. N., Yan, G., and Cowling, W. A. (2011). Production of viable male unreduced gametes in Brassica interspecific hybrids is genotype specific and stimulated by cold temperatures. *BMC Plant Biol.* 11, 103. doi: 10.1186/1471-2229-11-103

McClintock, B. (1984). The significance of responses of the genome to challenge. *Science* 226, 792–801. doi: 10.1126/science.15739260

Mehlferber, E. C., Song, M. J., Pelaez, J. N., Jaenisch, J., Coate, J. E., Koskella, B., et al. (2022). Polyploidy and microbiome associations mediate similar responses to pathogens in Arabidopsis. *Curr. Biol.* CB.32, 2719–2729.e5. doi: 10.1016/j.cub.2022.05.015

Meng, H., Jiang, S., Hua, S., Lin, X., Li, Y., Guo, W., et al. (2011). Comparison between a tetraploid turnip and its diploid progenitor (*Brassica rapa* L.): the adaptation to salinity stress. *Agr. Sci. China.* 10, 363–375. doi: 10.1016/S1671-2927(11)60015-1

Meru, G. M. (2012). "Polyploidy and its implications in plant breeding" in *Plant Breeding in the 21st Century*. eds. C. Mcgregor and C. Brummer (Athens, GA: University of Georgia)

Mishra, A., and Tanna, B. (2017). Halophytes: potential resources for salt stress tolerance genes and promoters. *Front. Plant Sci.* 8, 829. doi: 10.3389/fpls.2017.00829

Monda, K., Araki, H., Kuhara, S., Ishigaki, G., Akashi, R., Negi, J., et al. (2016). Enhanced stomatal conductance by a spontaneous Arabidopsis tetraploid, Me-0, results from increased stomatal size and greater stomatal aperture. *Plant Physiol.* 170, 1435–1444. doi: 10.1104/pp.15.01450

Mullan, D., and Pietragalla, J. (2012). "Leaf relative water content" in *Physiological breeding II: A field guide to wheat phenotyping*. eds. A. Pask, J. Pietragalla, D. Mullan and M. P. Reynolds (Mexico, D.F.: CIMMYT), 25–27.

Munns, R., and Tester, M. (2008). Mechanisms of salinity tolerance. *Annu. Rev. Plant Biol.* 59, 651–681. doi: 10.1146/annurev.arplant.59.032607.092911

Nieto Feliner, G., Casacuberta, J., and Wendel, J. F. (2020). Genomics of evolutionary novelty in hybrids and Polyploids. *Front. Genet.* 11, 1–21. doi: 10.3389/fgene.2020.00792

Niu, M., Huang, Y., Sun, S., Sun, J., Cao, H., Shabala, S., et al. (2018). Root respiratory burst oxidase homologue-dependent H_2O_2 production confers salt tolerance on a grafted cucumber by controlling Na^+ exclusion and stomatal closure. *J. Exp. Bot.* 69, 3465–3476. doi: 10.1093/jxb/erx386

Noctor, G., Mhamdi, A., and Foyer, C. H. (2014). The roles of reactive oxygen metabolism in drought: not so cut and dried. *Plant Physiol.* 164, 1636–1648. doi: 10.1104/pp.113.233478

Noggle, G. R. (1946). The physiology of polyploidy in plants: review of the literature. *Lloydia* 9, 153–173.

Nuismer, S. L., and Thompson, J. N. (2001). Plant polyploidy and non-uniform effects on insect herbivores. *Proc. R. Soc. B* 268, 1937–1940. doi: 10.1098/rspb.2001.1760

O'Hara, A., Headland, L. R., Díaz-Ramos, L. A., Morales, L. O., Strid, Å., and Jenkins, G. I. (2019). Regulation of Arabidopsis gene expression by low fluence rate UV-B independently of UVR8 and stress signaling. *Photochem. Photobiol. Sci.* 18, 1675–1684. doi: 10.1039/C9PP00151D

Osborn, T. C., Pires, J. C., Birchler, J. A., Auger, D. L., Chen, Z. J., Lee, H. S., et al. (2003). Understanding mechanisms of novel gene expression in polyploids. *Trends Genet.* 19, 141–147. doi: 10.1016/S0168-9525(03)00015-5

Oswald, B. P., and Nuismer, S. L. (2007). Neopolyploidy and pathogen resistance. *Proc. Biol. Sci.* 274, 2393–2397. doi: 10.1098/rspb.2007.0692

Oustric, J., Morillon, R., Luro, F., Herbette, S., Martin, P., Giannettini, J., et al. (2019). Nutrient deficiency tolerance in Citrus is dependent on genotype or ploidy level. *Front. Plant Sci.* 10, 127. doi: 10.3389/fpls.2019.00127

Paape, T., Akiyama, R., Cereghetti, T., Onda, Y., Hirao, A. S., Kenta, T., et al. (2020). Experimental and field data support range expansion in an allopolyploid Arabidopsis owing to parental legacy of heavy metal hyperaccumulation. *Front. Genet.* 11:565854. doi: 10.3389/fgene.2020.565854

Pan, Y. Q., Guo, H., Wang, S. M., Zhao, B., Zhang, J. L., Ma, Q., et al. (2016). The photosynthesis, Na^+/K^+ homeostasis and osmotic adjustment of *Atriplex canescens* in response to salinity. *Front. Plant Sci.* 7, 848. doi: 10.3389/fpls.2016.00848

Pan, Y., Wu, L. J., and Yu, Z. L. (2006). Effect of salt and drought stress on antioxidant enzymes activities and SOD isoenzymes of liquorice (*Glycyrrhiza uralensis* Fisch). *Plant Growth Regul.* 49, 157–165. doi: 10.1007/s10725-006-9101-y

Parisod, C., Salmon, A., Zerjal, T., Tenaillon, M., Grandbastien, M. A., and Ainouche, M. (2009). Rapid structural and epigenetic reorganization near transposable elements in hybrid and allopolyploid genomes in Spartina. *New Phytol.* 184, 1003–1015. doi: 10.1111/j.1469-8137.2009.03029.x

Paterson, A. H., Bowers, J. E., and Chapman, B. A. (2004). Ancient polyploidization predating divergence of the cereals, and its consequences for comparative genomics. *Proc. Natl. Acad. Sci. U. S. A.* 101, 9903–9908. doi: 10.1073/pnas.0307901101

Pecrix, Y., Rallo, G., Folzer, H., Cigna, M., Gudin, S., and Le Bris, M. (2011). Polyploidization mechanisms: temperature environment can induce diploid gamete formation in Rosa sp. *J. Exp. Bot.* 62, 3587–3597. doi: 10.1093/jxb/err052

Petersen, S. V., Dutton, A., and Lohmann, K. C. (2016). End-cretaceous extinction in Antarctica linked to both Deccan volcanism and meteorite impact *via* climate change. *Nat. Commun.* 7, 12079. doi: 10.1038/ncomms12079

Pfeil, B. E., Schlueter, J. A., Shoemaker, R. C., and Doyle, J. J. (2005). Placing paleopolyploidy in relation to taxon divergence: a phylogenetic analysis in legumes using 39 gene families. *Syst. Biol.* 54, 441–454. doi: 10.1080/10635150590945359

Podda, A., Checcucci, G., Mouhaya, W., Centeno, D., Rofidal, V., Del Carratore, R., et al. (2013). Salt-stress induced changes in the leaf proteome of diploid and tetraploid mandarins with contrasting Na^+ and cl-accumulation behaviour. *J. Plant Physiol.* 170, 1101–1112. doi: 10.1016/j.jplph.2013.03.006

Poorter, H., Niklas, K. J., Reich, P. B., Oleksyn, J., Poot, P., and Mommer, L. (2012). Biomass allocation to leaves, stems and roots: meta-analyses of interspecific variation and environmental control. *New Phytol.* 193, 30–50. doi: 10.1111/j.1469-8137.2011.03952.x

Prasad, M. N. V., and de Oliveira Freitas, H. M. (2003). Metal hyperaccumulation in plants: biodiversity prospecting for phytoremediation technology. *Electron. J. Biotechnol.* 6, 285–321. doi: 10.2225/vol6-issue3-fulltext-6

Qin, X., Yin, Y., Zhao, J., An, W., Fan, Y., Liang, X., et al. (2022). Metabolomic and transcriptomic analysis of *Lycium chinese* and *L. ruthenicum* under salinity stress. *BMC Plant Biol.* 22, 8. doi: 10.1186/s12870-021-03375-x

Quadrana, L., Etcheverry, M., Gilly, A., Caillieux, E., Madoui, M. A., Guy, J., et al. (2019). Transposition favors the generation of large effect mutations that may facilitate rapid adaption. *Nat. Commun.* 10, 1–10. doi: 10.1038/s41467-019-11385-5

Radziejwoski, A., Vlieghe, K., Lammens, T., Berckmans, B., Maes, S., Jansen, M. A., et al. (2011). Atypical E2F activity coordinates PHR1 photolyase gene transcription with endoreduplication onset. *EMBO J.* 30, 355–363. doi: 10.1038/emboj.2010.313

Rahman, K. M. A. and, Zhang, D. (2018). Effects of fertilizer broadcasting on the excessive use of inorganic fertilizers and environmental sustainability. *Sustainability*, 10, 759. doi: 10.3390/su10030759

Ramsey, J. (2011). Polyploidy and ecological adaptation in wild yarrow. *Proc. Natl. Acad. Sci. U. S. A.* 108, 7096–7101. doi: 10.1073/pnas.1016631108

Rao, S., Tian, Y., Xia, X., Li, Y., and Chen, J. (2020). Chromosome doubling mediates superior drought tolerance in *Lyciumruthenicum via* abscisic acid signaling. *Hortic Res.* 7, 1–18. doi: 10.1038/s41438-020-0260-1

Renny-Byfield, S., and Wendel, J. F. (2014). Doubling down on genomes: polyploidy and crop plants. *Am. J. Bot.* 101, 1711–1725. doi: 10.3732/ajb.1400119

Rieu, I., Twell, D., and Firon, N. (2017). Pollen development at high temperature: from acclimation to collapse. *Plant Physiol.* 173, 1967–1976. doi: 10.1104/pp.16.01644

Rizzini, L., Favory, J. J., Cloix, C., Faggionato, D., O'Hara, A., Kaiserli, E., et al. (2011). Perception of UV-B by the Arabidopsis UVR8 protein. *Science* 332, 103–106. doi: 10.1126/science.1200660

Robertson, F. M., Gundappa, M. K., Grammes, F., Hvidsten, T. R., Redmond, A. K., Lien, S., et al. (2017). Lineage-specific rediploidization is a mechanism to explain time-lags between genome duplication and evolutionary diversification. *Genome Biol.* 18, 111. doi: 10.1186/s13059-017-1241-z

Ruiz, M., Oustric, J., Santini, J., and Morillon, R. (2020). Synthetic polyploidy in grafted crops. *Front. Plant Sci.* 11:540894. doi: 10.3389/fpls.2020.540894

Ruiz, M., Quiñones, A., Martínez-Alcántara, B., Aleza, P., Morillon, R., Navarro, L., et al. (2016). Tetraploidy enhances boron-excess tolerance in Carrizo citrange (*Citrus sinensis* L. Osb.× *Poncirus trifoliata* L. Raf.). *Front. Plant Sci.* 7, 701. doi: 10.3389/fpls.2016.00701

Ruprecht, C., Lohaus, R., Vanneste, K., Mutwil, M., Nikoloski, Z., Van De Peer, Y., et al. (2017). Revisiting ancestral polyploidy in plants. *Science Adv.* 3, 1–7. doi: 10.1126/sciadv.1603195

Rus, A., Baxter, I., Muthukumar, B., Gustin, J., Lahner, B., Yakubova, E., et al. (2006). Natural variants of AtHKT1 enhance Na^+ accumulation in two wild populations of Arabidopsis. *PLoS Genet.* 2:e210. doi: 10.1371/journal.pgen.0020210

Saleh, B., Allario, T., Dambier, D., Ollitrault, P., and Morillon, R. (2008). Tetraploid citrus rootstocks are more tolerant to salt stress than diploid. *C. R. Biol.* 331, 703–710. doi: 10.1016/j.crvi.2008.06.007

Schlaepfer, D. R., Edwards, P. J., and Billeter, R. (2010). Why only tetraploid *Solidago gigantea* (Asteraceae) became invasive: a common garden comparison of ploidy levels. *Oecologia* 163, 661–673. doi: 10.1007/s00442-010-1595-3

Schranz, M. E., Mohammadin, S., and Edger, P. P. (2012). Ancient whole genome duplications, novelty and diversification: the WGD radiation lag-time model. *Curr. Opin. Plant Biol.* 15, 147–153. doi: 10.1016/j.pbi.2012.03.011

Schumann, G. L., and D'Arcy, C. J. (2006). *Essential Plant Pathology*. APS Press, St. Paul, MN.

Schwachtje, J., Whitcomb, S. J., Firmino, A. A. P., Zuther, E., Hincha, D. K., and Kopka, J. (2019). Induced, imprinted, and primed responses to changing environments: does metabolism store and process information? *Front. Plant Sci.* 10, 106. doi: 10.3389/fpls.2019.00106

Sehrish, T., Symonds, V. V., Soltis, D. E., Soltis, P. S., and Tate, J. A. (2014). Gene silencing *via* DNA methylation in naturally occurring *Tragopogon miscellus* (Asteraceae) allopolyploids. *BMC Genomics* 15, 701. doi: 10.1186/1471-2164-15-701

Shabala, S., and Pottosin, I. (2014). Regulation of potassium transport in plants under hostile conditions: implications for abiotic and biotic stress tolerance. *Physiol. Plant.* 151, 257–279. doi: 10.1111/ppl.12165

Shabala, L., Zhang, J., Pottosin, I., Bose, J., Zhu, M., Fuglsang, A. T., et al. (2016). Cell-type-specific H^+-ATPase activity in root tissues enables K^+ retention and mediates acclimation of barley (*Hordeum vulgare*) to salinity stress. *Plant Physiol.* 172, 2445–2458. doi: 10.1104/pp.16.01347

Shannon, M. C. (1998). Adaptation of plants to salinity. *Adv. Agron.* 60, 75–119. doi: 10.1016/S0065-2113(08)60601-X

Shi, T., Huang, H., and Barker, M. S. (2010). Ancient genome duplications during the evolution of kiwifruit (Actinidia) and related Ericales. *Ann. Bot.* 106, 497–504. doi: 10.1093/aob/mcq129

Sicilia, A., Testa, G., Santoro, D. F., Cosentino, S. L., and Lo Piero, A. R. (2019). RNASeq analysis of giant cane reveals the leaf transcriptome dynamics under long-term salt stress. *BMC Plant Biol.* 19, 355. doi: 10.1186/s12870-019-1964-y

Simonin, K. A., and Roddy, A. B. (2018). Genome downsizing, physiological novelty, and the global dominance of flowering plants. *PLoS Biol.* 16:e2003706. doi: 10.1371/journal.pbio.2003706

Soltis, P. S., and Soltis, D. E. (2009). The role of hybridization in plant speciation. *Annu. Rev. Plant Biol.* 60, 561–588. doi: 10.1146/annurev.arplant.043008.092039

Soltis, D. E., Visger, C. J., and Soltis, P. S. (2014). The polyploidy revolution then… and now: Stebbins revisited. *Am. J. Bot.* 101, 1057–1078. doi: 10.3732/ajb.1400178

Song, X.-M., Wang, J.-P., Sun, P.-C., Ma, X., Yang, Q.-H., Hu, J.-J., et al. (2020). Preferential gene retention increases the robustness of cold regulation in Brassicaceae and other plants after polyploidization. *Hort. Res.* 7, 20. doi: 10.1038/s41438-020-0253-0

Sora, D., Kron, P., and Husband, B. (2016). Genetic and environmental determinants of unreduced gamete production in *Brassica napus*, *Sinapis arvensis* and their hybrids. *Heredity* 117, 440–448. doi: 10.1038/hdy.2016.69

Springer, N. M., and Lisch, D. and, Li, Q. (2016). Creating order from chaos: epigenome dynamics in plants with complex genomes. *Plant Cell* 28, 314–325. doi: 10.1105/tpc.15.00911

Sreedharan, S., Shekhawat, U. K., and Ganapathi, T. R. (2013). Transgenic banana plants overexpressing a native plasma membrane aquaporin MusaPIP1: 2 display high tolerance levels to different abiotic stresses. *Plant Biotechnol. J.* 11, 942–952. doi: 10.1111/pbi.12086

Steudle, E. (2000). Water uptake by roots: effects of water deficit. *J. Exp. Bot.* 51, 1531–1542. doi: 10.1093/jexbot/51.350.1531

Sugiyama, S. (1998). Differentiation in competitive ability and cold tolerance between diploid and tetraploid cultivars in *Lolium perenne*. *Euphytica* 103, 55–59. doi: 10.1023/A:1018322821118

Sun, J., Chen, S., Dai, S., Wang, R., Li, N., Shen, X., et al. (2009). NaCl-induced alternations of cellular and tissue ion fluxes in roots of salt-resistant and salt-sensitive poplar species. *Plant Physiol.* 149, 1141–1153. doi: 10.1104/pp.108.129494

Sun, J., Wang, M. J., Ding, M. Q., Deng, S. R., Liu, M. Q., Lu, C. F., et al. (2010). H_2O_2 and cytosolic Ca^{2+} signals triggered by the PM H-coupled transport system mediate K^+/Na^+ homeostasis in NaCl-stressed *Populus euphratica* cells. *Plant Cell Environ.* 33, 943–958. doi: 10.1111/j.1365-3040.2010.02118.x

Tal, M., and Gardi, I. (1976). Physiology of Polyploid plants: water balance in autotetraploid and diploid tomato under low and high salinity. *Physiol. Plant.* 38, 257–261. doi: 10.1111/j.1399-3054.1976.tb04000.x

Talei, D., and Fotokian, M. H. (2020). Improving growth indices and productivity of phytochemical compounds in lemon balm (*Melissa officinalis* L.) *via* induced polyploidy. *BioTechnol* 101, 215–226. doi: 10.5114/bta.2020.97880

Tamayo-Ordóñez, M. C., Rodriguez-Zapata, L. C., Narváez-Zapata, J. A., Tamayo-Ordóñez, Y. J., Ayil-Gutiérrez, B. A., Barredo-Pool, F., et al. (2016). Morphological features of different polyploids for adaptation and molecular characterization of CC-NBS-LRR and LEA gene families in *Agave* L. *J. Plant Physiol.* 195, 80–94. doi: 10.1016/j.jplph.2016.03.009

Tardieu, F., Simonneau, T., and Muller, B. (2018). The physiological basis of drought tolerance in crop plants: a scenario-dependent probabilistic approach. *Annu. Rev. Plant Biol.* 69, 733–759. doi: 10.1146/annurev-arplant-042817-040218

te Beest, M., Le Roux, J. J., Richardson, D. M., Brysting, A. K., Suda, J., Kubešová, M., et al. (2012). The more the better? The role of polyploidy in facilitating plant invasions. *Ann. Bot.* 109, 19–45. doi: 10.1093/aob/mcr277

Thompson, J. N., Cunningham, B. M., Segraves, K. A., Althoff, D. M., and Wagner, D. (1997). Plant polyploidy and insect/plant interactions. *Am. Nat.* 150, 730–743. doi: 10.1086/286091

Thor, K. (2019). Calcium: nutrient and Messenger. *Front. Plant Sci.* 10, 440. doi: 10.3389/fpls.2019.00440

Tittel-Elmer, M., Bucher, E., Broger, L., Mathieu, O., Paszkowski, J., and Vaillant, I. (2010). Stress-induced activation of heterochromatic transcription. *PLoS Gen.* 6:e1001175. doi: 10.1371/journal.pgen.1001175

Tu, Y., Jiang, A., Gan, L., Hossain, M., Zhang, J., Peng, B., et al. (2014). Genome duplication improves rice root resistance to salt stress. *Rice* 7, 15. doi: 10.1186/s12284-014-0015-4

Van de Peer, Y., Ashman, T. L., Soltis, P. S., and Soltis, D. E. (2021). Polyploidy: an evolutionary and ecological force in stressful times. *Plant Cell* 33, 11–26. doi: 10.1093/plcell/koaa015

Van de Peer, Y., Maere, S., and Meyer, A. (2009). The evolutionary significance of ancient genome duplications. *Nat. Rev. Genet.* 10, 725–732. doi: 10.1038/nrg2600

Van de Peer, Y., Mizrachi, E., and Marchal, K. (2017). The evolutionary significance of polyploidy. *Nat. Rev. Genet.* 18, 411–424. doi: 10.1038/nrg.2017.26

Vanneste, K., Baele, G., Maere, S., and Van de Peer, Y. (2014a). Analysis of 41 plant genomes supports a wave of successful genome duplications in association with the Cretaceous–Paleogene boundary. *Genome Res.* 24, 1334–1347. doi: 10.1101/gr.168997.113

Vanneste, K., Maere, S., and Van de Peer, Y. (2014b). Tangled up in two: a burst of genome duplications at the end of the cretaceous and the consequences for plant evolution. *Phil. Trans. R. Soc. B.* 369, 20130353. doi: 10.1098/rstb.2013.0353

Vergara, F., Kikuchi, J., and Breuer, C. (2016). Artificial autopolyploidization modifies the tricarboxylic acid cycle and GABA shunt in *Arabidopsis thaliana* Col-0. *Sci. Rep.* 6, 26515. doi: 10.1038/srep26515

Verslues, P. E., Agarwal, M., Katiyar-Agarwal, S., Zhu, J., and Zhu, J. K. (2006). Methods and concepts in quantifying resistance to drought, salt and freezing, abiotic stresses that affect plant water status. *Plant J.* 45, 523–539. doi: 10.1111/j.1365-313X.2005.02593.x

Wang, L., Cao, S., Wang, P., Lu, K., Song, Q., Zhao, F.-J., et al. (2021). DNA hypomethylation in tetraploid rice potentiates stress-responsive gene expression for salt tolerance. *Proc. Natl. Acad. Sci. U. S. A.* 118:e2023981118. doi: 10.1073/pnas.2023981118

Wang, Z., Zheng, Q., Shen, Q., and Guo, S. (2013a). The critical role of potassium in plant stress response. *Int. J. Mol. Sci.* 14, 7370–7390. doi: 10.3390/ijms14047370

Wang, Q., Liu, H., Gao, A., Yang, X., Liu, W., Li, X., et al. (2012). Intergenomic rearrangements after polyploidization of *Kengyilia thoroldiana* (Poaceae: Triticeae) affected by environmental factors. *PLoS One* 7:e31033. doi: 10.1371/journal.pone.0031033

Wang, Z., Wang, M., Liu, L., and Meng, F. (2013b). Physiological and proteomic responses of diploid and tetraploid black locust (*Robinia pseudoacacia* L.) subjected to salt stress. *Int. J. Mol. Sci.* 14, 20299–20325. doi: 10.3390/ijms141020299

Wang, Z., Zhao, Z., Fan, G., Dong, Y., Deng, M., Xu, E., et al. (2018). A comparison of the transcriptomes between diploid and autotetraploid *Paulownia fortunei* under salt stress. *Physiol. Mol. Biol. Plants* 25, 1–11. doi: 10.1007/s12298-018-0578-4

Wargent, J. J., Gegas, V. C., Jenkins, G. I., Doonan, J. H., and Paul, N. D. (2009). UVR8 in *Arabidopsis thaliana* regulates multiple aspects of cellular differentiation during leaf development in response to ultraviolet B radiation. *New Phytol.* 183, 315–326. doi: 10.1111/j.1469-8137.2009.02855.x

Wei, N., Du, Z., Liston, A., and Ashman, T. L. (2020). Genome duplication effects on functional traits and fitness are genetic context and species dependent: studies of synthetic polyploid Fragaria. *Am. J. Bot.* 107, 262–272. doi: 10.1002/ajb2.1377

Wilkinson, S., and Davies, W. J. (2002). ABA-based chemical signalling: the co-ordination of responses to stress in plants. *Plant Cell Environ.* 25, 195–210. doi: 10.1046/j.0016-8025.2001.00824.x

Willing, E. M., Rawat, V., Mandáková, T., Maumus, F., James, G. V., Nordström, K. J., et al. (2015). Genome expansion of *Arabis alpina* linked with retrotransposition and reduced symmetric DNA methylation. *Nature Plants.* 1, 14023. doi: 10.1038/nplants.2014.23

Wójcik, D., Marat, M., Marasek-Ciołakowska, A., Klamkowski, K., Buler, Z., Podwyszyńska, M., et al. (2022). Apple autotetraploids – phenotypic characterisation and response to drought stress. *Agronomy* 12, 161. doi: 10.3390/agronomy12010161

Wu, M., Ge, Y., Xu, C., and Wang, J. (2020a). Metabolome and transcriptome analysis of hexaploid *Solidago canadensis* roots reveals its invasive capacity related to polyploidy. *Genes.* 11, 187.

Wu, S., Han, B., and Jiao, Y. (2020b). Genetic contribution of paleopolyploidy to adaptive evolution in angiosperms. *Mol. Plant* 13, 59–71. doi: 10.1016/j.molp.2019.10.012

Wu, Q., Su, N., Zhang, X., Liu, Y., Cui, J., and Liang, Y. (2016). Hydrogen peroxide, nitric oxide and UV RESISTANCE LOCUS8 interact to mediate UV-B-induced anthocyanin biosynthesis in radish sprouts. *Sci. Rep.* 6, 1–12. doi: 10.1038/srep29164

Xie, S., Khan, N., Ramanna, M. S., Niu, L., Marasek-Ciolakowska, A., Arens, P., et al. (2010). An assessment of chromosomal rearrangements in neopolyploids of Lilium hybrids. *Genome* 53, 439–446. doi: 10.1139/G10-018.

Xiong, Z., Gaeta, R. T., and Pires, J. C. (2011). Homoeologous shuffling and chromosome compensation maintain genome balance in resynthesized allopolyploid *Brassica napus*. *Proc. Natl. Acad. Sci. U. S. A.* 108, 7908–7913. doi: 10.1073/pnas.1014138108

Xiong, Y. C., Li, F. M., and Zhang, T. (2006). Performance of wheat crops with different chromosome ploidy: root-sourced signals, drought tolerance, and yield performance. *Planta* 224, 710–718. doi: 10.1007/s00425-006-0252-x

Xu, Y., Wei, H., Liu, J. H., Zhang, J. B., Jia, C. H., Miao, H. X., et al. (2014). A banana aquaporin gene MaPIP1: 1 is involved in tolerance to drought and salt stresses. *BMC Plant Biol.* 14, 59. doi: 10.1186/1471-2229-14-59

Xu, Y., Yang, F., Tian, X., Zhang, W., Wang, X., and Ma, G. (2011). Different patterns of transcriptomic response to high temperature between diploid and tetraploid *Dioscorea zingiberensis* CH. *Afri. J. Biotech.* 10, 8847–8854. doi: 10.5897/AJB11.384

Xue, H., Zhang, F., Zhang, Z., Fu, J., Wang, F., Zhang, B., et al. (2015). Differences in salt tolerance between diploid and autotetraploid apple seedlings exposed to salt stress. *Sci. Hortic.* 190, 24–30. doi: 10.1016/j.scienta.2015.04.009

Yaakov, B., and Kashkush, K. (2012). Mobilization of stowaway-like MITEs in newly formed allohexaploid wheat species. *Plant Mol. Biol.* 80, 419–427. doi: 10.1007/s11103-012-9957-3

Yamada, M., Morishita, H., Urano, K., Shiozaki, N., Yamaguchi-Shinozaki, K., Shinozaki, K., et al. (2005). Effects of free proline accumulation in petunias under drought stress. *J. Exp. Bot.* 56, 1975–1981. doi: 10.1093/jxb/eri195

Yang, P. M., Huang, Q. C., Qin, G. Y., Zhao, S. P., and Zhou, J. G. (2014). Different drought-stress responses in photosynthesis and reactive oxygen metabolism between autotetraploid and diploid rice. *Photosynthetica* 52, 193–202. doi: 10.1007/s11099-014-0020-2

Yang, C., Yang, Z., Zhao, L., Sun, F., and Liu, B. (2018). A newly formed hexaploid wheat exhibits immediate higher tolerance to nitrogen-deficiency than its parental lines. *BMC Plant Biol.* 18, 113. doi: 10.1186/s12870-018-1334-1

Yoo, M. J., Liu, X., Pires, J. C., Soltis, P. S., and Soltis, D. E. (2014). Nonadditive gene expression in polyploids. *Annu. Rev. Genet.* 48, 485–517. doi: 10.1146/annurev-genet-120213-092159

Yu, Y., Xiang, Q., Manos, P. S., Soltis, D. E., Soltis, P. S., Song, B., et al. (2017). Whole-genome duplication and molecular evolution in *Cornus* L. (Cornaceae) — insights from transcriptome sequences. *PLoS One* 12:e0171361. doi: 10.1371/journal.pone.0171361

Zhang, X. Y., Hu, C. G., and Yao, J. L. (2010). Tetraploidization of diploid Dioscorea results in activation of the antioxidant defense system and increased heat tolerance. *J. Plant Physiol.* 167, 88–94. doi: 10.1016/j.jplph.2009.07.006

Zhang, L., Ma, H., Chen, T., Pen, J., Yu, S., and Zhao, X. (2014). Morphological and physiological responses of cotton (*Gossypium hirsutum* L.) plants to salinity. *PLoS One* 9:e112807. doi: 10.1371/journal.pone.0112807

Zhang, G. B., Meng, S., and Gong, J. M. (2018). The expected and unexpected roles of nitrate transporters in plant abiotic stress resistance and their regulation. *Int. J. Mol. Sci.* 19, 3535. doi: 10.3390/ijms19113535

Zhang, F., Wang, Y., Yang, Y., Wu, H., Wang, D., and Liu, J. (2007). Involvement of hydrogen peroxide and nitric oxide in salt resistance in the calluses from *Populus euphratica*. *Plant Cell Environ.* 30, 775–785. doi: 10.1111/j.1365-3040.2007.01667.x

Zhang, F., Xue, H., Lu, X., Zhang, B., Wang, F., Ma, Y., et al. (2015). Autotetraploidization enhances drought stress tolerance in two apple cultivars. *Trees-Struct. Funct.* 29, 1773–1780. doi: 10.1007/s00468-015-1258-4

Zhao, Z., Li, Y., Liu, H., Zhai, X., Deng, M., Dong, Y., et al. (2017b). Genome-wide expression analysis of salt-stressed diploid and autotetraploid *Paulownia tomentosa*. *PLoS One* 12:e0185455. doi: 10.1371/journal.pone.0185455

Zhao, H., Liu, H., Jin, J., Ma, X., and Li, K. (2022). Physiological and transcriptome analysis on diploid and Polyploid *Populus ussuriensis* Kom. Under Salt stress. *Int. J. Mol. Sci.* 23, 7529. doi: 10.3390/ijms23147529

Zhao, C., Liu, B., Piao, S., Wang, X., Lobell, D. B., Huang, Y., et al. (2017a). Temperature increase reduces global yields of major crops in four independent estimates. *Proc. Natl. Acad. Sci. U. S. A.* 114, 9326–9331. doi: 10.1073/pnas.1701762114

Zhou, C., Liu, X., Li, X., Zhou, H., Wang, S., Yuan, Z., et al. (2021). A genome doubling event reshapes Rice morphology and products by modulating chromatin signatures and gene expression profiling. *Rice* 14, 72. doi: 10.1186/s12284-021-00515-7

Zhu, J. K. (2001). Plant salt tolerance. *Trends Plant Sci.* 6, 66–71. doi: 10.1016/S1360-1385(00)01838-0

Zhu, J. K. (2016). Abiotic stress signaling and responses in plants. *Cell* 167, 313–324. doi: 10.1016/j.cell.2016.08.029

frontiers | Frontiers in Plant Science

TYPE Original Research
PUBLISHED 09 September 2022
DOI 10.3389/fpls.2022.995402

OPEN ACCESS

EDITED BY
Jeremy Coate,
Reed College, United States

REVIEWED BY
Pui Ying Lam,
Akita University, Japan
Katharina Braeutigam,
University of Toronto
Mississauga, Canada

*CORRESPONDENCE
Wout Boerjan
wout.boerjan@psb.vib-ugent.be

†These authors have contributed equally to this work and share last authorship

SPECIALTY SECTION
This article was submitted to Plant Breeding, a section of the journal Frontiers in Plant Science

RECEIVED 15 July 2022
ACCEPTED 22 August 2022
PUBLISHED 09 September 2022

CITATION
Wouters M, Corneillie S, Dewitte A, Van Doorsselaere J, Van den Bulcke J, Van Acker J, Vanholme B and Boerjan W (2022) Whole genome duplication of wild-type and *CINNAMYL ALCOHOL DEHYDROGENASE1*-downregulated hybrid poplar reduces biomass yield and causes a brittle apex phenotype in field-grown wild types.
Front. Plant Sci. 13:995402.
doi: 10.3389/fpls.2022.995402

Whole genome duplication of wild-type and *CINNAMYL ALCOHOL DEHYDROGENASE1*-downregulated hybrid poplar reduces biomass yield and causes a brittle apex phenotype in field-grown wild types

Marlies Wouters[1,2], Sander Corneillie[1,2], Angelo Dewitte[3], Jan Van Doorsselaere[3], Jan Van den Bulcke[4], Joris Van Acker[4], Bartel Vanholme[1,2†] and Wout Boerjan[1,2*†]

[1]Department of Plant Biotechnology and Bioinformatics, Ghent University, Ghent, Belgium, [2]VIB Center for Plant Systems Biology, Ghent, Belgium, [3]Expertisecentrum Agro- en Biotechnologie, VIVES, Roeselare, Belgium, [4]Laboratory of Wood Technology, Department of Environment, Faculty of Bioscience Engineering, Ghent University, Ghent, Belgium

The potential of whole genome duplication to increase plant biomass yield is well-known. In Arabidopsis tetraploids, an increase in biomass yield was accompanied by a reduction in lignin content and, as a result, a higher saccharification efficiency was achieved compared with diploid controls. Here, we evaluated whether the results obtained in Arabidopsis could be translated into poplar and whether the enhanced saccharification yield upon alkaline pretreatment of hairpin-downregulated *CINNAMYL ALCOHOL DEHYDROGENASE1* (*hpCAD*) transgenic poplar could be further improved upon a whole genome duplication. Using a colchicine treatment, wild-type (WT) *Populus tremula* x *P. alba* cv. INRA 717-1B4, a commonly used model clone in tree biotechnology research, and *hpCAD* tetraploids were generated and grown in the greenhouse. In parallel, WT tetraploid poplars were grown in the field. In contrast to Arabidopsis, a whole genome duplication of poplar had a negative impact on the biomass yield of both greenhouse- and field-grown trees. Strikingly, field-grown WT tetraploids developed a brittle apex phenotype, i.e., their tip broke off just below the apex. In addition, the chromosome doubling altered the biomass composition of field-grown, but not of greenhouse-grown tetraploid poplars. More specifically, the lignin content of field-grown tetraploid poplars was increased at the expense of matrix polysaccharides. This increase in lignin deposition in biomass is likely the cause of the observed brittle apex phenotype, though no major differences in stem anatomy or in mechanical properties could be found between di- and tetraploid WT poplars grown in the field. Finally, without biomass pretreatment, the saccharification efficiency of greenhouse- and field-grown WT diploids was not different from that of tetraploids, whereas that of greenhouse-grown

hpCAD tetraploids was higher than that of greenhouse-grown diploids. Upon alkaline pretreatment, the saccharification yield of diploids was similar to that of tetraploids for all genotypes and growth conditions tested. This study showed that a whole genome duplication in hybrid WT and *hpCAD* poplar did neither result in further improvements in biomass yield, nor in improved biomass composition and, hence, saccharification performance.

KEYWORDS

polyploidy, field trial, CAD, lignin, saccharification

Introduction

Poplar (*Populus* spp.) is an ecologically and economically important tree genus widely grown in the northern hemisphere. Because of their fast growth, easy clonal propagation and amenability to genetic transformation, poplars have become the species of choice for genetics, physiology and biotechnology research on trees (Wullschleger et al., 2002; Singh et al., 2021). In addition, poplar woody biomass is increasingly gaining interest as a renewable feedstock for biorefineries, explaining the research efforts focusing on its secondary cell wall (Porth, 2015).

The plant secondary cell wall consists of large amounts of polysaccharides embedded in lignin. These polysaccharides can be enzymatically depolymerized—a process called saccharification—into monosaccharides that, in turn, can be fermented into yield biofuels or building blocks for all kinds of biobased products that are nowadays predominantly made from fossil sources (Vanholme et al., 2013). The major factor limiting efficient saccharification is lignin, hindering the access of depolymerizing enzymes to the polysaccharides (Chen and Dixon, 2007; Van Acker et al., 2013; Zeng et al., 2014). Lignin is a heterogeneous aromatic polymer composed of H, G and S units that are formed by combinatorial radical coupling of the monolignol building blocks *p*-coumaryl, coniferyl and sinapyl alcohol, respectively (Boerjan et al., 2003; Bonawitz and Chapple, 2010; Vanholme et al., 2019). Reducing the lignin amount or altering its composition by genetic engineering is a popular strategy to improve the saccharification efficiency of the lignocellulosic biomass (Chanoca et al., 2019; Bryant et al., 2020). However, reducing lignin content has its limit as this polymer plays a role in providing fiber strength and vessel hydrophobicity to the cell wall, ultimately resulting in a drop in biomass yield when lignin levels are too low (Muro-Villanueva et al., 2019; De Meester et al., 2020; De Vries et al., 2021). To fully unlock the potential of trees as biorefinery crops, both biomass yield and cell wall composition should be optimized. Using traditional breeding, such as interspecies hybridization, large improvements in biomass yield have been obtained, and genetic engineering strategies have proven to be successful in lowering the lignin amount without yield penalty (Van Acker et al., 2017; De Meester et al., 2020, 2021; Gui et al., 2020; Jang et al., 2021). The induction of artificial polyploidization might be an additional option to further improve the biomass yield and saccharification efficiency of trees.

Polyploidy typically increases cell size, known as the "*gigas*" effect of polyploidy (Stebbins, 1971). *In vitro* induction of allotetraploids in *P. alba x P. glandulosa* and (*P. pseudo-simonii x P. nigra*) *x P. beijingensis* resulted in larger and thicker leaves (Xu et al., 2016; Ren et al., 2021). In *Arabidopsis thaliana,* it has been found that artificial autotetraploids have a significant increase in stem height and dry weight, while the lignin content is reduced, resulting in an improved saccharification efficiency (Corneillie et al., 2019). A similar correlation between ploidy level and lignin content has been described for autotetraploid shrub willow, although the saccharification potential of the obtained biomass was not determined (Serapiglia et al., 2014, 2015). It has also been reported for autotetraploid acacia that the Kraft pulp yield is similar to that of diploid wood, but less alkali is consumed, indicating improved wood processing efficiency (Griffin et al., 2014).

To investigate the potential of polyploidization as a means to improve both the biomass yield and saccharification efficiency of poplar, colchicine-mediated induction of tetraploids was performed in the wild-type (WT) female hybrid *P. tremula* x *P. alba* cv. INRA 717-1B4, a well-studied model clone because of its high amenability to *Agrobacterium*-mediated transformation and the availability of a genome sequence (Leplé et al., 1992; Chupeau et al., 1994; Busov et al., 2011; Mader et al., 2016; Nietsch et al., 2017), and the transgenic hairpin-downregulated *CINNAMYL ALCOHOL DEHYDROGENASE1* (*hpCAD*), made in the same genetic background (Van Acker et al., 2017). CAD1 catalyzes the last step of the monolignol biosynthesis pathway, and downregulating *CAD1* in *P. tremula* x *P. alba* reduces the conversion of hydroxycinnamaldehydes to their respective

Abbreviations: 2x, diploid; 4x, tertraploid; CWR, cell wall residue; GC-MS, gas chromatography-mass spectrometry; *hpCAD,* hairpin-downregulated *CINNAMYL ALCOHOL DEHYDROGENASE1*; MOE, modulus of elasticity; MOR, modulus of rupture; MPS, matrix polysaccharides; TFA, trifluoroacetic acid; WT, wild type.

alcohols. Consequently, sinapaldehyde is incorporated in the lignin of *CAD1*-downregulated poplars resulting in (1) a higher proportion of free phenolic end-groups, making lignin more alkali-soluble, and (2) an increase in conjugated carbonyl functions that facilitate lignin cleavage under alkaline conditions (Baucher et al., 1996; Pilate et al., 2002; Lapierre et al., 2004; Van Acker et al., 2017). Accordingly, the saccharification yield of greenhouse-grown *hpCAD* poplars is increased by up to 81% compared with non-transgenic control lines upon an alkaline pretreatment (Van Acker et al., 2017).

Here, we studied the effect of whole genome duplication on the biomass yield, biomass composition and saccharification efficiency of WT and *hpCAD* allotetraploids that were grown in greenhouse conditions. In addition, a field trial was performed with the WT allotetraploids and their diploids controls.

Materials and methods

Plant material

The lines used were WT hybrid *P. tremula* x *P. alba* cv. INRA 717-1B4 and transgenic *hpCAD* line 19 as described in Van Acker et al. (2017).

Induction of polyploidy

Tetraploids were generated using a colchicine treatment. In brief, leaves of *in vitro* plantlets were removed and stems were cut in 1-cm pieces, each containing an axillary bud. Next, stem pieces were incubated (while shaking) in a 0.1% colchicine solution for 24 h, after which they were rinsed with sterile H_2O and transferred to M1/2 propagation medium [2.2 g/L MS; 1 mg/L cysteine; 0.2 g/L glutamine; 20 g/L sucrose; 5.5 g/L agar; 1% (v/v) Morel & Wetmore vitamins; 0.5 mg/L IAA; pH 5.9; adapted from Leplé et al. (1992)], allowing each axillary bud to grow into an independent *in vitro* plantlet.

Determination of the ploidy level

From the pool of colchicine-treated plantlets, diploid lines (2n = 2x), of which the treatment was not effective, and tetraploid lines (2n = 4x), of which the treatment was effective, were selected. The somatic ploidy level of all plantlets was determined using DNA flow cytometry, as described in Corneillie et al. (2019), and confirmed upon individual chromosome counting of chromosome spreads. Chromosome spreads were prepared according to Kirov et al. (2014) with an enzyme treatment of 1% cellulase and 1% pectolyase for 75 min.

Growth of trees in the greenhouse and the field, and biomass yield analyses

Three independent tetraploid WT lines and *hpCAD* lines—each with their diploid control line—were selected for analysis. Each line was *in vitro* propagated in clonal replicates, i.e., stems were cut into 1-cm stem pieces containing an axillary bud and each piece put on M1/2 medium (Leplé et al., 1992). After rooting, plantlets were transferred to soil. In the greenhouse (GH), 15 clonal replicates per line (di- and tetraploid WT and *hpCAD* lines) were grown in a randomized design. One *hpCAD*_4x biological replicate died and was left out the analyses. After an initial growth of 2 months in soil, all plants were cut back to ensure equal height of all trees at the start of the measurements. After resprouting from the stool, all shoots but the main new one were removed. The height of the main stem was monitored on a weekly basis for a period of 120 days. The growth speed was calculated by dividing the difference between the final height at day 120 and the initial height at day 21 by the analyzed period (99 days). At harvest time (day 120), the final height, the stem diameter 50 cm above soil level and the total dry weight of the debarked tree were measured.

In the field (F), 18 clonal replicates per di- and tetraploid WT line were grown in a randomized block design consisting of three blocks, each containing six clonal replicates per line (Supplementary Figure 1). The poplars were grown for 3 months in the greenhouse before they were planted at the field site located in Zwijnaarde, Belgium (51°00′00″ N, 3°42′60″ E) in May 2016. One WT_4x biological replicate snapped during planting and was left out the analyses. The height of the main stem was monitored at 11 time points over a period of 170 days. All trees that showed the brittle apex phenotype were excluded from further analyses of biomass yield. The growth speed was calculated by dividing the difference between the height at day 170 and day 9 by the period being analyzed (161 days). At day 170, the final height was measured. At harvest time in January 2017, after one growth season, the stem diameter 50 cm above soil level and the total dry weight of the debarked tree were measured.

Biomass composition analyses

All cell wall analyses were performed on purified cell wall residue (CWR) of the debarked bottom 50-cm part of the main stem harvested 10 cm above soil level. A subset of trees was made of which the dry stem weight was the closest to the average dry weight of that line (eight trees per line) for greenhouse-grown trees harvested at day 120; nine trees per line (three trees per block) for field-grown trees harvested in January 2017. A purified CWR of ground and sieved (0.5-mm mesh) stem material was prepared using sequential extraction

steps as described in Van Acker et al. (2013). The crystalline cellulose content was determined based on Updegraff (1969) as reported by Foster et al. (2010). Matrix polysaccharides (MPS, i.e., hemicellulose and pectin) were extracted from the CWR with 2 M trifluoroacetic acid (TFA) for 2 h at 99°C while shaking (750 rpm), dried under vacuum and weighed. The different monosaccharides present in the TFA extract were quantified *via* gas chromatography-mass spectrometry (GC-MS) as their corresponding alditol acetates as described by Foster et al. (2010). Response factors for each of the monosaccharides were taken from Van Acker et al. (2013). The lignin content was measured gravimetrically *via* the Klason method as essentially described by Ibáñez and Bauer (2014) and modified by Saleme et al. (2017). Klason data of greenhouse- and field-grown poplars were collected in different experiments and, therefore, cannot be compared. The lignin composition (traditional lignin units and S aldehyde marker for CAD1 deficiency) were quantified using thioacidolysis *via* GC-MS as their trimethylsilyl ether derivatives according to Robinson and Mansfield (2009). Response factors for H, G and S units, and the S aldehyde marker for CAD1 deficiency were taken from Van Acker et al. (2013). Thioacidolysis data of WT and *hpCAD* greenhouse-grown and WT field-grown poplars were collected in different experiments and, hence, cannot be compared.

Biomass saccharification assays

Saccharification assays were performed on the debarked bottom 50-cm part of the main stem of a subset of trees (see above) according to Van Acker et al. (2016). For alkaline pretreatment, ground and sieved (0.5-mm mesh) stem material was incubated in 62.5 mM NaOH for 3 h at 90°C. The enzyme mix added to each sample contained cellulase (from *Trichoderma reesei* ATCC 26921, Sigma Aldrich) and beta-glucosidase (Accellerase BG, Novozyme). Both enzymes were desalted over an Econo-Pac 10 DG column (Bio-Rad) and stacked with Bio-gel® P-6 DG gel (Bio-Rad) according to the manufacturer's guidelines. The activity of the enzyme mix was determined with a filter paper assay as described by Xiao et al. (2004). An activity of 0.01 filter paper units was added to each sample. Released glucose was measured after 10 h of saccharification *via* a quantitative color reaction and expressed as a percentage of dry weight. Saccharification data of greenhouse- and field-grown poplars were collected in different experiments and, hence, cannot be compared.

Microscopy

For microscopy, the main stem of field-grown WT trees was harvested 1 m above soil level in August 2017 of the second growth season. At that time, the WT tetraploids already showed the brittle apex phenotype. Harvested parts were fixed in 70% (v/v) ethanol. Multiple transversal stem sections of 20 μm thickness were made per plant using a Reichert-Jung 2040 Autocut Microtome (Leica) and stained with 0.5% (w/v) astra blue, 0.5% (w/v) chrysiodine and 0.5% (w/v) acridine red for 10 min. To prepare the triple staining solution, 0.5% (w/v) astra blue (Santa Cruz Biotechnology) in 2% tartaric acid was mixed with 0.5% (w/v) chrysoidine (Sigma Aldrich) in 5% (w/v) ammonium aluminum sulfate and 0.5% (v/v) glacial acetic acid and 0.5% (w/v) acridine red (Santa Cruz Biotechnology) in 5% ammonium aluminum sulfate and 0.5% (v/v) glacial acetic acid in a 4:1:1 ratio. After dehydration in isopropyl alcohol, the stained sections were mounted in Euparal mounting medium (Carl Roth). Images were acquired using a Zeiss Axioskop 2 microscope and processed using automated software described by Andriankaja et al. (2012) to quantify the average number and average area of vessels and fibers per selected area. The number of vessels was divided by the number of fiber cells to provide a ratio. The proportion of vessel lumen was defined as the total vessel area per selected area.

Three-point bending test

For the tree-point bending test, samples of the main stem of field-grown WT trees of approximately 50-cm in length were harvested in February 2022, when the trees were 4 years old. We sampled at the top and at the base of the stem, respectively, of di- and tetraploid poplars to obtain an as comparable as possible stem diameter range across all samples. The stem samples were debarked and dried at 40°C for 4 weeks. Three-point bending tests were performed using a universal testing machine (ZwickRoell). The span between the supporting pins was 340 mm, a pre-load of 30 N was applied and the actual bending was performed with a constant displacement of 8 mm/min of the central indenting pin until sample failure (30% decrease of the maximum applied force). The force-displacement data were exported to Excel.

The modulus of elasticity (MOE) was calculated using **Equation 1**:

$$MOE = \frac{sL^3}{12\pi r^4} \ (MPa)$$

with s the slope of the force-displacement curve in the elastic region (100 N–400 N), L the span between the supporting pins and r the radius of the stem sample (an average from two measurements taken in the center of the sample where the force by the central indenting pin was applied).

The modulus of rupture (MOR) was calculated using **Equation 2**:

$$MOR = \frac{8FL}{\pi d^3} \ (MPa)$$

with F the maximum applied force at failure, L the span between the supporting pins and d the diameter of the sample (a measurement taken in the center of the sample where the force by the central indenting pin was applied).

Statistical analyses

Greenhouse and field data were statistically analyzed by fitting (generalized) linear (mixed) models to the data. For a more detailed description of the models and the statistical tests, see Supplementary Materials and Methods 1.

Results

Generation of allotetraploid WT and *hpCAD* poplar lines

Allotetraploid *P. tremula x P. alba* WT and *hpCAD* poplar were obtained by incubating *in vitro* axillary buds of diploid plantlets with colchicine, an anti-mitotic agent. Subsequently, plantlets were grown from the colchicine-treated axillary buds and their ploidy levels were determined *via* flow cytometry (Figures 1A,B; Supplementary Figure 2). For both the WT and *hpCAD* genetic background, three tetraploid plantlets were clonally propagated as independent lines. All three tetraploid WT and *hpCAD* lines were grown in the greenhouse alongside their diploid control lines in a randomized design (15 trees per line). Simultaneously, a field trial was initiated with di- and tetraploid WT poplar lines (18 trees per line). Because transgenic *hpCAD* poplars need a regulatory permit to be tested in the field, we limited the field trial to the tetraploid WT lines and the corresponding diploid controls. The trees were planted in the field in May 2016 according to a randomized block design (three blocks of six trees per line; Supplementary Figure 1). In the meantime, to confirm the ploidy level of the selected lines, chromosome spreads were made to count the number of chromosomes (Figures 1C,D; Supplementary Figure 2). In line with the wild-type haploid chromosome number of 19 (Blackburn and Harrison, 1924), the chromosome numbers of di- and tetraploid lines were 38 and 76, respectively. However, one clonally propagated WT line turned out to be composed of both di- and tetraploid cells. Therefore, this mixoploid line—although initially planted in the greenhouse and field—was excluded from further analysis.

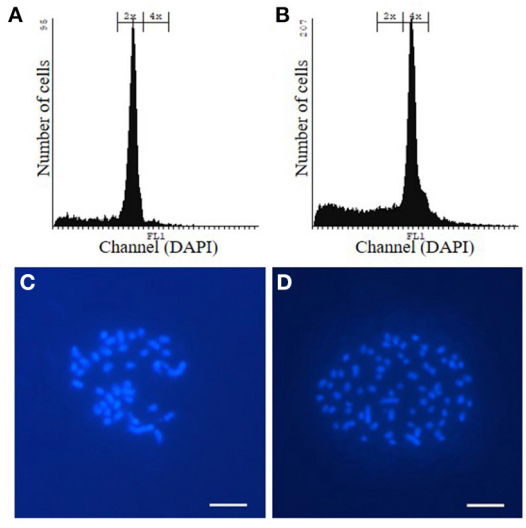

FIGURE 1
Confirmation of the ploidy level of WT poplar plantlets grown from colchicine-treated axillary buds *via* flow cytometry and chromosome spreads. **(A, C)** WT diploid poplar. **(B, D)** WT tetraploid poplar. Pictures are representative for the different independent tetraploid lines. The same way, the ploidy level of *hpCAD* di- and tetraploid poplar was verified (Supplementary Figure 2). Scale bars = 5 μm.

Biomass yield is reduced in greenhouse and field-grown allotetraploid poplars

To evaluate the effect of polyploidization on the biomass yield of hybrid *P. tremula x P. alba* trees, the greenhouse-grown trees were cut back after 2 months of growth to ensure uniform regrowth for the subsequent growth measurements. The height of the main stem resprouting from the stool was measured on a weekly basis over a period of 120 days (Figure 2A; Supplementary Table 1). As growth characteristics of the tetraploid lines with the same background (i.e., WT or *hpCAD*) were indistinguishable from one another over the period of observation, they were combined for data presentation and termed GH_WT_4x (30 replicates) and GH_*hpCAD*_4x (44 replicates).

First, we addressed the effect of whole genome duplication on biomass yield parameters in greenhouse-grown WT and *CAD1*-downregulated poplars. For WT trees, a decrease in height of tetraploids (vs. diploids) was apparent from day 63 onwards, whereas for *hpCAD* tetraploid trees, the difference was only significant from day 77 onwards. The decrease in height upon polyploidization was attributed to a reduction in growth speed of 14.78% for WT tetraploids and 16.22% for *hpCAD* tetraploids (Figure 2B; Supplementary Table 2). Accordingly, at the time of harvest (day 120), a negative impact of polyploidization on the final height was observed in the WT background (reduction of 15.11%) and the *hpCAD* background (reduction of 16.01%, Figure 2C; Supplementary Table 2). In contrast to their diploid counterparts, the stem diameter measured 50 cm above soil was 15.22% smaller in WT tetraploids and 19.48% smaller in *hpCAD* tetraploids at

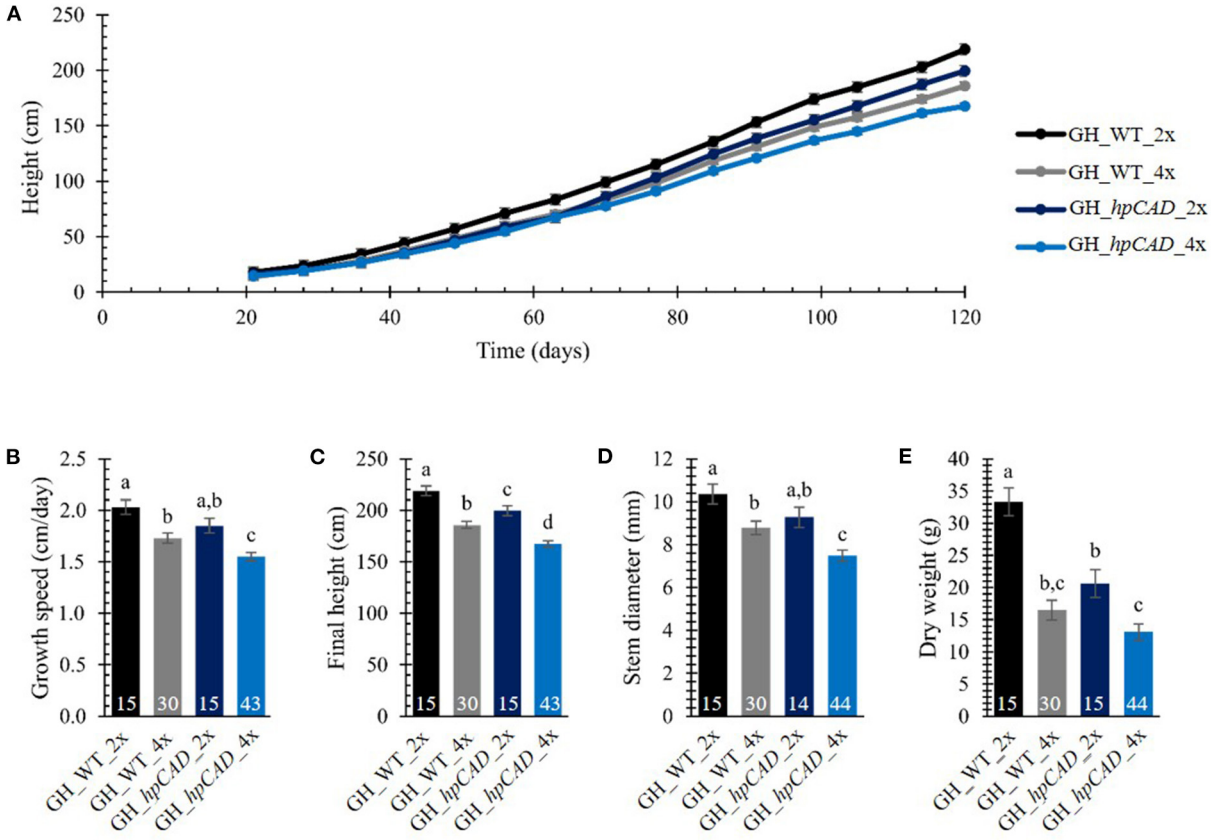

FIGURE 2
Biomass yield of greenhouse-grown di- and tetraploid poplar trees. **(A)** Height over time. The height of the main stem was measured on a weekly basis over a period of 120 days. **(B)** Growth speed. **(C)** Final height of the poplars measured at day 120. **(D)** Stem diameter measured at harvest time 50 cm above soil. **(E)** Total dry weight of the debarked tree measured at harvest time. The number of biological replicates is indicated in the bars. Data shown are adjusted mean ± standard error of the mean (SEM). Different letters represent significant differences at the 0.05 significance level. The significance differences for (A) are provided in Supplementary Table 1. For a detailed description of the models fitted to the data and the statistical tests used, see Supplementary Materials and Methods 1.

harvest time (Figure 2D; Supplementary Table 2). In addition, the total dry weight of the debarked trees at harvest time was reduced by 50.54% and 36.53% in WT and *hpCAD* tetraploids, respectively, compared with their diploid counterparts (Figure 2E; Supplementary Table 2).

Next, we studied the consequence of *CAD1*-downregulation. As a result of *CAD1*-downregulation, both *hpCAD* di- and tetraploid poplars started to show growth retardation from day 91 onwards, resulting in a reduction of the final height of respectively 8.85% and 9.82% compared with their WT counterparts (Figures 2A,C; Supplementary Tables 1, 2). Although the other parameters of biomass yield showed a similar trend for *CAD1*-downregulated trees, only the growth speed (reduction of 10.44%) and the diameter (reduction of 14.87%) of *hpCAD* tetraploids were significantly decreased compared with those of the WT tetraploids (Figures 2B,D; Supplementary Table 2). Inversely, only the total dry weight of the debarked trees (reduction of 38.14%) of *hpCAD* diploids was significantly lower compared with WT diploids (Figure 2E; Supplementary Table 2). Furthermore, debarked stems of the diploid *hpCAD* trees had the reddish colored xylem characteristic for *CAD1*-downregulated trees (Baucher et al., 1996; Van Acker et al., 2017), and this phenotype was maintained in the corresponding tetraploid lines (Figure 3).

Finally, we evaluated biomass yield parameters upon polyploidization in field-grown WT poplars. The biomass production of the field-grown di- and tetraploid WT trees was monitored over a period of 170 days. Strikingly, 50 days after planting, the apex of one of the tetraploid trees broke off 5–15 cm below the apex (Figure 4A). The frequency of tetraploids displaying this fragile or brittle apex phenotype gradually increased over time until 80% (28 trees out of 35) of the tetraploid poplars were affected at the end of the first growth season. The breaks were clean, leaving razor-cut-like

10.3389/fpls.2022.995402

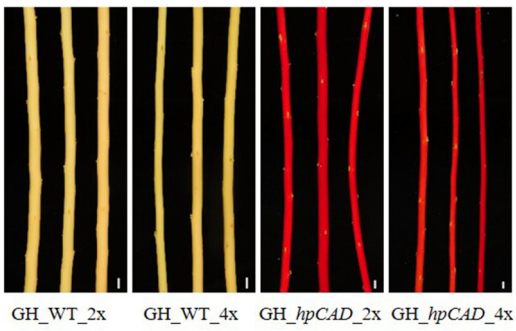

FIGURE 3
Xylem coloration of greenhouse-grown di- and tetraploid debarked poplar stems. The red xylem phenotype characteristic for *CAD1*-downregulation is maintained after whole genome duplication. Pictures are representative for the different independent lines. Scale bars = 1 cm.

edges. As a consequence of the damage, several axillary buds below the broken tip grew out, resulting in a bushy phenotype (Figure 4A). During the same period, only one out of 18 diploid trees (6%) had a broken tip (Figure 4B). This phenotype was never observed for greenhouse-grown trees, implying that some environmental factor(s) caused this phenotype. The emergence of the brittle apex phenotype was not related to the line nor the size of the plant, as it occurred on smaller trees (0.90 m) as well as trees of up to 1.90 m tall. Similarly as the greenhouse-grown trees, to quantify the growth parameters, the different lines of the WT tetraploid trees were combined and termed F_WT_4x. For the growth analyses, only those trees without broken tip were included (17 replicates for F_WT_2x and 7 replicates for F_WT_4x). Consistent with the results obtained from the greenhouse-grown trees, the tetraploid trees showed a yield penalty compared with their diploid counterparts. From day 43 onwards, the height of the main stem of the tetraploid poplars was significantly shorter as a result of polyploidization (Figure 4C; Supplementary Table 3). The growth speed of tetraploids was 29.71% slower and, hence, their final height (at day 170) was 28.69% shorter compared with the diploid trees (Figures 4D,E; Supplementary Table 2). At the time of harvest (January 2017), the stem diameter measured 50 cm above soil level and total dry weight of the debarked trees were reduced by respectively 14.69% and 47.20% in tetraploids vs. diploids (Figures 4F,G; Supplementary Table 2).

Taken together, these data show that polyploidization of WT and *hpCAD* hybrid *P. tremula x P. alba* results in a yield penalty, both when trees were grown in the greenhouse and in the field. In addition, the tetraploid WT poplar trees that were grown in the field were more susceptible to damage caused by environmental factors, as shown by the brittle apex phenotype.

Biomass composition is altered in field-grown, but not greenhouse-grown, allotetraploid poplars

Both the growth reduction as well as the brittle apex phenotype observed in tetraploid poplars grown in the field hinted toward increased susceptibility to biotic or abiotic stress. However, the tetraploid trees did not show any obvious signs of infection, making an abiotic stress factor such as mechanical stress due to wind or severe weather conditions a more likely cause for the phenotype. Because the mechanical properties of a plant are largely determined by the structure and composition of its cell walls (Horvath et al., 2010; Xi, 2018), a detailed cell wall characterization was performed on debarked stem segments sampled at the basis of the main stems of greenhouse- and field-grown di- and tetraploid trees. First, a crude cell wall extraction with water, ethanol, chloroform and acetone was performed on the dry biomass to prepare the CWR (Table 1). A small, but significant reduction of 1.14% in the amount of CWR was found between greenhouse-grown WT di- and tetraploids, but not between *hpCAD* di- and tetraploids. However, the greenhouse-grown *hpCAD* lines deposited less CWR compared with the WT (a reduction of 3.30% and 2.78% for di- and tetraploids, respectively). Similarly as for the greenhouse-grown trees, the CWR of field-grown WT tetraploid trees was reduced by a mere, albeit significant, 1.84% compared with the diploid field-grown control trees.

Next, the relative amounts of the main cell wall polymers (i.e., cellulose, MPS and lignin) were determined in the different biomass samples (Table 1). No significant differences for any of the cell wall polymers were observed in biomass from greenhouse-grown trees neither between diploids and tetraploids in WT and in *hpCAD* lines, nor between WT and *hpCAD* diploid lines. Only the lignin amount of *hpCAD* tetraploid lines was significantly decreased by 8.35% compared with that of WT tetraploid trees. Under field conditions, again, the cellulose content was not significantly affected as a result of polyploidization. However, field-grown tetraploid WT trees had a 4.88% decrease in MPS and a 9.36% increase in lignin compared with field-grown WT diploids.

Subsequently, the monosaccharide composition of the MPS was determined through analysis of the TFA extract by GC-MS. Xylose was the major constituent of the MPS, regardless of the ploidy level and the growth conditions (Table 2). Greenhouse-grown poplars had a significantly lower amount of MPS-glucose in WT tetraploids (a reduction of 55.58%) and of MPS-xylose in *hpCAD* tetraploids (a reduction of 3.58%) compared with their diploid counterparts. *CAD1*-downregulation, only affected the MPS-glucose levels in the diploid genetic background (a reduction of 63.30%). The arabinose, fucose, galactose, mannose and rhamnose content of the MPS were not significantly different after polyploidization, although a general trend toward

10.3389/fpls.2022.995402

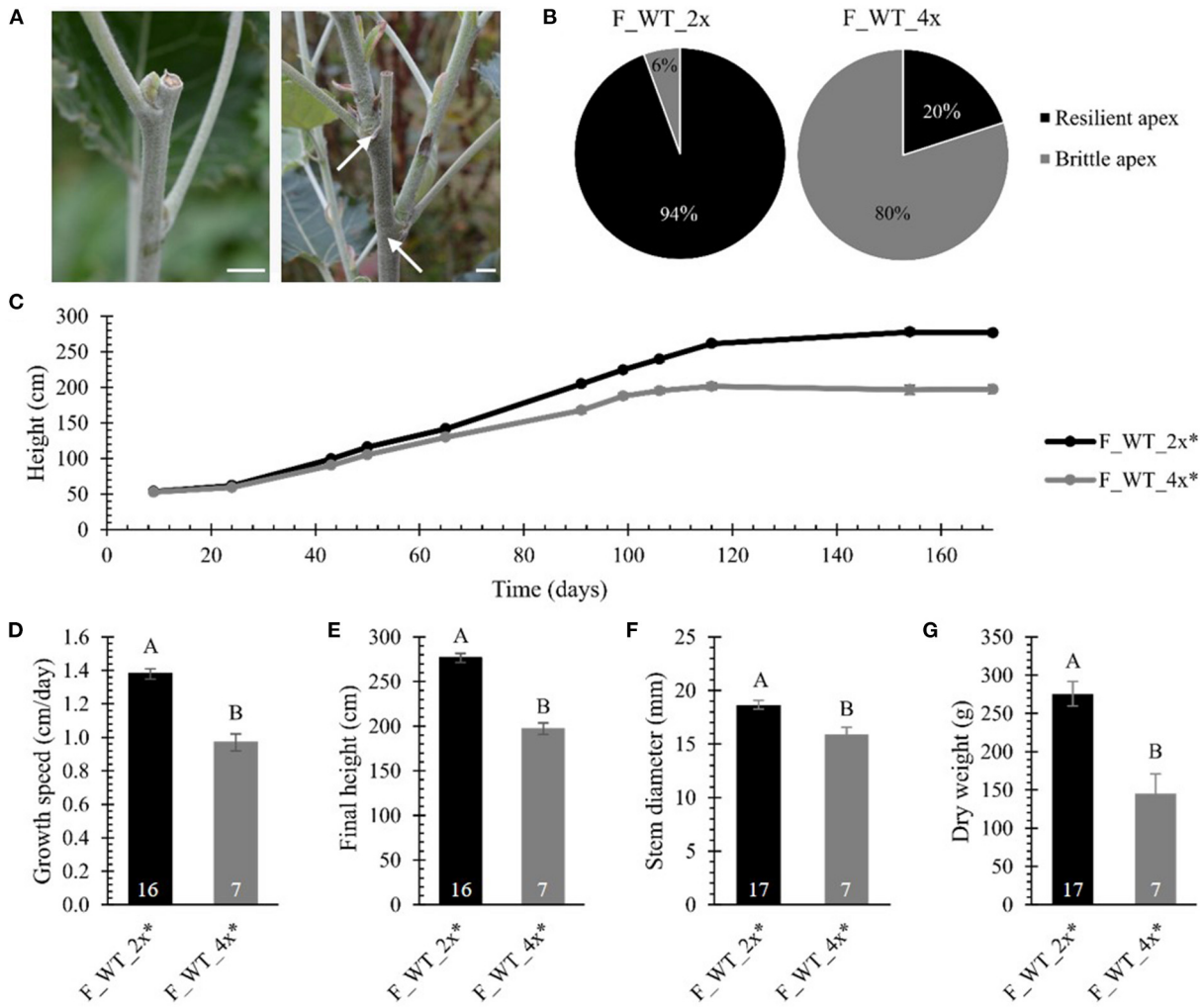

FIGURE 4
Biomass yield of field-grown di- and tetraploid poplar trees. **(A)** Broken tips of tetraploid poplar trees. Arrows point to axillary buds below the broken tip that grew out, resulting in a bushy phenotype. Scale bars = 1 cm. **(B)** Percentage of poplar trees showing the brittle apex phenotype (day = 170). **(C)** Height over time. The height of the main stem was measured at 11 time points over a period of 170 days. **(D)** Growth speed. **(E)** Final height of the poplars measured at day 170. **(F)** Stem diameter measured at harvest time 50 cm above soil. **(G)** Total dry weight of the debarked tree measured at harvest time. Only field-grown trees that did not develop the brittle apex phenotype were included in the analysis, as specified with the asterisk (*). The number of biological replicates is indicated in the bars. Data shown are adjusted mean ± standard error of the mean (SEM). Different letters represent significant differences at the 0.05 significance level. The significance differences for (C) are provided in Supplementary Table 3. For a detailed description of the models fitted to the data and the statistical tests used, see Supplementary Materials and Methods 1.

higher levels of these sugars was observed in greenhouse-grown WT and *hpCAD* tetraploids. Field-grown WT poplars had a significantly higher MPS-glucose (an increase of 87.39%) and a significantly lower MPS-xylose (a reduction of 3.11%) level in tetraploids compared with diploids. Similar to the MPS composition of the greenhouse-grown WT tetraploid poplars, the amount of the other MPS-sugars of field-grown WT tetraploid poplars did not differ significantly. In general, poplar polyploidization did not seem to affect the MPS composition much, except for the MPS-glucose levels that diminished in tetraploids grown in greenhouse conditions and increased in tetraploids grown in field conditions, and MPS-xylose levels that decreased in tetraploids grown in field conditions.

Finally, the lignin composition was quantified by thioacidolysis followed by GC-MS (Table 3). The thioacidolysis reaction releases the traditional lignin units (H, G, and S) that are linked by β-*O*−4-ether bonds in the lignin polymer. We found that the induction of polyploidy had no effect on the general lignin composition when trees were grown under greenhouse and field conditions. More specifically, the levels of the G and S

TABLE 1 Cell wall composition of di- and tetraploid poplar trees.

	CWR		Cellulose		MPS		Lignin	
Genotype	**n**	**(% DW)**	**n**	**(% CWR)**	**n**	**(% CWR)**	**n**	**(% CWR)**
GH_WT_2x	8	91.12 ± 0.26 (a)	8	54.18 ± 1.99 (a)	8	33.94 ± 0.97 (a)	7	18.27 ± 0.58 (a,b)
GH_WT_4x	16	90.08 ± 0.19 (b)	16	52.50 ± 1.40 (a)	16	33.86 ± 0.69 (a)	16	18.64 ± 0.38 (a)
GH_*hpCAD*_2x	8	88.12 ± 0.26 (c)	8	51.20 ± 1.99 (a)	7	36.18 ± 1.04 (a)	8	17.50 ± 0.54 (a,b)
GH_*hpCAD*_4x	24	87.58 ± 0.15 (c)	24	52.30 ± 1.15 (a)	24	34.03 ± 0.56 (a)	24	17.08 ± 0.31 (b)
F_WT_2x	9	87.75 ± 0.35 (A)	9	45.25 ± 0.78 (A)	9	41.73 ± 0.76 (A)	9	20.27 ± 0.27 (A)
F_WT_4x	18	86.13 ± 0.25 (B)	17	45.91 ± 0.56 (A)	17	39.69 ± 0.55 (B)	18	22.17 ± 0.19 (B)

The cell wall residue (CWR) was determined gravimetrically after a sequential extraction and is expressed as a percentage of dry weight (DW). Crystalline cellulose was determined with the Updegraff method, matrix polysaccharides (MPS) content was weighed after a TFA extraction and lignin content was analyzed with the Klason method. The amount of cellulose, MPS and lignin are expressed as a percentage of CWR. Data of greenhouse (GH)- and field (F)-grown poplars are separated by a black bar because they were collected in different experiments. The number of biological replicates (n) is indicated. Values given are adjusted mean ± standard error of the mean (SEM). Different letters represent significant differences at the 0.05 significance level. For a detailed description of the models fitted to the data and the statistical tests used, see Supplementary Materials and Methods 1.

units that make up the bulk of the lignin were not significantly different between di- and tetraploids. Besides the traditional lignin units, we also detected trace amounts (<1 mol%) of S aldehydes, characteristic for *CAD1*-downregulation, in lignin of both *hpCAD* diploids and *hpCAD* tetraploids, but not in lignin of WT. However, the levels of S aldehydes that were incorporated in the lignin did not change after polyploidization. The sum of all the released units is a good estimate of the total thioacidolysis yield and, hence, can be used as a measure for the lignin condensation. On the one hand, the total thioacidolysis yield of greenhouse-grown WT diploids and tetraploids was equal, whereas that of greenhouse-grown *hpCAD* tetraploids was significantly reduced by 19.18% compared with their diploid counterparts. On the other hand, the total thioacidolysis yield of field-grown WT tetraploids was significantly reduced by 15.03% compared with their diploid counterparts. The decrease in total thioacidolysis yield of greenhouse-grown *hpCAD* and field-grown WT tetraploids implies that their lignin is more condensed as a result of polyploidization.

Taken together, under greenhouse conditions, there is no significant effect on the cellulose, MPS and lignin amount, whereas under field conditions, the cell wall composition was altered upon whole genome duplication. Field-grown tetraploids had less MPS and more lignin than diploids. These data illustrate that there is a clear interaction between polyploidization and the environment on the deposition of cell wall polymers.

Saccharification efficiency is similar in greenhouse- and field-grown allotetraploid poplars

To evaluate the effect of polyploidy on downstream processing of poplar wood, we performed a saccharification assay and measured the glucose released after 10 h of enzymatic treatment (Figure 5; Supplementary Table 4). Saccharification assays were performed without and with alkaline (NaOH) pretreatment based on the positive effect of the latter on the saccharification yield of *hpCAD* lines (Van Acker et al., 2017). As expected, alkaline pretreatment of the biomass prior to saccharification improved the glucose release for all samples. In general, glucose levels were two- to fivefold higher for biomass pretreated with NaOH compared with biomass that was not pretreated. The positive effect of *CAD1*-downregulation on the saccharification yield after alkaline pretreatment could also be confirmed. Whereas without pretreatment the glucose release of *hpCAD* diploids and tetraploids was equal to that of their non-transgenic counterparts, the cellulose-to-glucose conversion upon alkaline pretreatment increased with 63.11% and 69.54%, respectively. Concerning the effect of polyploidization, no significant differences were observed between WT tetraploid poplars and their respective diploid counterparts, grown in either greenhouse or field conditions and irrespective of the inclusion of a pretreatment. In contrast, we found that greenhouse-grown *hpCAD* tetraploids released 32.43% more glucose without pretreatment, but not with an alkaline pretreatment, compared with greenhouse-grown *hpCAD* diploids.

Stem anatomy and mechanical properties are largely preserved in WT allotetraploid poplars

Field-grown WT tetraploids displayed a brittle apex phenotype. To investigate whether this phenotype is caused by anatomical abnormalities, transversal stem sections were made and triple stained with astra blue, chrysiodine and acridine red (Figure 6). For this, the main stem of di- and tetraploid trees was harvested 1 m above soil level in the second

10.3389/fpls.2022.995402

TABLE 2 Monosaccharide composition of the matrix polysaccharides of di- and tetraploid poplar trees.

Genotype	Arabinose		Fucose		Galactose		Glucose		Mannose		Rhamnose		Xylose	
	n	(mol%)	n	(mol%)	n	(mol%)	n	(mol%)	n	(mol%)	n	(mol%)	n	(mol%)
GH_WT_2x	8	0.66 ± 0.29 (a)	8	0.15 ± 0.14 (a)	8	4.55 ± 0.74 (a)	8	3.79 ± 0.67 (a)	8	0.80 ± 0.32 (a)	8	0.92 ± 0.34 (a)	8	89.17 ± 1.10 (a,b)
GH_WT_4x	15	0.86 ± 0.24 (a)	15	0.22 ± 0.12 (a)	16	5.81 ± 0.59 (a)	16	1.66 ± 0.32 (b)	16	1.22 ± 0.27 (a)	16	1.46 ± 0.30 (a)	16	88.79 ± 0.79 (a)
GH_*hpCAD*_2x	8	0.75 ± 0.31 (a)	8	0.16 ± 0.14 (a)	8	4.07 ± 0.70 (a)	8	1.38 ± 0.41 (b)	8	0.77 ± 0.31 (a)	8	0.95 ± 0.34 (a)	8	91.93 ± 0.96 (b)
GH_*hpCAD*_4x	24	0.93 ± 0.20 (a)	22	0.24 ± 0.10 (a)	22	5.71 ± 0.49 (a)	24	1.30 ± 0.23 (b)	23	0.99 ± 0.21 (a)	24	1.34 ± 0.23 (a)	24	88.64 ± 0.65 (a)
F_WT_2x	9	0.58 ± 0.25 (A)	9	0.14 ± 0.12 (A)	8	2.04 ± 0.50 (A)	9	2.38 ± 0.51 (A)	9	0.44 ± 0.22 (A)	9	0.61 ± 0.26 (A)	8	94.22 ± 0.83 (A)
F_WT_4x	18	0.57 ± 0.18 (A)	17	0.10 ± 0.08 (A)	18	2.78 ± 0.39 (A)	18	4.46 ± 0.49 (B)	15	0.33 ± 0.15 (A)	18	0.56 ± 0.18 (A)	16	91.29 ± 0.72 (B)

MPS content was determined gravimetrically after a TFA extraction (%arabinose + %fucose + %galactose + %glucose + %mannose + % rhamnose + %xylose = 100%). Data of greenhouse (GH)- and field (F)-grown poplars are separated by a black bar because they were collected in different experiments. The number biological replicates (n) is indicated. Values given are adjusted mean ± standard error of the mean (SEM). Different letters represent significant differences at the 0.05 significance level. For a detailed description of the models fitted to the data and the statistical tests used, see Supplementary Materials and Methods 1.

growth season (August 2017). At that time, the tetraploids already showed the brittle apex phenotype. Field-grown di- and tetraploids had an equal vessels to fibers ratio per selected area (Supplementary Table 5). In addition, no significant differences in the average vessel or fiber area per selected area were observed. However, stem sections of the tetraploid poplars showed a 47.98% increase in vessel lumen, i.e., the total vessel area per selected area as compared with the diploid trees. This means that these tetraploids have a higher proportion of cavities present in their stem, potentially weakening the trees when exposed to the environment.

To test whether the brittle apex phenotype might be explained by differences in mechanical strength, we performed a three-point bending tests on 4-year-old field-grown di- and tetraploid WT trees (Figure 7; Supplementary Table 6). To be able to make a valid comparison between di- and tetraploids that show a difference in biomass yield, we attempted to harvest stem samples with a comparable diameter for the three-point bending test (ten diploid samples harvested from the top and 20 tetraploid samples harvested from the base of the stem). For these tests, stems were mounted on two supporting pins, whereupon an increasing force was applied to the center *via* a third indenting pin until the sample breaks. A force-displacement curve was plotted for every sample (Supplementary Figure 3). Stem samples of diploids could resist a larger force than those of tetraploids because, despite our efforts to harvest stem samples with a comparable diameter, the stems of the diploid poplars had a larger diameter. We also observed that, in contrast to the diploids (0/10), the tetraploids had a different failure behavior (8/20), visible as sudden decreases in the force-displacement curve. These small cracks before fully breaking might be attributed to a higher brittleness and hint that the field-grown tetraploids are more fragile than the diploids when exposed to the environment (e.g., wind). From the force-displacement curves, two parameters of mechanical strength were calculated, the MOE and the MOR. Although the formulas for both parameters correct for the difference in diameter of di- and tetraploid poplar stems, they assume a perfect solid cylinder as sample, which was not the case for most of our stem samples. The MOE, derived from the elastic region of the curve is a measure for the resistance to non-permanent deformation: elastic materials have a small MOE, whereas stiff materials have a large MOE. The MOR, derived from the plastic region of the curve, is a measure for the bending strength at constant maximal force: materials with a small MOR break faster, whereas materials with a large MOR can withstand a larger force before breaking. No significant differences in the MOE and MOR were found between di- and tetraploid WT poplars grown in the field (Figures 7A,B). As such, the brittle apex phenotype observed in field-grown tetraploids cannot be explained by a difference in mechanical properties, at least not by those parameters deduced from the three-point

10.3389/fpls.2022.995402

TABLE 3 Lignin composition of di- and tetraploid poplar trees.

Genotype	Total thioacidolysis yield		Total thioacidolysis yield		H		G		S		S aldehyde		S/G
	n	(µmol / mg CWR)	n	(µmol / mg Klason lignin)	n	(mol%)	n	(mol%)	n	(mol%)	n	(mol%)	n	S/G
GH_WT_2x	6	0.44 ± 0.03 (a)	6	2.28 ± 0.24 (a)	7	1.11 ± 0.40 (a)	6	33.26 ± 1.92 (a)	6	65.49 ± 1.94 (a)	7	n.d.	6	1.97 ± 0.57 (a)
GH_WT_4x	15	0.45 ± 0.02 (a)	16	2.30 ± 0.15 (a)	16	1.32 ± 0.28 (a)	15	34.79 ± 1.23 (a)	15	63.87 ± 1.24 (a)	16	n.d.	15	1.84 ± 0.35 (a)
GH_*hpCAD*_2x	8	0.51 ± 0.02 (a)	8	2.92 ± 0.15 (a)	8	1.12 ± 0.37 (a)	8	37.69 ± 1.71 (a)	8	60.46 ± 1.73 (a)	8	0.73 ± 0.30 (a)	8	1.61 ± 0.45 (a)
GH_*hpCAD*_4x	24	0.40 ± 0.01 (b)	24	2.36 ± 0.09 (b)	22	1.83 ± 0.29 (a)	24	40.32 ± 1.00 (a)	24	57.18 ± 1.01 (a)	24	0.76 ± 0.18 (a)	24	1.42 ± 0.24 (a)
F_WT_2x	7	0.66 ± 0.02 (A)	7	3.23 ± 0.10 (A)	8	1.61 ± 0.44 (A)	8	29.48 ± 1.61 (A)	8	68.91 ± 1.64 (A)	8	n.d.	8	2.34 ± 0.54 (A)
F_WT_4x	17	0.58 ± 0.01 (B)	17	2.61 ± 0.07 (B)	17	1.52 ± 0.29 (A)	17	31.17 ± 1.09 (A)	17	67.31 ± 1.11 (A)	17	n.d.	17	2.16 ± 0.35 (A)

Lignin composition was determined with the thioacidolysis method (%H + %G + %S + %S aldehyde = 100%). The total thioacidolysis yield is the sum of H, G, S and S aldehyde content. Data of greenhouse (GH)-grown WT poplars, GH-grown *hpCAD* poplars and field (F)-grown poplars are separated by a black bar because they were collected in different experiments. The number of biological replicates (n) is indicated. Values given are adjusted mean ± standard error of the mean (SEM). Different letters represent significant differences at the 0.05 significance level. n.d., not detected. For a detailed description of the models fitted to the data and the statistical tests used, see Supplementary Materials and Methods 1.

bending test. However, the sudden decreases in the force-displacement curves of tetraploids do suggest some difference in mechanical properties.

Discussion

Whole genome duplication of *P. tremula* x *P. alba* cv. INRA 717-1B4 impairs vegetative growth

To study the effects of whole genome duplication on biomass yield and composition, allotetraploids were generated of hybrid *P. tremula* x *P. alba* cv. INRA 717-1B4, a model clone frequently used in tree biotechnology research. Under both greenhouse and field conditions, tetraploid poplar trees grew more slowly and had a significant yield penalty compared with their corresponding diploid counterparts. A similar slow vegetative growth has been observed in tetraploid poplars obtained after chromosome doubling of a diploid hybrid progeny (*P. pseudo-simonii* × *P. nigra* Zheyin3#) × (*P.* × *beijingensis*) and could be attributed to the upregulation of growth-promoting auxin- and gibberellin-related miRNAs and the downregulation of senescence-related miRNAs (Xu et al., 2020). This opposite trend in the expression of these two classes of differentially expressed genes decreased the photosynthetic rate, explaining the observed yield penalty (Xu et al., 2020).

The negative impact of whole genome duplication on growth speed and plant height is not limited to poplar, but has also been observed in empress tree, Rangpur lime, birch, acacia, willow and apple tree (Tang et al., 2010; Allario et al., 2011; Mu et al., 2012; Griffin et al., 2015; Dudits et al., 2016; Ma et al., 2016; Hias et al., 2017). Interestingly, in birch and willow, the reduction in growth speed and height was accompanied by a significant increase in stem diameter, resulting in an increase in total biomass (Mu et al., 2012; Dudits et al., 2016). We did not observe a similar compensation effect in the tetraploid poplar lines, indicating that the effect of whole genome duplication on plant growth is species- and genotype-dependent. On the other hand, the phenotypic differences between poplar and the other tetraploid woody species might find their origin in the nature of the parental line(s) used for tetraploidization, i.e. whether the tetraploid was derived from an intra- or interspecific hybrid. Indeed, whole genome duplication of *P. tremula* x *P. alba* cv. INRA 717-1B4 and (*P. pseudo-simonii* × *P. nigra* Zheyin3#) × (*P.* × *beijingensis*) resulted in allotetraploids, whereas autotetraploids were obtained in the case studies focusing on birch or willow. More systematic studies involving tetraploidization of pure and hybrid trees are needed to support or refute this hypothesis.

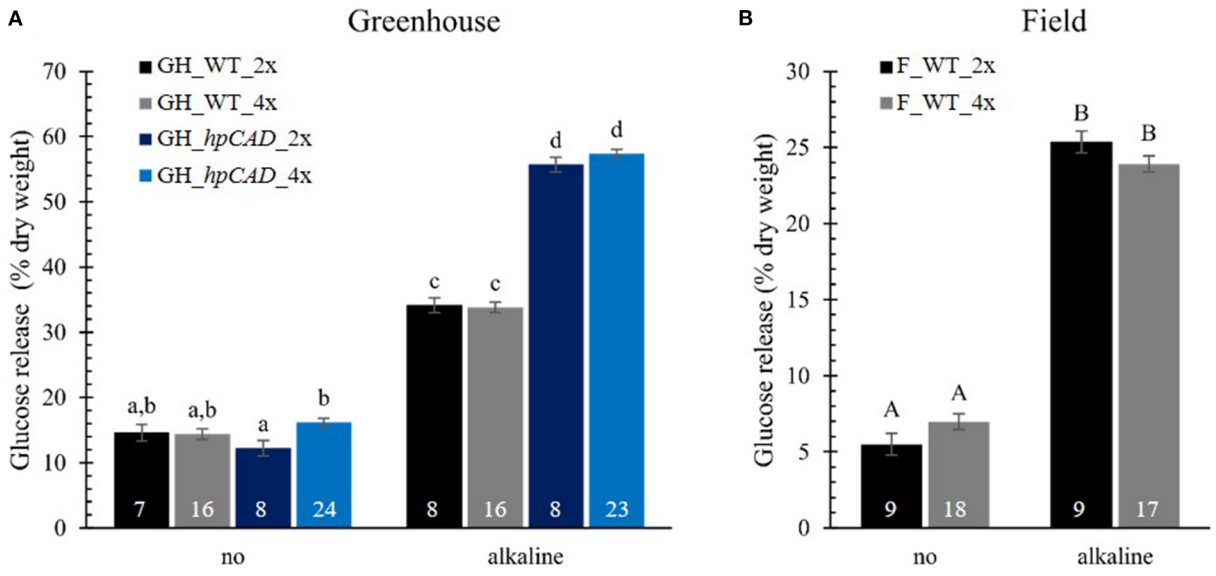

FIGURE 5
Saccharification yield of di- and tetraploid poplar trees. Glucose release without (no) and with alkaline pretreatment was determined after 10 h and expressed as % of dry weight. Data of greenhouse (GH)-grown **(A)** and field (F)-grown **(B)** poplars were collected in different experiments. The number of biological replicates is indicated in the bars. Data shown are adjusted mean ± standard error of the mean (SEM). Different letters represent significant differences at the 0.05 significance level. For a detailed description of the models fitted to the data and the statistical tests used, see Supplementary Materials and Methods 1.

Whole genome duplication of *P. tremula* x *P. alba* cv. INRA 717-1B4 affects biomass composition of field-grown WT tetraploids and causes a brittle apex phenotype

In *Arabidopsis thaliana*, ploidy level is negatively correlated with lignin content i.e., the higher the ploidy level, the lower the lignin content (Corneillie et al., 2019). Given that lignin is one of the main factors causing lignocellulosic biomass recalcitrance to enzymatic hydrolysis (Chen and Dixon, 2007; Van Acker et al., 2013; Zoghlami and Paës, 2019), the saccharification yield of low-lignin tetraploid Arabidopsis plants was higher than that of diploids (Corneillie et al., 2019). In contrast to Arabidopsis, the biomass composition (i.e. cellulose, MPS and lignin amount) of the greenhouse-grown di- and tetraploid WT and *CAD1*-downregulated poplar analyzed here was not different. Accordingly, also the saccharification yield remained equal, except for the small increase in glucose release observed in saccharifications without biomass pretreatment of tetraploid *hpCAD* poplars. Interestingly, a shift in biomass composition was observed for field-grown tetraploid poplars: the lignin content increased by 9.36% at the expense of MPS. In addition, the total thioacidolysis yield was reduced in field-grown—but not in greenhouse-grown—WT tetraploids in comparison with their diploid counterparts, implying that the lignin polymer is more condensed when tetraploids are grown in the field. However, this shift in lignin amount and condensation degree in field-grown tetraploid poplars did not translate into a difference in saccharification yield, regardless of a pretreatment. In contrast to our allotetraploid poplars, field-grown autotetraploid willows had a lower lignin content than diploids (Serapiglia et al., 2015), and for autotetraploid acacia, less alkali was consumed to yield similar amounts of Kraft pulp as diploids, indicating an increased biomass processing efficiency (Griffin et al., 2014). Again, these different findings indicate that the effect of whole genome duplication is not easily predictable, and most likely species- and genotype-dependent.

When grown in the field, the tetraploid *P. tremula x P. alba* cv. INRA 717 1B4 trees developed a brittle apex phenotype. Interestingly, some old studies on petunia and cassava mention a similar brittle phenotype upon whole genome duplication. In the case of petunia, tetraploids were described as "rather ugly plants, which were very fragile because after a storm great parts of the tetraploid material was broken, whereas the diploids were hardly damaged" (Levan, 1939), and tetraploid cassava plants were found to be "less vigorous, and their stem, although stouter is less hardy and more brittle" (Abraham et al., 1964). The fact that the brittle apex phenotype in our study was only present under field conditions makes it tempting to link the phenotype to the observed increase in lignin content in these plants, making them more sensitive to suboptimal growth conditions. A similar association between lignin content and brittleness was made

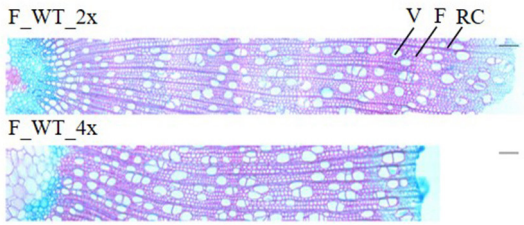

FIGURE 6
Stem anatomy of field-grown di- and tetraploid poplar trees. The main stem of field-grown WT trees was harvested 1 m above soil level in August 2017 of the second growth season. Transverse stem sections (from pith to bark) stained with astra blue, chrysiodine and acridine red are shown. Pictures are representative for the different independent lines. V, vessel; F, fiber; RC, ray cell. Scale bars = 100 μm.

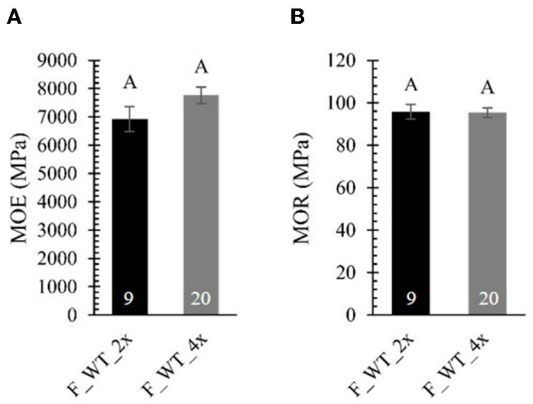

FIGURE 7
Mechanical strength of field-grown di- and tetraploid poplar trees. Stem samples were subjected to a three-point bending test. From the force-displacement curve, the modulus of elasticity [MOE, **(A)**] and the modulus of rupture [MOR, **(B)**] were calculated. The number of biological replicates is indicated in the bars. Data shown are adjusted mean ± standard error of the mean (SEM). Different letters represent significant differences at the 0.05 significance level. For a detailed description of the models fitted to the data and the statistical tests used, see Supplementary Materials and Methods 1.

before. For example, the *brittle stalk2* maize mutant, named after the fact that its aerial parts are easily broken in the field as a result of wind damage, has an enriched lignin content and a reduced mechanical strength compared with WT plants (Ching et al., 2006; Sindhu et al., 2007). Similarly, a brittle wood phenotype has been reported for *P. trichocarpa* downregulated in glycosyltransferase *8D1* and *8D2* genes implicated in xylan biosynthesis. The stem of this double mutant had a reduced modulus of elasticity (MOE) and modulus of rupture (MOR), which was correlated with a decrease in xylan content and an increase in lignin quantity (Li et al., 2011). Inversely, both in Arabidopsis and poplar, downregulation of lignin biosynthesis reduces cell wall stiffness as reflected in a decrease of the MOE (Köhler and Spatz, 2002; Koehler and Telewski, 2006; Bjurhager et al., 2010; Özparpucu et al., 2017; De Meester et al., 2018). Together, these data demonstrate that lignin plays an important role in cell wall stiffness. However, despite the increase in lignin content, no major differences in mechanical properties could be demonstrated between field-grown di- and tetraploid poplars. This could be a direct consequence of some technical limitations when performing the three-point bending test used to calculate MOE and MOR parameters. The three-point bending test and related calculations as performed here, require a sample that is a perfect solid cylinder for optimal performance. Our samples did not meet this criterion, because they contained the central pith and had a moisture content of 6%. In addition, in an attempt to analyze stem segments with a comparable diameter, diploid stem samples were harvested from the top of the stem, whereas tetraploid plants had to be sampled at the base of the stem. As such, the number and thickness of the year rings were also different between di- and tetraploid samples. Given all these limitations, the comparison of the obtained absolute values for MOE and MOR with literature should be made with caution. Nonetheless, the same order of magnitude was found by Horvath et al. (2010).

The environment has a strong effect on the biomass yield and composition of *hpCAD* poplar, whereas whole genome duplication does not

The diploid *hpCAD* line showed a biomass yield penalty, but no shift in lignin content compared with its WT counterpart when grown in the greenhouse. Similar results were obtained when this *hpCAD* line was grown for 3 years in the field (De Meester et al., 2022), whereas in another study no yield penalty and a 10% decrease in lignin content was obtained when this *hpCAD* line was grown under greenhouse conditions (Van Acker et al., 2017). Independent of these contradictory results, all these studies support a link between growth speed and lignin content in *CAD1*-downregulated poplars. Because plant growth and lignin biosynthesis compete for the same carbon resources, it is conceivable that when growth is slowed down, plants have more time to fully lignify their cell walls. Or vice versa, that a restored flux toward lignin has a negative impact on pant growth and, hence, on biomass yield. The dissimilarity in biomass yield and lignin content between the studies are likely due to differences in environmental factors such as irrigation frequency and temperature. An example illustrating this aspect even more profoundly is that of the *Medicago truncatula CAD* loss-of-function mutant. The plants appeared normal under standard conditions in the greenhouse, but were dwarfed when grown at

30°C (Zhao et al., 2013). Together, these studies demonstrate that caution is required when interpreting, comparing or extrapolating published results from lignin mutants, because the environment might influence biomass yield and composition, as also discussed by De Meester et al. (2022).

The generated tetraploid *hpCAD* poplars displayed a uniform red coloration of the xylem, incorporated sinapaldehydes into their lignin and had an increased saccharification yield upon alkaline pretreatment. These features have been described before for *CAD1*-downregulated lines and indicate that silencing of *CAD1* was maintained upon whole genome duplication. Similar to the greenhouse-grown WT poplars, chromosome doubling of *hpCAD* had a negative effect on biomass yield, but did not affect its composition. However, despite the absence of an effect on lignin content, saccharification yield without pretreatment slightly improved upon polyploidization.

P. tremula x *P. alba* cv. INRA 717-1B4 tetraploids may serve as parental germplasm to generate triploids

Triploid breeding is an excellent approach to improve lignocellulosic biomass yield and composition in shrub willow and poplar (Serapiglia et al., 2014, 2015; Kang, 2016). The surface area of poplar triploid leaves, as a consequence of cell size enlargement, is significantly larger than that of diploids (Nilsson-Ehle, 1936a; Zhang et al., 2019). The formation of these giant leaves with superior photosynthetic efficiency could be attributed to the upregulation of growth hormone-related and chlorophyll biosynthesis genes (Du et al., 2019; Wu et al., 2021). Moreover, most lignin biosynthesis genes are downregulated in triploid leaves compared with diploid leaves (Xu et al., 2022). Although biomass traits of some triploids are excellent, some may also have adverse characteristics, such as a low wood basic density and the potential to be easily broken by wind after planting. For this reason, allotriploids of *P. tremula* × *P. tremuloides* have been eliminated from most breeding programs (Kang, 2016).

Crossing diploid and tetraploid parents, i.e., hybridizing n with 2n gametes, is historically the most economic and fastest practice for triploid production (Ulrich and Ewald, 2014). A beneficial effect on biomass yield and composition has already been shown for triploids of *P. tremula* and *P. alba*, respectively. More specifically, in nature, a giant form of *P. tremula* was discovered with increased stem height, diameter and volume, which turned out to be a spontaneous triploid (Müntzing, 1936; Nilsson-Ehle, 1936b). And, comparative trials with a range of allotriploid clones involving *P. alba* showed that the stem volume and cellulose content were higher and the lignin content lower than those of the diploid controls (Kang, 2016). As such, combining both species like in the allotetraploid WT *P. tremula* x *P. alba* cv. INRA 717-1B4 generated in this study, may provide an important female parental germplasm for generating triploid poplars in the future. In addition, such crosses would allow investigating whether the reduction in biomass yield and the brittle apex phenotype of allotetraploid WT *P. tremula* x *P. alba* cv. INRA 717-1B4 are maintained in the triploids. Nevertheless, given the fact that the triploid offspring will all be genetically different, there is no reason to assume that this would be the case for all triploids when screening a large population.

In conclusion, we showed that combining polyploidy and heterosis in WT and *hpCAD* poplar did not result in a higher biomass yield, nor in an improved biomass composition for saccharification. Furthermore, we demonstrated that the outcome of a whole genome duplication is strongly dependent on the environment, highlighting the importance of field trials.

Data availability statement

The original contributions presented in the study are included in the article/Supplementary material, further inquiries can be directed to the corresponding author.

Author contributions

MW analyzed the data and wrote the article. SC designed and performed the experiments. JVD created the set of tetraploid poplars. AD performed the chromosome spreads. JVA and JVdB performed the three-point bending test and interpreted these results at UGent-Woodlab. BV and WB conceived the project, supervised the experiments and helped in writing the article. All authors contributed to the article and approved the submitted version.

Funding

This work was supported by grants from the Multidisciplinary Research Partnership Biotechnology for a Sustainable Economy (01MRB510W) of Ghent University. MW and SC were supported by the Research Foundation Flanders (FWO) for a predoctoral fellowship under project numbers 3S019619 and 3G032912, respectively. WB is indebted to the Energy Transition Funds project AdLibio and Adv Bio.

Acknowledgments

The authors would like to express their gratitude to Hilde Nelissen for providing the field facilities; to Stijn Willen

and Toon Gheyle for help in harvesting the field trial, preparation of the material and performing the thee-point bending tests; to Marnik Vuylsteke (GNOMIXX) for support in the statistical analyses and to Annick Bleys for critically reading the manuscript.

Conflict of interest

The authors declare that the research was conducted in the absence of any commercial or financial relationships that could be construed as a potential conflict of interest.

Publisher's note

Supplementary material

The Supplementary Material for this article can be found online at: https://www.frontiersin.org/articles/10.3389/fpls.2022.995402/full#supplementary-material

References

Abraham, A., Panicker, P. K. S., and Mathew, P. M. (1964). Polyploidy in relation to breeding in tuber crops. *J. Indian Bot. Soc.* 43, 278–282.

Allario, T., Brumos, J., Colmenero-Flores, J. M., Tadeo, F., Froelicher, Y., Talon, M., et al. (2011). Large changes in anatomy and physiology between diploid Rangpur lime (Citrus limonia) and its autotetraploid are not associated with large changes in leaf gene expression. *J. Exp. Bot.* 62, 2507–2519. doi: 10.1093/jxb/erq467

Andriankaja, M., Dhondt, S., De Bodt, S., Vanhaeren, H., Coppens, F., De Milde, L., et al. (2012). Exit from proliferation during leaf development in Arabidopsis thaliana: a not-so-gradual process. *Dev. Cell* 22, 64–78. doi: 10.1016/j.devcel.2011.11.011

Baucher, M., Chabbert, B., Pilate, G., Van Doorsselaere, J., Tollier, M. T., Petit-Conil, M., et al. (1996). Red xylem and higher lignin extractability by down-regulating a cinnamyl alcohol dehydrogenase in poplar. *Plant Physiol.* 112, 1479–1490. doi: 10.1104/pp.112.4.1479

Bjurhager, I., Olsson, A.-M., Zhang, B., Gerber, L., Kumar, M., Berglund, L. A., et al. (2010). Ultrastructure and mechanical properties of Populus wood with reduced lignin content caused by transgenic down-regulation of cinnamate 4-hydroxylase. *Biomacromolecules* 11, 2359–2365. doi: 10.1021/bm100487e

Blackburn, K. B. and Harrison, J. W. H. (1924). A preliminary account of the chromosomes and chromosome behaviour in the Salicaceae. *Ann. Bot.* 38, 361–378. doi: 10.1093/oxfordjournals.aob.a089900

Boerjan, W., Ralph, J., and Baucher, M. (2003). Lignin biosynthesis. *Annu. Rev. Plant Biol.* 54, 519–546. doi: 10.1146/annurev.arplant.54.031902.134938

Bonawitz, N. D. and Chapple, C. (2010). The genetics of lignin biosynthesis: connecting genotype to phenotype. *Annu. Rev. Genet.* 44, 337–363. doi: 10.1146/annurev-genet-102209-163508

Bryant, N. D., Pu, Y., Tschaplinski, T. J., Tuskan, G. A., Muchero, W., Kalluri, U. C., et al. (2020). Transgenic poplar designed for biofuels. *Trends Plant Sci.* 25, 881–896. doi: 10.1016/j.tplants.2020.03.008

Busov, V., Yordanov, Y., Gou, J., Meilan, R., Ma, C., Regan, S., et al. (2011). Activation tagging is an effective gene tagging system in Populus. *Tree Genet. Genomes* 7, 91–101. doi: 10.1007/s11295-010-0317-7

Chanoca, A., De Vries, L., and Boerjan, W. (2019). Lignin engineering in forest trees. *Front. Plant Sci.* 10, 912. doi: 10.3389/fpls.2019.00912

Chen, F. and Dixon, R. A. (2007). Lignin modification improves fermentable sugar yields for biofuel production. *Nat. Biotechnol.* 25, 759–761. doi: 10.1038/nbt1316

Ching, A., Dhugga, K. S., Appenzeller, L., Meeley, R., Bourett, T. M., Howard, R. J., et al. (2006). Brittle stalk 2 encodes a putative glycosylphosphatidylinositol-anchored protein that affects mechanical strength of maize tissues by altering the composition and structure of secondary cell walls. *Planta* 224, 1174–1184. doi: 10.1007/s00425-006-0299-8

Chupeau, M.-C., Pautot, V., and Chupeau, Y. (1994). Recovery of transgenic trees after electroporation of poplar protoplasts. *Transgenic Res.* 3, 13–19. doi: 10.1007/BF01976022

Corneillie, S., De Storme, N., Van Acker, R., Fangel, J. U., De Bruyne, M., De Rycke, R., et al. (2019). Polyploidy affects plant growth and alters cell wall composition. *Plant Physiol.* 179, 74–87. doi: 10.1104/pp.18.00967

De Meester, B., De Vries, L., Özparpucu, M., Gierlinger, N. Corneillie, S., Pallidis, A., et al. (2018). Vessel-specific reintroduction of CINNAMOYL-COA REDUCTASE1 (CCR1) in dwarfed ccr1 mutants restores vessel and xylary fiber integrity and increases biomass. *Plant Physiol.* 176, 611–633. doi: 10.1104/pp.17.01462

De Meester, B., Madariaga Calderón, B., De Vries, L., Pollier, J., Goeminne, G., Van Doorsselaere, J., et al. (2020). Tailoring poplar lignin without yield penalty by combining a null and haploinsufficient CINNAMOYL-CoA REDUCTASE2 allele. *Nat. Commun.* 11, 5020. doi: 10.1038/s41467-020-18822-w

De Meester, B., Van Acker, R., Wouters, M., Traversari, S., Steenackers, M., Neukermans, J., et al. (2022). *Field and Saccharification Performances of Poplars Severely Downregulated in CAD1. New Phytol*, in press. Available online at: https://www.ncbi.nlm.nih.gov/pubmed/35808905 (accessed July 8). doi: 10.1111/nph.18366

De Meester, B., Vanholme, R., De Vries, L., Wouters, M., Van Doorsselaere, J., and Boerjan, W. (2021). Vessel-and ray-specific monolignol biosynthesis as an approach to engineer fiber-hypolignification and enhanced saccharification in poplar. *Plant J.* 108, 752–765. doi: 10.1111/tpj.15468

De Vries, L., Brouckaert, M., Chanoca, A., Kim, H., Regner, M. R., Timokhin, V. I., et al. (2021). CRISPR-Cas9 editing of CAFFEOYL SHIKIMATE ESTERASE 1 and 2 shows their importance and partial redundancy in lignification in Populus tremula × P. *alba. Plant Biotechnol. J.* 19, 2221–2234. doi: 10.1111/pbi.13651

Du, K., Han, Q., Zhang, Y., and Kang, X. (2019). Differential expression of genes related to the formation of giant leaves in triploid poplar. *Forests* 10, 920. doi: 10.3390/f10100920

Dudits, D., Török, K., Cseri, A., Paul, K., Nagy, A. V., Nagy, B., et al. (2016). Response of organ structure and physiology to autotetraploidization in early development of energy willow Salix viminalis. *Plant Physiol.* 170, 1504–1523. doi: 10.1104/pp.15.01679

Foster, C. E., Martin, T. M., and Pauly, M. (2010). Comprehensive compositional analysis of plant cell walls (lignocellulosic biomass). Part II: carbohydrates. *J. Vis. Exp.* 37, e1837. doi: 10.3791/1837

Griffin, A. R., Chi, N. Q., Harbard, J. L., Son, D. H., Harwood, C. E., Price, A., et al. (2015). Breeding polyploid varieties of tropical acacias: progress and prospects. *Southern Forests-A J. Forest Sci.* 77, 41–50. doi: 10.2989/20702620.2014.999303

Griffin, A. R., Twayi, H., Braunstein, R., Downes, G. M., Son, D. H., and Harwood, C. E. (2014). A comparison of fibre and pulp properties of diploid and tetraploid Acacia mangium grown in Vietnam. *Appita: Technol. Innov. Manufact. Environ.* 67, 43–49.

Gui, J., Lam, P. Y., Tobimatsu, Y., Sun, J., Huang, C., Cao, S., et al. (2020). Fibre-specific regulation of lignin biosynthesis improves biomass quality in Populus. *New Phytol.* 226, 1074–1087. doi: 10.1111/nph.16411

Hias, N., Leus, L., Davey, M. W., Vanderzande, S., Van Huylenbroeck, J., and Keulemans, J. (2017). Effect of polyploidization on morphology in two apple (Malus× domestica) genotypes. *Hortic. Sci.* 44, 55–63. doi: 10.17221/7/2016-HORTSCI

Horvath, L., Peszlen, I., Peralta, P., Kasal, B., and Li, L. (2010). Mechanical properties of genetically engineered young aspen with modified lignin content and/or structure. *Wood Fiber Sci.* 42, 310–317.

Ibáñez, A. B. and Bauer, S. (2014). Downscaled method using glass microfiber filters for the determination of Klason lignin and structural carbohydrates. *Biomass Bioenerg.* 68, 75–81. doi: 10.1016/j.biombioe.2014.06.013

Jang, H.-A., Bae, E.-K., Kim, M.-H., Park, S.-J., Choi, N.-Y., Pyo, S.-W., et al. (2021). CRISPR-knockout of CSE gene improves saccharification efficiency by reducing lignin content in hybrid poplar. *Int. J. Mol. Sci.* 22, 9750. doi: 10.3390/ijms22189750

Kang, X. Y. (2016). "Polyploid induction techniques and breeding strategies in poplar," in *Polyploidy and Hybridization for Crop Improvement,* ed A. Mason (Boca Raton: CRC Press), 76–96. doi: 10.1201/9781315369259-5

Kirov, I., Divashuk, M., Van Laere, K., Soloviev, A., and Khrustaleva, L. (2014). An easy "SteamDrop" method for high quality plant chromosome preparation. *Mol. Cytogenet.* 7, 21. doi: 10.1186/1755-8166-7-21

Koehler, L. and Telewski, F. W. (2006). Biomechanics and transgenic wood. *Am. J. Bot.* 93, 1433–1438. doi: 10.3732/ajb.93.10.1433

Köhler, L. and Spatz, H.-C. (2002). Micromechanics of plant tissues beyond the linear-elastic range. *Planta* 215, 33–40. doi: 10.1007/s00425-001-0718-9

Lapierre, C., Pilate, G., Pollet, B., Mila, I., Leplé, J.-C., Jouanin, L., et al. (2004). Signatures of cinnamyl alcohol dehydrogenase deficiency in poplar lignins. *Phytochemistry* 65, 313–321. doi: 10.1016/j.phytochem.2003.11.007

Leplé, J. C., Brasileiro, A. C. M., Michel, M. F., Delmotte, F., and Jouanin, L. (1992). Transgenic poplars: expression of chimeric genes using four different constructs. *Plant Cell Rep.* 11, 137–141. doi: 10.1007/BF00232166

Levan, A. (1939). Tetraploidy and octoploidy induced by colchicine in diploid Petunia. *Hereditas* 25, 109–131. doi: 10.1111/j.1601-5223.1939.tb02689.x

Li, Q., Min, D., Wang, J.-P., Peszlen, I., Horvath, L., Horvath, B., et al. (2011). Down-regulation of glycosyltransferase 8D genes in Populus trichocarpa caused reduced mechanical strength and xylan content in wood. *Tree Physiol.* 31, 226–236. doi: 10.1093/treephys/tpr008

Ma, Y., Xue, H., Zhang, L., Zhang, F., Ou, C., Wang, F., et al. (2016). Involvement of auxin and brassinosteroid in dwarfism of autotetraploid apple (Malus x domestica). *Sci. Rep.* 6, 26719. doi: 10.1038/srep26719

Mader, M., Le Paslier, M.-C., Bounon, R., Berard, A. A., Faivre-Rampant, P., Fladung, M., et al. (2016). Whole-genome draft assembly of Populus tremula x P. Alba clone INRA 717-1B4. *Silvae Genet.* 65, 74–79. doi: 10.1515/sg-2016-0019

Mu, H.-Z., Liu, Z.-J., Lin, L., Li, H.-Y., Jiang, J., and Liu, G.-F. (2012). Transcriptomic analysis of phenotypic changes in birch (Betula platyphylla) autotetraploids. *Int. J. Mol. Sci.* 13, 13012–13029. doi: 10.3390/ijms131013012

Müntzing, A. (1936). The chromosomes of a giant populus tremula. *Hereditas* 21, 383–393. doi: 10.1111/j.1601-5223.1936.tb03206.x

Muro-Villanueva, F., Mao, X., and Chapple, C. (2019). Linking phenylpropanoid metabolism, lignin deposition, and plant growth inhibition. *Curr. Opin. Biotechnol.* 56, 202–208. doi: 10.1016/j.copbio.2018.12.008

Nietsch, J., Brügmann, T., Becker, D., and Fladung, M. (2017). Old methods rediscovered: application and improvement of two direct transformation methods to hybrid poplar (Populus tremula × P. alba). *Plant Cell Tissue Organ Cult.* 130, 183–196. doi: 10.1007/s11240-017-1214-7

Nilsson-Ehle, H. (1936a). Note regarding the gigas form of Populus tremula found in nature. *Hereditas* 21, 372–382.

Nilsson-Ehle, H. (1936b). Über eine in der natur gefundene gigasform von Populus tremula. *Hereditas* 21, 379–382. doi: 10.1111/j.1601-5223.1936.tb03205.x

Özparpucu, M., Rüggeberg, M., Gierlinger, N., Cesarino, I., Vanholme, R., Boerjan, W., et al. (2017). Unravelling the impact of lignin on cell wall mechanics: a comprehensive study on young poplar trees downregulated for CINNAMYL ALCOHOL DEHYDROGENASE (CAD). *Plant J.* 91, 480–490. doi: 10.1111/tpj.13584

Pilate, G., Guiney, E., Holt, K., Petit-Conil, M., Lapierre, C., Lepl,é, J.-C., et al. (2002). Field and pulping performances of transgenic trees with altered lignification. *Nat. Biotechnol.* 20, 607–612. doi: 10.1038/nbt0602-607

Porth, I. and El-Kassaby, Y. A. (2015). Using Populus as a lignocellulosic feedstock for bioethanol. *Biotechnol. J.* 10, 510–524. doi: 10.1002/biot.201400194

Ren, Y., Jing, Y., and Kang, X. (2021). In vitro induction of tetraploid and resulting trait variation in Populus alba × Populus glandulosa clone 84 K. *Plant Cell Tissue Organ Cult.* 146, 285–296. doi: 10.1007/s11240-021-02068-5

Robinson, A. R. and Mansfield, S. D. (2009). Rapid analysis of poplar lignin monomer composition by a streamlined thioacidolysis procedure and near-infrared reflectance-based prediction modeling. *Plant J.* 58, 706–714. doi: 10.1111/j.1365-313X.2009.03808.x

Saleme, M. L. S., Cesarino, I., Vargas, L., Kim, H., Vanholme, R., Goeminne, G., et al. (2017). Silencing CAFFEOYL SHIKIMATE ESTERASE affects lignification and improves saccharification in poplar. *Plant Physiol.* 175, 1040–1057. doi: 10.1104/pp.17.00920

Serapiglia, M. J., Gouker, F. E., Hart, J. F., Unda, F., Mansfield, S. D., Stipanovic, A. J., et al. (2015). Ploidy level affects important biomass traits of novel shrub willow (Salix) hybrids. *BioEnergy Res.* 8, 259–269. doi: 10.1007/s12155-014-9521-x

Serapiglia, M. J., Gouker, F. E., and Smart, L. B. (2014). Early selection of novel triploid hybrids of shrub willow with improved biomass yield relative to diploids. *BMC Plant Biol.* 14, 74. doi: 10.1186/1471-2229-14-74

Sindhu, A., Langewisch, T., Olek, A., Multani, D. S., Mccann, M. C., Vermerris, W., et al. (2007). Maize Brittle stalk2 encodes a COBRA-like protein expressed in early organ development but required for tissue flexibility at maturity. *Plant Physiol.* 145, 1444–1459. doi: 10.1104/pp.107.102582

Singh, R. K., Bhalerao, R. P., and Eriksson, M. E. (2021). Growing in time: exploring the molecular mechanisms of tree growth. *Tree Physiol.* 41, 657–678. doi: 10.1093/treephys/tpaa065

Stebbins, G. L. (1971). "The morphological, physiological, and cytogenetic significance of polyploidy," in *Chromosomal Evolution in Higher Plants (Contemporary Biology),* eds E. J. W. Barrington and A. J. Willis (London: Edward Arnold (Publishers) Ltd.), 124–154.

Tang, Z.-Q., Chen, D.-L., Song, Z.-J., He, Y.-C., and Cai, D.-T. (2010). In vitro induction and identification of tetraploid plants of Paulownia tomentosa. *Plant Cell Tissue Organ Cult.* 102, 213–220. doi: 10.1007/s11240-010-9724-6

Ulrich, K. and Ewald, D. (2014). Breeding triploid aspen and poplar clones for biomass production. *Silvae Genet.* 63, 47–58. doi: 10.1515/sg-2014-0008

Updegraff, D. M. (1969). Semimicro determination of cellulose inbiological materials. *Anal. Biochem.* 32, 420–424. doi: 10.1016/S0003-2697(69)80009-6

Van Acker, R., Déjardin, A., Desmet, S., Hoengenaert, L., Vanholme, R., Morreel, K., et al. (2017). Different routes for conifer- and sinapaldehyde and higher saccharification upon deficiency in the dehydrogenase CAD1. *Plant Physiol.* 175, 1018–1039. doi: 10.1104/pp.17.00834

Van Acker, R., Vanholme, R., Piens, K., and Boerjan, W. (2016). Saccharification protocol for small-scale lignocellulosic biomass samples to test processing of cellulose into glucose. *Bio-Protocol* 6, e1701. doi: 10.21769/BioProtoc.1701

Van Acker, R., Vanholme, R., Storme, V., Mortimer, J. C., Dupree, P., and Boerjan, W. (2013). Lignin biosynthesis perturbations affect secondary cell wall composition and saccharification yield in Arabidopsis thaliana. *Biotechnol. Biofuels* 6, 46. doi: 10.1186/1754-6834-6-46

Vanholme, B., Desmet, T., Ronsse, F., Rabaey, K., Van Breusegem, F., De Mey, M., et al. (2013). Towards a carbon-negative sustainable bio-based economy. *Front. Plant Sci.* 4, 174. doi: 10.3389/fpls.2013.00174

Vanholme, R., De Meester, B., Ralph, J., and Boerjan, W. (2019). Lignin biosynthesis and its integration into metabolism. *Curr. Opin. Biotechnol.* 56, 230–239. doi: 10.1016/j.copbio.2019.02.018

Wu, W., Liao, T., Du, K., Wei, H., and Kang, X. (2021). Transcriptome comparison of different ploidy reveals the mechanism of photosynthetic efficiency superiority of triploid poplar. *Genomics* 113, 2211–2220. doi: 10.1016/j.ygeno.2021.05.009

Wullschleger, S. D., Jansson, S., and Taylor, G. (2002). Genomics and forest biology: Populus emerges as the perennial favorite. *Plant Cell* 14, 2651–2655. doi: 10.1105/tpc.141120

Xi, E. (2018). Dynamic relationship between mechanical properties and chemical compo sition distribution of wood cell walls. *Wood Res.* 63, 179–192.

Xiao, Z., Storms, R., and Tsang, A. (2004). Microplate-based filter paper assay to measure total cellulase activity. *Biotechnol. Bioeng.* 88, 832–837. doi: 10.1002/bit.20286

Xu, C., Huang, Z., Liao, T., Li, Y., and Kang, X. (2016). In vitro tetraploid plants regeneration from leaf explants of multiple genotypes in Populus. *Plant Cell Tissue Organ Cult.* 125, 1–9. doi: 10.1007/s11240-015-0922-0

Xu, C., Zhang, Y., Han, Q., and Kang, X. (2020). Molecular mechanism of slow vegetative growth in Populus tetraploid. *Genes* 11, 1417. doi: 10.3390/genes11121417

Xu, T., Zhang, S., Du, K., Yang, J., and Kang, X. (2022). Insights into the molecular regulation of lignin content in triploid poplar leaves. *Int. J. Mol. Sci.* 23, 4603. doi: 10.3390/ijms23094603

Zeng, Y., Zhao, S., Yang, S., and Ding, S.-Y. (2014). Lignin plays a negative role in the biochemical process for producing lignocellulosic biofuels. *Curr. Opin. Biotechnol.* 27, 38–45. doi: 10.1016/j.copbio.2013.09.008

Zhang, Y., Wang, B., Qi, S., Dong, M., Wang, Z., Li, Y., et al. (2019). Ploidy and hybridity effects on leaf size, cell size and related genes expression in triploids, diploids and their parents in Populus. *Planta* 249, 635–646. doi: 10.1007/s00425-018-3029-0

Zhao, Q., Tobimatsu, Y., Zhou, R., Pattathil, S., Gallego-Giraldo, L., Fu, C., et al. (2013). Loss of function of cinnamyl alcohol dehydrogenase 1 leads to unconventional lignin and a temperature-sensitive growth defect in Medicago truncatula. *Proc. Natl. Acad. Sci. USA* 110, 13660–13665. doi: 10.1073/pnas.1312234110

Zoghlami, A. and Paës, G. (2019). Lignocellulosic biomass: understanding recalcitrance and predicting hydrolysis. *Front. Chem.* 7, 874. doi: 10.3389/fchem.2019.00874

frontiers | Frontiers in Plant Science

TYPE Original Research
PUBLISHED 11 October 2022
DOI 10.3389/fpls.2022.1029915

OPEN ACCESS

EDITED BY
Jen-Tsung Chen,
National University of Kaohsiung, Taiwan

REVIEWED BY
Erika Toda,
The University of Tokyo, Japan
Yavar Vafaee,
University of Kurdistan, Iran
Pandiyan Muthuramalingam,
Gyeongsang National University, South Korea

*CORRESPONDENCE
Rui-Zhen Zeng
zengrz@scau.edu.cn
Zhi-Sheng Zhang
zszhang@scau.edu.cn

†These authors have contributed equally to this work

SPECIALTY SECTION
This article was submitted to Plant Breeding, a section of the journal Frontiers in Plant Science

RECEIVED 28 August 2022
ACCEPTED 23 September 2022
PUBLISHED 11 October 2022

CITATION
Li M-M, Su Q-L, Zu J-R, Xie L, Wei Q, Guo H-R, Chen J, Zeng R-Z and Zhang Z-S (2022) Triploid cultivars of *Cymbidium* act as a bridge in the formation of polyploid plants. *Front. Plant Sci.* 13:1029915. doi: 10.3389/fpls.2022.1029915

Triploid cultivars of *Cymbidium* act as a bridge in the formation of polyploid plants

Man-Man Li[1†], Qing-Lian Su[2†], Jun-Rui Zu[1], Li Xie[1], Qian Wei[1], He-Rong Guo[1], Jianjun Chen[3], Rui-Zhen Zeng[1*] and Zhi-Sheng Zhang[1*]

[1]Guangdong Province Key Laboratory of Plant Molecular Breeding, College of Forestry and Landscape Architecture, South China Agricultural University, Guangzhou, China, [2]Guangzhou Flower Research Center, Guangzhou, China, [3]Mid-Florida Research and Education Center, Environmental Horticulture Department, Institute of Food and Agricultural Sciences, University of Florida, Apopka, FL, United States

Triploid is considered a reproductive barrier and also a bridge in the formation of polyploids. However, few reports are available in *Cymbidium*. In this study, diploid 'Xiaofeng', sexual triploid 'Yuchan' and 'Huanghe' of *Cymbidium* were used to evaluate hybridization compatibility of the triploids. Results showed that the sexual triploids were fertile whether they were used as male or female parents. 'Yuchan' produced male gametes of 1*x*, 1*x*~2*x*, 2*x*, 2*x*~3*x*, and 3*x* at frequencies of 8.89%, 77.78%, 6.67%, 3.33%, and 3.33%, respectively; while 'Huanghe' produced 3.33% 1*x*, 80.00% 1*x*~2*x*, 8.89% 2*x*, 5.56% 2*x*~3*x*, and 2.22% 3*x* male gametes. The cross of 'Xiaofeng' with 'Yuchan' produced progenies with a wide range of ploidy levels, including one diploid, 34 2×~3× aneuploids, 12 triploids, and one tetraploid, indicating that male gametes produced by sexual triploid were fertile and could be transmitted and fused with egg cells. On the other hand, 10 progenies obtained from the cross of 'Yuchan' × 'Xiaofeng' were all aneuploids. The cross of 'Yuchan' with 'Huanghe' produced 40 progenies including three 2×~3× aneuploids, nine 3×~4× aneuploids, 21 tetraploids, six 4×~5× aneuploids, and one pentaploid, suggesting that 2*x* gametes, instead of the unreduced ones played a more important role in the formation of tetraploids. The survival rates of the hybrids were all above 80.00%, with the tetraploids at 96.67%. Cytological analysis revealed that during meiosis of sexual polyploids, two chromosome sets of the 2*n* gamete were inclined to enter into the same daughter cell, resulting in the production of 2*x* gametes. Our results indicate that the triploid cymbidiums are not reproductive barrier but serve as a bridge in the formation of polyploid plants.

KEYWORDS

cross compatibility, *Cymbidium*, polyploidy, triploid bridge, unreduced gamete

Introduction

Polyploidy plays a major role in the evolution and diversification of plants (Thompson and Lumaret, 1992; Bretagnolle and Thompson, 1995; Kovalsky et al., 2018). In natural populations, polyploidy is formed by several different routes (Ramsey and Schemske, 1998). Among them, sexual polyploidy through unreduced gametes (2*n* gametes) is considered to be the main pathway (Bretagnolle and Thompson, 1995; Ramsey and Schemske, 1998; Xie et al., 2022). The union of reduced and unreduced gametes produces triploids, and the combination of two unreduced gametes forms tetraploids (Bretagnolle and Thompson, 1995; Husband, 2004). Owing to the limited chance in the fertilization between simultaneously formed unreduced male and female gametes, triploids are usually considered as the intermediate stage in the formation of stable tetraploids, and this pathway of tetraploid formation is known as the 'triploid bridge' (Ramsey and Schemske, 1998; Yamauchi et al., 2004; Jike et al., 2020).

Triploids play an important role in polyploidy dynamics of natural populations (Husband, 2004). For example, 1% tetraploid progeny were obtained by backcrossing a spontaneous triploid clone of *Populus tremula* with a diploid (Bergstrom, 1940). Henry et al. (2005) reported that triploid *Arabidopsis thaliana* plants were fertile and could lead to the formation of tetraploids because they act as bridges between euploid types. Schinkel et al. (2017) revealed that a female triploid produced through unreduced egg cells was the major cause of polyploidization in *Ranunculus kuepferi*. In the cross of 2× × 3×[2x] of *Chamerion angustifolium*, 65% progeny were triploids and 16% were tetraploids, while 45% triploid progeny and 35% tetraploid progeny were produced in the cross of 2× × 3×[4x] (Burton and Husband, 2001). Using triploid as parents, tetraploids and/or pentaploids were produced through the cross of triploid × diploid in *Hieracium echioides* (Peckert and Chrtek, 2006), *Phalaenopsis* (Zhou et al., 2009), *Tulipa* (Marasek-Ciolakowska et al., 2014), and *Phegopteris* (Nakato and Masuyama, 2021). Hexaploids were obtained from the selfing progeny of triploid *Phegopteris decursivepinnata* (Nakato and Masuyama, 2021).

A challenge to the formation of higher polyploidy *via* the 'triploid bridge' pathway is the occurrence in aneuploid gametes which can substantially reduce fertility (Ramsey and Schemske, 1998; Husband, 2004; Duszynska et al., 2019). However, increasing evidence has suggested that triploids can produce functional euploid (n = *x*, 2*x* or 3*x*) and aneuploid male gametes in some species (Ramsey and Schemske, 1998; Diao et al., 2009; Czarnecki et al., 2014; Kovalsky et al., 2018). Further studies show that pollen fertility (or percentage of viable pollen) in triploid plants varies among species and cultivars (Jones and Reed, 2007; Farco and Dematteis, 2014; Zhang et al., 2017; Alexander, 2020). Pollen fertilities in some triploid *Turnera sidoides* were found to be greater than 60% (Kovalsky et al., 2018; Alexander, 2020) and reach up to 80% in triploid *Hydrangea macrophylla* (Jones and Reed, 2007) and even 90% in triploid white poplar plants (Wang et al., 2010).

Another obstacle restricting the role of triploids in polyploid evolution is 'triploid block'. Triploid block, which prevents interploidy hybridization, is characterized by abnormal endosperm development and seed collapse (Johnston et al., 1980; Erilova et al., 2009; Koehler et al., 2010; Schinkel et al., 2017; Huc et al., 2022). It is well known that the endosperm may develop abnormally in interploidy-intraspecific crosses if the maternal and paternal genome deviates from 2:1 ratio (Johnston et al., 1980; Vinkenoog et al., 2003; Haig, 2013). However, some deviations from this ratio are found to be allowable in certain species as viable seeds were produced in *Zea mays* (Lin, 1984), *Solanum tuberosum* (Ehlenfeldt and Ortiz, 1995), *Arabidopsis thaliana* (Scott et al., 1998), and *Peperomia* (Friedman et al., 2008).

Orchids are plants belonging to the family Orchidaceae that are prized by their ornamental and medicinal value. There are 27,801 recognized species that are globally distributed with the exception of Antarctica (Vilcherrez-Atoche et al., 2022). Orchids have been used as models for studying plant evolutionary processes and adaptability to different environmental conditions. Polyploidy plays an important role during the evolution of orchids as sequence analyses showed that whole-genome duplication (WGD) occurred widely in orchids, including *Apostasia shenzhenica* (Zhang et al., 2017; Zhang et al., 2021), *Cymbidium ensifolium* (Ai et al., 2021), *Dendrobium chrysotoxum* (Zhang et al., 2021), and *Phalaenopsis* (Cai et al., 2015). A recent study showed that triploids clustered in an intermediate position between diploids and tetraploids in *Zygopetalum mackayi* (Moura et al., 2020). In the *Nigritella nigra* group, nuclear and plastid marker analysis showed that tetraploid *N. nigra* subsp. *austriacais* somewhat differentiated from the triploid subsp. *Nigra* at nuclear as well as plastid loci. The fusion of an unreduced egg cell from subsp. *Nigra* with a haploid microgamete from *Gymnadenia conopsea* gave rise to *Gymnigritella runei* (Hedren et al., 2018). In *Phalaenopsis*, diploids, triploids, pentaploids, and aneuploids were produced from the crosses of diploid × triploid or triploid × diploid. Triploids, tetraploids, octoploids, and aneuploids were identified in triploid × tetraploid crosses, while no hybrids were obtained from the cross of triploid × triploid (Zhou et al., 2009). Nevertheless, it is generally acknowledged that polyploids can be formed *via* polyspermy, unreduced gamete, hybridization and endopolyploidy in orchids (Okamoto et al., 2017; Vilcherrez-Atoche et al., 2022); but it is still unclear how each of these pathways contributes to the polyploidization in orchids.

Cymbidium Sw. is one of the most important orchids consisting of 74 species that are epiphytic, lithophytic, terrestrial or sometimes rarely leafless saprophytic (Ning et al., 2018; Thakur and Dutt, 2021). Among the terrestrial species, *C. sinense*, *C.*

ensifolium, C. goeringi, and *C. kanran* are the most popular flowering ornamental plants and widely cultivated for their beauty and fragrance (Huang et al., 2012). Our previous research identified 2*n* gamete occurrence in cultivated cymbidiums (Zeng et al., 2020). Hybridization among selected cultivars or species produced five triploid and two tetraploid progenies. Two of five triploids were propagated through *in vitro* culture and evaluated in shaded greenhouse for their aesthetic value. Results showed that they had improved ornamental traits displayed by rounder flowers with wider sepal, petals, and lips compared to the diploids. The occurrence of more triploids than tetraploids was intriguing. Since orchids do not have endosperm, triploid block due to the endosperm balance could not be great concern. Besides, triploid plants can be easily propagated through *in vitro* culture (Zeng et al., 2020). The higher frequency in triploid occurrence, the improved ornamental traits, and little concern over the triploid block prompted us to further analyze 2*n* gamete occurrence in cymbidiums and the implication of triploids as a bridge in the formation of polyploid plants.

The objectives of this study were to examine microsporogenesis and microgametogenesis behaviors of two sexual triploids, determine their pollen type and fertility, evaluate their crossability with either diploids or triploids, and analyze ploidy levels and the survival rates of their progenies. Results showed that the union of 2*x* gametes, which were derived from the unreduced gamete, was probably the key pathway for the formation of tetraploids through 'triploid bridge'. Our studies with cymbidium demonstrated the importance of triploids in the formation of polyploid plants.

Materials and methods

Plant materials

A total of seven cultivars were used in this study (Supplementary Figure S1). Two of them, 'Yuchan' and 'Huanghe', were sexual triploids. The remaining 'Xiaofeng', '11-65-1004', '13-44-5', '12L-2018-2', and 'Gongfenjiaren' were diploids. Plants were grown in a shaded greenhouse under a light intensity of 120 $\mu mol \cdot m^{-2} \cdot s^{-1}$, temperature ranging from 15°C to 30°C, and relative humidity varying from 70 to 80% at the Experimental Farm of South China Agricultural University, Guangzhou, China. At anthesis, the following studies were performed with selected cultivars.

Cytological observations of microsporogenesis and microgametogenesis

Microsporogenesis and microgametogenesis were observed using the method described by Zhu et al. (2014). The pollinia of 'Yuchan', 'Huanghe', and 'Xiaofeng' at different formation and developmental stages were collected and fixed at 4°C for 12-24 hours in fresh prepared Carnoy's solution. They were then transferred to 70% ethanol and stored at 4°C. The fixed pollinia were placed on a slide; after surface dried with filter paper, two drops of improved carbolic acid fuchsin or 4,6-diamidino-2-phenylindole (DAPI) [2 $\mu g.ml^{-1}$ DAPI, 1% Triton X-100 (v/v), and 1% sucrose (w/v)] staining solution were added, they were crashed with a forceps, and stained in the dark at room temperature for 5 min. A cover glass was applied and squeezed with pencil eraser, the slide was observed and photographed under either light or UV illumination with ZEISS microscope. For observation of each microsporogensis stage per hybrid progeny, at least nine slides were observed where three slides and 100 microsporocytes as a replicate. There were three replications for each hybrid progeny. For examining each microgametogensis stage of the hybrid progenies, at least ninety pollens were observed with thirty pollens as a replicate. The observations also had three replications. The percentage of meiosis abnormalities and each male gamete type were calculated as follows: (1) the percentage of meiosis abnormalities = (the number of abnormal microspore mother cell in a replicate/100) × 100% and (2) the percentage of each male gamete type = (the number of certain male gamete type in a replicate/30) × 100%.

For the calculation of dyad and triad occurrence, ten vision fields were photographed at 40× magnitude for each slide, one slide was regarded as a replicate, and each material was replicated three times. The frequencies of dyad and triad incidence were calculated according to the formula: $F_{Dy}(\%)$ = (Number of dyads/total microspore count observed)) ×100; $F_{Tr}(\%)$ = (Number of triads/total spore count observed) ×100.

Pollen viability determination

Pollinia of 'Yuchan' or 'Xiaofeng' were collected from the flowers that had opened for one day and placed on a slide. After two or three drops of 0.05% of 2, 3, 5-triphenyltetrazolium chloride solution were added, the pollinia were crashed with a forceps and kept in the dark at room temperature for 2-3 h. A coverslip was applied, and the slide was observed and photographed under photomicroscope (OlympusIX71, Japan). Pollen grains with red color were regarded as viable. About 1,000 pollens were counted per slide, one slide was regarded as a replicate, and three slides per cultivar were observed. The pollen fertility was calculated according to the formula: The pollen fertility (%) = (the number of stained pollen grains/total number of pollen grains observed) × 100.

Hybridization, seed germination, seedling production and transplanting

Methods of hybridization, seed germination, seedling production and transplanting were described previously (Zeng

et al., 2020). A total of 11 pairs of hybridization were made using the seven cultivars. The numbers of pollinated flowers and capsules produced from the pollinations were recorded, and fruit setting rates were calculated. Seeds harvested from the cross of 'Yuchan' × 'Xiaofeng', 'Xiaofeng' × 'Yuchan', and 'Yuchan' × 'Huanghe' were germinated *in vitro*. The protocorm like body or rhizome obtained from a seed was propagated, and test-tube seedlings were produced (Zeng et al., 2020). After the seedlings reached about 5 cm in height, they were used for identification of ploidy levels. When the seedlings were about 8 cm in height, they were removed from test tubes, rinsed with tap water, briefly air dried, and transplanted into small black plastic planting bags (100 mL). Each bag was filled with a substrate comprised of small pine bark (1 cm in length) and peat in a 3:1 ratio based on volume, one seedling per bag. Potted seedlings were grown in the aforementioned shaded greenhouse and fertigated with a Hyponex ($N–P_2O_5–K_2O$; 20–20–20) solution every 10 d. After 6 months of growth, they were transplanted into 2.6 L bags filled with the pine bark and granite substrate and grown in another shaded greenhouse under a light intensity of 300-400 μmol·m^{-2}·s^{-1}. A slow-release fertilizer ($N–P_2O_5–K_2O$; 20–20–20) was applied to each bag at 3-4 g each in March and September, respectively. Meanwhile, a solution containing 0.1% KH_2PO_4 (w/v) was sprayed monthly during growing season. Initially, a total of 90 seedlings from each hybrid were transplanted, and they were arranged as a randomized complete block design with three replicates. After 10 months of transplanting, the number of surviving seedlings were recorded, and the survival rate was calculated according to the formula: The survival rate (%) = (the number of seedlings survived in a replicate/30) × 100.

Flow cytometry analysis

The ploidy level of hybrid progenies was measured by flow cytometry (Cui et al., 2009; Zeng et al., 2020). For each individual, young leaves, about 0.5 cm^2, were placed in a one-off culture dish. After adding 0.4 mL of PartecHR-A extract, the leaves were chopped quickly with a blade, following by adding 1.6 mL of Partec HR-B (DAPI, 4,6-diamidino-2-phenylindole) solution as DNA staining agent. The mixture samples were filtered through 30 μm Partec Celltrics microporous membrane, stained in darkness for 5 min and analyzed by Partec flow cytometer using CyView8.5 software (PartecGmb H, Munster, Germany). The DNA histograms of nuclei from each sample were produced.

Chromosome counts

In order to further verify ploidy level of the hybrid progenies, the number of chromosomes in root tip cells was accounted by squash method (Zhou et al., 2009). The root tips with a length of 2~3 mm was cut from the newly formed root of *in vitro* grown seedlings and fixed in Carnoy's solution, which was consisted of 95% ethanol and glacial acetic acid in a 3:1 ratio based on volume, at 4°C for 12~24 h. The fixed material was washed with distilled water for 2~3 times, and then acidulated with 1 mL concentration of 1 mol·L^{-1} HCl in a constant temperature water bath at 60°C for about 8 minutes. The dissociated root tips were immersed in distilled water for 30 min, then stained with improved carbolic acid fuchsin staining solution, crushed with tweezers. The debris was discarded, and the sample was covered with a coverslip and observed at 100 × magnification using a photomicroscope (OlympusIX71, Japan). A digital camera system (Nikon) was used for photography. For each plantlet, at least 20 cells were observed. If more than 90% of the cells had a constant chromosome number, the chromosome number of the seedlings was confirmed. As diploid *Cymbidium* has somatic chromosome numbers of 40, we defined that chromosome numbers of 41-59, 61-79, and 81-99 were aneuploid of 2×~3 ×, 3×~4×, and 4×~5×, respectively.

Statistical analysis

All data were subjected to analysis of variance using Microsoft Office Excel 2019 and SPSS 26.0 (IBM Corporation, Somers, NY). When significance occurred, means were separated by Duncan's multiple range test at $P< 0.05$ level.

Results

Triploid pollen viability and hybridization compatibility

The intention of making the 11 crosses (Table 1) was to assess the hybridization compatibility of two sexual triploids 'Yuchan' and 'Huanghe'. As a result, capsules were obtained in all 11 cross combinations, and all capsules obtained had seeds. The seeds collected from the crosses of 'Yuchan' × 'Xiaofeng', 'Xiaofeng' × 'Yuchan', and 'Yuchan' × 'Huanghe' were geminated normally *in vitro*, and the seedlings grew vigorously (Supplementary Figure S2). These results suggested that sexual triploid *Cymbidium* had high hybridization compatibility and could be used as male or female parent for hybridization.

Ploidy levels of hybrid progenies

The ploidy levels of progenies derived from the crosses of 'Yuchan' × 'Xiaofeng' and 'Xiaofeng' × 'Yuchan' were analyzed by DNA flow cytometry and root tip chromosome count (Figure 1). Results showed that among 10 identified progenies of 'Yuchan' ×

TABLE 1 Fruit setting rates of 11 crosses made by using sexual triploid cultivars as one ortwo parents in *Cymbidium*.

Cross combination (♀ × ♂)	Year	No. of flowers Pollinated	No. of capsules obtained
'Yuchan' (3×) × 'Xiaofeng' (2×)	2018	1	1
'Xiaofeng' (2×) × 'Yuchan' (3×)	2018	2	2
'Yuchan' (3×) × 'Huanghe' (3×)	2018	1	1
'Xiaofeng' (2×) × 'Yuchan' (3×)	2019	1	1
'11-65-1004' (2×) × 'Yuchan' (3×)	2019	1	1
'Yuchan' (3×) × '13-44-5' (2×)	2020	1	1
'Yuchan' (3×) × '12L-2018-2' (2×)	2020	1	1
'Yuchan' (3×) × 'Gongfenjiaren' (2×)	2021	7	7
'Gongfenjiaren' (2×) × 'Yuchan' (3×)	2021	7	7
'Yuchan' (3×) × 'Yuchan' (3×)	2021	2	2
'Huanghe' (3×) × 'Yuchan' (3×)	2021	2	1

'Xiaofeng', nine were aneuploids of 2×~3×, and one was the aneuploid of 3×~4×. In the reciprocal cross of 'Xiaofeng' × 'Yuchan', the percentages of aneuploid of 2×~3×, diploid (2×), triploid (3×), and tetraploid (4×) in the hybrid progenies were 70.8%, 2.1%, 25.0%, and 2.1%, respectively (Table 2).

The ploidy levels of hybrid progenies from the cross of 'Yuchan'× 'Huanghe' were shown in Figure 1 and Table 2. They were aneuploids of 2×~3×, 3×~4×, and 4×~5×; tetraploid, and pentaploid. The proportion of tetraploid was the highest, accounting for 52.5%, followed by aneuploids of 2×~3×, 3×~4×, and 4×~5× with proportions of 7.5%, 22.5%, and 15.0%, respectively. The proportion of pentaploid was the lowest (2.5%). The occurrence in higher proportion of tetraploid in the triploid × triploid cross suggested that the cross between triploids was probably a main avenue for producing polyploids with higher ploidy levels in the natural population.

Types of male gamete and pollen fertility

In order to further understand how tetraploids were formed through 'triploid bridge', the types of male gametes and their fertilities were examined in sexual triploid and diploid parents. Results showed that 'Yuchan' and 'Huanghe' produced 1*x*, 2*x*, 3*x* (unreduced gamete) and aneuploid male gametes (Figures 2B–L; Supplementary Figure S3). The proportion of 1*x*~2*x* aneuploid gametophytes was 77.78% and 80.00% in 'Yuchan' and 'Huanghe', respectively (Table 3), which proved that the main type of male gamete produced by triploids was aneuploidy. The occurrence of 1*x* and 2*x* male gametes with a rather high proportion in sexual triploids suggested that the unreduced gamete was inclined to enter into the same daughter cell during meiosis, thus resulting in the formation of 2*x* male gamete (Figure 2J).

Diploid 'Xiaofeng' produced aneuploid gametes with chromosome number less than 20 (<1*x*), reduced male gametes (1*x*), aneuploid with chromosome number between 20 and 40 (1x–2x), and unreduced male gametes (2*x*) at 18.89%, 72.22%, 7.78%, and 1.11%, respectively (Table 3), which suggested that the main type of male gamete produced by 'Xiaofeng' was the reduced male gamete (1*x*).

The viability of pollen was investigated using 2, 3, 5-triphenyltetrazolium chloride staining method. Results showed that 67.88% pollen grains of 'Yuchan' were stained in red, indicating their viability (Figures 3A2, 3, 4). Similarly, 73.32% pollen grains of 'Xiaofeng' were viable (Figure 3A1). Besides, some pollen grains with different ploidy levels were also stained in red, suggesting that all types of male gametes were fertile or partial fertile (Figures 3A3, 4). Moreover, there was no significant difference in the percentage of stainable pollens between the diploid and sexual triploid (Figure 3B).

Meiotic abnormalities during microsporogenesis

Microsporogenesis of 'Yuchan', 'Huanghe', and 'Xiaofeng' were observed in order to gain a better understanding of cytological mechanisms behind the formation of different types of male gametes (Figure 4; Table 4 and Supplementary Figures S4, S5). The results indicated that meiotic abnormalities included meiosis asynchrony, lagging chromosomes, chromosome bridges, and abnormal orientation of spindles during the microsporogenesis. Univalents, bivalents, trivalents, and multivalents were observed at diakinesis of 'Yuchan' (Figure 4A). At metaphase I, there were 33.0% and 24.5% microspore mother cells of 'Yuchan' and 'Xiaofeng', respectively at either diakinesis or pachytene stage (Figure 4B; Table 4). Those microspore mother cells probably missed the meiosis I (Figure 4C) but proceeded with normal meiosis II (Figure 4D), which resulted in the formation of dyads (Figure 4E). Lagging chromosomes were noticed at every stage of meiosis from metaphase I to telophase II (Figures 4H, I, K, L). Chromosome bridges were found

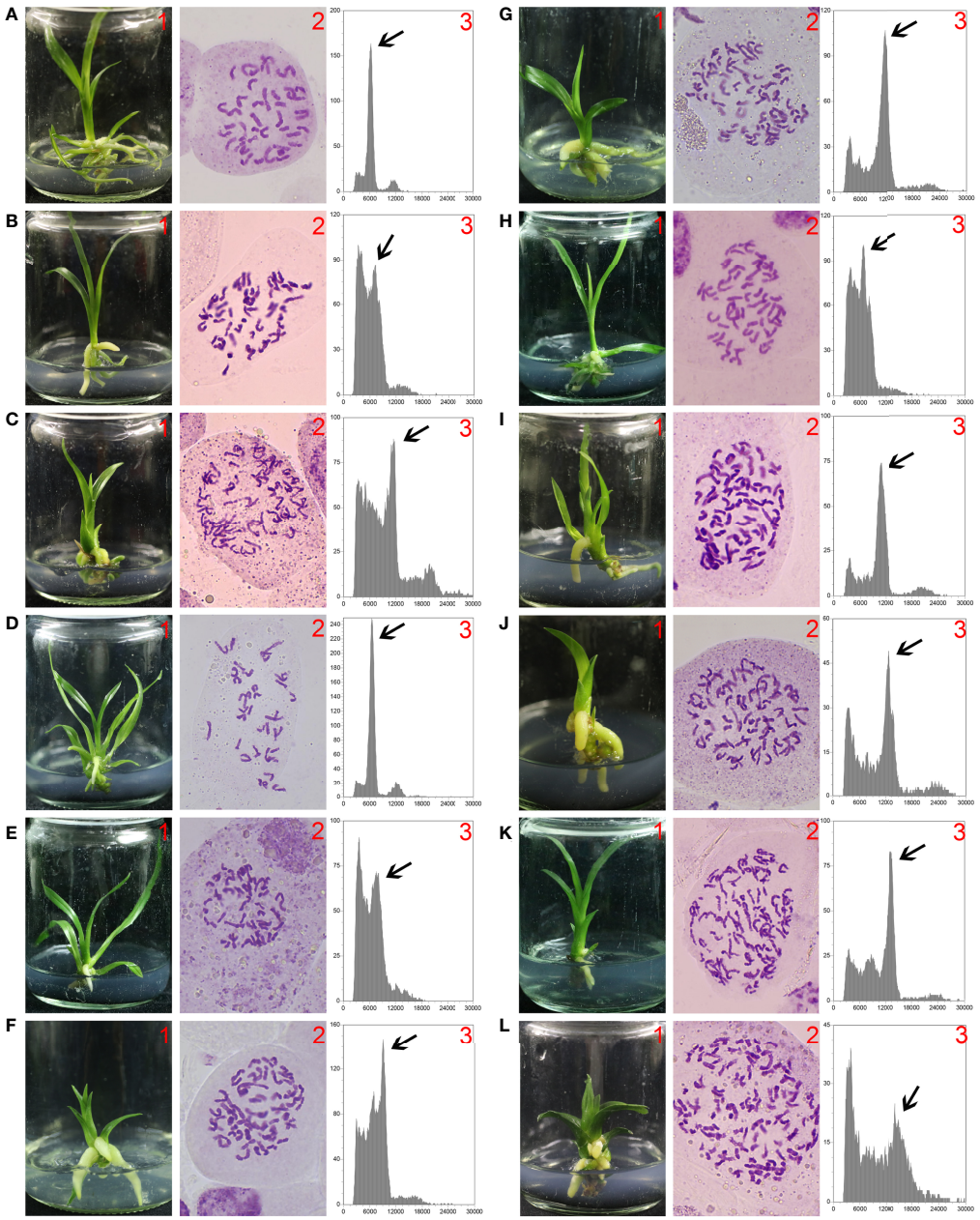

FIGURE 1
Ploidy identification of hybrid progenies. 1. *In vitro* cultured seedlings; 2. Chromosome numbers in a root tip cell; 3. Flow cytometry histogram of leaf tissue (arrow represents plant ploidy). **(A)** 'Xiaofeng' (diploid, 2*n* = 2× = 40). **(B, C)** Hybrid progenies of 'Yuchan' × 'Xiaofeng': **(B)** '18-21-8' (aneuploidy, 2*n* = 50), **(C)** '18-21-10' (aneuploidy, 2*n* = 75). **(D–G)** Hybrid progenies of 'Xiaofeng' × 'Yuchan' where **(D)** '18-50-1' (diploid, 2*n* = 2× = 40), **(E)** '18-50-86' (aneuploidy, 2*n* = 48), **(F)** '18-50-125' (triploid, 2*n* = 3× = 60), and **(G)** '18-50-140' (tetraploid, 2*n* = 4× = 80). **(H–L)** Hybrid progenies of 'Yuchan' × 'Huanghe' where **(H)** '18-24-50' (aneuploidy, 2*n* = 56), **(I)** '18-24-33' (aneuploidy, 2*n* = 72), **(J)** '18-24-15' (tetraploid, 2*n* = 4× = 80), **(K)** '18-24-1' (aneuploidy, 2*n* = 93), and **(L)** '18-24-172' (pentaploid, 2*n* = 5× = 100).

during anaphase I and telophase I, II (Figures 4J–L), which might lead to the formation of aneuploid male gametes and micronuclei (Figure 4M). The abnormal orientation of spindles was observed during metaphase II, including tripolar spindle (Figure 4N) and fusion spindle (Figure 4O), which resulted in the formation of triads (Figure 4P) and dyads (Figure 4E). The percentage of lagging chromosomes and chromosome bridges in sexual triploids was significantly higher than that in diploid. As a result, a higher percentage of aneuploid male gametes occurred in sexual triploids (Table 4).

10.3389/fpls.2022.1029915

TABLE 2 Ploidy level of hybrid progenies resulted from crosses with sexual triploid *Cymbidium*.

Cross combinations(♀ × ♂)	Total no. of plantlets evaluated	No. of plantlets with specified ploidy level						
		2×	2×~3×	3×	3×~4×	4×	4×~5×	5×
'Yuchan' (3×) × 'Xiaofeng' (2×)	10	0	9	0	1	0	0	0
'Xiaofeng' (2×) × 'Yuchan' (3×)	48	1	34	12	0	1	0	0
'Yuchan' (3×) × 'Huanghe' (3×)	40	0	3	0	9	21	6	1

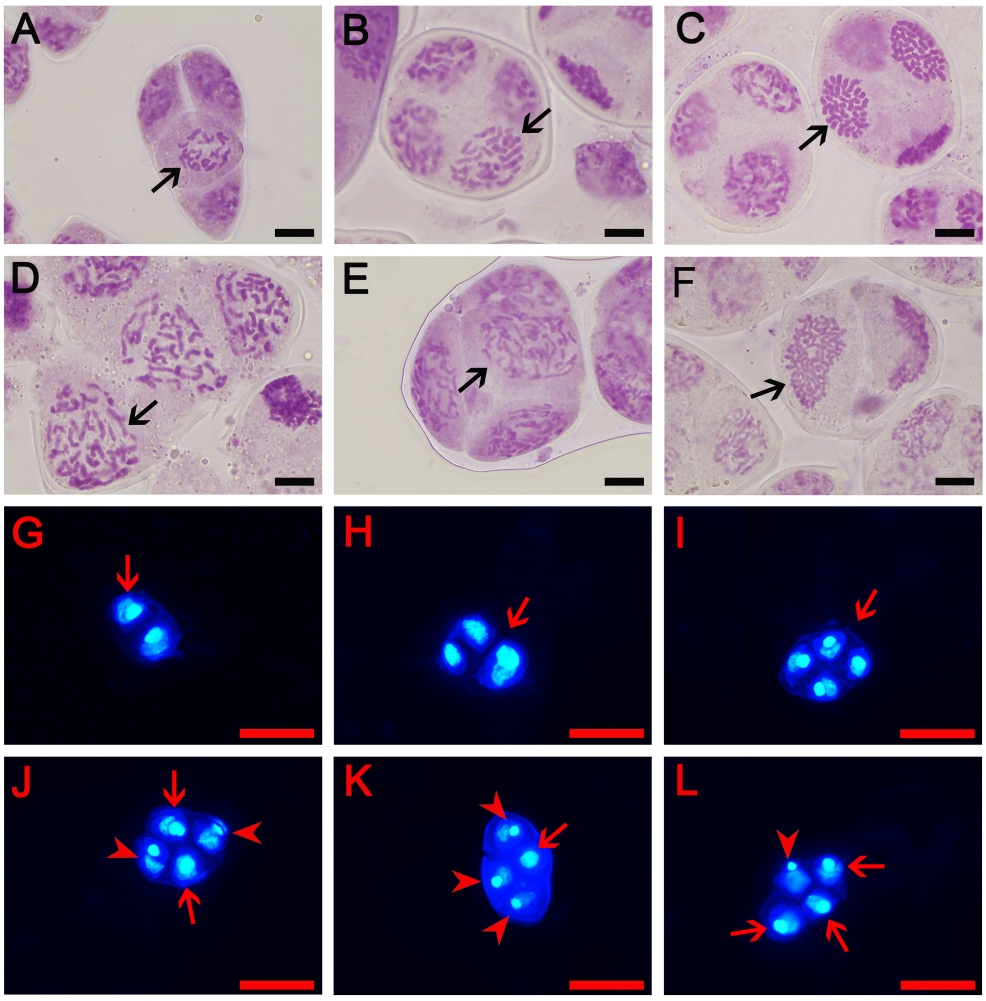

FIGURE 2
Types of male gametes in diploid and triploid cymbidiums. **(A–F)** represent early microspore stage where **(A)** The aneuploidy gamete of 'Xiaofeng': *x*-2 = 18 (arrow) and **(B–F)** The gamete of 'Yuchan': **(B)** 1*x* gamete: *x* = 20 (arrow), **(C)** Aneuploidy gamete: *x*+10 = 30 (arrow), **(D)** 2*x* gamete: 2*x* = 40 (arrow), **(E)** Aneuploidy gamete: 2*x* +2 = 42 (arrow), and **(F)** Unreduced gamete: 3*x* = 60 (arrow). Bar = 10 μm. Additionally, **(G–L)** represent mature pollens stained with 4, 6-diamidino-2-phenylindole (DAPI): **(G)** Dyad (arrow), **(H)** Triad (arrow), **(I)** Tetrad with the same size of nuclei (arrow), **(J)** Tetrad with two large (arrow) and two small nuclei (arrowhead), **(K)** Tetrad with one large (arrow) and three small nuclei (arrowhead), and **(L)** Tetrad with three large (arrow) and one small nuclei (arrowhead). Bar = 50 μm.

TABLE 3 Type and proportion (%) of male gametes in diploid and sexual triploid cymbidiums.

Parents	The proportion of gamete (%)					
	<1*x*	1*x*	1*x*~2*x*	2*x*	2*x*~3*x*	3*x*
'Yuchan'	0.00 ± 0.00^{b}	8.89 ± 3.85^{b}	77.78 ± 5.09^{a}	6.67 ± 3.33^{a}	3.33 ± 3.33^{a}	3.33 ± 3.33^{a}
'Huanghe'	0.00 ± 0.00^{b}	3.33 ± 0.00^{b}	80.00 ± 10.00^{a}	8.89 ± 1.92^{a}	5.56 ± 3.85^{a}	2.22 ± 1.92^{a}
'Xiaofeng'	18.89 ± 3.85^{a}	72.22 ± 1.92^{a}	7.78 ± 3.85^{b}	1.11 ± 1.92^{b}	0.00 ± 0.00^{b}	0.00 ± 0.00^{a}

Values represent mean ± standard error. Different letters behind the values within the same column indicate significant difference among cultivars based on Duncan's multiple range test at $P < 0.05$ levels.

Statistical analysis of survival rate of plantlets with different ploidy levels

To determine the survivability of plantlets, the survival rates of plantlets with different ploidy levels grown in the shaded greenhouse were evaluated. The survival rate of tetraploid plants was 96.67%, which was significantly higher than that of triploids. Interestingly, the survival rates of 2×~3× and 3×~4× aneuploid plants were also significantly higher than that of triploids. There was no significant difference in the survival rate between 4×~5× aneuploid and triploid plants (Figure 5).

Discussion

Polyploidization is considered as an important evolutionary force. The most common mechanism of polyploid origin is believed to be through production of unreduced gametes (Clo et al., 2022). There are two main models explaining the pathways of polyploid formation in diploid populations: (i) frequency-dependent minority cytotype exclusion (Levin, 1975; Husband, 2000) and (ii) the 'triploid bridge' hypothesis (Ramsey and Schemske, 1998; Burton and Husband, 2001; Husband, 2004; Peckert and Chrtek, 2006; Schinkel et al., 2017). According to the 'triploid bridge' hypothesis, triploids are first formed *via* the union of reduced and unreduced gametes. Subsequently, backcrosses of triploids to diploids or crosses between triploids can generate tetraploids (Bretagnolle and Thompson, 1995; Ramsey and Schemske, 1998). In the present study, we documented that sexual triploid cymbidiums produced functional 1*x*, 2*x*, 3*x*, and aneuploid gametes after backcross to diploids or through the cross between triploids. We further showed the triploid cross resulted in the formation of tetraploids at a high percentage and also pentaploids. Our results demonstrate that the sexual triploids act as a bridge for efficiently producing tetraploid and even polyploid with higher ploidy level in *Cymbidium*.

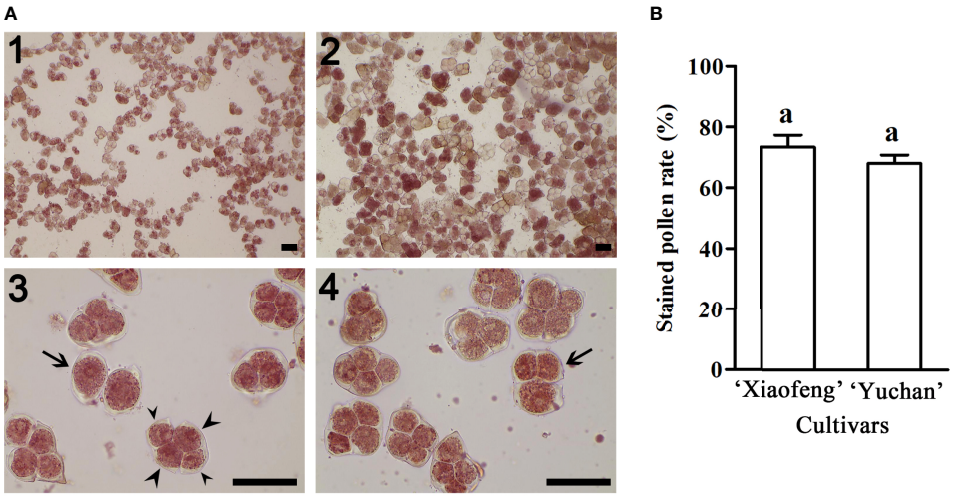

FIGURE 3
Pollen fertility of 'Xiaofeng' and 'Yuchan'. **(A)** Pollen stained with 2, 3, 5-triphenyltetrazolium chloride: Pollen grains of (1) 'Xiaofeng' and (2) 'Yuchan', (3) 'Yuchan' pollens showed dyad (arrow) and tetrad with two small nuclei (small arrowhead) and two big nuclei (big arrowhead), and (4) 'Yuchan' pollens with triad (arrow). Bar=50 μm. **(B)** The percentage of stained pollens of 'Xiaofeng' and 'Yuchan', the same letter above the bars indicates no significant difference between cultivars analyzed by Duncan's multiple range test at $P< 0.05$ level.

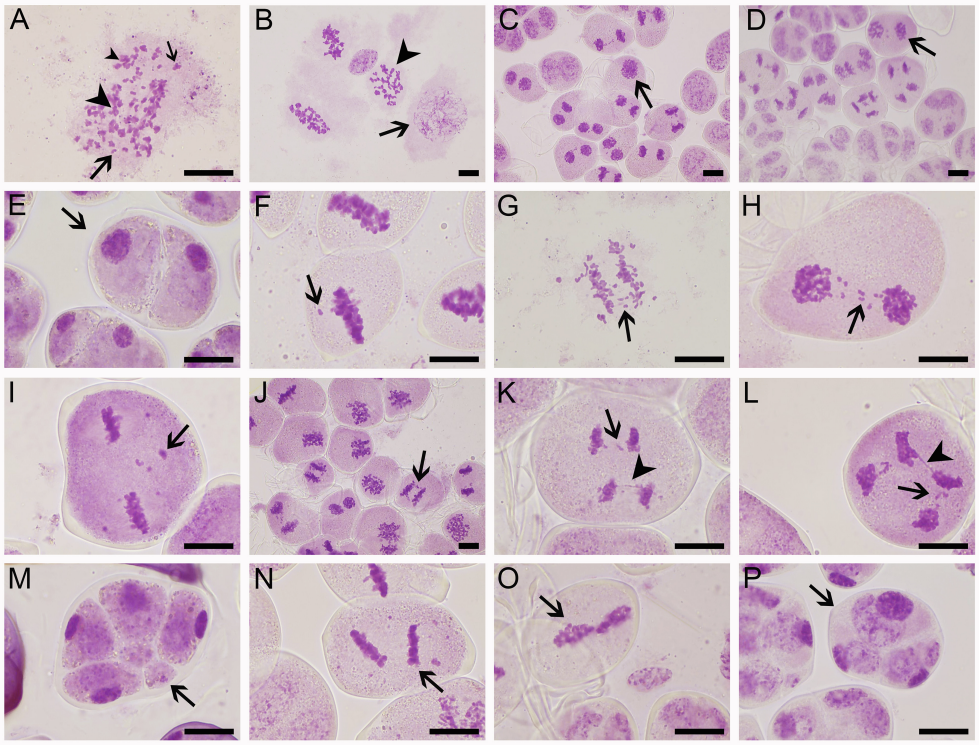

FIGURE 4
Meiotic abnormalities of sexual triploid 'Yuchan'. **(A)** Univalent (big arrow), bivalent (small arrow), trivalent (big arrowhead), and multivalent (small arrowhead) observed at diakinesis. **(B)** Metaphase I, microspore mother cells at pachyten (arrow) or diakinesis (arrowhead) stage were observed. **(C)** Telophase I: microsporocyte failed to carry out meiosis I (arrow). **(D)** Telophase II: microsporocyte that missed meiosis I but proceeded with normal meiosis II (arrow), which resulted in the formation of dyad (arrow) **(E)**. **(F–I)** Lagging chromosomes (arrow) at metaphase I, anaphase I, telophase I, and metaphase II. **(J)** Chromosome bridge (arrow) at anaphase **(I)**. **(K)** Lagging chromosomes (arrow) and a chromosome bridge (arrowhead) at anaphase II. **(L)** Lagging chromosomes (arrow) and a chromosome bridge (arrowhead) at telophase II. **(M)** Tetrad stage: indicating micronucleus (arrow). **(N)** Metaphase II: tripolar spindles (arrow). **(O)** Metaphase II: fused spindles (arrow). **(P)** Tetrad stage, indicating triad (arrow). Bar = 20 μm.

The production of functional *x*, 2*x*, 3*x*, and aneuploid gametes is important for triploids to fulfil the role as a bridge (Burton and Husband, 2001; Peckert and Chrtek, 2006; Marasek-Ciolakowska et al., 2014; Li et al., 2017; Zhang et al., 2017; Trankner et al., 2020). The percentages in occurrence of different types of gametes depended on plant species, origin of triploids, and gamete types (Marasek-Ciolakowska et al., 2014; Geng et al., 2019; Trankner et al., 2020). In general, there was a low frequency in occurrence of *x*, 2*x*, and 3*x* gametes but a high frequency with aneuploid gametes in triploids. For example, the percentages of *x*, 2*x*, and aneuploid gametes produced by triploid *Datura stramonium* were 2.6%, 1.2%, and 96.2%, respectively (Satina and Blakeslee, 1937) and by triploid *Pennisetum glaucum* were 1.85%, 1.85%, and 96.3%, respectively (Dujardin and Hanna, 1988). The percentages of *x* and 2*x* in autotriploid cucumber were 1.44% and 1.44% (Diao et al., 2009). Our results primarily concurred with the above reports and showed that the percentages of *x*, 2*x*, 3*x*, and aneuploid male gametes in 'Yuchan' were 8.89%, 6.67%, 3.33%, and 81.11%, respectively and in 'Huanghe' were 3.33%, 8.89%, 2.22%, and 85.56% (Table 3). The occurrence of 2*x* gametes in triploids is critical as it allows to the establishment of balanced tetraploid progenies from 3*x*-4*x* (Vuylsteke et al., 1993; Ramsey and Schemske, 1998; Ramanna and Jacobsen, 2003) or 3*x*-3*x* crosses demonstrated in this study.

Duo to the formation of functional gametes, triploids may produce tetraploid offspring through backcrosses with diploids or crossing with other triploids (Husband, 2004). In *Hieracium echioides*, the cross of 2× × 3× resulted in largely diploid progenies (92%); while in the cross of 3× × 2×, 56% hybrids were tetraploids, and the cross of 3× × 3× produced 60% tetraploids, 26% pentaploids, and 7% hexaploids (Peckert and Chrtek, 2006). In *Tulip*, one tetraploid and four pentaploids were produced in 3× × 2× crosses. In contrast, no tetraploids were obtained in 2× × 3× and 3× × 3× crosses (Marasek-Ciolakowska et al., 2014). In *Populus*, however, a cross of 2× × 3× produced 4% tetraploid hybrids (Wang et al., 2017). In *Echinacea purpurea*, tetraploids were generated in both 2× × 3× and 3× × 2× crosses (Li et al., 2017), while in

10.3389/fpls.2022.1029915

TABLE 4 Meiotic abnormalities in cymbidium 'Yuchan', 'Huanghe', and 'Xiaofeng'.

Stage	Percentage of abnormal behavior during meiosis (%)	Parents		
		'Yuchan'	'Huanghe'	'Xiaofeng'
Metaphase I	Meiotic asynchrony	33.00 ± 5.00^{a}	–	24.5 ± 6.36^{a}
	Lagging chromosomes	5.00 ± 1.00^{a}	–	1.33 ± 0.57^{b}
Anaphase I	Lagging chromosomes	21.50 ± 3.54^{a}	16.00 ± 1.41^{a}	5.50 ± 0.71^{b}
	Chromosome bridges	4.50 ± 0.71^{a}	2.00 ± 1.41^{ab}	0.5 ± 0.71^{b}
Telophase I	Lagging chromosomes	25.67 ± 2.89^{a}	12.50 ± 3.54^{b}	2.5 ± 0.71^{c}
	Meiotic asynchrony	26.00 ± 6.08^{ab}	32.33 ± 0.58^{a}	18.00 ± 1.41^{b}
Metaphase II	Lagging chromosomes	8.33 ± 1.15^{a}	7.50 ± 0.71^{a}	4.00 ± 1.41^{b}
	Tripolar spindles	7.00 ± 1.00^{a}	5.50 ± 0.71^{ab}	3.00 ± 1.41^{b}
	Fused spindles	1.67 ± 0.58^{a}	0.67 ± 0.58^{ab}	0.00 ± 0.00^{b}
Anaphase II	Lagging chromosomes	26.67 ± 3.06^{a}	19.33 ± 1.53^{b}	16.33 ± 2.52^{b}
	Chromosome bridges	9.33 ± 1.53^{a}	5.33 ± 0.57^{b}	0.00 ± 0.00^{b}
Telophase II	Lagging chromosomes	16.67 ± 1.53^{a}	15.33 ± 2.31^{ab}	12.33 ± 0.47^{b}
	Chromosome bridges	6.33 ± 1.53^{a}	1.33 ± 0.58^{b}	2.67 ± 0.94^{b}
	Meiotic asynchrony	30.67 ± 0.58^{a}	21.67 ± 2.08^{b}	12.00 ± 2.83^{c}
Tetrad period	Micronuclei	8.30 ± 1.53^{a}	8.67 ± 1.53^{a}	3.00 ± 1.00^{b}
	Dyad	3.93 ± 0.06^{a}	2.42 ± 0.09^{b}	1.40 ± 0.33^{b}
	Triad	3.76 ± 0.04^{a}	3.33 ± 0.54^{a}	0.58 ± 0.19^{b}

"-" indicates that data were not collected. Values represent mean ± standard error. Different letters within the same row indicate significant differences among cultivars based on Duncan's multiple range test at P< 0.05 level.

Phegopteris decursivepinnata, both tetraploid and pentaploid were formed in the 3× × 2× cross (Nakato and Masuyama, 2021). These results showed that tetraploids were produced more frequently in crosses of 3× × 2× and 3× × 3× than that of 2× × 3×. Our results indicated that albeit tetraploids were formed in combinations of diploid × triploid, however, the frequency (2.08%) was low. On the contrary, the percentage of tetraploids in the hybrids of triploid × triploid was very high (52.5%), suggesting that hybridization

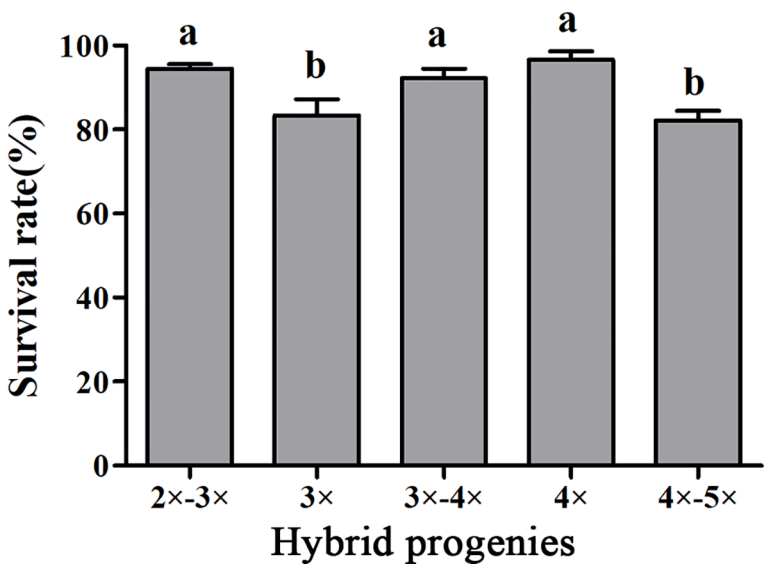

FIGURE 5
Survival rates of hybrid seedlings with different ploidy levels after being transplanted to plastic bags containing a substrate and grown in a shaded greenhouse. Bars represent standard error, and different letters on the top of bars indicate significant difference in survival rates among hybrid progenies analyzed by Duncan's multiple range test at *P*< 0.05 level.

between sexual triploids could be a principal way of producing tetraploid through 'triploid bridge' in *Cymbidium*.

In theory, triploids are sterility due to the unbalanced meiotic chromosome segregation, which resulted in the production of aneuploid gametes (Kohler et al., 2010; Wang et al., 2017; Zhang et al., 2017). But in practice, a lot of triploids can produce functional euploid gametes, especially for *x* and 2*x* gametes in different proportions, which can be used as male or female parent in cross breeding programs (Lim et al., 2003; Hayashi et al., 2009; Zhou et al., 2009; Nakato and Masuyama, 2021). Why does a triploid produce euploid gametes and why is it regarded as a bridge in polyploid evolution? Thus far, little information is available to the questions. Here we propose a hypothesis of coordinate actions of unreduced gamete to address the questions: During meiosis of a sexual polyploid, two chromosome sets of the 2*n* gamete are inclined to be assorted to a daughter cell, resulting in the production of 2*x* gamete, such a chromosome behavior during meiosis mainly depends on the genetic relationship of the parents who provide the chromosome set. When the genetic relationship is very close, such as sexual autopolyploid, the main chromosome pairing configuration at diakinesis is trivalent (sexual autotriploid) or quadrivalent (sexual autotetraploid); when the genetic relationship is far different, such as sexual allopolyploid, the main chromosome pairing configuration is a univalent and a bivalent (sexual allotriploid) or two bivalents (sexual allotetraploid). In fact, the meiotic configuration 8I+8II+2III was the most common in two natural triploid populations of *Campuloclinium macrocephalum*, and their pollen fertilities were 44.74 and 52.69%, respectively (Farco and Dematteis, 2014). Similar results were obtained in allotriploid *P. alba* × *P. berolinensis* 'Yinzhong' (Wang et al., 2017). Lavia et al. (2011) reported that the main chromosome paring configuration in sexual autotriploid *Arachis pintoi* was trivalent, and the pollen grain viability was 42.47%. Ramanna et al. (2003) reported that most *Alstroemeria* interspecific F_1 hybrids of Chilean-Brazilian species simultaneously produced 2*n* male and female gametes; and all the F_2 progeny plants, which were resulted from self-pollination of the F_1 hybrids, were typical allotetraploids. Additionally, most of them formed 16 bivalents and a small proportion formed multivalents during metaphase I stages of meiosis. Triploids that originated through the fusion of 2*n* × *n* gametes of the same taxon showed more regular meiotic behavior and higher fertility than triploids from the contact zone of diploids and tetraploids or triploids of hybrid origin (Kovalsky et al., 2018). Natural *Dactylis* polyploids exhibited successful chromosome pairing during meiosis, whereas artificial polyploids did not, suggesting that there was a selection for sexual fertility in order to stabilize meiosis in natural polyploids (Lumaret and Retired, 1988). Our results indicated that both sexual triploids 'Yuchan' and 'Huanghe' produced *x* and 2*x* male gamete (Figure 2J) with 2*x* gamete frequencies at 6.67% and 8.89%, respectively, and the percentage of viable pollen was 67.88% in 'Yuchan'. These results further proved that two chromosome sets of the 2*n* gamete were inclined to be assorted to a daughter cell. However, due to the sophisticated origin of 2*n* gamete and sexual triploid, the chromosome paring configuration was not typical and the occurrence percentage of 2*x* and *x* gametes was not high. Nevertheless, due to the occurrence in 2*n* gametes, triploids play an important role in polyploid evolution.

Our results indicated that in the cross of 2× × 3×, 25% hybrids were triploids, which was similar to the results in *Tulip* (Marasek-Ciolakowska et al., 2014) and *Populus* (Wang et al., 2017). These triploids were probably formed by the fusion of a 2*x* male gamete produced by the triploid with a haploid female gamete from the diploid or originated from the fusion of a haploid male gamete from the triploid with unreduced female gamete from the diploid. A tetraploid was also obtained in the cross of 2× × 3×, which was likely formed by the fusion of an unreduced male gamete (3*x*) produced by the triploid with a haploid female gamete from the diploid or originated from the fusion of 2*x* male gamete from the triploid with unreduced female gamete from the diploid. In the cross of 3× × 3×, 52.5% progenies were tetraploids, and these tetraploids probably originated from the fusion of an unreduced gamete produced by one parent with a haploid gamete from the other or the fusion of two 2*x* gamete from the parents. Similar results were reported in *H. echioides* where 3× × 3× produced 60% tetraploid (Peckert and Chrtek, 2006). Because of the low percentage of occurrence in euploid gametes in triploid, the aneuploid gametes might play an important role in the production of tetraploids. The possible pathways of producing tetraploids through 'triploid bridge' in *Cymbidium* are illustrated in Figure 6.

A long-standing problem in polyploid breeding is triploid block, which is a reproductive barrier caused by malfunction of endosperm. The endosperm supports the development of the embryo by providing nutrients for its growth, and the genetic relationship between the endosperm and the embryo is important for higher plants evolution (Johnston et al., 1980; Koehler et al., 2010; Stoute et al., 2012; Huc et al., 2022). In the majority of plants, the maternal and paternal chromosome dosages in the endosperm are considered to be critical for seed development and fertility (Vinkenoog et al., 2003; Koehler et al., 2010; Schinkel et al., 2017). However, orchid seeds have rudimentary embryo and lack of endosperm (Yeung, 2017; Chen et al., 2018). Seed germination and seedling establishment depend on the successful interaction between protocorms and mycorrhizal fungi either *in vitro* or *ex vitro*, thus endosperm is not a limiting factor affecting seed germination (Chugh et al., 2009; Xu et al., 2011; Yeung, 2017; Yeh et al., 2019; Bhatti and Thakur, 2022). Our study showed that hybrid seeds derived from the crosses of 3× × 2×, 2× × 3×, and 3× × 3× were well developed and able to germinate normally on culture medium. Plantlets with different ploidy levels grew healthy in greenhouse. Thus, triploid block is not a concern in *Cymbidium* as sexual triploids can produce seeds through

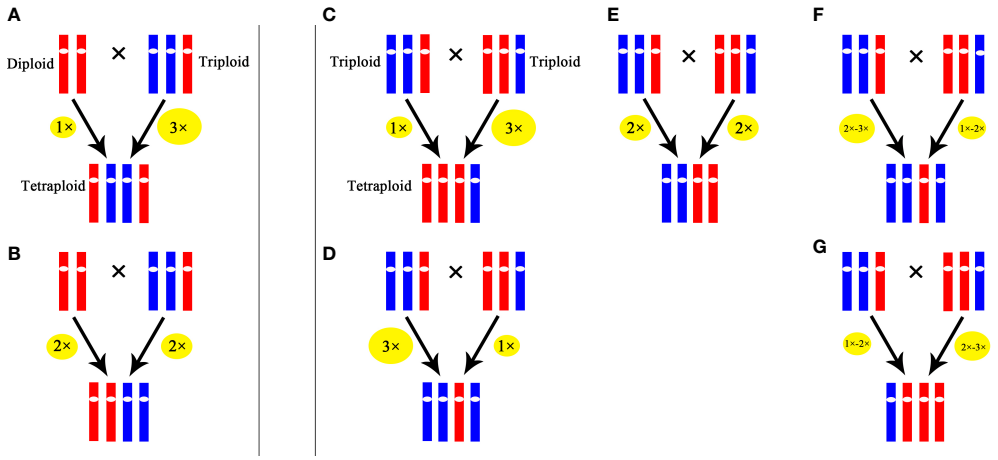

FIGURE 6
Possible pathways for producing tetraploid through 'triploid bridge'. **(A)** and **(B)** represent possible pathways in the cross of 2××3×. **(C–G)** represent possible pathways in the cross of 3××3×. The size of ellipse represents ploidy level of gamete, the larger the size is, the higher the ploidy level is.

hybridization with appropriate parents and the seeds can readily germinate.

Cymbidium is a renowned genus in the orchid family that distributed in tropical and subtropical areas of Asia, Papua New Guinea, and Australia (Ai et al., 2021). It exhibits distinctive ecological diversification and occurs in terrestrial, epiphytic, lithophytic, and saprophytic life forms (Yukawa and Stern, 2002; Ning et al., 2018). The cross compatibility between different species was reported to be high, and even an increasing number of interspecific and intergeneric hybrids has been obtained through artificial pollination (Li et al., 2014; Ogura-Tsujita et al., 2014; Joffard et al., 2022). These interspecific hybrids have a high percentage in occurrence of 2*n* gametes and have been successfully employed to create sexual polyploids in breeding programs (Zeng et al., 2020; Kondo et al., 2022). However, because of reproductive isolation caused by geographical, temporal, and spatial isolations, the interspecific hybrids are rare in nature. The triploid crossability and 2*n* gamete formation demonstrated in the present study may represent a viable way for creating new polyploid cymbidium through hybridization.

Conclusion

As far as is known, this is the first investigation of the crossability of sexual triploids in cymbidiums. Our study documented that both triploid 'Yuchan' and 'Huanghe' were fertile and able to be used as male or female parents in cross breeding. Sexual triploid cymbidiums produced fertile male gametes of 1*x*, 1*x*~2*x*, 2*x*, 2*x*~3*x*, and 3*x*. The production of 2*x* male gametes could be resulted from the probability that two chromosome sets of the 2*n* gamete were inclined to enter into the same daughter cell during meiosis. The cross of diploid × triploid generated diploid, triploid, and tetraploid with frequencies at 2.1%, 25.0%, and 2.1%, respectively. The cross of triploid × triploid produced tetraploid and pentaploid hybrids with proportions of 52.5% and 2.5%, respectively. The survival rate of tetraploid was significantly higher than that of triploid. Our results indicate that the triploid cymbidiums are not reproductive barrier but act as a bridge in the formation of polyploid plants. A hypothesis of coordinate actions of unreduced gamete was proposed to explain why sexual triploids produce 1*x* and 2*x* euploid gametes. Further research with more sexual polyploids including auto and allopolyploids, along with the use of genomic *in situ* hybridization (GISH) should be conducted to test this hypothesis.

Data availability statement

The original contributions presented in the study are included in the article/Supplementary Material. Further inquiries can be directed to the corresponding authors.

Author contributions

Z-SZ and R-ZZ designed the study. M-ML, R-ZZ, LX, H-RG, and J-RZ performed the experiment. M-ML, R-ZZ, and LX carried out and analyzed the data. M-ML and Q-LS wrote a first draft of the manuscript that was further critically reviewed and edited by JC, R-ZZ, LX, QW, H-RG, and J-RZ. All authors contributed to the article and approved the submitted version.

Funding

This work was supported by the Research and Development Plan in Key Area of Guangdong Province, China (2022B0202080004), Special Project of Agriculture Science Independent Innovation of Guangzhou Agricultural Bureau (21102422), Science and Technology Program of Guangzhou (202002030068) and Project of Guangdong Provincial Key Laboratory of Plant Molecular Breeding (GPKLPMB202206).

Conflict of interest

The authors declare that the research was conducted in the absence of any commercial or financial relationships that could be construed as a potential conflict of interest.

Publisher's note

All claims expressed in this article are solely those of the authors and do not necessarily represent those of their affiliated organizations, or those of the publisher, the editors and the reviewers. Any product that may be evaluated in this article, or claim that may be made by its manufacturer, is not guaranteed or endorsed by the publisher.

Supplementary material

The Supplementary Material for this article can be found online at: https://www.frontiersin.org/articles/10.3389/fpls.2022.1029915/full#supplementary-material

SUPPLEMENTARY FIGURE 1
Cymbidium cultivars used for hybridization.

SUPPLEMENTARY FIGURE 2
Morphology of seeds, test-tube seedlings and transplanted seedlings.

SUPPLEMENTARY FIGURE 3
Types of male gametes at early microspore stage in diploid and triploid Cymbidium.

SUPPLEMENTARY FIGURE 4
Meiotic abnormalities of sexual triploid 'Huanghe'.

SUPPLEMENTARY FIGURE 5
Meiotic abnormalities of diploid 'Xiaofeng'.

References

Ai, Y., Li, Z., Sun, W. H., Chen, J., Zhang, D. Y., Ma, L., et al. (2021). The *Cymbidium* genome reveals the evolution of unique morphological traits. *Hortic. Res.* 8, 255. doi: 10.1038/s41438-021-00683-z

Alexander, L. (2020). Ploidy level influences pollen tube growth and seed viability in interploidy crosses of *Hydrangea macrophylla*. *Front. Plant Sci.* 11. doi: 10.3389/fpls.2020.00100

Bergstrom, I. (1940). On the progeny of diploid × triploid *Populus tremula* with special reference to the occurrence of tetraploidy. *Hereditas* 26, 191–201. doi: 10.1111/j.1601-5223.1940.tb03231.x

Bhatti, S. K., and Thakur, M. (2022). An overview on orchids and their interaction with endophytes. *Bot. Rev.* doi: 10.1007/s12229-022-09275-5

Bretagnolle, F., and Thompson, J. D. (1995). Gametes with the somatic chromosome number: mechanisms of their formation and role in the evolution of autopolyploid plants. *New Phytol.* 129, 1–22. doi: 10.1111/j.1469-8137.1995.tb03005.x

Burton, T. L., and Husband, B. C. (2001). Fecundity and offspring ploidy in matings among diploid, triploid and tetraploid *Chamerion angustifolium* (Onagraceae): consequences for tetraploid establishment. *Heredity* 87, 573–582. doi: 10.1046/j.1365-2540.2001.00955.x

Cai, J., Liu, X., Vanneste, K., Proost, S., Tsai, W., Liu, K. W., et al. (2015). The genome sequence of the orchid *Phalaenopsis equestris*. *Nat. Genet.* 47, 65–72. doi: 10.1038/ng.3149

Chen, Y., Zhang, C., Wang, X. F., and Ao, C. Q. (2018). Fertilisation of polar nuclei and formation of early endosperms in *Dendrobium catenatum*: evidence for the second fertilisation in orchidaceae. *Aust. J. Bot.* 66, 354–359. doi: 10.1071/BT17211

Chugh, S., Guha, S., and Rao, I. U. (2009). Micropropagation of orchids: a review on the potential of different explants. *Sci. Hortic.* 122, 507–520. doi: 10.1016/j.scienta.2009.07.016

Clo, J., Padilla-Garcia, N., and Kolar, F. (2022). Polyploidization as an opportunistic mutation: The role of unreduced gametes formation and genetic drift in polploid establishment.*J. Evol. Biol.* 35, 1099–1109. doi: 10.1111/jeb.14055

Cui, J., Chen, J. J., and Henny, R. (2009). Regeneration of aeschynanthus radicans *via* direct somatic embryogenesis and analysis of regenerants with flow cytometry. *In vitro cell. Dev. Biol.-Plant.* 45, 34–43. doi: 10.1007/s11627-008-9147-9

Czarnecki, D. M., Hershberger, A. J., Robacker, C. D., Clark, D. G., and Deng, Z. A. (2014). Ploidy levels and pollen stainability of *Lantana camara* cultivars and breeding lines. *HortScience* 49, 1271–1276. doi: 10.21273/HORTSCI.49.10.1271

Diao, W. P., Bao, S. Y., Jiang, B., Cui, L., and Chen, J. F. (2009). Primary trisomics obtained from autotriploid by diploid reciprocal crosses in cucumber. *Sex Plant Reprod.* 22, 45–51. doi: 10.1007/s00497-008-0090-z

Dujardin, M., and Hanna, W. W. (1988). Cytology and breeding behavior of a partially fertile triploid pearl millet. *J. Hered.* 79, 216-218. doi: 10.1093/oxfordjournals.jhered.a110499

Duszynska, D., Vilhjalmsson, B., Bravo, R. C., Swamidatta, S., Juenger, T. E., Donoghue, M. T. A., et al. (2019). Transgenerational effects of inter-ploidy cross direction on reproduction and F2 seed development of *Arabidopsis thaliana* F1 hybrid triploids. *Plant Reprod.* 32, 275–289. doi: 10.1007/s00497-019-00369-6

Ehlenfeldt, M. K., and Ortiz, R. (1995). Evidence on the nature and origins of endosperm dosage requirements in *Solanum* and other angiosperm genera. *Sex Plant Reprod.* 8, 189–196. doi: 10.1007/BF00228936

Erilova, A., Brownfield, L., Exner, V., Rosa, M., Twell, D., Scheid, O. M., et al. (2009). Imprinting of the polycomb group gene *MEDEA* serves as a ploidy sensor in *Arabidopsis*. *PLoS Genet.* 5, e1000663. doi: 10.1371/journal.pgen.1000663

Farco, G. E., and Dematteis, M. (2014). Meiotic behavior and pollen fertility in triploid and tetraploid natural populations of *Campuloclinium macrocephalum* (Eupatorieae, asteraceae). *Plant Syst. Evol.* 30, 1843–1852. doi: 10.1007/s00606-014-1011-2

Friedman, W. E., Madrid, E. N., and Williams, J. H. (2008). Origin of the fittest and survival of the fittest: Relating female gametophyte development to endosperm genetics. *Int. J. Plant Sci.* 169, 79–92. doi: 10.1086/523354

Geng, X. N., Han, Z. Q., Yang, J., Du, K., Han, Q., and Kang, X. Y. (2019). The different origins of artificially-induced unreduced female gametes and their effect on transmitted parental heterozygosity in *Populus*. *Euphytica* 215, 181. doi: 10.1007/s10681-019-2501-7

Haig, D. (2013). Kin conflict in seed development: an interdependent but fractious collective. *Annu. Rev. Cell Dev. Biol.* 29, 189–211. doi: 10.1146/annurev-cellbio-101512-122324

Hayashi, M., Kato, J., Ohashi, H., and Mii, M. (2009). Unreduced 3× gamete formation of allotriploid hybrid derived from the cross of *Primula denticulata* (4×) x *P. rosea* (2×) as a causal factor for producing pentaploid hybrids in the backcross with pollen of tetraploid *P. denticulata*. *Euphytica* 169, 123–131. doi: 10.1007/s10681-009-9955-y

Hedren, M., Lorenz, R., Teppner, H., Dolinar, B., Giotta, C., Griebl, N., et al. (2018). Evolution and systematics of polyploid *Nigritella* (Orchidaceae). *Nord. J. Bot.* 36, e01539. doi: 10.1111/njb.01539

Henry, I. M., Dilkes, B. P., Young, K., Watson, B., Wu, H., and Comai, L. (2005). Aneuploidy and genetic variation in the *Arabidopsis thaliana* triploid response. *Genetics* 170, 1979–1988. doi: 10.1534/genetics.104.037788

Huang, W. T., Fang, Z. M., Zeng, S. J., Zhang, J. X., Wu, K. L., Chen, Z. L., et al. (2012). Molecular cloning and functional analysis of three *FLOWERING LOCUS T (FT)* homologous genes from Chinese *Cymbidium*. *Int. J. Mol. Sci.* 13, 11385–11398. doi: 10.3390/ijms130911385

Huc, J., Dziasek, K., Pachamuthu, K., Woh, T., Kohler, C., and Borges, F. (2022). Bypassing reproductive barriers in hybrid seeds using chemically induced epimutagenesis. *Plant Cell* 34, 989–1001. doi: 10.1093/plcell/koab284

Husband, B. C. (2000). Constraints on polyploid evolution: a test of the minority cytotype exclusion principle. *Proc. R. Lond.* 267, 217–223. doi: 10.1098/rspb.2000.0990

Husband, B. C. (2004). The role of triploid hybrids in the evolutionary dynamics of mixed-ploidy populations. *Biol. J. Linn. Soc* 82, 537–546. doi: 10.1111/j.1095-8312.2004.00339.x

Jike, W., Li, M. G., Zadra, N., Barbaro, E., Sablok, G., Bertorelle, G., et al. (2020). Phylogenomic proof of recurrent demipolyploidization and evolutionary stalling of the "Triploid bridge" in arundo (Poaceae). *Int. J. Mol. Sci.* 21, 5247. doi: 10.3390/ijms21155247

Joffard, N., Olofsson, C., Friberg, M., and Sletvold, N. (2022). Extensive pollinator sharing does not promote character displacement in two orchid congeners. *Evolution* 76, 749–764. doi: 10.1111/evo.14446

Johnston, S. A., den Nijs, T. P., Peloquin, S. J., and Hanneman, R. E. J. (1980). The significance of genic balance to endosperm development in intraspecific crosses. *Theor. Appl. Genet.* 57, 5–9. doi: 10.1007/BF00276002

Jones, K. D., and Reed, S. M. (2007). Analysis of ploidy level and its effects on guard cell length, pollen diameter, and fertility in *Hydrangea macrophylla*. *HortScience* 42, 483–488. doi: 10.21273/HORTSCI.42.3.483

Koehler, C., Scheid, O. M., and Erilova, A. (2010). The impact of the triploid block on the origin and evolution of polyploid plants. *Trend. Genet.* 26, 142–148. doi: 10.1016/j.tig.2009.12.006

Kondo, H., Deguchi, A., Kikuchi, S., and Miyoshi, K. (2022). Two pathways of 2*n* gamete formation and differences in the frequencies of 2*n* gametes between wild species and interspecific hybrids. *Plant Cell Rep*. doi: 10.1007/s00299-022-02915-5

Kovalsky, I. E., Luque, J. M. R., Elias, G., Fernandez, S. A., and Neffa, V. G. S. (2018). The role of triploids in the origin and evolution of polyploids of *Turnera sidoides* complex (Passifloraceae, turneroideae). *J. Plant Res.* 131, 77–89. doi: 10.1007/s10265-017-0974-9

Lavia, G. I., Ortiz, A. M., Robledo, G., Fernandez, A., and Seijo, G. (2011). Origin of triploid *Arachis pintoi* (Leguminosae) by autopolyploidy evidenced by FISH and meiotic behaviour. *Ann. Bot.* 108, 103–111. doi: 10.1093/aob/mcr108

Levin, D. A. (1975). Minority cytotype exclusion in local plant populations. *Taxon* 24, 35–43. doi: 10.2307/1218997

Li, Q. L., Jiang, W. Z., Ren, Y., Chen, R., Li, X. L., Yang, Y. S., et al. (2017). *In vitro* cloning potential and phytochemical evaluations of aneuploid individuals produced from reciprocal crosses between diploid and triploid in *Echinacea purpurea* l. *Acta Soc Bot. Pol.* 86, 1-16. doi: 10.5586/asbp.3556

Lim, K. B., Ramanna, M. S., Jacobsen, E., and van Tuyl, J. M. (2003). Evaluation of BC2 progenies derived from 3x-2x and 3x-4x crosses of *Lilium* hybrids: a GISH analysis. *Theor. Appl. Genet.* 106, 568–574. doi: 10.1007/s00122-002-1070-6

Lin, B. Y. (1984). Ploidy barrier to endosperm development in maize. *Genetics* 107, 103–115. doi: 10.1007/BF00056440

Li, X. B., Xiang, L., Wang, Y., Luo, J., Wu, C., Sun, C. B., et al. (2014). Genetic diversity, population structure, pollen morphology and cross-compatibility among Chinese cymbidiums. *Plant Breed.* 133, 145–152. doi: 10.1111/pbr.12125

Lumaret, R., and Retired, M. B. (1988). Cytology, genetics and evolution in the genus *Dactylis*. *Crit. Rev. Plant Sci.* 7, 55–91. doi: 10.1080/07352688809382259

Marasek-Ciolakowska, A., Xie, S. L., Arens, P., and van Tuyl, J. M. (2014). Ploidy manipulation and introgression breeding in Darwin hybrid tulips. *Euphytica* 198, 389–400. doi: 10.1007/s10681-014-1115-3

Moura, Y. A., Alves-Pereira, A., da Silva, C. C., Souza, L. M., de Souza, A. P., and Koehler, S. (2020). Secondary origin, hybridization and sexual reproduction in a diploid-tetraploid contact zone of the facultatively apomictic orchid *Zygopetalum mackayi*. *Plant Biol.* 22, 939–948. doi: 10.1111/plb.13148

Nakato, N., and Masuyama, S. (2021). Polyploid progeny from triploid hybrids of *Phegopteris decursivepinnata* (Thelypteridaceae). *J. Plant Res.* 134, 195–208. doi: 10.1007/s10265-021-01255-x

Ning, H. J., Ao, S. Y., Fan, Y. R., Fu, J. X., and Xu, C. M. (2018). Correlation analysis between the karyotypes and phenotypic traits of Chinese cymbidium cultivars. *Hortic. Environ. Biote.* 59, 93–103. doi: 10.1007/s13580-018-0010-6

Ogura-Tsujita, Y., Miyoshi, K., Tsutsumi, C., and Yukawa, T. (2014). First flowering hybrid between autotrophic and mycoheterotrophic plant species: breakthrough in molecular biology of mycoheterotrophy. *J. Plant Res.* 127, 299–305. doi: 10.1007/s10265-013-0612-0

Okamoto, T., Ohnishi, Y., and Toda, E. (2017). Development of polyspermic zygote and possible contribution of polyspermy to polyploid formation in angiosperms. *J. Plant Res.* 130, 485–490. doi: 10.1007/s10265-017-0913-9

Peckert, T., and Chrtek, J. (2006). Mating interactions between coexisting diploid, triploid and tetraploid cytotypes of *Hieracium echioides* (*Asteraceae*). *Folia Geobot.* 41, 323–334. doi: 10.1007/BF02904945

Ramanna, M. S., and Jacobsen, E. (2003). Relevance of sexual polyploidization for crop improvement - a review. *Euphytica* 133, 3–18. doi: 10.1023/A:1025600824483

Ramanna, M. S., Kuipers, A. G. J., and Jacobsen, E. (2003). Occurrence of numerically unreduced (2n) gametes in *Alstroemeria* interspecific hybrids and their significance for sexual polyploidisation. *Euphytica* 133, 95–106. doi: 10.1023/A:1025652808553

Ramsey, J., and Schemske, D. W. (1998). Pathways, mechanisms, and rates of polyploid formation in flowering plants. *Annu. Rev. Ecol. Syst.* 29, 467–501. doi: 10.1146/annurev.ecolsys.29.1.467

Satina, S., and Blakeslee, A. F. (1937). Chromosome behavior in triploids of *Datura* stramonium. i. the male gametophyte. *Am. J. Bot.* 24, 518–27. doi: 10.2307/2437074

Schinkel, C. C. F., Kirchheimer, B., Dullinger, S., Geelen, D., De Storme, N., and Hoerandl, E. (2017). Pathways to polyploidy: indications of a female triploid bridge in the alpine species *Ranunculus kuepferi* (Ranunculaceae). *Plant Syst. Evol.* 303, 1093–1108. doi: 10.1007/s00606-017-1435-6

Scott, R. J., Spielman, M., Bailey, J., and Dickinson, H. G. (1998). Parent-of-origin effects on seed development in *Arabidopsis thaliana*. *Development* 125, 3329–3341. doi: 10.1242/dev.125.17.3329

Stoute, A. I., Varenko, V., King, G. J., Scott, R. J., and Kurup, S. (2012). Parental genome imbalance in *Brassica oleracea* causes asymmetric triploid block. *Plant J.* 71, 503–516. doi: 10.1111/j.1365-313X.2012.05015.x

Thakur, S., and Dutt, H. C. (2021). *Cymbidium macrorhizon* lindl. (Orchidaceae): a new record for flora of jammu and Kashmir, India. *Natl. Acad. Sci. Lett.* 44, 271–274. doi: 10.1007/s40009-020-00985-1

Thompson, J. D., and Lumaret, R. (1992). The evolutionary dynamics of polyploid plants: origins, establishment and persistence. *Trends Ecol. Evol.* 7, 302–307. doi: 10.1016/0169-5347(92)90228-4

Trankner, C., Gunther, K., Sahr, P., Engel, F., and Hohe, A. (2020). Targeted generation of polyploids in *Hydrangea macrophylla* through cross-based breeding. *BMC Genet.* 21, 147. doi: 10.1186/s12863-020-00954-z

Vilcherrez-Atoche, J. A., Iiyama, C. M., and Cardoso, J. C. (2022). Polyploidization in orchids: from cellular changes to breeding applications. *Plants* 11, 469. doi: 10.3390/plants11040469

Vinkenoog, R., Bushell, C., Spielman, M., Adams, S., Dickinson, H. G., and Scott, R. J. (2003). Genomic imprinting and endosperm development in flowering plants. *Mol. Biotechnol.* 25, 149–184. doi: 10.1385/MB:25:2:149

Vuylsteke, D., Ortiz, R., Pasberg-Gauhl, C., Gauhl, F., and Speijer, P. (1993). Plantain and banana research at the international research institute of tropical agriculture. *HortScience* 28873, 970–971. doi: 10.21273/HORTSCI.28.9.874

Wang, J., Huo, B. B., Liu, W. T., Li, D. L., and Liao, L. (2017). Abnormal meiosis in an intersectional allotriploid of *Populus* l. and segregation of ploidy levels in 2× x 3×progeny. *PLoS One* 12, e0181767. doi: 10.1371/journal.pone.0181767

Wang, J., Kang, X. Y., and Zhu, Q. (2010). Variation in pollen formation and its cytological mechanism in an allotriploid white poplar. *Tree Genet. Genomes* 6, 281–290. doi: 10.1007/s11295-009-0248-3

Xie, L., Ke, L. Z., Lu, X. Q., Chen, J. J., and Zhang, Z. S. (2022). Exploiting unreduced gametes for improving ornamental plants. *Front. Plant Sci.* 13. doi: 10.3389/fpls.2022.883470

Xu, X. W., Cai, M. L., Yang, Y. P., Peng, K. K., Zeng, A. P., Jiang, N., et al. (2011). Hybridization and *in vitro* seed germination of *Cymbidium kanran* (in Chinese). *Acta Hortic. Sin.* 38, 2010–2016. doi: 10.16420/j.issn.0513-353x.2011.10.023

Yamauchi, A., Hosokawa, A., Nagata, H., and Shimoda, M. (2004). Triploid bridge and role of parthenogenesis in the evolution of autopolyploidy. *Am. Nat.* 164, 101–112. doi: 10.1086/421356

Yeh, C. M., Chung, K., Liang, C. K., and Tsai, W. C. (2019). New insights into the symbiotic relationship between orchids and fungi. *Appl. Sci.* 3, 585. doi: 10.3390/app9030585

Yeung, E. C. (2017). A perspective on orchid seed and protocorm development. *Bot. Stud.* 58, 33. doi: 10.1186/s40529-017-0188-4

Yukawa, T., and Stern, W. L. (2002). Comparative vegetative anatomy and systematics of *Cymbidium* (Cymbidieae: Orchidaceae). *Bot. J. Linn. Soc* 138, 383–419. doi: 10.1046/j.1095-8339.2002.00038.x

Zeng, R. Z., Zhu, J., Xu, S. Y., Du, G. H., Guo, H. R., Chen, J. J., et al. (2020). Unreduced male gamete formation in *Cymbidium* and its use for developing sexual polyploid cultivars. *Front. Plant Sci.* 11. doi: 10.3389/fpls.2020.00558

Zhang, X. Q., Cao, Q. Z., Zhou, P., and Jia, G. X. (2017). Meiotic chromosome behavior of the male-fertile allotriploid lily cultivar 'Cocossa'. *Plant Cell Rep.* 36, 1641–1653. doi: 10.1007/s00299-017-2180-6

Zhang, G. Q., Liu, K. W., Li, Z., Lohaus, R., Hsiao, Y., and Niu, S. C. (2017). The *Apostasia* genome and the evolution of orchids. *Nature* 549, 379–383. doi: 10.1038/nature23897

Zhang, W. X., Zhang, G. Q., Zeng, P., Zhang, Y. Q., Hu, H., Liu, Z. J., et al. (2021). Genome sequence of *Apostasia ramifera* provides insights into the adaptive evolution in orchids. *BMC Genomics* 22, 536. doi: 10.1186/s12864-021-07852-3

Zhang, Y. X., Zhang, G. Q., Zhang, D. Y., Liu, X. D., Xu, X. Y., Sun, W. H., et al. (2021). Chromosome-scale assembly of the *Dendrobium chrysotoxum* genome enhances the understanding of orchid evolution. *Hortic. Res.* 8, 183. doi: 10.1038/s41438-021-00621-z

Zhou, J. J., Zeng, R. Z., Liu, F., Yi, M. S., Li, Y. H., and Zhang, Z. S. (2009). Investigation on chromosome ploidy of the hybrids of *Phalaenopsis* polyploids (in Chinese). *Acta Hortic. Sin.* 10, 1491–1497. doi: 10.16420/j.issn.0513

Zhu, J., Liu, Y. Y., Zeng, R. Z., Li, Y. H., Guo, H. R., Xie, L., et al. (2014). Preliminarily study on formation and cytological mechanism of unreduced male gametes in different ploidy *Phalaenopsis* (in Chinese). *Acta Hortic. Sin.* 10, 2132–2138. doi: 10.16420/j.issn.0513-353x.2014.10.019

Frontiers in
Plant Science

Cultivates the science of plant biology and its applications

The most cited plant science journal, which advances our understanding of plant biology for sustainable food security, functional ecosystems and human health.

Discover the latest Research Topics

See more →

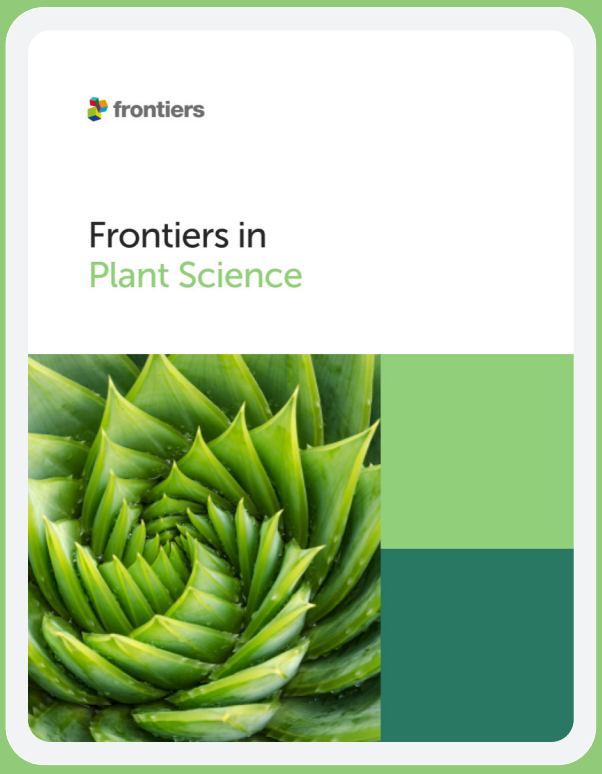

Frontiers

Avenue du Tribunal-Fédéral 34
1005 Lausanne, Switzerland
frontiersin.org

Contact us

+41 (0)21 510 17 00
frontiersin.org/about/contact